

2000 USNC/URSI National Radio Science Meeting

2000+

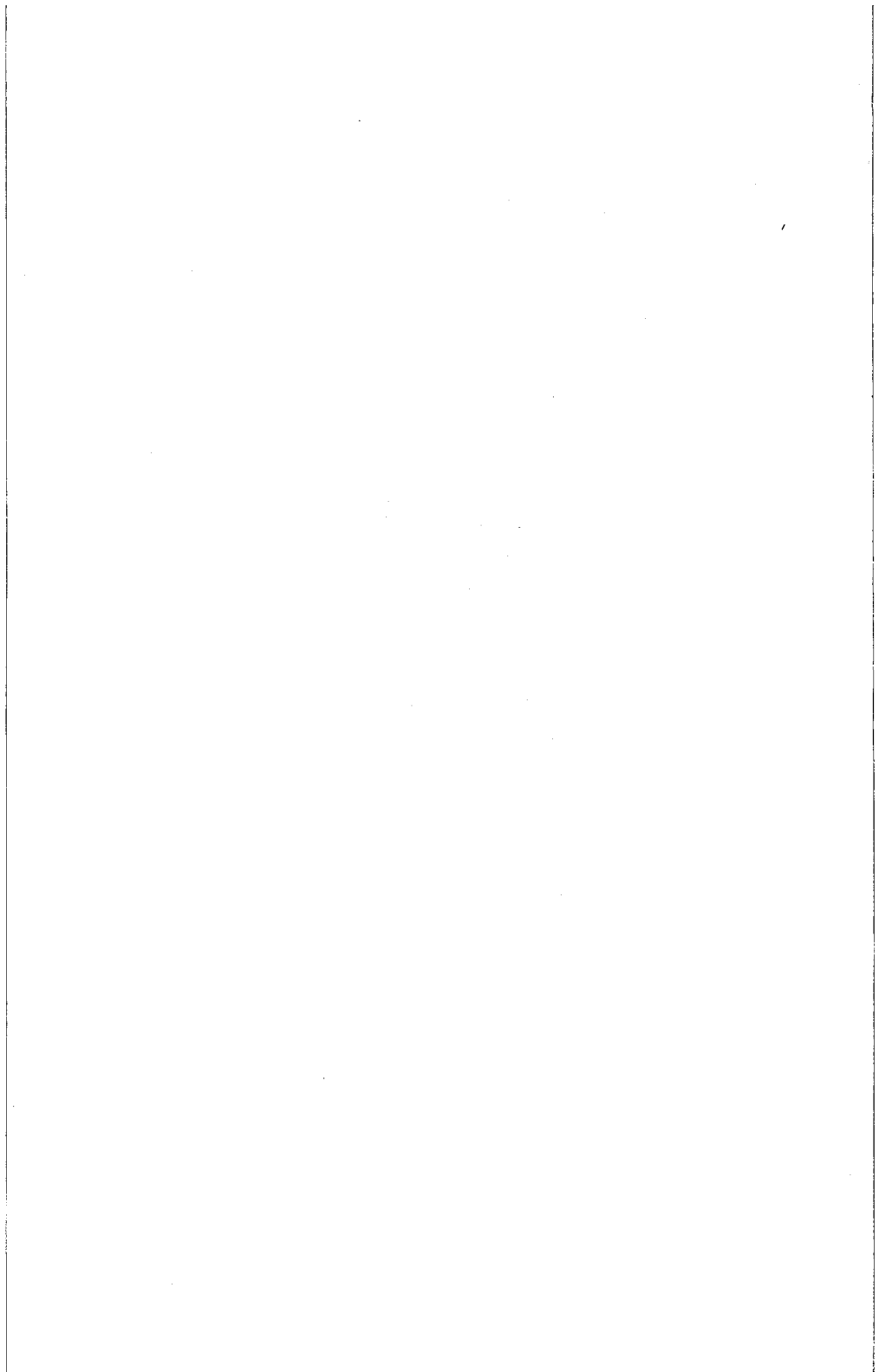
Transmitting
Waves of Progress
to the Next Millennium



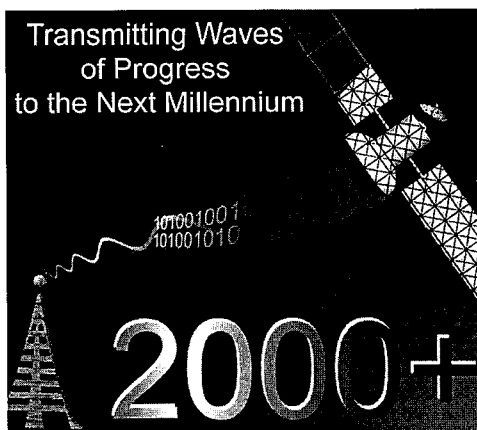
Salt Lake City, Utah
Doubletree Hotel
July 16-21, 2000

URSI DIGEST





USNC/URSI National Radio Science Meeting



July 16-21, 2000
Salt Lake City, Utah



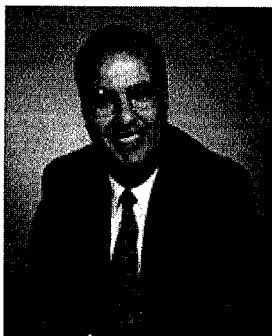
2000 Digest

Held in conjunction with:
**IEEE Antennas and Propagation Society
International Symposium**



Chair's Welcome

Welcome to the 2000 IEEE AP-S Symposium and USNC/URSI Meeting



A Wholehearted Welcome to Salt Lake City

On behalf of the Steering Committee and the IEEE community in Utah, I am delighted with the opportunity to welcome you, your families, and friends to Salt Lake City, the home of the new millennium IEEE AP-S Symposium and URSI meeting. The theme of this year's conference is "Transmitting Waves of Progress to the Next Millennium," and every effort was made to reflect this theme in the preparation of the technical and social programs.

For the technical program, a millennium session has been scheduled to reflect on the innovative contributions made by members of our society and their impact on modern progress in areas such as wireless communications, satellites, propagation and remote sensing, and education. Keynote speakers were invited to lead presentations in some of the scheduled sessions, and other special sessions were organized by leading members of our society. The "Interactive Forum" was scheduled daily during an extended lunch period in a friendly and highly interactive environment, and a complimentary light lunch will be served. I truly hope that you will enjoy a stimulating and highly informative technical program that includes more than 900 technical papers for both interactive and platform presentations.

For the social program, we went all out and, with the help of our corporate sponsors, were able to schedule a daily major social event during your four-day stay at the conference. On Sunday, you will enjoy meeting old friends and making new ones during the opening reception. On Monday, you will enjoy one of our major social events, a gala at Red Butte Gardens and a visit to the Rice-Eccles Stadium, home of the opening and closing ceremonies of the 2002 Winter Olympic Games. On Tuesday, we will take you to a western extravaganza at the Snowbird Resort in beautiful Little Cottonwood Canyon. You will enjoy the mountain air, a western barbecue buffet, live entertainment, and a scenic ride on the aerial tram. Several other tours of the city and the surrounding national parks are also scheduled during the conference week. On Wednesday, we invite you and your family to join us in the traditional awards banquet, which will culminate a whole day of millennium presentations. The daily and highly entertaining subsidized social events should make your stay both informative and enjoyable. Just plan on coming, bring along families and friends, and we will take good care of you.

Please consider an extended vacation and visit our national parks and the unique, breathtaking sights of the Wasatch Mountains and the exceptional outdoor activities available in Utah. Also try to take advantage of your stay to search for your family tree and discover your roots in the Family Search Center in Salt Lake City, the largest public genealogical facility in the world. The conference hotel is located at the heart of the downtown area and is one block away from historic Temple Square. This makes it easy to enjoy the city with its breathtaking sites and historical traditions.

We look forward with pleasure to welcoming you, your family, and friends to Salt Lake City in July. Have a safe trip and please let us know if we can be of assistance.

Magdy F. Iskander

Steering Committee

General Chair

Magdy F. Iskander
University of Utah
Phone: 801-581-6944
iskander@ee.utah.edu

Co-Chair

Richard W. Grow
University of Utah
Phone: 801-581-7634
grow@ee.utah.edu

Technical Program Committee Co-Chairs

Om P. Gandhi
University of Utah
Phone: 801-581-7743
gandhi@ee.utah.edu

Michael A. Jensen
Brigham Young University
Phone: 801-378-5736
jensen@ee.byu.edu

Special Sessions Co-Chairs

David V. Arnold
Brigham Young University
Phone: 801-378-3262
arnold@ee.byu.edu

Mikel J White
Raytheon Systems Co.
Phone: 972-344-5219
m-white1@raytheon.com

Exhibits Chair

Steven M. Blair
University of Utah
Phone: 801-585-6157
blair@ee.utah.edu

Workshops Co-Chairs

Randy Haupt
Utah State University
Phone: 435-797-2840
haupt@ece.usu.edu

Shane M. Bringhurst
Raytheon Systems Co.
Phone: 972-344-3548
s-bringhurst1@ratheon.com

Student Paper Contest Co-Chairs

J. Mark Baird
University of Utah
Phone: 801-581-6952
baird@ee.utah.edu

Cynthia Furse
Utah State University
Phone: 435-797-2870
furse@ece.usu.edu

Finance Chair

Michael G. Kay
University of Utah
Phone: 801-581-8258
mkay@coe.utah.edu

Publications Chair

Rex Jameson
Omega Performance
Phone: 801-483-9683
rex.jameson@omega-multimedia.com

Local Arrangement Co-Chairs

Sonia E. Iskander
Phone: 801-272-7240

Holly H. Cox
Phone: 801-581-3843
cox@ee.utah.edu

URSI Liaison

Douglas A. Christensen
University of Utah
Phone: 801-581-7859
christen@ee.utah.edu

Technical Program Committee for AP-S and URSI

Kenneth Anderson	Anthony Martin
J. Mark Baird	Krzysztof A. Michalski
Constantine Balanis	Robert Nevels
Frank Barnes	Cam Nguyen
Jennifer T. Bernhard	Michal Okoniewski
Ioannis Besieris	Dharmesh Patel
Steve Blair	Andrew F. Peterson
Shane Bringham	Yahya Rahmat-Samii
Gary Brown	Sembiam R. Rengarajan
Kai Chang	Shashi M. Sanzgiri
Indira Chatterjee	Guy A. Schiavone
Douglas A. Christensen	Rainee N. Simons
Samir El-Ghazaly	John K. Smith
Steve Frasier	W. Ross Stone
Cynthia Furse	Maria Stuchly
Om P. Gandhi	Warren Stutzman
Richard W. Grow	Dennis Sullivan
Susan C. Hagness	Mike Thursby
James Harvey	P. L. E. Uslenghi
Randy Haupt	Kathleen Virga
Akira Ishimaru	John Volakis
Magdy F. Iskander	Parveen Wahid
David R. Jackson	Ed Westwater
Ramakrishna Janaswamy	James C. Wiltse
Michael Jensen	Jeffrey L. Young
Jianming Jin	Zhengqing Yun
Linwood Jones	Amir I. Zaghlool
Motohisa Kanda	Zhijun Zhang
Stan J. Kubina	Ahmed Zooghy
Gianluca Lazzi	
Ronald J. Marhefka	

Corporate Sponsors

On behalf of the IEEE Antennas and Propagation Society and the United States National Committee (USNC) of the International Union of Radio Science (URSI), the Steering Committee gratefully acknowledges the gracious support of the following corporations in sponsoring this conference:

Agilent Technologies
Hewlett-Packard Co.
Kennecott Utah Copper
L-3 Communications
MOOG Inc.
Motorola
Raytheon Systems Co.

Exhibitors

In addition to exhibits by the corporate sponsors, the following organizations registered (as of June 5, 2000) as exhibitors in the conference.

Ansoft Corporation
Artech House Publishers
Comlab, Inc.
EM Software & Systems
EMAG Technologies
GIL Technologies
IEEE Press
John Wiley & Sons, Inc.
Nearfield Systems, Inc.
Prentice Hall
Sonnet Software, Inc.
TICRA
TRW, Specialized Services & Products
Vector Fields, Inc.
Zeland Software, Inc.

IEEE 2000 Awards

2000 IEEE Heinrich Hertz Medal

Arthur A. Oliner

for many outstanding contributions to the theory of guided waves and antennas, with emphasis on the fundamentals and applications of leaky waves

2000 IEEE Electromagnetics Award

Roger F. Harrington

for pioneering the application of the Method of Moments to computational electromagnetics, and contributions to electromagnetics education

2000 IEEE Medal for Radar Technologies and Applications

Merrill Skolnik

for outstanding leadership of Navy radar research, authorship of widely used books on radar, and personal contributions to the advancement of radar technology and systems

Antennas and Propagation Society 2000 Awards

2000 Distinguished Achievement Award

Thomas B. A. Senior

for outstanding contributions to the theory of diffraction and scattering of electromagnetic waves, and leadership in education and laboratory direction

2000 S. A. Schelkunoff Transactions Prize Paper Award

Giorgio Franceschetti, Stefano Marano, and Francesco Palmieri

for the paper "Propagation Without Wave Equation Toward an Urban Area Model," September 1999

Honorable Mention for Schelkunoff Award

Jean-Pierre Béranger

for the paper "Evanescent Waves in PML's: Origin of the Numerical Reflection in Wave-Structure Interaction Problems," October 1999

2000 H. A. Wheeler Applications Prize Paper Award

Jack J. Schuss, Jeffrey Upton, Bruce W. Myers, Thomas Sikina, Alan B. Rohwer,
Patrick J. Makridakis, Robert E. Francois, N. Leon Wardle, and Ralph Smith

for the paper "The IRIDIUM Main Mission Antenna Concept," March 1999

Honorable Mentions for Wheeler Award

Rocco Pierri, Giuseppi D'Elia, and Francesco Soldovieri

for the paper "A Two Probes Scanning Phaseless Near-Field Far-Field Transformation Technique," May 1999

Pawel Kabacik and Marek E. Bialkowski

for the paper "The Temperature Dependence of Substrate Parameters and Their Effect on
Microstrip Antenna Performance," June 1999

2000 R. W. P. King Prize Paper Award

Peter M. Johansen

for the paper "Time-Domain Version of the Physical Theory of Diffraction," February 1999

2000 IEEE Graduate Teaching Award

Weng Cho Chew

2000 IEEE Fellows

Yahia M. M. Antar
John S. Asvestas
Gilles Y. Delisle
Alan J. Fenn

Inder J. Gupta
Randy L. Haupt
Lars G. Josefsson
Giuseppi Pelosi

Andrew F. Peterson
Sadasiva M. Rao
Hung Yu David Yang

2000 IEEE Third Millennium Medals

Constantine A. Balanis
Gary S. Brown
Chalmers M. Butler
David Chang
Peter J. B. Clarricoats
Robert E. Collin
Donald G. Dudley
Robert S. Elliott
Ronald L. Fante
Leopold B. Felsen
Edmond S. Gillespie
Robert C. Hansen

Roger F. Harrington
Akira Ishimaru
Oren B. Kesler
Robert G. Louyoumjian
Stuart A. Long
Allan W. Love
Robert J. Mailloux
Ronald J. Marhefka
Raj Mittra
Prabhakar H. Pathak
L. Wilson Pearson
Irene C. Peden

Ronald J. Pogorzelski
David M. Pozar
Yahya Rahmat-Samii
Daniel H. Schaubert
Helmut E. Schrank
Thomas B. A. Senior
W. Ross Stone
Warren L. Stutzman
Piergiorgio L.E. Uslenghi
Donald R. Wilton

Short Courses and Workshops

Development of an Unconditionally Stable Finite-Difference Time-Domain Scheme for Solving Full-wave Maxwell's Equations, Zhizhang Chen, Dalhousie University, Canada; Takefumi Namiki, Fujitsu Ltd., Japan

A Pragmatic Approach to Smart Antennas, Tapan Sarkar, Syracuse University

Radiation Physics and Bistatic k -Space Imaging, John Shaeffer, Marietta Scientific, Inc., Marietta, GA; Edmund K. Miller, Los Alamos National Laboratory (Retired), Santa Fe, NM

Electromagnetics in Biology and Medicine, Om Gandhi, University of Utah

Smart Antennas for Wireless Systems, Jack Winters, AT&T Labs Research

Theory, Techniques and Applications of Electromagnetic Visualization, Edmund K. Miller, Los Alamos National Laboratory (Retired), Santa Fe, NM; John Shaeffer, Marietta Scientific, Inc., Marietta, GA

Artificial Neural Network Approaches for RF and Microwave CAD, K. C. Gupta, University of Colorado at Boulder

The Finite-Difference Time-Domain Method, Omar M. Ramahi, Compaq Computer Corporation, Marlborough, MA

MEMS/Micro-machining for Antenna Applications, Gabriel M. Rebeiz, University of Michigan

Practical Considerations in the Design of Antennas for Wireless Communications, Naftali (Tuli) Herscovici, Spike Technologies, Inc.

UHF Propagation for Modern Wireless Applications, Henry L. Bertoni, Polytechnic University, Brooklyn, NY

Application of the Finite Element Method to the Solution of Frequency Domain and Time Domain Electromagnetics Programs, Magdalena Salazar-Palma, Universidad Politecnica de Madrid, Spain; Luis-Emilio Garcia-Castillo, Universidad de Alcala, Madrid, Spain; Tapan K. Sarkar, Syracuse University, NY, USA

EMI/EMC Computational Modeling for Real-World Engineering Problems, Omar M. Ramahi, Compaq Computer Corporation, Marlborough, MA; Bruce Archambeault, IBM, RTP, NC

Foundations of Antennas with Mathcad, Per-Simon Kildal, Chalmers University of Technology, Sweden

Genetic Algorithm Design of Antennas, Derek Linden and Randy Haupt, Utah State University

An Introduction to Radar Cross Section, John Shaeffer, Marietta Scientific, Inc., Marietta, GA

Recent Advances in Fast Algorithms for Computational Electromagnetics, Weng Cho Chew, Jianming Jin, Eric Michielssen, and Jiming Song, University of Illinois at Urbana-Champaign

Wavelets for EM, Device, and Circuit Modeling, James F. Harvey, U.S. Army Research Office, USA; Wolfgang J. R. Hoefler, University of Victoria, Canada

TABLE OF CONTENTS

Session		Title	Page
<u>Monday</u>			
Session 2	AP/URSI B and D (Special)	Multimedia Education in Electrical Engineering	1
Session 5	URSI B	Antenna Analysis and Interactions	9
Session 6	URSI B	Recent Developments in the FDTD Method	21
Session 9	URSI B	Transient Electromagnetics (I)	33
Session 10	URSI F	Propagation over Land and Water	39
Session 11	URSI B	High-Frequency Techniques	45
Session 12	AP/URSI B	Electromagnetic Theory	57
Session 16	URSI K	RF/Microwave Interactions with Biological Media	69
Session 17	URSI B	Microstrip Antenna Analysis	75
Session 18	URSI B	Time-Domain PDE Methods	83
Session 19	AP/URSI B	Reconfigurable Aperture Antennas	95
Session 20	AP/URSI B	Array Design	101
Session 22	AP/URSI A	Electromagnetic Properties of Materials	109
Session 24	URSI F	Remote Sensing of the Earth's Surface and Atmosphere	111
Session 26	URSI B	Numerical Methods	123
<u>Tuesday</u>			
Session 31	URSI B	Adaptive and Beam Forming Arrays	131
Session 34	AP/URSI B	Recent Developments in Theoretical Electromagnetics	139
Session 35	URSI K	Medical Applications and Biological Effects	149
Session 37	URSI B	Fast Integral Equation Methods	161
Session 38	AP/URSI	Time-Domain Numerical Methods	173
Session 44	AP/URSI B	Smart Antennas, Arrays, and Diversity for Wireless Communications	185
Session 45	AP/URSI A, B, and D (Special)	Ferroelectric Technology for Phased-Array Antennas	187
Session 46	AP/URSI B (Special)	CAD Tools for Antennas and Microwave Circuit Modeling	197
Session 49	URSI A	Characterization of Materials and EMC	207
<u>Wednesday</u>			

Session 54	AP/URSI (Special)	A Century of Progress at the Dawn of a New Millennium (I)	218
Session 55	URSI B	PIFA and Small Antennas	219
Session 60	URSI B	Scattering	231
Session 61	URSI F	Indoor, Urban, and Mobile Propagation	243
Session 62	URSI B	Hybrid Numerical Methods	255
Session 63	AP/URSI B and D	Electronics and Photonics	267
Session 72	AP/URSI (Special)	A Century of Progress at the Dawn of a New Millennium (II)	278
Session 74	AP/URSI B	Fractal Antennas	279
Session 77	AP/URSI B and D (Special)	Advances on Theory and Applications of Wave (Photonic) Band-Gap Technology	283
Session 78	URSI B	LGA Rough Surface Scattering	291

Thursday

Session 82	AP/URSI (Special)	Wireless Communications Systems and Applications	299
Session 83	URSI B	Microstrip Element and Array Design	309
Session 86	URSI B	Periodic Structures	321
Session 92	AP/URSI B	Rough Surfaces and Random media	329
Session 94	AP/URSI A	Ultra-Wideband Systems and Measurements	339
Session 95	URSI B	Integral Equation Methods	347
Session 99	URSI B	Conformal Arrays and Elements	359
Session 101	URSI B	Specialized Antennas	367
Session 102	URSI B	Guiding Structures and Circuits	375
Session 104	AP/URSI B	Radar Cross Section	387
Session 105	URSI B	Inverse Scattering	393

Multimedia Education in Electrical EngineeringOrganizers and Chairs: P. Uslenghi, University of Illinois at Chicago
M. Iskander, University of Utah Page

- | | | | |
|---|-------|---|----|
| 1 | 8:00 | The impact of the Internet on engineering education, <i>B. Oakley II*</i> ,
<i>University of Illinois, USA</i> | 2 |
| 2 | 8:40 | Multimedia- and computer-based education in electromagnetics, <i>M.</i>
<i>Iskander*</i> , <i>University of Utah, USA</i> | 3 |
| 3 | 9:00 | A fresh paradigm for teaching sciences, <i>Z. Fazarinc*</i> , <i>Portola Valley, CA,</i>
<i>USA</i> | 4 |
| 4 | 9:20 | A Master of Engineering degree program on the internet, <i>D. Erricolo, R.</i>
<i>Matthes, S. Naylor, P. Uslenghi*, C. Williams, University of Illinois at</i>
<i>Chicago, USA</i> | 5 |
| | 9:40 | Break | |
| 5 | 10:00 | AntenNet: a web-based Method of Moments solver for antenna education, <i>AP</i>
<i>N. Schuneman, S. Fisher, E. Michielssen*, University of Illinois at Urbana-</i>
<i>Champaign, USA</i> | AP |
| 6 | 10:20 | Antenna analysis and design exercises using windows-based software for
senior/graduate level classes, <i>I. Chatterjee*, University of Nevada, USA, D.</i>
<i>Kokotovic, Norwegian University of Technology and Science, Norway</i> | AP |
| 7 | 10:40 | Software and hardware infrastructure for operating online engineering
laboratories, <i>D. Naylor*, S. Werges, University of Illinois at Chicago, USA</i> | 6 |
| 8 | 11:00 | Visualization of electromagnetic fields using MATLAB, <i>P. Wahid*, S.</i>
<i>Datta, M. Burke, University of Central Florida, USA</i> | 7 |
| 9 | 11:20 | Using commercial software in advanced electromagnetic courses, <i>D.</i>
<i>Worasawate, A. Ugur, K. Ozdemir*, S. Arvas, T. Buber, E. Arvas, Syracuse</i>
<i>University, USA</i> | 8 |

THE IMPACT OF THE INTERNET ON ENGINEERING EDUCATION

Burks Oakley II

Associate Vice President for Academic Affairs, University of Illinois

Professor of Electrical Engineering and Computer Science, UIC

Professor of Electrical and Computer Engineering, UIUC

oakley@uillinois.edu

In this presentation, it is shown how networked personal computers can be used to implement innovative teaching and learning environments in engineering education. Many engineering courses have been restructured to take advantage of the ability of such computers to provide learners with increased access both to learning materials and to people. This new approach to teaching and learning has been termed "Asynchronous Learning Networks", or ALN (see: <http://www.aln.org/>).

Many ALN courses have learning materials, such as movies of experiments, Java- and Mathematica-based simulations, mini-lectures with streaming audio and video, and interactive tutorials available on the World Wide Web. Some of these courses also have online homework and quizzes that are computer-graded in real time, providing rapid feedback to students. In addition, it is now possible to provide access to actual physical laboratory equipment via the Web, thus making it possible for students to conduct experiments from any location and at any time.

Asynchronous conferencing, using web-based software such as WebBoard, provides students with increased access to subject matter experts and to other students. It has been found to build community, to promote peer-peer learning, and to enable increased team-based activities. Overall, the application of ALN techniques enables the creation of new learning environments that are more active and student-centered than many traditional, lecture-based courses. A survey of ALN courses has found increases in student retention and performance, as well as enhanced student satisfaction with the learning process.

The presentation will include an online demonstration of the ALN techniques used in a variety of engineering courses. Some of these courses use ALN approaches to supplement lecture-based courses taken by on-campus students, while other courses are totally online, do not have lectures, and are taken by students far away from campus. Important peripheral issues will also be discussed, such as: faculty incentives and workload, ownership of intellectual property, and academic freedom in ALN programs. See the following websites for additional information:

<http://www.online.uillinois.edu/>

<http://www.online.uillinois.edu/oakley/>

<http://www.ivc.uillinois.edu>

Multimedia- and Computer-Based Education in Electromagnetics

Magdy F. Iskander

CAEME Center for Multimedia Education and Technology

Electrical Engineering Department

University of Utah

(801) 581-6944

Email:iskander@mail.een.utah.edu

Abstract

Multimedia technology provides a valuable resource to boost interest in engineering education and enhance the ability to effectively teach and learn engineering subjects. The ability to combine visualization of complex mathematical and abstract subjects, gain experience with visual laboratories, develop guided use of simulation software, and the ability to even experience virtual participation in practical applications are among the many advantages of technology-based education. In this presentation, features of some of the multimedia CD-ROM products developed by the CAEME Center for Multimedia Education and Technology will be demonstrated and preliminary results from controlled assessment experiments illustrating advantages of multimedia-based teaching will be discussed. CAEME multimedia CD-ROMs include *The Calculus Castle*, the *Physics Museum*, and a genetics CD-ROM, and focus will be placed on the most recent CD-ROMs on engineering electromagnetics.

For the CD ROMs on electromagnetics, the CAME Center developed two CD ROMs that include topics covering at least two introductory courses in this area. The first is a junior level course starting from vector analysis (graphical visualization and animation) and including topics such as electro- and magneto-statics (video clips and virtual labs), Maxwell's equations (virtual labs), wave propagation (animation and video clips), dielectric properties of materials (animation and virtual participation in practical applications), transmission lines (virtual labs, and simulation software including Smith chart and reflection diagram), and antennas (animation's, and virtual indoor antenna range). This CD ROM also includes virtual instruments such as Time Domain Reflectometer (TDR), slotted transmission line for impedance measurements, and several equipment for antenna measurements. The second CD ROM, which may be used for undergraduate senior level course, will include topics on antennas and numerical techniques. Simulation packages on Method of Moments, Finite Element, Finite Difference, and Finite Difference Time Domain have been developed with sufficient tutorial material to provide their self study and use.

Features of these CD ROMs will be demonstrated and suggestions for in- and out- of classes use will be discussed.

A FRESH PARADIGM FOR TEACHING SCIENCES

**Zvonko Fazarinc
880 La Mesa Drive
Portola Valley, CA 94028
Phone: (650)854 4111
E-mail: zvonko_f@pacbell.net**

Mathematical models of natural phenomena are irreplaceable tools to the scientist and the engineer in their daily practice. But they are not very suitable for teaching science concepts because they model only the externally observed behavior. The conceptual understanding of science and engineering requires a comprehension of the underlying mechanisms, which govern this behavior. Access to these mechanisms is not easy via the mathematical models but is very straightforward through physical models which rest on first principles of Nature. The approach enables the mathematically non-initiated to answer a number of open questions.

Why should a high school student not understand the inner workings of the process like boiling of liquids without having to deal with the diffusion equation? Does the liquid in the heated pot solve this equation? Why shouldn't a high school student understand reflections and the skin effect in wires without first solving Maxwell's equations? Does the wire or the electrons solve them while conducting electric current?

We could generate a long list of similar pairs of questions and always the answer to the second one would be an emphatic NO. When we eventually accept the fact that Nature blatantly ignores our equations, we are quickly led to the question of what Her inner workings really are. The answer holds the key to a better way of teaching natural sciences, which is not only accessible to pre-calculus students but is also rigorous.

Nature is governed by the first principles that fall into three categories: conservation, forces and non-classical. In the conservation category we have the energy, momentum and charge, among the forces we know the gravitational, electrical and nuclear and in the non-classical category we have relativity, duality, exclusion and uncertainty. Enforcing these laws on groups of elementary particles, which we can follow on the computer screen, allows us to observe their collective behavior. This is exactly what our mathematical models describe. In other words we have imitated Nature, gained insight into Her inner workings and are now in a position to develop the mathematical models from it.

The current teaching sequence goes from the mathematical model to understanding. The new paradigm reverses it to what it used to be in the early days of scientific endeavor. The presentation will elaborate on this paradigm and will illustrate it with some non-trivial examples.

A MASTER OF ENGINEERING DEGREE PROGRAM ON THE INTERNET

D. Erricolo, R. A. Matthes, S. Naylor, P. L. E. Uslenghi*, C. C. Williams
College of Engineering, University of Illinois at Chicago
851 South Morgan Street, Chicago, Illinois 60607-7043, USA

In Fall 1999, the College of Engineering of the University of Illinois at Chicago initiated a Master of Engineering professional degree program that is offered entirely on the web. This program has several interesting features. It consists entirely of courses that may be taken asynchronously from any location in the world where a web connection exists, and is therefore ideally suited to the educational needs of people who are located in geographical areas removed from centers of higher learning, or are disabled, or cannot attend classes in a synchronous learning environment because of work or family obligations. The program does not have a research component and is very flexible, in that it allows students to design their own curricula according to their professional needs and to select courses outside engineering to complement their technical skills, e. g. courses in business administration or law. All students are required to complete a common core of three courses: engineering law, project management, and an executive seminar based on case studies in the engineering profession.

The variety of technical disciplines participating in this program makes it mandatory that a variety of multimedia environments be utilized, while maintaining a common structure in the offering and administration of the various courses. Several examples will illustrate how different instructors have developed their educational material in electrical engineering courses such as: electromagnetic field theory, quasi-static electric and magnetic fields, electromagnetic scattering, microdevices and micromachining technology, and wireless communication networks. A great advantage of web-based courses is the opportunity that the instructor has to improve and modernize the material on a continuous basis, e. g. by adding interactive examples, hyperlinks, etc. A web-based course is like a textbook in continuous evolution, with the added advantage of a multimedia environment.

Software And Hardware Infrastructure For Operating Online Engineering Laboratories

D.L. Naylor, S.C. Werges

Dept. of EECS, University of Illinois at Chicago, IL 60607-7053, USA

The Interactive Electronics Laboratory (IEL) is the first of likely many online laboratory facilities deployed using online laboratory access infrastructure developed in the Interactive Systems Laboratory at the University of Illinois at Chicago. The characteristics and use of the IEL may be illustrated by the following examples of laboratory exercises:

1. Design a circuit for measuring the slew rate of an operational amplifier. The slew rate is the maximum rate at which the output voltage can vary with time. Measure this parameter for one of the available op-amps. This is an example of an experiment involving both design and non-ideal behavior of a component.
2. Measure current vs. applied voltage for a diode. Export the data to a spreadsheet containing theoretical equations. Vary the value of key parameters in the formula to find a good fit between experiment and theory. Observe the range of input values for which the theoretical expression provides a good fit and the nature of the deviations from simple predicted behavior.
3. Design and build a differential amplifier using a matched pair of transistors. Measure the differential gain (agrees well with theory and or simulators), and measure the so-called common-mode gain, which is a non-ideal behavior that is not well handled by simulators unless they are rigged to provide a set answer.

The collection of equipment currently available in the IEL that supports these kinds of experiments include ac and dc voltage sources, transient and dc voltage measuring devices, a programmable resistor system, a library of electronic components and an electrical switching matrix which interconnects components as required for the user designed circuit.

The current software environment that has been developed unfortunately only allows students to perform a small fraction of the experiments that are physically possible with the hardware system that has been made available. As a result of this software limitation a major software revision is currently underway with the intent of: supporting a broader range of laboratory equipment; enabling a broader range of tasks with the current equipment; and providing greater flexibility for customization of the user interface during the phases of configuring an experiment and analyzing the resultant data. The rationale and approach for the current software revision will be detailed along with the new kinds of experiments and associated instructional media that will be made possible by this new distributed software environment.

VISUALIZATION OF ELECTROMAGNETIC FIELDS USING MATLAB

P. F. Wahid*, S. Datta and M. Burke
Electrical Engineering Department
University of Central Florida
Orlando, Florida 32816
407-823-2610 wahid@mail.ucf.edu

Students in the required undergraduate Engineering Electromagnetics course often have difficulty grasping the abstract concepts introduced in the course. A large majority of the universities around the country offer this course over one semester. This makes the course rather fast-paced adding to the student's difficulty in understanding the material.

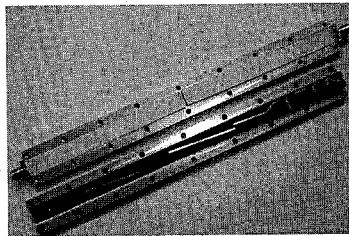
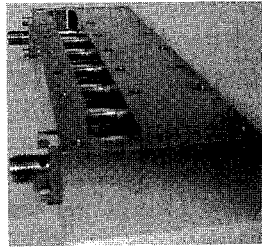
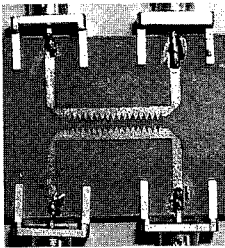
The authors of this paper have developed a demonstration package using the student version of MATLAB. MATLAB provides a good platform since it is supported by several numerical, graphical and engineering toolboxes. The demo package titled 'Visualization of Electromagnetic Fields' is designed to give a complete introduction to electromagnetic theory with simple definitions and examples. The package covers electrostatics, magnetostatics and uniform plane waves and will be expanded to cover antennas and transmission lines. In addition there are two chapters, which cover the basics of MATLAB and a review of vector analysis and the coordinate systems.

Each chapter has a consistent link of the topic from start to finish. Each topic has several subtopics that contain examples and simple problems for the student to solve. Solutions and illustrations are linked by different pushbuttons with appropriate labels on them on all the windows throughout the package. A demonstration of this package will be given at the conference.

Using Commercial Software In Advanced Electromagnetic Courses

Denchai Worasawate, Alper Ugur, Kemal Ozdemir*, Serhend Arvas,
Tekamul Buber, and Ercument Arvas
EECS Dept, 121 Link Hall, Syracuse University, Syracuse, NY 13244

Commercial software packages (Serenade, Ensemble, Ansoft HFSS, Sonnet, Micro-Stripes, etc) have been successfully used in antenna and microwave courses at Syracuse University to simulate various practical problems including amplifiers and oscillators. 2-D Microwave structures have been analyzed using Ensemble and Sonnet whereas 3-D microwave structures have been analyzed using Ansoft HFSS and Micro-Stripes. These circuits have been built and tested at Syracuse University Microwave Labs. It has been shown that the simulation results of different software packages agree among themselves as well as with the measurements. Antenna and scattering problems have also been simulated and compared with results from the literature. Very good agreement has been observed. Photos below show a wiggly line coupler, a combline filter, and a bandpass filter that is designed. These and other problems will be presented in our RF/Microwave Group Web site in detail. Step by step instructions from constructing the models to obtaining the results and analyzing them are included on the web pages.



Antenna Analysis and Interactions

Co-chairs: O. P. Gandhi, University of Utah
P. Wahid, University of Central Florida

Page

1	8:00	The folded dipole, a self-balancing antenna, <i>C. Buxton*</i> , <i>W. Stutzman</i> , <i>Virginia Polytechnic Institute and State University, USA</i>	10
2	8:20	Contribution on time-domain analysis of non-symmetrical cylindrical antennas in non-harmonious net using approximation for potential functions, <i>L. Ololoska*</i> , <i>L. Janev</i> , <i>University Sts. Kiril and Metodij, Macedonia</i>	11
3	8:40	Electromagnetic-circuit modeling of active antennas using Method of Moment network characterization technique, <i>M. Abdulla*</i> , <i>Yazaki North America, Inc., USA</i>	12
4	9:00	Modelling the performance of an antenna located inside a vehicle, <i>C. Coleman*</i> , <i>The University of Adelaide, Australia</i>	13
5	9:20	Theoretical analysis of dipole antenna in a borehole, <i>Y. Long</i> , <i>Zhongshan University, Guangzhou</i> , <i>B. Rembold</i> , <i>RWTH-Aachen, Germany</i>	14
	9:40	Break	
6	10:00	Coupling of mobile telephone antennas and a human head: theory and experiment, <i>B. Notaros*</i> , <i>University of Massachusetts Dartmouth</i> , <i>S. Whalen</i> , <i>S. Djukic</i> , <i>Allgon Telecom Ltd., USA</i>	15
7	10:20	Helical antenna optimization by genetic algorithms, <i>R. Lovestead*</i> , <i>A. Safaai-Jazi</i> , <i>Virginia Polytechnic Institute and State University, USA</i>	16
8	10:40	Numerical simulation of self-structuring antennas based on a genetic algorithm optimization scheme, <i>J. Ross*</i> , <i>John Ross & Associates</i> , <i>E. Rothwell</i> , <i>C. Coleman</i> , <i>Michigan State University</i> , <i>L. Nagy</i> , <i>Delphi Automotive Systems, USA</i>	17
9	11:00	An effective procedure of steepest descent method for the fast synthesis of shaped reflector antennas in the contoured and multiple beam applications, <i>H-T. Chou*</i> , <i>Yuan-Ze University, Chung-Li</i>	18
10	11:20	Analytical and numerical methods in the problem of synthesis antennas with planar aperture, <i>V. Kravchenko*</i> , <i>E. Zelkin</i> , <i>P. Toroshchin</i> , <i>Russian Academy of Sciences, Russia</i>	19

The Folded Dipole, a Self-Balancing Antenna

C. G. Buxton* and W. L. Stutzman

The Bradley Department of Electrical and Computer Engineering
Virginia Polytechnic Institute and State University
Blacksburg, VA 24061-0111

Dipole antennas are typically balanced structures but in practice they are connected to unbalanced feed lines resulting in an unbalanced configuration. A common example of an unbalanced feed line is a coaxial cable where one arm of the dipole is connected to the outer conductor and other to the inner conductor. To compensate for this imbalance a balun is placed between the coaxial feed line and the antenna, resulting in an overall balanced configuration. A sleeve balun is often used to balance dipole antennas. For wideband antennas, a balun must be designed to function over the entire bandwidth, which can be a challenge to design.

The folded dipole is a popular antenna design because of its high impedance relative to a dipole. An often-overlooked characteristic of the folded dipole is the self-balancing property due to the geometry. The currents on the feed lines and the antenna arms even remain balanced when fed from an unbalanced source.

The folded dipole is often described as an unbalanced transmission line with unequal currents. The currents can be separated into transmission line (TL) and antenna mode currents. The radiation from TL mode currents tend to cancel in the far field. The radiation from the antenna mode currents tend to add.

An unbalanced dipole antenna has unequal currents on the arms of the dipole and unequal currents on the feed lines. The unequal currents on the arms of the dipole create a far field pattern scanned off axis. The unequal currents on the parallel conductors or on outer and inner conductors of a coaxial line give rise to undesirable radiation from the transmission line. Therefore, an unbalanced dipole leads to undesirable pattern degradation.

An unbalanced folded dipole has unequal and asymmetric currents on the parallel wires, however when the wire currents are superposed the net current is symmetric, giving rise to a symmetric far field pattern. The currents on the transmission lines are also equal, eliminating unwanted radiation due to the transmission line imbalance. Because of this balanced current characteristic the folded dipole is a self-balancing antenna.

The dipole and folded dipole were modeled for cases of a balanced, parallel feed line and an unbalanced coaxial feed line. The feed line currents and antenna currents will be presented for both configurations as well as the resulting far field patterns.

Contribution on Time-Domain Analysis of Non-Symmetrical Cylindrical Antennas in Non-Harmonious Net Using Approximation for Potential Functions

L. Ololoska*, Lj. Janev
Faculty of Electrical Engineering Karpos II bb. 91000 Skopje, Macedonia
E-mail: labteh@mpt.com.mk

In this paper, transient analysis of non-symmetrical cylindrical antennas is based on time-domain analysis. First, for this purpose, potential functions values along the antenna are obtained, using the method of characteristics. Then, a method for determination of current distribution on the antenna is developed, when the source is ideal voltage generator. For this analysis, as a model, a non-symmetrical cylindrical antenna with arm's length h_1 and h_2 and radius r is taken. During the analysis, the antenna can be divided in pieces Δz and the analysis can be done in time steps Δt . So there is a relation between Δz and Δt , $\Delta z = v\Delta t$, (v is the velocity of propagation). Then, we say that the analysis is in harmonious net. The potential functions in selected points along the antenna are obtained as result of their values in the same points in previous times, using the method of characteristics. That means that the situation in time t can be obtained in base on the situation in time $t - \Delta t$. This enables to determine the values of the potential functions in selected points in space and time. The current distribution is approximated with in parts linear function, and it is developed in row of basic functions in form

$$i(x) = \sum_{i=N_1-k}^{N_1-k} f_i(x) i(t - |i|\Delta t, z + i\Delta z), \text{ where the } f_i(x) \text{ value is given. } N_1 \text{ and } N_2 \text{ is the}$$

number of parts on which the antenna arms are divided. Then, the magnetic vector potential and current distribution along the antenna can be found.

If the relation between the pieces Δz and the time steps Δt , is not valid, the analysis is in non-harmonious net. It is clear that during the analysis with optional time step Δt , requested values of the potential functions are not known, so the equations for potential functions could not be used directly. The requested values can be calculated using approximate functions for potential functions. Here, we use

approximation by time, which is in form $A(x) = \sum_{i=0}^N p_i x^i$. During this analysis, the current distribution is approximated with in parts linear function also.

As illustration of the exactness of presented method, an input admittance of non-symmetrical cylindrical antenna is obtained, using FFT. Those results are compared with results obtained with another method. Comparing the results for admittance, it can be concluded that the relative deviation in most cases is around and under 1%. Contented accuracy when the antenna admittance is computed, shows that the presented method for antenna analysis can be successfully used.

Electromagnetic-Circuit Modeling of Active Antennas Using Method of Moment Network Characterization Technique

Mostafa N. Abdulla
 Electronics, Instrumentation & Switch Department
 Yazaki North America, Inc.
 Canton, MI 48187

Electromagnetic modeling of active antenna systems along with linear and nonlinear circuit components is emerging as one of the great challenge in microwave and millimeter-wave computer aided engineering. Tight coupling between circuit and electromagnetic (EM) fields, integrated active array, circuit field interaction, global modeling, and compatibility of the circuit and EM simulators still need to be under investigation.

In this paper, an active-passive method of moment (MoM) analysis technique is represented to simulate active and passive circuits simultaneously. As a simple application, the technique is used to simulate a spatial power amplifier unit cell shown in Fig. 1. This amplifier unit cell consists of two orthogonal folded-slot antennas. The active device is connected to the antennas by CPW lines. One of the antennas is used as a receiving antenna and the other as a transmitting antenna in the orthogonal polarization to minimize the coupling effect between the two fields.

In this technique, first, the extraction of the passive parameters is performed using the MoM technique. This results in MoM excitation vectors (V_1^e and V_2^e) and Z or Y passive network parameters as shown in Fig.2. Using a circuit simulator, the exact currents and voltages at the device terminals are obtained. Then again, the MoM field simulator is used to calculate the exact fields and evaluate the antenna parameters but in this case, the exact excitation vectors are used. Fig.3 shows the agreement between the calculated and measured effective isotropic power gain (EIPG) of the amplifier. More results and details will be presented at the conference.

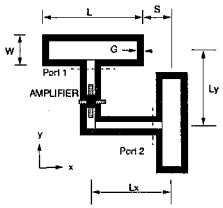


Fig.1 CPW-Slot antenna spatial amplifier

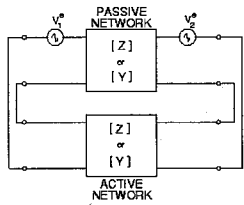


Fig.2 Circuit Model

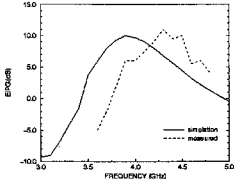


Fig.3 EIPG of the amplifier

Modelling the Performance of an Antenna Located Inside a Vehicle

C.J.Coleman

Department of Electrical and Electronic Engineering, The University of Adelaide,
Adelaide, South Australia 5005, Australia

The increased use of personal communications, and other forms of body born radio devices, has given rise to a need for a better understanding of their operation in less than ideal circumstances. Perhaps the most demanding situation is when the device is required to operate from within a vehicle. The vehicle has the potential to severely modify both the polarisation characteristics and pattern of the radiation field. At times, this modification can be so extreme as to completely invalidate system budgets based on the free space performance of the device. Consequently, it is important to understand the causes of the undesirable radiation in order to devise operating practices that will produce more desirable radiation.

In order to investigate the modified radiation fields, it is necessary to build an electromagnetic model of the vehicle and consider it when excited by radiation from the device antenna. Since the characteristics of importance will be the overall radiation pattern and the input impedance, a wire grid model is normally sufficient. In the present work, the electric field integral equation formulation is employed and discretised through a Galerkin procedure with currents represented by piecewise sinusoidal functions. In order to improve the modelling of solid panels, however, the currents on the wire grid are spread over the neighbourhood of each wire. The major problem is the extremely large number of elements required to adequately model the vehicle at UHF frequencies and above. Fortunately, the Galerkin procedure produces a symmetric system matrix which consequent reduction in memory requirement. Additional reductions are achieved by solving the system equations by means of a preconditioned conjugate gradient procedure. This approach only requires the system matrix to be stored in single precision as the matrix remains unmodified throughout the solution procedure. The downside, however, is a significant increase in arithmetic operations over those required by a Gauss-Jordan procedure and hence a increased solution time. Representative results are presented (including gain patterns and current distributions) and some conclusions are drawn concerning operational procedures.

Theoretical Analysis of a Dipole Antenna in a Borehole*

Yunliang Long

Dept. of Electronics, Zhongshan University, Guangzhou, 510275, P. R. of China

Bernhard Rembold

Institute of High Frequency Technology, RWTH-Aachen, 52056, Aachen, Germany

ABSTRACT

The theoretical analysis of an electric drill-rod telemetry system is necessary, but very complicated. As we known, when the analysis of an electromagnetic problem is concerned with the earth, the earth is often assumed simply as a homogeneous dissipative medium. But in the analysis of a drill-rod telemetry system, because the drill-rod is very long and buried in the earth, a more precise model of the earth is needed. The earth should be thought as a stratified medium, at least, two-layer lossy medium, one soil and one rock. Furthermore, there is a cylindrical boundary due to the existence of the mud (see Fig.1). So this electromagnetic problem is always connecting with both planar and cylindrical boundaries. In general, there are two sorts of exciting source used in telemetry system:

loop antenna and dipole antenna. In the first

case, the drill-rod is excited by a ring current. A modified perturbation method has been presented to deal with this case(Y. Long et al., *IEEE Trans. on GRS*, **34**, 33-35, 1996). For the latter, the drill-rod is excited by a δ voltage source, and the drill-rod itself is used as a dipole antenna. In this paper, an equivalent method is given to remove the mud layer. Then this telemetry system problem is switched to a so-called 'boundary-penetrating antenna' (BPA) problem in three-layer medium(Y. Long and H. Jiang, *Electron. Lett.*, **34**, 711-712, 1998). The Sommerfeld-type integrals involved in the current integral equations are simplified to the closed-form formulas when the frequency used is extremely low. A quasi-static approximation formula is used to obtain the electromagnetic fields due to the dipole antenna in the borehole. Finally, the input impedance of the antenna and the electromagnetic fields on the surface of the earth are given.

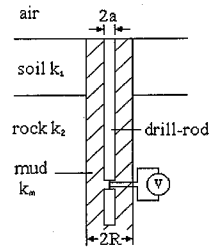


Fig.1 Geometric configuration.

* This work is sponsored jointly by Krupp Foundation of Germany, Chinese Scholarship Council and the National Natural Science Foundation of China (49604058).

Coupling of Mobile Telephone Antennas and a Human Head: Theory and Experiment

Branislav M. Notaros*, University of Massachusetts Dartmouth, ECE Dept.,
285 Old Westport Road, North Dartmouth, MA 02747

Stephen C. Whalen, Slavko Djukic, Allgon Telecom Ltd. – Allgon Mobile
Communications, 7317 Jack Newell Blvd. North, Fort Worth, TX 76118

Introduction. It has become standard that handset-unit antennas for cellular wireless communications have to be analyzed and designed in their real operating environment, i.e., together with nearby human tissues. This involves both antenna performance and health hazard aspects. This paper presents our on-going theoretical and experimental research efforts in efficient, accurate, and reliable characterization of the electromagnetic interaction between mobile-telephone antennas and a human head at 835 MHz and 1900 MHz (frequency bands allocated for wireless communications in North America).

Theoretical model. Our theoretical model is based on a large-domain (high-order expansion) surface-integral-equation moment-method computational approach (B.M. Notaros, B.D. Popovic, R.A. Brown, and Z. Popovic, 1999 IEEE MTT-S IMS Digest, pp.1665-1668). The boundary surfaces of a homogeneous approximation of a head, a phone box, and an antenna are modeled by electrically large bilinear quadrilateral surface elements, and the equivalent electric and magnetic surface current density vectors over the elements are approximated by high-order polynomial basis functions. The technique is extremely efficient, enabling the analysis of the phone/head system on a PC within minutes.

Experimental setup. Our experiments are performed on an anatomically shaped phantom head (a plastic container filled with a solution that resembles the dielectric and conductive properties of a human head). A mobile phone (real phone prototype with different antennas) is attached near the right or left ear of the phantom head, and the following quantities are measured in Allgon, Fort Worth: the antenna reflection coefficient (S_{11}), the E-field and specific absorption rate (SAR) inside the phantom (in a SAR Laboratory with a fully automated robotic system), and the antenna radiation patterns (in a computerized anechoic chamber).

Results and discussion. Theoretical and experimental results will be presented for the antenna reflection coefficient, SAR distributions, and antenna radiation patterns for mobile phone prototypes with different dual-frequency antennas at 835 MHz and 1900 MHz. Design issues will be discussed ranging from the antenna performances to safety compliance considerations. It will be demonstrated that both theory (efficient numerical modeling) and experiment (sophisticated measurement techniques) are necessary for successful market-oriented antenna/tissue interaction characterization.

Helical Antenna Optimization by Genetic Algorithms

Raymond A. Lovestead* and Ahmad Safaai-Jazi

Bradley Department of Electrical and Computer Engineering
Virginia Polytechnic Institute and State University
Blacksburg, Virginia 24061-0111, USA

The genetic algorithm (GA) is used to design helical antennas that provide a significantly larger bandwidth than conventional helices with the same size. Over the bandwidth of operation, the GA-optimized helix offers considerably smaller axial ratio and slightly larger gain than the conventional helix. Also, the input resistance remains nearly constant over the bandwidth. On the other hand, for nearly the same bandwidth and gain, the GA-optimized helix offers a size reduction of 2:1 relative to a conventional helix. The optimization is achieved by allowing the genetic algorithm to control a polynomial that defines the envelope around which the helix is wrapped. The GA-optimized helix has continuously varying radius and pitch angle. The fitness level is defined as a combination of gain, bandwidth, and axial ratio as determined by an analysis of the helix using the Numerical Electromagnetic Code, version 2 (NEC-2).

To experimentally verify the optimization results, a prototype 12-turn, GA-optimized helix was built and tested on the Virginia Tech outdoor antenna range. Far-field radiation patterns were measured over a wide frequency range. The axial-ratio information is extracted from the measured pattern data. Comparison of the measured and NEC-2 computed radiation patterns show excellent agreement. The agreement between the measured and calculated axial-ratio results is reasonable. The prototype GA-helix provides a peak gain of more than 13 dB and an upper-to-lower frequency ratio of 1.89. The 3-dB bandwidth of the antenna is 1.27 GHz (1.435 GHz – 2.705 GHz). Over this bandwidth the computed gain varies less than 3 dB and the axial ratio remains below 3 dB.

NUMERICAL SIMULATION OF SELF-STRUCTURING ANTENNAS BASED ON A GENETIC ALGORITHM OPTIMIZATION SCHEME

J.E. Ross*
John Ross & Associates
350 W 800 N, Suite 317
Salt Lake City, UT 84103

E.J. Rothwell, C.M. Coleman
ECE Dept.
Michigan State University
E. Lansing, MI 48824

L.L. Nagy
Delphi Automotive Systems
30500 Mound Road
Warren, MI 48090-9055

The self-structuring antenna is a new class of adaptive antenna that changes its electrical shape in response to the environment by controlling electrical connections between the components of a skeletal "template." The template can be highly structured or random and can be placed on a planar or a conformal surface. An example template is shown in Figure 1. The lines represent conductors and the dots switches or relays. A wide variety of shapes can be achieved by opening or closing the switches.

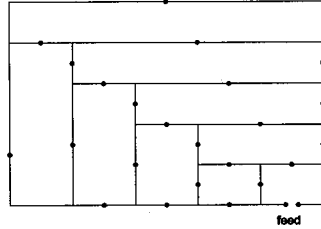


Figure 1. Example antenna template.

As shown in Figure 2, the switches are controlled using an embedded microprocessor and feedback signals from the receiver to optimize one or more performance criteria. Multiple feedback signals can be used when several qualities are desired – e.g., high signal strength,

good audio clarity, efficient multipath suppression, etc. Performance of the antenna is dependent on the control algorithm and template design. A trade-off exists between the "diversity" – i.e., the number of possible configurations - and the complexity of searching for the optimum structural arrangement. Antennas with a higher level of diversity can provide better performance, but require longer search times. The antenna of Figure 1 has 23 switches which provide 8.4 million possible configurations. In this situation, exhaustive and random searching is impractical. Thus modern search methods like genetic algorithms and simulated annealing are employed.

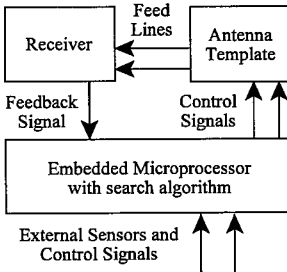


Figure 2. Block diagram.

The goal of this research is to simulate the example template as well as other templates in free space and in the presence of other antennas and conducting objects. The simulations are performed using computer tools developed for automated design of vehicular antennas. These tools use the NEC-4 program as the EM solver and the Delphi AntennaCAD program (Ross, Nagy and Szostka, URSI National Radio Science Meeting, Poznan, Poland, 1999) for pre-processing, post-processing and visualization. The effect of the feedback-control network is simulated using the Delphi GA-NEC program. This program uses a genetic algorithm, similar to the one used in the embedded microprocessor, coupled with the NEC program to efficiently search for optimum switch configurations.

**An Effective Procedure of Steepest Decent Method for the Fast Synthesis
of Shaped Reflector Antennas in the Contoured and Multiple Beam
applications**

Hsi-Tseng Chou

Dept. of Electrical Eng., Yuan-Ze University, Chung-Li 320, Taiwan

Steepest decent method (SDM) is a widely used optimization technique, and has been successfully employed in the synthesis of shaped reflector antennas to generate contoured beams in the applications of satellite communications. The SDM is very efficient in terms of computational convergence. However, SDM is more likely considered as a local search technique because it highly depends on an initial starting point and very easily reaches a local optimum. As a result, hybrid combinations with other global search techniques such as genetic algorithm (GA) to come out with a nice initial starting point have also been proposed, which in turn increase the complexity of the computation and number of iterations required in the synthesis procedure. Moreover, a global optimization technique like GA does not guarantee convergence and might converge very slowly. In this paper, a simple and effective procedure of SDM is proposed for the synthesis of offset single shaped reflector antennas illuminated by a single feed for the contoured and multiple beam applications, which tends to converge smoothly to a more acceptable optimum without any initial guess from other algorithms. This procedure is based on the physical behavior of wave propagation while the surface profile of the reflector antennas is varying, and subsequently adjusts the synthesizing variables while a local minimum is reached. A progressive starting point can therefore be smoothly created and employed in the refinement of the SDM synthesis, which in turn makes SDM converge smoothly to a more global optimum. The proposed procedure is particularly useful for an antenna designer since only a simple criterion need to be implemented. Implementation procedure will be discussed in the presentation and validated by the numerical examples in the applications of contoured and multiple beams.

ANALYTICAL AND NUMERICAL METHODS IN THE PROBLEM OF SYNTHESIS ANTENNAS WITH PLANAR APERTURE.

Victor F. Kravchenko, Efim G. Zelkin, and Pavel E. Toroshchin

Institute of Radio Engineering and Electronics of the Russian Academy of Sciences. 103907, Center, GSP - 3, ul. Mokhovaya, 11, Moscow, Russia.

Tel: +7 (095) 9024737, 9214837; Fax: +7 (095) 9259241

E-mail: kvf@mx.rphys.mipt.ru

In the first part of our report we will develop the necessary theory for calculating the radiation field distribution over the aperture of antenna in terms of an assumed known the directional diagram of antenna. The using mathematical approach is the method of equivalent linear aperture. (1. **E.G. Zelkin and V.G. Sokolov**, *Methods of Synthesis Antennas*, Moscow, *Sovetskoe Radio*, 1980. 2. **V.F. Kravchenko, and V.V. Timoshenko**, *Electromagnetic Waves and Electronic System*, vol. 4, no. 5, 21-32, 1999. 3. **V.F. Kravchenko**, *Proceeding of the 3rd International Conference on Antenna Theory and Techniques, Sevastopil, Ukraine*, 8-11 Sept., 55-61, 1999. 4. **V.F. Kravchenko, E.G. Zelkin, and V.V. Timoshenko**, *Proceeding of the 3rd International Conference on Antenna Theory and Techniques, Sevastopil, Ukraine*, 8-11 Sept., 124-126, 1999.). After the basic theory has been developed, we will apply it to analyze some of the more important features associated with a planar aperture antennas.

In second part of our report we will calculating the radiation field distributions over the aperture of antennas according to the fixed directional diagrams including diagrams given by Atomic Functions. Also in work compared properties of different diagrams.

This results can be used for various applications of the problem of synthesis antennas. Especially, in methods used the Atomic Function for approximation a directional diagram of antenna.

Recent Developments in the FDTD Method

Co-chairs: S. Bringham, Raytheon Systems
J. B. Schneider, Washington State University

			Page
1	8:00	Convergence properties of the non-orthogonal FDTD algorithm, <i>R. Schuhmann*</i> , <i>M. Hilgner</i> , <i>T. Weiland</i> , <i>Darmstadt University of Technology, Germany</i>	22
2	8:20	Plane waves and planar boundaries in FDTD simulations, <i>J. Schneider*</i> , <i>R. Kruhlak</i> , <i>Washington State University, USA</i> ,	23
3	8:40	Spherical wave sources for near field modeling in the total/scattered FDTD formulation, <i>M. Potter*</i> , <i>University of Victoria</i> , <i>M. Okoniewski</i> , <i>University of Calgary, Canada</i>	24
4	9:00	Accurate modeling of material boundaries with FDTD, <i>A. Christ*</i> , <i>C. Schuster</i> , <i>N. Kuster</i> , <i>Swiss Federal Institute of Technology, Switzerland</i>	25
5	9:20	Treatment of thin, arbitrary shaped PEC sheets with FDTD, <i>D. Reinecke*</i> , <i>P. Thoma</i> , <i>T. Weiland</i> , <i>CST GmbH, Germany</i>	26
	9:40	Break	
6	10:00	A FDTD study of Yee cell modifications for modeling curved surfaces, <i>J. Nehrbass</i> , <i>The Ohio State University, USA</i>	27
7	10:20	A sub-cellular algorithm to model a thin slot diagonal to the FDTD grid, <i>C. Mason</i> , <i>M. Okoniewski*</i> , <i>University of Calgary, Canada</i>	28
8	10:40	A new absorbing boundary condition for FDTD, <i>S. Sachdeva*</i> , <i>N. Balakrishnan</i> , <i>Indian Institute of Science, India</i> , <i>S. Rao</i> , <i>Auburn University, USA</i>	29
9	11:00	Modeling parallel and series RLC loads in a 1-D FDTD transmission line, <i>T. Montoya*</i> , <i>University of Tennessee</i> , <i>W. Scott</i> , <i>Georgia Institute of Technology, USA</i>	30
10	11:20	The modeling of lumped elements using the Haar wavelet multiresolution time domain technique, <i>S. Ju*</i> , <i>D. Bae</i> , <i>H. Kim</i> , <i>Hanyang University, Korea</i>	31

Convergence Properties of the Nonorthogonal FDTD Algorithm

Rolf Schuhmann*, Michael Hilgner, Thomas Weiland

Darmstadt University of Technology, Germany, Fachgebiet Theorie Elektromagnetischer Felder

One of the major disadvantages of the classical FDTD algorithm is its restriction to Cartesian grid doublets, leading to considerable geometrical errors, if curvilinear or oblique material interfaces or boundaries have to be modeled. Many extensions have been presented in the literature to overcome this difficulty, the most flexible among which is the usage of structured nonorthogonal grid systems (first proposed by Holland, IEEE Trans. Nucl. Sc., **30**, 4589-4591, 1983).

The basic idea is to apply a spatial interpolation scheme of both neighboring field components and metric coefficients (grid angles and lengths) in the mesh. This scheme can be included in the matrix-vector notation of the Finite Integration Technique (FIT), leading to so-called generalized material matrices with a special block-band format. If the usage of nonorthogonal grids is combined with the concept of triangular sub-fillings, even strongly twisted and rounded structures can be modeled with well-balanced grids, which is a basic prerequisite for an efficient time stepping procedure (Schuhmann/Weiland, IEEE Trans. Magn., **35**, 1470-1473, 1999).

The price to pay for the improved modeling accuracy is on the one hand an increase of the numerical cost, which is still linear in the number of unknowns. On the other hand, a new type of error is introduced by the method itself and its interpolation formulas. It can be shown, that this error shows a second order convergence in the interior of smooth nonorthogonal grids, and thus should not considerably decrease the overall convergence of the method.

However, the situation is worse, if perfectly electric conducting (PEC) materials or boundaries have to be considered: As the contravariant electric field components associated to grid edges along such boundaries are not available, the interpolation scheme for the neighboring normal components remains incomplete, leading to local field errors. As shown in Fig.1, such local errors can deteriorate the convergence behavior also of global quantities, here demonstrated in terms of the resonance frequencies of several eigenmodes in an oblique cavity (see inlet).

As a remedy, we propose two types of correction schemes: In the first approach, a locally asymmetric scheme is applied, where the missing components are compensated by simply increasing the weights of the remaining terms in the interpolation formula. In the second, more physical approach, the weighting coefficient of just one component (the contravariant component 'normal' to the boundary) is adjusted, taking into account the actual behavior of the electric fields in the vicinity of the PEC material. As with the latter approach only the main-diagonal entry of the discrete material operator is changed, the symmetry of this operator matrix is preserved.

Fig. 1 shows typical convergence curves for the original and the modified algorithm: The correction of the local field errors at the boundaries leads to an enhancement of the overall convergence rate due to the simulation, which is nearly second order (the theoretical limit due to the dispersion relation).

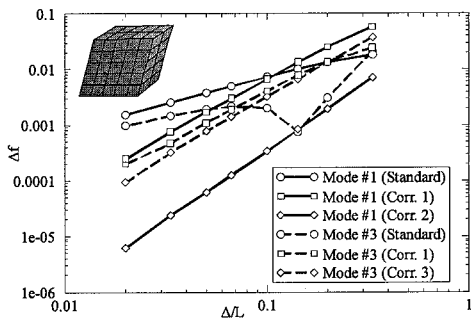


Fig. 1: Convergence curves for the computation of resonance frequencies in an oblique cavity (relative frequency error versus normalized mesh step size). The uncorrected ('Standard') scheme exhibits a very low convergence rate due to the local field errors at the boundaries. Both correction schemes lead to a regular 2nd-order convergence.

Plane Waves and Planar Boundaries in FDTD Simulations

John B. Schneider*

School of Elec. Eng. & Comp. Sci.
Washington State University
Pullman, WA 99164-2752

Robert J. Kruhlak

Nonlinear Optics Lab.
Dept. of Physics
Washington State University
Pullman, WA 99164-2814

Harmonic analysis has been used extensively to study the behavior of finite-difference time-domain (FDTD) grids. For example, it has been used to obtain the reflection coefficients from absorbing boundary conditions as well as the numerical dispersion relation and the stability criterion for the Yee FDTD grid. In this paper we use harmonic analysis to study fundamental properties of the Yee FDTD grid pertaining to plane waves and planar boundaries. For instance, we show that, unlike in the continuous world, arbitrary uniform plane waves do not necessarily have mutually orthogonal electric field, magnetic field, and propagation vectors.

An FDTD-specific version of the Fresnel equations and Snell's Law are derived for planar interfaces in the Yee grid. When modeling dielectric boundaries, nodes at the interface are often assigned the arithmetic mean of the permittivities to either side of the interface. Application of the FDTD Fresnel equations clearly shows that the arithmetic mean (as opposed to, say, a geometric mean) is, in fact, the optimum value for the permittivity approximation. Because of the staggering of electric and magnetic nodes in the Yee grid, when a material boundary produces a discontinuity in permittivity and permeability this must be modeled in the FDTD grid as either a change in permittivity followed by a change in permeability or, conversely, as a change in permeability followed by a change in permittivity. The errors associated with the transmission and reflection of plane waves for the two realizations are not the same and can be analyzed using the FDTD Fresnel equations. In all cases the error shows second-order convergence to zero as the discretization goes to zero.

Spherical Wave Sources for Near Field Modeling in the Total/Scattered FDTD Formulation

M.E. Potter

Dept. of Electrical and Computer
Engineering, University of Victoria Victoria
BC V8W 3P6
mpotter@ece.uvic.ca

M. Okoniewski

Dept. of Electrical and Computer
Engineering, University of Calgary, Calgary
AB T2N 1N4
michal@enel.ucalgary.ca

Since its introduction by Yee, the FDTD method has been used extensively to model electromagnetic field interactions with complex heterogeneous structures. A number of excitation techniques have been developed over the years, including the total/scattered field formulation [Taflov, *Computational Electrodynamics: the FDTD Method*]. The total/scattered FDTD algorithm allowed for efficient implementation of arbitrarily directed uniform plane waves, and for a considerable numerical dynamics in the computed fields. The efficient implementation of source fields on the Huygen's surface is not restricted to plane waves however. We have recently shown that with slight modifications the fields from an infinite line source can be implemented [*Electron. Lett.*, 34, 2216-2217, 1998]. This allowed for exposure modeling of humans close to power lines.

The restriction with plane wave sources is that they inherently model the far field of an electromagnetic source. If one wishes to model in the near field, then multiple plane wave modes could be used, but an unrealistically large number of modes would be required to accurately model the source of interest (e.g. an antenna). However, such sources can be accurately modeled in the near field by using spherical wave expansions instead. In this case, the number of modes required for the same accuracy is substantially reduced over the plane wave case.

In this work we then describe a method whereby a model of a source incorporating spherical waves is implemented in the total/scattered FDTD. Much like the plane wave sources in this FDTD method, the spherical wave modes are time-stepped on 1-D alternate source grids, representing mode propagation in free space. Spherical wave modes are then interpolated and summed up on the Huygens' surface. It is assumed that the object of interest lies not closer than in the radiative near field of the source, and therefore there is no significant coupling between source and object.

Accurate Modeling of Material Boundaries with FDTD

Andreas Christ, Christian Schuster, and Niels Kuster
Swiss Federal Institute of Technology (ETH)
8092 Zürich, Switzerland

Phone:+41-1 632 2736, Fax:+41-1 632 1057, e-mail: christ@itis.ethz.ch

Introduction

The Finite-Difference Time-Domain method (FDTD) allows a comparatively simple generation of a model of the structure to be simulated: The electrical parameters of the model are assigned to the updating coefficients at their particular locations in a rectangular mesh. This enables the correct propagation of waves within a domain with homogeneous material distribution. But the FDTD algorithm does not necessarily fulfill the boundary conditions of the electric and magnetic fields at material interfaces.

Usually, the update coefficients for the material boundaries are calculated by averaging the material parameters of the materials on both sides of the interface. This idea has been extended to the modeling of tilted surfaces by evaluating the flux integral over the cross section of the cell which the boundary transverses.

Method

In this paper, a novel approach is proposed. An analytical expression for the numerical reflection coefficient at a material interface has been derived as a function of the FDTD update coefficients. It shows that the error of the reflection coefficient depends not only on the discretization but also on the frequency of the incident wave. Based on this analysis, modified update coefficients are derived which make the FDTD algorithm exactly fulfill the boundary conditions at a frequency of optimization. Moreover, a general error reduction above a certain frequency limit is achieved.

Application

The proposed method has been used to simulate a vertical-cavity surface-emitting laser (VCSEL). For the simulation of the highly reflective mirrors used in VCSELs, the numerical phase errors in the materials and at their boundaries must be considered. Keeping these errors within sufficient limits with the conventional FDTD method, usually requires a very small mesh step (approximately $\lambda/40$). The application of the proposed boundary correction method allows precise results to be obtained with a significantly increased mesh step of $\lambda/10$.

Conclusion

The numerical reflection coefficient of an FDTD model of a material interface has been derived analytically. Thus the optimization of the update coefficients could be determined such that FDTD fulfills the boundary conditions at one frequency. The success of these findings was demonstrated with the help of the simulation of a VCSEL. The developed method allows a significant reduction of the computational expenses while retaining the numerical accuracy of a high resolution model.

Treatment of Thin, Arbitrary Shaped PEC Sheets with FDTD

D. Reinecke*, P. Thoma and T. Weiland
 CST GmbH, BÜdinger Str. 2a, D-64289 Darmstadt, e-mail: Reinecke@CST.de

In this paper we will present a cell splitting algorithm to treat thin, perfectly conducting sheets in a FDTD scheme. It is an extension of the Perfect Boundary Approximation (PBA), a stable method to approximate curved PEC-Surfaces within a normal cartesian mesh (B. Krietenstein, R. Schuhmann, P. Thoma, T. Weiland, *LINAC 98, Chicago, USA, 1998*, The Perfect Boundary Approximation Technique Facing the Big Challenge of High Precision Field Computation).

In standard FDTD simulations, the spatial resolution is directly related to the chosen grid. The smallest structural element to be resolved, defines the smallest grid step. For the discretization of thin PEC sheets this leads to a grid density that would not be necessary to resolve the fields or to calculate the Scattering matrices to a reasonable accuracy. The demands on the memory and simulation time might also become a serious problem. The only alternative is to accept a considerable error in the structure's approximation. Even when using a method which allows fractional fillings of mesh cells.

The cell splitting algorithm avoids this overhead of mesh points or loss of approximation accuracy.

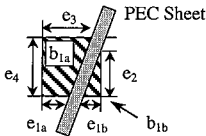


Fig. 1. Mesh cell surface cut by a PEC sheet. The voltage e_1 is split up to e_{1a} and e_{1b} as well as the magnetic flux b_1 is split up into b_{1a} and b_{1b}

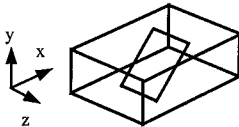


Fig. 2. Simulated waveguide. The ports are located at x_{min} and x_{max} .

Transmission coefficients

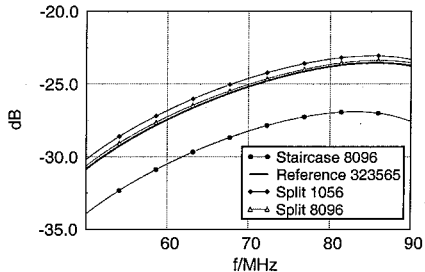


Fig. 3. Results of the simulated waveguide. The numbers in the legend field are the mesh points used for the simulation.

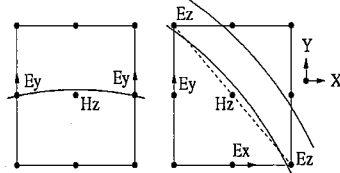
State values, such as the magnetic flux or the electric voltage, that are cut by a PEC sheet, are split up and treated independently as can be seen in Fig.1. For all split state values a new Curl operator is created. This operator is chosen in a way that the algorithm remains stable and that the fields of both sides of the sheet are completely separated. In fact our method treats the concerned cell surfaces as if they were two surfaces. One on the first side of the PEC Sheet and one on the other.

As an example of the considerable increase in simulation accuracy when using the split algorithm, a Waveguide with a sloping, infinitesimally thin metallic sheet inside has been simulated (Fig. 2). Two simulations with staircase approximation and two with the split algorithm have been made. One of the staircase simulations has been made with a very high number of mesh points to be used as a reference. The results in Fig. 3 show that the split algorithm converges much faster to the reference result than the staircase approximation. With only 8096 mesh points the split algorithm produces a difference to the reference simulation of only 0.1 to 0.2 dB, while the staircase approximation is of about 2.8 to 3.2 dB away. The split algorithm, therefore, proves itself to be a very promising method for the solving of all kinds of thin sheet problems, such as microstrip applications or conformal patch antennas.

A FDTD Study of Yee Cell Modifications for Modeling Curved Surfaces

Dr. John W. Nehrbass

Ohio Supercomputer Center; The Ohio State University
ASC/HP 2435 5th Street,
Wright-Patterson AFB, Ohio 45433-7802
nehrbass@osc.edu



Abstract - In this paper the RCS of a squat cylinder (4.5 inches in diameter by 2.1 inches high) is modeled with the FDTD method by using a uniform rectangular grid composed of modified Yee cells. Valid RCS results accurate to within a tenth of a dB over the bandwidth of 100 MHz to 18 GHz in 10MHz increments are desired. The FDTD results are verified for accuracy by comparing them to reference data obtained from: anechoic chamber measurements, and calculations from two frequency domain body of revolution codes which agreed to well within 0.1 of a dB of each other. It took several months for the 1790 frequency runs of these codes to generate the required reference data while the FDTD method could generate the entire bandwidth in a few hours. The FDTD method accuracy is improved by choosing Yee cells sufficiently small. For 3D systems, reducing the Yee cells by half increases the number of total cells by a factor of 8 and decreases the time increment by 2. For this study optimized PML absorbers are used to minimize artificial reflections. The cylinder is modeled as a PEC material and total field formulations are used. As observed, small changes when gridding the cylinder produced large changes in the RCS. PEC cells are selected when the center of the Yee cell resides within the cylinder. This suggests that tangent and normal components (E_y above) may incorrectly both be set to zero. When the cylinder boundary crosses the corner of a cell, it may not be necessary to model the entire cell as a PEC. Improved grids are achieved when each edge is determined PEC or not. Special care must be taken to assure that one does not model fins on a cylinder. The goal still remains to accurately model the physical curvature consequently the surface must remain as smooth as possible. Note that if one could cut the Yee cell diagonally in half, as shown by the dashed line above, this would improve curvature modeling. This change would not alter the evaluation of the electric fields but would modify magnetic (H_z) field formulas. The magnetic field is computed as the line integral of the electric field surrounding it. As the area is effectively cut in half, the magnetic field (H_z) is modified by replacing its permeability value with half the value used for a full cell. By appropriately choosing these diagonal cuts, the accuracy of the grid is further improved. Finally, note that as a symmetric target, the backscatterer RCS is not a function of angle about the cylinder axis. However, when the cylinder is modeled with rectangular cells it is not perfectly symmetric and thus the backscatterer RCS will be a function of angle. Further analysis is achieved by varying the angle of incidence with respect to the grid and minimizing any variations in the RCS. The final details of this study will be presented at this talk, with specific PML details, computational size, CPU timing, and the final grid chosen to achieve the desired accuracy.

A Sub-cellular Algorithm to Model a Thin Slot Diagonal to the FDTD Grid

Chris Mason and Michal Okoniewski
 Department of Electrical and Computer Engineering
 University of Calgary
 Calgary, Alberta, Canada T2N 1N4

Finite-Difference Time-Domain (FDTD) analysis is a popular technique that is used to model microwave circuits, antennas, and other high speed devices. One drawback of this technique is that current FDTD equations cannot model thin slots passing through the FDTD grid at an angle. By increasing the cell resolution, angled slots can be approximated with a staircase, however, this method introduces inaccuracies into the calculations and is computationally inefficient.

To solve the angled slot problem, a contour integral is applied to the cells shown in Figure 1. Two algorithms were developed. The first one uses a simple contour integral approach and neglects the conductor edge singularities. In this approach, the electric fields between the conducting sheets are placed perpendicular to the sheet edge to allow for a rectangular path of integration. To obtain the update equation for magnetic field, contour C1 is used:

$$H_z^{n+1}(i, j, k) = H_z^n(i, j, k) + \frac{\Delta t}{\mu} \frac{[E_r(d-1, k) - E_r(d, k)]}{\sqrt{\Delta x^2 + \Delta y^2}}$$

The update equation for electric fields is generated using a diagonal contour C2. Interpolation is used to calculate magnetic fields on the contour. The resulting formula is as follows:

$$E_r^{n+1}(d, k) = E_r^n(d, k) + \frac{\Delta t}{\epsilon} \left[\frac{H_z(i+1, j-1, k) - H_z(i, j, k)}{\sqrt{\Delta x^2 + \Delta y^2}} + \frac{H_r(d, k+1) - H_r(d, k-1)}{\Delta z} \right]$$

A more accurate approach enhances the above equation by accounting for singularities on the metal edges in a manner similar to the enhanced thin-slot formalism equations. (Wang, B.-Z., "Enhanced Thin-Slot Formalism for the FDTD analysis of thin-slot penetration," *IEEE Microwave and Guided Wave Letters*, Vol. 5, 1995 pp. 142-143.)

The initial results of these equations look promising, though work is still in progress. The equations appear to be time stable and significantly reduce overall computing time when used to model antennas that contain thin slots diagonal to the FDTD grid.

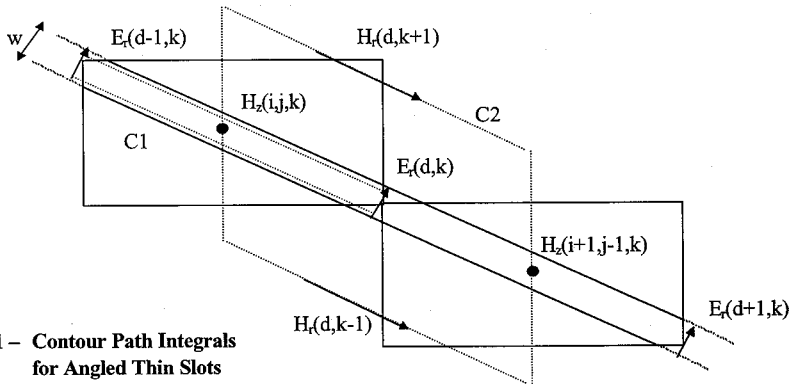


Figure 1 – Contour Path Integrals for Angled Thin Slots

A New Absorbing Boundary Condition for FDTD

N. Sachdeva* and N. Balakrishnan
Department of Aerospace Engineering,
Indian Institute of Science,
Bangalore — 560 012, INDIA

S. M. Rao,
Department of E & CE,
Auburn University, Auburn, AL 36849.

The Finite-Difference Time-Domain (FDTD) method is a differential equation based technique used for solving electromagnetic wave interaction problems for open as well as closed region problems. In order to facilitate a numerical solution for open region problems, it is necessary to incorporate artificial boundaries to simulate the infiniteness of the problem. These boundaries must satisfy certain conditions like the following:

1. They must simulate the outer boundary in such a way that it appears as though the domain is extending to infinity.
2. They must permit waves to travel in only one direction, that is, outwards only.
3. They should work for any direction of incidence.
4. They should work over a wide frequency band.
5. They could be placed as close to the scatterer as possible.

As it stands today, the Perfectly Matched Layer (PML) boundary condition seem to satisfy most of these requirements. It provides maximum absorption and independent of the frequency of operation and the angle of incidence. The boundary layers can also be placed very close to the scatterer. However, in this work we propose and implement a new absorption layer based on chiral materials, in particular, a material called ChiroSorbTM. The main advantage of this material is that it has the property of zero reflection. Keeping this in mind, the use of chiral materials to terminate the FDTD mesh has been taken up. When a linearly polarised electromagnetic wave propagates through a chiral medium the plane of polarisation of the transmitted wave gets rotated. The chiral material also has the property of having different absorptions for left- and right-circularly polarised waves.

A comparison of the far-field calculated using the FDTD with chiral boundary and the Time Domain Integral Equation (TDIE) method, has been carried out. The comparison is made via standard canonical shapes, a cube and a sphere, both for conducting as well as dielectric material bodies.

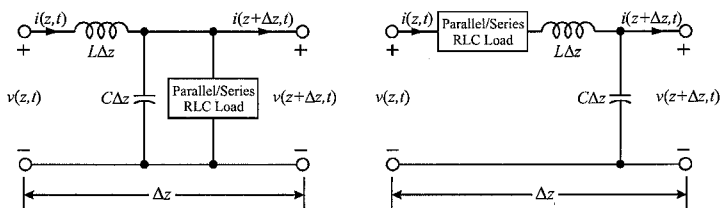
Modeling Parallel and Series RLC Loads in a 1-D FDTD Transmission Line

Thomas P. Montoya*
Dept. of Electrical & Comp. Eng.
University of Tennessee
Knoxville, TN 37996-2100

Waymond R. Scott, Jr.
School of Electrical & Comp. Eng.
Georgia Institute of Technology
Atlanta, GA 30332-0250

A one-dimensional (1-D) finite-difference time-domain (FDTD) model for a simple, lossless transmission line has been developed (J. G. Maloney, K. L. Shlager, and G. S. Smith, *IEEE Trans. Antennas Propag.*, **42**, 289-292, 1994). This 1-D FDTD transmission line model was extended (T.P. Montoya and G.S. Smith, *Microwave Optical Tech. Lett.*, **21**, 105-114, 1999) to implement single, passive, lumped circuit elements (e.g., capacitors, inductors, and resistors) placed in parallel or series with the transmission line. In addition to being useful in modeling various problems, the 1-D FDTD transmission line model is useful in teaching students about the FDTD method. The 1-D geometry allows for the simple presentation of the temporal- and spatial-stepping, and the minimal computational demands allows for real-time displays of pulse propagation along a transmission line.

This presentation will present the FDTD update equations necessary to implement parallel or series RLC loads placed in parallel or series with the transmission line. The figure shows the parallel or series RLC loads placed in parallel (left) and series (right) in an incremental section of the 1-D transmission line. These RLC loads can be part of a voltage source, a terminating load, or located at some arbitrary point in the transmission line. Selected results will be shown to demonstrate the accuracy and validity of the update equations by comparison with analytic results.



THE MODELING OF LUMPED ELEMENTS USING THE HAAR WAVELET MULTIREOLUTION TIME DOMAIN TECHNIQUE

Saehoon Ju*, Duck-ho Bae, and Hyeongdong Kim
 Computational Electromagnetics Laboratory
 Department of Electrical and Computer Engineering
 Hanyang University, Seoul 133-791, Korea

Phone/Fax: 82-2-2290-0373/82-2-2298-0373, e-mail: hdkim@email.hanyang.ac.kr

The Finite Difference Time Domain (FDTD) method has been used widely in solving applied electromagnetic problems. Recently, to improve the computational efficiency the multiresolution theory has been applied to the FDTD method and leads to Multiresolution Time Domain (MRTD) techniques (M. Krumpholz and L. P. B. Katehi, *IEEE Microwave and Guided Wave Lett.*, 5, 382-384, 1995). MRTD techniques using the Battle-Lemarie, Daubechies, and Haar wavelets have been applied to analyze various electromagnetic structures with success. Although these techniques need less computational effort than the conventional FDTD method, the latter method is easier to implement boundary conditions than the former methods. Therefore, the MRTD scheme combined with the local FDTD boundary conditions can be used to get the advantages of both the methods.

In this work, to analyze the microstrip structure with lumped elements, the conventional FDTD scheme (the physical domain) is used to describe the characteristics of the lumped elements, while the Haar-wavelet MRTD scheme (the wavelet domain) is applied to the remained computational domain. The main distinction between this work and earlier ones is the boundary conditions. The MRTD's temporal discretization width is twice as large as the FDTD's one to combine both the methods. To show the validity and the advantage of the proposed scheme, numerical results for microstrip structures with lumped elements (a diode and a capacitor) are presented and compared to those obtained by the use of the conventional FDTD scheme. Fig. 1 shows the 3-D microstrip structure with lumped element of interest. The perfect electric conductor and absorbing boundary condition are treated as described in the previous work (M. Fujii and W. J. R. Hofer, *IEEE Trans. Microwave Theory Tech.*, 46, 2463-2475, 1998). A microstrip line with a diode ($I_s = 10^{-14}$ amps) is simulated by the proposed method. For comparison, the conventional FDTD approaches are also applied to the problem. As shown in Fig. 2, the proposed method gives very good results compared with the FDTD fine mesh result. The computation time of the methods is shown in the Table 1.

Table 1. Comparison of computation time



Fig. 1. Microstrip Structure with Lumped Elements

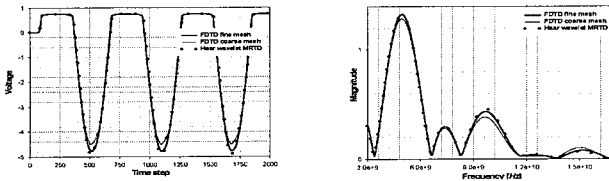


Fig. 2. The voltage across a diode (a) time domain (b) Frequency Domain

Transient Electromagnetics (I)

Chair: E. Heyman, Tel Aviv University, Israel

Page

- | | | | |
|---|------|---|----|
| 1 | 8:00 | A unified kinematic theory of transient array, <i>A. Shlivinski*</i> , <i>E. Heyman, Tel Aviv University, Israel</i> | 34 |
| 2 | 8:20 | Chaotic wave propagation and synchronization through planar transmission lines and discontinuities, <i>T. Wu, S. Yang*</i> , <i>University of Central Florida, USA</i> | 35 |
| 3 | 8:40 | Physical insight into an automated E-pulse scheme by analytical evaluation, <i>J. Mooney*</i> , <i>L. Riggs, Auburn University, Z. Ding, University of Iowa, USA</i> | 36 |
| 4 | 9:00 | Modeling high-speed gas discharge switching for wideband and ultra-wideband applications using a transient, full-wave electromagnetic solver with an integrated gas-discharge physics model, <i>R. Pate, D. Riley*</i> , <i>P. Patterson, Sandia National Laboratories, E. Kunhardt, Stevens Institute of Technology, T. Hussey, Air Force Research Lab., USA, S. MacGregor, A. Dick, University of Strathclyde, UK</i> | 37 |
| 5 | 9:20 | Use of time-frequency distributions and genetic algorithms in electromagnetic target feature extraction and K-pulse shaping, <i>G. Turhan-Sayan*</i> , <i>Middle East Technical University, Turkey</i> | 38 |

A UNIFIED KINEMATIC THEORY OF TRANSIENT ARRAY

A. Shlivinski* and E. Heyman

Department of Physical Electronics, Tel Aviv University

Tel Aviv 69978, Israel

Fax: +972-3-6423508, e-mail: heyman@eng.tau.ac.il

We present a unified framework for the kinematic analysis of transient arrays, i.e., arrays driven by pulsed waveforms and controlled by the time shifts between the array elements. The properties of the radiated field depend on the waveform parameters: the center frequency f_0 ; the fractional bandwidth of the waveforms B/f_0 ; the pulse repetition rate f_p ; the interelement spacing d and the total number of elements N . Following a previous work (A. Shlivinski, E. Heyman & R. Kastner, IEEE Trans. Antennas Propagat., AP-45, 1140-1149, 1997) we present here a unified parameterization for the kinematic properties that covers the entire parameter range, from the conventional monochromatic dense array to the ultra wideband sparse array. The radiation pattern consists of an interlace of grids of lobes, generated by different mechanisms: In addition to the *side-lobes* and the *grating-lobes* grids, which are mainly monochromatic phase-interference phenomena extended to the wideband regime, we also identify a grid of *cross-pulse-lobes* which is an intrinsic wideband phenomenon. The total lobe structure represents an interplay of all three phenomena that depends on the ratio between the parameters mentioned above.

Having established a unified representation we then focus on the ultra wideband regime where the lobe structure is dominated by the cross-pulse-lobes that are mainly controlled by the pulse repetition rate f_p , the d and the total number of elements N . It is shown that under certain conditions one may design a sparse array (with interelement spacing much larger than the wavelength for all frequencies in the band) which basically does not suffer from these lobes. These results are demonstrated both theoretically and numerically in the L_2 and L_∞ detector (norm) spaces.

Chaotic Wave Propagation and Synchronization Through Planar Transmission Lines and Discontinuities

Thomas X. Wu and Sarah X. Yang*
School of Electrical Engineering and Computer Science
University of Central Florida
Orlando, FL 32816

Chaotic communication has caught the attention of many researchers [see e.g., S. Hayes, *Physical Review Letters* **70**, 3031(1993)], especially since the robust synchronization property of chaos was discovered [see e.g., L. Pecora and T. Carroll, *Phys. Rev. Lett.*, **64**, 821(1990)]. This has piqued interest in new, non-linear devices and systems for communications and other applications. We note that chaotic wave propagation is important in the design of secure communication systems [T. Wu and D. Jaggard, *Microwave and Optical Technology Letters* **21**, 448(1999)].

In this talk, we discuss chaotic wave propagation and synchronization through planar transmission lines, which is of potential importance to build solid-state chaotic microwave system. We have used microstrip line and coplanar waveguide (CPW) as examples in the discussion. A baseband chaotic wave is generated and used as incident wave to discuss how waveguide dispersion and attenuation will affect synchronization. We will also discuss the influence of discontinuities on the distortion of chaotic signal and destruction of synchronization.

Since a chaotic signal can be used as a clock signal or a carrier through synchronization, the recovery of synchronization from a distorted signal after propagation is an important research topic. In the following figure, we discuss the general idea of synchronization recovery. A chaotic signal u_1 generated by the drive system (transmitter) propagates through a channel, which consists of planar transmission line discontinuities. \tilde{u}_1 which is a distorted version of u_1 is obtained. We cannot get chaotic synchronization if we use \tilde{u}_1 to drive the response system (receiver) if \tilde{u}_1 is a seriously distorted version of u_1 . Here, we use a genetic algorithm to design a recovery system to synchronize the chaotic signal. We use the *synchronization mismatch* (defined as the normalized average absolute value of the output u_2 and input \tilde{u}_1 of the response system) as the cost function in the genetic algorithm.

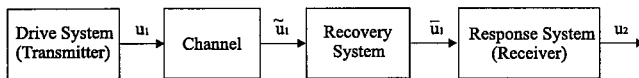


Figure 1: A typical synchronization recovery system.

Physical Insight into an Automated E-pulse Scheme by Analytical Evaluation

Jon E. Mooney* and Lloyd Riggs
Dept. of Elec. and Comp. Engineering
Auburn University
Auburn University, AL 36849

Zhi Ding
Dept. of Elec. and Comp. Engineering
University of Iowa
Iowa City, IA 53346

As demonstrated by the many papers on the subject, the E-pulse and S-pulse techniques are popular and viable methods for performing resonance based, aspect independent target discrimination. The E-pulse and S-pulse techniques, which provide a basis for target discrimination by selectively annihilating the resonant modes from the transient response of a specific target, were first described in the works by Rothwell *et al.* (*IEEE Trans. Antennas and Propagat.*, **33**, 929-937, 1985 and **35**, 426-434, 1987). In these works and others, the discrimination performance of the E/S pulse methods were validated using theoretical as well as measured signature data. Recently, Mooney *et al.* (*IEEE Trans. Antennas and Propagat.*, **48**, 2000) demonstrated how to analytically evaluate the performance of an automated E-pulse scheme when the scattering data is corrupted with white Gaussian noise.

The performance of an automated E-pulse scheme is quantified through the use of energy discrimination numbers (EDN's). The EDN represents how much of the received signal is present after having been passed through an E-pulse filter designed to annihilate the resonances of a specific target in the target library. By computing the probability density functions of the EDN's, one can establish a performance measure (in terms of probability of identification) for the E-pulse scheme.

Not only do the probability densities of the EDN's lead to a performance measure, they also effectively extend one's ability to understand and gain physical insights into how complex electromagnetic interactions ultimately affect the E-pulse technique. Since the EDN's are dependent on different variables of the electromagnetic interaction problem (such as resonances), one can study the probability densities to understand how the performance of the E-pulse technique varies with respect to these parameters. In this paper, a parametric analysis of thin cylinders of varying lengths will be performed. From this analysis, we will show how the probability densities of the EDN's effectively characterize the performance of the E-pulse discrimination scheme.

MODELING HIGH-SPEED GAS DISCHARGE SWITCHING FOR WIDEBAND AND ULTRA-WIDEBAND APPLICATIONS USING A TRANSIENT, FULL-WAVE ELECTROMAGNETIC SOLVER WITH AN INTEGRATED GAS-DISCHARGE PHYSICS MODEL

Ron Pate, Doug Riley*, and Paull Patterson

Sandia National Laboratories
Albuquerque, NM 87185-1152

Eric Kunhardt
Stevens Institute of Technology
Hoboken, NJ

Tom Hussey
Air Force Research Laboratory
Kirtland AFB, NM

Scott MacGregor and Andrew Dick
University of Strathclyde
Glasgow, Scotland, UK

ABSTRACT

High-voltage gas discharge switching has performed successfully over the years as a key component in many high power electromagnetic pulse generator systems. Recently there has been increasing interest in improving the performance and expanding the applications of pulsed high power microwave (HPM), wideband (WB), and ultra-wideband (UWB) source technologies. Despite gas switch limitations and the great advances being made in solid-state and other competing switch technologies, high-voltage gas discharge switching often remains the best option for various high-power pulsed electromagnetic applications.

High-power WB and UWB applications, in particular, require switching relatively low-energy (tens of Joules or less), short duration (on the order of nanoseconds or less) pulses with sub-nanosecond rise-times within relatively low-impedance circuits (on the order of ten ohms or less) operating at high voltages (tens to hundreds of kilovolts). Switch turn-on speed and energy loss behavior become critical system design and performance issues within this demanding hard-discharge regime of operation. Currently, gas discharge switch modeling and performance prediction as a function of detailed switch configuration, gas type, gas pressure, and drive circuit parameters are not well developed for this operating regime.

The authors are currently engaged in a coordinated analytical, experimental, and computer-modeling investigation of the early time behavior of high-power gas discharge switching. The effort is directed toward the development of improved design and modeling capabilities for simulating the performance of gas discharge switching. This paper describes the integration of a 3-D, transient finite-element electromagnetic solver, with an improved, two-fluid model of the gas-discharge channel physics during switch turn-on. The integration provides a self-consistent feedback loop that uses the channel-physics model as a source-term for the electromagnetic solver, and the local electromagnetic fields around the discharge as a source term for the channel-physics model. Experimental test results provide actual data for validation and verification of the simulation approach.

Use of Time-Frequency Distributions and Genetic Algorithms in Electromagnetic Target Feature Extraction and K-Pulse Shaping

Gönül Turhan-Sayan

Middle East Technical University, Electrical and Electronics Eng. Dept. &
TÜBİTAK-BYLTEN (Information Technologies and Electronics Research Inst. of the
Turkish Scientific and Technical Research Council), Ankara, TURKEY
E-mail: gtsayan@ed.eee.metu.edu.tr

Target recognition from measured data either in microwave or optical frequencies has been an important problem of applied electromagnetics. The most critical step in the solution of this general problem is to extract a proper set of target features for effective characterization. These features should represent the target in a unique way if possible, or otherwise should strongly emphasize the differences of that target from the other candidate targets. In addition to being physically meaningful, the extracted features should be compatible with the rest of the computational process and with the specific methods (statistical methods, neural network methods, natural response annihilation methods, etc.) to be used in target recognition.

Feature extraction from available data needs intensive use of signal processing techniques. Therefore, target recognition can be considered as an interdisciplinary area making use of both electromagnetics and signal processing. The conventional signal processing techniques, such as the Fourier transform, are useful for the analysis of stationary signals but not for that of non-stationary signals. Time-frequency representation (TFR) techniques must be utilized in the latter case to see the distribution of total signal energy with respect to time and frequency, simultaneously. In case of target recognition from scattered electromagnetic data, target pole strings on the complex frequency plane play a very important role in characterizing the target in an aspect and polarization independent manner. In a previous research which was focused on the design of Neural Network target classifiers by the help of TFR techniques (Turhan-Sayan, et.al., *Microwave and Optical Tech. Lett.*, 21(1), 63-69, 1999) the Wigner Distribution, a well-known TFR technique, was found quite useful to locate the poles and to extract feature vectors related to the distribution of signal energy in two-dimensional time-frequency plane.

The purpose of this paper is to extend the use of TFR's to target recognition techniques which are based on the natural response annihilation method, such as the K-Pulse technique. In the problem of multi-aspect K-Pulse shaping by Genetic Algorithms, selection of design aspects will be accomplished by using TFR analysis to ensure that almost all the target poles within the frequency band of the measurements will be properly represented by the design data. That approach will improve the results obtained in a previous K-Pulse design research (Turhan-Sayan, et.al., *Microwave and Optical Tech. Lett.*, 17(2), 128-132, 1998). The TFR analysis will also be used to check the validity of the designed K-pulse waveforms. Demonstrations involving both canonical and complicated target geometries will be presented.

Propagation over Land and Water

Chair: Y. Antar, Royal Military College of Canada

Page

- | | | | |
|---|------|---|----|
| 1 | 8:00 | Adaptive parabolic equation techniques for wave propagation over arbitrary irregular terrain, <i>T. Eibert*</i> , <i>Technologiezentrum, Germany</i> | 40 |
| 2 | 8:20 | Comparison of various propagation models on real terrain: difficulties and remedies, <i>A. Altintas*</i> , <i>M. Aksun</i> , <i>S. Topcu</i> , <i>H. Koymen</i> , <i>V. Yurchenko</i> , <i>E. Yetginer</i> , <i>O. Yilmaz</i> , <i>Bilkent University, Turkey</i> | 41 |
| 3 | 8:40 | Short range communication near the earth at 2.4GHz, <i>W. Merrill*</i> , <i>Sensor.com, USA</i> | 42 |
| 4 | 9:00 | Performance of site diversity and up-link power control techniques in Singapore: preliminary results, <i>J. Ong</i> , <i>K. Timothy*</i> , <i>E. Choo</i> , <i>Nanyang Technological University, Singapore</i> | 43 |

Adaptive Parabolic Equation Techniques for Wave Propagation over Arbitrary Irregular Terrain

Thomas F. Eibert
Technologiezentrum, E45g,
T-Nova Deutsche Telekom Innovationsgesellschaft mbH,
64307 Darmstadt, Germany,
email: thomas.eibert@telekom.de

In most cases, practical wave propagation techniques for mobile communication and radio broadcasting services are still based on so-called semi-empirical algorithms which were originally derived from the evaluation of measured data. Even though, these approaches are often upgraded by theoretical ingredients such as knife-edge diffraction or the uniform geometrical theory of diffraction for the treatment of wedges or cylinders, their accuracy is limited and optimizations of the inherent parameters are only valid for certain application areas. However, it is the superb computational speed of the semi-empirical approaches which makes them an indispensable tool for the planning and optimization of terrestrial radio services in large service areas with many transmitters. On the other hand, many attempts have been made to tackle the irregular terrain wave propagation problem by full-wave low-frequency techniques such as the method of moments as applied to integral equation formulations or the finite difference technique. Such attempts are plagued by three severe problems: 1) The required geometric data bases with resolutions on the order of fractions of a wavelength are not available. 2) Unavoidable numerical errors in the huge computational domain (with respect to wavelength) can cause stability problems and approximations are usually necessary to achieve a useful solution at all. 3) The required computational resources are prohibitively large.

In this contribution, we consider a rigorous solution of the wave propagation problem which is based on a reduced-accuracy geometric model of the problem at hand. To this end, we restrict ourselves to the two-dimensional (2D) problem: wave-propagation along the great circle cut between transmitter and receiver. The resulting 2D profile is then approximated by bridged knife-edges where different terrain classes are modeled as planar multilayered media consisting of different homogeneous dielectric and lossy layers. For each section of the profile, the exact layered medium Green's function is derived in the spectral domain. Then, it is recognized that the (exact) spectral representation can be combined with a Fourier split-step parabolic equation technique (PET) to obtain the forward-propagation solution over the whole 2D profile in a very efficient manner. In contrast to other PETs, which usually include several approximations (due to knife edges in free space or due to a position-dependent refractive index resulting from transformations of the irregular profile), this PET approach is absolutely robust and allows for very flexible adaptive step-size selection dependent on the spatial variability of the profile. Consequently, the required computational resources can be considerably lower than for previous PETs which can often only be optimized for a fixed (relatively short) step-size. Once the fields above the considered terrain are determined, the receiver field intensities are obtained for the required antenna heights, where this final step considers the local terrain usage (open field, forest, city, ...) in an appropriate manner.

Computational results and comparisons with measured data will be given in the presentation.

COMPARISON OF VARIOUS PROPAGATION MODELS ON REAL TERRAIN: DIFFICULTIES AND REMEDIES

A. Altýntap*, M.I. Aksun, S. Topçu, H. Köymen, V. Yurchenko,
E. Yetginer, and Ö. Yýlmaz

Bilkent University, Communication and Spectrum Management Research
Center (ISYAM) Bilkent TR-06533 Ankara, Turkey

Various propagation models are available for the VHF and UHF bands and higher frequencies. In the range of these frequencies, we compare the field attenuation predicted by the multiple diffraction algorithms of Epstein-Peterson, Deygout, and Vogler on the real terrain data. Since these algorithms are based on the knife-edge diffraction model, some of them may not be sufficiently accurate for real terrain. Besides, multiple-edge diffraction models such as the Vogler method, do not specify how to choose significant knife edges for simulations when the terrain data are available in the form of an elevation database. To this end, an original selection procedure has been developed which accounts for both the distance and the depth of the valley between local terrain maxima considered as potential knife edges for being accounted in simulations.

Another issue of our research has been a comparison of the knife edge diffraction models with the parabolic wave equation approximation. The comparison is of importance for the selection of significant maxima for multiple knife edge diffraction models and for studying the effect of the terrain between the selected knife-edges for such models. Parabolic wave equation has been solved by the Crank-Nicholson finite-difference method. Conformal mapping that depends on the terrain profile has been introduced in order to increase the stability and accuracy of the solution by simplifying the shape of the mesh and computational domain.

For actual field strength predictions, these multiple diffraction losses are added to the losses predicted by the CCIR curves. These curves may be modified by including terrain roughness factor, clearance angle and mixed path conditions.

Short Range Communication near the Earth at 2.4GHz

William M. Merrill
Sensor.com
3000 Ocean Park, Blvd, Suite 3030
Santa Monica, CA, 90405. williamm@sensorweb.com

As the Internet expands to allow remote monitoring of sensors and appliances, wireless communication on a micro cell scale becomes increasingly important. This paper focuses on characterizing the short range (1-100m) radiation and propagation characteristics of antennas operating in the 2.4GHz ISM band in close proximity to the earth. Sommerfeld's theoretical solution (A. Sommerfeld, *Partial Differential Equations in Physics*, Academic Press, 1949, New York) of the radiated fields due to infinitesimal radiators over a lossy half-space is applied to describe short-range communication. In addition measurements are presented to demonstrate the characteristics of non-infinitesimal antennas in a variety of environments. Radiation from a quarter-wave monopole antenna and microstrip patch is considered in conjunction with a frequency hopped wireless 2.4GHz modem.

Any antenna may be decomposed into a sum of infinitesimal radiating dipoles by the principle of superposition. The problem of infinitesimal dipoles radiating in close proximity to the earth was first rigorously treated by Sommerfeld, in which he represented the earth as a flat lossy half-space. Since Sommerfeld published his formulation multiple refinements have been made to include the earth's curvature, reflections off the ionosphere, surface roughness, and shadowing due to the earth's surface. Sommerfeld's original analysis provides a picture of the fundamental effects due to radiation in close proximity to the earth. In this paper the asymptotic solutions of Sommerfeld's flat half-space analysis is compared at 2.4GHz with measurements of the fall off between two antennas at short range.

Measurements over a flat grassy field, over a flat asphalt surface, and in a cluttered indoor environment are presented. In all measurements the same 2.4GHz system was utilized which provided average spread spectrum received signal strength over 100 frequency hops in the 2.4GHz to 2.4875GHz ISM band. Comparison of the asymptotic half-space solution over the grassy field, and $r^{-\alpha}$ fall off with α from 2 to 4 in all cases, is demonstrated. The substantial influence of antenna height off the ground and importance of cancellation of the incident and reflected term fields along grazing rather than the Norton surface wave response, are shown.

**Performance of Site Diversity and Up-link Power Control Techniques in Singapore:
Preliminary Results**

J. T. Ong, K. I. Timothy and E. B. Choo
School of Electrical and Electronic Engineering
Nanyang Technological University
Singapore 639798.
ekudari@ntu.edu.sg

Abstract

The application of "site diversity" and "up-link power control" techniques to counter the severe rain attenuation has been investigated at Ku Band frequency. The site diversity experiments are carried in Singapore, which has an equatorial climate, using the INTELSAT beacon with receivers at two stations separated by 10kms. The up-link power control technique has been implemented in the ST-1 beacon receiver, which is also operating at Ku-band. This paper describes preliminary results on these two techniques.

High-Frequency Techniques

Chair: D. Erricolo, University of Illinois at Chicago

			Page
1	12:00	Experimental validation of diffraction coefficients for dielectric screens, <i>F. Mioc, R. Tiberio*, A. Toccafondi, University of Siena, Italy</i>	46
2	12:00	High-frequency scattering from a grounded semi-infinite thick dielectric slab, <i>B. Polat*, Faculty of Engineering, Istanbul, L. Pearson, Clemson University, USA</i>	47
3	12:00	Physical optics models for backscatter response of road surface faults at millimeter-wave frequencies, <i>E. Li*, National Chi Nan University, Nantou, K. Sarabandi, University of Michigan, USA, T-C. Chiu, National Central University, Chung-Li</i>	48
4	12:00	Large axial distance evaluation of magnetic fields due to a magnetic source located on a conducting circular cylinder, <i>C. Tokgoz*, P. Pathak, R. Marhefka, The Ohio State University, USA</i>	49
5	12:00	Numerical comparison of eigenfunction and asymptotic (high-frequency) radiated fields from a class of open, convex structures, <i>D. Chatterjee*, University of Missouri-Columbia at Kansas City, USA</i>	50
6	12:00	Propagation path loss - a comparison between ray-tracing approach and empirical models, <i>D. Erricolo*, V. Garg, P. Uslenghi, University of Illinois at Chicago, USA</i>	51
7	12:00	Electromagnetic pulse wave propagation over land-sea mixed-path, <i>T. Ishihara*, R. Yoshioka, National Defense Academy, Japan</i>	52
8	12:00	Gaussian beam tracking through a curved interface: comparison with the Method of Moments, <i>D. Lugara*, Institut National des Telecommunications, France, A. Boag, Tel Aviv University, Israel, C. Letrou, Institut National des Telecommunications, France</i>	53
9	12:00	A Fast Physical Optics (FPO) algorithm for high frequency scattering, <i>A. Boag*, Tel Aviv University, Israel</i>	54
10	12:00	Two-mirror open resonators with spherical mirrors made from limited conductivity materials, <i>D. Afonin*, Moscow State University, V. Kravchenko, Russian Academy of Sciences, Russia</i>	55

Experimental validation of Diffraction Coefficients for Dielectric Screens

F. Mioc, R. Tiberio, A. Toccafondi

*Dept. of Information Engineering, University of Siena,
Via Roma 56, 53100 Siena Italy,
E-mail: tiberior@diu.unisi.it*

Most of the diffraction coefficients available within the framework of the Uniform Geometrical Theory of Diffraction (UTD) are relevant to perfectly electric conducting (p.e.c.) canonical configurations, and are found very accurate when dealing with diffraction phenomena arising from metallic bodies. However, there are several important practical applications that involve large complex dielectric structures. Significant examples are found in describing the electromagnetic propagation in urban and indoor environments for mobile and wireless communications. Rigorous solutions are available for the case of impenetrable wedges with impedance b.c., that have been developed by applying the method introduced by Maliuzhinets (Maliuzhinets, *Sov. Phys. Dokl.*, 3, 752-755, 1958). However, they lead to rather involved formulations, that are not suitable to treat edges in penetrable panels.

In order to broaden the applicability of UTD it is desirable to develop efficient formulations of high-frequency diffraction coefficients for edges in penetrable non perfectly conducting surface. To this end a heuristic solution has been inferred from the rigorous analysis of related problems (F.Mioc A.Toccafondi R.Tiberio AP-S Symposium, Orlando, 1999) which provides useful tools to treat practical applications, with an adequate degree of accuracy. Simple high-frequency expressions of a UTD dyadic diffraction coefficient for thin dielectric screens were obtained by conveniently modifying the UTD formulation for a p.e.c. half plane. This formulation, which represents a significant improvement to that suggested by Burnside et al (W. D. Burnside, K. W. Burgener, *IEEE Trans. Ant. Prop.*, 31, 1, 1983), provides a uniform description of the field across the SB, explicitly satisfies reciprocity and, to a first order, the b.c. at the faces of the screen.

In this paper, the results of an experimental validation of our heuristic solution are presented and discussed.

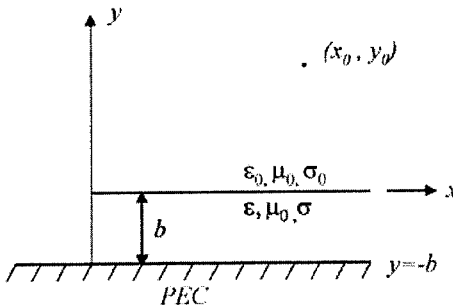
High-Frequency Scattering from a Grounded Semi-Infinite Thick Dielectric Slab

B.Polat*, Electronics Engineering Department, Faculty of Engineering, Istanbul University, TR-34850. Avcilar, Istanbul, TURKEY (bpolat@istanbul.edu.tr)
and

L. W. Pearson, Holcombe Department of Electrical and Computer, Clemson University, Clemson, South Carolina 29634-0915 (pearson@ces.clemson.edu)

The problem of electromagnetic scattering by truncated dielectric slabs is a canonical problem which has been investigated by numerous researchers in literature. In broad terms, we can divide such studies into two groups with respect to the electrical thickness of the slab. The case where the slab is electrically small utilizes approximate boundary conditions for modelling thin slabs with severe limitations. (Cf., R. G. Rojas and Z. Al-hekail, *Radio Science* (24), 1989, 1-12.) The case where the slab is electrically thick employs a rigorous Wiener-Hopf formulation and requires considerable numerical processing of integrals to evaluate the spectral objects that arise. (Cf., C. P. Bates and R. Mittra, *Radio Science*, (3), 1968, 251-266.) Pearson and Whitaker (, *Radio Science* (26), 1991, 169-174) introduced what they termed the "transverse aperture integral equation (TAIE) method" as a direct numerical means of localizing edge details in the diffraction process. The problem is formulated formally as an integral equation on an infinite-extend domain. Asymptotic anticipation is employed to reduce the solution domain to a region localized near the diffracting edge, thereby making the problem numerically tractable. The asymptotically anticipated terms can be integrated analytically through the use of spectral methods. This obviates the common difficulty of arduous integrals arising in asymptotic anticipation.

The TAIE method has been exercised only in limited cases to date. This presentation compares the results of the TAIE and the Wiener-Hopf method for a thick, grounded dielectric slab. Details of the computational features of the TAIE are discussed.



Physical Optics Models for Backscatter Response of Road Surface Faults at Millimeter-wave Frequencies

Eric S. Li*, Department of Electrical Engineering, National Chi Nan University
Nantou, Taiwan, R.O.C.

Kamal Sarabandi, Department of Electrical Engineering and Computer Science
The University of Michigan, Ann Arbor, MI 48109-2122

Tsen-Chieh Chiu, Department of Electrical Engineering, National Central University
Chung-Li, Taiwan, R.O.C.

The growing demands on driving safety issues have motivated the development of radar sensors for automotive application. One of the goals set for the radar sensors by the automotive industries is the capability of target recognition. Radar polarimetry is among several techniques proposed to achieve this goal. A complete polarimetric characterization of targets and clutter in highway environment is required to apply the technique of radar polarimetry for target recognition. Many scattering models were developed to accurately predict the backscatter response of various road surfaces and typical debris encountered on road surfaces (K. Sarabandi and E. S. Li, *IEEE Trans, Antennas Propagat.*, vol. 45, no. 11, 1997 and vol. 47, no. 5, 1999). Another common targets observed on highways are road surface faults, such as surface cracks and potholes. Two analytical models based on diffraction from impedance wedges and scattering from impedance cylinders at normal incidence condition were derived by Sarabandi and Li to predict the backscatter response of road surface cracks perpendicular to antenna boresight direction. A simpler and more accurate model based on physical optics (P.O.) approximation is presented in this paper. At millimeter-wave frequencies, the sizes of the surface faults of interest are large compared to the wavelength and the pavement materials is considered relatively lossy, thus P.O. model can provide precise results. Scattering at normal incidence from a horizontal circular cylinder whose radius is determined by the particle size distribution of the pavement materials is considered here. The technique of stationary phase approximation can be employed to derive a compact analytical expression for the scattering amplitude. The approach to estimate the radar cross sections (RCSs) of potholes is to approximate their shapes by polygons (e.g., round potholes approximated by hexagons or decagons). Scattering from each side of a polygon can be calculated by applying the P.O. model to the aforementioned cylinder at normal and oblique incidence conditions. The RCS of a pothole can be obtained by adding the scattered fields from each side coherently. The validity of the theoretical models will be examined by comparing the simulation results with the experimental data from the University of Michigan where extensive backscatter measurements at W-band were conducted to obtain the backscatter response of typical road surface faults at near grazing incidence angles ($76^\circ - 86^\circ$).

Large Axial Distance Evaluation of Magnetic Fields due to a Magnetic Source Located on a Conducting Circular Cylinder

Çağatay Tokgöz*, Prabhakar H. Pathak and Ronald J. Marhefka

The Ohio State Univ., Dept. of Electrical Eng., ElectroScience Lab.
1320 Kinnear Rd., Columbus, OH, 43212-1191, U.S.A.

Asymptotic analysis of surface fields by the Uniform Theory of Diffraction (UTD) may not yield accurate results in the paraxial region of a circular cylinder where evaluation of Fock type integrals by residue series expansion becomes ineffective. Although these integrals can be approximated by another expansion (P. H. Pathak and N. Wang, *IEEE Trans. Antennas Propagat.*, vol. AP-29, pp. 911-922, Nov. 1981) or some correction terms obtained by another technique can be added to obtain better accuracy (S. W. Lee and S. Safavi-Naini, *IEEE Trans. Antennas Propagat.*, vol. AP-26, pp. 593-598, July 1978) for a conducting circular cylinder, there is no general approach for the representation of the surface fields in the paraxial region of a circular cylinder. Therefore, an alternative solution is needed not only for a conducting circular cylinder but also for impedance and coated circular cylinders to obtain accurate results in this region.

The circumferential eigenfunction solution for a circular cylindrical geometry involves an infinite summation of inverse Fourier integrals corresponding to different modes. In the paraxial region of a circular cylinder, the addition of a few leading terms in the summation may be sufficient to yield satisfactory results with the idea that waves will be guided mostly along the axial direction. The inverse Fourier integrals can be evaluated in approximate closed form by employing the asymptotic representations of Bessel and Hankel functions for a fixed order and a small argument and assuming that the axial separation between source and observation points is large. A magnetic source located on the surface of a conducting circular cylinder will be assumed to generate the magnetic fields whereas the observation point can be either on or somewhat off the surface. Therefore, this alternative solution is useful for the representation of the magnetic fields that are close to the surface as well as the surface magnetic fields. The solution may be extended to the analysis of the fields in the paraxial region of an impedance circular cylinder.

Numerical Comparison of Eigenfunction and Asymptotic (High-Frequency) Radiated Fields from a Class of Open, Convex Structures

D. Chatterjee

370-H Robert H. Flarsheim Hall
Electrical and Computer Engineering Dept.
University of Missouri-Columbia at Kansas City (UMKC)
5100 Rockhill Road, KC, MO 64110-2499
Tel: (816)235-1276, Fax: (816)235-1260
e-mail: chatd@umkc.edu

An interesting canonical problem is to determine the variation of the source-excited radiated fields with respect to the height of a receiver moving normally away from a curved convex surface. The well-known Uniform Theory of Diffraction (UTD) [P. H. Pathak, *Proc. IEEE*, pp. 44-65, Jan. 1992] applies asymptotic solutions to find a *uniform* representation of the fields in the "lit" and "shadow" region of the convex surface. This UTD solution is not uniform when the receiver moves along the outward normal to a curved, convex surface. It is primarily because of this reason that these well-known UTD curved surface solutions, as implemented in the NEC-Basic Scattering Code [E. H. Newman and R. J. Marhefka, *Proc. IEEE*, pp. 700-708, May 1989], do not admit solutions for fuselage-mounted aircraft antennas. The different approximations to the eigenfunction solution for the scattering problem results in the various UTD solutions [P. H. Pathak, *op. cit.*]. The subject of this presentation is to present a parametric study for a class of curved surface solutions for future development of new forms of asymptotic solutions.

Following a recent study [D. Bouche, F. Molinet and R. Mittra, *Asymptotic Methods in Electromagnetics*, Springer, USA, 1997], it was concluded that the fields in the *close neighborhood* of the curved surface are largely confined within a *boundary layer*. The height of this boundary layer depends of the principal electrical radii of curvatures describing the curved surface. In the NEC-Basic Scattering Code [Newman and Marhefka, *op. cit.*] this distance is heuristically set to $\frac{\lambda}{4}$. The validity of this boundary layer thickness can be reasonably carried out by a numerical comparison of the eigenfunction and the corresponding UTD solutions. The purpose of this presentation is to compare eigenfunction solutions for the scattering problem, by varying receiver height off the curved surface for increasing principal electrical radii of curvature. This result can provide a benchmark against an earlier result obtained via UTD solutions for a circular cylinder [D. Chatterjee, *M.A.Sc Thesis*, ECE Dept., Concordia University, Montréal, Canada, 1992].

The eigenfunction solution requires accurate computation of Bessel functions [S. Zhang and J. Jin, *Computation of Special Functions*, John-Wiley, NY, USA, 1996] and the *Stokes Phenomenon* [C. J. Howls and A. B. Olde Daalhuis, *Proc. Roy. Soc. Lond.*, A, pp. 3917-3930, Nov. 1999]. Appropriate eigenfunction results, for a dielectric-coated PEC cylinder, shall be presented and compared against the corresponding UTD scattering solutions when $\epsilon_r \rightarrow 1$.

Propagation Path Loss - A Comparison between Ray-tracing Approach and Empirical Models

D. Erricolo (*), V. K. Garg, P. L. E. Uslenghi
Dept. of EECS, University of Illinois at Chicago, IL 60607-7053, USA

Radio waves arrive at a mobile station receiver from different directions with different time delays and polarization. As a result, a receiver at one location may experience a signal strength quite different from a similar receiver located only a short distance away. As a mobile station moves from one location to another, substantial amplitude and phase fluctuations may occur, and signals are subjected to fading.

Empirical propagation models are often used to determine how many cell sites are required to provide the coverage needed for a wireless network. The propagation model also helps to determine where cell sites should be located to achieve an optimal position in the network. If the propagation model used is not effective in providing a realistic path loss estimate, the probability of incorrectly deploying a cell site is high. The performance of the wireless network is affected by the propagation model chosen because the model is used for interference prediction. Based on traffic loading conditions, designing for high SNR could negatively affect financial feasibility. On the other hand, designing for a low SNR would degrade the quality of service.

Several empirical propagation models based on limited experimental data have been used. No propagation model accounts for all variations experienced in practice, hence the limitations of these models must be known, in order to achieve a good RF engineering design of a wireless network. Also, calibrating the empirical models against an analytical model and/or actual propagation environment is helpful in gaining confidence in these models. Therefore, a two-dimensional ray-tracing simulator has been developed to compute the trajectories between arbitrary locations of transmitter and receiver, and to provide results in terms of both path loss and time delay of each trajectory. The simulator applies to an arbitrary terrain profile obtained by a cut with a vertical plane passing through transmitter and receiver. The result is a polygonal line, each segment of which is characterized by an appropriate value of surface impedance. The simulator computes the trajectories according to the UTD, neglecting only most backscattered rays. Because of the use of second-order diffraction coefficients, the simulator is applicable to all vertical locations of transmitter and receiver.

We use several well-known empirical models for an urban environment (i.e., Hata-Okumura, Walfisch-Ikegami, Lee, Parson, ITU) and compare the results against the analytical results obtained from our two-dimensional ray-tracing approach. The comparison is carried out by examining the diagrams of path-loss vs. distance and/or time delay.

ELECTROMAGNETIC PULSE WAVE PROPAGATION OVER LAND-SEA MIXED-PATH

T. Ishihara* and R. Yoshioka
Department of Electrical Engineering
National Defense Academy
Hashirimizu, Yokosuka, 239, Japan

Ground wave propagation in urban area has shown an unexpected attenuation in some parts of the propagation path and an anomalous variation pattern of the electromagnetic field with distance [J. H. Causebrook, Proc. IEE, Vol.125, No.9, pp. 804-808(1978)]. It has been shown theoretically that, in contrast to the homogenous earth's surface, the electromagnetic field over a highly inductive inhomogeneous earth's case behaves in a peculiar manner due to interference between the conventional Norton ground wave and the trapped surface wave [D. A. Hill and J. R. Wait, Radio Science, Vol. 15, No.3, pp. 637-643(1980)]. Also, the ground wave propagation is strongly influenced when the surface impedance along the propagation path changes abruptly as it occurs when the radio wave traverses a coastline from land to sea or vice versa [James R. Wait, IEEE Antennas and Propagation Magazine, Vol. 40, No. 5, pp.7-24(1998), Levent Sevgi and Leopold B. Felsen, Int. J. Numer. Model., Vol. 11, pp. 87-103(1998)]. Ground wave propagation will continue to be one of the most important means for a long distance communication.

Recently, we have derived the field representation for the ground wave propagation along the inhomogeneous impedance surface with the surface duct appeared over the mixed-path [T. Ishihara and Y. Mukai, ISAP'96, CHIBA, JAPAN, pp. 297-300(1996)]. We have also derived a uniform time-domain solution for the scattered electromagnetic field when the electromagnetic wave radiated from the vector point source is incident on the plane dielectric boundary [T. Ishihara and Y. Miyagawa, Trans. of IEICE, Vol. J82-C-I, No.2, pp.62-73(1999), T. Ishihara and Y. Miyagawa, Proc. of USNC/URSI Radio Science Meeting, Orlando, Florida, p.16,1999]. In this research, we shall derive the asymptotic solution for the ground wave propagation in time-domain from the previously obtained frequency-domain solution by applying the saddle point technique. Comparison of our results with the reference solutions calculated numerically by applying the First Fourier Transform confirms the validity and utility of the proposed time-domain asymptotic solution.

Gaussian beam tracking through a curved interface: comparison with the Method of Moments

D. Lugara*, A. Boag†, C. Letrou

I.N.T., 9 rue Charles Fourier, 91011 Evry Cedex, France
Observatoire de Paris, DEMIRM, 61 avenue de l'Observatoire, 75014 Paris, France

† Dept. of Physical Electronics, Tel Aviv University, 69978 Tel Aviv, Israel

When transparent structures such as lens antennas or radomes are electrically large yet not in the far field of the source, their analysis by classical methods such as Physical Optics, Uniform Theory of Diffraction, Method of Moments, or Finite Elements method may be either inaccurate or numerically untractable. While hybridization of these techniques is an active field of research, an alternative approach, referred as discrete phase space methods, has also been proposed to address this problem (e.g., P. D. Einziger et al., *JOSA A*, **3**, 508-522, 1986). The key feature of this approach is that it employs field representation comprising discrete superpositions of a moderate number of shifted and tilted elementary Gaussian beams, which can easily be tracked in a complex environment.

However, the so-called Gabor representation, which has been used to discretize source fields, is numerically unstable. In recent contributions, we have shown that the use of a Gabor frame based representation provides a stable and efficient decomposition of source fields (D. Lugara and C. Letrou. *Electron. Lett.*, **34**, (24), 2286-2287, 1998) and that it leads to correct results when combined with asymptotic beam field expressions to calculate the fields transmitted through the curved interface of a large substrate lens type configuration.

The objective of the present work is to address the range of applicability of the closed form asymptotic expressions used to represent the fields resulting from the transmission of an elementary Gaussian beam through a curved dielectric interface. The validity of those expressions is studied by comparison with a numerically rigorous solution, namely, the Moment Method applied on the curved boundary. The configuration under study is analog to the one encountered in substrate lens antenna modeling but, for the sake of simplicity, we limit the presentation to 2D configurations. In this work, we evaluate the accuracy of the asymptotic expressions versus various critical parameters such as the angle of incidence, the radius of curvature of the interface, and the Gaussian beam width, relative to the wavelength. Previous works (e.g., Y. Ruan and L.B. Felsen, *JOSA A*, **3**, 566-579, 1986) have studied the influence of various degrees of paraxial approximations on the results obtained for transmitted or reflected fields, in a given configuration (convex interface, radius of curvature much larger than the wavelength, fixed angle of incidence). We compare our conclusions with theirs as much as possible.

A Fast Physical Optics (FPO) Algorithm for High Frequency Scattering

Amir Boag

Department of Electrical Engineering –Physical Electronics
Tel Aviv University, Tel Aviv 69978, Israel

Conventionally, the high frequency scattering by arbitrary shaped bodies is analyzed using the Physical Optics (PO) approximation augmented by the Physical Theory of Diffraction (PTD) and probably additional correction terms. For electrically large scatterers, the computation time is dominated by the PO integration time.

In this paper, we address the issue of numerically efficient evaluation of the pertinent PO integral. The number of field sampling points N on the scatterer surface is proportional to its illuminated area (normalized to the wavelength squared). In order to sufficiently resolve the two-dimensional structure of the scattering pattern, the latter should be evaluated over a sphere at a number of points, also, proportional to the scatterer area (dimensions squared). Of course, the proportionality factors depend on the acceptable error level and the specific quadrature rule used, as well as, on the desired level of oversampling of the scattering pattern. Thus, the computational cost of the straight-forward PO integration for $O(N)$ far-field directions each using $O(N)$ field samples amounts to $O(N^2)$ operations. On the other hand, the conventional Fast Fourier Transform (FFT) far field evaluation for planar apertures achieves an $O(N \log^2 N)$ computational complexity. Here, we propose a novel domain decomposition algorithm aimed at achieving a high computational efficiency similar to the FFT. The proposed approach is closely related to the Fast Far-Field Approximation introduced in the context of the MoM analysis of scattering problems (C.-C. Lu and W. C. Chew, *Microwave Opt. Technol. Lett.*, vol. 8, no. 5, April 5 1995, pp. 238-241). The algorithm is based on the observation that the fields on the scatterer surface serving as the equivalent sources of radiation are sufficiently smooth and we can safely assume that no “super-gain” distributions are present. Under these conditions, the scattering pattern can be “fully described” by its samples at a number of points proportional to the area of the surface domain comprising the equivalent sources. By “fully described” we mean that the pattern at an arbitrary point can be evaluated (with a prescribed error) by interpolation from the samples. With this in mind, we decompose the scatterer surface into smaller subdomains and compute the corresponding scattering patterns and, later, aggregate these patterns into the final pattern of the scatterer as a whole. The scattering patterns of the subdomains are evaluated at a smaller number of points, thus providing the computational savings. The aggregation step involves computational inexpensive phase correction, interpolation and addition. The single-level decomposition reduces the computational cost from $O(N^2)$ to $O(N^{3/2})$. The multilevel algorithm is formed by starting with small subdomains and repeating the aggregation step, while gradually increasing subdomain sizes. The multilevel algorithm attains the $O(N \log^2 N)$ asymptotic complexity and, interestingly, its overall structure resembles that of the FFT.

TWO-MIRROR OPEN RESONATORS WITH SPHERICAL MIRRORS MADE FROM LIMITED CONDUCTIVITY MATERIALS

Afonin D.G.* , Kravchenko V.F.**

*119899, Vorob'evy Gory, Moscow State University, Physics Faculty, Russia
(phone: (095)939-2094, e-mail: afonin@radi1.phys.msu.su)

**103907, Mokhovaya Street 11, Institute of Radio Engineering and
Electronics, Russian Academy of Sciences, Moscow, Russia
(phone: (095)921-48-37, e-mail: kvf@mx.rphys.mipt.ru)

Development of new devices for millimeter and submillimeter-wave band requires researchments for electrodynamic systems. The most perspective are opened resonator (OR) systems.

In this work with the help of the methods mentioned before (V.F.Kravchenko, A.B.Kazarov. *Radiotekhnika*, N9, p.21-27, 1997) new equations were received and electrodynamic characteristics were accounted - spectrum, Q-factor for two-mirror OR with confocal spherical mirrors from the materials with limited conductivity. Special attention was paid to resonators with superconductor mirrors while analyzing received results.

The accounts, which were made, showed that in millimeter - wave band Q-factor of these resonators for superconductivity one-layer mirrors decreases with the wavelength decreasing (for high temperature materials in the interval: $2 \cdot 10^5 \div 3 \cdot 10^4$, for low-temperature Nb - $10^7 \div 10^6$), and for the normal conductivity material mirrors (Cu) - increases (in the interval $(4 \div 8) \cdot 10^5$). In submillimeter-wave band this way of Q-factor changing maintains with decreasing of the wavelength.

When using OR with multylayers mirrors the dependence of Q-factor on wavelength gets oscillation character. The value of Q-factor can change more then in degree.

Using an automatic device in millimeter-wave band (D.G.Afonin, A.É.Malyshkin, *Pribori i tekhnika eksperimenta*, N3, p.81-85, 1999) experiments for OR with spherical confocal mirrors were made. Good coincidence of the theory and experiments of resonance frequencies was received; experimental values of Q-factor differed in some cases from theory more then in two degrees. It can be explained because the theory didn't take into account connection losses and oscillation types degeneration.

The results for concentric OR with spherical mirrors were also achieved.

Electromagnetic Theory

Co-chairs: R. Janaswamy, Naval Postgraduate School
B. Gilbert, Mayo Foundation **Page**

- 1 12:00 Ideal boundary conditions in electromagnetics, *I. Lindell**, Helsinki University of Technology, Finland 58
- 2 12:00 Anomalous behavior of the solution to the problem of plane wave scattering from a cylinder at grazing incidence, *R. Mittra**, *D. Werner*, *Y. Yang*, The Pennsylvania State University, USA 59
- 3 12:00 Propagation of line source fields over a non-constant admittance plane, *R. Janaswamy**, Naval Postgraduate School, USA 60
- 4 12:00 A class of surface boundary conditions for complex structures, *R. Cicchetti**, University of Rome "La Sapienza", Italy, *A. Faraone*, Motorola Florida Research Labs, USA 61
- 5 12:00 Equivalent current field generation null spaces, *M. Morgan**, *D. Steenman*, Naval Postgraduate School, USA 62
- 6 12:00 Complex dielectric constant measurements and model comparison of lossy dielectric materials, *S. Lee**, *Y. Kuga*, University of Washington, *E. Savrun*, Sienna Technologies, Inc., USA 63
- 7 12:00 Quasi-static permittivity of a lattice of complex-shaped 3-D particles, *K. Whites**, *F. Wu*, University of Kentucky, USA 64
- 8 12:00 Mode orthogonality in pseudochiral planar waveguides, *A. Topa**, *C. Paiva*, *A. Barbosa*, Technical University of Lisbon, Portugal 65
- 9 12:00 Integral operator method for determining the impedance of isolated and coupled stripline structures, *D. Infante**, *D. Nyquist*, Michigan State University, USA 66
- 10 12:00 Resonant mode suppression for Helmholtz boundary value problems, *G-T. Lei**, *R. Techentin*, *B. Gilbert*, Mayo Foundation, USA AP
- 11 12:00 Time domain electromagnetic fields due to a vertical electric dipole in front of two layer planar dielectric media, *G. Rafi**, Zanjan University, *R. Moini*, Amirkabir University of Technology, *R. Dana*, University of Tehran, Iran 67
- 12 12:00 Green's function for EM field in a parallel-plate environment with imperfectly conducting walls using a Hertzian-potential impedance boundary condition, *M. Havrilla**, *D. Nyquist*, Michigan State University, USA 68

Ideal Boundary Conditions in Electromagnetics

I.V. Lindell,

Electromagnetics Lab., Helsinki University of Technology
PO Box 3000, FIN-02015HUT, Espoo, Finland

The concept of 'boundary' in electromagnetic theory relates to a surface which does not let electromagnetic fields pass through it. Mathematically, the fields are related by boundary conditions at the surface. In contrast, the interface of two media is defined by conditions of continuity or discontinuity of the fields at the surface. Boundary is normally an approximation to the interface giving mathematical convenience and can be applied under certain restrictions.

Assuming time-harmonic fields with time dependence $e^{j\omega t}$, the concept of 'ideal boundary' is defined so that the complex Poynting vector $\mathbf{S} = \frac{1}{2}\mathbf{E} \times \mathbf{H}^*$ has no component normal to the surface of the boundary for any possible fields. This definition is tighter than that of the 'lossless boundary', in which case the real part of the Poynting vector has no component normal to the boundary. The two basic ideal boundary conditions most often encountered in electromagnetics are the perfect electric and magnetic conductor (PEC and PMC) conditions defined by $\mathbf{n} \times \mathbf{E} = 0$ (PEC) and $\mathbf{n} \times \mathbf{H} = 0$ (PMC). Obviously, in both of these cases we have $\mathbf{n} \cdot \mathbf{E} \times \mathbf{H}^* = 0$, whence the complex Poynting vector has no normal component. Yet another type of ideal boundary is the so-called soft-and-hard (SHS) boundary (P.S. Kildal, *IEEE Trans. Ant. Prop.*, **38**(10), 1537-1544, 1990) defined by the conditions $\mathbf{v} \cdot \mathbf{E} = 0$, $\mathbf{v} \cdot \mathbf{H} = 0$, where \mathbf{v} is a real unit vector tangential to the surface S , i.e., satisfying $\mathbf{n} \cdot \mathbf{v} = 0$.

It is of interest to see whether there are more general ideal boundary conditions. In fact, it can be shown that there exists a generalization to the ideal SHS conditions as $\mathbf{a} \cdot \mathbf{E} = 0$, $\mathbf{a}^* \cdot \mathbf{H} = 0$, where \mathbf{a} is a complex vector satisfying $\mathbf{n} \cdot \mathbf{a} = 0$. Such a surface will be called the generalized soft-and-hard surface (GSHS). Basic properties for a plane wave reflecting from a GSHS plane are derived. It is shown that TE and TM components (with respect to the complex vector \mathbf{a} and its complex conjugate \mathbf{a}^* , respectively), of a plane wave are reflected from a GSHS plane as from respective PMC or PEC planes. Image theory for the GSHS plane is suggested with an example. Finally, possible realization of a GSHS plane and its application in polarization transformation are briefly discussed.

Anomalous Behavior of the Solution to the Problem of Plane Wave Scattering from a Cylinder at Grazing Incidence

R. Mittra*, D. H. Werner, and Yi Yang
Electromagnetic Communication Laboratory
Department of Electrical Engineering
The Pennsylvania State University, University Park, PA 16802, USA
Email: rxm53@psu.edu or dhw@psu.edu

The problem of plane wave scattering from a cylinder at oblique incidence is a classical one and its solution can be found in any number of standard textbooks, e.g., (R. F. Harrington, *Time-Harmonic Electromagnetic Fields*, 1961) and (C. A. Balanis, *Advanced Engineering Electromagnetics*, 1989). A close examination of this solution reveals that the series representation for the induced current on the cylinder, given below, becomes singular as the incident angle approaches grazing (i.e., $\theta \rightarrow \theta'$).

$$J_z = H_\phi^{total} \Big|_{\rho=a} = \frac{2E_o}{\pi a \omega \mu \sin \theta_i} e^{j\beta z \cos \theta_i} \sum_{n=-\infty}^{\infty} j^{-n} \left[\frac{e^{jn\phi}}{H_n^{(2)}(\beta a \sin \theta_i)} \right] \quad (1)$$

This result, predicted by the analytical formula in (1), must be non-physical and, therefore, incorrect. This poses a dilemma and prompts one to raise the question: What causes the analytical solution for this canonical problem to break down near grazing incidence?

The purpose of this paper is to examine this question carefully, to provide an explanation for this curious phenomenon, which, to the best of our knowledge has not been observed before, or been reported in the literature.

The paper then goes on to discuss an approach to constructing the solution for the limiting case of grazing incidence, one that not only yields a result that is free of singularity, but also the correct solution for this case.

Propagation of Line Source Fields Over a Non-Constant Admittance Plane

R. Janaswamy
Code EC/Js, Department of Electrical & Computer Engineering
Naval Postgraduate School, Monterey, CA 9394
Email: janaswam@ece.nps.navy.mil,

The problem of electromagnetic wave propagation over a constant impedance plane has been investigated by several researchers in the past (see for example, R. J. King, *Radio Science*, 4 (3), 255-268, 1969). The study is relevant to the propagation of radio waves over the surface of the earth. In the study of electromagnetic propagation over a random rough surface such a sea, it is a common practice to replace the rough surface with a constant impedance plane provided that the r.m.s. roughness height is less than some fraction of the radio wavelength (F. G. Bass and I. M. Fuks, *Wave Scattering from Statistically Rough Surfaces*, New York: Pergamon Press, 1979). When the roughness heights are large, it is still possible to extract an equivalent impedance for the rough surface as far as the specular component is concerned, particularly for low grazing angles (R. Janaswamy, *URSI Meeting*, paper F3-5, Boulder, CO, January 4-8, 2000). However, the impedance varies with the grazing angle of the wave and a single impedance value to represent the rough surface is no longer possible.

In the present work we study the problem of electromagnetic wave propagation of line source fields over a non-constant admittance plane. Due to the non-constant admittance of the plane, it is no longer possible to specify an impedance type boundary condition that relates the field to its normal derivative. Instead the nature of the plane is specified in terms of the specular reflection coefficient for plane waves impinging on it. Expressions are provided for the near and far-fields. A spectral decomposition of the fields is done to permit a direct use of the reflection coefficient.

A Class of Surface Boundary Conditions for Complex Structures

Renato Cicchetti* and Antonio Faraone²

Dept. of Electronic Engineering, University of Rome "La Sapienza", Italy

²Motorola Florida Research Labs, Fort Lauderdale, Florida, USA

Introduction

Surface boundary conditions exhibit extremely advantageous features in the solution of many electromagnetic problems. Standard and Tensor Impedance Boundary Conditions (S/TIBC's) are employed to model thin-coated objects, when the coating exhibits high refraction index or ohmic losses. Higher-Order Impedance/Admittance BC's (HOI/ABC's) were introduced to describe the non-local nature of surface boundary conditions. Recently, we have derived exact and higher-order boundary conditions to model complex-geometry objects. These conditions allow accurate analysis of curved objects, which may exhibit discontinuities at the boundary and may support surface-waves. In this communication, we demonstrate the application of these conditions to model efficiently complex guiding and radiating structures.

Methodology

The exact surface boundary condition are expressed by a dyadic integral operator that links the tangential electric and magnetic fields

$$\hat{n} \times E_t(r) = \oint_S \mathbf{Z}(r/r') \cdot H_t(r') dS' \quad (1)$$

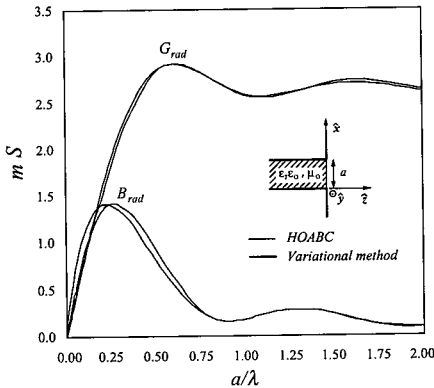


Fig. 1 Radiation admittance of a parallel-plate guide radiating into free-space.

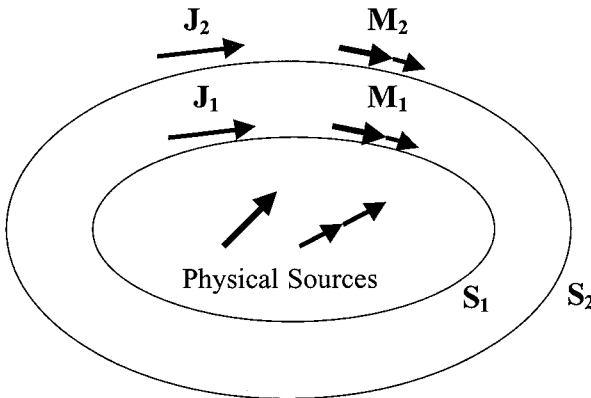
where the dyadic surface impedance $\mathbf{Z}(r/r')$ depends upon the dielectric characteristics and the geometry of the medium enclosed in the boundary surface S . Evidently, (1) describes the global dependence of the condition in r . Quasi-local approximations of (1) yielding HOIBC's are derived by means of suitable asymptotic techniques to allow efficient solutions of complex electromagnetic problems. In Fig. 1 we present the behavior of the radiation admittance vs. electrical aperture dimension for a parallel plate waveguide loaded with a dielectric material having $\epsilon_r = 10$, which was obtained by means of a HOABC that includes diffraction effects due to the sharp edges. The agreement with the variational solution (N. Marcuvitz, *Waveguide Handbook*, McGraw-Hill, 1951) is excellent.

Equivalent Current Field Generation Null Spaces

Michael A. Morgan and Daryl G. Steenman
Electrical and Computer Engineering Department
Naval Postgraduate School
833 Dyer Road, Room 437, Monterey, CA 93943

Tangential fields used to form equivalent currents \mathbf{J} and \mathbf{M} on, say S_2 in the figure below can be generated by near-field integration of the physical sources or by integration of enclosed equivalent sources, such as those on S_1 . This Green's function integration from inner surface \mathbf{J}_1 and \mathbf{M}_1 to obtain the outer surface \mathbf{J}_2 and \mathbf{M}_2 forms a numerical transfer function operator.

The inversion of this operator was investigated as a means to back-propagate measured fields toward the source between surfaces having electrically small separations. The objective was to obtain a high resolution mapping of the physical source distribution by employing a very close conformal inner surface. The inversion process was expected to be somewhat ill-conditioned, but manageable by use of spatial filtering and SVD processing. Trial inversions indicated extreme ill-conditioning, irrespective of the surface separations. A simple proof is presented using the Equivalence Theorem to demonstrate exact null space properties resulting from equivalent current based field generation.



COMPLEX DIELECTRIC CONSTANT MEASUREMENTS AND MODEL COMPARISON OF LOSSY DIELECTRIC MATERIALS

Sangil Lee* and Yasuo Kuga
Department of Electrical Engineering
University of Washington
Seattle, WA 98195-2500

Ender Savrun
Sienna Technologies, Inc.,
19501 144th Avenue NE, Suite F-500
Woodinville, WA 98072

It is known that lossy dielectric materials can be designed by adding conducting particles into a host dielectric material. Conductor-loaded lossy dielectric materials have been used for microwave applications including microwave absorbing materials and EMI shields. In recent years, several models have been proposed to describe the complex dielectric constant of conductor-loaded materials. In this paper, we present the complex dielectric constant measurements of lossy dielectric materials. Based on the measurements, the models for the complex dielectric constant of lossy dielectric materials are compared and their limitations are discussed.

The complex dielectric constants are measured using the transmission/reflection method and genetic algorithms as an inversion process at X-band. Both transmission and reflection methods can be used to estimate the complex dielectric constant. However, for lossy dielectric materials, the transmission methods may yield better results such as low sensitivity due to the measurement errors. Based on our measurements, several models are compared. One model is a logarithmic law used by Neelakanta (*IEEE Trans. On MTT*, 43, (6), 1381-1389, 1995) and the other is an extension of the Maxwell Garnet mixing formula or Lorentz-Lorentz equation applied by Doyle and Jacobs (*J. Appl. Phys.* 78, (10), 6165-6169, 1995). Recently, Matsumoto and Miyata suggested (*IEEE Trans. On Dielectrics and Electrical Insulation*, 6, (1), 27-34, 1999) a new model based on a equivalent circuit model. Even though some of models may show partial success to obtain the real part, they fail in obtaining reasonable values for the imaginary part. We will show the applicability of different mixing formulas for the estimation of the complex dielectric constant of lossy dielectric materials.

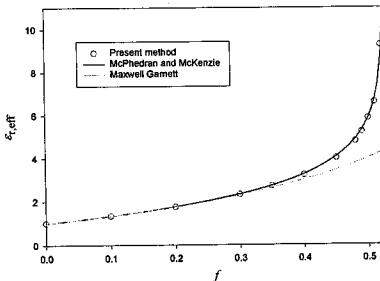
Quasi-Static Permittivity of a Lattice of Complex-Shaped 3-D Particles

Keith W. Whites* and Feng Wu
Department of Electrical Engineering
University of Kentucky
453 Anderson Hall
Lexington, KY 40506-0046
(whites@enr.uky.edu)

Computing the effective permittivity ϵ_{eff} for a lattice of particles (and other similar material parameters) has application in a number of industries including remote sensing, nondestructive test/evaluation and non-reflective coatings, among others. This problem is a challenging one. Lord Rayleigh was the first to present analysis for lattices of separably-shaped objects (round and elliptic cylinders, spheres and ellipsoids) that included some effects of interaction between the particles, though a complete solution was not obtained (*Phil. Mag.*, vol. 34, pp. 481-502, 1892 and *Ibid.*, vol. 44, pp. 28-57, 1897).

More recently, accurate numerical solutions for ϵ_{eff} have been obtained for certain separably-shaped objects. McPhedran, McKenzie, et al. presented numerical solutions and some measured results for ϵ_{eff} of two-phase cubic lattices of spheres (*Proc. R. Soc. Lond.*, vol. A. 359, pp. 45-63, 1978 and *Ibid.*, vol. A. 362, pp. 211-232, 1978). Additionally, we have recently completed the accurate computation of ϵ_{eff} for lattices of multiphase round cylinders and spheres (*IEEE APS Inter. Symp. Dig.*, Orlando, FL, pp. 1934-1937, 1999 and *URSI National Radio Sci. Meet. Dig.*, Orlando, FL, p. 246, 1999).

Our research is ongoing in this area. In this paper, we will present a technique for computing the quasi-static permittivity for a lattice of complex-shaped particles including the effects of mutual interaction. That is, essentially arbitrarily shaped particles that may not be of separable shape (for example, cubes). This technique employs the moment method to obtain an integral equation solution for the dipole



moment of the dielectric or conducting particles. The results shown in this figure are $\epsilon_{r,\text{eff}}$ versus volume fraction f of conducting spheres in a 3-D simple cubic lattice. This comparison serves as a strong validation of our integral equation solution even for large f where the separation between particles is extremely small and the mutual coupling is large.

Mode Orthogonality in Pseudochiral Planar Waveguides

António L. Topa*, Carlos R. Paiva, and Afonso M. Barbosa
*Departamento de Engenharia Electrotécnica e de Computadores
and Instituto de Telecomunicações,*

Instituto Superior Técnico, Technical University of Lisbon, PORTUGAL

In this paper we derive orthogonality relations for the modes supported by general inhomogeneous pseudochiral planar waveguides. These wave-guiding structures consist of a multi-layered planar waveguide involving one or more omega media layers (N. Engheta and M. M. I. Saadoun, *Proc. PIERS'91*, 339, 1991). Orthogonality relations are essential to expand arbitrary electric and magnetic fields in terms of a complete set of mutually orthogonal modes. As in our previous work (A. L. Topa, C. R. Paiva, and A. M. Barbosa, *Progress in Electromagnetics Research*, 18, EMW Publishing, Cambridge, MA, Chapter 5, 85-104, 1998) the linear-operator formalism is used, by means of which the problem of guided electromagnetic wave propagation is reduced to an eigenvalue equation related to a 2×2 matrix differential operator. This formalism, which is applicable to multi-layered pseudochiral planar waveguides, reduces to an algebraic 2×2 coupling matrix eigenvalue problem when considering homogeneous layers.

In this paper, a different orientation for the omega particles is considered. In fact, instead of being in the horizontal plane, the omega particles locate in the transverse plane. A system with four coupled differential equations leads to six-component hybrid modes. However, after a suitable choice of a state vector Φ in the EH representation, the problem of electromagnetic wave propagation is reduced to the following rank-two eigenvalue problem:

$$\overline{\mathcal{L}} \cdot \Phi = \beta^2 \overline{\mathcal{W}} \cdot \Phi, \quad (1)$$

where $\overline{\mathcal{L}}$ is a linear differential operator and $\overline{\mathcal{W}}$ is the weight operator. Here, $\beta = k / k_0$ is the normalized propagation constant, with k being the longitudinal wavenumber. The electromagnetic problem herein obtained is the dual problem of the one presented before. This fact is useful in the characterization of the adjoint problem, and simple orthogonality relations can be derived.

Integral Operator Method for Determining the Impedance of Isolated and Coupled Stripline Structures

David J. Infante* and Dennis P. Nyquist
 Department of Electrical and Computer Engineering
 Michigan State University
 East Lansing, MI 48824

A full-wave, integral operator method for determining the complete propagation-mode spectrum of an isolated stripline structure has previously been presented by the authors.

This involved developing a Hertzian potential Green's function for a generalized impressed current source suspended in the space between two infinitely wide, perfectly-conducting ground planes. This Green's function was then specialized to a stripline structure by enforcing boundary conditions for tangential fields at the perfectly conducting surface of the center conductor. This resulted in an electric field integral equation (EFIE) for currents on the stripline. Guided mode solutions for this EFIE were determined by Fourier transforming on the axial variable, and examining the resulting EFIE

$$\hat{t} \cdot (k^2 + \tilde{\nabla} \tilde{\nabla} \cdot) \int_{-a}^a \tilde{g}_\zeta(\bar{\rho} | \bar{\rho}') \cdot \bar{k}_p(x') dx' = 0.$$

Here \hat{t} is a unit tangent vector, $\tilde{\nabla}$ is the transform domain gradient operator, \tilde{g}_ζ is the transform domain Green's function, \bar{k}_p is the transform domain current, and the center conductor is defined to extend from $-a$ to a . This EFIE for discrete stripline modes has non-trivial solutions that exist only for $\zeta = \zeta_p$, and was converted to matrix form and solved numerically via a Galerkin's method using Cheybechev basis functions. This technique was later extended by the authors to the case of a stripline structure having a pair of coupled center strips.

Because most stripline devices are operated in such way that only the fundamental TEM mode is excited, a TEM specialization of the stripline full-wave theory is developed for both isolated and coupled stripline structures. This is accomplished by recognizing that for the TEM mode $\zeta = k_0$, and only axial currents exist. These assumptions result in a simplified fundamental EFIE for isolated stripline

$$\lim_{y \rightarrow 0} \int_{-a}^a k_z(x') \tilde{g}_\zeta'(x, y | x', 0) dx' = C$$

where C is a constant which is proportional to the potential difference that exists between the center conductor and ground planes. This is again extended for the case of coupled stripline. A Galerkin's method numerical solution results in a forced matrix equation, yielding the current distribution associated with the TEM mode. For the case of an isolated stripline this current distribution is used to determine a unique characteristic impedance. For the case of coupled stripline an impedance matrix results.

Time Domain Electromagnetic Fields Due to a Vertical Electric Dipole in Front of two-Layer Planar Dielectric Media

Gh. Z. Rafi*, R. Moini**, R. Faraji Dana***

* Zanzan University

Email: r7323939@cic.aku.ac.ir

** Amirkabir University of Technology

*** University of Tehran

Abstract: The time domain response of a dipole antenna in the presence of stratified media has been subject of continuing interest. Most of the past contributions dealt with the case of a dipole with two dielectric half-space [1-2], and the fields were calculated in some special cases.

In this paper we use a new approach to determine the time domain response of a impulsive vertical electric dipole over two-layer dielectric media. For the same geometry Ezzeddine et. al. derived an analytical solution for early-time response by using asymptotic techniques and Fourier transformation [3]. Time domain solution of this problem can be used in different areas of electromagnetics, such as wave propagation, printed antennas, wave scattering, electromagnetic effects of lightning, etc.

Our mathematical formulation of the problem is developed for the magnetic vector potential in time domain, whose solution is derived in a new approach using two dimensional spatial Fourier transforms. The main emphasis here is to derive new expressions for the vector potential and reflected and transmitted electromagnetic fields. In particular, an efficient numerical method is given for computing transient transmitted electromagnetic fields for vertical electric dipole.

References:

- [1] K. Nikoskenin, I. Lindell, "Time Domain Analysis of Sommerfeld VMD Problem with Exact Image Theory," *IEEE Trans. Antenna Propagat.* Vol. Ap-39, pp. 241- 250, Feb. 1990.
- [2] Gh. Z. Rafi, , "A Novel Transient Analysis of Vertical Magnetic Dipole Radiation in the Vicinity of a Planar Dielectric Interface", *In Proc. ICEAA 99*, Torino, Sept. 1999
- [3] A. Ezzeddine, J. A. Kong, and L. Tsang, "Transient Fields of a Vertical Electric Dipole Over a Two-layer Nondispersive Dielectric", *J. Appl. Phys.* vol. 52, pp. 1202- 1208, March 1981

Green's Function for EM Field in a Parallel-Plate Environment with Imperfectly Conducting Walls using a Hertzian-Potential Impedance Boundary Condition

Mike Havrilla* and Dennis Nyquist

Department of Electrical Engineering
Michigan State University
East Lansing, MI 48824

Transmission line structures having metallic boundaries can exhibit significant losses at high operational frequencies if the conductors are imperfect. A common example is the strip transmission line in a parallel-plate environment. Since this structure has an excitatory current located between parallel plates having finite conductivity, it is necessary to determine the Green's function for this geometry if wall loss is to be accounted for. Thus, the purpose of this paper is to develop the Green's function for a general three-dimensional current immersed between two parallel plates that are imperfectly conducting.

The above Green's function can be identified by investigating the solution of the Hertzian potential Helmholtz equation $\nabla^2 \vec{\pi} + k^2 \vec{\pi} = -\vec{J} / j\omega\epsilon$ subject to the impedance boundary condition $\vec{E}_{\text{tang}} = Z_m \hat{n} \times \vec{H}_{\text{tang}}$ at the imperfectly-conducting walls where \hat{n} is the unit normal pointing out of the conductor and $Z_m = (1 + j)\sqrt{\omega\mu_0 / 2\sigma}$ is the surface impedance of the metal (i.e., conducting) plates. Using $\vec{E} = k^2 \vec{\pi} + \nabla(\nabla \cdot \vec{\pi})$ and $\vec{H} = \nabla \times \vec{\pi} / j\omega\epsilon$, it will be shown that the impedance boundary condition in terms of Hertzian potentials can be written as

$$\pi_x = \pm \frac{1}{\sigma Z_m} \frac{\partial \pi_x}{\partial y}, \quad \pi_z = \pm \frac{1}{\sigma Z_m} \frac{\partial \pi_z}{\partial y}, \quad \frac{\partial \pi_y}{\partial y} = \pm j\omega\epsilon Z_m \pi_y - \frac{\partial \pi_x}{\partial x} - \frac{\partial \pi_z}{\partial z}$$

where π_x and π_z are components tangential to the imperfectly conducting plates, π_y is the normal component and the \pm sign is used for $\hat{n} = \pm \hat{y}$. Enforcement of these boundary conditions will result in a solution for $\vec{\pi}$ in terms of a Hertzian potential dyadic Green's function, that is

$$\vec{\pi}(\vec{r}) = \int_V \vec{G}(\vec{r}, \vec{r}') \cdot \frac{\vec{J}(\vec{r}')}{j\omega\epsilon} dV'$$

The dyadic Green's function for the electric and magnetic fields can then be determined through careful application of the above expressions for \vec{E} and \vec{H} . One can also find the Green's function by treating the problem as a symmetric slab waveguide and examining the solution as the outer slab regions become good conductors.

The Hertzian-potential impedance boundary conditions at the surface of an imperfect conductor will be determined and the Hertzian-potential and electric-field dyadic Green's function for the parallel-plate waveguide will be developed. In addition, a perturbational analysis will be performed in order to determine how the conductor losses influence the ideal propagation constant (i.e., the propagation constant when the plates are perfectly conducting).

RF/Microwave Interactions with Biological Media

Chair: M. Wagner, Agilent Technologies

			Page
1	12:00	A study on shielding effects on field distributions in human model tilted 45° exposed to handset, <i>W. Dou, National University of Singapore, Singapore</i>	70
2	12:00	A study of near field shielding effect measurement for elliptical human phantom model using the resistive sheet, <i>S. Nishizawa*, I. Wu, O. Hashimoto, Aoyama Gakuin University, Japan</i>	71
3	12:00	A planar antenna for multifrequency microwave radiometry, <i>A. Vagnoni, DISP, Universita' di Roma Tor Vergata, P. Tognolatti, DIE, Universita' dell'Aquila, F. Bardati*, Universita' di Roma Tor Vergata, Italy</i>	72
4	12:00	Microwave imaging of radially inhomogeneous cylindrical bodies, <i>M. Akhtar*, A. Omar, University of Magdeburg, Germany</i>	AP
5	12:00	Modelling of real neurals vibrations frequency spectrum transformation in the process of interaction with electromagnetic signal, <i>V. Spitsyna*, N. Spitsyna, Tomsk State University, Russia</i>	73
6	12:00	Effects of UHF-impulsive noise on low-power telemetry systems, <i>A. Riemann*, Cetecom GmbH Essen, Germany, N. Evans, University of Ulster, UK</i>	74

A study on shielding effects on field distributions in human model tilted 45° exposed to handset

Weiping Dou

Centre for Wireless Communications, National University of Singapore

Abstract: Shielding is studied to reduce electromagnetic radiation from handsets with finite-difference time-domain (FDTD) method in this paper. It is shown that some shielding modes decreases both electric and magnetic field distributions in most parts of human model, and that absorbed energy and SARs of some parts of human model are also reduced.

Summary

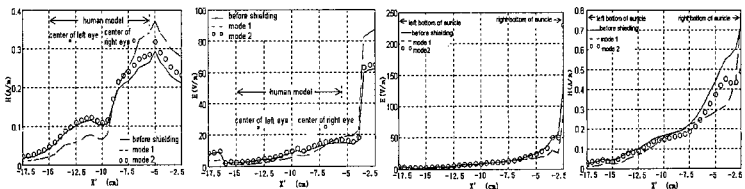
In recent years, there are numerous experiments and calculations on the interaction between human and electromagnetic wave emitted by handsets. Many of them show that a lot of radiated energy of handsets is absorbed by human, and even SARs at some places of human exceed limits of standard ANSI/IEEE C95.1-1992. It is reported that energy disposition in human may induce some diseases or other unhealthy effects.

For sake of safety or health, many methods have been taken to reduce electromagnetic fields in human body, such as new antenna design, lower radiation power, longer distance between handsets and human, some protection products. For protection products, some measurement results show copper is better than both iron and absorbing materials, about 3dB. The main purpose of the paper is to concern shielding effects of conductors, and perfect conductor is chosen for convenience to analyze.

Human model includes head, neck and right hand of an average man with 1.75m high. It simulates 15 different tissues and neck 3 tissues. Hand simulates 2/3 of electromagnetic parameters of muscle. A model of handset is used here, whose radiation power is 0.6W and frequency is 835 MHz. It is held by right hand. The angle is 45° and distance is 2.5cm between feeding point and the bottom of auricle.

Two shielding modes are given and field distributions at these modes are calculated and analyzed using FDTD method. Mode 1 is that shielding plane is placed closely on the nearest side of the handset's box to human model and is grounded. Mode 2 is that the shielding plane is raised up to shield the whole antenna. Figures give electric and magnetic field distributions in human model before shielding. Comparing with those, electric and magnetic fields of most parts at two shielding modes decrease, especially at the mode 1. Electric field collapses at the first 5mm distance (-3cm < X' < -2.5cm) when electromagnetic wave emitted from the handset enters into human. It shows most of electric energy is absorbed during a very short period, whenever shielding or not. However, magnetic field decreases at a slower speed. In addition, It is also shown human affects electric field distribution more than magnetic. Electric field pattern shows an irregular ellipse. It just likes rough shape of this cross-section of human model, and position is same. But magnetic field pattern does not.

After shielding, absorbed energy ratios of human model and head model descend, especially at mode 1. For example, energy absorbed by head changes from 21.2% before shielding to 13.0%. Average and peak SARs of eyes reduce at mode 1.



Centre for Wireless Communications, National University of Singapore, 20 Science Park Road, #02-34/37, TeleTech Park, Singapore Science Park II, Singapore 117674.
Tel: +658709165, Fax: 657795441, Email: douwp@cw.c.nus.edu.sg

A Study of Near Field Shielding Effect Measurement for Elliptical Human Phantom Model using the Resistive Sheet

S.NISHIZAWA* I.WU O.HASHIMOTO

Aoyama Gakuin University

6-16-1 Chitosedai, Setagaya-ku, 157-8572 Tokyo, Japan
 Tel : +81-3-5384-1111(Ex.23422) , Fax : +81-3-5384-1121
 E-Mail: s-nishi@ee.aoyama.ac.jp

With the explosively increasing of mobile communications, the human shield, which protects the human effect from the electromagnetic waves has been investigated. Most of these researches have been conducted by the numerical calculation[1][2], however, few investigation is done for the human shield measurement, and also the comparison between the calculated and measured results, for the validity of the measurement method[3]. In this study, the resistive sheet (Surface resistance: $R=0.1 \Omega/\square$) is located in front of the elliptical human phantom model and the near field shielding effect is measured for several shield lengths, which varied the gap distance between the human model and shield.

Fig.1 shows the measurement setup, and the Fig.2 shows the measured and calculated results. For the calculation method, the FDTD (Finite Difference Time Domain) method is used, which applied the equivalent approximate equation for the resistive sheet[4]. From these results, more than 30 dB of the shielding effect is observed for the small gap distances between the shield and phantom model, with the square shield length of 1.0λ . On the other hand, very little and also the negative shielding effect is observed for the square shield length of 0.25λ , because of the diffracted wave from the shield. Furthermore, due to the good agreement between the measured and calculated results, the validity of our measurement method is confirmed.

Acknowledgement

This work is supported by Grant-in-Aid for Scientific Research.

Reference

1. T.Nakamura,S.Tokumaru: IEICE Trans.,Vol.J78-B-II,No.3,pp.200-207(March 1995).
2. S.Nishizawa,O.Hashimoto: IEEE Trans. on MTT,Vol.47,No.3,pp.277-283(March 1999).
3. Y.Tarusawa,Y.Suzuki,T.Nojima: 1996 Autum Natl. Conv. Rec. IEICE Japan,B-296.
4. T.Inumaru,O.Hashimoto: IEICE Trans.,Vol.J81-B-II,No.7,pp.719-724(July 1998).

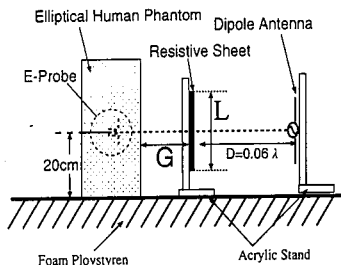


Fig.1 Measurement setup.

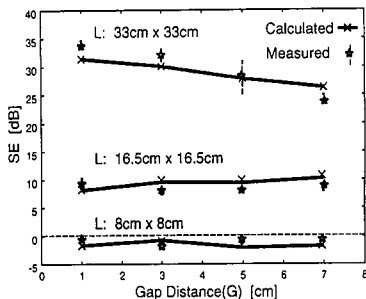


Fig.2 Measured and Calculated results.

A Planar Antenna for Multifrequency Microwave Radiometry

Andrea Vagnoni¹, Piero Tognolatti², Fernando Bardati¹
¹DISP Universita' di Roma Tor Vergata, 00133 Roma, Italy
²DIE, Universita' dell'Aquila, 67100 L'Aquila, Italy

A dual-mode dielectric-filled truncated rectangular waveguide is commonly used as receiving antenna in contacting microwave radiometry for temperature measurements in medical applications (Y. Hamamura *et al.*, *Automedica*, 8, 213-232, 1987). This antenna has several interesting features, including wide-band operation and deep sensing capability, however it is bulky, heavy and costly. Mechanical and thermal perturbations of contacted surfaces are further effects we have to face when using this kind of antennas especially in paediatric subjects, while the resort to a bolus simply reduces these drawbacks. Radiometric patch antennas have been proposed (L. Dubois *et al.*, *IEEE Trans. MTT*, 44, 1755-1760, 1996). Their thermal and mechanical impact on the body can be strongly lower than the corresponding effect for waveguide devices. Weight and cost also are lower, while conformability can be achieved by flexible substrates. However, important drawbacks of planar antennas are i) less deep-sensing capability, ii) narrow-band operation.

In this paper we propose a radiometric antenna design based on radiation from a slot in a coaxially-fed microstrip structure (Fig. 1). Similar configurations have been successfully exploited for application to radio-frequency hyperthermia (P.R. Stauffer *et al.*, *IEEE Trans. BME*, 45, 605-613). In order to predict feed-point impedance, a lumped-element circuit model has been developed by modal decomposition. The circuit is the series connection of sub-blocks, where each sub-block corresponds to a microstrip guided mode (Fig. 2). The m -th mode interaction with the lossy biological medium is modelled by an impedance, Z_m . The m -th mode propagation in the microstrip is modelled by three sections of lossless transmission lines of suitable parameters and lengths. Any change in the geometrical parameters of the structure produces a change of the equivalent circuit parameters, which can be taken easily into account. The proposed model enables the antenna to be designed by methods of circuit optimisation. Multiband operation can be easily achieved. Once the geometrical parameters have been determined, a fullwave (FDTD) analysis will provide the electromagnetic field pattern inside the sensed biological medium for radiometric weighting functions computation.

The deep sensing capability for this type of sensors can be slightly increased by interposing a thin dielectric layer between the antenna and the body. The use an array of parallel slots has been investigated. Preliminary experimental measurements will be shown.

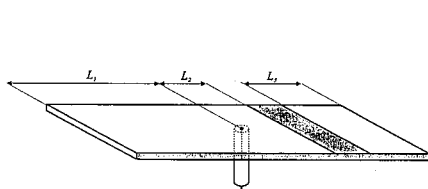


Fig. 1

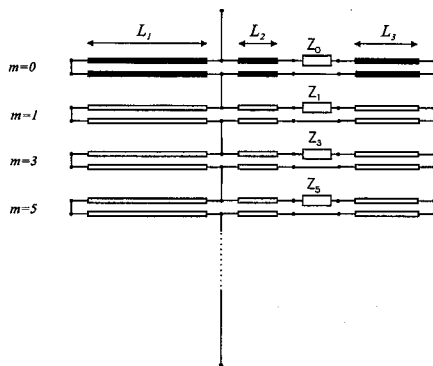


Fig. 2

**Modelling of Real Neurons Vibrations Frequency Spectrum
Transformation in the Process of Interaction
with Electromagnetic Signal**

Vladimir G. Spitsyn, Nataliya V. Spitsyna
Tomsk State University, Siberian Physical and Technical Institute,
Revolution square, 1, Tomsk, 634050, Russia,
Tel: 7-3822-412797, Fax: 7-3822-233034,
e-mail: spic@elefot.tsu.ru

In this investigation is suggested the numerical model of multiple interaction of electromagnetic signal with oscillator neural network. For solving this problem is applied the method of numerical analysis of electromagnetic signal interaction with active random media (V.G. Spitsyn, IEEE AP-S Intern. Sympos., Atlanta, USA, 1, 112-115, 1998).

We consider the propagation of signal in the three dimensional oscillator neural network with stochastic connections. Every oscillator has possibility connection with all another oscillators. Here there are investigated the process of signal interaction with point oscillators, disposed in spherical region. Every act interaction of signal with oscillator is accompanied by displacement the frequency of signal and oscillator vibrations.

In this work there are considered the isotropic indicatrix of over-radiation of oscillators. The initial frequency spectrum of oscillator vibration is defined on the base of discretization of real neural potential dependence from time (H.D.I. Abarbanel, et al, Physics-Uspeschi, 166, 363-390, 1996) and its spectral transformation. In the process of multiple interaction of signal with oscillator real neural network there are take place the transformation of frequency spectrums of signal and oscillators and in the limit its synchronization.

Effects of UHF-Impulsive Noise on Low-Power Telemetry Systems

*A.I. Riemann
Cetecom GmbH Essen
Im Teelbruch 122
45219 Essen
Germany

N.E. Evans
School of Electrical
& Mechanical Engineering,
University of Ulster
Northern Ireland, UK, BT37 0QB

Tel: +492054951943, FAX: +492054951913, e-mail: AI.Riemann@IEEE.ORG

Background

The potential of low-cost radio biotelemeters using basic modulation schemes such as PWM, PPM and FSK is limited by the effect of impulsive electrical noise mainly generated by electrical plant and radiated by equipment wiring and in-building cables. The resultant interference corrupts the weaker RF signals input to the telemetry receiver's detector stage, inducing output waveform distortion in analogue signals and bit errors in transmitted digital data streams. The telemedicine industry is already exploiting RF links in both hospital- and home-based patient monitors, but the nature of the electrical environment hosting these systems is largely unknown. This paper reports on the characteristics of the impulsive noise found in two acute hospitals, one located in Berlin, Germany and the other in Belfast, N. Ireland, in the 450 MHz band.

Measurement Procedure

The 10.7 MHz IF output of a modified ICOM IC-R7000 receiver tuned to 450 MHz was connected to a specialist logarithmic demodulator and the baseband signal was digitised with 12 bit accuracy at 750 k-samples/sec. The resultant data were streamed to a hard disk for later evaluation. The system was set up at the Martin Luther Krankenhaus in Berlin; initially the 50 Ω antenna input port was resistively terminated and 6 minutes of output data recorded to establish the system's (mainly thermal) background noise floor. Afterwards a resonant $\lambda/2$ folded dipole was connected to the receiver's input port and two consecutive 12-minute measurements were carried out, one each for vertical and horizontal polarisations.

Observations

An initial measurement campaign indicated diurnal variations in both noise pulse density and amplitude (A.I.Riemann and N.E.Evans, MEP, 21, 8, pp 569-574, 1999); the temporal changes reflected the working shifts and associated personnel activity in each hospital. An enhanced measurement procedure was therefore carried out over a 5 day period, with two measurement sessions completed per day, one at a likely noisy time (12 noon) and the other at a potentially quiet time (midnight). APD plots indicated that for levels above -85 dBm horizontally polarised noise was dominant, contrary to the popular belief that man-made noise is predominantly vertically polarised. The presentation will expand on statistical analyses performed on the measurement data.

Microstrip Antenna Analysis

Co-chairs: W. Davis, Virginia Polytechnic Institute and State University
H. Nakano, Hosei University, Japan **Page**

- | | | | |
|---|------|--|----|
| 1 | 1:50 | A proposal for a standard microstrip satellite antenna, <i>M. Sultan*</i> , <i>Benha Higher Institute of Technology, Egypt</i> | 76 |
| 2 | 2:10 | Comparative study of analysis techniques and measurement methods for a canonical microstrip antenna, <i>K. Takamizawa*</i> , <i>N. Cummings, W. Stutzman, W. Davis, Virginia Polytechnic Institute and State University, USA</i> | 77 |
| 3 | 2:30 | Shape optimization of printed patch structures using the Genetic Algorithm, <i>H. Choo*</i> , <i>T. Su, The University of Texas at Austin, USA, L. Trintinalia, Escola Politécnica da USP, Brazil, H. Ling, The University of Texas at Austin, USA</i> | 78 |
| 4 | 2:50 | Moment Method analysis of an aperture coupled patch antenna in a cylindrical PEC structure with arbitrary cross section, <i>P. Slattman*</i> , <i>REMEC Magnum, USA, B. Lindmark, Allgon System, Sweden</i> | 79 |
| 5 | 3:10 | Hybrid MoM/Green's function analysis of printed antennas mounted on large coated cylinder, <i>V. Erturk, R. Rojas*</i> , <i>The Ohio State University, USA</i> | 80 |
| | 3:30 | Break | |
| 6 | 3:50 | Theory and experiment on microstrip patch antennas with shorting walls, <i>K. Lee*</i> , <i>University of Missouri-Columbia, USA, Y. Guo, City University of Hong Kong, Hong Kong, J. Hawkins, University of Missouri-Columbia, USA, R. Chair, K. Luk, City University of Hong Kong, Hong Kong</i> | 81 |
| 7 | 4:10 | Accurate computation of radiation pattern of a linearly and an exponentially tapered slot antennas, <i>S. Jang, T. Sarkar, Syracuse University, USA</i> | 82 |

A PROPOSAL FOR A STANDARD MICROSTRIP SATELLITE ANTENNA

MOHAMMED A. SULTAN

Department of Electronics and Electrical Technology
Benha Higher Institute of Technology
Benha , Egypt

In the past analysis of microstrip antennas, a considerable amount of work has been done on the radiation characteristics of closed-ring microstrip antennas. The radiation fields have been evaluated by utilizing a host of techniques ranging from the use of a simple cavity model to the use of the spectral domain technique in Fourier-Hankel transform domain and the use of the method of matched asymptotic expansion. As a result, expressions for all radiation characteristics are now available either in a closed form expression or in a form of converging series. This made it possible to propose the closed-ring antenna to be a standard element.

In this paper, known closed form expressions for radiation fields and radiated power (based on the cavity model) of the proposed standard element are used to derive a general expression for radiated power of any other antenna configuration with known radiation fields. This gives an equivalent solution for the surface integral of the Pointing vector over a closed spherical surface for the antenna of the unknown characteristics . As a consequence, the expressions for radiation resistance, directivity, bandwidth and other radiation characteristics are determined in a straight forward manner. The method is valid for all modes of excitation and can be used in the field of satellite communications.

Details of this method and its results would be discussed.

Comparative Study of Analysis Techniques and Measurement Methods for a Canonical Microstrip Antenna

K. Takamizawa*, N. P. Cummings, W. L. Stutzman, and W.A. Davis

Antenna Group
The Bradley Department of Electrical and Computer Engineering
Virginia Polytechnic Institute and State University
Blacksburg, VA 24061-0111
<http://www.ee.vt.edu/antenna>

Microstrip patch antennas are quickly becoming the most attractive solutions for the applications requiring small sizes and integration with radio electronics. Rapid and accurate prediction of patch antenna performance is critical to successful design. In addition, analysis tools can be used in conjunction with optimization routines for performance improvement of particular designs. As analysis accuracy improves, less time and effort is needed for post fabrication trimming of patches for the performance enhancement or adjustments.

Many electromagnetic analysis techniques have been developed in the last forty years. Some of these techniques have matured and have been implemented as commercially available codes. Unfortunately, there is no single method or code that can completely predict all performance parameters of any patch antenna.

This paper reports on comparative studies of a microstrip antenna using commercially available codes as well as experimental evaluation. An edge-fed square microstrip patch antenna implemented on a substrate is used for the comparison. Four popular analysis techniques for the microstrip antennas are considered: Method of Moments, Finite Elements, Finite Difference Time Domain, and Cavity Model. Antenna parameters such as radiation pattern, gain, input impedance, and impedance bandwidth will be compared. The effects of finite ground plane on the above parameters will also be considered. Computational requirements such as processor time and memory size will also be discussed. Results will be presented for comparisons of computed parameters to measurements conducted on outdoor and indoor far-field ranges as well as in a near-field range.

Shape Optimization of Printed Patch Structures Using the Genetic Algorithm

Hosung Choo*, Tao Su, Luiz Cezar Trintinalia⁺ and Hao Ling

Department of Electrical and Computer Engineering
The University of Texas at Austin
Austin, TX 78712 U.S.A

⁺Department of Telecommunications and Control
Escola Politécnica da USP, Brazil.

Patch structures printed on thin material substrates such as microstrip antennas and grating absorbers are known to exhibit narrow frequency bandwidth. In this work, we explore the use of the genetic algorithm (GA) to design patch shapes for broadband applications. Our approach is to use a full-wave electromagnetic solver to predict the performance of patch structures of arbitrary shape. We implement a two-dimensional GA algorithms in which the discretized patch shape information is encoded into binary bits.

We employ an electromagnetic solver capable of computing the scattering from an infinite layered coating with embedded periodic metal structures. The formulation of the code is similar to that described in T. Cwik and R. Mittra, *IEEE Trans. Antennas Propagat.*, 35, 1226-1234, 1987. The roof-top basis function is used to expand the unknown current on the metal patch and the boundary condition on the patch is enforced through the electric-field integral equation. The periodic Green's function for layered coatings is the kernel of the integral equation and FFT is used to accelerate the computation of the matrix elements.

In the GA procedure, the discretized patch shape is encoded into binary bits to form a chromosome, with metal sub-patches represented by ones and non-metal areas represented by zeros. The cost function is defined to be the difference between the computed and the desired frequency response. The number of samples in the population is chosen depending on the number of data bits in the chromosome. It is more desirable to obtain optimized patch shapes that are well-connected from the manufacturing point of view. Therefore, a 2D median filter is applied to the chromosomes to create a more realizable population at each generation of the GA.

The results of the GA design will be presented. Physical interpretation for the optimized structures will also be discussed and compared with baseline results obtained by using rectangular shaped patches of different sizes.

Moment Method Analysis of an Aperture Coupled Patch Antenna in a Cylindrical PEC Structure with Arbitrary Cross Section

Peter Slettman, REMEC Magnum, 1990 Concourse Drive, San Jose, CA 95131

pslettman@remecmagnum.com

Björn Lindmark, Allgon System, P.O. Box 541, SE 183 25 Täby, Sweden

bjorn.lindmark@allgon.se

The motivation for this work is to study radiation from aperture coupled patch elements in linear array base station antennas. In base station antenna design it is important to meet the requirements on sector coverage in azimuth and to minimize the spill-over into adjacent sectors. To accurately predict the radiation pattern in azimuth it is necessary to include the shape of the cross-section of the structure that the antenna elements are mounted on in the analysis. The commonly used analysis technique for aperture coupled patch antennas is to employ the so called spectral domain approach which assumes an infinite planar layered structure. The technique is very successful for calculating input impedance in an accurate and efficient manner, but fails to account for edge effects in the structure. This is a draw back when analyzing radiation from linear arrays of patch antennas, since the finite cross-section of the antenna influences the radiation heavily in azimuth.

The purpose of this presentation is to describe the formulation, implementation, and validation of an aperture coupled patch antenna in a cylindrical perfectly conducting structure. The formulation is general in the sense that no restrictions are put on the geometry of the patch, the slot, or the cross-section of the cylindrical scatterer, i.e. the cylinder does not have to be circular. The cylinder is assumed to be infinitely long which enables us to analyze the problem in the spectral domain, (x, y, k_z, α) . The resulting field problem is solved by a two-stage moment method procedure: one in the cylindrical spectral domain to calculate the coupling between the basis functions on the patch and the slot modes, and one in the spatial domain to calculate the currents on the patch for each slot mode. In this work we use only the fundamental slot mode for calculating the radiation pattern, but we are currently working on calculating the slot admittance where more modes are needed. In the implementation of the algorithm we put some restrictions on the patch and slot geometries and make a certain choice of basis functions. The motivation is two-fold: to keep the resulting computer program as simple as possible and to make it run faster.

The resulting computer program can be used to analyze and design linear arrays of aperture coupled patches with restrictions on sector coverage and front-to-back ratio. The program is not only capable of analyzing aperture coupled patches at finite size ground planes, but to analyze *any* cross-sectional shape of the structure. This extra degree of freedom can be used to shape the structure/reflector to meet very tough requirements on the azimuth pattern.

Hybrid MoM/Green's Function Analysis of Printed Antennas Mounted on Large Coated Cylinder

V.B. Ertürk and R.G. Rojas*

Dept. Electrical Engineering, ElectroScience Laboratory
The Ohio State University
Columbus, Ohio 43212-1191

There has been a major advance in the area of computer aided design (CAD) technology due to the development of efficient numerical methods for the design and analysis of planar microstrip elements and arrays. Some work has also been done for conformal antennas, however, most of the developed methods are valid for electrically small structures. This necessitates the development of efficient and accurate analytical and numerical tools for antennas conformal to electrically large cylindrically shaped substrates.

In this paper, an efficient and accurate hybrid method based on the combination of method of moments (MoM) with a special cylindrical Green's function in the spatial domain will be presented to analyze antennas and array elements conformal to electrically large material coated circular cylinders. The efficiency and accuracy of the method depends strongly on the computation of the Green's function which is the kernel of an integral equation solved via MoM (where a Galerkin testing scheme is employed) for the unknown equivalent currents concerning only the antenna elements. Therefore, three type of spatial domain cylindrical Green's function representations are used interchangeably, based on the computational efficiency of their calculation and the region where they remain highly accurate. The first and the most frequently used one is a Steepest Descent Path (SDP) representation of the Green's function which reduces to the UTD-based Green's function in the limiting case of large separations between the source and observation points. It is valid everywhere except when the observation point is in the vicinity of the source point (i.e. electrically small separations), and when the observation point is in the paraxial (i.e. near axial) region of the source point. For electrically small separations as well as the evaluation of the self impedance term, an efficient integral representation of the of the planar microstrip dyadic Green's function is used. Finally, to calculate the mutual coupling between two current modes in the paraxial region, a third, asymptotic-based, spatial domain Green's function representation is employed. Consequently, combining different Green's function representations with MoM, a computationally optimized analysis tool for conformal microstrip antennas is obtained.

To validate the proposed method, numerical results involving the input impedance of a microstrip antenna, as well as mutual coupling between two microstrip antennas conformal to an electrically large circular cylinder will be presented.

Theory and Experiment on Microstrip Patch Antennas with Shorting Walls

K. F. Lee,^{*1} Y. X. Guo², J. A. Hawkins¹, R. Chair², K. M. Luk²

¹Department of Electrical Engineering, University of Missouri-Columbia

²Department of Electronic Engineering, City University of Hong Kong

There have recently been extensive studies on size reduction techniques for microstrip patch antennas. The earliest design that results in a reduced size patch is the quarter-wave shorted patch. Although this design has been around for quite some time, certain basic properties of the shorted patch remain unclear. For example, is the bandwidth of the quarter-wave patch smaller or larger than the regular half-wave patch? What is its typical gain? What is the effect of a partial short on the bandwidth? Can the concept be applied to reduce the sizes of wideband and dual-frequency patch antennas?

In this paper, we present experimental and calculated results which address these questions. The calculated results are based on a FDTD code developed in house. It is found that, for foam substrate ($\epsilon_r \approx 1.08$), the bandwidths of quarter wave patches are significantly larger than half-wave patches. On the other hand, for microwave substrates with $\epsilon_r = 2.33$ and 4.0, the bandwidths of quarter wave patches are about 20% less than those of half-wave patches. This is attributed to surface waves. The maximum gain in the case of foam substrate is in the range of 2-3 dBi, occurring 30-45° from broadside. When a partial short is used, the resonant frequency is reduced, resulting in further size reduction. However, this is accompanied by a reduction in bandwidth.

We have successfully applied the shorting wall technique to reduce the size of the L-probe wideband patch antenna and the slot loaded dual frequency patch antenna. In the former case, an impedance bandwidth of 39% is obtained for a quarter-wave patch on a foam substrate of thickness $\approx 0.1\lambda_0$. In the latter case, by controlling the width of the shorting plane, the two resonant frequencies, f_{10} and f_{30} , can be significantly reduced and the frequency ratio f_{30}/f_{10} is tunable in the range 1.6 – 2.2.

Accurate Computation of Radiation Pattern of a Linearly and an Exponentially Tapered Slot antennas

Seong-man Jang, Tapan K. Sarkar
Department of Electrical Engineering and Computer Science
Syracuse University
121 Link Hall
Syracuse, NY 13244-1240
Tel : (315) 443-3775
Fax : (315) 443-4441
Email : tksarkar@mailbox.syr.edu
sejang@mailbox.syr.edu

The accurate computation of radiation pattern for the tapered slot antenna (TSA) using WIPL is presented. This includes the analysis of exponentially tapered slot antenna (Vivaldi) and linearly tapered slot antenna (LTSA). Theoretical results of them are compared with experimental data for frequency range (8GHz ~12GHz).

The tapered slot antenna consists of a tapered slot in a thin film of metal with or without an electrically thin substrate. A traveling wave propagates along the slot and radiated along the end-fire direction. These kinds of antenna have high directivity for a given cross section, good crosspolarization characteristics and low sidelobes. Another merit is that it is easy to integrate with other printed circuits, such as mixer or amplifier devices.

WIPL is a software package for electromagnetic modeling of composite metallic and dielectric structures. In WIPL, electric and magnetic surface currents are approximated by an entire domain polynomial expansion and the unknown expansion coefficients are determined by applying the Galerkin method to the corresponding surface integral equation. All other quantities of interest such as radiation field, gain are obtained using the calculated current distribution.

The theoretical result for the LTSA in fig. 1 is compared with the experimental data (Fig.2). Dielectric constant of the substrate is 2.55, its thickness is 0.030", opening angle of the slot is 35degree, and the operating frequency is 12GHz. The result shows a good agreement.

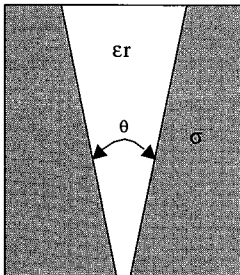


Fig. 1 Linearly tapered slot antenna (LTSA)

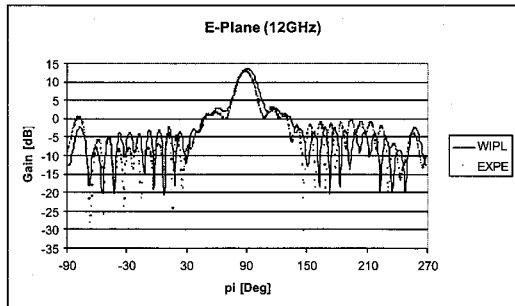


Fig. 2 Comparison of the result at 12 GHz

Time-Domain PDE Methods

Co-chairs: J. M. Baird, University of Utah
F. El-Hefnawi, Electronic Research Institute, Egypt

			Page
1	1:50	FDTD analysis of a short dipole immersed in space plasma, <i>C. Furse*</i> , <i>J. Olakangil</i> , <i>C. Swenson</i> , <i>Utah State University, USA</i>	84
2	2:10	Modification of the PLRC algorithm for the analysis of propagation through Van Vleck-Weisskopf media, <i>D. Kelley*</i> , <i>R. Luebbers</i> , <i>The Pennsylvania State University, USA</i>	85
3	2:30	Advantages and limitations of FDTD subgrid schemes for EM transmitters operating within highly complex environments, <i>N. Chavannes*</i> , <i>N. Kuster</i> , <i>Swiss Federal Institute of Technology, Switzerland</i>	86
4	2:50	Comparison of FDTD and MoM for the analysis of multifinger FET, <i>B. Cetiner*</i> , <i>R. Coccioli</i> , <i>B. Housmand</i> , <i>T. Itoh</i> , <i>University of California, Los Angeles, USA</i>	87
5	3:10	FDTD analysis of modes & mutual coupling between waveguide slots, <i>V. Cable*</i> , <i>D. Nestico</i> , <i>Lockheed Martin Skunk Works, USA</i>	88
	3:30	Break	
6	3:50	FDTD modeling near-fields of helical antennas on a handset, <i>K. Caputa*</i> , <i>M. Stuchly</i> , <i>University of Victoria, Canada</i> , <i>M. Kanda</i> , <i>Motorola Research Laboratories, USA</i>	89
7	4:10	Three-dimensional cylindrical FDTD algorithm using alternating-direction implicit method, <i>S. Ow*</i> , <i>S. Judah</i> , <i>University of Hull, U.K.</i>	90
8	4:30	A Comparison of FDTD-PML with TDIE, <i>S. Rao</i> , <i>Auburn University, USA</i> , <i>N. Sachdeva</i> , <i>N. Balakrishnan*</i> , <i>Indian Institute of Science, India</i>	91
9	4:50	MRTD scattering computations with bi-orthogonal wavelets, <i>T. Dogaru</i> , <i>L. Carin*</i> , <i>Duke University, USA</i>	92
10	5:10	Scaling and wavelet function based multiresolution time-domain scheme for electromagnetic wave applications, <i>Q. Cao</i> , <i>M. Yang</i> , <i>Y. Chen*</i> , <i>Hong Kong Polytechnic University, Hong Kong</i>	93

FDTD ANALYSIS OF A SHORT DIPOLE IMMERSERD IN SPACE PLASMA

Cynthia Furse*, Joseph Olakangil, Charles Swenson
Department of Electrical and Computer Engineering
4120 Old Main Hill
Utah State University, Logan, Utah 84322-4120,
phone : (435) 797-2870, fax (435) 797-3054, furse@ecc.usu.edu

Introduction

The Plasma Frequency Probe (PFP) makes use of a short dipole antenna (approx. 1 meter long) to probe ionospheric plasmas. This measurement technique has been flown on sounding rockets by the Space Dynamics Laboratory and Utah State University for over three decades. These probes are used to measure the electron density, temperature, and collision frequency of the ionosphere based on the change of the electrical impedance of the antenna in contact with the space plasma. The data analysis for these probes has traditionally been based on analytical theory and several simplifying assumptions including cold plasma, antenna fully aligned with the earth's magnetic field, and an approximate prescribed current density on the antenna. This paper describes a new formulation using the Finite Difference Time Domain (FDTD) method that allows full-wave analysis of the PFP in space plasma including the effects of variable magnetic field orientation, plasma temperature, and physical antenna current distributions. This can provide improved resolution and understanding of the measurements. This formulation, which is based on the fluid model of plasma, is different than previous plasma simulations (Nickisch and Franke, *IEEE AP Mag.*, 5, 33-40, 1992; Luebbers, et al., *IEEE TAP*, 1, 29-34, 1991; Hunsberger, et al., *IEEE TAP*, 12, 1489-1493, 1992; Kashiwa, *IEEE TAP*, 8, 1096-1105, 1988) that have been made with the FDTD method.

Fluid Model of Plasma

Maxwell's equations in the time domain (including the plasma current term in the Faraday equation) are used:

$$\nabla \times \vec{E} + \frac{1}{c} \frac{\partial \vec{B}}{\partial t} = 0 \quad \nabla \times \vec{B} - \frac{1}{c} \frac{\partial \vec{E}}{\partial t} = \frac{4\pi}{c} (nq\vec{u} + \vec{J}_{ext})$$

along with the current continuity equation :

$$nm \frac{\partial \vec{u}}{\partial t} + kT \nabla n - nq \left(\vec{E} + \frac{1}{c} \vec{u} \times \vec{B} \right) = -m\vec{u}$$

and the charge continuity equation:

$$\frac{\partial n}{\partial t} + \nabla(n\vec{u}) = 0$$

where E,B are the electric and magnetic fields, n is the number of electrons (based on electron density), and u is the vector velocity. The differentials in these equations are converted to the difference form, using the central difference method, in the same way as the traditional FDTD equations are derived.

The simulation was tested for a magnetized plasma with no antenna, verifying that that cyclotron resonance, the plasma resonance, and the damping due to ionic collisions were predicted correctly. The impedance of the probe was then predicted for a wide range of plasma and collision frequencies, and compared with analytical theory developed by Balmain (*IEEE TAP*, 5, 605-617, 1964). The agreement was found to be excellent. Efforts to calibrate the existing library of measured data to simulation data will be described.

MODIFICATION OF THE PLRC ALGORITHM FOR THE ANALYSIS OF PROPAGATION THROUGH VAN VLECK-WEISSKOPF MEDIA

David F. Kelley* and Raymond J. Luebbers
Department of Electrical Engineering
The Pennsylvania State University
University Park, PA 16802

The piecewise linear recursive convolution (PLRC) algorithm has gained widespread acceptance as an accurate and efficient means for analyzing propagation through linear isotropic dispersive dielectrics using the finite difference time domain (FDTD) method. The original PLRC algorithm and most of the other approaches that have appeared in the literature have been applied only to materials characterized by the Debye and Lorentz frequency-domain permittivity functions. However, a commonly-used model of atmospheric absorption in the upper microwave and millimeter-wave frequency ranges, known as the Van Vleck-Weisskopf line shape function, is based upon a third permittivity function that is unfamiliar to many investigators in the FDTD community. This paper outlines a modification of the PLRC algorithm that adds to it the capability of analyzing propagation through Van Vleck-Weisskopf media. Although the presentation focuses on the PLRC formulation, a similar approach should be applicable to other dispersive media modeling methods.

The PLRC formulations for Debye and Lorentz media take advantage of the fact that the time-domain susceptibility functions corresponding to each material type can be represented as either a real or a complex exponential function. This property makes possible the development of a highly efficient recursive convolution scheme. A similar exponential behavior is found in the Van Vleck-Weisskopf case, except that the susceptibility function exhibits a constant phase shift. A recursive convolution approach can therefore be derived for Van Vleck-Weisskopf media as well. An interesting result is that the new algorithm uses update equations that are identical in form to those used in the algorithm for Lorentz media; it is necessary only to compute different values for the update equation coefficients. Consequently, the required modifications to computer programs that already incorporate the PLRC algorithm are minimal.

Advantages and Limitations of FDTD Subgrid Schemes for EM Transmitters Operating Within Highly Complex Environments

Nicolas Chavannes and Niels Kuster
Swiss Federal Institute of Technology (ETH)
8092 Zurich, Switzerland

Phone:+41-1-632 2755, Fax:+41-1-632 1057, e.mail: chavanne@itis.ethz.ch

Introduction

In recent years, numerical modeling using the Finite-Difference Time-Domain method has been widely used to analyze various electromagnetic problems. Although the method has gained increasing interest for the calculation of various structures, limited resolution makes it more difficult to simulate very fine or grid non-conformal objects. This restriction makes the common FDTD method unsuitable for the reliable analysis of detailed EM transmitter structures embedded within highly complex environments. An efficient way to overcome these limitations is the use of local grid refinement schemes, such as subgrid algorithms which have been reported in the literature, e.g. in (M.Okoniewski et al., IEEE-AP,45,422-429,1997). These algorithms can be combined with advanced CAD environments to enable the creation of complex models with high resolution.

In this study a novel and robust 3-D FDTD subgrid scheme (N.Chavannes et. al.,Proc. Mill. Conf. on AP,2000) is applied in order to point out advances and limitations of subgrid methods for the characterization of EM transmitters in FDTD.

Objectives

The objective of this study was the characterization of FDTD subgrid schemes with enhanced modeling capabilities for the analysis of electromagnetic transmitters embedded in complex environments.

Methods

A novel subgrid scheme was implemented into a state of the art Yee-grid based FDTD simulation platform (A.Christ et. al., Proc. Mill. Conf. on AP, 2000). It enables an easy and flexible modeling of various geometric structures due to CAD capabilities and a fully automated grid generation.

In a first approach the coupling mechanisms between the parameter sensitivity and intensity of modeling detail was assessed for basic antenna types like monopoles and helices using the subgrid. Antenna parameters from the near- and far-field are compared for various antenna discretizations, modeling types and applications of the subgrid algorithm. Finally, the drawn conclusions were applied to the characterization of a previously defined generic phone (M. Burkhardt et al.,Proc. Int. Conf. on Appl. Electr. and Comm., 83-86,1997) equipped with a helical antenna. The initially mismatched phone was rebuilt based on the results from the simulation and matched for a variety of configurations for free space as well as close to a flat phantom at different distances. All results from the simulations were validated by measurements from a physical model of the generic phone using the near-field scanning system DASY3 (T.Schmid et. al., IEEE-MTT,1,105-113,1996) and were in excellent agreement.

Results and Discussion

The common FDTD method is of limited use for profound antenna analysis due to limited resolution. The method's modeling capabilities can be greatly enhanced by the implementation of subgrid schemes as well as CAD and automated meshing support. The subgrid algorithm must perform high stability and low reflection to support the needed efficiency. It must be locally adapted to the configuration which is examined and combined with special treatments for materials which traverse the interface region. Whereby for the far-field pattern no major influence can be observed with respect to modeling detail, parameters like feedpoint impedance and close near-field distribution show strong variation. The analysis of these characteristics revealed the needs of improved FDTD modeling features, in particular for the simulation of EM transmitters embedded in highly complex environments.

Comparison of FDTD and MoM for the analysis of multifinger FET

B.A. Cetiner, R. Coccioli, B. Housmand, T. Itoh
Electrical Engineering Department, University of California, Los Angeles
405 Hilgard Avenue, Los Angeles, CA 90095
Tel: (310) 206-1710, Fax: (310) 206-4819, e-mail: bedri@ucla.edu

The performance optimization of large multifinger, power FET devices require a full 3-D electromagnetic analysis. Although CAD tools based on finite numerical techniques are routinely employed and are an industry standard for the analysis of microwave passive circuits, comprehensive 3D electromagnetic modeling for active circuits is still a topic of intensive research.

In this work, the passive part of an X-band MMIC pre-matched power cell built on a 25 μm thick GaAs ($\epsilon_r=12$) substrate has been investigated. The structure differs from a similar one previously investigated (S.-H. Chang, R. Coccioli, B. Housmand, T. Itoh, *IEEE MTT-S International Microwave Symposium 99*, Anaheim, California, June 12 - 19, 1999) because of the thinner substrate, suitable for flip-chip assembling, a different connection topology of source fingers to ground, and the presence of a metallic bridge (not shown in Fig. 1 for sake of clarity) connecting the source fingers.

To implement an efficient CAD tools based on extended FDTD, the MIM capacitor of the input matching network must be replaced with their equivalent lumped element circuits. This is necessary to avoid a exceedingly small discretization step that would lead to an unacceptable small time step with consequent increase in the running time. To this end, the equivalent circuit of the MIM capacitors has been derived from numerical results obtained from the MoM based Sonnet simulator and used in the FDTD based simulator.

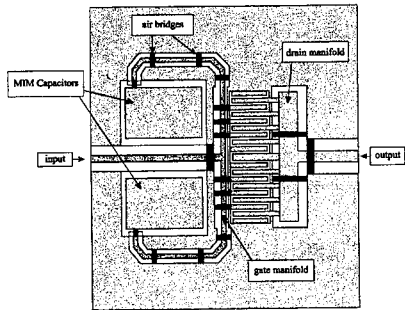


Fig. 1 – Schematic of Pre-matched Power Cell.

Additionally, the results obtained with the extended FDTD relative to the passive part of the FET have been compared with the analysis of the whole cell obtained with Sonnet. The two methodologies gave results in good agreement, thus confirming the validity of the assumptions made to set up the model used in the extended FDTD.

As last step of the analysis of the complete cell, we plan to introduce the effects of the intrinsic non-linear part of the active device following the methodologies introduced for the large signal analysis of microwave amplifiers (C.N.Kuo, B.Houshmand, T.Itoh, *IEEE MTT*, vol. 45, 819-826, May 1997) and modeling of interaction of FET and MMIC (A.Cidronali, G.Collodi, G.Vannini, *IEEE MTT*, vol.47, June 1999).

FDTD Analysis of Modes & Mutual Coupling Between Waveguide Slots

**Vaughn Cable* & David Nestico
Lockheed Martin Skunk Works
Palmdale, CA 93599**

The simplicity of FDTD and yet its ability to handle complex structures has makes it a desirable tool for analyzing many difficult guided wave problems. For example, S. T Chu, et al. [MTT, Nov. '90], E. A. Navarro, et al. [IEE Proceedings – H, Dec. '92], and others have applied FDTD to composite guiding structures, some with radiation, as well as to modal analysis of waveguides and waveguide discontinuities. In many cases, resonant frequencies and/or cutoff frequencies were computed 2D FDTD with the usual assumption that evanescent modes are not explicitly modeled (e.g., calculation of s-parameters). These techniques also often utilize impulsive excitation and Discrete Fourier Transforms to determine the spectrum of propagating modes which are possible. In this paper, we present results for the extraction of local evanescent waveguide modes in the vicinity of a discontinuity using 3D FDTD. The geometry consists of a single length of standard waveguide with a probe feed at one end and a termination at the other. A pair of broadwall slots is located midway between the ends of the guide. The mutual coupling between and the radiation from these slots is the target application for this work. In this calculation, the steady state total field solutions are generated and processed using orthogonality and correlation relationships to separate propagating, evanescent and radiating modes in and around the structure. Based on these results, the mutual coupling and radiation are derived for changes in frequency as well as for changes in slot orientation. The changes in mutual coupling with the introduction of a dielectric sheet over the radiating slots are also investigated and discussed.

FDTD Modeling Near-Fields of Helical Antennas on a Handset

K. Caputa*, M. A. Stuchly,
University of Victoria, ECE Dept., Victoria, BC, V8W 3P6,
and M. Kanda,
Motorola Research Laboratories, Plantation, FL.

Evaluation of performance of wireless telephones in proximity of the human head is essential for various purposes. Some of them are (1) evaluation of power deposition in the head for compliance assessment, (2) antenna design, and (3) electromagnetic interference (EMI) evaluation. Compliance evaluation can be performed experimentally. However, in the two other problems, numerical evaluation is either the only possible solution or the preferred one. Numerical modeling that includes models of the human body or its parts is usually done using the FDTD (finite-difference time-domain) method.

One of the most critical issues in the FDTD modeling is a correct representation of the antenna. This is particularly challenging for helical antennas. Such antennas can be modeled by staircase approximation of helix by square loops and straight conductor sections [J. S. Colbourn and Y. Rahmat-Samii, *IEEE Trans Antennas Propag.* vol. 46(6), pp. 813-820, 1998]. Near field of the helix has also been represented by sub-cell models [G. Lazzi and O. P. Gandhi, *IEEE Trans. Antennas Propag.* vol. 46(4), pp. 525-530, 1998.]. The latter method is useful for efficient computation of fields and power deposition in the head. On the other hand, it does not allow for determination of input impedance of the antenna.

In this research we demonstrate how the staircase approximation can ensure reliable representation of an actual antenna by adjusting the helix pitch. The antenna length and diameter are maintained the same as the actual physical dimensions, and so are the dielectric cover dimensions. An adjustment of the helix pitch is made to obtain the same resonant frequency (or frequencies in the case of an antenna with more than one helix) and input impedance in free space. Staircasing and FDTD grid changes accompany a pitch change. To determine the actual input impedance and resonant frequencies, a vector network analyzer is used to measure the actual antenna on the handset. We have performed modeling using two FDTD codes. Computed electric and magnetic fields within 1 to 4 cm away from a handset have been compared with those measured in Motorola laboratory for the same handset. A very good agreement has been obtained. A relative difference between the mean measured and computed fields for a surface of about 15-cm x 10-cm is of the order of 2%. The mean absolute error is 15% in the plane 1-cm away from the handset and 9% at 4 cm.

Three-dimensional Cylindrical FDTD Algorithm Using Alternating-Direction Implicit Method

S.C.Ow* and S.R.Judah
School of Engineering, University of Hull, U.K.

The finite-difference time-domain (FDTD) method has been widely used in solving a broad range of electromagnetic problems. However, the accuracy of any model can be greatly improved with the use of finer spatial increments especially where there are discontinuities in the structure. In order to avoid intensive use of memory storage, a computational domain can be sub-divided into regions, each with a different mesh size; finer mesh size is used for regions with high irregularity and larger mesh size for the rest of the domain.

In the past, to maintain stability as defined by the Courant-Friedrich-Levy (CFL) condition, either the time step corresponding to the smallest mesh size is used, or the time steps are set separately for each mesh region. For a large object with highly irregular structure, the first method can be computationally expensive. Using the second method, the mesh sizes have to be such that the time steps are integer multiples of one another while in a graded mesh, several different time steps have to be used in a simulation.

With the ADI-FDTD method, the Courant stability constraint is eliminated and therefore a single time step can be used for all mesh sizes throughout the model. This is very useful when modelling a probe-fed circular patch where the probe is extremely narrow when compared to the diameter of the patch. In order to represent the effective input impedance of the probe-fed circular patch accurately, a high FDTD mesh density is applied in the vicinity of the probe and the mesh density decreases gradually away from the probe.

In this paper, the three-dimensional cylindrical FDTD algorithm based on the alternating-direction implicit (ADI) method is used to model a probe-fed circular patch to demonstrate the use of cylindrical ADI-FDTD in a graded mesh. Although the ADI method has been applied on the Cartesian coordinate FDTD (T.Namiki, IEEE MTT, vol.47, no.10, pp.2003-2007, 1999), it is useful, however, to apply the ADI-FDTD method within the cylindrical coordinate system so that circular structures can be modelled with an exact boundary definition. This then avoids the application of a staircase approximation or conformal mapping technique at structural boundaries, whilst retaining the advantages that the ADI method provides.

A Comparison of FDTD-PML with TDIE

S. M. Rao,
Department of E & CE,
Auburn University, Auburn, AL 36849.

N. Sachdeva and N. Balakrishnan*
Department of Aerospace Engineering,
Indian Institute of Science,
Bangalore — 560 012, INDIA

In this work, we present a comparison of two popular and widely different numerical methods *viz.* the Finite-Difference Time-Domain (FDTD) method and the Time Domain Integral Equation (TDIE) method. To the best of our knowledge, a thorough comparison of these two techniques for three-dimensional bodies has not been made and this work is aimed at filling up this gap. It is also hoped that this comparison might help while choosing one method over the other for a given situation.

As is well known, the FDTD method is a differential equation based technique used for solving electromagnetic wave interaction problems for open as well as closed region problems. When applied to open region problems, FDTD requires a suitable absorbing boundary condition. At present, the most popular and accurate boundary condition seems to be the Perfectly Matched Layer (PML) which is incorporated in the present work. On the other hand, as the name implies, TDIE is an integral equation based technique which incorporates radiation condition in the formulation itself. For numerical solution of TDIE, we model the scattering structure with planar triangular patches and employ the RWG basis functions on triangular patches to approximate the spatial variation of the induced current. For the temporal variation we use linear interpolation.

The comparison is made for standard canonical shapes, *viz.* a cube and a sphere, both for conducting as well as dielectric material bodies. In our comparison we address such issues as the factors affecting accuracy, efficiency of each method and required computer resources.

MRTD Scattering Computations with Bi-Orthogonal Wavelets

Traian Dogaru and Lawrence Carin
Department of Electrical and Computer Engineering
Duke University
Box 90291
Durham, NC 27708-0291

The multi-resolution time domain (MRTD) method performs a time and spatial expansion of the electromagnetic fields in Maxwell's equations, using a wavelet (multi-resolution) basis. The advantage of this approach is that wavelets can be added in localized regions for which higher resolution is required, and scaling functions can be applied in regions for which less resolution is sufficient. The sampling rate of the wavelets is dictated by the smoothness of the scaling and wavelet functions. For example, Haar wavelets have sharp corners, and are therefore not particularly smooth. Consequently, the MRTD with Haar expansion functions can be related directly to the traditional Yee finite difference time domain (FDTD) formalism. Researchers have employed smoother scaling and wavelet functions, with the goal of reducing the required sampling rate (in space, and possibly in time as well). A difficulty with the traditional orthogonal wavelets is that, to increase the smoothness, one generally must increase the scaling and wavelet filter lengths. While this does not constitute a problem to the MRTD in general, it increases the complexity of ultimate MRTD implementation. In this context, the Haar-based MRTD is particularly simple to implement, based on the compact support of the associated scaling and wavelet functions. It is desirable to combine smoothness with compact support.

If one relaxes the requirement that the scaling and wavelets must be orthogonal, there are greater degrees of freedom available in the wavelet design, toward a particular task. In particular, biorthogonal wavelets can be applied to simultaneously achieve smoothness and compact support (*vis-à-vis* orthogonal wavelets). In this paper we demonstrate that MRTD based on biorthogonal wavelets is not particularly different than its counterpart with orthogonal wavelets. However, the biorthogonal wavelets provide greater flexibility in MRTD implementation. The basic formulation is discussed, as are example scattering results.

Scaling and Wavelet Function Based Multiresolution Time-Domain Scheme for Electromagnetic Wave Applications

Qunsheng Cao, Mingwu Yang, and Yinchao Chen
Department of Electronic and Information Engineering
Hong Kong Polytechnic University, Hong Kong

Abstract – In this research, we explore a hybrid scaling and wavelet based multiresolution time domain (MRTD) scheme for electromagnetic wave applications. In particular, we simultaneously chose the cubic spline *Battle-Lemarie* scaling function $\phi(x)$ and wavelet function $\psi_m(x)$ as expansion bases. We construct the fields dominantly by the scaling function expansions and use the wavelet contributions to describe a fine variation of fields. We apply this MRTD algorithm to analyze a transient electromagnetic pulse propagating through a one or multi-layered dielectric system. For the purpose of efficient computation, we only apply the wavelet expansions in the close region of the dielectric-air discontinuity part where the electromagnetic fields change dramatically, and use the scaling function in the entire computational domain. Through the orthogonal relations between the basis functions and the calculated expansion coefficients, we derive the field leapfrog update relations. It has been found that the computed results for all cases investigated in this research are excellently agreement with those derived from other methods, while the MRTD method is much more efficient than the conventional FDTD in terms of the computational CPU time and memory space with the same or better accuracy.

Reconfigurable Aperture Antennas

Organizer and Chair: J. K. Smith, DARPA

Page

1	1:50	Reconfigurable antenna program, <i>J. K. Smith, Defense Advanced Research Project Agency, USA</i>	96
2	2:10	Switched fragmented aperture antennas, <i>J. Maloney, M. Kesler, L. Lust, L. Pringle, T. Fountain, P. Harms, Georgia Tech Research Institute, G. Smith, Georgia Institute of Technology, USA</i>	AP
3	2:30	Reconfigurable aperture decade bandwidth array, <i>J. Veihl*, R. Hodges, D. McGrath, C. Monzon, Raytheon Electronic Systems, USA</i>	AP
4	2:50	A reconfigurable slot aperture, <i>R. Gilbert*, D. Kopf, Sanders, A Lockheed Martin Co., J. Volakis, University of Michigan, USA</i>	97
5	3:10	Multi-mode microstrip antennas for reconfigurable aperture, <i>J. Sor, Y. Qian, M. F. Chang, T. Itoh, University of California, Los Angeles, USA</i>	AP
	3:30	Break	
6	3:50	Reconfigurable aperture antennas using RF MEMS switches for multi-octave tunability and beam steering, <i>J. H. Schaffner*, R. Y. Loo, D. F. Stevenpiper, F. A. Dolezal, G. L. Tangonan, J. S. Colburn, J. J. Lynch, HRL Laboratories, J. J. Lee, S.W. Livingston, R. J. Broas, Raytheon, M. Wu, UCLA, USA</i>	AP
7	4:10	Silicon based reconfigurable antennas, <i>A. Fathy, A. Rosen, F. McGinty, G. Taylor, S. Perlow, Sarnoff Corp., M. ElSherbiny, Future Technologies Inc, USA</i>	AP
8	4:30	Design of frequency-reconfigurable rectangular slot ring antennas, <i>K. Gupta*, J. Li, R. Ramadoss, C. Wang, Y. Lee, V. Bright, University of Colorado, Boulder, USA</i>	AP
9	4:50	Modeling and design of reconfigurable antenna arrays including MEMS switches, <i>K. Sabet*, T. Ozdemir, J. Cheng, EMAG Technologies, K. Sarabandi, L. Katehi, The University of Michigan, G. Creech, P. Watson, Air Force Research Laboratory, USA</i>	98
10	5:10	TM mode analysis of a Sievenpiper high-impedance reactive surface, <i>R. Diaz*, J. Aberle, Arizona State University, W. McKinzie, Atlantic Aerospace Electronics, USA</i>	AP
11	5:30	Mechanically conformal and electronically reconfigurable apertures using low voltage MEMS and flexible membranes for space based radar applications, <i>J. Bernhard*, N.-W. Chen, R. Clark, M. Feng, C. Liu, P. Mayes, E. Michielssen, University of Illinois at Urbana-Champaign, J. Mondal, Northrop Grumman Corporation, USA</i>	99

MEMs in Microwave Antennas

John K. Smith
DARPA
Arlington, VA 22203

This talk will discuss the use of MicroElectroMechanical (MEMs) devices in future microwave antennas. MEMs are important because they are built using low cost integrated circuit processing technology. In recent years, advanced radar has come to mean solid state electronically scanned Array (Active ESAs). MEM RF switches and components may provide a cheaper, lighter alternative for some applications. This talk discusses large ESAs which use MEMs components, such as the MEM-tenna. This concept will bring down the cost, weight, and power consumption of these radars, while retaining many of the high-end capabilities including beam agility. Additionally the use of MEMs in wide bandwidth antennas and geometrically re-configurable antennas is being explored in the RECAP program. Application in high impedance surfaces, Reconfigurable elements, tunable filters, multilayer interconnects, and flexible substrates will be discussed.

A Reconfigurable Slot Aperture

R. Gilbert⁺⁺, D. Kopf⁺⁺ and J. Volakis^{**}

⁺⁺ Sanders, A Lockheed Martin Co.
95 Canal Street
P.O. Box 868
Nashua, NH 03060-0868

^{**} Radiation Laboratory
Electrical Engineering and Computer Science Dept.
University of Michigan
1301 Beal Ave
Ann Arbor, MI 48109-2122

The increasing demand for RF connectivity to support the bandwidth requirements of modern platforms, which have reduced real estate for antennas, must be met with new apertures that have broad instantaneous and reconfigurable bandwidth, reduced volume, and increased efficiency. The Sanders/University of Michigan Reconfigurable Aperture (RECAP) concept is addressing this need with a structurally integrated antenna that is comprised of an array of dual-polarized slot antenna elements whose dimensions can be altered with photonically activated RF MEMs switches. These elements are integrated into the top layer of a multilayered composite structure comprised of passive frequency selective surfaces (FSS) that form a broadband ground plane system that presents a constant impedance surface to the slot radiators over the whole operational frequency band. Therefore, the effective electrical height of the radiator above the ground plane remains the same in terms of wavelength as the operating frequency changes. A reduction in the overall array thickness is realized as a result of the increased artificial dielectric constant of the FSS ground plane. The reconfiguration of cavities behind the slot elements is being investigated as an additional degree of freedom to improve element gain and efficiency. The array is capable of scanning grating lobe-free beams over more than two octaves bandwidth while maintaining near $\lambda/2$ spacing between elements. The reconfigurable aperture concept is described in this paper and predicted performance data from a 3×3 -element array panel operating from 800 MHz to 3500 MHz will be presented.

MODELING AND DESIGN OF RECONFIGURABLE ANTENNA ARRAYS INCLUDING MEMS SWITCHES

Kazem F. Sabet[§], Tayfun Ozdemir[§], Jui-Ching Cheng[§], Kamal Sarabandi^{§§}, Linda P.B. Katehi^{§§}, Gregory L. Crech^{§§§} and Paul M. Watson^{§§§}

[§] EMAG Technologies, 3055 Plymouth Rd, Suite 205, Ann Arbor, MI 48105

^{§§} Dept. of EECS, The University of Michigan, Ann Arbor, MI 48109-2122

^{§§§} Air Force Research Laboratory, AFRL/SNDM, Wright-Patterson AFB, OH 45433-7327

With the growing demand for diverse communication services, the ability to transmit and receive multiple frequency bands has become an urgent priority. Reconfigurable antennas offer a viable solution to the problem of wavelength diversity. A reconfigurable antenna is one that can be changed in near-real time to match more than one operating wavelength. The concept of aperture reconfiguration can be extended to include control of radiation pattern through changing the receiving/transmitting elements of the antenna in near-real time. The leading technology for a reconfigurable antenna system is based on switchable antenna elements in conjunction with multilayer substrate configurations. The design of the antenna array, its associated switching and bias control network, and the underlying multilayer substrate is a complex electromagnetic design problem. The design of these antennas requires rigorous full-wave numerical techniques to account for the electromagnetic coupling among various constituents of the structure.

In a reconfigurable antenna array, switching the radiating elements on and off varies the overall aperture size to accommodate different operational wavelengths or to achieve different pattern characteristics. With the recent advances in micro-electromechanical systems (MEMS), miniature micromechanical switches with low actuation voltages have been developed that rival the performance of conventional microwave solid-state switching devices such as pin diodes. The design of reconfigurable systems involving MEMS switches must take into account the presence of such devices and their bias circuits as they may couple electromagnetically to the radiating elements. The switches by themselves exhibit non-ideal characteristics such as fringing capacitance. As such, the use of ideal ON/OFF switch models for the design of the array may lead to inaccurate results.

In this paper, we present a hybrid approach to the modeling and design of complex reconfigurable antenna arrays. The radiating elements and their corporate feed network are modeled using the method of moments (MoM) for fast and accurate results. The MEMS switches and their bias circuits are modeled using the finite element method (FEM). Equivalent circuits or lumped element models are developed for the switching devices using analytical and neural network techniques. If necessary, the assembly of the radiator/switch (compound element) may be modeled together to account for any coupling effects. Then, macromodels are generated for the circuit and radiation characteristics of the compound elements based on full-wave simulation data. Moreover, full-wave-based macromodels are also developed to characterize the coupling among adjacent compound elements. These models are then combined to provide a fast solution of the problem within a good approximation including inter-element coupling effects. The overall array is optimized to achieve the given circuit and radiation characteristic goals using optimization techniques based on genetic algorithms and neural network models.

**MECHANICALLY CONFORMAL AND ELECTRONICALLY
RECONFIGURABLE APERTURES USING LOW VOLTAGE
MEMS AND FLEXIBLE MEMBRANES
FOR SPACE BASED RADAR APPLICATIONS**

J. Bernhard*, N.-W. Chen, R. Clark, M. Feng, C. Liu, P. Mayes, E. Michielssen,
*Department of Electrical and Computer Engineering
University of Illinois at Urbana-Champaign
and J. Mondal
Northrop Grumman Corporation*

A new integrated wide band reconfigurable aperture array with associated wide band T/R functions on a flexible and foldable/rollable substrate for space based radar applications is proposed.

Advanced MEMS and packaging techniques are used to make the antenna array light weight, mechanically and electrically reliable, and reproducible. Soft flexible substrates make the antenna foldable/rollable with the associated electronics on the opposite side of the substrate. The individually reconfigurable antenna element, which is suitable for inclusion in a large array, uses MEMS switches to select frequency bands of operation. These MEMS switches have low actuation voltages and stress-free operation, improving the reliability of individual array elements and the array as a whole.

The reconfigurable antenna element is based on a low-profile conical radiator that provides greatly increased instantaneous bandwidth over microstrip patch antennas currently in place for phased array applications. Voltage-controlled MEMS switches are utilized so that the antenna element is capable of covering multiple bands, either contiguous or disparate, with each band having broad instantaneous bandwidth.

Preliminary experiments have produced antenna elements with over 15% instantaneous bandwidth and 23% effective bandwidth achieved with one reconfiguration (3 switches). (The goal for contiguous effective bandwidth is 50%.) Design parameters under investigation include the element's shape, its position relative to the ground plane, the feed point design, and the number of sub-radiators included in the antenna as well as tuning element values and their positions on the antenna structure. The experimental results are backed up by computational data obtained using a novel low frequency, integral equation-based time domain solver.

Array Design

Co-chairs:	S. Sanzgiri, Boeing Defense and Space Group	Page
	T. Milligan, Milligan & Associates	
1	1:50 X band aperture coupled active microstrip patch antenna array, <i>H. da Silva*</i> , Instituto Superior de Engenharia de Lisboa, M. Rosario, C. Peixeiro, Instituto Superior Tecnico, Portugal	102
2	2:10 An alternating-phase feed for single-layer slotted waveguide arrays, <i>J. Coetzee*</i> , H. Xu, National University of Singapore, Singapore	103
3	2:30 Using reconfigurable PBG structures for phase shifting in a planar phased array, <i>B. Elamran, I-M. Chio, L-Y. Chen, J-C. Chiao*</i> , University of Hawaii, USA	104
4	2:50 Adaptive antenna concept based on actively driven non continuous elements for handset configuration, <i>L. Desclos*</i> , NEC USA Inc., USA, E. Hankui, T. Harada, NEC, Japan, M. Madhian, NEC USA Inc., USA	105
5	3:10 Analysis of arrays of smoothly flared rectangular corrugated horns, <i>L. Salghetti*</i> , A. Freni, University of Florence, S. Maci, University of Siena, Italy	106
	3:30 Break	
6	3:50 All-angle grating lobe suppression for fixed-beam arrays with wide element spacing, <i>A. Hart*</i> , L. Pearson, Clemson University, USA	107
7	4:10 Antenna aspects of Techsat21 - a distributed space-based radar system, <i>J. Schindler, H. Steyskal*</i> , P. Franchi, R. Mailloux, Air Force Research Laboratory, USA	108
8	4:30 Coaxial continuous transverse stub (CTS) array, <i>Z. Zhang*</i> , M. Iskander, Z. Yun, University of Utah, USA	AP

X Band Aperture Coupled Active Microstrip Patch Antenna Array

Henrique José da Silva^{1*}, Maria João Rosário², Custódio Peixeiro²
Instituto de Telecomunicações, Lisboa, Portugal

¹*Instituto Superior de Engenharia de Lisboa,
Lisboa, Portugal*

²*Instituto Superior Técnico
Lisboa, Portugal*

Active microstrip patches are widely used in the nowadays very hot topic of adaptive (smart) antennas. Following previous studies, aiming low costs production and ideal trade-offs for the active circuits and antenna substrates (H. J. da Silva, M. J. Rosário, C. Peixeiro, *X Band Aperture Coupled Active Microstrip Antenna*, to be presented at AP2000 Conference, Davos, Switzerland, April 2000), this work presents the design of an X band aperture coupled active microstrip patch antenna array, for reception. The simulated and measured results are commented and compared to the results obtained with an identical passive array, also designed and tested in the scope of this presentation.



Figure 1: Prototype of the X band active array. Front and back view

Both, the passive and the active arrays, are linear and composed by four 7.5 mm square radiating patches, printed on a RT/Duroid 5880 ($\epsilon_r=2.2$) substrate, with a thickness of 1575 μm . The microstrip feed lines are printed on a RT/Duroid 6010 ($\epsilon_r=10.2$) substrate, with a thickness of 1270 μm . The distance between the elements is $\frac{3}{4}\lambda_0$. To reinforce the contact, mainly at the slot and patch zone, the patch substrate has been smoothly curved, operating has a spring, and five plastic screws force the substrates one against the other. The active device to be integrated in each one of the patches, is an LNA, designed and fabricated with a standard 0.5 μm GaAs-MESFET technology. It presents a noise figure of 3.5 dB, 15 dB controllable gain, 2 GHz bandwidth, simultaneously input port signal and noise match and S_{22} better than -10 dB. This amplifier is chip on board assembled and wire bond connected to the feed lines, considering a new interconnection model for higher thickness, lower permittivity substrates.

The described active array presents a high improvement of gain, an input return loss less than -10 dB in a 20 % bandwidth, and the H plane beam width is 20° in opposition to the 120° beam width of the E plane.

An Alternating-Phase Feed for Single-Layer Slotted Waveguide Arrays

J.C. Coetzee* and H.Y. Xu

Department of Electrical Engineering, National University of Singapore, 4 Engineering Drive 3, Singapore 117576

A planar slot array consists of a number of slotted waveguides (branch lines) placed in a side-by-side configuration. Conventionally, branches are shorted at both ends, while they are fed by means of a separate feed waveguide (main line) running beneath and at a right angle to the branch lines, while inclined coupling slots connect each branch line to the main line. The manufacturing of this configuration is complex, and generally not suitable for mass production. Single-layer arrays have the advantages of a low profile, and generally being easier to manufacture. In the design of planar arrays, it is desirable to have the freedom of varying the power levels fed into each branch, and also to allow for unmatched branch line input impedances. This affords greater control over the radiating slot offsets from the branch centerline and avoids the necessity of, and problems associated with, excessively large or small offsets for radiating elements. This paper describes the design and analysis of a single-layer alternating-phase array feed where the main line feeds the branches via a series of T-junctions, as shown in Fig. 1. The design procedure accommodates varying branch line input admittances and arbitrary power split ratios, while ensuring an impedance match at the input of the feed waveguide. A simple equivalent network approach for the off-center frequency analysis of the feed network is also proposed. Measured results for a prototype feed network confirm the theory.

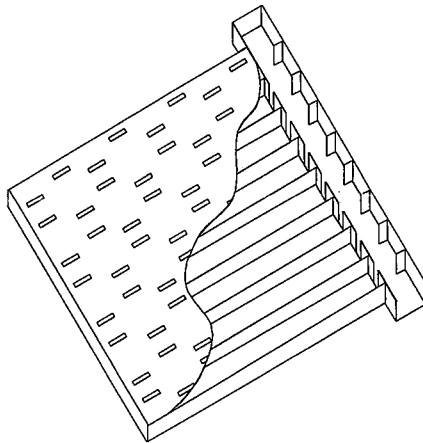


Fig. 1 A planar slotted waveguide array fed by a single-layer alternating-phase feed network.

Using Reconfigurable PBG Structures for Phase Shifting in a Planar Phased Array

Balasundaram Elamaram, Iao-Mak Chio, Liang-Yu Chen and Jung-Chih Chiao*
 Department of Electrical Engineering, University of Hawaii at Manoa

Electronic beam-steering allows radiation beams shift fast so that targets can be tracked more efficiently in the radar applications and networks can be reconfigured with high efficiency and flexibility in the wireless communication applications. Electronic beam-steering can be achieved by linear phase variation, provided by phase shifters in the feed networks, across an antenna array. However, this usually requires many phase shifters and the number of phase shifters scales with the number of antennas in the array. Solid-state phase shifters are expensive and have high losses at millimeterwaves. In this work, we demonstrated the feasibility of using switches to reconfigure the arrangement of a photonic band gap (PBG) structure in the ground plane of microstrip lines to achieve phase shifting for the phased-array antennas. Because the reconfiguration is done in the ground plane, the insertion loss should be lower than the one of solid-state phase shifters. Microstrip-line photonic band gaps are periodic metal patterns in the ground plane. [“Novel architectures for high-efficiency amplifiers for wireless applications,” *IEEE Trans. Microwave Theory Tech.*, Nov. 1998] They have been shown to produce frequency dependent amplitude characteristics. In this work, we present the phase characteristics of PBG and use this feature to provide phase shifts for a patch-antenna beam-steering array.

Figure 1 shows the configuration of a patch-antenna array with PBG holes in the ground plane under each microstrip line fed to the antenna. The propagation constant of a microstrip line with etched PBG holes in the ground plane is higher than the one with a normal ground plane. A four-element microstrip patch-antenna array was designed to operate at 5.6GHz with 18 PBG periods for each feed line. A Duroid board with $\epsilon_r=2.2$ and a thickness of 0.508mm was used. The PBG period is 10.9mm and the radius of the holes is 2.7mm. Fig.2 shows the measured phase shifts at 5.6GHz for different numbers of PBG periods. The maximum phase shift for 18 periods is 232° . The phase shifts are proportional linearly to the numbers of PBG periods.

Discrete beam-steering patterns were obtained by covering linearly-varying numbers of PBG periods among four antenna elements with conductive tape. The conductive tape imitates the closed state of switches across the PBG holes. The steered patterns are shown in Fig.3. The patterns are individually normalized, however, the relative peak powers of different patterns vary by less than 2 dB, which indicates the maximum insertion loss added by 18 PBG phase-shifting periods. The beam-steering angle varies linearly as the number of PBG periods is varied and a maximum beam-steering of 35° is obtained. Theoretical patterns, calculated by the phased-array factors and the patch antenna pattern, agree with the measurements. E- and H-plane patterns with both co- and cross-polarizations were measured for each case. The co-/cross-pol isolation is better than 12dB in all cases.

The effective distances between PBG holes change as the operating frequency changes. Therefore, for a fixed configuration of PBG arrangement, the beam can be steered with carrier frequencies. A beam-steering angle of 15° was achieved by changing the operating frequency from 5 GHz to 6 GHz.

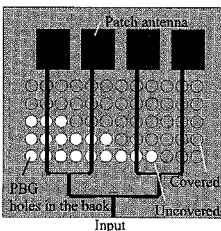


Figure 1: The 4-element patch-antenna array with the PBG holes in the ground plane.

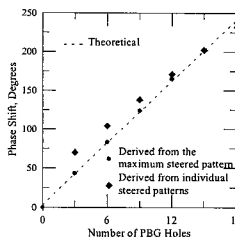


Figure 2: Measured phase shifts for different numbers of PBG holes in the ground plane.

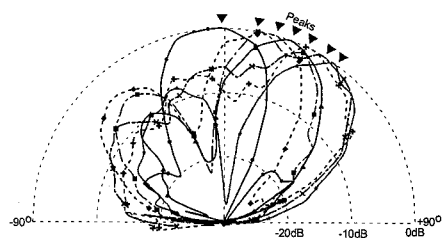
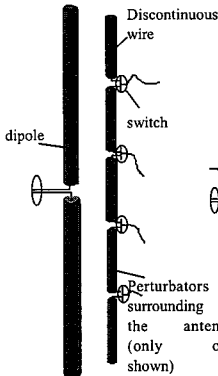


Figure 3: Measured beam patterns for different ground-plane configurations. The array steers in increments of approximately 6° . The maximum steering angle is 35° for an 18-period PBG ground plane.

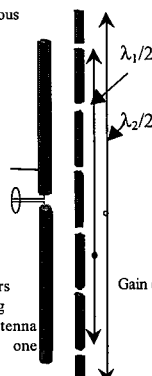
Adaptive antenna concept based on actively driven non continuous elements for handset configuration

L.Desclos, E. Hankui*, T. Harada*, M. Madihian
 NEC USA Inc., CCRL, Princeton, * NEC, EMC Engineering Center, Japan

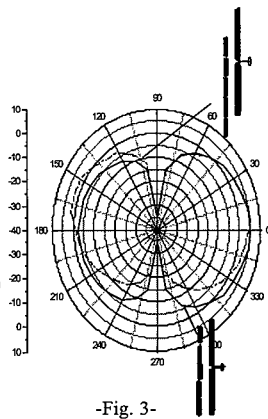
Summary: The multimedia communication systems require more and more features from the antenna such as diversity or multi frequency. One of the main concerns for the actual handset or portable antenna is how to cope with possible obstacle in near field as well as multi-frequency transmission support. Several authors have already addressed these points independently. However, none of them has addressed both problems at the same time. One of the aims of this presentation is to introduce a configuration - Fig. 1- based on an active principle, commuting continuous wires to discontinuous ones. Switches are used in this case to control the beam of a surrounded dipole. When the discontinuous wires assembly surrounds the dipole (or other antenna), the perturbing elements are not resonating at the working frequency. Therefore the radiation of the primary source is unchanged. However, as the wires are used as resonating perturbators the diagram will be changed. As the wires surrounding the emitting/receiving antenna are discontinuous ones or not, the control of the beam is achieved. This duality could be obtained by connecting active elements between each portion of wire and through a control voltage allowing turning them short or open, i.e. continuous or discontinuous. An advantage over already published work [R.G. Vaughan, IEEE TAP, Feb. 1999] is that, by switching the parasitic elements on and controlling independently the lengths of the antenna perturbators it is possible to adjust to different frequencies -Fig.2-. Since, in a dipole case the perturbator could be adjusted at $\lambda/2$ or $\lambda/4$ and in a monopole case it is at $\lambda/4$ or $\lambda/2$. The source in this case could be a multi frequency broadband dipole or monopole or any multi frequency element. Also, by making longer the perturbator the beam can be steered in a vertical direction too- Fig.3-, as the resonating length could be electronically moved from up to down position. In this case the pattern in Fig.3 shows a modification in elevation as the perturbing elements are in regards or slightly above the dipole. Experiments have been conducted on a dipole working at 900 MHz, surrounded by short wires of 1mm diameter placed as less than 1 cm and connected with FET's as switches. Measurements in near field show that it is possible to control actively the distribution of energy therefore the beam. Several considerations on the implementation will be shown in the conference.



- Fig. 1-



-Fig.2-



-Fig. 3-

ANALYSIS OF ARRAYS OF SMOOTHLY FLARED RECTANGULAR CORRUGATED HORNS

L. Salghetti*, A. Freni

Dept. of Electronic Engineering, University of Florence
Via S.Marta 3, I-50139 Florence, Italy
Email: luca.salghetti@cse.it, freni@unifi.it

S. Maci

Dept. of Information Engineering, University of Siena
Via Roma 56, I-53100, Siena, Italy
Email: macis@ing.unisi.it

Rectangular horn antennas are widely used as primary feed for reflector antennas. In particular, because of their property of having different beamwidths in the two principal planes of radiation, the rectangular horn is the right candidate for the use as feed for elliptical reflectors. In order to predict the performance of a reflector antenna accurately, it is important to have an accurate characterization of the feed horn. Feed characterization is particularly important for accurate prediction of the cross-polar power level of a reflector, because this latter is in most of part determined by the cross-polar field radiated by the feed horn. It is then important the development of accurate and efficient electromagnetic algorithms for the design of these antennas. To this end the generalized admittance matrix (GAM) method seems to be the most adequate technique. In [L.D. Salghetti, A. Freni and S. Maci, "A CAD oriented, Generalized Admittance Matrix approach for arbitrarily corrugated Eplane sectoral horns," *IEE Microwave Antennas and Propagation*, vol. 146, n. 5, 1999, pp. 329-334] the GAM method was efficiently used to study E-plane corrugated sectoral horns; in most practical applications it is convenient to realize in these horn a gradual smooth flare in the other plane in order to enhance directivity. In this paper, the algorithm is then extended to E-plane corrugated horns smoothly flared on the H-plane and to H-plane corrugated horns smoothly flared on the E-plane. The GAM is formulated here by using longitudinal section electric (LSE) modes to expand the tangential field in the internal part of the horn. For this internal part, the two sets of LSE modes (LSE^x and LSE^y) are rigorously uncoupled, and the only coupling between the two basis is obtained when the Green's function of the free space is used in the analysis the radiating aperture. In this way the behavior of the horn in terms of reflection coefficient and radiation pattern can be accurately predicted without a relevant numerical effort. When a flare in both planes is realized, the assumption of uncoupling between LSE^x and LSE^y mode expansion loses validity. However, for small flare angles these cross-polarized modes are weakly excited thus yielding a negligible influence on the input reflection coefficient and a minimum contribution on the cross-polar power radiated by the feed. On the other hand, the approximation introduced significantly reduces the overall computation time. As application of the proposed method the design of an array of mixed E-plane and H-plane corrugated horns will be presented. The cross coupling between LSE^x and LSE^y modes pertaining to different apertures are been taken into account by properly including in the integral equation analysis which represents the continuity of the magnetic field through the apertures, the reaction integral calculated on the basis of [T. Bird, "Analysis of mutual coupling in finite arrays of different-sized rectangular waveguides," *IEEE Trans. Antennas Propagat.*, vol. AP-38, 1990, pp. 166-172].

All-Angle Grating Lobe Suppression for Fixed-Beam Arrays with Wide Element Spacing

A. K. Hart* and L. W. Pearson, Holcombe Department of Electrical and Computer, Clemson University, Clemson, South Carolina 29634-0915
(pearson@ces.clemson.edu)

Sehm, Lehto, and Raisanen (*IEEE Trans. Antennas and Propagat.*, 47 (1), July, 1999, pp. 1125-1130) have devised two means of suppressing grating lobes that arise in a large, fixed-beam array with element spacing of 1.8λ in one dimension. These authors employ two tools simultaneously in achieving principal-plane grating lobe suppression. First, they employ a so-called box horn element in the array (Silver, *Microwave Antenna Theory and Design*, Peter Perigrinus, 1984) to place element pattern nulls at the precise angles at which the array factor presents grating lobes. Second, they subdivide the array and introduce a lateral shift between the two resulting subarrays. This shift may be chosen so that the array factor associated with interaction between the two subarrays possesses a null at the location of the grating lobes in the principal planes of the array.

In this presentation, we demonstrate that for a separable array excitation, one can, in principle, design *separable aperture distributions* in the elements, and pair factors in such a way that

$$F_{\text{tot}} = F^H(\gamma_x)F^E(\gamma_y)AF^H(\gamma_x)AF^E(\gamma_y),$$

where F and AF are respectively element and array factor patterns, each of which has been factored. The superscripts designate E - and H -plane factors, while $\gamma_x = kd_x \cos \phi \sin \theta$ and $\gamma_y = kd_y \sin \phi \sin \theta$ are the x - and y -oriented far-field wavenumbers. Clearly by pairing like orientations of element factors and array factors, and placing zeros in the element pattern at the grating lobe peak in the array factor, one can achieve grating lobe suppression for *all* γ_x and γ_y and hence for all observation angles (θ, ϕ) .

The forgoing discussion clearly holds in principle, but raises questions regarding the realizability of the necessary separable element patterns. Their separability can be ensured by restricting their aperture distributions to comprise only a select set of modal patterns. Any field constituents apart from the acceptable mode set constitutes "contamination" field, which compromises the grating-lobe cancellation originally sought.

Computed examples are presented to support the assertions here and to evaluate the practicability of all-angle grating lobe suppression.

Antenna Aspects of TechSat21 – A Distributed Space-Based Radar System

J. Schindler, H.Steyskal*, P. Franchi, R. Mailloux,
AF Research Lab./SNH, Hanscom AFB, MA 01731, USA

The TechSat21 concept involves a distributed cluster of small satellites operating cooperatively to perform a surveillance mission. The primary focus is for Moving Target Indication (MTI) radar mode. A baseline assumption is, similar to the French RIAS system (Dorey et al: RIAS, Radar a Impulsion et Antenne Synthetique. Int'l Conf. on Radar, Paris, Apr. 1989), that the individual satellites transmit different frequencies, but receive all the reflected signals at the frequencies transmitted by the other satellites in the cluster. In addition, it is assumed that the positional accuracy can be sensed to within a fraction of a wavelength so that signals can be combined coherently.

Each satellite has roughly a 4 m² phased array operating at about 10 GHz, other typical parameters are 4 to 20 satellites per cluster, cluster diameters 100 to 1000 meters, and orbits 700 to 1000 km above Earth. Orbital mechanics constrain the satellites to move either linearly along track or to local orbits around a reference point in a global orbit, such that their projections on a vertical plane form 2:1 ellipses.

The cluster forms essentially a multi-element interferometer, whose diameter is driven by the high angular resolution corresponding to the desired minimum detectable doppler velocity. The grating lobes inherent in an interferometer pose significant problems in avoiding ambiguities and achieving the desired radar performance. Research studies are ongoing to explore pattern synthesis in angle-frequency space to resolve these problems.

Our present approach considers a vertical planar 19-element array with a triangular lattice, such that the grating lobes are highly periodic in angle. This imposes a periodicity on the doppler spectrum of the received clutter signal. A second periodicity is imposed by the radar pulses which are transmitted periodically in time. By judicious choice of the pulse repetition frequency these two periodic signal frequencies can be aligned and suppressed by a common doppler filter. This would then leave "windows" between these spectral lines through which targets can be detected.

Although simple in principle, the approach is complicated due to the curvature and rotation of the Earth and the rotation of the array around its geometric center, which continuously changes the grating lobe structure. – Results of this ongoing study will be reported.

Electromagnetic Properties of Materials

Chair: M. Stuchly, University of Victoria, Canada

Page

- | | | | |
|---|------|---|-----|
| 1 | 1:50 | On the relations of microscopic and averaged material parameters in composite media, <i>P. Belov*</i> , <i>CR. Simovski</i> , <i>M. Kondratjev</i> , <i>St. Petersburg Institute of Fine Mechanics and Optics, Russia</i> | AP |
| 2 | 2:10 | Electromagnetic characterisation of building materials at 5.8 GHz using transmission and reflection measurements, <i>I. Cuinas*</i> , <i>M. Sanchez</i> , <i>Universidade de Vigo, Spain</i> | AP |
| 3 | 2:30 | Calculation of effective permittivity for a 2-D periodic composite, <i>F. Wu*</i> , <i>K. Whites</i> , <i>University of Kentucky, USA</i> | AP |
| 4 | 2:50 | Phase characterization of ferromagnetic materials using a coplanar waveguide, <i>A. Brown*</i> , <i>University of Michigan</i> , <i>L. Kempel</i> , <i>Michigan State University</i> , <i>J. Volakis</i> , <i>University of Michigan, USA</i> | AP |
| 5 | 3:10 | Computation of the effective propagation constants for a planar interface between two lossy uniaxial media, <i>J. Roy*</i> , <i>Communications Research Centre Canada, Canada</i> | AP |
| | 3:30 | Break | |
| 6 | 3:50 | SrTiO ₃ multilayers for microwave applications: fabrication and dielectric properties, <i>P. Joshi*</i> , <i>M. Cole</i> , <i>E. Ngo</i> , <i>C. Hubbard</i> , <i>US Army Research Laboratory, USA</i> | 110 |
| 7 | 4:10 | Fabrication and characterization of doped barium strontium titanate thin films for tunable device applications, <i>M. W. Cole*</i> , <i>P. C. Joshi</i> , <i>US Army Research Laboratory, USA</i> | AP |

SrTiO₃ multilayers for microwave applications: Fabrication and dielectric properties

P. C. Joshi*, M. W. Cole, E. Ngo, and C. Hubbard
US Army Research Laboratory,
Weapons and Materials Research Directorate,
Aberdeen Proving Ground, MD 21005

SrTiO₃ is an attractive material for the development of tunable microwave devices due to field dependent dielectric permittivity, low dielectric loss, good insulating behavior, and good high-frequency characteristics. SrTiO₃ is expected to retain its good dielectric properties at microwave frequencies. However, it is important to reproduce the bulk properties in thin films as the thin film properties are strongly influenced by the method of preparation, nature of substrate, growth and microstructure, film-substrate interfacial characteristics, and contact metallization. In the present paper, we report on the fabrication of SrTiO₃ thin films by metalorganic solution deposition technique using room temperature processed carboxylate-alkoxide precursor solution. The films have been fabricated on Pt-coated silicon, bare silicon, and MgO substrates. The films have been characterized in terms of microstructural, dielectric, and insulating properties. The electrical measurements have been conducted on films in metal-insulator-metal (MIM) and metal-insulator-semiconductor (MIS) configurations. The tunability of the films has been calculated from capacitance-voltage (C-V) characteristics. The effects of film thickness and post-deposition annealing temperature on the microstructural and electrical properties have been analyzed. The temperature and bias-stability of the dielectric properties have also been analyzed. Dielectric loss and tunability are the two most important parameters for the realization of SrTiO₃ thin film based microwave devices. Attempts have been made to enhance the dielectric properties of SrTiO₃ thin films by using several multilayer schemes involving amorphous and crystalline dielectric layers. The dielectric and insulating properties of various SrTiO₃ multilayers have been compared to establish the potential of SrTiO₃ thin films for integrated microwave devices.

Remote Sensing of the Earth's Surface and Atmosphere

			Page
Co-chairs:		P. Pampaloni, CNR-IROE, Italy	
		D. Long, Brigham Young University	
1	1:50	Model-based Sea Winds on QuikSCAT ground station calibration analysis, <i>P. Yoho*</i> , <i>A. Anderson</i> , <i>D. Long</i> , Brigham Young University, USA	112
2	2:10	SeaWinds views Greenland, <i>I. Ashcraft*</i> , <i>D. Long</i> , Brigham Young University, USA	113
3	2:30	A scanning radar altimeter for geographic terrain monitoring and mean sea level data collection, <i>D. Zaugg*</i> , <i>D. Arnold</i> , <i>M. Jensen</i> , Brigham Young University, USA	114
4	2:50	An improved model for determining the electromagnetic bias, <i>F. Millet*</i> , <i>D. Arnold</i> , Brigham Young University, USA	115
5	3:10	YINSAR: A compact, low-cost interferometric synthetic aperture radar - current status, <i>D. Thompson</i> , <i>R. Lundgreen*</i> , <i>D. Arnold</i> , <i>D. Long</i> , Brigham Young University, USA	116
	3:30	Break	
6	3:50	Stationary "cross-track" interferometry for ocean wave measurement, <i>D. Thompson*</i> , <i>D. Arnold</i> , Brigham Young University, USA	117
7	4:10	A low cost, radio controlled blimp as a platform for remote sensing, <i>B. Walkenhorst*</i> , <i>G. Miner</i> , <i>D. Arnold</i> , Brigham Young University, USA	118
8	4:30	Modeling backscattering from leafy vegetation, <i>G. Macelloni</i> , CNR-IROE, Italy, <i>F. Marliani</i> , ESA-ESTEC, The Netherlands, <i>S. Paloscia</i> , <i>P. Pampaloni*</i> , CNR-IROE, Italy	119
9	4:50	Carrier-to-interference (C/I) statistics on a dual polarized double diversity satellite system including ice crystals and raindrop canting angle effects, <i>J. Kanellopoulos</i> , <i>T. Kritikos</i> , <i>A. Panagopoulos*</i> , National Technical University of Athens, Greece	120
10	5:10	Slant path measurements at 50 GHz in Madrid: attenuation by gases and clouds, <i>K. Al-Ansari</i> , <i>P. Garcia</i> , <i>J. Riera</i> , <i>A. Benarroch*</i> , Polytechnic University of Madrid, Spain	121
11	5:30	Determining snow accumulation and ablation rates on the Greenland ice sheet using SSM/I radiometer and ERS scatterometer data, <i>J. Pack*</i> , <i>J. Wallace</i> , <i>M. Jensen</i> , Brigham Young University, USA	122

Model-based SeaWinds on QuikSCAT Ground Station Calibration Analysis

Peter Yoho*, Arden Anderson, David G. Long
Brigham Young University, 459 Clyde Building, Provo, UT 84602
Telephone (801) 378-4884, Facimile (801) 378-6586

SeaWinds on QuikSCAT is the latest of NASA's wind-observing scatterometer missions. It was launched in June of 1999 with the goal of accurately measuring wind fields over all the oceans. It has also proven to be valuable in monitoring ice changes in polar regions. The value of such data necessitates an extremely accurate and precise calibration of both satellite performance and instrument measurements. In order to assure optimal performance a Calibration Ground Station was constructed, which provides direct measurements of the instrument transmissions.

The Calibration Ground Station, or CGS, is located in White Sands, NM. Each time the spacecraft flies overhead, approximately twice a day, the CGS passively captures microwave pulses transmitted from QuikSCAT. The data is then used with various processing and analysis techniques. As part of the calibration analysis, a software simulation model of the instrument system has been constructed. This model is able to simulate critical instrument systems and path loss characteristics and thus predict CGS receive data for any given satellite pass. By comparing model-based simulation data with actual recorded CGS data, calibration of parameters such as timing, power, attitude, and Doppler compensation can be accurately determined.

Initial calibration revealed a one second spacecraft time tag error, which was subsequently corrected. The analysis has also been able to validate the antenna rotation speed and mounting alignment, STALO drift, the Doppler/range compensation algorithm, and other key system operational parameters.

A major contribution of the CGS-based analysis is demonstration of pointing accuracy and overall system stability of SeaWinds. By employing a variance minimization technique between simulated and actual data, the QuikSCAT platform is shown to be extremely stable. This has allowed for precision measurement of ocean wind vectors and polar ice formation, key factors in the global weather cycle.

SeaWinds Views Greenland

Ivan S. Ashcraft and David G. Long
Brigham Young University
459 Clyde Building
Provo, UT 84602

ashcraft@ee.byu.edu voice: (801) 378-4381 fax: (801) 378-6586

The location of key snow and ice zones, or facies, in Greenland is considered a sensitive indicator of global climate change. Data from NASA's new Ku-band SeaWinds scatterometer has been used to map the extent of the facies in Greenland. The wide swath, rapid coverage, and dense sampling of the SeaWinds scatterometer has made it possible to produce daily morning and evening radar backscatter images of Greenland. This provides an unprecedented opportunity to investigate the diurnal variations over the summer melt extent and derive error bars on facies estimates made using multi-day periods as has been done with previous scatterometers. Using resolution enhancement techniques, the spatial resolution of these images has been increased from the native ~25 km resolution of the raw SeaWinds measurements to a pixel resolution of 4.5 km.

The temporal signature of the SeaWinds measurements has been used to map the extent of the different Greenland snow zones. The wet snow zone was identified by a significant drop in the radar backscatter measured by SeaWinds over the melt period. This decrease in backscatter is a result of the liquid moisture content in the melting snow. The end of a melt period is indicated by a sharp increase in the backscatter caused by the formation of ice pipes and lenses, a result of the liquid moisture percolating down through the snow during the melt event. Using these aspects of the temporal signature of the SeaWinds data, the length in days of the summer melt event for each pixel was determined. Using the diurnal temporal resolution of the SeaWinds data, the extent of the daytime melt and night-time freeze for each day has also been measured.

The estimated facies map derived from SeaWinds data has been compared with facies maps derived from ERS, NSCAT, and SASS data to evaluate possible changes in the facies location over a multi-decade period. The possibility of using SeaWinds data to determine snow accumulation over the percolation and dry snow zones has also been investigated.

A Scanning Radar Altimeter for Geographic Terrain Monitoring and Mean Sea Level Data Collection

David A. Zaugg*, David V. Arnold, Michael A. Jensen
CERS Lab, Brigham Young University

A scanning radar altimeter has been built which will be used in two experiments being conducted in remote sensing, one to improve the electromagnetic (EM) bias estimate, and the other to improve the technology for geographic terrain monitoring. It will be used to monitor the ocean off the coast of San Diego and map out a land slide area in Colorado over a period of time. For both of these experiments, the altimeter will be mounted on a blimp. In the EM bias experiment, different sea states will be monitored from the blimp-borne altimeter. The blimp-borne instrument will allow evaluation of the bias from different altitudes, and therefore will afford studies of the effect of radar footprint size on the bias. In the land slide experiment, the scanning capability of the altimeter will be used to create a topographical image of the surface. Images will be taken over a period of time to determine the characteristics of the land slide. Improving the EM bias estimate will improve the accuracy of the mean sea level data currently being taken by the TOPEX/Poseidon satellite and, in late 2000, to be taken by the Jason 1 satellite. The instrument for these studies exploits advanced system architectures with multiple receive channels to provide high resolution scanning capability at low cost. This research is being funded by NASA in support of the upcoming NASA/CNES Jason mission.

The scanning radar altimeter is capable of obtaining a topographical image of the target area or simply altimetry or backscatter data. It mixes a transmitted, chirped pulse with the returned copy of itself to find its range to the target. Since the chirp is linear, the result of the mixdown is a tone. The frequency of this tone can be used to find the range to the target. Several different interesting hardware solutions are used in the altimeter to achieve its objectives. The transmitter is an inexpensive linear chirp generator. The transmitter consists of feedback circuitry that linearizes the pulse. When the instrument calibrates itself, it counts the frequency of the VCO output at a sequence of different input voltages. By doing this, it generates a table of VCO input voltages that will produce a linearly chirped pulse on the output of the VCO.

The transmit and receive antennas are designed so that beamforming and timing information can be used to calculate the direction of the return from different points on the ground. The transmit antenna is a slotted rectangular waveguide array antenna. The field distribution is designed to provide a narrow beamwidth in the direction of travel of the blimp and a wide beamwidth perpendicular to the direction of travel. The receive antenna consists of an array of sixteen independently fed printed-slot loop antennas on PC board. The return received through each of these antennas is mixed with the transmitted signal, and the resulting tones are sampled. The data is recorded and post-processed. Beamforming is used to generate the topographical image in the axis perpendicular to the direction of travel by combining relative phase offsets with each of the signals and adding them together. Time-of-arrival information is used to generate the image in the axis along the direction of travel.

An improved model for determining the electromagnetic bias

Floyd Millet* and David Arnold
Center for Earth Remote Sensing
Brigham Young University
Provo, UT 84602

Traditional estimation models of the electromagnetic bias have focused on the correlation of the bias with wind speed, significant wave height, or a combination of the two. Recently, other studies have focused on correlations between other wave characteristics. Most notably wave slope and wave age have been used to estimate electromagnetic biases.

Recent literature has shown that wave slope characteristics are more highly correlated with electromagnetic bias than either wind speed or significant wave height. The analysis of two different experiments, the Gulf of Mexico Experiment (GME) and the Bass Strait, Australia Experiment (BSE), show a strong correlation between wave slope and electromagnetic bias. Determining which frequencies are most correlated to the electromagnetic bias have also increased the ability to determine the electromagnetic bias. Characteristics of the wave age have also been shown to improve the correlation of the data sets to the measured electromagnetic bias. An accurate determination of the correlation between the wave characteristics of slope and wave age will improve the ability to model the electromagnetic bias in the oceans of the world.

Additionally, a comparison of the wave characteristics from the GME and BSE revealed that there were fundamental differences in the wave spectra of these two areas of the world. These differences point to the possibility of regional differences in electromagnetic bias and wave slopes in the oceans of the world. Frequency component analysis of the GME and BSE data reveal profound differences in the data sets. Taking in to account these regional differences brings with it the possibility of creating a model based on the specific wave characteristics of each area of the world.

This project is funded by NASA in support of the upcoming Jason-1 satellite altimeter mission.

YINSAR: A Compact, Low-Cost Interferometric Synthetic Aperture Radar –Current Status

Douglas G. Thompson, Richard B. Lundgreen* , David V. Arnold, David G. Long
The Center for Earth Remote Sensing
Brigham Young University
459 CB
Provo, UT, USA 84602

Synthetic Aperture Radar (SAR) data is used to study many different aspects of the earth's surface. Many applications would benefit from a low-cost SAR that is simple to deploy. The low cost of deployment allows repeated imaging of a given area, at a cost within the budget of many small operations. Applications that may benefit from repeat-pass investigation include land change detection, landslide measurement and detection, mining, forestry, and archaeology. The theoretical possibility of using SAR data for many of these applications has been demonstrated, but the high cost of obtaining SAR data has prevented a full demonstration of the feasibility and practicality of the application of SAR data on a regular basis in these areas.

To address this need, BYU has developed a compact, low-cost interferometric SAR called YINSAR. Using commercial off-the-shelf components and standard PC parts throughout the system has kept the initial cost low. The instrument is carried in a small aircraft, which allows very low operational cost for data collection. Recent advancements in computer technology have made it feasible to use a standard PC for high-speed data storage. At the same time, improvements in digital-to-analog and analog-to-digital converters and other components of the digital data collection system allow us to build the chirp generation system and the entire IF portion of the radar digitally. Similar advances in RF components and circuitry allow these portions of the system to be built from semi-standard parts, reducing the size significantly while keeping the cost reasonable. The low altitude of the small aircraft allows us to use a relatively low-power transmitter. The low altitude can also improve the interferometric height resolution.

This paper presents the current status of YINSAR and shows images demonstrating the resolution of YINSAR and its potential for use in scientific studies. This project is funded by two NASA grants, the first to develop the instrument and the second to demonstrate its usefulness in geography and archaeology.

Stationary "Cross-track" Interferometry for Ocean Wave Measurement

Douglas G. Thompson, David V. Arnold
The Center for Earth Remote Sensing
Brigham Young University
459 CB
Provo, UT, USA 84602

Knowing the relationship between ocean wave characteristics and radar return is important in interpreting the data from scatterometers and altimeters. This paper describes and discusses a new method of characterizing that relationship using the ideas of cross-track interferometry in a stationary instrument. We use a real aperture radar with a narrow fan-beam antenna, mounted on a platform above the surface of the ocean. Range gating and matched filtering are used to obtain high resolution in the range direction, and the fan beam is narrow enough to illuminate a small spot in the cross-range dimension. Thus we obtain the radar returns from the water's surface in a plane formed by the range direction and the vertical axis. A second identical receiver is placed a short distance above the first, giving an interferometric baseline which is used to infer the wave height at each point. In this manner, we will be able to find repeated snapshots of the shape of the waves approaching the platform.

This instrument will be coupled with altimeters and scatterometers to study the relationship between the shape of the waves and the backscatter to each type of instrument. In this paper, we analyze the interferometric instrument through numerical simulations, probability theory, and actual data. Given a simulated wave shape, we determine the radar return from each point by assuming there are short waves riding on longer waves. The reflective properties of the short waves are affected by their position on the long waves, in a way described by a modulation transfer function. We use these principles to find the power returned from each point along the wave, then combine all these simulated returns to get the total simulated receive signal. The two channels are then combined interferometrically to generate the estimated wave shape, which is compared to the original. This process is repeated for various wave shapes, signal power, and noise power to see how each factor affects the height accuracy. We also analyze the instrument using the theoretical probability distribution functions associated with the problem for another estimate of the height accuracy and its dependence on various parameters.

The prototype version of this instrument will soon be deployed on a test platform at the edge of Utah Lake. We will use this test deployment to confirm the operation of the system and the theoretical height accuracy. The instrument we will use is a modified version of the railroad track hazard detection system recently developed for the Canadian National Railway.

A Low Cost, Radio Controlled Blimp as a Platform for Remote Sensing

Brett T. Walkenhorst*, Gayle F. Miner, David V. Arnold
Center for Earth Remote Sensing
Brigham Young University

With increasing interest, much of the electrical engineering community is turning to remote sensing for its varied uses in the areas of scatterometry, radiometry, altimetry, and others.

Among the current methods for deployment of these radars are satellites, platforms, and airplanes. We propose a small, unmanned, remote controlled blimp as a new platform for microwave remote sensing. Although blimps of this kind have been used for aerial photography, they have not as yet been applied in precision remote sensing. Among the advantages suggested are low cost, low maintenance, ease of deployment, and minimal personnel requirements.

Applications are given of typical radar systems for which a remotely controlled blimp is a suitable platform. Among these systems, we suggest microwave radar systems such as synthetic aperture radars (SAR), altimeters, and scatterometers. Such radar systems are currently used for archaeological and geological studies typically from aircraft or satellites, but we propose using a blimp as a low cost alternative for these systems.

As an example, we present an altimeter system designed to support NASA's Jason-1 launch. In support of this launch, testing is scheduled for work on landslide detection and mean sea level measurement. For the altimeter, the remote controlled blimp will be used as the platform to take these measurements.

The blimp's trajectory will be controlled by a computer controlled feedback loop to ensure stability. Testing for the blimp will be conducted as it is used in this altimetry study and the testing and the stability issue will be further discussed.

Modeling backscattering from leafy vegetation

Giovanni Macelloni¹, Filippo Marliani², Simonetta Paloscia¹ and Paolo Pampaloni^{1*}

¹ CNR-IROE, via Panciatichi 64, 50127, Florence, Italy.

² ESA-ESTEC, TOS-EEE, PB 299 -NL-2200 AG Noordwijk, The Netherlands

The availability of a considerable amount of Synthetic Aperture Radar data, obtained in recent years from airborne and spacecraft systems, has stimulated significant research for the purposes of interpreting backscattering data and investigating the potential of radar remote sensing for various applications. Vegetation has been one of the subjects most studied; however, most of the work has been carried out in forestry while less attention has been paid to agricultural crops. Experimental research has demonstrated that the microwave backscattering coefficient is sensitive to crop biomass, and is affected by the shape and dimensions of plant constituents (leaves and stems). On "broad leaf" crops, such as sunflower, backscattering increases with an increase in the biomass, as it is typical of media in which scattering is dominant. On the contrary, on "narrow leaf" plants, such as wheat, the trend is flat or decreasing, denoting a major contribution of absorption.

Theoretical simulations were performed with an incoherent radiative transfer model and with a coherent approach in which the scattered fields are added coherently and the attenuation in the canopy is computed by means of Foldy's approximation. In the latter case the field scattered by a collection of plants within the radar footprint can be computed in two steps: by applying the coherent model to a single crop plant and, by then performing a Monte Carlo simulation over a large number of plants generated from ground truth measurements or derived from an architectural growth model (fractal model, for instance). In both models leaves and stems were approximated by dielectric disks and cylinders. The scattering matrices of these elements were obtained by using the finite cylinder approximation for the cylinders and the Rayleigh Gans approximation for the disks, while the underlying soil was represented by a semi-empirical model valid for gentle rough surface.

Simulations performed with the simple radiative transfer model for two typical crops, that are well representative of the two categories investigated, confirmed the trends of the experimental data and made it possible to evaluate the contribution of single plant constituents (stems and leaves) to total backscattering. On the other hand, the coherent model was found able to simulate scattering from various types of canopies and to obtain a detailed description of the main scattering mechanisms that contribute to the backscattering coefficient.

Carrier-to-interference (C/I) statistics on a dual polarized double diversity satellite system including ice crystals and raindrop canting angle effects.

by

J.D. Kanellopoulos, T.D. Kritikos and A.D. Panagopoulos*

**Division of Electrosience
Department of Electrical and Computer Engineering
National Technical University of Athens
9 Iroon Polytechniou Street
GR-15773, Athens-Greece
Email :ikanell@cc.ece.ntua.gr**

Abstract

For frequencies above 10GHz which are of high importance in current satellite systems, the dominant sources of interference are the following: interference due to differential rain attenuation induced by an adjacent satellite operating in the same frequency [E. Matricciani and M. Mauri, Int. Jour. on Sat. Commun. 14, 71-76, 1996; E. Matricciani, Int. Jour. on Sat. Commun., 15,65-71, 1997] and crosstalk between orthogonally polarized signals. One of the most effective techniques to overcome potential fade margins and to decrease the outage time is site diversity. The reliable design of a modern satellite communication system must further take into account the interference effects. In the present paper, a method for the prediction of the carrier-to-interference statistics (C/I) on a dual polarized double diversity system interfered by an adjacent satellite path [Kanellopoulos et al , Radio Sci., vol. 34, No 4, pp.967-981, 1999] is properly modified in order to include ice crystals and canting angle effects. These novel assumptions reflect upon the more accurate estimation of cross polarization discrimination (XPD). The lognormal form for both the unconditional (including non-raining time) point rainfall rate R and attenuation A distribution is adopted and finally the convective raincell model [S.H.Lin, Bell Syst. Tech. Jour., 54,1051-1086, 1975] is employed for the description of the horizontal variation of the rainfall medium. Numerical results taken from the present procedure are compared with existing predictive results for various geographic latitudes and climatic zones. The sensitivity of various parameters affecting the interference performance is also investigated. Some very useful conclusions are deduced towards the reliable and economic design of the future communication systems where orbital and frequency congestion is quite expectable.

SLANT PATH MEASUREMENTS AT 50 GHZ IN MADRID: ATTENUATION BY GASES AND CLOUDS

K.H. Al-Ansari, P. Garcia, J.M.Riera, A. Benarroch*
Polytechnic University of Madrid, Spain

After performing slant path propagation measurements at 50 GHz using a radiotelescope during several years, a full-time experiment has been started recently in Madrid using a purposely built propagation receiver. The objective of this experiment is to investigate various atmospheric effects on the Italsat 50 GHz beacon received in the climatic conditions which may occur in Madrid. The main effects to be considered are: attenuation by rain, clouds and atmospheric gases, scintillation and depolarization. The measurement system includes a radiometer at the same frequency employed to obtain a reference for the beacon measurements and also to carry out attenuation measurements. A detailed description of the receiver can be found elsewhere (J.M.Riera, K.H. Al-Ansari, J.L. Besada, A. Benarroch, Propagation Experiment at 50 GHz in Madrid, Proceedings of URSI Commission F, Aveiro, 304-307, 1998).

Recent ITU-R and COST 255 (European Commission research project) documents have stressed the need to extend existing prediction methods and models to higher frequencies, asking collaborating countries to verify such models in any climate above Ka band.

In this paper, the results on gases and clouds attenuation, both from the beacon receiver and the radiometer, available at the time of the APS/URSI Conference will be presented. Experimental results will be compared to attenuation predicted by various methods and models which use meteorological surface and radiosonde data. Surface data are available from a meteorological station located by the beacon receiver/radiometer. The radiosonde data correspond to Madrid Airport, about 14 Km away from the experiment site.

The experimental attenuation by gases is being compared to attenuation predicted by the ITU-R methods using surface and radiosonde meteorological data, obtaining good agreement between experimental and predicted attenuation so far. The possible effects of the large seasonal variability of meteorological parameters, characteristic of a continental climate (such as Madrid's climate), and also of the diurnal variability, on atmospheric attenuation are being investigated. These aspects will also be commented in the paper.

Determining Snow Accumulation and Ablation Rates on the Greenland Ice Sheet Using SSM/I Radiometer and ERS Scatterometer Data

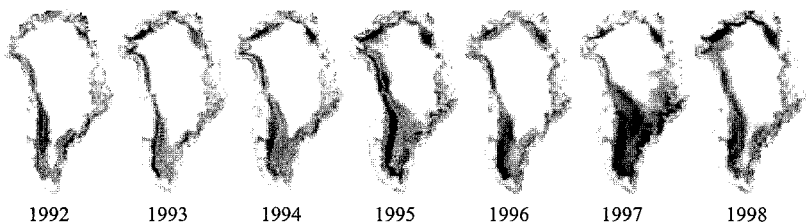
Jed D. Pack*, Jon W. Wallace, and Michael A. Jensen
Department of Electrical and Computer Engineering
Brigham Young University
Provo, UT 84602

Historical scientific observations illustrate that temporal changes in the Greenland ice sheet provide a sensitive indicator of global climate change. As a result, researchers in the remote sensing community have focussed considerable attention toward mapping the evolution of ice facie boundaries and estimating snow accumulation and ablation rates. For example, one recent study examined the trends in normalized radar cross section (NRCS) from ERS scatterometer data, pointing out a sudden increase in backscatter observed when a brief melt event precedes the formation of a rough, reflective firn layer on the surface. As snow accumulates on top of this surface, the resulting absorption is manifest as a gradual decline of the NRCS with time. This study used a very simple layered dielectric model to estimate the accumulation resulting from the NRCS curves.

In this work, we couple passive radiometer data from SSM/I with the ERS scatterometer record to more clearly identify melt events, accumulation, and ablation on the Greenland ice sheet. Our findings indicate that the passive record shows increased sensitivity to melt events, showing a sudden *decrease* in brightness temperature as the wet surface tends to reduce the emission from the underlying snow pack. Spatial mappings (see figure) of the magnitude of this melt discontinuity have been generated and been used to indicate areas of atypical melt for each summer from 1992 to 1998, with significant melting appearing during the summers of 1995 and 1998. This technique has also been used to monitor the changes in location of the "melt line" during this time period. Use of this methodology with combined SSM/I and SSMR records allows examination of the melt characteristics over a nearly continuous time period from 1978 to present.

To more closely examine the relation between snow accumulation and observed microwave responses, we have developed a radiative transfer model combining surface and volume scattering. Using this advanced model, we have been able to provide estimates of snow accumulation rates that are lower than those predicted by past studies, with the results matching well with existing in-situ data and precipitation maps. The model also confirms that a saturation effect in the changing NRCS/brightness temperature plots occurs once the snow accumulation reaches a certain critical depth. Details of this modeling and data analysis effort will be provided as part of the presentation.

Magnitude of Melt Discontinuity in SSM/I Data



Numerical Methods

Co-chairs:			Page
	A. Peterson, Georgia Institute of Technology		
	A. Cangellaris, University of Illinois at Urbana-Champaign		
1	1:50	Effect of higher-order surface discretization and grid uniformity on CEM code efficiency, <i>K. Hill*</i> , <i>Air Force Research Laboratory, S. Bindiganavale, Northrop Grumman Corporation, USA</i>	124
2	2:10	Electromagnetic modeling of interconnects and embedded passives in layered media, <i>F. Caliskan*</i> , <i>A. Peterson, Georgia Institute of Technology, USA</i>	125
3	2:30	Rapid calculation of closed-form electromagnetic Green's functions in layered media, <i>A. Cangellaris*</i> , <i>V. Okhmatovsky, University of Illinois at Urbana-Champaign, USA</i>	126
4	2:50	A sheet impedance approximation for shielding by a multilayered box, <i>E. Newman*</i> , <i>Ohio State University, USA</i>	127
5	3:10	Shielding effectiveness, statistical characterization, and the simulation of a two-dimensional reverberation chamber using finite element techniques, <i>C. Bunting*</i> , <i>Old Dominion University, USA</i>	128
6	3:30	Validation of coupling models for shielded cables in high-Q cavities, <i>W. Johnson*</i> , <i>R. Jorgenson, L. Warne, J. Kotulski, H. Hudson, S. Stronach, Sandia National Laboratories, USA</i>	129

EFFECT OF HIGHER-ORDER SURFACE DISCRETIZATION AND GRID UNIFORMITY ON CEM CODE EFFICIENCY

Kueichien C. Hill*
Air Force Research Laboratory
Sunil S. Bindiganavale
Northrop Grumman Corporation

The advent of parallel computers in the 90's has contributed to the advancement of computational electromagnetics (CEM) technology by allowing problems of practical size to be solved. As the computer power increases, our desire to solve even larger and more complex CEM problems increases as well. Unfortunately, the problem size scales as frequency to the 6th power using integral equation technique with direct LU solvers. In other words, if one wants to solve a problem at ten times its original frequency within the same time, an order of six reduction in computational time would need to be realized. Based on current technology, the speed-up due to faster chip and more compute nodes may account for an order of two reduction in computational time. The emerging fast iterative solver technology may account for an additional order of two reduction. To further reduce the run time, the CEM community has started to employ higher-order basis functions which require less unknowns. Thus, the need for superior basis functions is necessitated by the inability of just better computer resources and fast methods to meet the analysis requirements. However, it is not clear at this point how much benefit higher-order techniques can offer.

In this paper, we study the effect of curvilinear surface discretization and grid uniformity on CEM code efficiency by comparing the number of unknowns required to produce a converged solution using integral equation based CEM codes. Since we are interested only in the unknown reduction due to the higher order geometry effect, we use linear rooftop current expansion for all test runs. Two CEM codes, CARLOS and SWITCH, are used to predict the radar cross section (RCS) of a set of canonical targets with varying degrees of curvature. The effect due to grid uniformity on convergence rate is also examined. We use only the EFIE formulation to avoid the different convergence rates exhibited by using different integral equation formulations. In a previous study (Hill *et al*, AIAA Paper 2000-0957), we chose a flat plate, a circular cylinder, and an almond as the test targets. We confirmed that there is benefit to use higher order geometry for targets with curvatures, but the benefit is not as significant as we had hoped for. This study is an extension to the previous study by including additional test targets with more curvatures. The electric size of the test targets is also increased to more accurately determine the benefit of non-uniform gridding.

Electromagnetic Modeling of Interconnects and Embedded Passives in Layered Media

Fatma Çalışkan*, Andrew F. Peterson
Packaging Research Center
School of Electrical & Computer Engineering
Georgia Institute of Technology
Atlanta, GA, 30332

The electrical design of passive microelectronic devices in electronic packaging is complicated because of nonideal attributes of the actual circuit realization. Electromagnetic modeling offers the possibility of accurately predicting the electrical performance of the devices and reducing the cost associated with the design process. The method of moments (MoM) is utilized as a technique in modeling and analyzing these designs.

The first step of the MoM formulation is to write an integral equation describing the electromagnetic problem, which is the mixed potential integral equation (MPIE) in this work. These integral equations require related Green's functions of the vector and scalar potentials. The derivation of the closed-form Green's functions in the spectral domain eliminated the computationally expensive evaluation of the Sommerfeld integrals to obtain the Green's functions in the spatial domain using the generalized pencil of functions (GPOF) algorithm [G. Dural and M. I. Aksun, *IEEE Trans. Microwave Theory Tech.*, vol. 43, pp. 1545-1552, July 1995]. MoM formulations using rooftop basis and testing functions were implemented and a method was introduced which provides the analytical evaluation of the matrix elements involved in the MoM formulations [L. Alatan, M. I. Aksun, K. Mahadevan and M. T. Birand, *IEEE Trans. Microwave Theory Tech.*, vol. 44, pp. 519-525, Apr. 1996].

In this presentation, we consider applying the above techniques to problems in package designs, which often involve multilayer structures, solid or perforated ground planes, embedded passive devices such as capacitors and spiral inductors, and interconnects in horizontal or vertical directions. Several examples will be used to illustrate the modeling.

RAPID CALCULATION OF CLOSED-FORM ELECTROMAGNETIC GREENS FUNCTIONS IN LAYERED MEDIA

Andreas C. Cangellaris* and Vladimir Okhmatovsky
Center for Computational Electromagnetics
Department of Electrical & Computer Engineering
University of Illinois at Urbana-Champaign
1406 West Green Street, Urbana, IL 61801, U.S.A.

Tel: 217-333-6037; Fax: 217-333-5962; E-mail: cangella@uiuc.edu

A novel methodology is presented for the rapid calculation of closed-form expressions for spatial electromagnetic Green's functions in layered media. Availability and expedient numerical calculation of such Green's functions is highly desired for the modeling of electromagnetic field interactions in a variety of applications such as scattering by targets in the vicinity of a layered earth, radiation coupling to wire structures in the vicinity of layered earth, radiation coupling to interconnections in multi-layered printed circuit boards, design of integrated, planar microwave circuits and antenna arrays. A variety of methodologies have been proposed over the years for the efficient calculation of the Sommerfeld-type integrals associated with such Green's functions. Among them, the so-called discrete complex image method (DCIM) (D. G. Fang et al, *Inst. Elect. Eng. Proc.*, vol. 135, pt. H, 297-303, Oct. 1998) appears to be the most popular for handling an arbitrary number of layers. DCIM and its variants are based on the approximation of the kernel in the Sommerfeld integrals by a sum of complex exponentials. Such an approximation is effected using, for example, the generalized pencil-of-function method (T. K. Sarkar and O. Pereira, *IEEE Antennas & Propagation Magazine*, vol. 37, 48-55, Feb. 1995). However, for this method to work effectively and accurately, the quasi-static contributions and the surface wave contributions need be extracted first from the spectral kernel.

The proposed new method does not rely on the approximation of the integral kernels by complex exponentials. In fact, the analytic form of the spectral Green's function is not needed. Thus, the extraction of the quasi-static terms and the surface wave contributions are avoided. Instead, a discrete approximation of the governing differential equation in the spectral domain is used as the vehicle for the development of a rational function approximation of the spectral form of the Green's function at all planes at which it is required. A closed-form expression of the spatial Green's function in the form of a finite sum of Hankel and modified Hankel functions of zero order is then obtained in a straightforward manner from the Hankel transform of the pole-residue representation of the aforementioned rational function approximation of the spectral Green's function. The proposed methodology is straightforward, computationally efficient, and very accurate. In order to demonstrate the validity and accuracy of the proposed method, results from its application to the calculation of electromagnetic fields due to both vertical and horizontal electric dipoles in layered media will be presented and compared with those obtained through direct integration of the Sommerfeld integrals.

A Sheet Impedance Approximation for Shielding by a Multilayered Box

E.H. Newman

Ohio State University

Department of Electrical Engineering, ElectroScience Lab

1320 Kinnear Rd., Columbus, OH 43212

Tele: (614)292-4999 Fax: (614)292-7297

newman@ee.eng.ohio-state.edu

This paper will illustrate the use of the sheet impedance concept to develop a relatively simple and efficient method of moments (MM) solution for electrically thick material shields. The shield wall thickness must be very small in terms of the free space wavelength, but it may be large in terms of the material shield wavelength. The sheet impedance, which reduces a volume problem to a surface problem, is obtained from the relatively simple problem of a plane wave normally incident upon a planar 1D multilayered material slab. For a homogeneous slab it is shown that the well known sheet impedance relation for electrically thin slabs will also apply to electrically thick slabs, by simply replacing the constant electric field of the thin slab by the average electric field of the thick slab. If the slab is also magnetic, a simple relation is obtained between the electric and magnetic currents representing the slab.

By assuming the results obtained for the 1D slab hold on a local basis, an integral equation and MM solution is developed for closed shields. A single surface integral equation, which is a simple modification of that for a perfect electric conducting surface, is obtained for the electric currents. The magnetic currents are included in this integral equation as a dependent unknown, thus avoiding the need to solve coupled integral equations, and reducing the number of unknowns in the MM solution. Once the MM currents are known, the numerical problems associated with computing the small interior fields are avoided by employing an equivalent problem in which the interior surface of the shield is replaced by a perfect electric conductor. Numerical results are shown for a 2D cylindrical shield and a 3D box.

Shielding Effectiveness, Statistical Characterization, and the Simulation of a Two-Dimensional Reverberation Chamber using Finite Element Techniques.

Charles F. Bunting, Ph.D.
Old Dominion University, Dept. of Eng. Technology
Norfolk, VA 23529
e-mail: cbunting@odu.edu
(757) 683-4719

A reverberation chamber is an enclosure consisting of metal walls with a metallic stirrer essentially forming a high quality factor (Q) cavity with continuously variable boundary conditions. Reverberation chambers are attaining an increased importance in determination of electromagnetic susceptibility of avionics equipment. Given the nature of the variable boundary condition, the ability of a given source to couple energy into certain modes, and the passband characteristic due the chamber Q, the fields are typically characterized by statistical means. Specifically the probability density functions for the real and imaginary and quadrature components of the electric and magnetic fields are normally distributed. Reasonable statistical agreement in a source free environment has been obtained and was the primary emphasis of the work presented by the author [C. F. Bunting, et.al. *IEEE Trans. Electromag. Compat.*, vol. 41, pp. 280-289].

The major emphasis of this work is to apply finite element techniques at cutoff to the analysis of a two-dimensional structure to examine the notion of shielding effectiveness issues in a reverberating environment. The two-dimensional structure as depicted below represents a means of investigating the coupling from the stirred region (1) into the unstirred region (2) through the aperture and the resulting field characteristics including shielding effectiveness and the statistical characteristics of both the stirred and unstirred regions. The work is intended to provide further refinement in the consideration of shielding effectiveness in complex electromagnetic environment. Frequency stirring and mechanical stirring will be employed to obtain a statistical field distribution.

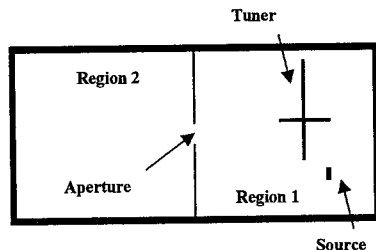


Figure 1. 2D Reverberation chamber geometry.

Validation of Coupling Models for Shielded Cables in High-Q Cavities¹
W. A. Johnson*, R. E. Jorgenson, L. K. Warne, J. D. Kotulski, H. G. Hudson and
S. L. Stronach
Sandia National Laboratories, P. O. Box 5800, Albuquerque, NM 87185-1152
wajohns@sandia.gov

This paper reports on the progress that has been made toward modeling canonical coupling through thin-slots to a shielded cable in a high-Q cavity with the EIGER (Electromagnetic Interactions GenERalized) code. EIGER is an object oriented, frequency domain code written in FORTRAN90 which runs on the massively parallel tera-flop computer at Sandia National Laboratories. We will first review the formulation and validation of thin-slot sub-cell models. Comparisons from computer simulations, analytic theory, and experiment will be shown.

Next we will show comparisons of modeling the coupling to a perfectly conducting wire connected to one side of the cavity and terminated by a 50 Ohm load on the other side. It has been observed that small perturbations in the cavity volume yield significant changes in results. An attempt to explain the reasons for this sensitivity will be made.

As first step towards modeling the coupling to shielded cables, the modeling of a calibration tube in our cable test facility will be carried out. This modeling will be carried out both with slot sub-cell models and dipole moment approximations for low frequency coupling. Results obtained will be compared to both analytical models and experiments.

¹ Sandia is a multiprogram laboratory operated by Sandia Corporation, a Lockheed Martin Company for the United States Department of Energy under Contract No. DE-AC04-94AL85000.

Adaptive and Beam Forming Arrays

Chair: T. Sarkar, Syracuse University

Page

- | | | | |
|---|------|---|-----|
| 1 | 8:00 | A direct data domain approach to space-time adaptive processing, <i>J. Koh, T. Sarkar, Syracuse University, USA</i> | 132 |
| 2 | 8:20 | An efficient DFT-UTD based array synthesis via the successive projection method for contoured beam applications, <i>H-T. Chou*, Yuan-Ze University, Chung-Li, P. Nepa, University of Pisa, Italy, P. Pathak, P. Janpugdee, The Ohio State University, USA</i> | 133 |
| 3 | 8:40 | An effective beam forming algorithm and its applications in the design of adaptive array antennas, <i>H-T. Chou*, Y-Y. Lin, S-W. Sun, Yuan-Ze University, Chung-Li</i> | 134 |
| 4 | 9:00 | Adaptive antenna array system for down link beam-forming using a closed loop, <i>S. Choi*, J. Choi, J. Choi, Hanyang University, Korea</i> | 135 |
| 5 | 9:20 | Quasi-optical reconfigurable beam-forming grids, <i>J. Mazotta, L. Chen, J-C. Chiao*, University of Hawaii, USA</i> | 136 |
| 6 | 9:40 | Cellular system capacity increase using spatially distributed adaptive array systems, <i>M. da Silveira*, Nortel Networks, Canada, J. Odendaal, J. Joubert, University of Pretoria, South Africa</i> | 137 |

A Direct Data Domain Approach to Space-Time Adaptive Processing

Jinhwan Koh and Tapan K. Sarkar
Department of Electrical Engineering & Computer Science
121 Link Hall
Syracuse University
Syracuse, New York 13244-1240
Phone : 315-443-3775
Fax : 315-443-4441
Email : jjkoh@mailbox.syr.edu, tk Sarkar@mailbox.syr.edu

A directive data domain approach to adaptively receiving a signal is presented for enhancing signals in a non homogeneous environment. Conventional space-time adaptive processing (STAP) utilizes statistical methodology based on estimating a covariance matrix of the noise. A wide sense stationary process has been assumed while estimating a covariance matrix, the statistical approach method cannot handle where the noise statistics changes rapidly. The direct data domain approach is ideal for the case of a highly non-stationary environment, particularly in the presence of blinking jammers and for the problems where the clutter characteristics changes rapidly. As direct data domain approach, two methods have been presented in this paper. One is based on the calculation of a generalized eigenvalue equation and the other is based on the solution of a set of block Hankel structure. The conjugate gradient method and the Fast Fourier transform can be utilized for efficient solving of the block Hankel structure. In the numerical examples, the Multichannel Airborne Radar Measurements (MCARM) database is utilized to demonstrate an applicability of the presented approach.

1. Topic : B1.3 Antenna arrays
2. Presentation equipment : 35mm slide projector
3. Jinhwan Koh and Tapan K. Sarkar
Department of Electrical Engineering & Computer Science
121 Link Hall Syracuse University
Syracuse, New York 13244-1240
Phone : 315-443-3775
Fax : 315-443-4441
Email : jjkoh@mailbox.syr.edu, tk Sarkar@mailbox.syr.edu

An Efficient DFT-UTD Based Array Synthesis via the Successive Projection Method for Contoured Beam Applications

Hsi-Tsung Chou¹, P. Nepa², P.H. Pathak³, P. Janpugdee³

¹ Dept. of Electrical Eng., Yuan-Ze University, Chung-Li 320 Taiwan

² Dept. of Information Eng., University of Pisa, via Diotisalvi, 2-5612 Pisa, Italy

³ ElectroScience Lab., Dept. of Electrical Eng., The Ohio State University,
1320 Kinnear Rd., Columbus, Ohio 43212

Contoured beam forming is an important application of antenna arrays in satellite communications. In practice, a very large array which consists of numerous antenna elements, with appropriately synthesized current amplitudes, is placed on a satellite for producing a desired contoured beam that is typically confined to a very narrow angular space for illuminating a specified region on the earth. As a result, an efficient array synthesis algorithm is very desirable, because conventional methods require intensive computations of the radiation patterns from all the array elements at each step in the iterative algorithm until the desired synthesis goal is achieved. In this paper, a novel synthesis which employs the DFT-UTD solution for array fields is proposed. This approach employs a finite series whose number of terms exactly equals the number of array elements (although only a small fraction of these are really significant) for representing the array element weights where the series coefficients are obtained via DFT from the element weights, and vice versa [P. Nepa, P. Pathak, P. Janpugdee, "An Extended Spectral UTD Analysis of Large Finite Antenna Arrays," *ICEAA Conference Proceedings*, pp. 229-236, Torino, Italy, Sep. 1999]. In the synthesis procedure, where the successive projection method (SPM) is employed [G.T. Poulton, "Power Pattern Synthesis using the Method of Successive Projections," *1986 IEEE AP Symp. Digest*, 2, pp. 667-670.], the coefficients of the DFT basis representation for the array weights now serve as the unknown variables in contrast to conventional approach that directly employs the element weights as the unknowns. There are two important advantages in this proposed approach. First, each DFT term works as a global basis function on the array and it consists of a constant amplitude and linearly impressed phase distribution on the entire array, and it generates a directional narrow beam, which now serves as a radiation type basis function in the contoured beam synthesis; this is in contrast to a very broad beam radiated from each individual array element that is utilized in the conventional element by element summation approach. It is noted that a very broad beam may be viewed as a global basis radiation function, and a narrow beam as a local radiation field basis function. Local radiation type basis functions tend to be better adapted to contoured beam synthesis since the radiation from only a few number of DFT terms (which are less than 25% of the total number of array elements) are usually sufficient to cover the confined angular space of the contoured beam, and outside the required beam area the synthesized pattern automatically drops to a very low level. Secondly, a closed form asymptotic UTD ray solution can be employed to directly and efficiently find the radiation pattern due to each term in the series of global DFT basis functions for the array weights; thus the local radiation basis function radiated by each global DFT basis on the whole array is now a simple UTD array field in closed form. Numerical examples will be presented to validate the proposed approach. It will be shown that contoured beams for continental USA and Taiwan, for example, need less than a hundred unknown DFT coefficient terms to be solved for an array size of 100×100 elements.

An Effective Beam Forming Algorithm and its applications in the Design of Adaptive Array Antennas

Hsi-Tseng Chou, Yo-Ye Lin and Shih-Wei Sun

Dept. of Electrical Eng., Yuan-Ze University, Chung-Li 320 Taiwan

The applications of adaptive array antennas in the wireless communications are very popular for many purposes including directional beam forming as in the smart antenna systems. With the increasing availability of beam forming network in the market, an effective algorithm to create a directional beam pattern with best performance becomes most desirable. Conventional approach of phased array antennas is the most popular method which gives rise to a maximum gain in the desired beam direction in the case that the arrays are located in the free space. However, the performance will be degraded when the environmental factors come into effect including the geometrical problems caused in the environments surrounding the arrays. One important example is the array fed reflector antenna systems where the phased array concept becomes inapplicable due to the existence of reflector surface. A universal algorithm is thus desired. In this paper, an effective beam-forming algorithm, previously developed in software radio applications, is employed to synthesize a directional beam with best gain performance. Focus will be in its applications in the array fed reflector antenna system to create a directional beam in addition to its general application descriptions. This algorithm employs the field patterns radiated from the array elements in the desired beam direction in a "matched" fashion analogous to the concepts of matched-filter in the applications of signal processing, and is more general than the phased array concepts. As a result, the beam-forming network can self-adjust the weighting of the array elements according to the received signals or their radiation patterns. Auto gain control (AGC) in addition to the directional beam forming can be therefore achieved. This algorithm is incorporated and interfaced with several NEC codes such as NEC-BSC code and reflector codes for the effective directional beam forming. Numerical experience has also found that side lobe levels can also be reduced simultaneously in addition to the best gain achievement in the beam direction. Several numerical examples will be presented to demonstrate its application procedure and validity.

ADAPTIVE ANTENNA ARRAY SYSTEM FOR DOWN LINK BEAM-FORMING USING A CLOSED LOOP

Seungwon Choi, Jinwoo Choi and Jaehoon Choi

School of Electrical & Computer Engr., Hanyang Univ., Haengdang 17, Seongdong, Seoul, 133-791, Korea T. +82-2-290-0366, F. +82-2-296-8446,

E-mail choi@dsplab.hanyang.ac.kr, H.P. <http://dsplab.hanyang.ac.kr>

This paper presents a systematic procedure of computing the weight vector \underline{w} for the base station (BS) to properly weight each transmitting signal in such a way that the signal power at the receiving mobile station (MS) be maximized. Though the weight vector is adopted at the transmitting BS, the information about the optimal weight vector is prepared at the receiving MS based on the received signals at the MS. In most cases, the weight vector itself is fed back from the MS to the BS. However, in order to avoid using a separate channel for sending the computed weights, the MS might send a compressed information with a minimal number of bits. Therefore, we deal with two tasks in the down-link beam-forming: one is to compute the weight vector itself and the other is to send the resultant vector from the MS to the BS without fully occupying a separate channel. Suppose a signal $s(t)$ is to be transmitted to a target subscriber. For simplicity, we assume a single propagation path between each antenna element and the subscriber. The same concept can be adopted in multipath signal environments for each path. The signal $s(t)$ passes through a processing unit before transmission in order to orthogonalize the signal at each antenna element for a preset period of time slot. This procedure is needed in order for the receiving MS to be able to separately extract the signal from each antenna element. The received power can be written as $|\underline{y}|^2 = \underline{w}^H \underline{R}_{hh} \underline{w}$ where \underline{y} is the received signal and \underline{R}_{hh} ($= \underline{h}^H \underline{h}$) denotes the matrix consisting of the channel parameter of each antenna element with the superscript H being the Hermitian operator. Since the transmitted signal at each antenna element is orthogonal to each other, as mentioned above, it is possible to form the matrix \underline{R}_{hh} at the receiving MS. The maximization of the functional can be found with a linear complexity utilizing the methods given in [1]-[3].

References

- [1] S. Choi and D. Yun. "Design of adaptive antenna array for tracking the source of maximum power and its application to CDMA mobile communications." IEEE Trans. Antennas. Propagat., vol. 45, No.9, pp. 1393-1404, Sept. 1997.
- [2] S. Choi and D. Yun. "Design technique of an array antenna. and telecommunication system and method utilizing the array antenna." USA patent 5999800. 9-101999 in Japan. 96-12172 in Korea.
- [3] S. Choi. "Signal processing apparatus and method for reducing the effects of interference and noise in wireless communications utilizing antenna array." USA patent 5808913. 9-172729 in Japan. 97 1 12119.2 in China. 97108432.2 in 11 European countries. 96-17931 in Korea.

Quasi-Optical Reconfigurable Beam-Forming Grids

John Mazotta, Liang-yu Chen, Jung-Chih Chiao*
 Department of Electrical Engineering, University of Hawaii – Manoa

Quasi-optical reconfigurable beam-forming grids with large apertures have been demonstrated using unit blocks, in which each consists of $n \times n$ unit cells, to compose one- or two-dimensional arrays. The functionality of producing multiple output beams from a single source; beam focussing; beam divergence; multiple-beam steering; single-beam two-dimensional steering; and multiple-beam switching were demonstrated in both one- and two-dimensional arrays. The discrete phase shifting by reconfiguring metal patterns in unit cells has been demonstrated in ["Quasi-Optical Discrete Beam Steering Grids," *IEEE-MTT-IMS 99*]. In this work, double-side metal patterns (Figure 1), with capacitive patterns in the back and switches to close inductive strips in the front, were used to increase phase shifts.

For a unit-block with 6×6 unit cells, two-beam steering was achieved in a 1×3 -block grid with E-plane steering at $(+18^\circ, -15^\circ)$ and H-plane steering at $(+20^\circ, -18^\circ)$. The 3-dB beam widths for two main beams are 10.8° and 11.2° . Beam focussing was demonstrated with a focal length of 137cm and 3-dB beamwidths of 9.6° in both E- and H-planes. Without the focussing, the E- and H-plane main beams have 3-dB beamwidths of 53.6° and 70.8° . The 1×3 unit-block arrays had higher sidelobes so 1×4 unit-block arrays were used to improve the focussed patterns. The E-plane main beam has a 3-dB beamwidth of 11.6° . The sidelobes are 4.5dB lower than the main beam. The 10-dB beam width is reduced from 68.4° to 42.8° . The H-plane main beam has a 3-dB beamwidth of 12.8° , with reduced sidelobes of -3.8 dB. Using the same size of aperture, H- and E-plane two-beam steering was achieved at $\pm 18^\circ$ and $\pm 20^\circ$, respectively.

3×3 - and 5×5 -block grids were constructed to demonstrate two-dimensional reconfigurable apertures. For a 3×3 -block grid, Fig. 2 (a) shows E- and H-plane steered beams at $\pm 15^\circ$ and $\pm 18^\circ$, respectively. The 3-dB beamwidths for the main beams are 10° . Fig. 2 (b) shows the focussed patterns. The E- and H-plane main beams both have a 3-dB beamwidths of 9.6° . The sidelobes are reduced to less than -4.2 dB. Four beams at $\pm 18^\circ$ and $\pm 20^\circ$ in the E- and H-planes, respectively, were produced by a 5×5 array. These four beams were then switched to $\pm 18^\circ$ in two 45° -cutplanes, as shown in Fig. 3. 3-D radiation patterns were measured in both cases. Beam focussing was achieved with 3-dB beamwidths of 10.8° and 21.6° in the E- and H-planes, respectively, using the same array, compared to the unfocussed 3-dB beamwidths of 37.2° and 49.6° .

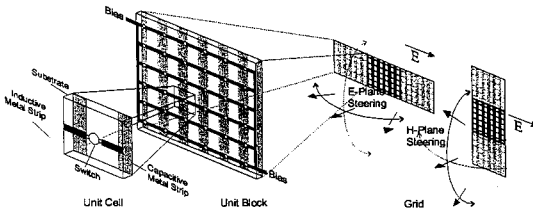


Figure 1: A reconfigurable grid. Each unit block has 6×6 unit cells. The blocks can be assembled into a larger aperture such as a 1×3 -block grid.

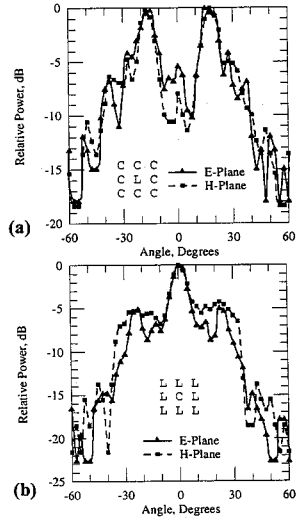


Figure 2: (a) The steered and (b) focussed patterns. The legends show the 3×3 unit-block configurations. "L" and "C" are for the inductive and capacitive unit blocks, respectively.

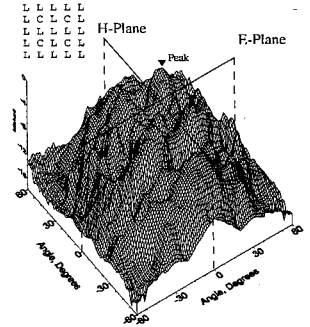


Figure 3: 3-D pattern for multiple-beam switching.

Cellular System Capacity Increase Using Spatially Distributed Adaptive Array Systems

M da Silveira*

Nortel Networks, TDMA Basestation Systems Design, Nepean, ON, Canada

JW Odendaal, J Joubert

Dept. Department of Electric and Electronic Engineering
University of Pretoria, Pretoria, 0002, South Africa

The radiation pattern of an antenna array can be adapted to the mobile environment by changing the amplitude and phase (or steering vector) at each array element. The radiation pattern can be shaped to reduce the interference from multiple co-channel users. Interference from co-channel mobiles in the same cell as well as adjacent cells are decreased by reducing the received energy in the angular direction of these interferers in the uplink, while maximizing the received signal in the direction of the desired mobiles. The result will be an increase in the signal to interference ratio at the base station, improving the signal quality. The number of mobiles can be increased up to the point where the same signal to interference ratio is reached (acceptable to the cellular system) compared to a system without an adaptive antenna array, with the result that the system capacity is increased. The angular location of the mobiles can be determined using the uplink information. Knowing the angular positions of the mobiles, energy can be directed towards the desired mobiles and reduced towards the interfering mobiles. In this scenario spatial channels are formed, which allows a further increase of the capacity of a system.

In the current literature adaptive array antennas are located at the centre of the cell. Antenna arrays located in the cell center forms these spatial channels in angle from the base station to the mobiles. The ability of this array configuration to form spatial channels between desired and interfering mobiles are reduced when the mobiles are located close to each other in angle.

The concept proposed in this paper overcome this limitation. A spatially distributed array is formed by three sub-arrays at the border of a hexagonal cell, with a 120-degree angle between the sub-arrays. Each sub-array determines the angle between the sub-array and all the desired and interfering mobiles (using methods such as ESPRIT). Mobiles located too close to each other in angle for the individual base stations to resolve, are resolved with two or all three of the antenna sub-arrays together. The spatial geometry of these antenna sub-arrays allows them to resolve the mobiles not only in angle, but also in distance. The result of this is a further increase in the capacity of a cellular system. Using a known bit sequence (typically the training sequence in GSM), the complex steering vector for each sub-array is determined by means of the least mean squares algorithm. The outage probability of the proposed system is compared to conventional linear and circular arrays located at the cell center. It will be shown how the outage probability of the proposed system can be increased by 60%, under certain conditions, compared to an array at the cell center.

Recent Developments in Theoretical Electromagnetics

Organizer and Chair: N. Engheta, University of Pennsylvania

Page

1	8:00	Elliptic integrals in diffraction theory, <i>S. Legault*</i> , <i>T. Senior, University of Michigan, USA</i>	140
2	8:20	Exact scattering by a ridge on a metal plane with isorefractive quadrants, <i>D. Erricolo, University of Illinois at Chicago, USA</i> , <i>F. Miot, University of Siena, Italy</i> , <i>P. Uslenghi*</i> , <i>University of Illinois at Chicago, USA</i>	141
3	8:40	Generalizing the TE/TM decomposition for electromagnetic fields, <i>I. Lindell*</i> , <i>L. Puska, Helsinki University of Technology, Finland</i> , <i>F. Olyslager, University of Ghent, Belgium</i>	142
4	9:00	Maximization of information content in polarimetric measurements, <i>J. Tyo*</i> , <i>US Naval Postgraduate School, USA</i>	143
5	9:20	PBG, PMC and PEC ground planes: a case study of dipole antennas, <i>Z. Li, Y. Rahmat-Samii*</i> , <i>University of California, Los Angeles, USA</i>	AP
	9:40	Break	
6	10:00	Nonlinear spatial-temporal solitary waves in millimetre-wave planar waveguides, <i>J. Arnold*</i> , <i>University of Glasgow, UK</i>	144
7	10:20	Bouncing-ray chaos for smart media, <i>V. Fiumara, University of Salerno, Italy</i> , <i>V. Galdi, Boston University, USA</i> , <i>V. Pierro, I. Pinto*</i> , <i>University of Sannio at Benevento, Italy</i>	145
8	10:40	On the accuracy of asymptotic approximations in ultrawideband signal, ultrashort-pulse, time-domain electromagnetics, <i>K. Oughstun*</i> , <i>University of Vermont</i> , <i>P. Smith, Micro Communications, USA</i>	146
9	11:00	Fractional stages in scattering problems, <i>N. Engheta*</i> , <i>University of Pennsylvania, USA</i>	147

Elliptic Integrals in Diffraction Theory

Stéphane R. Legault* and Thomas B.A. Senior
Radiation Laboratory
Department of Electrical Engineering and Computer Science
University of Michigan, Ann Arbor, MI 48109-2122

Maliuzhinets' technique (G. D. Maliuzhinets, *Sov. Phys. Doklady* **3**, pp. 752-755, 1958) remains today the most general approach for solving diffraction problems in wedge-shaped regions typically characterized by impedance boundary conditions. The technique leads to a pair of first order difference equations for the spectra of the total fields and their period is related to the open angle of the wedge. For all solutions completed thus far, the equation pair is decoupled or can be made so by choosing a suitable linear combinations of the spectral functions and the polarization independent wedge recently treated by Bernard (J. M. L. Bernard, *J.Phys. A* **31**, pp. 595-613, 1998) provides a good example. In general, however, the equation pair cannot be decoupled and we are left with having to solve a second order difference equation with functional coefficients. There is no established method to solve such equations but a technique has recently been developed by Senior and Legault (*Radio Sci.*, accepted for publication). The proposed approach is conceptually simple and requires the use of elliptic integrals of the first and third kind to construct solutions with the desired analytical requirements.

The equation considered here is

$$t(\alpha + 5\pi) - 2 \left\{ 1 - 2 \frac{\cos^2 \theta - \cos^2 \theta'}{\cos^2 \alpha - \cos^2 \theta'} \right\} t(\alpha + \pi) + t(\alpha - 3\pi) = 0,$$

an extension of the one obtained by Demetrescu *et al.* (*Radio Sci.* **33**, pp. 39-53, 1998) where θ and θ' are specified parameters such that $0 < \text{Re}.\theta \leq \pi/2$ and $0 \leq \text{Re}.\theta' < \pi/2$. We seek two linearly independent solutions of the above which are free of branch points for all α , free of poles and zeros for $|\text{Re}.\alpha| \leq 2\pi$, and of specified order as $|\text{Im}.\alpha| \rightarrow \infty$. The second order difference equation can be factored to obtain a pair of difference equations involving a branched function $u(\alpha)$. Application of a logarithmic derivative to the first order difference equations shows that their solution $w(\alpha, u)$ may be written as

$$w(\alpha, u) = \exp \int_{(0, u(0))}^{(\alpha, u(\alpha))} \left\{ \rho_0(\alpha') + \rho_1(\alpha') + \rho_2(\alpha') \right\} d\alpha',$$

where the dependence on the choice of the branch of $u(\alpha)$ is explicitly shown. The branched function $\rho_0(\alpha)$ follows directly from the logarithmic derivative operation and the 4π periodic branched functions $\rho_{1,2}(\alpha)$ are used to construct solutions having appropriate analytical properties. Specifically, $\rho_1(\alpha)$ is used to cancel the poles of $\rho_0(\alpha)$ whereas $\rho_2(\alpha)$ is used to cancel the periodicity modules that arise in the strip due to the branch points of $u(\alpha)$. It is shown that $\rho_2(\alpha)$ is a linear combination of elliptic integrals of the first and third kind and its form is specified by enforcing vanishing periodicity modules in the strip. This results in a well defined integral expression for $w(\alpha, u)$ and, using specific symmetric forms, acceptable branch-free solutions of the second order difference equation can then be constructed. The overall procedure will be described and sample results presented.

Exact scattering by a ridge on a metal plane with isorefractive quadrants

D. Erricolo (1), F. Mioc (2), P. L. E. Uslenghi (*1)

(1) Department of ECE, University of Illinois at Chicago, Illinois 60607, USA

(2) Department of Information Engineering, University of Siena, Italy 53100

The scattering of the primary field produced by a plane wave or a line source by a metal-dielectric structure is considered, in the frequency domain. The structure consists of an infinite planar boundary separating the perfectly conducting half-space $x < 0$ from the penetrable half-space $x > 0$. The metal plane has a PEC bulge, or ridge, consisting of a semi-elliptic cylinder whose axis is the z -axis of a rectangular coordinate system and whose cross section in a $z = \text{constant}$ plane is a semi-ellipse located in the $x > 0$ half-space with its major axis along the x axis. As limiting cases, one has a metal strip in contact with a metal plane and perpendicular to it, or a semi-circular metal ribbon on a metal plane. The $y = 0$ plane divides the penetrable half-space $x > 0$ in two quadrants filled with linear, homogeneous and isotropic materials that are isorefractive to each other. The primary plane wave propagates in a direction perpendicular to the z -axis, whereas the primary line source is parallel to the z -axis. Thus, the boundary value problem is two-dimensional in nature.

First, we consider the geometrical-optics fields that would exist in the absence of the ridge; these are obtained via simple geometrical optics considerations and, for plane-wave incidence, do not satisfy the radiation condition. To these fields, the scattered field produced by the ribbon, which must satisfy the radiation condition, is added. The total field is then required to satisfy the boundary conditions. In order to do so, both geometrical optics and scattered field are expanded in terms of Mathieu functions, and analytical expressions are obtained for the unknown coefficients in the expansions. The ensuing exact solution to the boundary-value problem is compared to previously known solutions for limiting cases. Numerical results are also presented. A similar technique may be used for dipole sources, in which case, however, the boundary-value problem becomes tri-dimensional and the field expansions involve both infinite series and definite integrals.

Generalizing the TE/TM Decomposition for Electromagnetic Fields

I.V. Lindell*, L.H. Puska

Electromagnetics Lab., Helsinki University of Technology

PO Box 3000, FIN-02015 HUT, Espoo, Finland

F. Olyslager

Dept. Information Technology, University of Ghent

St-Pietersnieuwstraat 41, B-9000 Ghent, Belgium

The classical TE/TM decomposition of electromagnetic fields with respect to a fixed direction in space is known to be applicable to solving electromagnetic problems when either sources or boundaries of the problem are invariant with respect to this direction, i.e., to two-dimensional sources and/or axial wave-guiding structures. Also, the same principle applies when the medium is uniaxially anisotropic, i.e., permittivity and/or permeability are uniaxial dyadics. In the 1970's the decomposition was generalized so that the fields can be TE and TM with respect to different directions in space.

More recently, these authors have taken a task to generalize the decomposition principle further to involve a class of linear media as general as possible. In the process the class of 'decomposable' media has become more general over the years and the decomposition is not valid for the electric and magnetic fields but for their linear combinations. In the most general case so far, applicable for a quite general set of bi-anisotropic media depending on four arbitrary directions in space, any field outside of its sources can be decomposed in two independent (non-coupling) electromagnetic fields labeled as a- and b-fields. The a-field depends on two vectors $\mathbf{a}_1, \mathbf{a}_2$ so that $\mathbf{a}_1 \cdot \mathbf{E} + \mathbf{a}_2 \cdot \mathbf{H} = 0$. Similarly, the b-field satisfies $\mathbf{b}_1 \cdot \mathbf{E} + \mathbf{b}_2 \cdot \mathbf{H} = 0$.

There are some interesting basic properties associated with these classes of decomposable media:

- (1) Fields can be decomposed in two independent partial fields.
- (2) For the decomposed fields the media can be replaced by equivalent media characterized by simpler medium dyadics
- (3) Green dyadics can be expressed in analytic form for these equivalent bi-anisotropic media
- (4) The fourth-order scalar Helmholtz determinant operator, governing the electromagnetic fields in bi-anisotropic media, can be factorized, expressed as a product of two second-order operators.
- (5) The fourth-order dispersion surface for a plane wave becomes a combination of two second-order surfaces.

Because it appears extremely difficult to find analytic solutions to Green dyadics for bi-anisotropic media, the method of decomposition could be of help by splitting the problem in two parts each associated with a simpler bi-anisotropic medium with an analytic Green dyadic.

Maximization of Information Content in Polarimetric Measurements

J. Scott Tyo

Department of Electrical and Computer Engineering,
US Naval Postgraduate School, Monterey, CA 93943

Imaging polarimeters have been developed for use in remote sensing applications and have been demonstrated to improve target contrast, reduce clutter, aid in the defeat of intervening scatterers, and provide orientation information about target features. Polarimeters employ strategies motivated by ellipsometry to measure components of the Stokes vector at each pixel in a frame; however, there are significant differences between ellipsometric and imaging applications that drive the design to fewer measurements. The question remains as to how to best choose the individual measurements to optimize information content and make the most reliable reconstruction of the Stokes vector.

This question has been addressed in the past from the points of view of system condition (Ambirajan and Look, *Opt. Eng.* **34** p. 1651, 1995), measurement decorrelation (Tyo, *JOSA A*, **15**p. 359, 1998), and noise minimization (Sweatt, *et al.*, 1999 OSA Annual Meeting) for specific imaging systems. In this talk, the process of minimizing condition number will be linked to noise reduction and maximization of information content. The coverage on the Poincaré sphere of particular polarimeter strategies will be discussed, and a single strategy is developed to design an optimum polarimeter configuration for *any* dimensionality, *any* imaging strategy, and *any* number of measurements.

To optimize a general polarimetric imaging system, one need only make the N individual measurements that go into reconstructing the Stokes vector need to be maximally decorrelated, and this is equivalent to saying that the measurements must be maximally spaced within the region of the Poincaré sphere that can be reached by the imaging method. Certain 4-dimensional systems allow enough flexibility to inscribe a regular tetrahedron in the Poincaré sphere (variable retardance, dual-rotating-compensator), while others do not, and hence are sub-optimal (rotating quarter-waveplate). Three-dimensional systems, that measure only linear polarization information give access to only the equatorial plane of the Poincaré sphere. For maximal decorrelation, the measurements must be spread out around the equator of the Poincaré sphere. Optimum 2-dimensional systems give access to a diameter, and maximal decorrelation is obtained when the measurements are at opposite ends.

NONLINEAR SPATIAL-TEMPORAL SOLITARY WAVES IN MILLIMETRE-WAVE PLANAR WAVEGUIDES

J. M. Arnold

Department of Electronics and Electrical Engineering
University of Glasgow
Glasgow G12 8LT, UK

Abstract

Monolithic MOS capacitors fabricated on planar semiconductor substrates can exhibit very large dependences of capacitance on applied bias voltage. This renders guided-wave propagation in the parallel-plate quasi-TEM mode between the capacitor electrodes highly nonlinear, since the local phase velocity is strongly dependent on the local voltage between the electrodes. The phenomenon of strongly nonlinear propagation expected to exist in the MOS capacitor environment suggests that regimes of ultra-fast pulsed spatial soliton propagation are accessible at modest voltage excitations. In fact it is known that these waves can be described in the lowest order of nonlinearity by the Kadomtsev-Petviashvili (KP) equation [1], which permits exact spatial-temporal solitons as solutions, exhibiting lateral self-guidance in the direction parallel to the waveguide plane as well as temporal self-stabilisation in a short soliton pulse.

In this paper the electromagnetic theory leading to these expectations will be developed, including an assessment of the effects of perturbations of the KP solitons caused by a non-ideal environment in the semiconductor substrate.

BOUNCING-RAY CHAOS FOR SMART MEDIA

Vincenzo Fiumara

Waves Group, D.I.³.E., University of Salerno, I-84084 Fisciano, ITA

Vincenzo Galdi¹

Dept. Elec. and Compu. Eng., Boston University, Boston, MA 02215, USA

Vincenzo Pierro and Innocenzo M. Pinto*

Waves Group, University of Sannio at Benevento, I-82100 Benevento, ITA

Two dimensional ray paths in an exponentially graded-index slab backed by a sinusoidal reflecting surface are similar to the trajectories of a ball (massive point particle) bouncing on a time-harmonically moving table, under the effect of gravity. This latter is a well known paradigm of chaos (A.J. Lichtenberg and M.A. Liebermann, *Regular and Stochastic Motion*, Springer, NY, 1983). Not unexpectedly, regular (space-periodic), almost-periodic and chaotic ray-path regimes are observed. These latter are *generic*, i.e., do occur for *almost all* initial condition (injection direction). As a result, a number of interesting features are observed. The ray exit-angle distribution is essentially uniform in the external half space; the ray path-length distribution in the slab is such that the exit phase is uniformly distributed in $(0, 2\pi)$. For a lossy dielectric, the power deposition in the slab is fairly uniform, and the exit amplitude distribution is such that the scattered field can be highly attenuated. These properties suggest a number of possible applications, including radar-countermeasures and smart absorbers. Preliminary results from a hybrid (analytical/numerical) full-wave analysis substantially confirm the above scenario.

¹ On leave of absence from the Waves Group, University of Sannio at Benevento, I-82100 Benevento, Italy.

On the Accuracy of Asymptotic Approximations In Ultrawideband Signal, Ultrashort-Pulse, Time-Domain Electromagnetics

Kurt E. Oughstun
College of Engineering & Mathematics
University of Vermont
Burlington, Vermont 05405-0156
oughstun@emba.uvm.edu

Paul D. Smith
Micro Communications
P. O. Box 4365
Manchester, New Hampshire 03108

After an ultrashort pulse (or an ultrawideband signal) has propagated a sufficiently large distance into a dispersive, attenuative material its spatio-temporal dynamics settle into a relatively simple (or mature) behavior for the remainder of the propagation. In this so-called mature dispersion regime the field becomes locally quasimonochromatic with fixed local frequency, wavelength, and attenuation in small regions of space that propagate with their own characteristic constant velocity. The modern asymptotic description of the dynamical evolution of an ultrashort electromagnetic pulse (or an ultrawideband electromagnetic signal) as it propagates through a homogeneous, isotropic, locally linear, temporally dispersive medium provides a detailed characterization of the entire temporal field evolution for all propagation distances that are in the mature dispersion regime (K. E. Oughstun and G. C. Sherman, *Electromagnetic Pulse Propagation in Causal Dielectrics*, Springer-Verlag, 1994). The modern asymptotic theory shows that the temporal field evolution for sufficiently large propagation distances $z > 0$ in the dispersive material is critically dependent upon the presence of any pole singularities in the initial pulse spectrum $\tilde{f}(\omega)$ as well as upon the saddle points of the complex phase function $\phi(\omega) = i(c/z)(\tilde{k}(\omega)z - \omega t)$. The pole singularities (if any) describe the steady-state field behavior in the dispersive material and are a characteristic of the input pulse. The saddle points, whose locations in the complex- ω plane vary with both the propagation distance z and the time t , describe the transient field behavior and are a characteristic of the material dispersion. The accuracy of this asymptotic description is critically dependent upon the accuracy with which the saddle point dynamics may be determined. The rms error is found to decrease monotonically as the propagation distance increases, in keeping with Poincaré's definition of an asymptotic expansion. Although it is satisfying to know that the accuracy of the asymptotic description of dispersive pulse propagation behaves as it should, it is still desirable to obtain improved accuracy at relatively small absorption depths ($z/z_d \sim 1$) into the medium. In order to accomplish this, improvements need to be made in the asymptotic theory about several critical points in the field evolution. The most notable of these is in the small space-time interval about the pole arrival.

Fractional Stages in Scattering Problems

Nader Engheta

University of Pennsylvania

Moore School of Electrical Engineering

Philadelphia, Pennsylvania 19104, U.S.A.

Tel: +1 (215) 898-9777, Fax: +1 (215) 573-2068

E-mail: engheta@ee.upenn.edu

Web: <http://www.ee.upenn.edu/~engheta/>

In the past few years, we have been exploring the possible applications of fractionalization of operators in electromagnetic problems and have been studying and developing the topic of *fractional paradigm in electromagnetic theory* [N. Engheta, "Fractional Paradigm in Electromagnetic Theory" a chapter in *Frontiers in Electromagnetics*, D. H. Werner and R. Mittra (eds.), IEEE Press, New York, chapter 12, pp. 523-552, (2000)]. For instance, we have applied the tools of fractional differentiation and fractional integration in various problems in electromagnetic fields and waves, and have obtained interesting results with notable features and potential applications. Since fractional derivatives/integrals are effectively the result of fractionalization of differentiation and integration operators, we have also explored the notion of fractionalization of some other linear operators in electromagnetic theory, which has led us to interesting solutions in radiation and scattering problems.

In this talk, we discuss one of our present studies on analyzing some of these fractionalized operators in scattering problems. In particular, the attention is paid to the effect of these operators on the induced current on the scatterer. Specifically, consider the current induced on the surface of a perfectly conducting object when it is illuminated by a plane wave. If one applies a fractional operator (e.g., fractional derivative/integral along one of the axes in the Cartesian coordinate system) on the scattered and incident fields, the resulting functions will, under certain mathematical conditions, satisfy Maxwell's equations and they thus represent another set of incident and scattered electromagnetic fields. However, the same fractional operator does apply on the induced current as well, and it is of interest to study the new current distribution. The resulting current, which is obtained by applying the fractional operator on the original induced current, may represent an "intermediate stage" between two limiting scattering problems, i.e., the original problem and another problem for which the fractionalization parameter is taken to be unity. Therefore, application of such fractional operators on fields and induced currents in a given scattering problem may provide us with "fractional stages" in that scattering problem. These issues, along with physical insights, will be discussed in this talk.

Medical Applications and Biological Effects

Co-chairs:			Page
	M. Stuchly, University of Victoria, Canada		
	S. Hagness, University of Wisconsin, Madison		
1	8:00	Evaluation of spatial peak 1g and 10g average SAR in homogeneous phantoms, <i>A. Brehonnet*</i> , <i>A. Drossos, Nokia Research Center, Finland</i>	150
2	8:20	Synthetic model of base station antennas for dosimetric analysis using the genetic algorithm, <i>Z. Altman, CNET France, A. Karwowski, Wroclaw & Silesian University of Technology, Poland, M. Wong, J. Wiart, CNET, France</i>	151
3	8:40	An improved human-head model for cellular telephone antenna designs, <i>A. Hirata*</i> , <i>S. Mori, Osaka University, Y. Horii, Kansai University, T. Shiozawa, Osaka University, Japan</i>	152
4	9:00	Calculation and experimental validation of induced EM fields inside a human head: a study at ultra high-field MRI, <i>T. Ibrahim*</i> , <i>R. Lee, B. Baertlein, P. Robitaille, The Ohio State University, USA</i>	153
5	9:20	Microwave discrimination between malignant and benign breast tumors: a computational and experimental feasibility study, <i>K. Leininger, X. Li, S. Hagness*, University of Wisconsin, Madison, USA</i>	154
	9:40	Break	
6	10:00	Temperature calculations in the human eye exposed to EM waves from 600 MHz to 6 GHz, <i>A. Hirata*</i> , <i>S. Matsuyama, T. Shiozawa, Osaka University, Japan</i>	155
7	10:20	Modeling of induced potentials on implanted cardiac pacemaker electrodes by 60Hz electric field sources, <i>T. Dawson*</i> , <i>M. Stuchly, K. Caputa, University of Victoria, Canada, A. Sastre, A.S. Consulting and Research, Inc., R. Shepard, University of Alabama, Birmingham, R. Kavet, EPRI, USA</i>	156
8	10:40	Improvement of heating patterns by using a coaxial-dipole antenna for microwave coagulation therapy, <i>K. Saito*</i> , <i>S. Hosaka, T. Tanigughi, H. Yoshimura, K. Ito, Chiba University, Japan</i>	157
9	11:00	In vitro effects of 60 Hz magnetic fields on the differentiation and proliferation of friend leukemia cells, <i>E. Rothwell*</i> , <i>K. Chen, J. Suk, C. Chang, J. Trosko, G. Chen, B. Upham, W. Sun, Michigan State University, USA</i>	158
10	11:20	Time domain analysis of the human body exposed to the EMP excitation using the human equivalent antenna model, <i>D. Poljak*</i> , <i>University of Split, Croatia, C. Tham, University of Wales, UK, V. Roje, University of Split, A. Sarolic, University of Zagreb, Croatia</i>	159
11	11:40	Corticonic networks for automatic learning and recognition of spatio-temporal signals, <i>N. Farhat*, University of Pennsylvania, USA</i>	160

Evaluation of spatial peak 1g and 10g average SAR in homogeneous phantoms

A. Brehonnet(*), A. Drossos
Nokia Research Center
P.O Box 407, FIN-00045 NOKIA GROUP Finland
Tel: +358 40 703 8162; Fax: +358 9 4376 6858
E-mail: arnaud.brehonnet@nokia.com

Introduction

The evaluation of spatial peak 1g and 10g average Specific Absorption Rate (SAR) in homogeneous phantoms for compliance testing of cellular phones with electromagnetic safety limits requires a certain number of steps. First, a coarse grid is performed for the determination of the maximum SAR value on the phantom surface. Then, a cubic grid with dimensions exceeding considerably the dimensions of 1g and 10g cubes is centered on the maximum point measured during the coarse grid. The three-dimensional matrix is then interpolated to an adequate step and extrapolated to the phantom surface. 1g and 10g average SAR are finally evaluated with appropriate averaging algorithms.

Objectives

The primary objective for this study was the comparison of algorithms utilized in Nokia Research Center's E-field automatic scanner for the evaluation of 1g and 10g average SAR with other existing algorithms of commercial systems.

Furthermore, various extrapolation algorithms were investigated, since, in most of the systems, extrapolation to the phantom surface is inevitable due to the fact that dipole sensors of E-field probes are always located few millimeters away from the probe tip.

Methods

In another research work conducted by Nokia ("Statistical measurement uncertainty of SAR evaluations", A. Drossos, XXVIth General Assembly of URSI, 1999), the spatial peak 1g and 10g average SAR were evaluated for 6 GSM phones using a DASY 3 system. Each phone was measured 6 times thus a total of 36 evaluations was generated. From these measurements, 6 files, containing the cubic grid local SAR values, were used as an input to our software for the re-evaluation of spatial peak 1g and 10g average SAR. The re-evaluation of 1g and 10g average SAR was performed with two algorithms. The first one simply centers a cube of 1g or 10g mass around the extrapolated SAR local peak. The second scans the entire interpolated cubic matrix and searches for the maximum cubic volume with a corresponding mass of 1g or 10g. A similar procedure was followed for 36 evaluations of 6 devices of the same GSM phone measured with a DASY 2 system.

For the extrapolation to the phantom surface, polynomials utilized in our software were compared with the built-in extrapolation algorithm of DASY 3 systems.

Results

When no scans of the entire cubic interpolated matrix were performed with our software, the 1g and 10g average SAR varied considerably (mean difference of 1.5% in cubes of 1g and 3.4% in cubes of 10g) when compared to DASY 2 and 3 results. On the contrary, when the entire cubic interpolated matrix was scanned, a very good agreement (mean difference of 0.9% in cubes of 1g and 0.3% in cubes of 10g) on the spatial peak 1g and 10g average SAR between our software and DASY was recorded.

Concerning the extrapolation algorithms, our investigation showed that the use of a fourth-order polynomial was appropriate to describe the fast decaying E-field in the proximity of the phantom inner surface.

Synthetic Model of Base Station Antennas for Dosimetric Analysis Using the Genetic Algorithm

Zwi Altman⁽¹⁾, Andrzej Karwowski⁽²⁾, Man-Fai Wong⁽¹⁾ and Joe Wiart⁽¹⁾

⁽¹⁾ CNET, France Telecom, 38-40 rue du General Leclerc, 92794 Issy les Moulinaux, France

⁽²⁾ Wroclaw & Silesian University of Technology, Akademicka 16, 44-100 Gliwice, Poland

International recommendations such as the ICNIRP guidelines have defined exposure levels for electromagnetic fields that should be verified for both the general public and workers. The purpose of this work is to propose a simple model for Base Station (BS) panel antennas that allows one to accurately calculate the radiated electromagnetic fields and to verify their compliance to these exposure levels.

The model proposed in this work, denoted as the synthetic model, satisfies the manufacturer specifications for the maximum gain and for the 3 dB aperture in the *E*- and *H*- planes. The synthetic model is generated from a unit cell element of the antenna array that is optimized using the Genetic Algorithm to give the correct 3 dB aperture in the *H*- plane and a suitable maximum gain. Instead of adding the field contributions of different unit cells of the antenna array at a given point, we superpose the contributions of one unit cell at vertically shifted points. Since only one unit cell is modeled, the computation time is negligible.

Comparisons of the synthetic model with both full antenna model (Figs. 1,2), and with measurements have shown excellent agreement and the results will be included in the presentation.

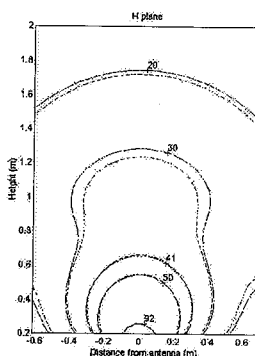
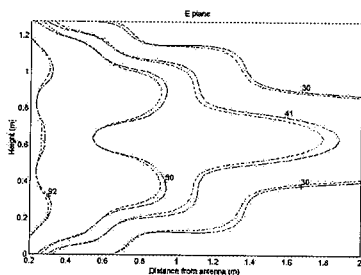


Fig. 1. *E* field iso-lines in the *E*-plane. Fig. 2. *E* field iso-lines in the *H*-plane.

An Improved Human-Head Model for Cellular Telephone Antenna Designs

*A. Hirata†, S. Mori†, Y. Horii†, and T. Shiozawa‡

†Department of Communication Engineering, Osaka University, Japan.

‡Faculty of Informatics, Kansai University, Japan.

A considerable amount of the EM power emitted from the antenna of a cellular telephone is absorbed in the human head and hand, leading to much modification of the antenna pattern. Therefore, it is desirable to design antennas by taking the influence of the human body into account. In recent years, the interaction between an antenna and the human head has been investigated theoretically and experimentally. In experimental approaches, however, a homogeneous head model is often used, because it is very difficult to make an inhomogeneous phantom. Similarly, it is not so easy to construct an anatomically-based model for theoretical calculations. The use of a homogeneous model causes some errors in numerical calculations of the antenna pattern, the amount of EM power deposited in the human head, and the SAR distribution in the human head. However, the correctness not in the SAR distribution but in the antenna pattern and the deposited power is more essential for antenna designs. Thus, in this paper, we propose a new head model which is relatively easy to make, and satisfies the two requirements mentioned above.

The model which we propose in this paper consists of only two kinds of tissues, that is, skin and an imaginary tissue. The material constants of the imaginary tissue are determined so that the radiation characteristics obtained by using the proposed head model come close to those by the anatomically-based model. From numerical results, the differences in the antenna pattern and the amount of EM power deposited in the model between the anatomically-based model and the proposed model are fairly suppressed, as compared with those between the anatomically-based model and a homogeneous model. Thus, one can apply the simplified model proposed in this paper for cellular telephone antenna designs.

Calculation and Experimental Validation of Induced EM Fields Inside a Human Head: A Study at Ultra High-Field MRI

Tamer S. Ibrahim⁺⁺, Robert Lee⁺, Brian Baertlein⁺, and P.M.L. Robitaille[!]

Departments of Electrical Engineering⁺ and Radiology[!]
The Ohio State University
Columbus, Ohio 43210

Since the start of magnetic resonance imaging (MRI), there has been a constant push towards more powerful (higher static field strength) systems. These systems enable obtaining images with much greater details than the ones with the conventional 1.5 Tesla magnets. On the other hand, as the static field increases the Larmor frequency rises and human head size becomes comparable to the operational wavelength. As a result, the design of radiofrequency (RF) coils has become a major challenge for high field imaging, especially > 7 Tesla systems. These coils are required to have good signal to noise ratio, reasonable homogeneity of the tangential magnetic field distribution (B_1), and low specific absorption rate (SAR). In this work, we evaluate the performance of a TEM resonator (J. T. Vaughan et al. MRM 32:206-218, 1994) loaded with a newly developed anatomically detailed human head model at ultra high-field (> 7 Tesla) using the finite difference time domain method. Also, the numerical results are compared to experimental data obtained at 8 Tesla.

An anatomically detailed human head mesh was developed from MRI images for use in FDTD simulations. The model consists of eighteen tissue types in addition to air and has a resolution of $2\text{mm} \times 2\text{mm} \times 2\text{mm}$. The greater detail in the model provides additional details in the internal fields especially for the SAR calculations. The three-dimensional FDTD model of the TEM resonator was developed and evaluated with the aforementioned human head model while considering the interactions between the coil and the head. While the TEM resonator was loaded with the human head, the coil was tuned numerically to the frequencies of interest: 300, 340, and 469 MHz as a representation of 7, 8, and 11 Tesla systems respectively. The B_1 field and the SAR were then obtained at these frequencies.

The results show that while the homogeneity of the B_1 field deteriorates as the frequency of operation increases, a significant improvement was obtained using different excitation techniques other than the conventional quadrature drive. These excitations include 4-port quadrature and phase/magnitude-optimized 4-port drives. As a result, acceptable quality images especially at 7 and 8 Tesla systems were obtained. The SAR values were significantly dominated by the coupling between the tissue and source/coil. Therefore the locations of the excitations sources had a large effect on the SAR peak values especially on the surface of the human head.

Microwave Discrimination Between Malignant and Benign Breast Tumors: A Computational and Experimental Feasibility Study

Kristen M. Leininger¹, Xu Li², and Susan C. Hagness^{1,2,*}

(1) Dept. of Electrical and Computer Engineering, (2) Dept. of Biomedical Engineering
University of Wisconsin, Madison, WI 53706-1691
hagness@engr.wisc.edu

Previous dielectric spectroscopy studies at frequencies up to 1 GHz indicate a significant dielectric contrast between malignant and normal breast tissue that greatly exceeds the usual tissue variability (Surowiec et al, *IEEE Trans. Biomed. Eng.*, 35:257-263, 1988; Joines et al., *Med. Phys.*, 21:547-550, 1994; Chaudhary et al., *Ind. J. Biochem. Biophys.*, 21:76-79, 1984). Based on this data, there is a strong probability that malignant breast tumors have a relatively large microwave scattering cross section. For this reason, several microwave breast cancer detection approaches are under investigation.

A recently introduced confocal microwave imaging approach (Hagness et al., *IEEE Trans. Biomedical Engineering*, 45:1470-1479, 1998; Hagness et al, *IEEE Trans. Antennas and Propagation*, 47:783-791, 1999) has shown much promise as a non-ionizing, non-invasive alternative to X-ray mammography. Here, the uncompressed breast is illuminated with a low-power synthetically focused microwave pulse. Acquisition of backscattered waveforms and a subsequent synthetic scan of the focal point permits the detection of strong scattering sites in the breast.

Since little is known about the dielectric properties of benign breast tumors, a key question is whether there exists a systematic and significant contrast in the dielectric properties of benign and malignant breast lesions at microwave frequencies. If so, then confocal microwave imaging would permit not only the detection of malignant tumors but also discrimination between malignant and benign lesions, as only malignant tumors would act as strong scattering sites in the breast. If not, then more elaborate signal processing schemes would be required to extract information from the backscattered signals about the detected scattering site.

To begin to answer this question, we have conducted a pilot study whereby the microwave dielectric properties of freshly excised breast biopsy tissue specimens have been measured at the University of Wisconsin Hospitals and Clinics using an open-ended coaxial needle probe in conjunction with a commercial vector network analyzer. The dielectric properties for each lesion have been correlated with pathology results and sorted into two groups: malignant (infiltrating or in situ carcinomas), and benign (fibroadenomas or other benign tissue including cysts, hyperplasia, fibrosis, and fibrocystic change). We have also developed 3-D FDTD models using breast MRI scans to calculate the backscatter from the different types of lesions. These computational tools have provided an efficient means for exploring the merits of various signal processing strategies. The results of these experimental and computational studies suggest that microwave discrimination between malignant and benign breast tumors should indeed be feasible through both intensity-based and spectral-based signatures.

Temperature Calculations in the Human Eye exposed to EM Waves from 600 MHz to 6 GHz

*A. Hirata, S. Matsuyama, and T. Shiozawa

Department of Communication Engineering, Osaka University, Japan.
e-mail: hirata@comm.eng.osaka-u.ac.jp, FAX:+81-6-6879-7735

The human eye is one of the most hazardous organs for the EM exposure because it has neither blood flow to carry away the heat evolved nor skin layer to protect it. Therefore, several theoretical and experimental work have been done on the temperature rise in the human or animal eye exposed to EM waves for assessing the possibility of microwave-induced cataract formation. In this paper, with the aid of the FDTD method, we calculate the SAR and the temperature distributions in the human eye for exposure to the EM wave in the frequency range between 600 MHz and 6 GHz, which covers the hot spot range (Schwan, *J. Microwave Pow.*, 1982). Note that for this calculation we constructed an anatomically-based whole head model composed of 17 tissues. In particular, we investigate the dependence of the thermal distribution in the human eye on the polarization of the EM wave. Additionally, we discuss the effect of the height of nose on the thermal distribution. Note that this effect is not negligible as pointed out by Bernardi *et al* (*IEEE Trans. MTT*, 1998).

We show in Fig.1 the dependence of the temperature rises in the human eye on the frequency and the EM polarization. As seen from the figure, the temperature rises greatly depend on the EM polarization. Additionally, we found that the height of nose changes the SAR distribution significantly. However, the SAR averaged over the human eye does not change so much.

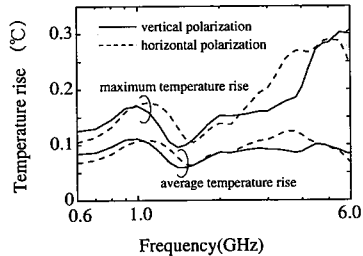


Fig.1 Dependence of the temperature rise in the human eye on the frequency and the EM polarization.

Modeling of Induced Potentials on Implanted Cardiac Pacemaker Electrodes by 60Hz Electric Field Sources

T.W. Dawson*, M. A. Stuchly, K. Caputa,
ECE Department, University of Victoria, Victoria, BC, Canada
A. Sastre, A.S. Consulting & Research, Inc., Overland Park, KS
R. B. Shepard, Dept. Cardiothoracic Surgery, Univ. of Alabama, Birmingham, AL
and R. Kavet, EPRI, 3412 Hillview Ave., Palo Alto, CA

Recent progress in computational dosimetry at power-line frequencies has resulted in the availability of heterogeneous models of the human body, and of efficient computational methods for evaluating exposures to electric and magnetic fields. One important issue not yet resolved is protection against electromagnetic interference (EMI) with implanted cardiac pacemakers. This is particularly critical for workers in strong fields. Previously tests of EMI have and could only be done after implantation (Astridge, P.S., et. al., *P.A.C.E.*, 1993. Vol. 16: 1966-1974, Kaye, G.C., et al. *P.A.C.E.*, 1988.vol. 11: 999-1008).

The objective of the research presented is twofold. First, organ and tissue dosimetry in terms of induced electric fields under exposure to 60-Hz vertical electric fields is compared to those produced by head and shoulder current injection electrodes. Second, potential differences are evaluated for the various EMI scenarios for a few clinically relevant pacemaker electrode placements. A high-resolution model of the human body, modified to include a pacemaker, together with previously developed and verified computational methods (Dawson, T.W., et. al., *J. Computational Physics*, 1997. Vol. 136: 640-653) are used. The computational code is modified to include current injection sources. Exposure is modeled and quantified in terms of the short circuit current to ground. The following configurations of the electric field source are considered: exposure to uniform electric field of a frequency of 60 Hz, two current electrodes placed symmetrically on the shoulders and two electrodes placed on the feet, and two asymmetric configurations.

The evaluations have shown that contact electrode excitation is a practical and convenient way to approximate the effects of external electric source fields. There are, however, differences in the total vertical current flow in the head and upper torso for the electric field source, in comparison with contact electrodes on the shoulders and feet. Based on the maximum practical bipolar electrode separation, voltages of the order of 0.2 (0.1) mV have been estimated for the ventricular (atrial) placements. These values are for a short-circuit current of 100 μ A for the shoulder electrodes and a grounded average male exposed to a 9.1-kV/m. The corresponding unipolar potentials are 0.9 (0.4) mV for ventricular (atrial) placement.

Improvement of Heating Patterns by Using a Coaxial-Dipole Antenna for Microwave Coagulation Therapy

Kazuyuki SAITO¹*, Sumie HOSAKA¹, Takeshi TANIGUCHI¹,
Hiroyuki YOSHIMURA², and Koichi ITO²

¹ Graduate School of Science and Technology, Chiba University

² Faculty of Engineering, Chiba University

1-33 Yayoi-cho, Inage-ku, Chiba 263-8522, JAPAN

In recent years, various types of applications of electromagnetic techniques to microwave thermal therapy have been developed. The authors have been studying thin coaxial antennas for the minimally invasive microwave thermal therapy. In particular, we have applied the antennas to the applicators of the microwave coagulation therapy (MCT). In this study, we improved the heating performances of the antennas for the MCT.

The MCT has been used mainly for the treatment of hepatocellular carcinoma. In the treatment, the thin microwave antenna is inserted into the tumor and the microwave energy heats up the tumor to produce the coagulated region including the cancer cells. We have to heat the cancer cells up to at least 60 °C above which the cells are coagulated. At present, there are some problems to be improved for the conventional MCT antennas. Particularly, there is a problem that length of the coagulated region becomes long in the antenna insertion direction. In this study, we employed the coaxial-dipole antenna to solve this problem. Figure 1 shows a structure of the coaxial-dipole antenna.

We investigated the heating characteristics of the coaxial-dipole antenna by conducting the phantom experiments, the coagulation experiments using the liver of pig, and the numerical simulations using the FDTD method. From the results, we could confirm that the heating region exists only around a tip of the coaxial-dipole antenna. This result means that the coaxial-dipole antenna is very useful in the MCT. As a further study, we should optimize the structural parameters of the coaxial-dipole antenna.

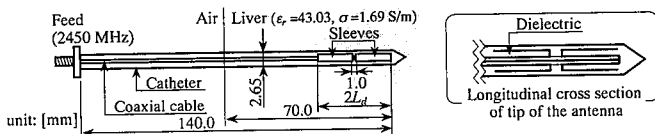


Fig. 1 Basic structure of the coaxial-dipole antenna.

In Vitro Effects of 60 Hz Magnetic Fields on the Differentiation and Proliferation of Friend Leukemia Cells

E.J. Rothwell*, K.M. Chen, and J. Suk
Department of Electrical and Computer Engineering
C.C. Chang, J.E. Trosko, G. Chen, B.L. Upham, and W. Sun
Department of Pediatrics and Human Development
Michigan State University
East Lansing, MI 48824

There has been a suspected link between childhood cancer and the exposure to electromagnetic fields ever since 1979, when epidemiological studies showed that proximity to power lines corresponded to a two to three times higher incidence of Leukemia. Subsequent studies have produced varying results, and whether exposure to EM fields is correlated with human cancer is controversial.

Leukemia results when the differentiation process in blood cells is supplanted by cell proliferation. To investigate the possible effect of EM fields on cell differentiation and proliferation, Friend erythroleukemia cells were induced to differentiate by exposure to the chemicals dimehtyl sulfoxide (DMSO) and hexamethylene bis-acetamide (HMBA) and then exposed to 60 Hz magnetic fields for four days. The resulting amount of differentiation was determined both by measuring the hemoglobin content within the cells (high in differentiated cells) and by measuring telomerase activity (high in undifferentiated cells). The amount of cell proliferation was determined by measuring DNA activity (high in proliferating cells).

A dose-response curve was obtained by measuring hemoglobin content at 0, 0.01, 0.025, 0.05, 0.10, 0.50, 1.0, and 10.0 G magnetic field strengths. It was found that differentiation of Friend leukemia cells was inhibited by exposure to magnetic fields, with the level of inhibition dependent on the exposure level. At 0.025 G and below, there was no inhibition. Between 0.05 G and 1.0 G the exposed cells differentiated at a rate roughly 34% lower than the unexposed cells, while at 10 G this rate had risen to 50% lower than the unexposed cells.

Telomerase activity was reduced 100 times by exposure to DMSO, indicating a high level of cell differentiation. When exposed to both DMSO and 1.0 G magnetic fields, the reduction was only 10 times, indicating a much lower level of differentiation. Finally, the DNA marker increased 1.5 times for cells exposed to 1.0 and 10.0 G fields, indicating an increase in proliferation.

**TIME DOMAIN ANALYSIS OF THE HUMAN BODY EXPOSED TO THE EMP
EXCITATION USING THE HUMAN EQUIVALENT ANTENNA MODEL**

¹Dragan Poljak¹, Choy Yoong Tham², Vesna Roje¹, Antonio Šarolić³

¹Department of Electronics, University of Split, Croatia, Email: dpoljak@fesb.hr

²Department of Electrical and Electronic Engineering, University of Wales, Swansea, UK,

³Faculty of Electr. Eng. and Computing, Univ. of Zagreb, Croatia

The electromagnetic pulse (EMP) coupling to human body results in transient currents induced inside the standing man (J.Y. Chen, O.P. Gandhi, *IEEE Trans. MITT*, **1**, 31-39, 1991). Determining this current it is possible to do some biological studies pertaining to the electromagnetic radiation exposures. Through the frequency domain analysis some analytical formulas were provided for ELF and VLF radiation (R.W.P. King, *Proc. IEEE 23rd Bioeng. Conf.*, Piscataway, NJ 1997) and the problem was also handled numerically using the FDTD technique (O.P. Gandhi, J.Y. Chen, *Bioelectromagnetics*, **1**, 43-60, 1992). A frequency domain thick wire antenna model of the human body exposed to ELF, VLF (D.Poljak, V.Roje, *Proc. 20th Int. Conf. IEEE/EMBS*, Hong-Kong, 1998.) and RF radiation (D.Poljak, R.Šimundić, *XXVth General Assembly, URSI*, Ontario, Canada 1999) was reported recently. Though very efficient in frequency domain calculations the thick wire representation of the human body was not shown to be numerically stable in the time domain study (D.Poljak et al., *Proc. 4th EBEA*, Zagreb, 1998). On the other hand, a human equivalent antenna model has been proposed for experimental dosimetry (O.P. Gandhi, US patent, 1995). This equivalent antenna model of the human body is stated to be valid in the frequency region from 50Hz to 110MHz.

The goal of this work is to perform a time domain simulation of the body exposed to the EMP radiation using the human equivalent antenna model. Namely, dimensions of the human equivalent antenna stay within the thin wire approximation which enables one to obtain stable numerical results in the time domain simulations.

Transient current induced in the person is obtained by solving the time domain integral equation:

$$\int_0^{2h} \frac{I(z', t-R/c)}{4\pi R} dz' = F_0(t - \frac{z}{c}) + F_1(t - \frac{2h-z}{c}) + \frac{1}{2Z_0} \int_{z'}^{inc} E_z(z', t - \frac{|z-z'|}{c}) dz'$$

where $I(z', t-R/c)$ is the unknown current, $E_z^{inc}(t)$ is the incident field and h is the height of the body. The equation (1) is solved by the boundary element/time marching procedure (D.Poljak, *Journ. Electromagn. Waves and Applic.*, **6**, 775-787, 1998).

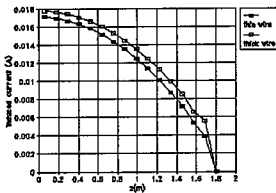


Fig. 1 Induced current in the body (f=30MHz, $E^{inc} = 1V/m$)

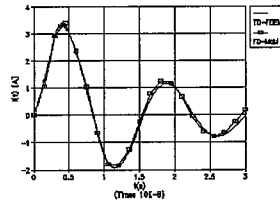


Fig. 2 Induced transient current in the body exposed to the EMP waveform

Fig. 1 shows the computed current distribution along the cylinder via frequency domain boundary element code (D.Poljak, V.Roje, *IEE Proc. Microw. Antennas Propag.*, **6**, 435-440, 1995) using the thick wire and thin wire model. Fig. 2 shows the transient current induced in the waist. The height of the body is $h=1.8m$, and the standard EMP waveform is used: $E_z^{inc}(t) = E_0(e^{-at} - e^{-bt})$, where $E_0 = 1kV/m$, $a = 4 \cdot 10^8$, $b = 4.76 \cdot 10^8$. The results obtained by the time domain code and frequency domain code are in close agreement.

CORTICONIC NETWORKS FOR AUTOMATIC LEARNING AND RECOGNITION OF SPATIO-TEMPORAL SIGNALS

Nabil H. Farhat
The Moore School of Electrical Engineering
University of Pennsylvania
200 South 33rd Street
Philadelphia, PA 19104
e.mail: farhat@ee.upenn.edu

Corticonics is the art of identifying anatomical and physiological attributes of cortical organization to be abstracted and used in the modeling and simulation of the cortex. The cortex is the seat of all higher-level brain function and understanding its workings can have significant scientific, technological, and clinical implications.

The challenge in cortical modeling and simulation is to determine what are the essential features of cortical tissue and organization one needs to incorporate in the model in order to reproduce and predict known functional attributes of the cortex. An important question then is whether the behavior produced by the model is artefact of the model itself or is true reflection of the thing being modeled. This translates often into the level of detail of cortical organization one may include without complicating the model to a point where it becomes cumbersome and ineffective. Ideally, the goal is to obtain a simple description that captures as much of the known cortical dynamics and function as possible.

I will describe a macroscopic dynamical brain theory with holographic undertones that constitutes a useful step towards achieving this goal. The theory draws on concepts from nonlinear dynamics, bifurcation theory, and chaos. It leads to functional models of the cortex with remarkable explanatory, predictive, and synthesizing power which is a good indicator of its viability. The basis, rationale, and consequences of the theory can be summarized as follows: Holographic models of the brain that were proposed in the sixties and seventies had limited success because they did not account for (a) the nonlinearity of cortical tissue, and (b) the temporal dimension of cerebral events. Our theory uses both of these fundamental properties to produce model networks (corticonic networks) capable of imitating important known functional attributes of the brain/cortex. This includes: (a) ability to handle dynamic stimulus i.e. spatio-temporal input patterns of the kind encountered in radar, sonar, speech recognition, and other applications, (b) selective autonomous learning driven by mutual information and coherence that distinguishes automatically between novel and familiar (already learned) stimuli (inputs) by learning the novel and producing the correct learned response for the familiar, (c) memory formation with no cross-talk that is anticipated to lead to immense memory capacity even in networks of modest size, and (d) computing with diverse attractors i.e. with both static (fixed-point) and dynamic (periodic and chaotic) attractors. These attributes suggest that corticonic networks will be the basis for designing a new generation of machines with functional capabilities and brain-like levels of intelligence that are not possible with present neural net and connectionist models because these compute with static attractors only. For these reasons corticonic networks are expected to impact the design and enhance the performance of automated object recognition in Radar and Sonar and other applications involving the classification and recognition of spatio-temporal signals.

Fast Integral Equation Methods

Co-chairs: S. Rengarajan, California State University, Northridge
D. R. Wilton, University of Houston Page

- | | | | |
|----|-------|--|-----|
| 1 | 8:00 | On using approximate factorization preconditioners with the MLFMA boundary integral formulation of time-harmonic scattering, <i>R. Adams*</i> , <i>Virginia Tech</i> , <i>T. Xie</i> , <i>L. Carin</i> , <i>Duke University, USA</i> | 162 |
| 2 | 8:20 | An improved parallelization strategy for MLFMA on distributed memory computers, <i>S. Velampambal*</i> , <i>W. Chew</i> , <i>J. Song</i> , <i>University of Illinois at Urbana-Champaign, USA</i> | 163 |
| 3 | 8:40 | Multi-level fast-multipole algorithm for scattering from dielectric and conducting targets above or embedded in a lossy half space, <i>J. He</i> , <i>L. Carin*</i> , <i>Duke University, USA</i> | 164 |
| 4 | 9:00 | Comparison of three-dimensional frequency and time-domain modeling of electromagnetic scattering from buried mines, <i>X. Zhu*</i> , <i>J. He</i> , <i>L. Carin</i> , <i>Duke University, USA</i> | 165 |
| 5 | 9:20 | Fast evaluation of transient fields in the presence of two half spaces using a plane wave time domain algorithm, <i>M. Lu*</i> , <i>A. Ergin</i> , <i>E. Michielssen</i> , <i>University of Illinois at Urbana-Champaign, USA</i> | 166 |
| | 9:40 | Break | |
| 6 | 10:00 | Basis-pursuits matrix compression for Moment Method scattering analyses, <i>L. Li</i> , <i>L. Carin*</i> , <i>Duke University, USA</i> | 167 |
| 7 | 10:20 | On the convergence properties of the Multiple Sweep Method of Moments (MSMM), <i>D. Colak*</i> , <i>R. Burkholder</i> , <i>E. Newman</i> , <i>J. Johnson</i> , <i>The Ohio State University, USA</i> | 168 |
| 8 | 10:40 | Reduction of sampling density in CGFFT method: application of FFT algorithm for discontinuous functions, <i>G-X. Fan*</i> , <i>Q. Liu</i> , <i>X. Xu</i> , <i>Duke University, USA</i> | 169 |
| 9 | 11:00 | An efficient approach to Moment Method analysis of large antenna arrays, <i>M. Hurst*</i> , <i>The Boeing Company, USA</i> | 170 |
| 10 | 11:20 | Solution of large dense complex matrix equations using a Fast Fourier Transform (FFT) based wavelet-like methodology, <i>K. Kim</i> , <i>T. Sarkar*</i> , <i>Syracuse University, USA</i> | 171 |

On Using Approximate Factorization Preconditioners with the MLFMA Boundary Integral Formulation of Time-Harmonic Scattering

Robert J. Adams*

Bradley Department of Electrical and Computer Engineering
Virginia Tech, Blacksburg, VA 24061-0111

Tony Xie and Lawrence Carin

Department of Electrical and Computer Engineering
Duke University, Durham, NC 27708-0291

The MoM solution of the time-harmonic boundary integral equation (BIE) generally results in a linear system of equations, with the MoM impedance matrix typically dense. The total computational cost associated with iteratively solving such an equation is approximately proportional to the product of (1) the cost of computing a matrix-vector product, and (2) the number of iterations required to achieve a given residual error level. In this presentation we consider the integration of complementary methods for reducing the individual components of the total computational cost, thereby obtaining a composite algorithm with reduced computational complexity for multi-aspect simulations of scattering from large targets.

The multiple-level fast multipole algorithm (MLFMA) provides a general method for reducing the cost of computing the matrix-vector product operation from $O(S^2)$ to $O(S \log S)$ where S is the electromagnetic surface area of a target. Although the MLFMA significantly reduces the cost of a matrix-vector product, it does not change the conditioning of the original BIE. This leads to an overall simulation cost that approximately scales as $O(S^{1+\alpha} \log S)$ with $0.25 < \alpha < 0.5$ for large targets.

Approximate factorization preconditioners (AFPs) provide a general framework for reducing the number of iterations required to iteratively solve the BIE formulation of a scattering problem. These techniques are based on an approximate factorization of a BIE into a product of one-way scattering operators, effectively re-summing many of the physically important scattering interactions. The resulting renormalized integral equation typically has a significantly lower condition number than the original form of the BIE.

In this presentation we discuss the modifications to the standard implementation of MLFMA required to combine the method with the integral equations obtained using AFPs to renormalize the standard BIE formulations of scattering from open and closed targets in free space. Significant modifications of the standard MLFMA are necessary due to the manner in which an AFP continuously updates the source vector during a single iteration. This property of AFPs leads to an interdependence between the near-group and distant-group interactions of the MLFMA. Near and far interactions are independent in the standard implementations of MLFMA.

The computational costs of the composite MLFMA+AFP algorithm are compared to results obtained using more traditional preconditioners in conjunction with the MLFMA. The impact of using various Krylov algorithms will also be discussed.

An Improved Parallelization Strategy for MLFMA on Distributed Memory Computers

Sanjay Velamparambil*, Weng Cho Chew, Jiming Song
Center for Computational Electromagnetics
Department of Electrical and Computer Engineering
University of Illinois
Urbana, IL 61801, USA

In this presentation, we shall report a new, radically different strategy for the parallelization of dynamic Multilevel Fast Multipole Algorithm (MLFMA) as implemented in ScaleME [1, 2]. This new scheme exploits certain insights gained while solving large-scale problems on distributed memory environments and can be shown to have better communication performance than the previously reported methods. The parallelization strategy used in original ScaleME suffers from performance degradation due to lengthy messages for very large scale problems. This is basically due to the large sizes of radiation and receiving patterns of boxes at the coarse levels of the MLFMA tree. We shall show that better communication performance can be achieved by distributing the radiation and receiving patterns of large boxes across processors, thereby maintaining a reasonable grain size. We shall discuss the various issues related to the implementation and the integration of this new scheme with the existing one, which is near optimal for small to medium scale problems. The new hybrid parallelization scheme is currently being implemented in ScaleME.

We shall demonstrate the performance of the new scheme by solving electromagnetic scattering problems involving perfectly conducting scatterers. To this end, we shall use a new distributed memory method of moments code which uses ScaleME as its MLFMA kernel along with a parallel GMRES solver. We shall also compare the results with the parallelization strategy used in original ScaleME [1].

References

- [1] S. Velamparambil, J. Song, and W. C. Chew, "ScaleME: A Portable, Distributed Memory Multilevel Fast Multipole Kernel for Electromagnetic and Acoustic Integral Equation Solvers," Tech. Rep. CCEM-23-99, Center for Computational Electromagnetics, Dept. of Electrical and Computer Engineering, University of Illinois at Urbana-Champaign, Urbana, IL, 1999. (Under the review of SIAM J. Scientific Computing).
- [2] S. Velamparambil, J. Song, W. Chew, and K. Gallivan, "ScaleME: A portable, scalable multipole engine for electromagnetic and acoustic integral equation solvers," *IEEE Antennas Propagat. Symp.*, vol. 3, pp. 1774-1777, 1998.

Multi-Level Fast-Multipole Algorithm for Scattering from Dielectric and Conducting Targets Above or Embedded in a Lossy Half Space

Jiangqi He and Lawrence Carin

Department of Electrical and Computer Engineering
Duke University
Box 90291
Durham, NC 27708-0291

The FMM and MLFMA models exploit a particular expansion of the free-space Green's function, and therefore virtually all implementations to date have been relegated to the case of targets in free space. The difficulty of directly applying the FMM or MLFMA formalism to three-dimensional layered-medium problems resides in the fact that the layered-medium Green's function is a dyadic, each term of which represented in terms of a generally complicated Sommerfeld integral. We have developed an approximate means of handling the dyadic half space Green's function, with application to the FMM. In particular, the near FMM terms are evaluated via use of the exact dyadic Green's function, the latter evaluated efficiently via the complex-image technique. The far terms, evaluated efficiently via the clustering algorithm, employ an approximation to the exact dyadic Green's function. In particular, each component of the approximate Green's function is expressed in terms of the direct-radiation term plus radiation from an image source in *real* space. We have previously presented a FMM model for perfectly conducting targets above or below a half space, using the aforementioned scheme for efficient evaluation of the Green's function. In that work we employed an electric-field integral equation, which limited its applicability somewhat, due to possible internal resonances for closed targets. In the work presented here, we extend our previous work to the case of a MLFMA formalism, employing electric-field, magnetic-field and combined-field integral equations, the latter eliminating internal resonances. After validating the MLFMA model, through comparison with results from a rigorous but relatively inefficient MoM algorithm, we consider several targets of interest to radar-based remote sensing. In particular, we consider scattering from a realistic three-dimensional vehicle, buried unexploded ordnance (UXO), and dielectric tree trunks.

Comparison of Three-Dimensional Frequency and Time-Domain Modeling of Electromagnetic Scattering from Buried Mines

Xianyang Zhu, Jiangqie He and Lawrence Carin

Department of Electrical and Computer Engineering
Duke University
Box 90291
Durham, NC 27708-0291

Over the last several years there has been a dramatic improvement in the capabilities of numerical modeling tools for electromagnetic scattering from subsurface targets. There have traditionally been two approaches to this problem: (1) frequency-domain techniques such as the method of moments (MoM), which employ a layered-medium dyadic Green's function, and (2) general time-domain techniques such as the finite difference time domain (FDTD). Both the MoM and FDTD algorithms have been extended of late to improve their numerical efficiency. In particular, the memory and CPU requirements of the MoM have been improved dramatically through recent development of the multi-level fast multipole algorithm (MLFMA), while the numerical efficiency of FDTD has been extended through development of a wavelet-based multi-resolution time-domain (MRTD) algorithm.

The time-domain and frequency-domain approaches involve very different techniques, and therefore it is of interest to investigate under which circumstances each approach is optimal. Such a comparison is the focus of this paper. We consider wideband scattering from general subsurface targets (e.g. mines, UXO, rocks, etc.), embedded in a layered, dispersive soil medium. We address issues of calculating scattering due to a distant source (plane-wave excitation) as well as GPR systems for which the target is close to the soil interface. In addition to analyzing such scattering scenarios, we also address the merits of these two approaches in the context of resonant-mode characterization. Both flat and rough air-ground interfaces are considered.

Fast Evaluation of Transient Fields in the Presence of Two Half Spaces Using a Plane Wave Time Domain Algorithm

M. Lu*, A. A. Ergin, and E. Michielssen
Center for Computational Electromagnetics
Department of Electrical and Computer Engineering
University of Illinois at Urbana-Champaign, Urbana, IL 61801.
mingyulu@uiuc.edu

The recently developed plane wave time domain (PWTD) algorithm permits the efficient evaluation of transient wave fields that are generated by known and bandlimited source configurations residing in free space [A. A. Ergin, B. Shanker, and E. Michielssen, *Journal of Computational Physics*, **146**, 157-180, 1998]. In this study, the PWTD scheme is extended to allow for the evaluation of transient fields due to sources residing in an unbounded medium comprised of two half spaces. Both the fields that are reflected from and transmitted through the interface between the two half spaces can be cast in terms of plane wave expansions, and assuming that both the source and observers reside in the denser of the two half spaces, a diagonal translator can be constructed that is reminiscent of the free-space PWTD translator. Use of this diagonal translator greatly accelerates the evaluation of the transient response. Unlike in free space, however, the transient fields due to a source residing in the presence of two half spaces are not localized in time. In contrast, these fields have an infinitely long temporal tail. It turns out that this tail can be represented efficiently in terms of a Hilbert transformed plane wave expansion, similar to PWTD schemes for two-dimensional wave fields [M. Lu, J. Wang, A. A. Ergin, and E. Michielssen, accepted for publication of *Journal of Computational Physics*]. The proposed PWTD scheme reduces the computational complexity associated with the evaluation of fields in a half space configuration from $O(N_s^2 N_t^2)$ to $O(N_s N_t \log N_s \log N_t)$, where N_s is the number of the spatial sources and N_t is the total number of time steps. This study is a first step towards realizing a fast integral equation based scheme for analyzing transient scattering problems involving planarly layered media.

Basis-Pursuits Matrix Compression for Moment Method Scattering Analyses

Ling Li and L. Carin
Department of Electrical and Computer Engineering
Duke University
Box 90291
Durham, NC 27708-0291

The method of moments (MoM) is one of the most popular techniques for electromagnetic scattering and propagation problems. However, a principal limitation of this technique is the $O(N^2)$ RAM requirements for storage of the $N \times N$ impedance matrix, for N unknowns. In the work presented here, we apply techniques developed in the signal-processing community for compact signal representation. The objective is to adaptively design a basis set with which the unknown surface currents can be represented compactly, thereby significantly reducing the number of unknowns N .

The idea of tailoring the basis set to a particular problem has received wide attention. For example, for canonical scatterers, researchers have used physical-optics-like basis functions over relatively smooth and electrically large portions of the target, with GTD and UTD basis functions in the vicinity of edges and other discontinuities. Such techniques have dramatically reduced the number of basis-function coefficients that need be solved for. However, the physical optics (PO), GTD, and UTD basis functions are difficult to define for general, non-canonical targets. Here we therefore examine adaptive techniques for determination of such basis functions. In this context, the usual subsectional basis functions are applied initially, at a given frequency. An adaptive algorithm, such as matching pursuits, is then used to define an alternative, compact basis set, parametrized to the frequency under consideration. These compact basis functions are then used to solve the scattering problem at other frequencies.

On the Convergence Properties of the Multiple Sweep Method of Moments (MSMM)

D. Çolak*, R.J. Burkholder, E.H. Newman, and J.T. Johnson
The Ohio State University ElectroScience Laboratory
1320 Kinnear Road, Columbus, Ohio 43212

The Multiple Sweep Method of Moments (MSMM) analysis of radiation and scattering from electrically large bodies has recently been introduced (D. Torrungrueng and E.H. Newman, AP-45, Aug. 1997) and extended for the analysis and design of the three dimensional (3D) geometries (D. Çolak, and E.H. Newman, AP-46, Sept. 1998). In the MSMM, the body is split into P sections and the currents on these sections are found in a recursive fashion. Although the MSMM is a frequency domain method, it has a time domain interpretation. The first sweep includes the dominant scattering mechanisms and each subsequent sweep includes higher order mechanisms.

This paper presents an investigation of the convergence properties of the MSMM. The method is formulated in a matrix notation as a stationary iterative algorithm. It is shown that the MSMM is mathematically equivalent to a block Jacobi preconditioned system of equations that result from the moment method, and solved via block symmetric successive over-relaxation (SSOR) with relaxation factor $\omega = 1$ (i.e. Back and Forth Seidel method). The MSMM first sweep, which uses R-cards to isolate the sections, is viewed as an initial guess vector. The Method of Ordered Multiple Interactions (MOMI) (and hence the Forward-Backward method) is shown to be equivalent to the MSMM with the MSMM section size equal to the MM segment size and zero initial guess vector. The convergence properties of the MSMM and the MOMI are compared for various 2D scattering geometries. Our results show that the MSMM converges for problems that the MOMI (and FB) fails to converge. Examples include a rough surface with a target on it, or when the surface becomes multi-valued which causes large off-diagonal elements in the interaction matrix. The effect of the initial guess vector on the convergence of the MSMM is also investigated. It is shown that using the MSMM first sweep current (which uses R-cards) as an initial guess vector for the iterative method yields the best convergence compared to PO and zero initial guess vectors. This is due to the fact that the MSMM first sweep includes the dominant scattering mechanisms.

Reduction of Sampling Density in CGFFT Method: Application of FFT Algorithm for Discontinuous Functions

Guo-Xin Fan, Qing Huo Liu, and Xue Min Xu
Department of Electrical and Computer Engineering
Duke University
Durham, NC 27708-0291

Large-scale scattering problems have been one of important topics in computational electromagnetics. Among the integral equation and differential equation solvers for large-scale problems, the conjugate gradient-fast Fourier transform (CGFFT) method has an $O(N)$ memory requirement, and is thus attractive for many applications.

In the CGFFT method, the FFT is used to evaluate the pertinent convolution integrals. As is well known, for a smooth periodic function, the FFT provides a high accuracy of the Fourier spectrum. However, if the function has singularities, such as jump discontinuities, the accuracy of the FFT results will be greatly reduced. For the problems involving inhomogeneous media and/or scatterers, since both the Green's function and the current density function have the discontinuities, the accuracy of their spectral functions obtained by the standard FFT limits the accuracy of the CGFFT method. Therefore, in practical CGFFT computation, the sampling density requires to be more than 10 points per wavelength, and the contrast of the medium parameters cannot be large.

Recently, we developed an efficient FFT algorithm for piecewise smooth functions. In this work, we apply this algorithm to the CGFFT method. For the one-dimensional scattering problems, it is observed that the sampling density in our new CGFFT method reduces to half of that in the conventional CGFFT method, and the contrast of the medium parameters can be much higher. New development and results will be reported in this presentation.

This work was supported by EPA through a PECASE grant CR-825-225-010, and by NSF through a CAREER grant ECS-9702195.

An Efficient Approach to Moment Method Analysis of Large Antenna Arrays

Michael P. Hurst
The Boeing Company
St. Louis, MO 63166

This paper describes a method for radically reducing the order of the general moment method (i.e., faceted geometry) system matrix for antenna arrays while retaining the accuracy of the solution. Hi-fidelity modeling of large antenna arrays has been beyond the reach of conventional low frequency methods because of the intractably large system matrices which arise. Modern arrays for aerospace applications often have more than 1000 antenna elements and several thousand facets may be required to capture the geometrical detail of a single element, resulting in millions of unknowns. "Fast" numerical methods which work well for large smooth bodies cannot achieve the same efficiency in antenna array problems, because the electrical separation between current subdomains is much shorter on average and more of the coupling is in the near field. Because detailed electromagnetic analyses have not been available, gain pattern predictions typically have been done by simply summing isolated element patterns and ignoring mutual coupling effects. Input impedance predictions have relied on periodic formulations which assume an infinite array and neglect edge effects, curvature and platform interactions.

The method described in this paper achieves high efficiency by converting a subdomain current expansion to a modal expansion. It has long been known that modal expansions (i.e., specialized basis functions tailored to a particular geometry) can be more efficient than general faceted models. This is because one can use physical insight to reduce the degrees of freedom to a bare minimum by building the physics into the basis function. In most practical cases, however, it is not apparent what the appropriate modal basis functions should be, nor is it desirable to write a new code for every new geometry. The present approach is to construct a modal basis set using facets as building blocks. A large number of the original edge current unknowns on an antenna element are replaced by a few *macro basis function* unknowns in the moment method system matrix. Each macro basis function corresponds to a natural mode of the antenna and is defined as a weighted collection of the original edge currents. The weights are determined empirically by solving for the currents which arise on an antenna element in a small array under various excitations (e.g., driven in antenna mode, illuminated by a neighbor, etc.). Currents on different antenna elements remain independent and may use different macro basis functions. The original faceted description is retained for portions of the geometry which do not lend themselves to modal expansion. The success of this approach depends on finding a set of expansion functions which spans the physical solution space. Examples will be given which show a two order-of-magnitude reduction in unknowns between the present approach and the standard moment method.

SOLUTION OF LARGE DENSE COMPLEX MATRIX EQUATIONS USING A
FAST FOURIER TRANSFORM (FFT) BASED WAVELET-LIKE
METHODOLOGY.

Kyungjung Kim
Tapan K. Sarkar
Department of Electrical Engineering & Computer Science
Syracuse University: Syracuse, NY 13244-1240
121 Link Hall
Syracuse University
Syracuse, NY 13244-1240
Phone : 315-443-3775
Fax : 315-443-441
Email : kkim08@mailbox.syr.edu
tk Sarkar@mailbox.syr.edu

Abstract

The Wavelet-like transformations have been used in the past to compress dense large matrices into a sparse system to solve a large of complex matrix equation. However, they generally are implemented through a finite impulse response filter realized through the formulation of Daubechies. In this paper, we propose an alternate methodology to the FIR Daubechies filters. This alternate procedure is based on the classical Fast Fourier Transform (FFT). The computationally efficient FFT is used to carry out the multiresolution analysis instead of the FIR Daubechies filters. The goal of this new implementation is not only to establish a computationally efficient methodology but a numerically stable result for higher order FIR filter. The advantage and disadvantage of this new procedure based on the classical FFT is illustrated through the solution of a large dense complex matrix equation in the numerical examples. The disadvantage of the FFT procedure is that due to the introduction of the Gibb's phenomenon, the reconstruction error is slightly higher. To reduce Gibb's phenomenon this methodology is achieved through the symmetric extension of the functions. Even though the FFT implementation of the DWT displays Gibb's phenomenon, it can still achieve compression > 99% of a 4096 by 4096 complex dense matrix that arises in a typical electromagnetic scattering problem. It has been performed that the result of the FFT becomes better, the larger the size of the matrix equations. Hence, the large complex dense matrix which needs to be stored on a disk for solution purpose can be stored entirely in the main memory without resulting in as significant loss in accuracy.

Time-Domain Numerical Methods

Co-chairs: J. L. Young, University of Idaho
W. Hoefer, University of Victoria, Canada

			Page
1	12:00	Volume integral equation based method for transient scattering from nonlinear penetrable objects--TM case, <i>J. Wang, M. Lu, E. Michielssen*</i> , University of Illinois at Urbana-Champaign, USA	AP
2	12:00	A hybrid time domain technique combining the Finite Element, Finite Difference and Integral Equation methods, <i>A. Monorchio*</i> , University of Pisa, Italy, <i>A. Rubio Bretones, R. Gomez Martin</i> , University of Granada, Spain, <i>G. Manara</i> , University of Pisa, Italy, <i>R. Mittra</i> , Pennsylvania State University, USA	AP
3	12:00	Novel 2D transient EFIE, MFIE, and CFIE solvers based on the multilevel plane wave time domain algorithm, <i>M. Lu*</i> , University of Illinois at Urbana-Champaign, <i>B. Shanker</i> , Iowa State University, <i>A. Ergin, E. Michielssen</i> , University of Illinois at Urbana-Champaign, USA	AP
4	12:00	An accurate discretization scheme for the numerical solution of time domain integral equations, <i>D. Weile*</i> , <i>A. Ergin</i> , University of Illinois at Urbana-Champaign, <i>B. Shanker</i> , Iowa State University, <i>E. Michielssen</i> , University of Illinois at Urbana-Champaign, USA	AP
5	12:00	Fast transient analysis of electromagnetic scattering from three-dimensional dielectric inhomogeneities using a volume integral equation, <i>N. Gres*</i> , University of Illinois at Urbana-Champaign, <i>B. Shanker</i> , Iowa State University, <i>A. Ergin, E. Michielssen</i> , University of Illinois at Urbana-Champaign, USA,	AP
6	12:00	Transient analysis of scattering from arbitrarily shaped perfectly conducting bodies at very low frequencies, <i>N. Chen*</i> , <i>K. Aygun, E. Michielssen</i> , University of Illinois at Urbana-Champaign, USA	AP
7	12:00	Characteristic-based time-domain method for electromagnetic analysis, <i>D. Jiao*</i> , <i>J-M. Jin</i> , University of Illinois at Urbana-Champaign, <i>J. Shang</i> , Air Force Research Laboratory, USA	AP
8	12:00	A MoMTD/FDTD hybrid method to calculate the SAR induced by a base station antenna, <i>D. Lautru*</i> , <i>J. Wiart</i> , France Télécom, <i>W. Tabbara, Supelec</i> , France, <i>R. Mittra</i> , Pennsylvania State University, USA	AP
9	12:00	A systematic and memory-saving scaling function based multiresolution scheme, <i>M. Yang, Q. Cao, Y. Chen*</i> , Hong Kong Polytechnic University, Hong Kong	AP
10	12:00	Generalized Z-domain absorbing boundary conditions for time-domain Finite-Element method, <i>Z. Shao, W. Hong*</i> , Southeast University, Nanjing	AP
11	12:00	A time domain integral equation method for wide-band scattering problems, <i>T. Van, A. Wood*</i> , Air Force Institute of Technology, USA	175

12	12:00	Time domain integral equation analysis of hybrid inhomogeneous dielectric and conducting surface wire structures, <i>K. Aygün*</i> , <i>N. Gres</i> , <i>University of Illinois at Urbana-Champaign</i> , <i>B. Shanker</i> , <i>Iowa State University</i> , <i>E. Michielssen</i> , <i>University of Illinois at Urbana-Champaign, USA</i>	176
13	12:00	A predictor-corrector technique for the accurate solution of electromagnetic time-domain integral equations, <i>D. Weile*</i> , <i>University of Illinois at Urbana-Champaign</i> , <i>B. Shanker</i> , <i>Iowa State University</i> , <i>A. Ergin</i> , <i>E. Michielssen</i> , <i>University of Illinois at Urbana-Champaign, USA</i>	177
14	12:00	Analysis of transient scattering from multiregion bodies using the plane wave time domain algorithm, <i>B. Shanker*</i> , <i>University of Iowa</i> , <i>A. Ergin</i> , <i>E. Michielssen</i> , <i>University of Illinois, Urbana-Champaign, USA</i>	178
15	12:00	Analysis of transient scattering from real complex structures composed of conducting and dielectric bodies, <i>T. Sarkar*</i> , <i>W. Lee</i> , <i>Syracuse University, USA</i>	179
16	12:00	A study of ABCs for the PITD method, <i>J. Miller*</i> , <i>R. Nevels</i> , <i>Texas A&M University, USA</i>	180
17	12:00	An explicit full wave path integral method for electromagnetic scattering, <i>R. Nevels*</i> , <i>J. Miller</i> , <i>Texas A&M University, USA</i>	181
18	12:00	An improved pseudospectral time-domain method for perfect conductors, <i>Q. Liu*</i> , <i>G-X. Fan</i> , <i>Duke University, USA</i>	182
19	12:00	Comparison of two Chebyshev PSTD algorithms for inhomogeneous media, <i>B. Tian*</i> , <i>Q. Liu</i> , <i>Duke University, USA</i>	183

A Time Domain Integral Equation Method for Wide-Band Scattering problems

Tri Van and Aihua W. Wood
Department of Mathematics and Statistics
Air Force Institute of Technology / ENC
2950 P Street
Wright-Patterson AFB, OH 45433-7765
email: Tri.Van@afit.af.mil, Aihua.Wood@afit.af.mil

To advance the state-of-the-art in low observables (LO) prediction technology demands the development of accurate and efficient simulation tools. Computational modelling provides an avenue to improve the efficiency of the LO design process. However, conventional frequency-domain computational electromagnetics (CEM) techniques are too computationally expensive to be used to generate accurate radar signature predictions of large targets over wide frequency bands. Current time-domain methods fail to satisfy LO accuracy requirements due to the artificial boundary condition used to model the infinite physical domain with a finite computational domain.

Recently, Ammari, Bao and Wood developed a set of frequency-domain integral equations that govern the scattering of electromagnetic waves by a cavity embedded in a ground plane ("An Integral Equation Method for the Electromagnetic Scattering from Cavities", preprint). By introducing a *transparent boundary condition* the infinite geometry was reduced to a bounded domain. In this paper, based on a similar approach, we develop a set of time-domain integral equations (TDIE) for broad-band scattering problems. We also establish the well-posedness of the problem by proving existence and uniqueness of the solution. Using the exact time domain integral equations to capture the outgoing behavior of the scattered waves, we reduce the computational effort to a bounded domain which contains the scatterer.

The new TDIEs we develop here leads naturally to the development of a new and accurate computational method, combining the strengths of finite element time-domain and time-domain integral equation (FETD/TDIE) methods, for wide-band applications. The new simulation tool will be especially useful in LO applications such as cavity-backed antennas and jet engine inlet and exhaust ducts. The numerical implementation will be reported elsewhere.

Time Domain Integral Equation Analysis of Hybrid Inhomogeneous Dielectric and Conducting Surface-Wire Structures

K. Aygün*†, N. Gres†, B. Shanker‡, and E. Michielssen†

†Center for Computational Electromagnetics
Department of Electrical and Computer Engineering
University of Illinois at Urbana-Champaign
1406 W. Green St., Urbana, IL 61801
e-mail: aygun@uiuc.edu

‡Electrical and Comp. Engineering Dept.
Material Assessment Research Group
Iowa State University
372 Durham Center, Ames, IA 50010

In this paper, a novel method for analyzing transient electromagnetic phenomena involving complex structures comprised of arbitrarily shaped inhomogeneous dielectric bodies and/or perfect electrically conducting (PEC) surfaces and wires, is proposed. The proposed scheme solves a hybrid volume-surface time domain integral equation (TDIE) using a marching on in time (MOT) algorithm. Specifically, the MOT algorithm computes the time dependent electric flux density throughout the dielectric bodies and electric currents on the PEC surfaces and wires by simultaneously solving a set of coupled volume-surface TDIEs. In the MOT algorithm, volumetric tetrahedral and surface triangular rooftop basis functions are used to describe the spatial dependency of the electric flux in the dielectrics and currents on the PEC surfaces, respectively. The temporal dependency of all quantities is modeled using piecewise polynomial basis functions.

The above MOT scheme has been accelerated with the recently developed plane wave time domain (PWTD) algorithm (A. A. Ergin, B. Shanker, and E. Michielssen, *IEEE Antennas and Propagat. Mag.*, **41**, 39-52, 1999) to facilitate the analysis of realistic problems involving complex geometries described in terms of a large number of basis functions. For a problem described by N_s spatial and N_t temporal unknowns, the computational complexity of the PWTD enhanced hybrid volume-surface MOT scheme scales as $O(N_s N_t)$ compared to $O(N_s^2 N_t)$ of the classical MOT scheme.

The proposed technique has been applied to the analysis of radiation and scattering from and signal propagation on printed circuit boards, dielectric resonators, and the design of novel broadband antennas. Numerical results illustrating the efficacy of the method will be presented at the conference.

A Predictor-Corrector Technique for the Accurate Solution of Electromagnetic Time-Domain Integral Equations

Daniel S. Weile^{†*}, Balasubramaniam Shanker[‡], A. Arif Ergin[†], and Eric Michielssen[†]

[†]Center for Computational Electromagnetics
Dept. of Electrical and Computer Engineering
University of Illinois at Urbana-Champaign
1406 W. Green St., Urbana, IL 61801
E-mail: dsw@decwa.ece.uiuc.edu

[‡]372 Durham
Dept. of Electrical and Computer Engineering
Iowa State University
Ames, IA 50011

Though largely ignored in the past, applications of time-domain integral equation (TDIE) methods to the solution of electromagnetics problems have become more common in the past few years. The rekindling of interest in techniques such as marching-on-in-time (MOT) was made possible by two recent advancements: the introduction of implicit time-stepping schemes that enhance the stability of MOT, and the advent of fast solution schemes that make the MOT solution of large problems feasible. Despite this progress, however, the accuracy and stability of MOT methods is still not well understood, and the construction of a reliable temporal basis remains an elusive goal.

Most current MOT schemes rely on piecewise Lagrange interpolation polynomials as temporal basis functions. The basis functions themselves must be anticausal by exactly one time step. Using more anticausal bases makes the current at any given time step dependent on future currents that are not yet known, and using less anticausal bases eliminates the modeling of interactions between different portions of the scatterer. Moreover, because of the spatial discretization of the scatterer, the incident (and hence the scattered) wave must be approximately band-limited. Not only are piecewise polynomials inefficient in interpolating band-limited functions, but they also introduce enormous amounts of extra frequency content not present in the fields themselves.

Functions specifically designed for the interpolation of band-limited temporal signatures (such those used in the approximate prolate series (J. J. Knab, *IEEE Trans. Inf. Theory*, 6, 717-720, 1979)) can solve both of these problems. In general, such functions require many fewer samples of a function than piecewise polynomials to produce an accurate interpolant. Additionally, these band-limited interpolation functions (BLIFs) are themselves band-limited, making it possible to control the frequencies introduced into the simulation by the basis. Unfortunately, BLIFs are always more than just one step anticausal, making their direct inclusion in standard MOT techniques impossible.

In this study, a predictor-corrector technique is used to allow for BLIF temporal modeling in an MOT scheme. Specifically, one-step anticausal functions are used to march forward in time and compute approximate values of the future current. Past values are then corrected using these predictions and the BLIFs for temporal modeling. By constantly correcting current values at past times, the stability and accuracy of MOT codes with large time steps is greatly improved. Numerical results demonstrating the technique will be given at the presentation.

Analysis of Transient Scattering from Multiregion Bodies Using the Plane Wave Time Domain Algorithm

Balasubramaniam Shanker^{†*}, A. Arif Ergin[‡], and Eric Michielssen[‡]

[†]Dept. Elec. & Comp. Engg.
Iowa State University
Ames, IA 50011
Email: shanker@iastate.edu

[‡] Dept. Elec. & Comp. Engg.
University of Illinois at Urbana
1406 W. Green St., Urbana, IL
61801

Integral equation based methods for time domain scattering analysis are computationally intensive with a cost scaling of $\mathcal{O}(N_t N_s^2)$, where N_s represents the number of surface unknowns modeling the current on the body, and N_t denotes the number of time steps that the analysis is carried out for. With the introduction of the plane wave time domain (PWTd) algorithm (A. A. Ergin, B. Shanker and E. Michielssen, *IEEE Antennas Propagat. Mag.*, 41, 39-52, 1999) this cost can be reduced to $\mathcal{O}(N_t N_s \log^2 N_s)$. In electromagnetics, the PWTd algorithm has been used in accelerating the analysis of scattering and radiation from perfect electrically conducting (B. Shanker, A. A. Ergin and E. Michielssen, *Proceedings of IEEE Antennas and Propagation Society International Symposium*, 2, 1342-1345, 1999) and penetrable bodies (B. Shanker, A. A. Ergin, and E. Michielssen, *26th General Assembly Abstracts*, URSI, 112, 1999).

In this paper, a novel time domain integral equation technique, that is developed for analyzing transient scattering from arbitrarily shaped bodies that comprise of different regions, will be presented. The regions could be either conducting or penetrable or partially penetrable. The analysis proceeds as follows: In each region, time domain Stratton-Chu integral equations are reduced to matrix equations. Boundary conditions at the interfaces of two regions and other constraints are imposed via multiplication with auxiliary matrices. For a simple dielectric interface, it can be shown that using appropriate auxiliary matrices, one can obtain matrix equations that correspond to the weak forms of either the PMCHW or the Müller integral equations. This procedure yields a scheme that is in spirit akin to the frequency domain algorithm that was proposed by Medgyesi-Mitschang *et. al.* (L. N. Medgyesi-Mitschang, J. M. Putnam, and M. B. Gedera, *J. Opt. Soc. Am. A*, 11, 1383-1398, 1994). While the above set of equations can be solved using the classical marching-on-in-time (MOT) method, the computational cost of which is prohibitive. This is alleviated using the multilevel PWTd algorithm. To accommodate the PWTd algorithm, each region is assigned its own fast PWTd kernel that is responsible for propagating the fields within that region. This kernel performs the following tasks: (i) divides the region into a number of subregions, (ii) generates a multilevel tree depending on a predefined separation criterion, and (iii) computes the interaction between subregions at the lowest level of the tree using the MOT algorithm, and between those at higher levels using the multilevel PWTd algorithm. It is necessary that each region have its own kernel as the wave speed in each region differs. Boundary conditions are imposed using the methodology mentioned earlier. This technique has been applied to the analysis of scattering from electrically large multiregion bodies. Details of the method and numerical results that demonstrate its efficiency will be presented at the conference.

ANALYSIS OF TRANSIENT SCATTERING FROM REAL COMPLEX STRUCTURES COMPOSED OF CONDUCTING AND DIELECTRIC BODIES

*Tapan K. Sarkar and Wonwoo Lee
Department of Electrical Engineering & Computer Science
121 Link Hall, Syracuse University
Syracuse, New York 13244-1240
Phone : 315-443-3775
Fax : 315-443-4441
Email : wlee01@mailbox.syr.edu, tk Sarkar@mailbox.syr.edu

Sadasiva M. Rao
Department of Electrical Engineering
Auburn University,
Auburn, AL 36849
e-mail: rao@eng.auburn.edu

A time-domain surface integral equation approach based on the electric field formulation is utilized to calculate the transient scattering from both conducting and homogeneous dielectric bodies consisting of large complex structures. The method involves the triangular patch modeling of arbitrary shaped surfaces because of their ability to conform easily to any geometrical boundary or surface. The numerical solution is based on the method of moment and an implicit time-domain integral-equation technique to solve the coupled integral equations that can be derived utilizing the equivalence principle for the combined conducting and dielectric bodies. This approach is efficient for large values of the time step and even for the large real complex structures. The usual late time instabilities associated with the time domain integral equations are avoided by using an implicit scheme.

In the recent literature, some kinds of simple structures like wires, plates, or spheres were considered to apply to either of conducting or dielectric bodies. The arbitrarily shaped-structure used in this paper is a model of an aircraft that has many different shaped triangular patches to make close enough to the real aircraft even in the case that one part of the structure is conducting body and the other part is dielectric body, which are combined each other. Mathematical steps and numerical solutions are presented to illustrate the efficiency of this analysis and may be used to obtain the surface current density and the near or far scattered fields, and simulation results of the example are presented to verify this method.

A Study of ABCs for the PITD Method

J. A. Miller* and R. D. Nevels
Department of Electrical Engineering
Texas A&M University
College Station, Texas 77843-3128

The Path Integral Time-Domain (PITD) method is a full wave electromagnetic scattering technique (R. D. Nevels, J. A. Miller, and R. E. Miller, "A Path Integral Time Domain Method for Electromagnetic Scattering", IEEE Trans. Antennas Propagat., April, 2000). It is based on a Feynman path integral formulation, which yields a propagator solution to the time domain form of Maxwell's differential equations. The essence of the PITD method is that the present time electric and magnetic field components are first Fourier transformed into the spectral domain, then multiplied by a state transition matrix and finally inverse transformed back to the real space-time domain. Each repetition of this set of operations advances the field a single time step.

The use of a discrete Fourier transform and a numerical grid throughout the computational space present difficulties in the numerical implementation of the PITD method. As with other time domain techniques, the scattered field reflects from the numerical grid boundary. In addition, the periodic nature of the discrete Fourier transform causes a "wrap around" effect on waves incident on the numerical grid boundary. For example, a wave propagating to the right will leave the numerical space and re-enter at the left numerical boundary. Both of these problems can be resolved by implementing an absorbing boundary condition (ABC).

In this presentation, three classes of ABCs will be considered. The first is the Null Boundary Condition, in which all field components are set to zero at the edges of the numerical space. This boundary condition can be implemented in a single cell layer around the boundary. The second includes a wide range of simple impedance tapers in which the conductivity of successive cells increases in the ABC region. The number of required boundary cells and the design (parabolic, exponential, etc.) of the taper will be discussed. It will be shown that the overall best choice in this class is a one in which $\sigma/\epsilon = \rho^*/\mu$ where σ is the electric conductivity, ϵ is the permittivity, ρ^* is the magnetic resistivity, and μ is the permeability. The last class is a Berenger type perfectly matched layer boundary condition. The absorbing material will be similar to that used in the class of impedance tapers, but applied to split field components in the absorbing boundary region. Reflection and transmission error will be presented for one and two-dimensional grids.

An Explicit Full Wave Path Integral Method For Electromagnetic Scattering

R. D. Nevels* and J. A. Miller
Department of Electrical Engineering
Texas A&M University
College Station, Texas 77843-3128

A full wave Feynman Path Integral for the electromagnetic field has recently been derived based on the time domain form of Maxwell's differential equations (R. D. Nevels, J. A. Miller, and R. E. Miller, "A Path Integral Time Domain Method (PITD) for Electromagnetic Scattering", IEEE Trans. Antennas Propagat., April, 2000). The solution is in a form known as a phase space path integral. For the electromagnetic field this means that in order to complete one time step, the initial time electric and magnetic field components are first Fourier transformed into the spectral domain, then multiplied by a state transition matrix and finally inverse transformed back to the real space-time domain. Each repetition of this set of operations advances the field another time step.

A numerical method for evaluating the phase space path integral is easily devised. In fact one can simply select a fixed time step, determined by the size and physical complexity of the scattering object, and replace the forward and inverse Fourier transforms with discrete Fourier transforms (DFT's). A more sophisticated method, which allows speedier computation, relies on the fast Fourier transform (FFT) rather than the DFT. In either case the numerical method can be described as being *implicit* because it is necessary to process all of the field components in the numerical scattering region before the field is known at any spatial point at the next time step. There are also numerical difficulties that must be overcome when using numerical Fourier transforms because their periodic nature leads to aliasing errors and what is known as the "wrap around" effect, a phenomena in which waves exiting one side of the numerical space reappear on the adjacent side.

In this presentation we will describe an *explicit* method for evaluating the time domain path integral derived in the above referenced paper. Since this is an explicit method, only a knowledge of the previous time field at points in the immediate vicinity are required to determine the field at a particular point in the present time. It will be shown that the mathematical expressions are exact in 1-dimension and rely on only two integrations in 2- and 3-dimensions. In the latter two cases the integrations can be replaced by accurate numerical approximations. The explicit and implicit forms will be compared in terms of accuracy, dispersion and stability and results will be given for electromagnetic scattering from canonical structures, including a half space and a dielectric cylinder.

An Improved Pseudospectral Time-Domain Method for Perfect Conductors

QING HUO LIU AND GUO-XIN FAN

DEPARTMENT OF ELECTRICAL AND COMPUTER ENGINEERING
DUKE UNIVERSITY
DURHAM, NC 27708-0291

The pseudospectral time-domain (PSTD) algorithm was developed as an alternative to the finite-difference time-domain (FDTD) method for the simulation of electromagnetic wave propagation and scattering. This technique uses the fast Fourier transform (FFT) algorithm for the spatial derivatives and uses the perfectly matched layer (PML) to eliminate the wraparound effect due to the spatial periodicity introduced by FFT. Because of its highly accurate spatial derivatives, the PSTD algorithm requires a very small number of grid points per wavelength, and hence can be orders of magnitude more efficient than the FDTD method for large-scale problems. So far the PSTD method has been successfully applied to multidimensional inhomogeneous, anisotropic, and dispersive media.

The success of the PSTD largely relies on the fact that the tangential electric and magnetic field components are continuous across an interface between two different materials. However, one important limitation of the previous PSTD algorithm is that it cannot treat perfect conductors. This is due to the Gibbs' phenomenon associated with the discontinuities of some tangential magnetic field component at the PEC boundary. In this work, we address this problem by analyzing the singularity of the fields near a PEC interface. We propose a novel singularity subtraction method, which makes the field component continuous. Thus, the fast Fourier transform can be again used to obtain the spatial derivatives of electromagnetic fields without producing the Gibbs' phenomenon. We will demonstrate this technique by several numerical examples.

This work was supported by U.S. EPA through a PECASE grant CR-825-225-010, and by the NSF through a CAREER grant ECS-9702195.

Comparison of Two Chebyshev PSTD Algorithms for Inhomogeneous Media

Bo Tian and Qing Huo Liu

Department of Electrical and Computer Engineering

Duke University

Durham, NC 27708

In this work we develop and compare two Chebyshev pseudospectral time-domain (PSTD) methods for electromagnetic waves in inhomogeneous media. Because of its use of fast cosine transform (FCT), the conventional Chebyshev PSTD method has to use grid points located at the Chebyshev Gauss-Lobatto points $x_j = \cos \frac{\pi j}{N}$. Hence it cannot be directly applied to media with several regions of inhomogeneities or with complex geometry. The two methods developed here aim to overcome the limitations of the conventional Chebyshev PSTD method.

One way to deal with such problems is the multidomain Chebyshev pseudospectral time domain (PSTD) method, which splits the whole domain into several homogeneous subdomains. Field values across the interfaces of subdomains are coupled via characteristics matching conditions. Uniform FCT is applied in every subdomain with the regular Chebyshev grid.

Recently, nonuniform fast cosine transform (NUFCT) algorithms has been developed to allow a fast cosine transform of nonuniformly sampled data with $O(N \log_2 N)$ arithmetic operations. With these NUFCT algorithms, we can now develop a Chebyshev PSTD method for inhomogeneous media with one grid. The grid points are not necessarily located at the Chebyshev Gauss-Lobatto points. Depending on the property of inhomogeneous medium and its geometry, we can define a proper grid to avoid the dispersion errors around the interfaces of different materials and treat the entire computational region as one domain. In this work, we will calculate the field distribution and compare the numerical results of these two Chebyshev PSTD algorithms.

Smart Antennas, Arrays, and Diversity for Wireless Communications

Co-chairs: M. Crozzoli, CSELT, Italy Page
E. S. Gillespie, California State University, Northridge

- | | | | |
|----|------|---|-----|
| 1 | 1:50 | A dual-linear polarized microstrip array for fully-adaptive GSM antenna systems, <i>A. Ansbro, M. Crozzoli*, L. Destro, D. Forigo, R. Vinassa, CSELT, Italy</i> | AP |
| 2 | 2:10 | Improving the reverse link capacity of CDMA systems using macrodiversity, <i>S. Hum*, TRILabs, A. Host-Madsen, M. Okoniewski, University of Calgary, Canada</i> | AP |
| 3 | 2:30 | Space, polarization, and angle diversity for cellular base stations operating in urban environments, <i>B-K. Kim*, W. Stutzman, D. Sweeney, J. Reed, Virginia Polytechnic Institute & State University, USA</i> | AP |
| 4 | 2:50 | Mobile transmit diversity and TDD downlink performance for smart antennas in fast fading scenarios, <i>A. Kavak, Samsung Telecom, M. Torlak, University of Texas at Dallas, G. Xu, W. Vogel, University of Texas at Austin, USA</i> | AP |
| 5 | 3:10 | Key techniques for actualizing smart antenna hardware, <i>T. Hori*, K. Cho, Y. Takatori, K. Nishimori, Nippon Telegraph and Telephone Corp., Japan</i> | AP |
| | 3:30 | Break | |
| 6 | 3:50 | Implementation of a smart antenna test-bed, <i>H-J. Im, Seungwon Choi*, Hanyang University, Korea</i> | AP |
| 7 | 4:10 | Smart antenna application on vehicles with low profile array antennas, <i>R. Kronberger*, Fuba Automotive, H. Lindenmeier, L. Reiter, J. Hopf, University of the Bundeswehr Munich, Germany</i> | AP |
| 8 | 4:30 | A 120-degree sector beam from a transverse slot on the corner of a triangular waveguide for a base station antenna in millimeter-wave subscriber radio system, <i>H. Maejima*, J. Hirokawa, M. Ando, Tokyo Institute of Technology, Japan</i> | AP |
| 9 | 4:50 | Forward transfer function and carrier correlation measurements of broadband wireless systems, <i>T. Wong*, L. Chen, M. Yan, Illinois Institute of Technology, USA</i> | 186 |
| 10 | 5:10 | Active metallic photonic band-gap materials used for polarization diversity, <i>G. Poilasne*, University of California, Los Angeles, L. Desclos, NEC, USA</i> | AP |
| 11 | 5:30 | A planar diversity antenna for wireless handsets, <i>S. Ko*, R. Murch, Hong Kong University of Science and Technology, Hong Kong</i> | AP |

FORWARD TRANSFER FUNCTION AND CARRIER CORRELATION MEASUREMENTS OF BROADBAND WIRELESS SYSTEMS

Thomas Wong*, Ling Chen, and Ming Yan
Department of Electrical and Computer Engineering
Illinois Institute of Technology
Chicago, Illinois 60616
U. S. A.

Broadband wireless communication systems often need to accommodate a variety of baseband signal formats and modulation schemes to meet with the requirements of the subscribers, while maintaining high efficiency in spectrum usage. Conventional measurements of system performance in terms of the degradation of signal set with specific modulation and fixed network configuration become rather limited in their scope to provide a comprehensive assessment of system throughput.

To the RF engineer, a method to characterize the RF portion of the channel independent of the baseband format would appear attractive, for it will enable one to observe the intrinsic characteristics of the RF sections in the communication system, while allowing the implications of the measurement results to be translated to effects on the baseband signal when one desires to make the substantiation. In addition, specifications on the RF sections may be stipulated on the measurements to enable effective technical interactions between the RF engineer and engineers responsible for other portions of the system. This paper describes two measurement schemes to characterize the RF sections of a broadband wireless system. The first scheme provides information on gain flatness, channel dispersion, and nonlinear effects resulting from saturation of power devices and frequency conversion elements. This is accomplished by measuring the forward transfer function of the system from transmitter IF to receiver IF as the excitation is swept across the band. The second scheme provides information on the ability of the RF channel in preserving the coherence of two carriers under various system load conditions. This is achieved by observing the degradation in the cross correlation of two carrier tones after they are recovered by the receiver.

Both measurement schemes employ standard equipment with little modification on the method of excitation. Results of measurements performed on a broadband millimeter-wave system with over 1 GHz instantaneous bandwidth will be presented along with the interpretation of the data in the context of link budget, data throughput, and spectral efficiency.

Ferroelectric Technology for Phased-Array Antennas

Organizers and Chairs:			Page
		J. Synowczynski, ARL	
		D. Patel, NRL	
		B. Gersten, ARL	
1	1:50	Evaluating ferroelectric-based electronic scanning antenna array performance using measured material properties, <i>S. C. Tidrow, E. D. Adler, D. M. Potrepka, A. Tauber, D. D. Brickerd, A. Lee, B. Rod, M. S. Patterson, J. Synowczynski, US Army Research Laboratory, USA</i>	188
2	2:10	Phased-array antenna using the ferroelectric lens, <i>J. Rao*, D. Patel, Naval Research Laboratory, USA</i>	189
3	2:30	Low cost planar lens ESA, <i>P. Park*, S. Kim, J. Gandolfi, R. Tadaki, J. Zelik, T. Dougherty, Raytheon Electronic System, D. Patel, J. Rao, Naval Research Laboratory, L. Sengupta, Paratec Company, S. Wolf, D. Treger, DARPA, USA</i>	AP
4	2:50	Transitioning low loss Ferroelectric BaSrTiO ₃ /MgO composites into electronic scanning antennas, <i>J. Synowczynski, B. Gersten, Army Research Laboratory, Z. Yun, Z. Zhang, M. Iskander, University of Utah, USA</i>	190
5	3:10	Design of a low-cost 2D beam steering antenna using ferroelectric material and the CTS technology, <i>M. Iskander, Z. Yun, Z. Zhang, University of Utah, USA</i>	AP
	3:30	Break	
6	3:50	RF tunability measurements of ferroelectric ceramics, <i>W. McKinzie, 191 Atlantic Aerospace Electronics Corp., R. Geyer*, National Institute of Standards and Technology, USA</i>	
7	4:10	(Ba,Sr) TiO ₃ thin films for tunable microwave applications, <i>J. Horwitz, W. Kim, W. Chang, J. Pond, S. Kirchoefer, H. Wu, D. Chrisey, S. Qadri, Naval Research Laboratory, USA</i>	192
8	4:30	Thin-film phase shifters for low-cost phased arrays, <i>R. York*, A. Nagra, Y. Liu, E. Erker, T. Talor, P. Periaswamy, J. Speck, University of California, Santa Barbara, USA</i>	193
9	4:50	Thin film ferroelectric phase shifters for direct radiating and reflective phased array antennas, <i>R. Romanofsky, F. Van Keuls, F. Miranda, NASA Glenn Research Center, USA</i>	194
10	5:10	Ferroelectric thin films on Ferrites for phase shifters, <i>S. W. Kirchoefer, J. M. Pond, H. S. Newman, W. J. Kim, and J. S. Horwitz, Naval Research Lab., USA</i>	195
11	5:30	Electrophoretic deposition of ferroelectric composites for applications in electronic scanning systems, <i>E. Ngo*, P. C. Joshi, M. Cole, C. Hubbard, US Army Research Laboratory, USA</i>	196

Evaluating Ferroelectric-based Electronic Scanning Antenna Array Performance Using Measured Material Properties

S. C. Tidrow,* E. D. Adler, D. M. Potrepka, A. Tauber, D. D. Brickerd, A. Lee, B. Rod, M. S. Patterson, U. S. Army Research Laboratory, AMSRL-SE-RE, 2800 Powder Mill Road, Adelphi, MD, and J. Synowczynski, U. S. Army Research Laboratory, AMSRL-WM-MD, Aberdeen Proving Ground, MD

There is a need to quantify the performance of ferroelectric-based electronic scanning antenna arrays for radar and communication applications. For passive antenna arrays, the isotropic radiated power (EIRP), a measure of transmitter power, and G/T (antenna gain/effective system temperature), a measure of the system output signal-to-noise ratio, are used as accurate gauges for comparing electronic scanning antenna performance. Using the properties of the ferroelectric materials, EIRP and G/T can be estimated using commercially available simulation software and thus reasonable phase shifter architectures can be defined. For ferroelectric phase shifters, the relevant material properties are loss tangent ($\tan \delta$), dielectric constant (ϵ) and material tunability for predefined bias conditions. In this paper, we utilize the temperature and frequency dependent dielectric constant and loss tangent measurements of a barium-titanate-based field-tunable material to develop initial phase shifter parameters. We further use the reported material temperature dependent low frequency tunability to estimate the total expected phase shift of the ferroelectric device. Based on these phase shifter parameters, we then can extract performance metrics for an electronic scanning antenna.

PHASED-ARRAY ANTENNA USING THE FERROELECTRIC LENS

Jaganmohan B. L. Rao* and Dharmesh P. Patel
Radar Division, Naval Research Laboratory, Washington, DC 20375

A phased-array antenna can rapidly scan its beam without mechanical movement. Each radiating element of a phased array is usually connected to a phase shifter and a driver, which determine the phase of the signal at each element to form a beam at the desired angle. The cost of a phased array mainly depends on the cost of the phase shifters and drivers. A typical array may have several thousand elements and that many phase shifters and drivers; hence, it is very expensive. Therefore, reducing the cost and complexity of the phase shifters, drivers and controls is an important consideration in the design of phased arrays.

The ferroelectric lens phased-array antenna uniquely incorporates bulk phase shifting with ferroelectric material; the array does not contain individual phase shifters. This reduces the number of phase shifters from $(n \times m)$ to $(n + m)$, where n is the number of columns and m is the number of rows in a phased array. The number of phase shifter drivers and phase shifter controls is also reduced by the same factor using row-column phase control. This leads to a substantial reduction in the total cost of a phased-array antenna. A single ferroelectric lens provides one-dimensional electronic beam scanning. Two-dimensional beam scanning can be achieved by cascading two ferroelectric lenses or using one ferroelectric lens in a hybrid configuration with a phased array that can scan the beam in one plane.

In this presentation, we will review the ferroelectric lens concept and show how it can be used as a low-cost phased array. We will describe the bulk ferroelectric ceramics that we used. We will present experimental results of one column of the lens at X band and C band. Radiation patterns of a two-column interferometer demonstrating electronic beam scanning at 10 GHz will also be presented.

TRANSITIONING LOW LOSS FERROELECTRIC BaSrTiO₃ / MgO COMPOSITES INTO ELECTRONIC SCANNING ANTENNAS

^AJ. Synowczynski, ^AB. Gersten, ^BZ. Yun, ^BZ. Zhang and ^BM. F. Iskander

^A AMSRL-WMR-MD, Army Research Laboratory, APG, MD USA

^B Electrical Engineering, University of Utah, Salt Lake City, Utah USA
jenns@arl.mil

The Army has been developing low cost electronic scanning antenna technology for Comm-on-the-Move communication systems. Ferroelectric materials offer an inexpensive phase shifting alternative to MMIC, MEMS and ferrite phase shifting. However, the ferroelectric insertion losses and temperature stability issues prohibited demonstration until the discovery of BaSrTiO₃ / MgO composite materials. By compositing BaSrTiO₃ with low loss MgO, the ferroelectric behavior is preserved while the average materials losses are reduced. However, there are obstacles to integrating these phase shifters into conventional antenna architectures. These include problems in synchronization between the phase shifters which result from temperature variations in the lattice and individual phase shifter reliability. These issues will be discussed in detail in terms of their origin in the materials processing. One potential solution to these materials barriers is to use an integrated antenna architecture such as the Continuous Transverse Stub Antenna Array. An overview of the CTS design using ferroelectric material will also be discussed.

RF TUNABILITY MEASUREMENTS OF FERROELECTRIC CERAMICS, W. McKinzie, Atlantic Aerospace Electronics Corp., Greenbelt, MD 20770; R. G. Geyer*, Radio Frequency Technology Division, M.S. 813.01, National Institute of Standards and Technology, Boulder, CO 80303, (303) 497-5852

Tunability is needed in many areas of microwave electronics such as radar, communications, and test systems. Ferroelectric materials, nonlinear dielectrics possessing an electric field-dependent permittivity, may be used over a wide frequency spectrum and do not have low frequency limits like tunable ferrites. Inexpensive, lightweight tunable capacitors, filters, resonators, phase-shifters, and voltage controlled oscillators incorporating ferroelectric materials can be developed for microwave applications. Although larger tunability is a desirable feature for most microwave applications, a ferroelectric material with larger tunability usually has greater dielectric loss. Optimizing tunability and dielectric loss to meet the needs of a particular microwave application remains a challenging task. A modified doubly reentrant coaxial cavity for characterizing tunability of ferroelectric ceramics at rf frequencies is discussed.

Richard G. Geyer, National Institute of Standards and Technology, MS 813.01, 325 Broadway, Boulder, CO 80303, (303) 497-5852, FAX: (303) 497-3122

Will McKinzie, Atlantic Aerospace Electronics Corporation, 6404 Ivy Lane, Suite 300, Greenbelt, MD 20770

(Ba,Sr)TiO₃ THIN FILMS FOR TUNABLE MICROWAVE APPLICATIONS

J.S. Horwitz, W.J. Kim, W. Chang, J.M. Pond, S.W. Kirchoefer, H. D. Wu, D.B. Chrisey,
and S.B. Qadri

Naval Research Lab, Washington DC 20375

Ferroelectric thin films are currently being used to develop a new class of frequency agile microwave devices such as broad band phase shifters and low phase noise, voltage controlled oscillators. Oriented, single phase (Ba,Sr)TiO₃ (BST) thin films (≤ 5000 Å) have been deposited onto dielectric substrates using pulsed laser deposition (PLD). BST is a solid solution ferroelectric that exhibits an electric field dependent dielectric constant and composition dependent (Ba/Sr) Curie temperature. Thick ($>1\mu\text{m}$) interdigitated Ag capacitors have been deposited on top of the BST films to characterize the dielectric properties of the BST film. The capacitance and dielectric Q ($1/\tan\delta$) of the interdigitated structure have been measured at room temperature and at microwave frequencies (1-20 GHz) as a function of electric field (0-80 kV/cm). The measured dielectric properties were observed to strongly depend on film composition, substrate type and post-deposition processing. In the heteroepitaxial growth of BST on MgO and LaAlO₃ substrates, the lattice mismatch between the film and the substrate creates a strained interface and a tetragonally distorted BST film structure. High-resolution X-ray diffraction measurements have shown that the magnitude of the strain in the BST film is correlated with the dielectric tuning and dielectric loss. BST films deposited by PLD are oxygen deficient. On MgO, the lattice constants for the film are enlarged relative to the bulk material and the film is in compressive stress. Post-deposition annealing films in oxygen can be used to fill oxygen vacancies, which reduces the lattice parameter of the film and changes the film stress to tension. By controlling the oxygen deposition pressure during film growth, strain free films can be deposited onto non-lattice matched substrates. These films have higher dielectric constants and lower dielectric loss compared to films that are tetragonally distortion. Strain free films have a higher overall figure of merit ($Q \times \% \text{Tuning}$) for the tunable microwave device. BST films with low stress will be required for the development of next generation frequency agile microwave electronics.

Thin-Film Phase Shifters for Low-Cost Phased Arrays

Robert A. York^{1*}, Amit S. Nagra¹, Yu Liu¹, E. Erker¹, Troy Taylor²,
Padmini Periaswamy², James S. Speck²

¹*Department of Electrical and Computer Engineering,* ²*Materials Science*
University of California, Santa Barbara, CA 93106

ABSTRACT:

Drastic cost reduction of phased-arrays will require a significant shift in current design strategy. The emphasis must be on removing expensive active components, not developing more highly integrated components or exotic packaging techniques. The phase shifter circuits—an essential active component—are the primary obstacle in decreasing the cost and number of active components in a phased-array. The problem is multi-faceted: (1) current phase-shifter components are themselves MMICs, which are expensive (~40% of the total receive-array cost) and require complex packaging; and (2) current phase shifters have significant RF loss and therefore amplification (i.e. even more MMICs) must be provided in front of the phase shifter (in a receiving application) to compensate for this loss, which in turn may require limiting circuits in situations with strong local interference. If a phase shifter could be designed with little or no loss, it is believed that up to 80% of the active devices in a typical phased-array could be deleted from the design.

Two new technologies—thin-film nonlinear dielectrics and MEMS—have recently emerged and show significant promise for implementation of low-loss and low-cost phase shifters. Both technologies appear capable of ultimately providing <3dB insertion loss for a 360 degree phase shifter at considerably lower cost than existing MMIC designs. This paper will focus mostly on developments in thin-film phase shifter circuits using monolithic Barium Strontium Titanate (BST) varactors on inexpensive substrates. Enhanced MEMS circuits using such thin-film dielectrics will also be discussed and contrasted with the nonlinear dielectric approaches in terms of electrical performance and practical considerations for use in low-cost phased-arrays. The thin-film nonlinear dielectrics have been grown by both MOCVD-grown and RF magnetron-sputtering, and can now be obtained commercially. They are very inexpensive, can be deposited on inexpensive Silicon or ceramic substrates, and are compatible with most standard monolithic processes with considerably looser lithography requirements as compared with MMICs. Current progress in materials and projected performance limits will be discussed.

Thin Film Ferroelectric Phase Shifters for Direct Radiating and Reflective Phased
Array Antennas

R.R. Romanofsky, F.W. Van Keuls, and F.A. Miranda
NASA Glenn Research Center
Cleveland, Ohio

Our group at NASA Glenn has developed novel coupled microstripline phase shifters based on thin ferroelectric films (F.W. VanKeuls et al., IEEE MTT-S Digest, 1999, pp. 737-740). These phase shifters are designed to enhance the performance of direct radiating arrays and enable a new type of reflectarray at K-band frequencies. These $\text{Ba}_{1-x}\text{Sr}_x\text{TiO}_3$ on LaAlO_3 phase shifters exhibited performance as good as ≈ 6 dB of loss with ≈ 360 degrees of phase shift when operated in the transmit mode. Using these phase shifters we demonstrated a 16 element linear array employing a conventional beam forming manifold at 23.675 GHz. When operated in the reflective mode these phase shifters enable another type of scanning antenna called the ferroelectric reflectarray. We have designed a 2832 element reflectarray at 19.0 GHz where phase shifters have demonstrated a figure of merit of $74^\circ/\text{dB}$. The design and performance of the linear array and the design details of the reflectarray will be discussed.

FERROELECTRICS THIN FILMS ON FERRITES FOR PHASE SHIFTERS

S. W. Kirchoefer, J. M. Pond, H. S. Newman, W. J. Kim and J. S. Horwitz
Naval Research Laboratory, Washington, DC 20375

Wideband tunable phase shifters are being developed using ferroelectric thin films for operation at room temperature. Our efforts have focused on pulsed-laser deposition of thin films of barium strontium titanate which are being optimized to simultaneously possess low dielectric loss tangent and reasonable modulation of the relative permittivity with an applied dc field. These films are used to fabricate wideband distributed transmission lines. Ferroelectric/ferrite material combinations are being developed in order to mitigate the deleterious effects of modifying the capacitance per unit length on the impedance match of the transmission line. The addition of a ferrite will make it possible to independently tune both the inductance per unit length and capacitance per unit length. In principle, this will permit tuning of the phase velocity while maintaining the transmission line characteristic impedance. Barium strontium titanate has been successfully deposited on YIG. Initial microwave measurements have indicated that both magnetic and electric tuning mechanisms are active and that the phase velocity can be tuned equally well by either magnetic or electric field. An equivalent differential phase shift can be achieved with a magnetic bias on the order of 100 Oersteds as has been achieved with an electric field bias of 21 KV/cm (40 Volts)

Electrophoretic Deposition of Ferroelectric Composites for Applications in Electronic Scanning Systems

Eric Ngo,* P. C. Joshi, M. Cole, C. Hubbard
U. S. Army Research Laboratory, Weapons and Materials Directorate, APG, MD

In the last decade, the need to miniaturize electronic components has generated tremendous interest, especially in the thick/thin film research and development. The Army Research Laboratory have formulated and patented various composites of Barium Strontium Titanate (BSTO) combined with other nonelectrical oxide ceramics in the form of bulk and thin films. These materials possess superior electronic properties that can be controlled and tailored for use in different electronic devices, particularly in phase array antennas.

In this study, we have investigated the electrophoretic deposition (EPD) method as a low cost and conformal way of depositing thin films of the composites of barium strontium titanium oxide. The materials were deposited on platinum substrate in an acetone base slurry under bias and at controlled rate. A study on the dispersing media was done to optimize the deposition rate. Electronic properties at low frequency of the EPD films were compared with those of the bulk ceramics. Additional analyses including surface roughness, SEM, FT-IR and AFM will also be discussed.

CAD Tools for Antennas and Microwave Circuit Modeling

Organizer and Chair: R. Mittra, Pennsylvania State University

Page

1	1:50	Current developments and future trends in antenna software user interfaces, <i>P. Frandsen, K. Pontoppidan*, TICRA, Denmark</i>	198
2	2:10	3D-CAD tools for antenna design, <i>J-P. Martinaud*, Thomson-CSF Detexis, France</i>	199
3	2:30	Finite Element tools for antenna and microwave circuit design, <i>T. Cwik*, Jet Propulsion Laboratory, USA</i>	200
4	2:50	Genetic algorithms in engineering electromagnetics: antenna design applications, <i>Y. Rahmat-Samii*, University of California, Los Angeles, USA</i>	201
5	3:10	CAD for frequency selective surface, <i>C. Chan*, K. Lam, K. Chan, City University of Hong Kong, Hong Kong</i>	202
	3:30	Break	
6	3:50	CAD tools for antennas and microwave circuit modeling: industry perspective, <i>P. Tirkas*, R. Kuroda, Kyocera America, Inc., USA</i>	203
7	4:10	A conformal FDTD software package for modeling RF antennas and microstrip circuit components, <i>W. Yu*, R. Mittra, The Pennsylvania State University, USA</i>	204
8	4:30	Neural networks for knowledge-based RF and microwave designs, <i>K. Gupta*, University of Colorado at Boulder, USA, Q. Zhang, Carleton University, Canada</i>	205

Current Developments and Future Trends in Antenna Software User Interfaces.

Poul Erik Frandsen and Knud Pontoppidan,
TICRA, Kronprinsensgade 1, DK-1114 Copenhagen K, Denmark*

Since the beginning of the seventies a substantial amount of antenna analysis and synthesis software has been developed based on advanced and excellent electromagnetic and mathematical models. Traditional programs can perform the analysis of a single type of antenna or antenna component operating under often ideal conditions. Such programs have become indispensable tools for the designer. The continuously growing complexity of antenna systems makes them difficult or impossible to analyze with the traditional programs. Hence, it has become necessary to develop more sophisticated antenna software although the underlying models to a large extent remain unchanged. Further, since the design process often requires the execution of different software it is important that the programs can be combined with limited efforts.

Contemporary software must be able to manage complex antenna systems where for example the radiation from several antennas mounted on a spacecraft can be analyzed in different ways including the interaction between different antennas. Advanced antenna analysis software that possesses these features is, however, of limited value unless a matching user interface is supplied. The user interface must offer relatively simple but at the same time flexible means for controlling the software. The user must be allowed to define the antennas to be analyzed and their environments in a natural way using concepts which are well known and well defined in antenna engineering. The programs must assist the user in setting up the complete system geometry and provide rapid and easy means for visualizing the system. In the case of reflector antennas e.g. such items as reflectors, struts, plane scatterers of different shapes and feeds of different types must be easy to create and to position. Further, the software must enable the user to manage the required sequence of electromagnetic calculations.

In the near future it will be required that different programs can be combined in the design process with a minimum user effort. Data created by one program must be easily accessible to other programs without the need for user-made filters. Homogeneous, recognizable and standardized interfaces will be required for the different programs such that user can get acquainted with new software tools with very limited training. Standardized interfaces will also enable an easy integration of software tools into design frameworks. Also, client-server interfaces for intranet and possibly internet services will appear.

In this presentation one such flexible interface for reflector antenna analysis will be discussed and the ongoing development and future requirements will be considered.

3D-CAD TOOLS FOR ANTENNA DESIGN

Jean-Paul Martinaud
Antennas and Radomes Unit
Thomson-CSF Detexis
78852 Elancourt, France

Fierce international competition is exerting increasing pressure to reduce price levels and lead times, and manufacturers are increasingly forced to optimize their approaches to the market and seek the highest levels of excellence possible. In this difficult technical and economic context, any design shortcoming can ultimately prove disastrous.

Antenna design is in the critical path of RF systems such as Radar and electronic warfare systems. The use of antenna modeling in the different phases of the development (specification, industrialization ...) is one way to improve the design process.

Thomson-CSF, aware of the great implications in hand, has been using and developing software tools dedicated to the solution of Maxwell equations for more than twenty years. In this context, we have been lead to use several techniques for antenna simulation such as BEM and FE both in the frequency and in the time domain.

In this presentation, we will give first an analysis of the capabilities of these methods to give a response to the industrial needs. Second, we will identify the future directions of development or improvement of software tools that have to be explored from the antenna designer point of view.

This analysis will be mainly focused on fully 3D antennas with arbitrary shape and materials, either alone or in array, issued from real-life applications. We will provide with some comparisons between simulations and measurements.

Finite Element Tools for Antenna and Microwave Circuit Design

Tom Cwik
Jet Propulsion Laboratory
4800 Oak Grove Dr.
Pasadena CA 91109
cwik@jpl.nasa.gov

Among tools used in the computer-aided design of antenna and microwave circuits, the finite element method provides a versatile and powerful approach for high-fidelity modeling. The method is useful for a wide range of structures and applications including antenna elements and arrays, microwave circuits, waveguide structures and scattering problems. Advantages of the method include reliable modeling of curved shapes and materials, accurate source models for waveguide or antenna structures, and fidelity to geometry variations at various scales. A strong mathematical formulation also allows controlled accuracy in the solution. Disadvantages of the method flow from the need to provide the computer-aided design geometry format as input, and the associated three-dimensional mesh of the volumes where the electromagnetic fields are calculated. For exterior antenna or scattering problems, the computational expense in memory and time to hold the mesh data and create a solution can also be limiting.

This talk will examine the use of finite element tools for the design and analysis of antenna elements and arrays, and microwave circuits. Specifically the state-of-the-art will be examined, with current limitations and areas of future advancement being outlined. This will include areas of computer-aided design for geometry definition, mesh generation and associated finite element basis functions, solution methods with associated computer resources, and boundary conditions for materials and at mesh boundaries when radiation problems are solved. The use of adaptive refinement to control the solution accuracy while limited the number and size of finite elements will also be examined. Finally, the use of parameterized geometries and the integration of optimization methods for design will be examined. Examples will be drawn from antenna elements and arrays, periodic structures and microwave devices.

Genetic Algorithms in Engineering Electromagnetics: Antenna Design Applications

Yahya Rahmat-Samii

University of California, Los Angeles

Los Angeles, CA 90095-1594, U.S.A.

Tel: 310 206 3847, Fax: 310 206 8495, e-mail: rahmat@ee.ucla.edu

Concept and Implementation of GA:

Charles Darwin's notion of biological evolution has resulted into the argument that life in this world in all its diverse and amazing forms was evolved by natural selection and natural adaptation processes controlled by the survivability of the fittest species. With this acceptance has come the temptation that perhaps one might be able to utilize nature's "selection and adaptation implementation engine" and apply it to the solution of engineering problems via the applications of Genetic Algorithms (GAs). In a few words, the machinery of Genetic Algorithms utilizes an optimization methodology which allows a global search of the cost surface via the mechanism of the statistical random processes dictated by the Darwinian evolutionary concept (Y. Rahmat-Samii and E. Michielssen, *Electromagnetic Optimization by Genetic Algorithms*, John Wiley, 1999). In this presentation, some of the key features of the Genetic Algorithms are summarized in an innovative and illustrative fashion and then they are applied to facilitate the optimum design of a class of antennas and electromagnetic devices for communications and radar applications..

Applications of GA in Antenna Designs:

One of the objectives of this presentation is to highlight an up to date body of knowledge on the application of GA techniques to the synthesis and optimization of antenna designs. In particular, this talk will focus on:

- (a) A brief engineering introduction to the Genetic Algorithms,
- (b) Demonstration of the potential application of GAs to a variety of electromagnetic engineering designs including microstrip antennas, multi-band and wideband antennas, synthesis of non-planar radar absorbing materials for RCS applications, Luneburg lens antenna design, synthesis of reflector antennas, design of photonic bandgap structures, etc. and
- (c) Assessment of the advantages and the limitations of the technique and its future development areas.

CAD for Frequency Selective Surface

C. H. Chan*, K. W. Lam and K. F. Chan
Wireless Communications Research Center
Department of Electronic Engineering
City University of Hong Kong
Kowloon, Hong Kong

Frequency selective surface (FSS) has a wide variety of electromagnetic applications. It has been used extensively as antenna radomes and microwave and optical filters. More recent applications can be found in the design of microstrip reflectarrays and uni-planar photonic band-gap structures. Over the years, we have developed various efficient CAD tools for planar FSS analyses. The FSS may have several screens. Several layers of dielectric may be sandwiched between any two screens. These CAD tools share a common feature that they all require solving an integral equation. When a uniform discretization of the unknown induced surface current on the conducting screen is adopted, an electric-field integral equation will be solved in the spectral domain using the conjugate gradient method in conjunction with the fast Fourier transform algorithm (CG-FFT). On the other hand, a hybrid spatial/spectral domain approach will be used instead when a non-uniform discretization is more suitable. To develop a successful CAD tool, we need to address issues such as user friendliness, efficiency and accuracy of the tool.

We have developed a Java based graphical user interface (GUI) for our CAD tool so that it can be run on different computer platforms. All parameters can be entered easily by using pull-down menus. Using a pointing device and predefined shapes, the unit-cell geometry of each FSS screens can be drawn easily. The unit-cell geometry will then be discretized automatically. For certain applications in analyzing fractal FSS and out-of-band response, a fine discretization may be needed. The resolution of the unit-cell ranges from 8x8 pixels to 1024x1024 pixels. Each pixel assumes a binary value of either one or zero. If the location of the pixel coalesces to the metallic portion of the FSS screen, the pixel will assume a value of one and it will assume a value of zero otherwise. A parallel version of the CAD tool is also developed for situations that a high resolution is unavoidable. The parallel code entails the use of the message passing interface (MPI) and a MPI version of FFT. It can be run on a cluster of PC's connected together by a switching box. This parallel code is particularly useful when we perform FSS design using the parallel genetic algorithm (GA). Each row of 1's and 0's can be regarded as a string of genes in the parallel GA.

The uniform discretization may not be convenient when thin structures exist in the unit cell. A non-uniform discretization using RWG triangular discretization will be used instead. Several hybrid spectral/spatial domain approaches have been developed to solve the corresponding mixed-potential integral equation. For the same number of unknowns, these hybrid methods, however, require much longer CPU time than that of CG-FFT method employed for the uniform discretization. All our CAD tools yield results that compared favorably with measurement.

CAD Tools for Antennas and Microwave Circuit Modeling: Industry Perspective

P.A. Tirkas and R. Kuroda
Kyocera America, Inc.
Research and Development Department
8611 Balboa Avenue
San Diego, CA 92123

Abstract

Advances in computer technology and computational electromagnetic methods provide a unique opportunity for fast, accurate, and efficient design of antennas and microwave circuits. Commercially available, full-wave electromagnetic software packages based on Finite Element Method (FEM), Moment Method (MM) and Finite-Difference Time-Domain (FDTD) method are becoming standard design tools in industry. Such software packages are often installed on powerful, but yet inexpensive, personal computers which in many instances have more than one processor and in excess of one GByte of RAM.

This paper will review the application of such computational methods in the design of advanced package modules where the integration of the antenna with the electronic package and other microwave passive devices such as filters is desirable. The first example involves a TR module for a phased array in the Q band. The module consist of a linearly tapered slot antenna as the radiator which is fed by a stripline. A transition from stripline to a coaxial connector is also included in the module. This module was modeled using a full-wave electromagnetic analysis package based on the FEM. Mutual coupling effects with the radiating elements positioned in a triangular grid were also accounted for using the periodic boundary conditions available in the FEM package. This represents an example where the model complexity requirements are well matched by the available commercial FEM software package.

The second example involves a miniature antenna printed on a thick ceramic substrate. This antenna is intended for wireless applications in the 2-3 GHz frequency range. Some of the desired characteristics included an omnidirectional pattern, better than 10 dB return loss over 100 MHz of bandwidth and better than -5dBi gain. A MM based software package was used for designing this antenna. This software package assumes infinite substrate dimensions in the horizontal plane. Discrepancies between measured results and simulated results were attributed to the differences in the substrate size in the horizontal plane (infinite substrate extent in the model versus finite substrate extent in the prototype). An attempt to model this antenna with an FEM based software package resulted in a large computational problem due to the thick substrate involved and poor convergence.

A Conformal FDTD Software Package for Modeling RF Antennas and Microstrip Circuit Components

Wenhua Yu and Raj Mittra

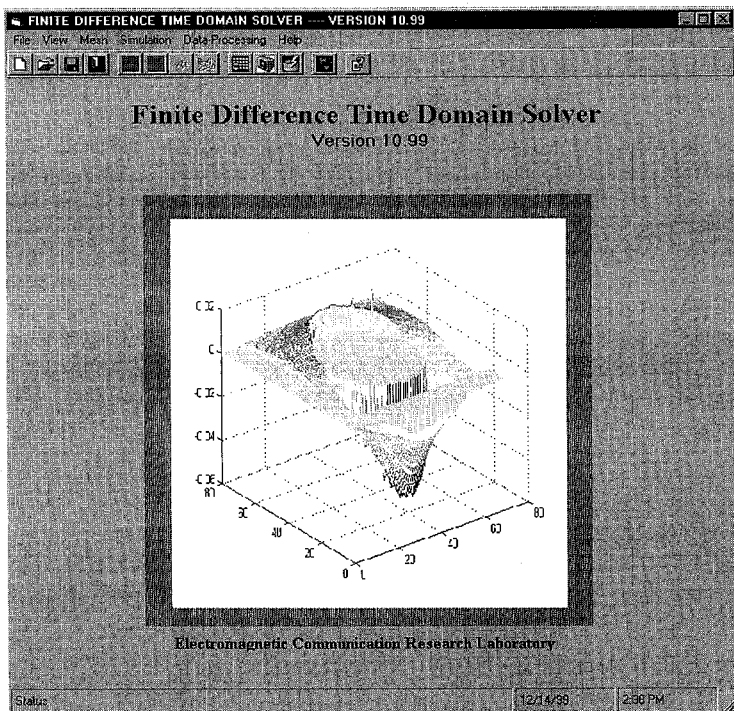
Electromagnetic Communication Laboratory, 319 EE East

The Pennsylvania State University

University Park, PA 16802

wxy6@psu.edu and rxm53@psu.edu

Abstract: This paper describes a conformal Finite Difference Time Domain (FDTD) software packaged and presents its applications to RF antennas and microstrip circuit components. The program includes a Visual Basic GUI for inputting object geometries, setting source and boundary conditions, generating a non-uniform mesh, and data post processing. A robust *conformal* finite difference time domain (CFDTD) technique is employed to handle conductors with curved surfaces and edges. Illustrative examples that show the application of the code for modeling antennas as well as microstrip discontinuities will be presented in the paper.



Neural Networks for Knowledge-Based RF and Microwave Designs

K.C. Gupta
University of Colorado at Boulder
Boulder, CO 80309-0425 USA

and

Q.J. Zhang
Carleton University
1125 Colonel By Drive, Ottawa, ON K1S5B6 Canada

Role of computational neural networks in modeling and optimization for RF and microwave designs has been well recognized in recent years. Another important task that is made convenient by usage of neural networks is embedding some specific knowledge in the design process leading to methodology for knowledge-based design.

The need for developing tools for knowledge-based design in various design domains is well appreciated. In this article we review various recent advances where existing RF/microwave knowledge is combined with neural networks. Starting with a brief description of knowledge issues in conventional neural network applications (e.g., pattern classification) and in microwave design, we discuss various effects of adding knowledge on the performance of the neural models such as, generalization ability, extrapolation ability, and model reliability, versus different sizes of training data needed in a knowledge based neural network (KBNN) technique. We also describe several ways of combining existing circuit models with neural networks, including the source difference method, the prior knowledge input method, and the space-mapped neural models. Finally, an advanced hierarchical neural network structure for the task of neural model library development is discussed.

The presentation concludes with some comments on how these recent research efforts could lead to development of knowledge based design tools for RF and microwave applications.

Characterization of Materials and EMC

Co-chairs:			Page
	D. A. Christensen, University of Utah		
	D. G. Bodnar, MI Technologies		
1	1:50	Using microwave sensors for determining physical properties of granular materials, <i>S. Trabelsi*</i> , <i>S. Nelson</i> , <i>US Department of Agriculture, O. Ramahi, Compaq Computer Corporation, USA</i>	208
2	2:10	Characterization of layered materials using a single, transient scattered field measurement, <i>E. Rothwell*</i> , <i>D. Nyquist</i> , <i>K. Chen</i> , <i>J. Meese</i> , <i>Michigan State University, L. Frasch, Boeing ISDS, USA</i>	209
3	2:30	On discriminating between buried metallic mines and metallic clutter using spatial symmetry and temporal exponential decay rates, <i>L. Riggs</i> , <i>L. Lowe*</i> , <i>T. Barnett</i> , <i>J. Mooney</i> , <i>J. Elkins</i> , <i>Auburn University, USA</i>	210
4	2:50	A theoretical investigation of pavement surface roughness using millimeter-wave interferometry technique, <i>S. Kim*</i> , <i>C. Nguyen</i> , <i>Texas A&M University, USA</i>	211
5	3:10	An experimental study of pavement macro texture using millimeter-wave step-frequency radar technique, <i>J. Park*</i> , <i>C. Nguyen</i> , <i>T. Scullion</i> , <i>Texas A&M University, USA</i>	212
	3:30	Break	
6	3:50	Coplanar sensors for thickness measurements, <i>C. Bassey</i> , <i>K. Caputa*</i> , <i>S. Stuchly</i> , <i>University of Victoria, Canada</i>	213
7	4:10	EMC effects of radiated fields coupling into electronic enclosures, <i>Z. Pantic-Tanner*</i> , <i>San Francisco State University, F. Gisin</i> , <i>Nortel Networks, USA</i>	214
8	4:30	Electromagnetic coupling to a wire residing inside a rectangular metallic box perforated with rectangular apertures, <i>M. Deshpande*</i> , <i>NYMA</i> , <i>C. Cockrell</i> , <i>F. Beck</i> , <i>NASA Langley Research Center, USA</i>	215
9	4:50	Wave absorber using transparent resistive-film for 1 GHz frequency band, <i>M. Hanazawa</i> , <i>K. Wada</i> , <i>O. Hashimoto*</i> , <i>Aoyama Gakuin University, Japan</i>	216
10	5:10	A broadband, calculable, disk-loaded, thick cylindrical dipole for validation of an EMC test site from 30 to 300 MHz, <i>W-S. Cho</i> , <i>Korea Institute of Industrial Technology, Korea</i> , <i>M. Kanda*</i> , <i>National Institute of Standards and Technology, USA</i>	217

Using Microwave Sensors for Determining Physical Properties of Granular Materials

Samir Trabelsi* and Stuart Nelson
U.S. Department of Agriculture
Agricultural Research Service
Richard B. Russell Agricultural Research Center
P. O. Box 5677, Athens, GA 30604-5677, U.S.A
e-mail: strabelsi@qaru.ars.usda.gov

Omar Ramahi
Compaq Computer Corporation
MR01-1/p5
2000 Forest St.
Marlborough, MA 01752, U.S.A

In many industries, such as agricultural, pharmaceutical and mining, nondestructive real-time sensing of physical properties of materials has become a necessity. Therefore, there is a real opportunity to develop a new generation of sensors that fulfills the requirements of highly automated industries. Microwave techniques based on the extraction of the desired physical properties from measurement of their dielectric properties have shown promise for achieving such goals (S. Trabelsi et al., IEEE Trans. Instrum. Meas., 47, 127-132, 1998). However, standardization and commercialization of microwave sensors, based on such principles, require development of reliable measurement techniques, efficient calibration methods and cost-effective assembly. In this paper, all of these aspects will be approached through measurements of the dielectric properties of cereal grains (corn, wheat and oats) and soybeans over wide ranges of frequency (2.5 GHz to 12.3 GHz), temperature (-14 °C to 50 °C), and bulk density and moisture content ranges of practical interest. The measurements were performed in free space with a sample-material placed between two horn/lens antennas facing each other and with time-domain application to the principal transmitted signal. The data collected are analyzed to define optimum operating conditions for a microwave sensor, and different calibration methods are explored. For a microwave sensor dedicated to moisture determination in granular materials, particular emphasis is placed on defining a "universal" calibration method which allows moisture content to be determined regardless of the kernel size, geometry and composition (S. Trabelsi et al., *Electronics Letters*, 35, 1346-1347, 1999). This will provide a solid background for the standardization of such measurement methods in industrial applications. In addition, as an example for the commercialization of cost-effective microwave sensors, use of microstrip antennas as sensing elements is considered. A three dimensional Finite-Difference Time-Domain (FDTD) method is used to simulate numerically the wave-material interaction for a material with dielectric properties and physical characteristics similar to those measured for corn, wheat, oats and soybeans. The material is assumed to be placed between two microstrip antennas facing each other with the possibility of being in contact with the transmitter and/or the receiver which can induce changes in their radiation characteristics. Results of the numerical simulation are compared to those obtained experimentally.

Characterization of Layered Materials Using a Single, Transient Scattered Field Measurement

E.J. Rothwell*, D.P. Nyquist, K.M. Chen, and J.D. Meese
Department of Electrical and Computer Engineering
Michigan State University
East Lansing, MI 48824

L.L. Frasch
Boeing ISDS
P.O. Box 3999
Seattle, WA 98124-2499

A system to measure the electromagnetic characteristics of layered material media is currently under development at the Boeing Company. This system radiates a wideband transient pulse that impinges on a layered medium from free space and analyzes the resulting scattered field return. For simplicity of use, the system is only configured for normally-incident illumination.

This paper examines an algorithm for extracting the complex permittivity and permeability of interrogated layers from a single transient scattered field measurement. Traditionally, two frequency-domain measurements of the complex scattered field are used to obtain the two complex quantities $\epsilon(\omega)$ and $\mu(\omega)$. These two measurements may be, for example, one reflection and one transmission measurement, two reflection measurements at different aspect angles, or two reflection measurements with known materials placed in front of the layered medium. In order to use a single measurement, the unknown permittivities and permeabilities are represented as an expansion over basis functions

$$\epsilon(\omega) = \sum_{n=1}^N a_n F_n(\omega), \quad \mu(\omega) = \sum_{m=1}^M b_m F_m(\omega)$$

where the total number of unknown coefficients is less than the number of frequency points available from the inverse Fourier transform of the transient signal. The values of the expansion coefficients (a_n, b_n) are then determined by minimizing the difference between the measured scattered field and the value predicted theoretically using a simple layered medium model.

The extraction procedure can be quite ill-conditioned – the scattered field may change only slightly for large changes in the unknown ϵ and μ . This suggests that the basis functions be chosen based on physical models of the materials, with information about the causal behavior of ϵ and μ built in (i.e., they should obey the Kronig-Kramers relationships.) Several models for ϵ and μ will be examined, and the effect of model choice on accuracy of extraction will be examined using both experimental and contrived data.

On Discriminating Between Buried Metallic Mines and Metallic Clutter Using Spatial Symmetry And Temporal Exponential Decay Rates

Lloyd Riggs, Larry Lowe*, Tom Barnett, Jon Mooney, and James Elkins
Electrical and Computer Engineering Department 200 Broun Hall
Auburn University, Alabama 36849

Last year we collected data at the JUXOCO test site located at Fort A. P. Hill with the U. S. Army's standard metal detector the AN/PSS-12. The AN/PSS-12 is a pulse-induction metal detector, and our instrumentation allowed us to collect "raw" data by amplifying and recording the time-domain response immediately following the metal detector's receiver coil. The JUXOCO test site has a calibration area and a large test grid made up of 980 adjacent 1 m square test locations (20 adjacent rows and each row has 49 test squares). At the center of each square there is nothing at all (a blank), a mine, or a clutter item (metallic trash). Time domain response data was collected at a number of different positions on an x-y grid centered over each square in the large test grid. Our presentation describes the signal processing algorithms that were used to discriminate among blanks, metallic mines, and metallic clutter.

The baseline receiver operating characteristic (ROC) curve (probability-of-detection versus probability-of-false alarm curve) for the AN/PSS-12 is shown to lie along the chance diagonal indicating that the instrument has no ability to discriminate between mines and clutter when used in its normal mode of operation (i.e. as a metal detector). We discovered that the spatial energy signature for mines is symmetrical, almost without exception, whereas in many instances the metallic clutter did not demonstrate this symmetry. This finding lead us to develop a very simple "symmetry detector" (algorithm) that enjoys a ROC curve well above the chance diagonal. Thus, by taking advantage of spatial information we were able to transform the AN/PSS-12 from a simple metal detector into a mine detector! Our paper will describe in greater detail the signal processing techniques that lead to the baseline and improved symmetry ROCs.

As pointed out by Baum (C. E. Baum, Interaction Note 499, November 1993) the low frequency response of highly, but not perfectly, conducting bodies is characterized by negative real natural frequencies that correspond to a damped exponential response in time domain. There is a unique correspondence between a metallic object's geometry (shape) and constitutive parameters (conductivity and permittivity) and its poles or time domain decay rates. This unique correspondence affords an opportunity for discrimination among metallic objects based on their negative real natural frequencies – a method referred to as magnetic singularity identification (MSI). We are currently working to use MSI to improve our symmetry ROC, and our presentation will summarize progress on this front.

**A THEORETICAL INVESTIGATION OF PAVEMENT
SURFACE ROUGHNESS USING MILLIMETER-WAVE
INTERFEROMETRY TECHNIQUE**

Seoktae Kim * and Cam Nguyen

Department of Electrical Engineering
Texas A&M University
College Station, Texas 77843-3128
E-mail: cam@ee.tamu.edu

ABSTRACT

Measurement of pavement surface roughness is critical for assessing highway safety. In this paper, we report for the first time an investigation of pavement surface roughness by the interferometry technique implemented using millimeter waves.

Single- and two-frequency systems have been investigated. The advantage of the two-frequency system as compared to the single-frequency counterpart is the surface to be measured can be referenced against itself, resulting to measurements almost insensitive to environmental and physical variations imposed on the system and imperfections of the scanning mechanism. However, the two-frequency system is more complex than the single-frequency system. The use of millimeter waves results in high resolution, which is needed for non-destructive, high-resolution surface roughness measurements. Various simulations have been performed at 35 GHz; and the preliminary results are promising, demonstrating that it is possible to characterize pavement surface roughness using millimeter-wave interferometers. System configurations, analysis, and results will be presented.

AN EXPERIMENTAL STUDY OF PAVEMENT MACRO TEXTURE USING MILLIMETER-WAVE STEP-FREQUENCY RADAR TECHNIQUE

Joongsuk Park ^{*1}, Cam Nguyen ¹, and Tom Scullion ²

¹Department of Electrical Engineering

²Texas Transportation Institute

Texas A&M University

College Station, Texas 77843-3128

E-mail: cam@ee.tamu.edu

ABSTRACT

The ability to measure pavement surface conditions such as transverse profiles, micro and macro textures, and segregation is important for transportation applications.

In this paper, we report for the first time an experimental investigation of pavement macro texture using step-frequency radar technique at millimeter-wave frequencies. Macro texture is a term relating to the coarseness of the road surface. The macro texture refers to the average height of the individual aggregates above the asphalt binder. Macro texture is a fundamental measurement of the surface condition and is critical to an assessment of the surface aggregate quality. Current efforts are only focused on lasers.

Our experimental system is based on the principle of step-frequency radar operating in the millimeter-wave regime. Millimeter waves have two distinct characteristics, which can be exploited for non-destructive, high-resolution surface texture measurements: higher frequencies and large (absolute) bandwidths leading to high angle- and range-resolution. Using Ka-band (26.5-40 GHz), we have examined the surfaces of several pavement samples. Preliminary measured results, with horizontal and vertical resolutions of around 7 and 0.375 mm, respectively, are promising, indicating that it is feasible to characterize macro textures with millimeter waves. Detailed system setup, pavement samples, and measured results will be presented.

Coplanar Sensors for Thickness Measurements

C. E. Bassey, K. Caputa* and S. S. Stuchly
Department of Electrical & Computer Engineering,
University of Victoria, Victoria, BC, V8W 3P6

The propagation of electromagnetic waves in a transmission line is affected by the geometry of the conductors and also by the dielectric constant and thickness of the test material. Thus, for a given line configuration, the thickness of the test material can be determined provided its dielectric constant is known. Various techniques have been developed for measurements of the thickness of dielectrics layers which include the UHF/microwave technique that measures the wave propagation velocity along a modified microstrip line (Hurley et. al., *Rev. Sci. Instrum.*, 61 (9), 2462-2465, 1990) and a vector reflectometer technique which utilizes a horn antenna to measure reflected signals from the test dielectric (Joseph et. al., *Microwave J.* (12), 84-90, 1994). These techniques are limited by multiple reflections between the test material and the transmission line and also by relatively weak coupling between the field and the test material.

We have developed a technique that uses a three and five-strip coplanar line as sensor, in conjunction with an Automatic Network Analyzer, to measure the dielectric constant of test materials (S. S. Stuchly and C. E. Bassey, *Meas. Sci. Technol.*, 9, 1324-1329, 1998). The coplanar line configuration is such that the test material is placed mainly on one side (conductor side) in contact with the sensor. In the coplanar sensor the energy is concentrated mainly above the line. This provides a characteristic that is perfectly suitable for interaction between the test and material and the sensor. This is contrary to microstrip where energy is concentrated inside the line. Numerical computations of propagation characteristics of both three-strip and five-strip coplanar lines have been carried out using design expressions obtained by quasi-static analysis (B.C Wadell, *Transmission Line Design Handbook*, Artech House, 87-88, 1991) and also by Finite Difference Time Domain (FDTD) modelling (K. Caputa and S. S. Stuchly, *URSI Gen. Ass. Abstract*, 5, 1999).

The objective of this work is to develop a technique for non-destructive measurements of the thickness of test dielectrics by utilizing the unique characteristics of the coplanar lines. Other applications of the sensor include moisture content measurements and liquid level gauging in tanks. Future research is aimed at utilizing the sensor as a device for monitoring the accumulation of ice on the wings of an airplane (M. A. Gottschalk, *Aerospace Design News*, 153-154, 1992).

EMC Effects of Radiated Fields Coupling Into Electronic Enclosures

*Dr. Z. Pantic-Tanner**
San Francisco State University
1600 Holloway Ave., SCI 165
San Francisco, CA 94132
(zpt@sfsu.edu)

Franz Gisin
Nortel Networks, SCI-2
4401 Great America Parkway
Santa Clara, CA 95054
(fgisin@nortelnetworks.com)

As digital circuits operate at higher and higher clock frequencies, they not only create more harmonic energy at higher frequencies, but also become more susceptible to high frequency signals from such applications as wireless radios, cellular telephone base stations, and high power broadcast stations. The enclosures that house these digital circuits generally have apertures (slots between two adjacent metallic pieces, cooling vents, etc.) that become more transparent as the frequency increases. Once the electromagnetic waves penetrate an aperture, it can excite standing waves in the cavities surrounding the digital circuits. All of these result in high levels of induced voltages and currents that can cause the digital circuits to malfunction. A similar failure mechanism also exists for analog circuits.

Several examples of small desktop and handheld electronic enclosures are simulated using the FDTD method to show how these effects can cause sensitive electronic circuits to malfunction. The enclosures were then built and their response to external electromagnetic waves were measured using a GTEM Cell operating in a radiated immunity configuration. The model and measured results are then analyzed and compared.

The analysis and measurement results show that cavity resonances dominate the fields inside the enclosure, and that the location and orientation of circuit boards, inside the enclosure can have a significant impact on the amount of noise induced into circuits mounted on the printed circuit boards. The orientation and location of enclosure apertures also plays a significant role in the overall coupling efficiency.

Electromagnetic Coupling to a Wire Residing Inside a Rectangular Metallic Box Perforated With Rectangular Apertures

M. D. Deshpande, NYMA Inc, C. R. Cockrell & F. B. Beck, NASA LaRC, Hampton, VA

Summary

Apertures in rectangular metallic boxes (housing electrical components) are used for reasons such as input and output connections, control panels, visual-access windows, ventilation panels, etc. Since these apertures at appropriate frequencies can behave as efficient antennas, they also become sources of electromagnetic interference (EMI) problems for both electromagnetic (EM) emission and susceptibility. In this situation there are two types of problems that must be addressed. First, a metallic wire residing inside a rectangular box and carrying electric current would radiate EM waves into its surroundings through these apertures which could cause interference with other equipment. Second, the EM waves that are present around the rectangular box would be coupled (through these apertures) to metallic wires/electronic circuits inside the box thus causing interference. In this presentation, the latter problem is addressed. EM coupling to a wire inside a perforated rectangular box illuminated by EM waves can be calculated using various numerical or analytical methods described in the literature. Numerical methods such as FDTD and FEM can model complex structures inside enclosure but often require large computing time and memory. For electrically large enclosures and apertures these methods though more accurate, become difficult for designers to use to investigate coupling to a wire inside a perforated rectangular box.

In the present paper a method for calculating current induced on a cylindrical wire in a large rectangular shaped enclosure having walls perforated with rectangular apertures is described. Using the equivalence principles and the rectangular cavity Green's functions, the electromagnetic fields inside the cavity due to the equivalent current sources are determined. By matching the tangential magnetic fields across the apertures and equating the total tangential electric field over the cylindrical surface of wire to zero, coupled integro-differential equations are obtained. The differential equations in conjunction with the Method of Moments (MoM) are then solved for unknown magnetic and electric current amplitudes. One of the advantages of the present approach is that it gives an accurate and efficient analytical model for the EM coupling studies which is computationally less intensive compared to other numerical methods. Figure 1 shows the open circuit voltage induced on a monopole wire residing inside an x-band sized rectangular cavity due to a normal incident plane wave.

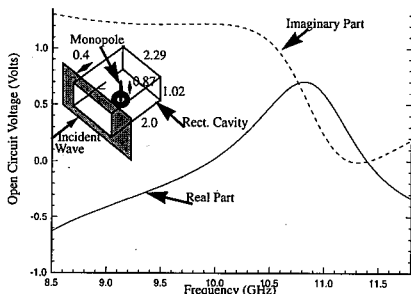


Figure 1 Open circuit voltage induced on monopole wire in rectangular cavity

Wave Absorber Using Transparent Resistive-Film for 1GHz Frequency Band

M.HANAZAWA K.WADA O.HASHIMOTO

Aoyama Gakuin University

6-16-1 Chitosedai, Setagayaku, 157-8572 Tokyo, Japan

Tel. & Fax. : +81-3-5384-1121

E-Mail : hana@ee.aoyama.ac.jp, wada@ee.aoyama.ac.jp,hasimoto@ee.aoyama.ac.jp

Microwave and millimeter-wave telecommunications have been attracted much attention because of the development of commercial communication technologies. The mobile communications therefore are now in the limelight all over the world. With the development of these communications, for instance, the electric wave hindrance frequently occurred. For overcoming the trouble, the research and development of a wave absorber are of considerable practical concern.

In our previous work, the 60GHz transparent wave absorber for future use in wireless local area network (LAN) has been realized [1][2]. The X-band transparent wave absorber for use at radar frequency band has also been examined[3]. The our wave absorber will be utilized not only for use in the floor and wall but also for windowpanes of indoors and the anechoic chamber because of the advantage of its transparency.

The absorber partly consists of a transparent resistive film made of indium-tin-oxide(ITO). The ITO film is a key material for our wave absorber, and it is also attractive material for development of super-twisted nematic (STN) or thin film transistor(TFT) liquid crystal display.

In the present paper, we propose the 1GHz wave absorber using the transparent ITO resistive film for commercial use. Figure 1 shows the structure of the wave absorber. The design of this absorber is carried out based on an equivalent transmission line model. Figure 2 shows the absorption characteristics of the present absorber are examined theoretically and experimentally. Consequently, we confirmed that the reflection loss of 20dB or more for the absorber was obtained between 1.32 and 1.60 GHz, and then the peak absorption of about 34dB was also realized at 1.46GHz.

References

1. K. Takizawa and O. Hashimoto, "The Transparent Wave Absorber Using Resistive Tin Film at V-band Frequency," IEEE Transaction Microwave Theory and Techniques, Vol.47, No.7,(1999).
2. O. Hashimoto, T. Abe, Y. Hashimoto, T. Tanaka, and K. Ishino, "Realization of Resistive-Sheet Type Wave Absorber in 60 GHz Frequency Band," Electronics letters, Vol.30,No.8, (1994).
3. O. Hashimoto, M. Haruta and K. Takizawa "A practical study of transparent wave absorber using resistive-film at X frequency band," Trans.IEE of Japan , Vol.119-A, No.4,(1999).

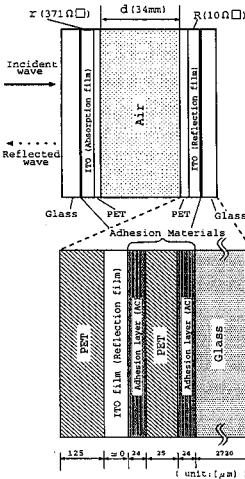


Fig.1. Structure of wave absorber

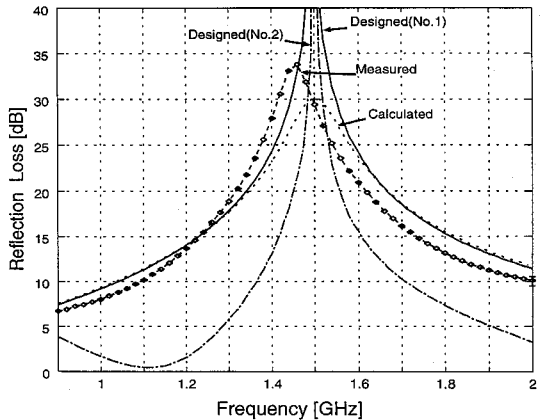


Fig.2. Absorption characteristics

A Broadband, Calculable, Disk-Loaded, Thick Cylindrical Dipole for Validation of an EMC Test Site from 30 to 300 MHz

Won-Seo Cho, Korea Institute of Industrial Technology, Seoul, Korea
Motohisa Kanda, National Institute of Standards and Technology, Boulder, Colorado

We propose a new broadband, short (80 cm long), calculable, disk-loaded thick cylindrical dipole (DTCD) antenna for validation of an EMC test site for the frequency range between 30 and 300 MHz. In order to achieve broadband characteristics, we have chosen a thick dipole as DTCD element. Disk loading has been applied to make this dipole shorter. To eliminate any ambiguity in balun characteristics, a commercially available hybrid junction is used as an antenna balun. Thus, the DTCD proposed in this paper is a very short, simple and well defined broadband antenna, which covers the frequency range between 30 and 300 MHz. The DTCD has an azimuthally symmetrical radiation pattern and thus, is very well suited for the validation of an EMC test site.

Fig. 1 shows the structure of the DTCD antenna used for site validation. This antenna uses hybrid junctions for the antenna balun. Equal-length, semi-rigid, twin coaxial cables from the dipole terminals to the hybrid junction form a 100 Ω balanced and shielded transmission line.

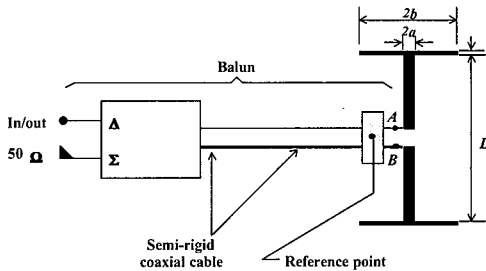


Fig.1. Structure of the DTCD antenna.

For the antenna analysis, cylindrical coordinates (ρ, ϕ, z) are oriented so that the vertical z -axis in Fig. 1 is centered through the linear portion of the antenna structure. Antenna length is given by L , while radii of the vertical stem and end-disk of thickness t are a and b respectively. The integral equation for the surface current on the DTCD antenna is given as

$$\bar{a}_0 \cdot \int_l I(l') \left[k^2 \bar{a}_l - \frac{\partial^2}{\partial l' \partial \rho} \bar{a}_\rho - \frac{\partial^2}{\partial l' \partial z} \bar{a}_z \right] G^* dl' = -j\omega \epsilon_0 E^{inc}(l) \quad (1)$$

where

$$G^* = \int_0^{2\pi} \frac{e^{-jkR}}{8\pi^2 R} d\phi \quad (2)$$

$$R = \sqrt{\rho^2 + \rho'^2 - 2\rho\rho' \cos(\phi) + (z-z')^2} \quad (3)$$

\bar{a}_0 represents the vector on the observation point inside the antenna, l is the total length along the antenna surface from the center of the outside of the bottom end-disk to that of the upper one and $k (= \omega\sqrt{\mu\epsilon})$ is the propagation constant. The current distribution problem for the DTCD antenna can be solved by the Method of Moments (MoM). In this paper, the solution described uses pulse subsection currents and the point-matching method, while the antenna is assumed to be excited by an idealized source, the magnetic frill generator. Once the current distribution is determined, the unknown antenna characteristics such as input impedance, antenna gain, and antenna factor can be found by solving the resulting equations.

A Century of Progress at the Dawn of a New Millennium (I)
Sponsored by MotorolaOrganizers and Chairs: Robert E. Collin, Case Western Reserve University
Yahya Rahmat-Samii, UCLA

			Page
	7:55	Opening Remarks	
1	8:00	Einstein looks at Maxwell's Legacy?, <i>J. Van Bladel, Ghent University, Belgium</i>	AP
2	8:20	Advances in Technology-Based Engineering Education, <i>M. Iskander, University of Utah, USA</i>	AP
3	8:40	Wire Antennas—Simple and Powerful, <i>C. Butler, Clemson University, USA</i>	AP
4	9:00	Antennas in Wireless Communication and Human Interaction, <i>M. Stuchly, University of Victoria, Canada</i>	AP
5	9:20	Reflector, Lenses and Horns—Past, Present and Future, <i>Y. Rahmat-Samii, University of California Los Angeles, USA</i>	AP
	9:40	Break	
6	10:00	Enabling Technologies for Broadband Communications, <i>K. Warble, Motorola, USA</i>	AP
7	10:20	Key Developments in Phased Arrays, <i>R. C. Hansen, Hansen Inc., USA</i>	AP
8	10:40	Deployable and Light-weight Array Antennas for Space Application, <i>J. Huang, A. Fera, B. Lopez, and M. Lou, JPL, USA</i>	AP
9	11:00	Smart Antennas and Digital Beam Forming, <i>T. K. Sarkar, R. Adve, J. Koh and S. Park Syracuse University, USA, and M. Salazar, Universidad Politecnica de Madrid, Spain</i>	AP
10	11:20	RF MEMS and Si-Micromachined Circuits for High-Frequency Applications, <i>L. Katehi and G. Rebeiz, University of Michigan, USA</i>	AP
11	11:40	Adjourn	

PIFA and Small Antennas

Co-chairs: E. Altshuler, Air Force Research Laboratory
W. Stutzman, Virginia Polytechnic Institute and State University

			Page
1	8:00	A new design method for single feed dual band PIFA, <i>G. Kadambi*, K. Simmons, J. Sullivan, T. Masek, M. Rohde, Centurion International, Inc., USA</i>	221
2	8:20	Designs of planar inverted F-antennas using genetic algorithms, <i>I. Gonzalez*, B. Alonso, J. Perez, M. Catedra, Universidad de Alcala, Spain</i>	222
3	8:40	Ground plane effects on PIFA antennas, <i>M. Huynh*, W. Stutzman, Virginia Polytechnic Institute and State University, USA</i>	223
4	9:00	Internal PIFA for laptop computer applications, <i>G. Kadambi*, K. Simmons, J. Sullivan, M. Rohde, Centurion International, Inc., USA</i>	224
5	9:20	The lower bound on Q for an electrically small dipole, <i>G. Thiele*, P. Detweiler, R. Penno, University of Dayton, USA</i>	225
	9:40	Break	
6	10:00	Very small genetic antennas, <i>E. Altshuler*, Air Force Research Laboratory, USA</i>	226
7	10:20	Fundamental limits on small antennas, <i>W. Davis, W. Stutzman, E. Caswell*, K. Takamizawa, Virginia Polytechnic Institute and State University, USA</i>	227
8	10:40	A simple, compact antenna for wireless communications, <i>R. Johnston, M. Okoniewski*, University of Calgary, Canada</i>	228
9	11:00	Integrated low-profile GPS and cellular antenna, <i>W. Stutzman, N. Cummings*, Virginia Polytechnic Institute and State University, USA</i>	229
10	11:20	Normal mode bent wire antennas, <i>T. Montoya*, M. Swiatkowski, University of Tennessee, USA</i>	230



A NEW DESIGN METHOD FOR SINGLE FEED DUAL BAND PIFA

Govind R. Kadambi*, Kenneth D. Simmons, Jon L. Sullivan, Thomas F. Masek, and
Monty D. Rohde

Centurion International, Inc.
3425 N. 44th Street, Lincoln, NE 68504, U.S.A.

The cellular communication industry has witnessed an increasing emphasis on internal antennas for cellular handsets instead of a conventional external wire antenna. Internal antennas have several advantageous features such as being less prone for external damage, a reduction in overall size of the handset with optimization, easy portability, and potential for low SAR Characteristics. The concept of internal antenna stems from the avoidance of protruding external radiating element by the integration of the antenna into the handset. Among the various choices for cellular internal antennas Planar Inverted F antenna (PIFA) appears to have great promise. Rapid expansion of the cellular communication industry in the recent past has created a need for multi frequency band operation cellular handsets to meet the ever-increasing subscriber demand. Dual band PIFA designs have been realized in the past by using a separate feed path for each band. There is a great concern for dual band PIFA design with separate feed paths having its performance compromised due to the mutual coupling and poor isolation of the various resonant bands. Consequently, the dual band PIFA with multiple feed paths has not been a logical choice for practical applications in dual frequency band cellular operations. Therefore the design of single feed dual band PIFA has been a topic of specific emphasis and special relevance to cellular communication.

This paper proposes a new method of design of a single feed dual band PIFA overcoming many of the limitations of the previous design techniques. In all the previous designs of dual band PIFA with dual and single feeds, the dual resonance has been realized through physical partitioning of the original single band PIFA structure [Z.D.Liu et al., IEEE- AP, October 1997, pp. 1451-1458; P.Kabacik and A.A. Kucharski, JINA Conference, 1998, pp. 655-658]. In these studies, slot (L or U shape) is used to partition the original single band structure to realize the dual resonance. The dimensions and the position of the slot determine the separation of the resonant bands. The available dual band PIFA configurations are not amenable for quick and easy method of varying the resonant frequency. The change in resonant frequency involves the change in the dimensions of the antenna itself. In the proposed design, a simplified dual band PIFA has been realized **without necessitating** a physical partitioning. In this design, the shorting pin and the feed pin are located along the centerline of the PIFA. The position of a shorting pin, which is placed away from the edge of PIFA controls the separation of resonant bands. Thus the design proposed in this paper has a merit of relative ease of controlling the separation of resonant bands. The placement of shorting pin away from the edge also demands the wider separation of the feed and shorting pins to get a good impedance match. Thus the return loss characteristics of dual band PIFA using the design proposed in this paper are less sensitive to feed positioning errors. An AMPS-PCS single feed dual band PIFA designed and developed using the above concept exhibits satisfactory bandwidth and gain performance. The techniques of capacitive and partial dielectric loading have also been invoked in the above design. The presented design technique has been extended to include the concept of slot loading as in C-Patch[C. Kossiavas et. al, Electronics Letters, February 16, 1989] for the design of a dual band PIFA resonating in GSM-DCS bands. This paper also presents the gain and the return loss characteristics of various dual band PIFAs. The effect of critical parameters on the impedance bandwidth is also discussed in this paper.

DESIGNS OF PLANAR INVERTED F-ANTENNAS USING GENETIC ALGORITHMS

I. González, Beatriz Alonso, Jesús Pérez, M.F. Cátedra

*Dept. Teoría de la Señal y Comunicaciones
Escuela Politécnica, Universidad de Alcalá
28871 Alcalá de Henares. Madrid. Spain
Fax: +34 91 885 6699. E-mail: felipe.catedra@uah.es*

A method to design Planar Inverted F-Antennas (PIFA) based on Genetic Algorithms (GA) is presented. MONURBS, a Moment Method code, has been used for the electromagnetic analysis that requires the GA application. MONURBS employs NURBS surfaces for the description of the geometry of the structures under analysis. MONURBS have a well-proved model for the electromagnetic treatment of the wire-surface junction that gives accurate results for input impedance calculations.

PIFA are defined by a plane patch above a ground plane where is attached by a short-circuited wire and a feed wire. Three parameters have been considered in the PIFA design: the height of the patch; the Voltage Stand Wave Ratio (VSWR) and the bandwidth. The VSWR must be lower than 2 in the working bandwidth. These parameters depend on the location of the wires. MONURBS code is used to obtain this dependence. The search of the best positions of the wires is the optimization problem to be solved. For simple PIFA antennas (one radiant element), our approach fixes the position of the feed wire and using the Genetic Algorithms optimizes the location of the short-circuited wire. The GA have been used, also, to design Dual-Band Array PIFA antennas. In this case there are two bands where the antenna has to work and two radiant elements in every band.

The method has been probed with prototype antennas achieving good agreement between the predicted values and the prototype measurements done by ERICSSON labs.

Ground Plane Effects on PIFA Antennas

M. T. Huynh* and W.L. Stutzman

Antenna Group
The Bradley Department of Electrical and Computer Engineering
Virginia Polytechnic Institute and State University
Blacksburg, VA 24061-0111
<http://lab.ant.ee.vt.edu>

The planar inverted-F antenna (PIFA) is of current interest for cellular communication applications because of its small size and wide bandwidth. Thorough analysis and design of a conventional PIFA mounted on an infinite ground plane has been performed [Hirisawa and Haneishi, *Analysis, Design, and Measurement of Small and Low-Profile Antennas*, Artech House, 1992, Chapter 5.] Cellular communication applications require antennas to be small in size. Antenna designs based on an infinite or very large ground plane cannot be used for applications with small ground planes. It has been shown that the performance of a PIFA mounted on a conductive housing of portable radio equipment, which acts as the ground plane, differs significantly from that of a PIFA mounted on a large ground plane. Understanding the effects of the ground plane on the PIFA is crucial in today's applications where miniaturization is important. Ground plane influence on PIFA antenna patterns and bandwidth has not been generally characterized. Investigations must be conducted for many possible geometries by trial-and-error.

Studies of the ground plane effects on a PIFA have not been found in the open literature. This paper reports on results from investigations on the performance of a conventional PIFA with ground planes of various sizes. Characteristics such as impedance and bandwidth are the primary concern. Theoretical and measured results are presented and compared. IE3D [Zeland Software], a MoM electromagnetic simulation engine, is the main tool for the numerical computation of the antenna characteristics.

Our investigations showed that the bandwidth of PIFA antennas is dramatically reduced if the ground plane size is reduced below a certain point. Details will be presented in the talk.

INTERNAL PIFA FOR LAPTOP COMPUTER APPLICATIONS

Govind R Kadambi*, Kenneth D. Simmons, Jon L. Sullivan and Monty D. Rohde
Centurion International Inc.,
3425 N. 44th Street, Lincoln, NE 68504, U.S.A.

With the rapid progress in wireless communication technology and the ever-increasing emphasis for its expansion, wireless modems on laptop computers and other handheld radio devices will be a common feature. The technology using short range radio link to connect devices such as cellular handset, Laptop computers and other handheld devices has already been demonstrated [Wireless Design On-line Newsletter, Vol. 3, Issue 5, November 22, 1999]. The ISM band (2.4- 2.5 GHz) is the allocated frequency band for such applications. The performance of the antenna placed on devices like Laptop computers is one of the critical parameters for the satisfactory operation of such a radio link. Therefore the performance characterization of the antenna located on Laptop computers assumes significant importance in the evolving technology of wireless modems. This paper presents the several designs and experimental studies of Planar Inverted F antenna (PIFA) for possible use as an internal antenna in wireless applications.

The internal antennas have several advantageous features such as being less prone for external damage, easy portability and a reduction in overall size with optimization. The internal antenna also ensures the absence of protruding radiating element. In recent years, the PIFA has been a topic of special relevance to both the Mobile Voice and RF Data communications. PIFA exhibits omnidirectional radiation patterns in orthogonal principal planes for vertical polarization. The primary objective of this paper is the design of a PIFA with wider bandwidth and structural simplicity. The improvement of bandwidth of a PIFA with a capacitive feed is discussed in [C.R. Rowell and R.D. Murch, IEEE-AP, Vol. AP-45, pp.837-842, May 1997]. The PIFA with a capacitive feed has the disadvantage of additional structural complexities and leads to a complicated fabrication process. This paper demonstrates the design of a PIFA with a bandwidth of about 260 MHz centered on the ISM band without resorting to capacitive feed technique. Another significant design aspect of this paper is the realization of wider bandwidth with a ground plane of small size. This paper also presents a comparative study of several designs with varying linear dimensions of the PIFA and its ground plane. Both the bandwidth and the gain performance of the PIFA are discussed in this paper. The range of size of the ground plane varies from 10mmX17mm to 10mmX42 mm. The radiation characteristics of a PIFA located in the hinge area of a typical Laptop computer are also illustrated through the experimental studies. The effect of display screen of the Laptop computer on the radiation patterns of the PIFA is also discussed. From the impedance bandwidth and the composite radiation pattern of the PIFA on a Laptop computer, it is inferred that the PIFA can be a potential internal antenna for wireless applications under study.

The structural configuration of the PIFA proposed in this paper is simple, lightweight, easy to fabricate and cost effective to manufacture. The design and experimental studies presented in this paper are likely to find utility in Wireless and Local Area Network (LAN) applications.

The Lower Bound on Q for an Electrically Small Dipole

G. A. Thiele, P. L. Detweiler, R. P. Penno
Department of Electrical & Computer Engineering
University of Dayton, Dayton, OH 45469-0226

In 1948 Chu (1) published a widely cited analysis which established the minimum radiation Q of an antenna which fits inside a sphere of the corresponding radius. This analysis was later corrected by McLean (2) in 1996. However, it is not clear how their theoretical analysis relates to the Q of an actual antenna since practical antennas are not able to achieve a Q as low as that predicted by the analysis. In 1998 Foltz and McLean (3) presented an analysis in which they used prolate spheroidal wave functions to expand the fields instead of spherical wave functions as used by Chu. This was an attempt to make the volume containing the antenna conform more closely to the actual shape of an antenna such as a thin linear antenna (e.g., dipole). Foltz and McLean presented a curve for correcting spherically derived Q to a prolate spheroidal derived Q. However, the relationship between that correction curve and an actual antenna, such as a dipole, is not obvious.

In this paper a different approach is used to obtain a lower bound on the Q of a dipole antenna. The approach is not restricted to dipole antennas, but the dipole is a particularly convenient antenna to examine because its far field pattern is known in analytical form for arbitrary dipole length. The approach here utilizes the fact that an electrically small dipole is superdirective and that the superdirectivity ratio is related to the radiation Q. Results will be presented that correlate well with the radiation power factor as defined by Wheeler (4), and which show the Q to be higher than in (1) and (2). The results may serve to set a new and practical lower bound on the radiation Q for electrically small dipoles.

- 1) L. J. Chu, "Physical Limitations of Omnidirectional Antennas," *J. Appl. Physics*, vol 19, pp. 1163-1175, December 1948.
- 2) J. S. McLean, "A Re-Examination of the Fundamental Limits on the Radiation Q of Electrically Small Antennas," *IEEE Trans Ant & Prop.*, vol 44, pp. 672-676, May 1996.
- 3) H. D. Foltz and J. S. McLean, "Limits on the Radiation Q of Electrically Small Antennas Restricted to Oblong Bounding Regions," *Digest of the 1999 AP-S Symposium*, Orlando, FL, pp. 2702-2704, July 1999.
- 4) H. A. Wheeler, "Fundamental Limitations of Small antennas," *Proc. IRE*, vol 35, pp 1479-1484, Dec. 1947.

VERY SMALL GENETIC ANTENNAS

Edward E. Altshuler
Air Force Research Laboratory
Sensors Directorate
Hanscom AFB, MA 01731-2909

Tel: 781 377 4662, Fax: 781 377 1074, e-mail: altshule@maxwell.rl.ph.af.mil

Abstract

One of the most challenging problems in antenna design is that of the electrically small antenna. Its size is usually defined in terms of a sphere of radius $a\lambda$, within which the antenna is enclosed. This definition is convenient for the analysis of antennas when the fields are represented by spherical wave functions. However, for this investigation we define the size of the antenna as that enclosed within a cube of height, h/λ over an infinite ground plane. Thus the total volume within which the equivalent antenna in free space is confined is $2(h/\lambda)^3$. This definition is chosen because the computations are done with the Numerical Electromagnetics Code (NEC), which uses Cartesian coordinates. The parameter which best characterizes the performance of a small antenna is the quality factor, Q , which is defined as the ratio of the resonant frequency of the antenna to the frequency difference at which the radiated power decreases to $1/2$ that at resonance. The main problem in small antenna design is that as the size of the antenna is decreased its radiation resistance approaches zero and its reactance approaches infinity. Small antennas are usually non-resonant, inefficient and require matching networks.

In this investigation we use a genetic algorithm (GA) in conjunction with the NEC to search for resonant wire configurations that best utilize the volume within which the antenna is confined. The objective of this optimization is to minimize the Voltage Standing Wave Ratio (VSWR) and corresponding Q of an electrically small resonant antenna. A steady state GA with 30% replacement and a 0.6% mutation rate was selected. Each antenna configuration was represented by a chromosome. The chromosomes having the best solutions were mated and after many generations converged to an "optimal" solution. In order to obtain a resonant antenna, the total length of the wire should be at least $\lambda/4$. Thus, as the size of the cube within which the antenna is enclosed is decreased, more wire segments have to be used. We investigated configurations having from 4 to 10 wire segments and for all cases resonant antennas were obtained. The GA optimization was done at 400 MHz. The minimum sized cubes decreased from about 0.06 to 0.03λ on edge as the number of wire segments increased. The corresponding Q s and VSWRs increased from about 40 and 9.0 to about 200 and 50 respectively. The radiation patterns for these antennas were elliptically polarized and had near hemispherical coverage.

The computed antenna designs have been built and tested. The impedance and VSWR were measured with a Hewlett-Packard Model 8510 Network Analyzer. The measured results compared very well with the computations, considering that the computations were made for an antenna over an infinite ground plane; also, these antennas, because of their very small size, could not be fabricated to the exact dimensions of the computed models. Future plans are to replace the thin wires with copper strips. Preliminary results indicate that this design will have a lower Q . Also being considered is the possibility of designing planar antennas that can be fabricated using printed circuits and dielectrics.

Fundamental Limits on Small Antennas

W.A. Davis, W.L. Stutzman, E.D. Caswell*, and K. Takamizawa
The Bradley Department of Electrical and Computer Engineering
Virginia Polytechnic Institute and State University
Blacksburg, VA 24061-0111

Many current applications for wireless communications require physically small antennas to be placed on or inside of compact terminals such as handheld transceivers. Directivity must be low to provide wide-angle coverage, but efficiency must be high. This implies a gain goal comparable to that for a half-wave dipole (2.15 dB). In addition, bandwidths of as much as 10% or more are often required. These efficiency and bandwidth specifications cannot be met with an antenna that is significantly less than a wavelength in extent. Unfortunately, the available volume for an antenna often dictates that an electrically small antenna be used. For example, at U.S. cellular telephone frequencies of 824 to 894 MHz the midband frequency is 859 MHz, corresponding to a wavelength of $\lambda = 35\text{cm}$, and the relative bandwidth is $BW = 70/859 = 8.1\%$. Typical antenna specifications on maximum dimensions are on the order of 25 mm, which is 0.07λ . This antenna size class is of enormous interest to the wireless community. It is, therefore, important to carefully examine the fundamental limits on achievable antenna size. When an antenna designer is familiar with the limits on antenna extent for a given bandwidth, the search for an impractical antenna can be avoided.

In this paper we review the theoretical limits on antenna size. These limits are based on assumptions that give rise to questions on how the limits apply to actual antennas. In addition, there are some steps that must be taken to calculate bandwidth based on the theoretical results. A time domain approach is used to re-derive the fundamental limit on radiation Q . In the time domain it becomes apparent that the electric and magnetic time-average stored energies are not completely orthogonal. This leads to the conclusion that the sum of the electric and magnetic stored energies rather than twice the peak electric stored energy should be used when computing radiation Q . The fundamental limit derived from the time domain method converges to the accepted limit for $ka \ll 1$ but deviates by approximately 31% at $ka = 1$. We also find that the radiation Q for a circularly polarized antenna is identical to that of a linearly polarized antenna. This differs from conclusions in previous papers but is a more intuitive result.

The fundamental limits are validated with several examples. The antennas selected are not limited to electrically small antennas in order to evaluate the validity of the classical fundamental limits for a variety of sizes and bandwidths. The result of this comparison for many practical antennas of various types demonstrates that the theoretical limits on antennas provide a practical limit on antenna size. That is, the commonly accepted theoretical size limits hold for all antennas, and for a given antenna type and bandwidth the antenna cannot be reduced in size below the theoretical limit without paying a penalty in efficiency. For most antennas, performance does not approach the theoretical limits very closely.

A Simple, Compact Antenna for Wireless Communications

Ronald H. Johnston and Michal Okoniewski
Department of Electrical and Computer Engineering
University of Calgary
Calgary, Alberta, Canada T2N 1N4

A novel antenna structure is proposed for wireless communications. The antenna comprises a metallic ground-plane and a folded patch (Fig.1). The antenna is fed by a coax line. The patch is short-circuited to the ground plane by two metal pins. A match to 50 Ω line can be easily achieved, as illustrated in Tab. 1. Our main interest in this work

was however not the antenna itself, but the study of the properties of small patch antennas with ground planes of limited size – a typical problem in wireless communications. The influence of the ground plane dimensions on the antenna is examined and compared with the theoretical limits [H.D.Foltz, J.S.McLean, “Limits on the Radiation Q of Electrically Small Antennas restricted to Oblong Bounding Regions, *Proc IEEE AP-S*, pp 2702, 1999].

Other parameters of the ground-plane, e.g. its thickness were also explored. In general, it is observed that for this antenna it is the ground-plane that assumes the role of the radiator, while the patch with its sub-systems becomes a complex feed. An interesting insight to the complex relations between the ground-plane and its feed is gained by examining the currents flowing on both surfaces of the ground-plane. Work is in progress to take advantage of these studies to modify the presented structure in such a way that significantly lower radiation towards the user’s head is achieved.

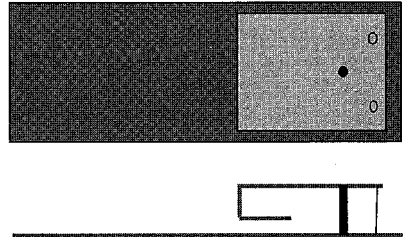


Fig 1. The geometry of the antenna

Ground plane size [mm]	100	110	120	130	140	150	160
Resonance f [MHz]	838	839	857	875	878	877	875
$ S_{11} $	0.26	0.08	0.02	0.05	0.18	0.30	0.39

Table 1. S_{11} and resonance frequency, as a function of the length of the ground-plane size

Integrated Low-Profile GPS and Cellular Antenna

W.L. Stutzman and N.P. Cummings*

The Bradley Department of Electrical Engineering
Virginia Polytechnic Institute and State University
Blacksburg, VA 24061-0111

In recent years the rapid decrease in size of personal communication devices has lead to the need for more compact antenna designs. At the same time, integration of existing wireless applications has driven the need for multifunctional antennas that operate over broad bands or even multiple independent bands. The civilian GPS system is quickly becoming the standard for personal and commercial navigation and location finding. The difficulty with GPS is that there is no return link. That is, a GPS terminal determines its position, but that position is known only to the terminal user. The next wide scale technology area for GPS is the integration of GPS with some type of wireless service to provide communication of the GPS - derived position as well as messaging. One of the most popular uses for this service is tracking of mobile cargo.

This paper presents a design for a compact, low-profile that operates at both the conventional cellular telephone band of 824 to 894 MHz and the civilian GPS L1 frequency of 1575 MHz. The combined antenna unit has a lateral diameter of less than 4 inches (10 cm) and its height is less than 2 inches (5 cm). The integrated unit is a hybrid design of two collocated antennas that operate at the two different bands. The planar inverted F antenna, PIFA, meets the specifications which are required in a reduced size environment. A nominal bandwidth of 8% is achieved in the cellular band. The GPS portion of the hybrid unit consists of a dielectrically loaded slotted patch located in a "piggyback" configuration on top of the top PIFA element.

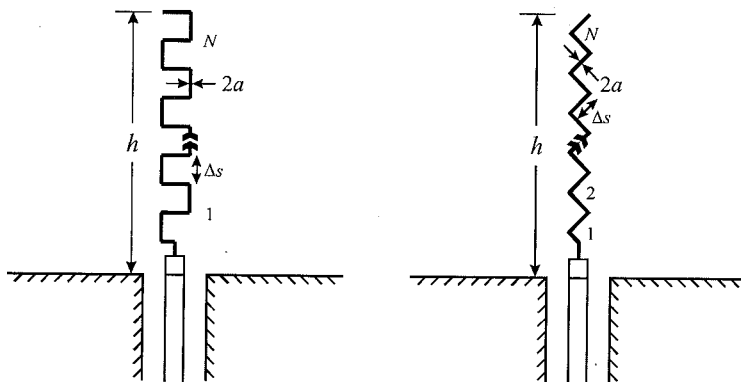
Computer simulation and design was performed using a combination of IE3D, a 2.5 dimensional moment method code, and Fidelity, a finite difference time domain code. Results will be presented from these calculations along with measurements on prototype antennas using both the Virginia Tech outdoor antenna range and the Virginia Tech near-field antenna range.

Normal Mode Bent Wire Antennas

Thomas P. Montoya* and Michael J. Swiatkowski
Department of Electrical & Computer Engineering
University of Tennessee
Knoxville, TN 37996-2100

Simple compact antennas that radiate omnidirectionally in the normal direction are attractive in numerous applications. Here, bent wire antennas with radiation characteristics similar to those of a linear wire $\lambda/2$ dipole ($\lambda/4$ monopole) antenna are desired. In particular, the two bent wire configurations examined are the meander (left of figure) and right-angle zigzag (right of figure) antennas. For these antennas, the axial length h is less than $\lambda/4$ and the step length Δs is much less than λ . The overall wire length is not restricted other than by the limitations to h and Δs . While wire antennas are considered, the meander and zigzag antenna geometries are readily implemented as flat metallic ribbons on a substrate (i.e., traces on a printed circuit board).

The goal is bent wire antenna designs where the axial length is less than half that of a comparable linear wire antenna. The electrical and radiation characteristics should be similar. The main parameters varied are the number of meander or zigzag steps or sections, the step length, the wire radius a , and feed geometry (i.e., should the antennas be centered as shown or allowed to be offset). The bent wire antennas are studied using the finite-difference time-domain (FDTD) method and the Method of Moments (MoM), using the Numerical Electromagnetics Code (NEC-4). Selected results, e.g., radiation patterns and input impedances, will be shown and contrasted with the comparable linear antennas.



Scattering

Chair: R. V. McGahan, Air Force Research Laboratory

Page

- | | | | |
|----|-------|--|-----|
| 1 | 8:00 | A time domain incremental theory of diffraction (TD-ITD), <i>F. Capolino*</i> , <i>R. Tiberio, Universita di Siena, Italy</i> | 232 |
| 2 | 8:20 | UAPO diffraction coefficients for penetrable and non-penetrable structures, <i>F. D'Agostino, C. Gennarelli, University of Salerno, G. Pelosi, University of Florence, G. Riccio*, University of Salerno, G. Toso, University of Florence, Italy</i> | 233 |
| 3 | 8:40 | RCS modeling of aircraft at radio frequencies, <i>B. Notaros*, University of Massachusetts Dartmouth, USA</i> | 234 |
| 4 | 9:00 | Radiation from parallel circular loops near a conducting sphere and/or caps, <i>H. Partal*, J. Mautz, E. Arvas, Syracuse University, USA</i> | 235 |
| 5 | 9:20 | Electromagnetic scattering from dihedral corner reflectors characterized by random surface impurities, <i>P. Corona, G. Ferrara, Istituto Universitario Navale, G. Toso*, Universita di Firenze, Italy</i> | 236 |
| | 9:40 | Break | |
| 6 | 10:00 | A new formalism for time dependent electromagnetic scattering from a bounded obstacle, <i>M. Recchioni, Universita di Ancona, F. Zirilli*, Universita di Roma "La Sapienza", Italy</i> | 237 |
| 7 | 10:20 | Genetic algorithm approach to extrapolation for fields scattered by large objects, <i>S. Chakravarty, R. Mittra*, E. Aydin, The Pennsylvania State University, USA</i> | 238 |
| 8 | 10:40 | Simulations of the delay spread and angle-of-arrival using physics-based propagation models, <i>B. Koala*, ATT Wireless, M. Curry, M. Ciccotosto, Y. Kuga, L. Tsang, University of Washington, USA</i> | 239 |
| 9 | 11:00 | Electromagnetic scattering analysis utilizing a near-field scanning microwave microscope, <i>W. Symons*, Virginia Polytechnic Institute and State University, K. Whites, University of Kentucky, USA</i> | 240 |
| 10 | 11:20 | Using physical optics, finite differences and Kirchhoff integral, in the time domain, to study electromagnetic fields in a complex environment, <i>M. Martinez-Burdalo, L. Nonidez*, A. Martin, R. Villar, Instituto de Física Aplicada, Spain</i> | 241 |

A Time Domain Incremental Theory of Diffraction (TD-ITD)

Filippo Capolino and Roberto Tiberio

Dip. Ingegneria dell'Informazione, Università di Siena, Via Roma 56, 53100 Siena, Italy.

ABSTRACT

A frequency domain (FD) incremental theory of diffraction (ITD) has been presented in [R. Tiberio et al., *IEEE Trans. Ant. Prop.*, **42**, 600-612,1994; **43**,87-97, 1995; and **44**,593-599, 1996] which provide effective tools for describing a wide class of high-frequency scattering phenomena. The method overcomes caustic singularities of ray techniques and extends the field prediction to observation aspects outside the diffraction cone. When elementary ITD contributions are distributed, and then integrated along the edges a curved wedge, they provide a high-frequency approximation of the total radiated field by the actual curved structure. The incremental field contribution at any point l on a generally curved edge, is defined by resorting to a convenient interpretation of the solution of the canonical problem of the locally tangent, infinite wedge at l . Recently, more refined ITD incremental fields have been obtained that overcome the limitations occurring in the formulation developed earlier. In particular, for the specific example of the wedge, these new incremental coefficients recover the spatial field superposition given by A. Rubinowicz [*Acta Physica Polonica*,**28**(12),841-860,1965].

In this paper, a time domain (TD) version of the ITD is presented which provides a self-consistent, high-frequency (early time) description of a wide class of transient phenomena. Explicit expressions of the incremental TD field contributions have been obtained for source and observer both at finite distance from the wedge, via direct Fourier inversion of the more recent version of FD-ITD incremental field contributions. According to the FD-ITD, the high-frequency diffracted field at curved wedges is given by $\psi = \int_L dl F(l) e^{-jk[r'(l)+r(l)]}/[r'(l)r(l)]$, where: \int_L represents integration along the curved edge; $F(l)$ is the incremental coefficient, and $r'(l)$ and $r(l)$ are the distances of the source and observer from a point l along the edge. In performing the TD Fourier inversion it is important to note that $F(l)$ is independent of the radian frequency ω which appear at the exponent $k = \omega/c$, with c the ambient wave speed. An early time TD field representation of the transient field radiated by a curved edge illuminated by an impulsive source $\delta(t)$, is then easily obtained as $\hat{\psi} = \int_L dl F(l) \delta[t - c^{-1}(r'(l) + r(l))]/[r'(l)r(l)]$ (the hat tags a time domain quantity). In this framework, the TD diffracted field $\hat{\psi}$ is represented as superposition of impulses retarded by the time $c^{-1}r'(l)$ needed by the incident field to reach the edge at l , plus the time $c^{-1}r(l)$ successively needed to reach the observer. The relevant expressions explicitly satisfy reciprocity. The impulsively excited wavefield $\hat{\psi}$ is valid only for *early times*, on and close to (behind) the wavefronts. However, convolution with an excitation waveform $\hat{G}(t)$ whose frequency spectrum $G(\omega)$ has no low-frequency components and is thus dominated by high frequencies may enlarge the range of validity of the resulting pulsed response to later observation times behind the wavefront. Accuracy and limits of the present TD-ITD formulation will be discussed during the oral presentation.

UAPO DIFFRACTION COEFFICIENTS FOR PENETRABLE AND NON-PENETRABLE STRUCTURES

F. D'Agostino (1), C. Gennarelli (1), G. Pelosi (2), G. Riccio* (1), G. Toso (2)

(1) D.I.I.E. – University of Salerno, via Ponte Don Melillo, 84084 Fisciano (SA), Italy.

(2) D.I.E. – University of Florence, via C. Lombroso, 50134 Florence, Italy.

Abstract.

The study of the electromagnetic scattering from penetrable and nonpenetrable structures represents a favorite research subject because of its importance in many application areas. However, the derivation of rigorous diffraction coefficients for edges in such structures is usually difficult, and sometime impossible. Moreover, if the final expressions require the calculus of special integral functions, the numerical efficiency of the solution is strongly reduced. Consequently, the derivation of high frequency approximated diffraction coefficients, which are efficient and easy to handle, becomes fundamental for predicting the scattering from the considered objects.

A Uniform Asymptotic Physical Optics (UAPO) technique has been recently proposed to obtain approximated diffraction coefficients for nonpenetrable half-planes characterized by anisotropic impedance boundary conditions (Gennarelli, Pelosi, Pochini and Riccio, *J. Electromagnetic Waves Appl.*, **13**, 963-980, 1999) and for penetrable resistive sheets forming a wedge (Gennarelli, Pelosi, Riccio and Toso, *IEEE Trans. Antennas Propagat.*, April 2000). Such a technique is based on a PO approximation of the surface current densities induced by an incident Geometrical Optics (GO) field. The related diffraction coefficients are obtained by performing a uniform asymptotic evaluation of the radiation integral, and are resulted to be efficient and accurate when compared with other available solutions, and simple to implement in a computer code.

Since the approach seems to be applicable in all the cases in which the GO field on the considered surface is known, aim of this work is to extend the considered technique to other scattering problems involving penetrable or nonpenetrable half-planes and wedges, and to prove its effectiveness.

RCS Modeling of Aircraft at Radio Frequencies

Branislav M. Notaros

University of Massachusetts Dartmouth, ECE Department
285 Old Westport Road, North Dartmouth, MA 02747

There have been tremendous research efforts in recent years in the area of radar cross section (RCS) analysis, measurement, and design. This includes the entire spectrum of methods and techniques for the computation and measurement of RCS of complex objects, which are necessary for the design and building of objects of desired, "optimized" RCS. One application, out of many, is the design of aircraft of as small as possible RCS ("stealth" technology).

This paper deals with the computation of RCS of aircraft at radio frequencies. In order to predict the RCS of civil and military airplanes at frequencies from about 100 kHz to about 300 MHz, we use a very efficient and accurate computational technique based on the method-of-moments (MoM) solution of electromagnetic-field equations (B.M. Notaros, M.Lj. Djordjevic, B.D. Popovic, and Z. Popovic, 1999 IEEE Radio and Wireless Conference – RAWCON'99 Digest, pp.167-170). For RCS modeling of aircraft at frequencies higher than 300 MHz, rigorous (full-wave) MoM techniques become computationally inefficient, and high-frequency asymptotic methods, such as the uniform geometric theory of diffraction (UTD) technique, may be used at those frequencies.

We model the aircraft geometry as a system of bilinear quadrilateral surface elements (plates) and approximate the induced surface current over the elements by 2D polynomials in local coordinates. The polynomial degrees can be high, enabling electrically large elements (large-domain MoM approach). The current-distribution coefficients are determined by a Galerkin-type solution of the electric field integral equation (EFIE). The scattered field and RCS are then easily found from current distribution. For example, we are able to accurately predict the RCS of a Boeing 737-300 at 100 MHz on a PC (AMD-K6 266 MHz) within only 12 minutes of CPU time. Once the analysis of the given aircraft at the specified frequency is performed, each new excitation requires practically negligible additional CPU time. This feature of the method is very important since RCS is often required for various directions of the plane-wave incidence.

The modeling results will be presented for RCS of aircraft at various radio frequencies, along with very useful and instructive color-scale pictures of the corresponding computed current distributions over airplanes. Several aircraft antenna simulations will also be presented. The necessity of the rigorous evaluation of currents (or associated fields) induced on an illuminated airplane at different frequencies will be discussed, and frequency range of applicability and effectiveness of our approach and technique will be demonstrated. Possibilities of using wire-grid modeling and high-frequency asymptotic methods at the lower and upper end of this range, respectively, will also be discussed.

RADIATION FROM PARALLEL CIRCULAR LOOPS NEAR A CONDUCTING SPHERE AND/OR CAPS

Hakan P. Partal*, Joseph R. Mautz, and Ercument Arvas
EECS Dept., Syracuse University, Syracuse, NY 13244

The radiation pattern of loop antennas may be reshaped by the presence of symmetrically placed conducting objects nearby. Here, radiation from parallel circular loops placed symmetrically near a conducting sphere and/or conducting caps is considered. The loops are assumed to have uniform currents. The loops may have different radii but all are parallel to the xy -plane with their centers on the z -axis. They may carry different currents. Figure 1 shows the geometry of a typical problem considered. The smaller cap may be a complete sphere. The fields in various regions are expressed by truncated eigenfunction series. Each loop is assumed to be on the same imaginary sphere centered at the origin. This sphere constitutes a boundary between two regions. The unknown coefficients are computed by satisfying the boundary conditions partly analytically and partly numerically. The numerical method uses the point matching technique. Computed results include the current induced on the conducting surfaces and the radiated far field pattern. Figure 2 shows the magnitude of the computed electric far field pattern when a loop is placed at different locations near a perfectly conducting sphere. The loop carries a uniform current of 0.1mA, and has a radius equal to one wavelength. The radius of the conducting sphere is 0.75 wavelength. The result for the case where $\theta_a = 90^\circ$ is in excellent agreement with the result published previously. It is observed that the presence of conducting objects changes the pattern in a way that cannot be predicted easily.

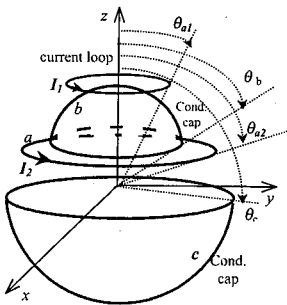


Figure 1

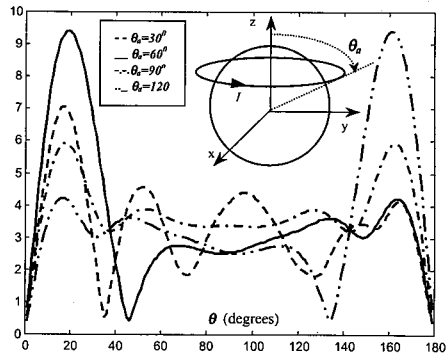


Figure 2

**ELECTROMAGNETIC SCATTERING FROM DIHEDRAL
CORNER REFLECTORS CHARACTERIZED
BY RANDOM SURFACE IMPURITIES**

P. Corona (1), G. Ferrara (1), G. Toso* (2)

(1) Istituto di Teoria e Tecnica delle Onde Elettromagnetiche, Istituto Universitario Navale,
Via Acton 38, 80133 Naples, Italy.

(2) Laboratorio di Microonde ed Elettromagnetismo, Dipartimento di Ingegneria Elettronica,
Università di Firenze, Via C. Lombroso 6/17, 50134 Florence, Italy.

Abstract.

In this paper the scattering from perfectly conducting dihedral corner reflectors (DCR) with randomly deformed faces is analyzed. DCRs are theoretically characterized by perfectly conducting and flat surfaces (P. Corona *et al.*, *Electromagnetics*, **13**, 23-36, 1993). However, common DCRs present surface deformations essentially due to a) manufacture errors and tolerances and b) the environment conditions where they have to operate. Recently, the scattering properties of DCRs characterized by parabolic or sinusoidal deterministic profiles have been studied by the same authors. However the surface profiles can be considered also from a statistical point of view. In general, especially in Remote Sensing applications, the surface statistic is used to describe the profile of distributed target as the ground or the sea. A DCR, despite their faces are quite large in terms of wavelengths, cannot be considered as a distributed target but its surface profile is equally depending on random effects. Resorting to a full-wave method of moments technique (G. Toso *et al.*, *Radio Sci.*, **32**, 4, 1347-1359, 1997) the scattering from perfectly conducting DCRs characterized by random profiles is studied.

**A new formalism for time dependent electromagnetic scattering
from a bounded obstacle⁺**

Maria Cristina Recchioni

Istituto di Teoria delle Decisioni e di Finanza Innovativa (DE.FIN)

Università di Ancona

Piazza Martelli 8, 60121 Ancona, Italy

email: recchioni@posta.econ.unian.it

Francesco Zirilli*

Dipartimento di Matematica "G. Castelnuovo"

Università di Roma "La Sapienza"

Piazzale Aldo Moro 2, 00185 Roma, Italy

email: f.zirilli@caspur.it

Abstract

We consider a time dependent three dimensional electromagnetic scattering problem. Let \mathbf{R}^3 be the three dimensional real Euclidean space filled with a medium of electric permittivity ϵ , magnetic permeability μ and zero electric conductivity. The quantities ϵ , μ are positive constants and there are no free charges in the space. Let $\Omega \subset \mathbf{R}^3$ be a bounded simply connected obstacle with a locally Lipschitz boundary $\partial\Omega$, that is assumed to have a nonzero constant boundary electromagnetic impedance. The limit cases of perfectly conducting and perfectly insulating obstacles are studied. We consider an incoming electromagnetic wave packet that hits Ω . We present a method that solves the Maxwell equations to compute the scattered electromagnetic field as a superposition of time harmonic electromagnetic waves. These time harmonic electromagnetic waves are the solutions of exterior boundary value problems for the vector Helmholtz equation with the divergence free condition and they are computed with an "operator expansion" method that generalizes the methods presented in [1] and [2]. The "operator expansion" method for time harmonic acoustic scattering from an unbounded surface was introduced for the first time by Milder [3]. The method proposed here is computationally very efficient. In fact it is highly parallelizable with respect to time and space variables. Several numerical experiments obtained with a parallel implementation of the method are shown. The numerical results obtained are discussed from the numerical and the physical point of

⁺ The numerical experience shown in this paper has been made possible by the support and sponsorship of CINECA - Casalecchio di Reno (BO) - Italy through a grant account on the T3E computer facility.

* Presenting author.

Genetic Algorithm Approach To Extrapolation For Fields Scattered By Large Objects

Sourav Chakravarty¹, Raj Mittra^{1*} and Elif Aydin^{1,2}

¹Electromagnetic Communication Laboratory, 319 EE East
The Pennsylvania State University
University Park, PA 16802

²On leave from Gazi University, Ankara, Turkey
sxc289@psu.edu, rxm53@psu.edu

In this paper we show how the Genetic Algorithm (GA) approach can be used to extrapolate, in frequency, the fields scattered by a large object in the asymptotic region, where the problem may be too large to be handled by direct numerical techniques.

The procedure for carrying out the extrapolation is as follows. First, we compute the scattered field from the object for frequencies up to the highest value possible. We then go to the far field at the look angle of interest, and track the frequency variation of the scattered field there. Typically, at high frequencies, this field will have the appearance of an interference pattern between signals originating from a fixed number of scattering centers.

Next, we process the frequency characteristics of the field to determine the components that comprise the scattered field. This is accomplished by first using the Prony's method, over a relatively narrow frequency window, to get an initial estimate of the exponents, and of their coefficients.

Next we use GA to refine these estimates and to fit the exponential series representation, with coefficients and exponents that are functions of frequency, to match the scattered field data over a wider range of frequencies than was originally used in the Prony's method. Once a good match has been found between the field data and the series representation, we can use this representation, with frequency-dependent exponents and coefficients, to extrapolate the field at higher frequencies. Two examples that illustrate the application of the procedure outlined above are presented in the figures below. Figure 1 shows the extrapolation results for a thin plate, and Fig. 2 presents the example of a line source located in the proximity of a wedge-shaped scatterer.

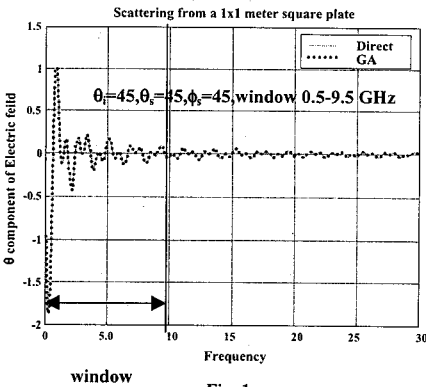


Fig. 1

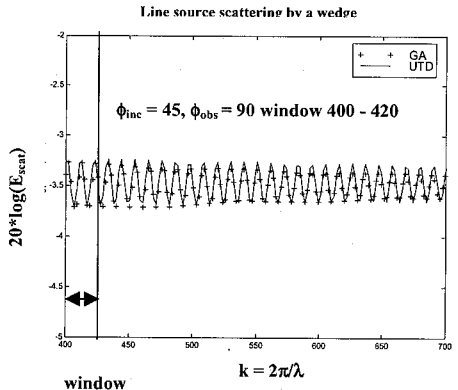


Fig. 2

SIMULATIONS OF THE DELAY SPREAD AND ANGLE-OF-ARRIVAL USING PHYSICS-BASED PROPAGATION MODELS

Bertin Koala*
ATT Wireless
Seattle, WA 98109

Mark Curry, Massimiliano Ciccotosto, Yasuo Kuga and Leung Tsang
Department of Electrical Engineering
University of Washington, Box 352500
Seattle, WA 98195-2500

In order to include the effects of man-made structures and natural media in communication channels and improve the current signal processing methods, the physics-based propagation models must be studied. One example of the physics-based models is the electromagnetic (EM) scattering from realistic trees based on Lindenmayer's L-system which has been applied extensively in remote sensing, and another example is an indoor EM wave propagation model.

We have developed a computer program to calculate the propagation of waves in an indoor environment for the study of angle-of-arrival (AOA) of signals. We used the ray tracing techniques and took into account diffraction, transmission, and reflection effects. Using this program, it was possible to simulate an antenna array receiving system and determine the angle-of-arrival of signals from a transmitter in an indoor building. Adaptive array processing and multi frequency averaging were used for processing data and analyzing a direction of the signal. Good agreement was obtained between the EM field strength measured at selected locations and the numerical simulations.

To estimate the effects of a forest on the signal delay spread in wireless communications, we have applied a tree-scattering code developed for remote sensing. The time-domain data is used to specifically determine the effect of the forest on the bit-error-rates for different modulation signals. A program was written to model the forest as a collection of dielectric cylinders and spheroids representing trees, branches and leaves. Using this model, we computed the forward scattering field and use such data to find the root-mean-square delay spread, and the mean excess delay for an EM wave propagating through a patch of trees. Initial results for a canopy of 50 trees with 64 branches each on a 100m x 100m area show an average delay spread of 23.7ns, and a mean excess delay of 20ns.

Electromagnetic Scattering Analysis Utilizing a Near-Field Scanning Microwave Microscope

W. C. Symons^{1*} and K. W. Whites²

¹The Bradley Department of Electrical and Computer Engineering
Virginia Polytechnic Institute and State University, Blacksburg, VA 24061-0111

²Department of Electrical Engineering
University of Kentucky, Lexington, KY 40506-0046

Near-field scanning microscopes utilize a subwavelength aperture placed within a wavelength of a sample to obtain image resolutions beyond the diffraction limit of $\lambda/2$. This mechanism allows a subwavelength resolution image to be obtained by raster scanning the aperture in a plane parallel to the sample while simultaneously recording the scattered power corresponding to each scan location. In this manner, the image resolution is determined by the aperture size, aperture/sample separation distance, and the step size of the raster scan. Although, near-field scanning microscopes have traditionally been implemented in the optical region of the electromagnetic spectrum, the subwavelength imaging effect is independent of wavelength. In general, size limitations imposed by optical wavelengths make it difficult to produce and manipulate subwavelength-sized samples. Because this size limitation does not apply to the X-band region of the electromagnetic spectrum, a near-field scanning microwave microscope (NSMM) has been constructed in the Electromagnetic Materials Laboratory at the University of Kentucky. The NSMM is composed of a transmit and a receive lensed horn antenna connected to an HP 8510B network analyzer. An aluminum plate containing a subwavelength aperture separates the two antennas. A positioning stage then allows the aperture to be scanned in a plane parallel to the sample of interest.

Under some circumstances, near-field scanning microscopes do not necessarily produce images that can be intuitively identified. For example, a thin-wire intensifies the transmitted power as opposed to blocking power and therefore could be misinterpreted as a slot. Therefore, in order to accurately interpret the image data of NSMM instruments, it is important to fully understand the near-field scattering characteristics of sample objects illuminated within the near-field of a subwavelength aperture. To this end, two numerical models have previously been developed based the physical attributes of an NSMM instrument. Specifically, both a moment method and a finite-difference time-domain model of an NSMM instrument have been utilized to investigate the near-field scattering phenomena. Images obtained from the actual NSMM instrument will be presented validating the computational models. The NSMM in conjunction with the computational models provides a better understanding of near-field optical imaging effects.

Using Physical Optics, Finite Differences and Kirchoff Integral, in the time Domain, to Study Electromagnetic Fields in a Complex Environment

M. Martínez-Búrdalo, L. Nonidez*, A. Martín and R. Villar
Consejo Superior de Investigaciones Científicas. Instituto de Física Aplicada
Serrano 144, 28006-Madrid, SPAIN
E-mail: mercedes@iec.csic.es

Physical Optics (PO) has been a widely used technique to study the scattering by large obstacles in the frequency domain. Its extension to the time domain has been used to solve some electromagnetic-scattering problems (E.Y. Sun and W.V.T. Rush, *IEEE Trans. Antennas Propagat.*, 42, 9-15, 1994).

In the last years, FDTD has been a widely used technique when dealing with electromagnetic compatibility problems and interaction of electromagnetic fields with biological tissues (A. Taflove, *Computational Electrodynamics: The Finite-Difference Time-Domain Method in Electromagnetics*. Norwood, MA: Artech House, 1995). It has the advantages that it can represent complex material properties and obtain broadband responses with a single analysis, but it has some limitations when calculating fields in large regions. In this last case, a Kirchoff integral derived from the Green's theorem in the time domain, combined with the FDTD method, has been used for calculating electromagnetic fields both in near- and far-zone in the time domain (M. Martínez-Búrdalo, L. Nonidez, A. Martín and R. Villar, *Microwave Opt. Technol. Lett.*, 22, pp. 74-78, 1999). The use of these techniques has demonstrated to be useful for large computational domains. When large distances and scatterers are involved we can take advantage of a high frequency approximation as the PO in the time domain (TDPO) to know the first order field scattered by obstacles. The efficiency and accuracy of TDPO in the region where PO is appropriated is demonstrated. In this work we have used a combination of all of the above techniques to analyze electromagnetic pollution in complex environments involving antennas, flat plates and dielectric materials. The results obtained and the saving of calculation time show the utility of these techniques.

Indoor, Urban, and Mobile Propagation

Chair: J. Volakis, University of Michigan

			Page
1	8:00	Prediction of radio wave propagation through manmade obstacles over impedance surfaces using exact image theory, <i>M. Casciato*</i> , <i>K. Sarabandi</i> , <i>University of Michigan, USA</i>	244
2	8:20	Building attenuation models, <i>A. Paul*</i> , <i>G. Hurt</i> , <i>U.S. Department of Commerce, USA</i>	245
3	8:40	Propagation in built-up areas with various terrain profiles, <i>N. Blaunstein*</i> , <i>D. Katz</i> , <i>Ben-Gurion University of the Negev, Israel</i>	246
4	9:00	Approximate integral methods for improved picocell modeling in wireless channels, <i>H. Syed*</i> , <i>Advanced Engineering Research Organization, Pakistan</i> , <i>J. Volakis</i> , <i>The University of Michigan, USA</i>	247
5	9:20	Novel approach to indoor semi-deterministic propagation prediction, <i>P. Pechac*</i> , <i>M. Klepal</i> , <i>M. Mazanek</i> , <i>Czech Technical University in Prague, Czech Republic</i>	248
	9:40	Break	
6	10:00	A system for measuring the indoor and outdoor MIMO wireless channel response, <i>J. Wallace*</i> , <i>M. Jensen</i> , <i>Brigham Young University, USA</i>	249
7	10:20	Geo-location of the mobile station with multiple base stations, <i>H. Li*</i> , <i>H. Lee</i> , <i>C. Lee</i> , <i>T. Liu</i> , <i>National Taiwan University, Taipei</i>	250
8	10:40	Mobile position in GSM system using the time advance, <i>C-C. Wang*</i> , <i>N-L. Hwang</i> , <i>National Cheng Kung University, Tainan</i>	251
9	11:00	Applying MLFMA to electromagnetic simulations in wireless communication, <i>Y. Zhang*</i> , <i>J. Song</i> , <i>W. Chew</i> , <i>University of Illinois at Urbana-Champaign, USA</i>	252
10	11:20	The frequency correct and analysis the L-CDMA system, <i>L. Daming*</i> , <i>Beijing Pacific Linkair Communications INC., Beijing</i>	253

Prediction of Radio Wave Propagation Through Manmade Obstacles Over Impedance Surfaces Using Exact Image Theory

Mark D. Casciato* *Student Member, IEEE* and Kamal Sarabandi *Fellow, IEEE*

Radiation Laboratory
Department of Electrical Engineering and Computer Science
University of Michigan
Ann Arbor, MI 48109-2122 USA
email: casciato@eecs.umich.edu, saraband@eecs.umich.edu

Of significant interest in the prediction of radio wave propagation is the effect of various scattering and diffraction mechanisms in an urban environment. The environment can include obstacles such as buildings, towers, and trees and also the effects of the surface on which they sit. Their effect on the radio signal can include phenomena such as scattering, diffraction, and reflection (multipath effects) between obstacles as well as from the impedance surface. Point to point transmission from within a city can only be accomplished at frequencies below UHF, however even at HF frequencies calculation of field interactions using the appropriate Green's function makes numerical techniques such as method of moments (MoM) impractical even for small structures. Because of this, high frequency techniques are usually applied. They can include methods such as ray-tracing and include the effects of shadowing and multi-path, however while simple to implement they are of limited accuracy for moderate size objects and tend to be computationally cumbersome. An approach is sought to compute the effects on the radio signal of moderate size structures such as buildings, and include the combined effects of both the structures and the impedance surface on which they sit, when excited by a small dipole near the surface.

MoM is an integral equation (IE) technique in which unknown currents are expanded in terms of a set of orthogonal basis functions and cast in the form of a matrix equation. As with all IE formulations the Green's function must be known and multiple integrations must be performed to calculate the field interaction between matrix elements. The Green's function appropriate for this problem is the classic Sommerfeld problem of a point source radiating above an impedance half-space. The Sommerfeld solution consists of integrals (Sommerfeld type integrals) which are highly oscillatory and difficult to evaluate numerically. The near-field interaction between matrix elements of the MoM formulation precludes asymptotic evaluation of these integrals and their slow convergence properties makes numerical evaluation of them impractical.

In order to improve the convergence properties of the Sommerfeld type integrals, and make them of practical use in a MoM formulation, they are modified by application of exact image theory. In this method an integral transform is applied to the Sommerfeld integrals and the resulting expressions converge extremely fast, up to two orders of magnitude faster than then the original formulation. This improvement allows them to be of practical use in calculating the field interactions in a MoM solution. In this work a MoM solution is implemented, using the exact image formulation for field interactions, to calculate the scattering and diffraction from an obstacle of moderate wavelength, such as a wall or walls of a building on an impedance surface. Results shown will include analysis of the effects of shadowing and diffraction on the radio signal.

BUILDING ATTENUATION MODELS

Alakananda Paul and Gerald F. Hurt
National Telecommunications and Information Administration
U.S. Department of Commerce, Washington, D.C.

Building attenuation models are needed for determination of coverage of wireless communications as well as for estimating interference levels in shared frequency bands. There are two types of building losses. The first is the loss through the outer wall or the **penetration loss** and the second is the loss inside the building or **in-building loss**. The building penetration losses are becoming increasingly important because of the following two reasons. First, it is essential to quantify the coverage of an external cell into different locations inside a building. Second, it is important to assess the level of interference from indoor devices, such as, RLAN transmitters to receivers located outside the buildings, when sharing the same frequency band. A large number of RLANs are intended to operate on an unrestricted manner and meant to be mostly in an indoor environment. The additional attenuation due to building penetration loss is likely to reduce the interference. For outdoor RLANs, the loss due to surrounding buildings and foliage need to be considered. The in-building losses are important for the estimation of total loss from an external base station to a mobile inside the building as well as for determination of coverage of indoor communication systems.

A large number of studies and measurements of building attenuation have been reported in open literature as well as in ITU-R Study Group 3 (Propagation) Recommendations and other documents. The Institute of Telecommunication Sciences (ITS) of NTIA has conducted extensive measurements of building penetration losses at several frequencies. There also has been an effort at NTIA to develop empirical models based on the measured data. More recently, there has been effort through ITU-R Study Group 3 to produce elevation angle dependent propagation models for building penetration losses, which takes into account the diversity of buildings and environments. It is agreed that there will be additional losses caused on low angle paths due to buildings, vegetation, hills etc. and may be quite large for some low-angle paths. Also, it is expected that over-all excess path loss from large number of RLANs deployed randomly in a large variety of buildings will have a continuous average variation with elevation angle.

The aim of this paper is to present the outcome of a study of building attenuation losses. The review will include the results of diverse measured data as well as empirical models.

Propagation in Built-Up Areas with Various Terrain Profiles

N. Blaunstein and D. Katz

Department of Electrical and Computer Engineering, Ben-Gurion
University of the Negev, P. O. Box 653, Beer Sheva 84105, Israel

Abstract

In this work we continue to investigate the 3D-model parametric model that combines both deterministic and statistical description of wave scattering and diffraction from randomly distributed buildings and other kind of obstacles placed on rough terrain taking into account the built-up terrain profile. The law of buildings' distribution is assumed to be Poissonian [1]. As in [1], an array of randomly distributed buildings and obstacles placed on the rough ground surface was considered. The height of the ground relief is described in the coordinate system (x, y, z) placed at the plane $z=0$ of ground surface by the generalized function $Z(x, y)$ which describes the non-regular rough ground surface relief $z=Z(x, y)$.

Using this statistical model and its input parameters, such as the buildings' spatial distribution, their density over the terrain, as well as each building's characteristic dimensions and the reflection properties of the buildings' walls, we describe the average field attenuation along the radio path and the coverage effects. Using this model we also obtain the characteristic scale of cellular maps of built-up areas for various situations of receiver and transmitter (stationary or moving, higher or lower with respect to building heights) in the urban scene.

We present a comparison between the theoretical predictions based on this statistical 3D-model and the results of numerous experiments carried out in various urban areas with non-regularly distributed buildings for different positions of transmitter and receiver antennas [2, 3]. The possibility of using the statistical approach for predicting loss characteristics in cluttered (NLOS) urban conditions is examined here.

Comparison between theoretical prediction and experimental data obtained for measurements in different kinds of built-up areas show that using the 3D-model we can very accurately predict the loss characteristics in built-up areas for various kinds of terrain profile and for different position of transmitting and receiving antennas with respect to rooftops.

References

- [1] Blaunstein, N., *Radio Propagation in Cellular Environments*, Artech Houses, Boston-London, 1999.
- [2] Blaunstein, N., M. Levin and M. Shalukhin, *Proc. of International URSI/IEEE Conference*, Athena, Greece, May 14-18, 1998, pp. 87-90.
- [3] Liang, G. and H. L. Bertoni, *Proc. IEEE, Antennas and Propagation*, vol. 46, No. 6, 1998, pp. 853-863.

Approximate Integral Methods for Improved Picocell Modeling in Wireless Channels

H.H. Syed* and J.L. Volakis

*Advanced Engineering Research Organization
P. O. Box 145, Haripur
Pakistan

Radiation Laboratory
Electrical Engineering and Computer Sci.
University of Michigan
1301 Beal Ave
Ann Arbor, MI 48109-2122

It is well recognized that propagation models will play an important role in the design of broadband wireless communication systems, either for planning purpose or to assess multipath and interference issues in wideband systems. By and large existing electromagnetic propagation models rely on high frequency methods which may incorporate fast raytracing methods and shadowing. Recent advances for fast shadowing using algorithms such as binary space partitioning (BSP), shadow volume BSP (SVBSP), Z-buffer, etc. have also been essential to making high frequency solutions practical for the characterization of site specific urban propagation models. The incorporation of diffraction in these models is typically difficult, but has been found essential to include diffraction from building/edges nearby the receiver to obtain acceptable accuracies. This is particularly the case for pedestrian to pedestrian communication in densely populated urban environments.

In this paper, we consider another approach for including diffraction effects from structures nearby the receiver for improving channel modeling in pedestrian to pedestrian communications at the picocell level. Instead of using diffraction coefficients to characterize scattering effects, a degraded form of integral methods is considered. In this context, we examine the minimum sampling requirements needed to obtain accuracies comparable to the geometrical theory of diffraction (GTD) under various illumination conditions. It will be shown that discretizations as low as 3 samples per linear wavelength can deliver accuracies comparable to the GTD. When combined with recent fast integral methods such low sampling criteria can allow for fast picocell region modeling with predictable accuracy. Moreover, the approach provides for ease in handling non-metallic structures and other details and interactions that are difficult to include in high frequency methods.

NOVEL APPROACH TO INDOOR SEMI-DETERMINISTIC PROPAGATION PREDICTION

***Pavel Pechač, Martin Klepal, Miloš Mazánek**

Czech Technical University in Prague, Dept. of Electromagnetic Field
Technická 2, 166 27 Praha 6, Czech republic

tel.: ++420 2 2435 2252, fax: ++420 2 311 9958, email: pechac@ieee.org

An indoor propagation prediction for personal communication systems is demanded. There are two general approaches to the modeling: empirical and deterministic. The empirical modeling based on very simple formulas with parameters obtained from measurements is very easy and straightforward to use. On the other hand the accuracy is not so excellent especially for complicated interiors and building structures where supplementary measurement is necessary. On the contrary the deterministic model - typically ray tracing - is characterized by a very good site-specific validity. The trade off is the model complexity, which requires very long computation time and a detailed description of analyzed scene. The challenge is to combine the two approaches into a semi-deterministic/empirical model, which features:

- sufficient site-specific accuracy (agreement with measurements)
- fast computation time (needed for software tools with complex iterative optimization processes of indoor systems)
- reasonable demands on input data complexity and precision
- reasonable demands on test calibration measurement.

The proposed paper presents a novel approach to the semi-deterministic modeling. The main idea is based on a ray tracing, Monte Carlo method and statistics. A uniform grid (2D or 3D) represents an analyzed area where all partitions and obstacles fill appropriate elements. The element dimensions are predetermined by a wavelength. According to the transmitter antenna radiation pattern rays are launched in the grid using simple pixel graphics algorithm. When a ray hits a filled element the elements in the vicinity of the hit point are separated into a matrix called motif. Then the most similar motif - specific pattern in the grid - is found in a motif database. To each motif in the database a probability function and random number generator are assigned mainly based on measurements. The motif plays the key role in the algorithm determining the ray direction or its end in a next step. Each free element in the grid records number of passed rays, which predicts relative signal strengths in the location after sufficient number of launched rays. The calibration measurement or calculation is then needed to obtain the actual signal strengths.

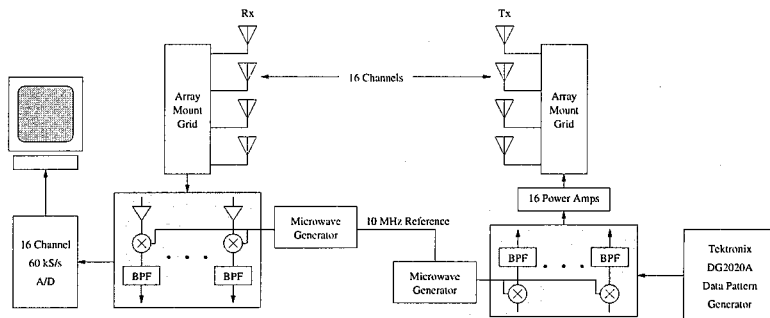
In addition to detailed description and functionality of the model the proposed paper presents also prediction results comparisons with measurements and basic empirical models which show good agreements.

A System for Measuring the Indoor and Outdoor MIMO Wireless Channel Response

Jon W. Wallace* and Michael A. Jensen
Department of Electrical and Computer Engineering
Brigham Young University
Provo, UT 84602

Recent years have witnessed an unprecedented growth in the area of wireless communications, with applications ranging from cellular phone technology to wireless networking. The resulting demand for increased communications bandwidth has motivated a search for new techniques that more efficiently exploit the available bandwidth. Recent research has demonstrated that the multiple-input-multiple-output (MIMO) channel exhibits a substantial increase in capacity over the single-input-single-output (SISO) channel when multipath fading exists (which is commonly the case). A variety of coding schemes are emerging which attempt to take advantage of increased capacity for the MIMO wireless channel. However, most coding development and performance assessment is based upon analytical channel models, such as Rayleigh or Ricean fading, under an assumption of independent signal statistics for each antenna. Since the spatial behavior of the indoor and outdoor wireless channel is not well understood, the ultimate applicability of such simple models to real MIMO channels remains uncertain. Further, the stationarity of these channels and the effect of multiple polarizations are not well understood.

To address this lack of fundamental understanding about the MIMO channel, we have developed a system capable of directly measuring the channel transfer matrix. Such measurement facilitates accurate assessment of various coding schemes and development of realistic models for the MIMO channel. The system (see figure) consists of 8 dual-polarization antennas at both transmit and receive ends for a total of 16 inputs and 16 outputs. The 16 transmit channels simultaneously radiate at the same carrier frequency of 2.45 GHz, with the signal from each channel being modulated with one of 16 orthogonal codes (30 kHz bandwidth). The transmitter and receiver local oscillators are phase locked to simplify the downconversion process. At the receiver, the 16 baseband signals are simultaneously sampled at 60 ksamples/s and stored to disk. The system is portable to allow measurement of a wide variety of channel scenarios. Channel transfer matrices constructed in a post-processing step can be analyzed to evaluate channel stationarity, the applicability of typical channel models, and the performance of existing coding schemes for real channels. The collected data is also being used to develop advanced channel models that capture the true spatial and polarization behavior of MIMO wireless environments.



Geolocation of the Mobile Station with Multiple Base Stations

Hsueh-Jyh Li*, Hsin-Yu Lee, Chi-Min Lee, Ta-Yung Liu
Graduate Institute of Communication Engineering
National Taiwan University
Taipei, Taiwan, R.O.C

The mobile station (MS) position can be located if times of arrival (TOA) and/or directions of arrival (DOA) of the direct paths from the MS to multiple base stations (BSs) are available. In the W-CDMA systems, the Q-channel can be used to estimate the channel parameters, where a matched filter is used to distinguish the desired user's signal from the co-channel interference and the time-domain output, or called the delay profile, gives the time delays of the multi-paths. If multiple antenna elements are employed in the BS, the DOA can be further obtained. In this paper we will propose signal-processing algorithms to locate the MS by using the data received by multiple BSs for the W-CDMA systems.

In the mobile environments, the MS signals usually arrive at the BS in clustering. Each cluster consists of multi-paths and each path subjects to fading. It is known that the more the number of BS that their shortest paths from the MS are correctly detected, the more that the MS can be accurately located. However, if the TOA of the wrong paths were used in the location process, the estimation error will be increased. In this paper we will propose algorithms to choose the correct paths.

If only the TOA is available in the measurement, the MS position can be estimated by the conventional method, where each TOA defines a circle (neglect the altitude dimension) around the BS, and the MS is located by the intersection of all circles. The more the number of circle is, the small the intersection area will be. However, the above statement is true only when the TOAs are all from the correct paths. In this paper we will propose algorithms to retain the correct paths and discard the incorrect ones.

If both the TOA and DOA are available, the MS can be located by using the parameters estimated by a single BS. If N BSs are used to locate the MS, then there are N location points. Some points may be wrong positions and are far away from the real MS position. In this paper we will propose a method to locate the MS from the N location points. Numerical results will be demonstrated at the presentation.

Mobile Position in GSM System Using the Time Advance

Chuen-Ching Wang*, Nan-Lu Hwang
Directorate General of Telecommunications
Ministry of Transportation and communications

Abstract--Due to the mobile telephones are widely used, the mobile position becomes more and more important for the requirement of supporting the Enhanced emergency call service. A roughly estimated data shows that in the major U.S metropolitan areas 10% of the emergency calls originate from mobile phones.

In the mobile position system the first step is to measure the raw data for the location calculation. Next, the raw data are transferred to the Operator of Maintenance Center (OMC) where these data can be further processed. In this paper, a method that based on the delay time and the signal level for locating the mobile phone will be presented. This delay time between the serving BS and mobile phone is also called the Time Advance (TA). Unlike the traditional method, the mobile phone is first modified by the embedded firmware so that the Time Advance, signal level and Cell Identifier (CI) can be detected. In practical, the embedded firmware enables the mobile phone to handshake with at most six cells at a time. Next, we use the Global Position System (GPS) to measure the position of all BS beforehand. Also, the distance between mobile phone and the BS can be estimated by the Time Advance. Further, we choose the two CI with larger signal level for doing the operation of mobile phone's position. The location can be made from solving the equation as follow:

$$\begin{aligned} L_p &= \sqrt{(x - Y_p)^2 + (y - Y_p)^2} \\ L_q &= \sqrt{(x - Y_q)^2 + (y - Y_q)^2} \end{aligned} \quad (1)$$

where (X_k, Y_k) represents the fixed coordinates of BS_k and L_k represents the propagation distance corresponding to the measured Time Advance from BS_k to mobile phone. The experimental result shows that this method is a simple and efficient strategy.

Applying MLFMA to Electromagnetic Simulations in Wireless Communication

Y. Zhang*, J. M. Song, and W. C. Chew
Center for Computational Electromagnetics
Department of Electrical & Computer Engineering
University of Illinois, Urbana, IL 61801, USA

The problem of electromagnetic simulations of indoor propagations in wireless communication is addressed. The operating frequencies of wireless communication span several bands, specifically within the range of personal communication, cellular phones and pagers work at 800MHz-900MHz, and latest dual band cellular phones occupy another band between 1800MHz and 1900MHz, corresponding to wavelengths around tens of centimeters.

Most research interests studying the indoor propagation of waves nowadays rely on the ray approximation of electromagnetic wave. Geometrical optics models are developed and ray tracing method is used. Finding new models that better describe the diffraction features of indoor wave propagation environment has attracted much attention of scientists. However, these high frequency models lose accuracy when taking into account that the size of many indoor structures is only several wavelengths. High frequency methods also encounter certain difficulties modeling material properties accurately.

It was once hard also to imagine solving the integral equations directly for better accuracy. The size of a building usually is tens of meters and our frequency of interest is not low enough to reduce the electrical size of the problem to a moderate scale, which allows solution with any existing method within affordable time and resource limit. The Fast Illinois Solver Code (FISC) (J. M. Song, C. C. Lu, W. C. Chew and S. W. Lee, *IEEE Antennas Propagat. Mag.*, vol. 40, no. 3, pp. 27-34, June 1998) successfully overcame this problem. The application of Fast Multipole Method(FMM) and Multilevel Fast Multipole Algorithm (MLFMA) in FISC vastly reduced the workload of a matrix-vector multiply and the memory requirement, thus making it possible to solve such electrically large problems on small computers. FMM/MLFMA has the advantage over high frequency methods for its ease of modeling different material properties regardless of the scales of the structures. Also, solving the integral equations directly gives more accurate results. Various cases are considered and results are shown to demonstrate the ability of MLFMA in wireless communication.

The Frequency correct and analysis the L-CDMA system

Li Daming Beijing Pacific Linkair Communications INC.

Abstract:

L-CDMA (large-area CDMA) system is a kind of synchronous CDMA communication system. The up and down links all adopt the way of synchronization. Using the method of Time Division Duplex. As employs a set of well-design spread spectrum multiple address codes with better correlation characteristic, compared with the IS-95 system, L-CDMA system has many advantages such as simpler structure and larger capacity, no need complex technology of interleaving and scrambling, less demand of the power control. In addition, since using a simple 4-th power frequency loop in the RAKE receiver of user station to recover the carry frequency and phase, hence, reducing the system's complexity efficiently.

The first part of this paper introduces simply the functions and performances of L-CDMA system, after that, a detailed theoretical analysis on the automatic frequency correction loop is presented. Two concrete methods of automatic frequency correction, i.e. L-th power loop and decision feedback loop, are put forward and their performances are carefully compared. Computer simulation of the automatic frequency correction loop is the kernel of this paper. By a vast amount of simulation considering various kinds of interference, we proposed an automatic frequency correction algorithm that works well in practical multi-path fading channels, and several methods of improvement are discussed. Finally, the detailed theoretical analysis of above topics is given. The conditions, steps and results of the computer simulation are also presented. Figures and graphs are attached, and references are listed.

The Introduce of the L-CDMA System Performances

At presently, L-CDMA system uses M special spread spectrum address codes and is especially designed for large area. The capacity of every base station at the same time is bigger than any publicized CDMA system's.

This system has following functions mostly:

- (1) To adopt the bi-direction double side synchronization and ideal address code, the function of system gets insure.
- (2) To have not use the complex technology such as the interleaving and scrambling, the complexity of system and the demand of power control are lower, the administer and control of system also are more simple.
- (3) More communication capability.
- (4) To adapt to different access rates, such as 16, 32, 64, 128, 256, 512, 1024, 2048Kbps.
- (5) Lower transmitting power, according to test, it is 3mw as the distance of 30km nearly and 10mw as the distance of 50Km, and insure the error probability lower 10.
- (6) Cost effective for every user in this system .

The Analysis of Frequency Correct Loop in the L-CDMA System

For resume the data message from signal sent by the Base station, the user station of CDMA system need to perform spread spectrum modulation to data sent by transmitter firstly, that is demodulation and despreading. For the demodulation, it is necessary that the carry frequency of local signal is same as the frequency of received signal basically, if it is bigger difference between them, the correct demodulation would don't had been got and result in higher error rate. Here, we should point out that the carry frequency of local signal is found based on the clock of user station, however the carry frequency of received signal is found on the clock of base station, even though the user station and base station all use the crystal of very stability and precision of oscillation frequency as clock, still there is difference with delay of time between them. We usually call the difference as frequency offset. Actually, it is necessity for the offset, if the corresponding measures have not been done, the offset would reach to the situation no endure. Aim at the L-CDMA system, to get the allowing rang of frequency offset, we have got a group of curves, which the error code performance is affected by the deferent frequency offset through the computer simulation.

To avoid the situation, the system should have the measure to overcome frequency offset. In tradition method, such as IS-95, to get the carry frequency of receiver signal, it set up a loop of resuming carry frequency on the every finger of RAKE receiver of user station, apparently, this way is very complex. We detect the frequency offset between user station and base station from the receiver signal of user station firstly, and then by mean of this message to control and improve the clock of user station. Next the user station demodulate according to the local signal of carry frequency adjusted, only if the user station communicate normally, above steps would repeat constantly, to insure that the user

station and base station have same clock.

As we know from the above represent, it is very important to detect the frequency offset between the user station and base station from the receiver signal. Therefore we have designed two methods for detecting frequency offset: (1) using L-th power loop, that is 4-th power loop in our system; (2) using decision feedback loop. Following is the theory analysis and compare of two frequency correct loop.

The Summarize and discuss:

- (1) To a band limit system with band broad B, the taps interval of RAKE receiver, Δ should not more than $1/B$.
- (2) The time spreading channel limited that max time spread is T_d , the fingers number K of RAKE receiver should not more than max integral of $T_d / \Delta + 1$. Because, if the K's value is bigger, it would increase the complication and noise of receiver, or vice versa, the system's performance would decrease.
- (3) Through using the time average rather than set average, we can have following results: for the RAKE receiver of ideal signal and better design, if its SNR is high enough and time is long enough, as $E\{F_1(\Delta f)\} \gg E\{F_2(\Delta f)\}$, so the frequency correct performance of L power loop is better than the decision feedback loop.

After we analyze the performance of two frequency correct loop in L-CDMA system and according to above results, we have done the computer simulation for frequency correct loop, due to the limit of length, and consider for the results of simulation all are some figures, so we will make them into some slides and bring the slides by myself when I go take part in meeting.

Hybrid Numerical Methods

Chair: T. Cwik, Jet Propulsion Laboratory

Page

1	8:00	3D higher order modeling in the BEM/FEM hybrid formulation, <i>P. Fink*</i> , <i>NASA-JSC, D. Wilton, University of Houston, USA</i>	256
2	8:20	A higher-order hybrid FEM/MLFMA for scattering and radiation analysis, <i>X. Yin*</i> , <i>J. Jin, J. Song, W. Chew, University of Illinois at Urbana-Champaign, USA</i>	257
3	8:40	Matrix solvers for computational electromagnetics, <i>C. Reddy*</i> , <i>Hampton University, C. Cockreel, F. Beck, NASA Langley Research Center, USA</i>	258
4	9:00	A higher-order FEM for computing the RCS of BORs, <i>E. Branch*</i> , <i>J-M. Jin, University of Illinois at Urbana-Champaign, USA</i>	259
5	9:20	A study of Webb's hierarchical vector shape functions for FEM solution of electromagnetic scattering problems, <i>T. Ezzedine*</i> , <i>A. Kouki, Ecole de Technologie Superieure, A. Khebir*</i> , <i>ElectroMagneticWorks Inc., Canada</i>	260
	9:40	Break	
6	10:00	Parallel implementation of a hybrid finite-element, finite-volume, and finite- difference transient electromagnetic simulation, <i>J. Kotulski*</i> , <i>D. Riley, C. Turner, Sandia National Laboratories, USA</i>	261
7	10:20	Domain decomposition method for the computation of scattering by inhomogeneous penetrable 3D objects, <i>B. Stupfel*</i> , <i>CEA/CESTA, France</i>	262
8	10:40	A study on the efficient FEM-based hybrid method for the open region problem and its applications to characterizing radiating slots in a broad wall of a rectangular waveguide, <i>J. Park*</i> , <i>H. Chae, S. Nam, Seoul National University, S. Korea</i>	263
9	11:00	Hybrid current-based formulation for modeling on board antennas, <i>F. Obelleiro*</i> , <i>J. Taboada, J. Rodriguez, Universidade de Vigo, Spain</i>	264
10	11:20	Scattering from 3D cavities with the Scheme FACTOPO. The effects of PO processes on the S matrix of the exterior domain, <i>V. Bazin*</i> , <i>G. Bobillot, A. Barka, P. Soudais, S. Langlet, Office National d'Etudes et de Recherches Aerospaciales, France</i>	265
11	11:40	On the use of spatiotemporal wavelet expansions in Method of Moments solutions for time-domain integral equations, <i>Y. Shifman*</i> , <i>Y. Leviatan, Technion--Israel Institute of Technology, Israel</i>	266

3D HIGHER ORDER MODELING IN THE BEM/FEM HYBRID FORMULATION

P. W. Fink*
NASA-JSC
Houston, TX 77058

D. R. Wilton
University of Houston
Houston, TX 77204-4793

Higher order divergence- and curl-conforming bases have been shown to provide significant benefits, in both convergence rate and accuracy, in the 2D hybrid finite element/boundary element formulation (P. Fink and D. Wilton, National Radio Science Meeting, Boulder, CO, Jan. 2000). A critical issue in achieving the potential for accuracy of the approach is the accurate evaluation of all matrix elements. These involve products of high order polynomials and, in some instances, singular Green's functions. In the 2D formulation, the use of a generalized Gaussian quadrature method was found to greatly facilitate the computation and to improve the accuracy of the boundary integral equation self-terms. In this paper, a 3D, hybrid electric field formulation employing higher order bases and higher order elements is presented. The improvements in convergence rate and accuracy, compared to those resulting from lower order modeling, are established. Techniques developed to facilitate the computation of the boundary integral self-terms are also shown to improve the accuracy of these terms. Finally, simple preconditioning techniques are used in conjunction with iterative solution procedures to solve the resulting linear system efficiently.

In order to handle the boundary integral singularities in the 3D formulation, the parent element—either a triangle or rectangle—is subdivided into a set of sub-triangles with a common vertex at the singularity. The contribution to the integral from each of the sub-triangles is computed using the Duffy transformation to remove the singularity. This method is shown to greatly facilitate the self-term computation when the bases are of higher order. In addition, the sub-triangles can be further divided to achieve near arbitrary accuracy in the self-term computation. An efficient method for subdividing the parent element is presented.

The accuracy obtained using higher order bases is compared to that obtained using lower order bases when the number of unknowns is approximately equal. Also, convergence rates obtained using higher order bases are compared to those obtained with lower order bases for selected sample problems. The convergence rates of the iterative procedure are compared for different preconditioners.

A Higher-Order Hybrid FEM/MLFMA for Scattering and Radiation Analysis

X. T. Yin*, J. M. Jin, J. M. Song, and W. C. Chew

Center for Computational Electromagnetics
Department of Electrical and Computer Engineering
University of Illinois
Urbana, Illinois 61801, USA

The computation of electromagnetic scattering/radiation from three-dimensional (3D) targets/antennas has been considered a challenging problem in the field of computational electromagnetics. One of the most suitable numerical techniques is the hybrid finite-element and boundary-integral (FE--BI) method (J. M. Jin *et al.*, *IEEE Antennas Propagat. Mag.*, vol. 33, no. 3, pp. 22-32, June 1991). This method first divides the problem into an interior and exterior problem. The field in the interior region is formulated using the finite-element method (FEM), and the field in the exterior region is represented by a boundary-integral equation (BIE). The interior and exterior fields are then coupled by the field continuity conditions. This method has been successfully applied to electrically small-size problems.

To apply the hybrid FE--BI method to electrically large problems, it is necessary to reduce the computational complexity associated with the BIE part. In a recent work (X. Q. Sheng *et al.*, *IEEE Trans. Antennas Propagat.*, vol. 46, no. 3, pp. 303-311, March 1998), this problem is solved by applying the multilevel fast multipole algorithm (MLFMA), which is based on the fast multipole method (FMM). The use of MLFMA reduces both the memory requirements and CPU time per iteration from $O(N^2)$ to $O(N \log N)$, where N denotes the number of unknowns in the BIE matrix.

In this paper, we will further enhance the efficiency and accuracy of the hybrid FEM/MLFMA by employing higher-order vector basis functions (R. D. Graglia *et al.*, *IEEE Trans. Antennas Propagat.*, vol. 45, no. 3, pp. 329-342, March 1997), which have been successfully implemented in the FEM and MLFMA in our center. The resulting method can accurately model the problem geometry as well the unknown fields. In addition, it exhibits fast convergence that permits obtaining an accurate solution with a smaller number of unknowns. A variety of scattering and radiation problems will be considered to demonstrate the capability of the higher-order hybrid FEM/MLFMA.

MATRIX SOLVERS FOR COMPUTATIONAL ELECTROMAGNETICS

C. J. Reddy*
Department of Electrical Engg.
School of Engineering & Technology
Hampton University, Hampton VA 23668

C. R. Cockrell and F. B. Beck
Electromagnetic Research Branch
NASA Langley Research Center
Hampton VA 23681

ABSTRACT:

Matrix methods to solve many problems in Computational Electromagnetics (CEM) have been very popular. The use of different frequency domain techniques such as Method of Moments (MoM), Finite Element Method (FEM) and hybrid Finite Element Method and Method of Moments (FEM/MoM) technique lead to a variety of complex matrices, which have to be solved using efficient matrix solvers to minimize the memory requirement and CPU time. Application of MoM results in complex, symmetric dense matrices, whereas application of FEM results in complex, sparse and symmetric matrices. A hybrid technique combining FEM and MoM to accurately model many EM problems, results in partly sparse and partly dense non-symmetric complex matrices. In this paper, various matrix techniques which are used to solve systems of simultaneous linear equations. To solve complex dense matrices, very efficient direct solvers, such as LAPACK are available in the public domain. But for the complex sparse matrices not many efficient direct solvers are available. But at the same time, sophisticated direct solvers are available for real sparse matrices. A technique to convert complex sparse matrices into real matrices and solve them using real sparse matrix solvers will be presented. Some results on the numerical experiments performed to compare the performance of various solvers will be presented. Limitations of various solvers will be discussed and efficiency of parallel solvers will also be presented.

A Higher-Order FEM for Calculating the RCS of BORs

Eric D. Branch* and Jian-Ming Jin
Center for Computational Electromagnetics
Department of Electrical and Computer Engineering
University of Illinois
Urbana, Illinois 61801

*Also affiliated with Air Force Research Laboratory at Wright-Patterson AFB, OH

Higher-order basis functions are applied to the finite element method (FEM) calculation of the radar cross section (RCS) of bodies of revolution (BORs). The FEM is used because it can model arbitrary bodies fairly easily, it does not involve the Green's function, and it is fairly easy to incorporate inhomogeneities into the formulation. Using symmetry, the FEM formulation for BORs can be reduced from a three-dimensional (3-D) problem to a two-dimensional (2-D) problem. A 2-D FEM BOR code can be used to calibrate RCS measurements and provide a benchmark for the validation of 3-D numerical simulations. Greater accuracy can be obtained by using higher-order basis functions for a given mesh, especially if the BOR has sharp edges or tips. The higher-order basis functions approximate the singular fields around edges and tips better than low-order basis functions. On the other hand, fewer elements, for the higher-order case, can be used in the mesh to obtain the same accuracy relative to the original mesh using the low-order basis functions.

The mixed-element formulation used in this work involves scalar basis functions for the azimuthal component and vector basis functions for the transverse components. Another well-known FEM for the BOR problem is the coupled azimuthal potential (CAP) formulation, but the singularities that occur in the CAP formulation are difficult to evaluate properly. This difficulty does not arise in the mixed-element formulation. The singularities that do occur in the mixed-element formulation can be evaluated by applying the z -axis boundary condition. Both the higher-order vector basis functions (R.D. Graglia, D.R. Wilton, and A.F. Peterson, *IEEE Trans. on Antennas and Propagation*, 45, 329-342, 1997) and the higher-order scalar basis functions (J. Jin, *The Finite Element Method in Electromagnetics*, 123-130, 1993) are interpolatory. The mesh is terminated by a perfectly matched layer (PML). PML allows the mesh to be terminated at a reasonable distance from the scatterer by reducing the amplitude of the reflections due to mesh truncation.

A number of examples computed using the higher-order basis functions are given for various BORs. The validity of the code will be shown by comparing the data against the Mie series and moment-method solutions.

A Study of Webb's Hierarchical Vector Shape Functions for FEM Solution of Electromagnetic Scattering Problems

Tahar Ezzedine*, Ammar B. Kouki,
Ecole de Technologie supérieure
1100, rue Notre-Dame Ouest
Montréal, Québec, H3C 1K3, Canada

and

Ahmed Khebir
ElectroMagneticWorks Inc.
5115 Trans Island Avenue, Suite 239
Montréal, Québec, H3W 2Z9, Canada

The finite-element method (FEM) is well suited to solve complicated electromagnetic (EM) problems. The recent introduction of the hierarchical tangential vector shape functions for tetrahedral elements has made the FEM even more suitable and attractive since they can be used for p -adaption (J. Webb, IEEE Trans. Antennas Propagat., vol. 47, No. 8, August 1999), (L. Andersen and J. Volakis, IEEE Trans. Antennas Propagat., vol. 47, No. 8, August 1999). Experience with nodal FEM for the solution of the scalar wave equation has led many researchers to believe that p -adaption is computationally very efficient. Examining the two publications, one realizes that even though the concept of hierarchy is the same, the shape functions suggested by Webb are quite different from the ones employed by Andersen *et al.* In this work, we intend to examine Webb's functions and study their use for EM scattering problems.

Webb's functions are of arbitrary order and provide separate representation of the gradient and rotational parts of the vector field, which introduces two orders for the high-order elements. As mentioned by Webb, the choice of these orders is not obvious and is problem dependent. This ambiguity comes from the fact that in vector EM, the curl of the field is often as important as the field itself. The question that remains open is whether to choose the same order p for both the gradient and rotational parts of the shape function. In this work, we will answer this question for EM scattering applications and report on our findings on related issues such as the dependence on the frequency, the angles of incidence, and the shape of the scatterer. We will also look at the effect of the mesh truncation using both the Absorbing Boundary Condition (ABC) and the Perfectly Matched Layer (PML) techniques in conjunction with these hierarchical vector shape functions.

A study of hierarchical shape functions or a use of an adaptive FEM requires the computation of a *posteriori* error estimator. Such error index is a measure of the accuracy of the FEM solution for a given mesh size or p -order of the shape functions. We derived an error functional appropriate for scattering problems that take into accounts both the volume and surface errors due the FEM discretization.

Parallel Implementation of a Hybrid Finite-element, Finite-volume, and Finite-difference Transient Electromagnetic Simulation¹

Joseph D. Kotulski*, Douglas J. Riley, and C. David Turner
Electromagnetics and Plasma Physics Analysis Department
Sandia National Laboratories
Albuquerque, NM 87185-1152

A transient solution of a general three-dimensional problem can be approached in a number of different manners. These include finite elements, finite volume, finite differences or combinations of either of these methods. For the finite-element formulation edge-based elements are normally used and the solution is implicit. This results in a matrix that is solved at each time step whose solution is fairly efficient by the use of conjugate-gradient methods.

Finite-volume methods can be considered to be a generalization of the straightforward finite-difference time-domain method. These methods introduce offset, or dual grids to perform the calculation for the field advancement. These algorithms are attractive because they are explicit and can be generalized to arbitrary cell types. Unfortunately the algorithm appears to be unstable for late times for cells other than hexahedral elements and stabilization schemes have been proposed and applied to circumvent this issue.

The next level of complexity would hybridize the finite-volume with finite-difference and finite-element techniques. These hybrid methods promise high accuracy and efficiency. The stability of this hybrid approach has and is being examined by a number of investigators.

The purpose of this presentation is to show a parallel implementation for this hybrid approach. The problem of interest contains an unstructured geometry that may be solved by finite-volume or finite-element approach. To solve this in parallel the mesh describing the unstructured region has to be decomposed and mapped to the available processors. Then appropriate communication maps have to be constructed. In addition, this geometry is embedded in a structured region. This region also has to be decomposed and appropriate communication maps constructed together with the interface between the two regions.

The strategy to accomplish the parallelization will be described and discussed. In addition the parallel efficiency will be presented for a number of processors and processor distributions.

¹Sandia is a multiprogram laboratory operated by Sandia Corporation, a Lockheed Martin Company for the United States Department of Energy under Contract No. DE-AC04-94AL85000.

DOMAIN DECOMPOSITION METHOD FOR THE COMPUTATION OF SCATTERING BY INHOMOGENEOUS PENETRABLE 3D OBJECTS

Bruno Stupfel

CEA/CESTA, Commissariat à l'Énergie Atomique, B.P. 2, 33114 Le Barp, France

The finite element method (FEM) is a powerful numerical technique for solving scattering problems involving inhomogeneous penetrable 3D objects. For open region problems, the radiation condition may be rigorously taken into account by prescribing an integral equation (IE) on the outer surface of the object. The corresponding hybrid FE-IE method yields a linear system constituted, essentially, by a sparse FE matrix and a dense MoM matrix. The usual procedure is either to solve the whole system in one piece or, by eliminating the volume unknowns, to invert the FE matrix and solve as many FE systems as there are surface unknowns. When the total number of unknowns is large, both techniques are quite demanding in computer resources.

A possible way to reduce the numerical complexity of the problem is to employ a domain decomposition method (DDM): The large FE problem is decomposed into several subproblems that can be solved independently. The computational domain is partitioned into concentric subdomains circumscribing the object. The propagation of the waves is accounted for by a Robin-type transmission condition (TC) prescribed upon the interfaces between these subdomains. An IE is implemented on the outermost boundary, and it has been proposed recently [Stupfel & Després, *J. Electromag. Waves and Appl.*, vol. 13, pp. 1553-1568 (1999)] to consider the exterior infinite free-space as an additional subdomain, related to the inner ones by a TC. It has been demonstrated mathematically that the corresponding iterative DDM algorithm converges to the solution of the original scattering problem if the dielectric permittivity and magnetic permeability tensors, constitutive of the inhomogeneous region, satisfy standard stability conditions, i.e., correspond to passive materials. As a consequence, the FE and MoM systems are decoupled, and can be solved independently.

Numerical results are presented that illustrate some of the possibilities of this technique.

A study on the efficient FEM-based hybrid method for the open region problem and its applications to characterizing radiating slots in a broad wall of a rectangular waveguide

Jongkuk Park*, Heeduck Chae, and Sangwook Nam

School of Electrical Engineering, Seoul National University

The finite element method has been utilized as a powerful tool for characterizing arbitrary-shaped objects in a shielded structure. However, for open region problems, since the mesh of the computational domain cannot be extended to infinity, appropriate boundary condition must be applied or another action must be taken in order to simulate the effect of the infinite domain. As known widely, the implementations of FEM for radiation and scattering have been limited primarily to FEBIM and the method incorporating ABCs. However, since each method has some shortcomings, many other techniques have been developed. As one of these methods, the iterative hybrid method was proposed to solve electrostatic and TM 2D scattering problems in open space (T. Roy, T. K. Sarkar, A. R. Djordjevic and M. Salaza, *IEEE Trans. Microwave Theory Tech.*, 1996, **44**, (12), pp. 2145-2151), and applied to characterize discontinuities in a rectangular waveguide as an example of 3D problems (Jongkuk Park, Heeduck Chae, and Sangwook Nam, *Electronics Letters*, vol.35, no. 14, pp. 1170-1171, Jul. 1999.). In the above method, with a small number of meshes around the scatterer, FEM is applied on the assumption that all the boundary fields are given as the Dirichlet type. Once all the field-components are determined, equivalent electric or magnetic current source can be calculated using the equivalence theorem. From this calculated equivalent source, the scattered field can be computed with an appropriate Green's function, and the Dirichlet boundary condition is updated. Through the iteration of this procedure, the converged solution can be obtained. However, while this method has given a good and efficient result, it is found to be not suitable for characterizing the scattering a electrically-large object due to internal resonance-like phenomena. Therefore, in this paper, to eliminate this phenomena, the radiation type boundary condition is proposed instead of the Dirichlet boundary condition. In the far-field region, Sommerfeld radiation condition is satisfied as follows. $\hat{n} \times \nabla \times \vec{E} + j k_0 \hat{n} \times \hat{n} \times \vec{E} = 0$. However, in this method, since the mesh is terminated near the scatterer, the boundary is not placed in the far field region. Therefore Sommerfeld radiation condition is not valid and must be reconstructed as $\hat{n} \times \nabla \times \vec{E} + j k_0 \hat{n} \times \hat{n} \times \vec{E} = \vec{U}$. This mixed boundary condition means that the left side of Sommerfeld radiation condition does not vanish in the near field region. The key idea in the proposed method is based on the update of this residual term. As an example of applications of this method, we analyzed arbitrary-shaped slots with resonant length in a broad wall of a rectangular waveguide. To show the validity, the proposed method is compared with FEBIM and gives an efficient result in good agreement with FEBIM

Hybrid current-based formulation for modeling on board antennas

F. Obelleiro*, J. M. Taboada, and J. L. Rodríguez

Dpto. Tecnoloxías das Comunicacións. Universidade de Vigo
ETSE Telecomunicación. Campus Universitario s/n. 36200 Vigo, Spain
e-mail: obi@tsc.uvigo.es

Phone: +34 986 812120, Fax: +34 986 812116

The development of numerical methods in order to estimate the interactions between on board antennas and complex structures (ships, aircrafts, automobiles, etc.) is of great interest for the electromagnetic community. Since conventional Moment Method (MM) limits the size of the structure to be modeled, hybrid techniques combining MM with asymptotic techniques have been developed in recent years. It is worth mention current-based hybrid methods, that combine unknown currents (MM currents) for some regions with ansatz-surface-currents obtained from approximations such as Physical Optics (PO), Fock theory, etc. A great variety of current-based hybrid methods have been applied to scattering calculations; regarding to 3-D problems, the first contribution can be found in (C. S. Kim and Y. Rahmat-Samii, "Low profile antenna study using the physical optics hybrid method", *Proc. IEEE Int. Symp. APS. Meet.*, London, ON, Canada, 1991), where the MM was combined with PO in the so called physical optics hybrid method (POHM).

In this work, we present an efficient and accurate procedure based on a hybrid MM-PO formulation, to obtain the coupling between different antennas mounted in a complex platform, as well as their respective radiation patterns and other magnitudes of interest. The proposed hybrid method is related to previous solutions, although there are some fundamental differences, mainly with regard to its practical implementation, which allows the method to be applicable to larger electromagnetic problems. Otherwise, the presence of more complex structures (containing edges, vertex, etc.), in which PO cannot provide an accurate result, is considered by including them into the MM region instead of performing an iterative solution for the MFIE (R. E. Hodges and Y. Rahmat-Samii, "An iterative current-based hybrid method for complex structures", *IEEE TAP*, **45**, 265-276, 1997) or using ansatz solutions for them (U. Jakobus and F. M. Landstorfer, "Improved PO-MM hybrid formulation for scattering from three-dimensional perfectly conducting bodies of arbitrary shape", *IEEE TAP*, **43**, 162-169, 1995). Some results will be shown to illustrate the capabilities of the proposed method.

Scattering from 3D cavities with the Scheme FACTOPO
The effects of PO processus on the S matrix of the exterior domain

Valérie Bazin*, Gérard Bobillot, André Barka, Paul Soudais, S. Langlet

Office National d'Etudes et de Recherches Aéronautiques
BP 72, 29 avenue de la Division Leclerc 92322 Chatillon CEDEX FRANCE
v.bazin@onera.fr, bobillot@onera.fr, barka@onera.fr, soudais@onera.fr

Increasing needs in knowing scattering mechanisms have made necessary the development of numerical software based on modelization of Maxwell's equations. Different techniques can be used such as FEM (Finite Element Method), FDTD (Finite Difference Time Domain), FMM (Fast Multipole Method) ... The study of the radar cross section (RCS) of a complex engine requires dealing with a complicated geometry and an accurate modelization. Hybrid Techniques that couple different methods are often used.

A multi-domain and multi-method coupling scheme called FACTOPO has been developed at ONERA. It is based on generalized scattering matrix computations on three dimensionnal subdomains. The global target is split in several subdomains, separated by fictitious surfaces, called interfaces. On the interfaces, a modal representation of the tangent field is used. Each subdomain is characterized by its Scattering matrix S , which is computed by any well suited numerical method (e.g. EFIE ...). The subdomains are connected by cascading the different S matrices.

This strategy reduces significantly the computational time compared to traditional hybrid methods for which a geometric or electromagnetic modification requires a new computation of the global object. In the paper (*A. Barka, P. Soudais, D. Volpert: Scattering from 3-D cavities with a Plug and Play Scheme Combining IE, PDE, and Modal Techniques (submitted to IEEE-AP)*), all S matrices are computed with different methods such as the three-dimensional FEM or the Electric Field Integration Equation (EFIE) combined with a efficient representation of the fields on the interfaces.

For high frequency domain, the computation of S_0 , the S matrix of the exterior volume (e.g. the complementary of the volume which involves the whole target) can be a problem for the FEM.

The paper will first discuss the computation of the S matrix S_0 with Physical Optics (PO) and the differences between S_0 , computed by FEM and by PO. Next, a comparison of responses of different cavities computed by the FACTOPO scheme using FEM for all subdomains and PO for the exterior volume is done. The limitations of the asymptotic hypotheses are given.

On the Use of Spatiotemporal Wavelet Expansions in Method of Moments Solutions for Time-Domain Integral Equations

Y. Shifman* and Y. Leviatan
Department of Electrical Engineering
Technion — Israel Institute of Technology
Haifa 32000, Israel
E-mail: shifman@iee.org

Numerical time-domain solutions for scattering of electromagnetic waves are essential for wide-band scattering problems, where frequency-domain analysis is expectedly inefficient. Commonly used time-domain methods such as the FDTD resort to solving the Time-Domain Differential Equation (TDDE), which is generally simpler than its counter part, the Time-Domain Integral Equation (TDIE). However, the TDDE may require the discretization of the entire domain under investigation and special care must be taken to comply with the radiation condition, while the TDIE is defined on a spatial domain of finite extent and has a built-in radiation condition in its Green's function. Conventional solution techniques for the TDIE employ the method of moments to reduce it to a matrix equation. Often an explicit discretization of the spatiotemporal domain, i.e., keeping the distance between two adjacent space samples larger than the distance traveled by the wave during the corresponding time step, is considered. In turn, a marching-on in time scheme is employed to sequentially solve the equation at each time step. While this method enables solving the TDIE virtually without any matrix inversion, it introduces inherent numerical instability. Moreover, the sequential solution technique requires passing through all intermediate time steps until the desired time step is reached.

The new approach presented here is to construct the implicit formulation of the TDIE using spatiotemporal wavelet expansion functions, and then solve it simultaneously at all the time steps within the time frame of interest. The implicit formulation allows the use of an increased spatial sampling rate while ensuring numerical stability. However, since the resultant matrix equation is usually very large, it is not solved directly. Instead, an iterative procedure is used, in which the set of spatiotemporal wavelet expansion functions is systematically increased until the desired level of fulfilling the TDIE operator equation is reached. In this manner, the unknown is determined by solving a series of smaller matrix equations whose solution altogether requires much less computational effort than the solution of the original matrix equation. Furthermore, since the implementation of these expansion functions is carried out via an efficient transformation algorithm, computational complexity is even further reduced.

The method is applied to a one-dimensional problem of electromagnetic plane wave interaction with a dielectric slab. A comparison of the computed results with results based on the analytic solution demonstrates the merits of this new method.

Electronics and Photonics

Chair: P. Savi, Politecnico di Torino, Italy

			Page
1	12:00	A novel integrated pulse generator and balun, <i>J-S. Lee*</i> , <i>C. Nguyen</i> , <i>Texas A&M University, USA</i>	268
2	12:00	A generic, low cost, compact FM/CW transmitter, <i>R. Smith*</i> , <i>D. Arnold</i> , <i>Brigham Young University, USA</i>	269
3	12:00	Cylindrical FDTD with uniaxial PML for modeling vertical-cavity surface-emitting lasers, <i>T. Lee*</i> , <i>S. Hagness</i> , <i>University of Wisconsin, Madison, USA</i>	270
4	12:00	Order reduction of electromagnetic circuit elements based on FIT discretization, <i>T. Wittig*</i> , <i>Darmstadt University of Technology, Germany</i> , <i>I. Munteanu</i> , <i>D. Ioan</i> , <i>Politehnica University of Bucharest, Romania</i> , <i>T. Weiland</i> , <i>Darmstadt University of Technology, Germany</i>	271
5	12:00	Characterization of a frequency doubler circuit using an FEM based method, <i>E. Yasan*</i> , <i>L. Katehi</i> , <i>The University of Michigan, USA</i>	272
6	12:00	A planar circuit design for suppressing the parasitic resonances in a packaged microstrip circuit, <i>H-H. Chen*</i> , <i>C-L. Weng</i> , <i>Huafan University, Taipei</i> , <i>S-J. Chung</i> , <i>National Chiao Tung University, Hsinchu</i>	273
7	12:00	Fabrication of polymer and elastomer-based photonic bandgap structures, <i>J. Schultz*</i> , <i>J. Maloney</i> , <i>M. Kesler</i> , <i>Georgia Tech Research Institute</i> , <i>J. Colton</i> , <i>Georgia Institute of Technology, USA</i>	274
8	12:00	Dielectric properties of a high-resistivity silicon wafer and its application to an optically tunable microwave attenuator, <i>S. Lee*</i> , <i>Y. Kuga</i> , <i>University of Washington</i> , <i>R. Mullen</i> , <i>Nextlink, USA</i>	275
9	12:00	A FEM high-order model for the analysis of LiNbO3 electro-optic modulators, <i>P. Savi*</i> , <i>Politecnico di Torino, Italy</i> , <i>I. Gheorma</i> , <i>Columbia University, USA</i> , <i>R. Graglia</i> , <i>G. Ghione</i> , <i>Politecnico di Torino, Italy</i>	276
10	12:00	Simple simulation of the Gunn effect with the FDTD method, <i>T. Hruskovec*</i> , <i>Dalhousie University, Canada</i> , <i>Z. Chen</i> , <i>The Hong Kong University of Science and Technology, Hong Kong</i>	AP
11	12:00	Open three-mirror systems investigation in the millimeter-wave band, <i>D. Afonin*</i> , <i>Y. Issaev</i> , <i>A. Malyshkin</i> , <i>Moscow State University, Russia</i>	277
12	12:00	A new investigation on low noise amplifiers for W-CDMA applications, <i>T. Denidni*</i> , <i>University of Quebec at Rimouski</i> , <i>F. Ghanem</i> , <i>INRS-Telecommunications</i> , <i>N. Hassaine</i> , <i>Harris Corporation, Canada</i>	AP
13	12:00	An FD/FDTD method for optical waveguide modeling, <i>J. Wallace*</i> , <i>M. Jensen</i> , <i>Brigham Young University, USA</i>	AP

A NOVEL INTEGRATED PULSE GENERATOR AND BALUN

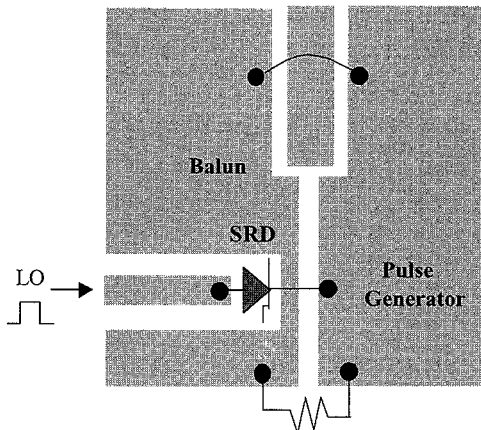
Jeong-Soo Lee* and Cam Nguyen

Department of Electrical Engineering
Texas A&M University
College Station, Texas 77843-3128
E-mail: cam@ee.tamu.edu

ABSTRACT

Integrated pulse generator and balun is a special microwave circuit that simultaneously provides both functions of generating a pulse and dividing it into two pulses of equal amplitude and 180-degree out-of-phase. This circuit is needed for various uses; for instance, a sampling down-converter in impulse radar. An integrated pulse generator and balun completely realized using uniplanar transmission lines are highly desirable because of ease in mounting solid-state devices, elimination of via holes, and requirement of only one-sided circuit processing, all leading to circuit simplicity and low cost.

In this paper, we report the study of a novel integrated pulse generator and balun utilizing step-recovery diode (SRD), coplanar waveguide, and slot line. The circuit is shown below, and is very simple and completely uniplanar, making it ideal for low-cost time-domain microwave applications. Our results show that the output pulses resemble closely the input pulse with reduced amplitudes and are 180-degree out-of-phase with respect to each other. Analysis, design, and performance of this circuit will be presented.



A Generic, Low Cost, Compact FM/CW Transmitter

*Ryan L. Smith, Microwave Earth Remote Sensing, Brigham Young University
David V. Arnold, Microwave Earth Remote Sensing, Brigham Young University

A generic, low cost, compact FM/CW transmitter has been developed for use from 2 to 18 GHz with a transmit bandwidth of up to 1 GHz. This generic design is currently being used in a railway hazard detection system, a synthetic aperture radar, a scatterometer, and an altimeter.

Capitalizing on the functionality and low cost of wireless communication parts, an inexpensive broad band linear frequency generator was developed which is extremely small in size and lightweight. This design incorporates the functionality of a microcontroller's counter to measure the frequency at a given voltage and thus calibrate a digital waveform to drive a VCO with linear frequency modulation. The microcontroller communicates with a host using a RS232 serial port, enabling the user to set parameters such as center frequency, bandwidth and repetition count. A trigger is outputted to synchronize receiver A/D conversions with the transmitted signal. Tests show the transmitter waveform has low deviation from linearity and level output power over the entire band.

This project was supported with funding from the Canadian National Railway and NASA.

Cylindrical FDTD with Uniaxial PML for Modeling Vertical-Cavity Surface-Emitting Lasers

Tae-Woo Lee* and Susan C. Hagness

Department of Electrical and Computer Engineering
University of Wisconsin, Madison, WI 53706-1691
tae-woo@cae.wisc.edu, hagness@engr.wisc.edu

For many optical communications and signal processing applications, high-power single-transverse-mode operation is desired in vertical-cavity surface-emitting lasers (VCSELs). Full-vector electromagnetics models, such as cylindrical-coordinate FDTD schemes, are needed to fully understand the complex nature of transverse-mode competition and polarization effects in VCSELs. For this purpose, we have developed an axially symmetric FDTD solver with uniaxial perfectly-matched-layer (UPML) boundary conditions that have recently been extended to cylindrical coordinates.

Many rigorous studies of the effectiveness of PML formulations in Cartesian coordinates have been conducted. Fewer studies have been done for UPML in cylindrical coordinates. In this paper, we present a rigorous global error analysis of the UPML performance in the radial direction of the axisymmetric FDTD grid. For the global error analysis, two FDTD grids are constructed, each of identical size in the z -direction: a test domain with the UPML treating the radial boundary and a benchmark domain which has a much larger radial size to mimic a domain of infinite extent. In each domain, the grid is terminated in the z -direction with PEC boundary conditions. Calculating the discrepancy between the FDTD solutions over the area common to both domains provides a measure of the spurious reflection caused by the UPML in the test domain.

Performance of the UPML is tested for vacuum, lossless dielectric, and lossy dielectric computational domains. Here, P is the physical length of the computational domain in the radial direction, d is the physical thickness of the UPML region, and Δr is the grid cell size. For vacuum, the UPML is investigated for three cases: 1) variable P , fixed d and Δr ; 2) variable d , fixed P and Δr ; 3) variable Δr , fixed P and d . For the lossless and lossy dielectric cases, UPML performance is compared to the vacuum case. The following polynomial grading for the UPML conductivity profile is used:

$$\sigma(r) = \sigma_{\max} \left(\frac{r}{d} \right)^m = -A \frac{(m+1) \ln(R)}{2\eta\epsilon_0 d} \left(\frac{r}{d} \right)^m$$

where $R = 10^{-5}$. Numerical experiments are required to determine the optimum choices for A and m . These parameters are chosen to minimize the global error.

Our analysis reveals that the optimum choice of parameters A and m are independent of the dielectric properties of the material(s) being simulated. For a UPML thickness of 10 to 20 cells and a reasonably fine grid resolution (10 to 20 points per smallest wavelength of interest), the optimum values of A and m are 1.25 and 3 respectively. Under these conditions, the normalized global error energy is on the order of 10^{-11} .

We are currently using the resulting FDTD-UPML algorithm to explore methods for achieving transverse-mode control in VCSELs.

Order Reduction of Electromagnetic Circuit Elements Based on FIT Discretization

T. Wittig^{1*}, I. Munteanu², D. Ioan², T. Weiland¹

¹ Darmstadt University of Technology, Germany, Theorie Elektromagnetischer Felder

² „Politehnica“ University of Bucharest, Romania, Electrical Engineering Department

Many approaches to solve electromagnetic field – electric circuit coupled problems were proposed over the last few years. The extraction of circuit parameters seems to be the most general and efficient technique to handle this task. The final solution of the coupled problem is thus obtained by connecting the equivalent circuit to the external one and by using a standard circuit simulator. This abstract presents a technique to generate the circuit parameters of a general electromagnetic device starting from a field equation formulation with certain boundary conditions, but without the need to actually solve the field problem.

The electromagnetic device is considered as a simply connected spatial domain with linear and time-invariant material parameters. A field representation of the device is obtained by discretization of the Maxwell's equations with the Finite Integration Technique (FIT) (T. Weiland, *Int. J. Num. Modelling*, 9, 295-319, 1996). These equations are derived in a matrix form, that is similar to the Modified Nodal Analysis formulation known from circuit theory.

In order to ensure the proper definition of electric terminals on the device's surface the Electromagnetic Circuit Element (ECE) boundary conditions (F. Hantila, D. Ioan, 6th *Int. IGTE Symp.*, Graz, Austria, 41-46, 1994) have to be applied to the system. They enforce the equipotentiality on each terminal, the magnetic decoupling and the total current flow through terminals only. These boundary conditions are imposed by constructing, on the domain's boundary, a tree for the electric and a dual tree for the magnetic fields. The final presentation will contain the description of the technique used to handle boundary trees and cotrees in the general n-port case, considering both voltage and current excitation. The total elimination process and the consideration of the terminal excitation is realized in a linear transformation. The system matrices are reformulated to get the well-known state-space form, which is finally reduced in order using the Padé Via Lanczos (PVL) method (M. Celik, C. Cangellaris, *IEEE Trans. Microwave Theory Tech.*, 44, 2525-2535, 1996).

For the purpose of algorithm validation a shielded T-shaped microstrip filter was analyzed. The dimensions are 10 x 14 x 6.5 mm, ϵ_r equals 10. The dimension of the initial state-space vector is 496. A Gaussian impulse was used as excitation current.

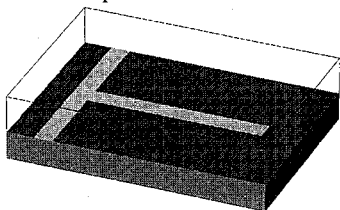


Fig. 1. Microstrip filter

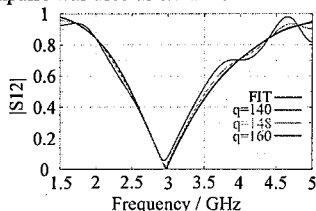


Fig. 2. Scattering parameter S_{12}

The time and frequency response of the system of order 160 is practically indistinguishable from the initial one, while the simulation time is a factor 12 faster.

Characterization of a Frequency Doubler Circuit Using an FEM Based Method

Eray Yasan* and Linda P. Katehi
Radiation Laboratory

Dept. of Electrical Engineering and Computer Sci.

The University of Michigan, Ann Arbor, MI 48109-2122, U.S.A.

Tel: 734-764-0502, Fax: 734-747-2106, Email: eray@engin.umich.edu

Finite Ground Coplanar (FGC) lines have found a wider application area recently due to their better performances over microstrip lines and Coplanar Waveguides (CPW). Since FGC line has narrower ground planes preventing parallel plate modes from propagating, it supports a TEM-like mode without a backside metallization. Also due to the minimal change in dielectric constant over a wide range of frequencies and scalability to higher frequencies have made FGC lines popular for frequency multiplier and mixer designs.

The circuit analyzed in this study is a W-Band doubler on a FGC line.

The linear passive part of the circuit is analyzed using the Finite Element Method (FEM). The circuit is treated as the collection of internal ports where the nonlinear elements are connected and the external ports where the input and output quantities of the circuit are calculated. Due to the difficulty of exciting the inner ports separately, combinations of open and short circuit terminations are used along with the excitement of external ports in order to derive the appropriate voltages and currents at all ports. The linear part of the circuit is characterized by the admittance parameters (Y- matrix). The difficulty of not having a well defined ground plane is accounted by treating the existing finite width ground planes separately and combining their effects through additional set of circuit parameters. Analysis has been carried out to account for the two modes of operation of FGC lines, namely slotline mode and coplanar waveguide mode. After characterization of the linear passive part of the circuit in terms of circuit parameters, the nonlinear elements are introduced to the internal ports along with their corresponding device characteristics using a software simulation package. A nonlinear analysis such as Harmonic Balance Method (HBM) gives the overall circuit performance.

The output parameters such as efficiency, return loss, output power vs. input power are given and compared with the experimental results for the GaAs 40-80 GHz frequency doubler under study. Results from this study will be presented and discussed in detail.

A Planar Circuit Design for Suppressing the Parasitic Resonances in a Packaged Microstrip Circuit

Hao-Hui Chen* and Ching-Liang Weng
 Dept. of Electric Eng., Huaan Univ.
 Taipei, Taiwan, R.O.C.

Shyh-Jong Chung
 Dept. of Communication Eng., Nat'l Chiao Tung Univ.
 Hsinchu, Taiwan, R.O.C.

In a packaged microware circuit, significant degradation of the circuit performance caused by the resonances of the enclosure have been found. Suitable approaches should be adopted to reduce these parasitic resonance effects. For a packaged microstrip circuit, it has been shown that the package resonances are due to the high quality resonator behavior of the metallic enclosure for the 2nd-order mode of the packaged microstrip (H.-H. Chen and S.-J. Chung, *IEEE MTT*, 46, 2124-2130, 1998). The package resonances can thus be suppressed by destroying the fields of the 2nd-order mode. In this paper, we propose a planar circuit design for suppressing the package resonances in a packaged microstrip circuit. Fig.1 shows this circuit design, where a packaged circuit element (CE), which may excite the 2nd-order mode and result in the package resonances, is designed to be located between two pairs of side metal patches. The side patches, after being designed appropriately, would substantially deform the field distributions of the 2nd-order mode (H.-H. Chen, C.-L. Wang and S.-J. Chung, *IEEE MTT*, 46, 2156-2159, 1998). The parasitic resonances can be then suppressed by these side patches.

To demonstrate the suppression effects of the side patches, the CE is represented by a microstrip bandpass filter, and the analyses are performed using the commercial software *em* by SONNET (Sonnet Software, Inc., Liverpool, NY.) in this paper. The microstrip having a width $w=0.635mm$ is fabricated on the substrate with dielectric constant $\epsilon_r=9.7$ and thickness $h=0.635mm$. The bandpass filter is designed with three end-coupling sections, a center frequency of 23.21GHz, and a bandwidth of 2%. The transmission characteristics (S_{21}) of the filter operated under the normal state (that is, the circuit without being affected by the package resonances) are illustrated by the solid line in Fig.2. When the circuit is enclosed in a metal package of the dimensions $6.35 \times 2.54 \times 22.1 mm^3$, substantial interferences caused by the package resonance on the circuit can be observed in Fig.2. (It has been found that a package resonance would occur at 23.25 GHz in such a package.) The performance of the filter is significantly disturbed and is displayed by the broken line in Fig.2. The undesirable interaction between the circuit and the package resonance can be suppressed by placing two pairs of side metal patches at suitable positions in the package. The sizes of the patches, after being carefully designed, are chosen to be $w_p \times l_p = 0.988 \times 2.34 mm^2$. The dotted line in Fig.2 depicts the transmission of the filter enclosed in such a package. Comparing the dotted line and the solid one, it is seen that the parasitic resonance effect is greatly suppressed and, thus, the circuit performance is almost resumed.

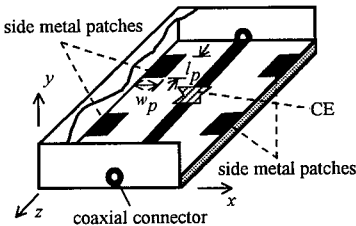


Fig. 1. A package with two pairs of side metal patches.

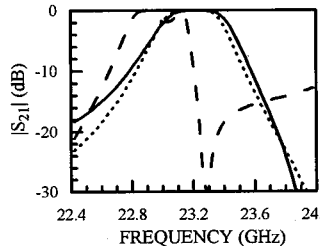


Fig. 2. Transmission characteristics of the packaged bandpass filters.

FABRICATION OF POLYMER AND ELASTOMER-BASED PHOTONIC BANDGAP STRUCTURES

John W. Schultz*, James G. Maloney, Morris P. Kesler
Georgia Tech Research Institute, Atlanta, Georgia 30332

Jonathan S. Colton
School of Mechanical Engineering
Georgia Institute of Technology, Atlanta, Georgia 30332

Three-dimensional periodic structures of two-phase materials with high dielectric contrast may be assembled as photonic bandgap (PBG) structures. These structures exhibit frequency regions in which electromagnetic propagation is prohibited, which provide electromagnetic characteristics that can be exploited as filters, waveguides, resonators, and antenna substrates. To date, methods for constructing microwave and millimeter wave PBG structures have been limited to expensive, time-consuming techniques such as machining, drilling, and stacking. Solid freeform fabrication techniques, such as stereolithography, have been proposed (Shepherd et al., *Electronics Lett.*, 34, 787-789, 1998), but they are limited in the availability of appropriate materials and are not appropriate for mass production quantities.

In this research, a low-cost, high-quantity manufacturing technique is described for fabricating PBG structures for microwave and millimeter-wave applications. The technique combines ceramic filled polymer resins with liquid molding techniques to create 3-D PBG crystals. High dielectric fillers enable the polymer mixtures to have permittivities approaching 10 with low fill fractions (20 vol%). This provides more than sufficient dielectric contrast to achieve bandgaps. Because of the low fill fraction, elastomer resins have been used to manufacture mechanically flexible PBG structures. Flexibility opens possible new applications in bendable groundplanes and conformal antennas. Prototype structures were manufactured with the 'woodpile' structure and with electromagnetic bandgaps in the 8-12 GHz frequency region.

Measured data and model calculations are presented. Measurements were made with a free-space, focused beam system and demonstrate the viability of the manufactured structures. Numerical results were predicted with FDTD models (Maloney et al., *Proc. USNC/URSI Mtg.*, June 1995) and predictions agree with measurement. FDTD modeling also was used to study the effects of moderate loss (e.g., some of the formulations had moderate loss: $\tan \delta \sim 0.04$). Moderate loss has negligible effect on reflection within the bandgap (8-12 GHz), but results in substantial absorption outside of the bandgap. Finally, the expected effects of curvature and imperfections (i.e., due to manufacturing tolerances) are presented.

DIELECTRIC PROPERTIES OF A HIGH-RESISTIVITY SILICON WAFER AND ITS APPLICATION TO AN OPTICALLY TUNABLE MICROWAVE ATTENUATOR

Sangil Lee* and Yasuo Kuga
Department of Electrical Engineering
University of Washington
Seattle, WA 98195-2500

Ruth Ann Mullen
Nextlink
500 108th Ave. NE, Suite 2200
Bellevue, WA 98004

The dielectric constants of a high-resistivity silicon wafer are measured with and without optical excitation in both the microwave range from 14 GHz to 40 GHz and the millimeter wave range from 75 GHz to 110 GHz. When a silicon wafer is excited by a laser, a large amount of free electrons are created and changes occur in the effective bulk dielectric constant of the silicon wafer. Thus, the optically excited silicon wafer shows a substantial increase in both the real and imaginary parts of the dielectric constant, which is consistent with that of a lossy dielectric material. The free-space dielectric constant measurement technique is applied, and genetic algorithms are used for the inversion process. An argon (Ar) laser is used for excitation and the complex dielectric constants are measured up to 40A excitation, which corresponds to 3.6W. For flexible applications, side areas of a silicon wafer are excited, and the results will be presented.

The dielectric constant changes due to the laser excitation can be exploited to create an optically tunable structure. Layered structures are commonly used as microwave frequency selective surfaces. However, these structures usually have fixed transmission characteristics, and it is difficult to control the pass- and stop-band responses without changing the physical spacing or surface patterns. In this paper, we present an optically reconfigurable attenuator using multi-layered structures. A two-layered structure, silicon with optical excitation, air between, and silicon without excitation is considered. The transmission characteristics of layered structures are calculated based on the estimated dielectric constants and measured. Both simulated and measured results show similar attenuation characteristics. The laser excitation of the layered structure leads to the change of the pass- and stop-band frequencies. To obtain sharper and better stop-band responses, layered structures having more than two layers are also suggested. The simulation results show substantial improvements of pass- and stop-band responses with the addition of an extra layer. The transmission characteristics are optimized by adjusting the separation and thickness of the layers.

A FEM High-Order Model for the Analysis of LiNbO₃ Electro-optic Modulators

P. Savi*, I-L. Gheorma[†], R.D. Graglia, G. Ghione

Politecnico di Torino, Dipartimento di Elettronica
Corso Duca degli Abruzzi 24, 10129 Torino, Italia
Tel: +39-011-5644074, Fax: +39-011-5644015, e-mail: savi@polito.it
+ Microelectronic Sciences Laboratory
Columbia University, New York, NY, email: isg12@columbia.edu

Electro-optic modulation is achieved by the synchronous coupling of an optical signal with the RF signal. An electro-optic modulator on LiNbO₃ substrate has the shape of a coplanar waveguide with the optical signal travelling in a diffused waveguide. The microwave effective refractive index is lowered by inserting low-epsilon buffer layers underneath the electrodes and by increasing the metallization thickness through electroplating up to 30 μ m. The line-to-ground spacing must be kept low (e.g. 10 μ m) in order to optimize the overlap between the microwave and optical fields. Hence, the resulting structures show unusual shape ratios for the center conductor and due to the very small gap width, such lines tend to exhibit high losses.

Among the most suitable methods (mode matching technique, the method of lines, the finite element method, the spectral domain approach and the integral equation method) to model waveguides of complex cross-section and to keep into account conductor and dielectric losses, anisotropies of both electric and magnetic kind, the Finite Element Method (FEM) is the most generally applicable and the most versatile. We provide a general FEM formulation of the lossy, anisotropic waveguide problem where the discretization is obtained by using higher-order interpolatory functions. In particular, the transversal components of the electric field E are modeled by interpolatory higher-order vector curl-conforming elements (R.D. Graglia et al., IEEE Trans. AP, 45, 329-342, 1997), whereas the longitudinal component E_z is modeled by higher-order nodal elements.

When the conductor thickness is comparable to the skin depth, the customary skin-effect approximation, based on an equivalent surface impedance, fails to provide meaningful results. In this case the finite thickness and the finite conductivity of the metallic regions should be exactly accounted for in the line modelling. Hence, the metallic regions of finite conductivity are discretized and the field in these regions is computed. This allows a precise evaluation of the loss phenomena at the expenses of introducing a higher number of unknowns; use of high-order elements permits to reduce the number of unknowns. Several results will be shown at the conference and compared with measured results, and the advantages of using high-order model will be discussed.

OPEN THREE-MIRROR SYSTEMS INVESTIGATION IN THE MILLIMETER-WAVE BAND

Afonin D.G., Issaev Yu.A., Malyshkin A.K.

119899, Vorob'evy Gory, Moscow State University,
Physics Faculty
(phone: (095)939-2094, e-mail: afonin@radi1.phys.msu.su)

One of the widely used and perspective electrodynamic elements in millimeter-wave band are the open resonance systems (ORS), the investigations of different modifications of which is a undoubted interest.

In this paper the subjects of investigations were the open 3-mirror system with mirrors of different shape.

The case of three-mirror ORS, consisted of plane (flat or with the metal lattice) mirror and 2 spherical mirrors, was considered. The connection with outer waveguide systems were made using the small circle holes in mirrors; so ORS was exited by means of such hole with the help of the outer generator, and through the analogous hole in the exit mirror the the signal entered the analyzing device. The falling angles, at which the system is exited, were defined; the spectra were obtained and the Q-factor values were calculated. The Q-factor values reached 10^3 - 10^4 . The simple theoretical calculation was made for such system spectrum and the satisfactory coincidence with the experiment was obtained. It is showed that the Q-factor increase take place in case of putting a small structure lattice on the flat mirror.

Also the system where spherical mirrors were replaced by cylinder ones was considered, and cases of different curvature were studied. The spectrum was obtained and Q-factor values were calculated for such system.

In our work an automated setup for electrodynamic characteristics investigations of ORS in frequency region 53-78 Ghz (D.G.Afonin, A.É.Malyshkin, *Pribori i tekhnika eksperimenta*, N3, p.81-85, 1999). The automated setup allows to obtain graphs of the transmission coefficient dependencies on frequency and on distance between ORS mirrors. Investigations of the resonance curves allows to obtain Q-factor values about 10^3 with the error less than 15%.

A Century of Progress at the Dawn of a New Millennium (II)
Sponsored by MotorolaOrganizers and Chairs: Robert E. Collin, Case Western Reserve University
Yahya Rahmat-Samii, UCLA

			Page
	1:45	Opening remarks	
1	1:50	Antenna Measurements -- A Historical Perspective, <i>S. Gillespie, CSUN, USA</i>	AP
2	2:10	Modern Near Field and Diagnostic Antenna Measurements, <i>G. Hindman, Nearfield, System Inc., USA</i>	AP
3	2:30	Radio Wave Propagation- 20th Century Highlights, <i>R. Collin, Case Western Reserve University, USA</i>	AP
4	2:50	Statistical Electromagnetic Propagation and Scattering in Random Media and Rough Surfaces, <i>A. Ishimaru, University of Washington, USA</i>	AP
5	3:10	Application of Diffraction Theory to Wireless Propagation problems, <i>H. Bertoni, Polytechnic University of New York, USA</i>	AP
	3:30	Break	
6	3:50	Analytical Techniques in Scattering, <i>T. B.A. Senior, University of Michigan, USA</i>	AP
7	4:10	High Frequency Diffraction, Focus on Ray Methods, <i>R. G. Kouyoumjian and P. H. Pathak, The Ohio State University, USA</i>	AP
8	4:30	The Method of Moments—A Personal Review, <i>R. F. Harrington, University of Arizona, USA</i>	AP
9	4:50	FDTD—How Complex a Problem Can We Solve? <i>A. Taflov, Northwestern University, M. Picket-May, University of Colorado, S. C. Hagness, University of Wisconsin, USA</i>	AP
10	5:10	Computational Electromagnetics at the Turn of the Millennium, <i>W. C. Chew, University of Illinois, USA</i>	AP
11	5:30	Concluding Remarks and Discussions	

Fractal Antennas

Co-chairs: J. Romeu, Universitat Politècnica de Catalunya, Spain
D. Werner, Pennsylvania State University Page

- 1 1:50 Fractal element antennas: a compilation of configurations with novel characteristics, *J. Gianvittorio**, *Y. Rahmat-Samii*, University of California, Los Angeles, USA AP
- 2 2:10 A design approach for dual-polarized multiband frequency selective surfaces using fractal elements, *D. Werner**, *D. Lee*, The Pennsylvania State University, USA AP
- 3 2:30 High directivity modes in the Koch island fractal patch antenna, *J. Romeu**, *C. Borja*, *S. Blanch*, Universitat Politècnica de Catalunya, Spain AP
- 4 2:50 Miniature wideband stacked microstrip patch antenna based on the Sierpinski fractal geometry, *J. Anguera**, *C. Puente*, Fractus S.A., *C. Borja*, *J. Romeu*, Universitat Politècnica de Catalunya, Spain AP
- 5 3:10 Fractal elements in array antennas: investigating reduced mutual coupling and tighter packing, *J. Gianvittorio**, *Y. Rahmat-Samii*, University of California, Los Angeles, USA AP
- 3:30 Break
- 6 3:50 Multiband Sierpinski fractal patch antenna, *C. Borja**, *J. Romeu*, Universitat Politècnica de Catalunya, Spain AP
- 7 4:10 Dual-band Sierpinski fractal monopole antenna, *J. Soler**, *J. Romeu*, Universitat Politècnica de Catalunya (UPC), Spain AP
- 8 4:30 A generalized fractal radiation pattern synthesis technique for the design of multiband and broadband arrays, *D. Werner**, *M. Gingrich*, *P. Werner*, The Pennsylvania State University, USA 281
- 9 4:50 A simplified Koch multiband fractal array using windowing and quantization techniques, *S. El-Khany*, Alexandria University, *M. Aboul-Dahab*, Arab Academy for Science and Technology and Maritime Transport, Egypt, *M. Elkashlan**, Arizona State University, USA AP



A Generalized Fractal Radiation Pattern Synthesis Technique for the Design of Multiband and Broadband Arrays

D. H. Werner*, M. A. Gingrich, and P. L. Werner
The Pennsylvania State University
Department of Electrical Engineering and
Applied Research Laboratory
University Park, PA 16802

The recent introduction of fractal geometry into antenna theory has led to a proliferation of new designs for antenna elements as well as arrays (D. H. Werner and R. Mittra, *Frontiers in Electromagnetics*, IEEE Press, 2000). The self-similarity property that is characteristic of many fractals has made them particularly attractive for application to the design of a new class of multiband and broadband antennas. In this paper we will focus on the application of fractal geometric concepts to the design of multiband/broadband antenna arrays.

It has been demonstrated that multiband properties can be achieved for certain self-scalable arrays, namely those which produce self-similar (i.e., fractal) radiation patterns in the limit of infinite array size. More specifically, two types of multifrequency arrays have been considered in the literature, one which generates Weierstrass fractal radiation patterns (D. H. Werner and P. L. Werner, *Radio Sci.*, **31**, 1331-1343, 1996) and the other which generates Koch fractal radiation patterns (C. Puente and R. Pous, *IEEE Trans. Antennas Propagat.*, **44**, 730-739, 1996). This paper will consider a unified approach to the design of multiband/broadband fractal arrays. It will be shown that the Weierstrass and Koch arrays, previously considered independent, are actually special cases of the more general design methodology introduced here. Also of equal importance is the fact that this new method circumvents past limitations associated with the practical application of fractal radiation pattern synthesis techniques based on either Weierstrass or Koch arrays.

Finally, the fractal antenna engineering design techniques developed in this paper will be illustrated by considering some specific examples of synthesized multiband as well as broadband arrays. These examples will include both linear and planar array configurations.

Advances on Theory and Applications of Wave (Photonic) Band-Gap Technology

Organizers and Chairs: D. Yang, University of Illinois at Chicago
D. Jackson, University of Houston

Page

1	1:50	Alternative graphical methods for describing leakage effects on open periodic structures, <i>A. Oliner*</i> , Polytechnic University, USA	284
2	2:10	The physics of endfire radiation from uniform and periodic leaky-wave antennas, <i>D. Jackson*</i> , University of Houston, <i>A. Oliner</i> , Polytechnic University, USA	285
3	2:30	Anomalous absorption of resonance-type periodic structures, <i>S. Peng</i> , <i>R. Hwang*</i> , <i>H. Shih</i> , National Chiao-Tung University, Hsinchu	AP
4	2:50	Fundamental characteristics of a printed antenna on planar structures with periodic metallic loading, <i>H. Yang*</i> , University of Illinois at Chicago, USA	286
5	3:10	Reconfigurable electromagnetic bandgap structures: modeling and experiments, <i>R. Ziolkowski*</i> , <i>M. Hill</i> , <i>J. Papapolymerou</i> , The University of Arizona, USA	287
	3:30	Break	
6	3:50	Integration of planar antennas and defect resonators in two-dimensional EBG substrates, <i>W. Chappell*</i> , <i>M. Little</i> , <i>J. Shumpert</i> , <i>L. Katehi</i> , University of Michigan, USA	288
7	4:10	Low-profile cavity-backed slot antenna using UC-PBG substrate, <i>F. Yang</i> , <i>Y. Qian</i> , <i>T. Itoh*</i> , University of California, Los Angeles, USA	AP
8	4:30	Surface wave mitigation using photonic bandgap structures, <i>P. Kelly</i> , <i>T. Kutrumbos</i> , <i>T. Lammers</i> , <i>M. Piker-May*</i> , University of Colorado, USA	289
9	4:50	Analysis of microstrip dipoles on planar artificial periodic dielectric structures, <i>H. Yang*</i> , University of Illinois at Chicago, USA	AP

Alternative Graphical Methods for Describing Leakage Effects on Open Periodic Structures

Arthur A. Oliner

Polytechnic University, NY

Certain methods of displaying data are superior to other methods depending on the nature of the physical problem and on the features to be stressed. To put it another way, certain behavior becomes transparent when the results are displayed in the right way.

When analyzing the leakage behavior of open periodic structures, various alternative graphical methods have been used, and each has its own special virtues. This talk, which is largely tutorial, will first offer perspectives on some of the most commonly used graphical representations, such as the dispersion plot in the form of β/k_0 vs. frequency, the steepest-descent plane, the k_z (longitudinal-wavenumber) plane, the k_x (transverse-wavenumber) plane, and the Brillouin diagram, in the form of a plot of k_0 vs. β but modified for open structures. The virtues and limitations of these alternatives will be summarized, and the talk will then explain why the Brillouin diagram, as modified, presents the most information in a compact form and is the most useful representation for obtaining insights into the radiation behavior.

The k_0 vs. β diagram has been known for many years, and its usefulness for open periodic structures has also been appreciated, but incompletely. This talk will present a systematic explanation of how the Brillouin diagram should be modified to apply to open structures. The triangular regions within which all solutions are purely real (except those within spectral gaps occurring at the sides of the triangles) will be reviewed, and it will be seen how one can easily tell which space harmonics are radiating and which are not. One can, at a glance, observe how the radiation behavior changes with frequency, which beams are in the forward or the backward direction, the angles of each beam, the nature of the stop bands, the frequencies and wavenumbers at which couplings between space harmonics occur, and so on.

The Physics of Endfire Radiation From Uniform and Periodic Leaky-Wave Antennas

D. R. Jackson, University of Houston, TX

A. A. Oliner, Polytechnic University, NY

Many people believe that when a radiating beam goes through endfire the process occurs smoothly. We demonstrate here that for leaky-wave antennas this is not so, and that in the neighborhood of endfire the variation of propagation wavenumber with frequency is rather complicated. In fact, the solution is nonphysical over a small frequency range near endfire. This frequency range is known as a "spectral gap." Furthermore, the physical leaky mode corresponding to the radiated beam does not mathematically transition smoothly into a bound surface-wave solution as endfire is approached; a surface-wave mode emerges from a nonphysical leaky mode instead.

This behavior has been found to occur on simple structures such as grounded dielectric layers (H. Ostner, J. Detlefsen, and D. R. Jackson, IEEE Trans. Antennas Propagat., vol. AP-43, pp. 331-339, April 1995) where, as the frequency is lowered, a higher-order surface wave passes through a spectral gap as the surface wave goes through cutoff and becomes a leaky wave. It has also been observed on *uniform* leaky-wave antennas where, as the frequency is increased, the radiating beam reaches endfire (P. Lampariello, F. Frezza and A. A. Oliner, IEEE Trans. Microwave Theory Tech., vol. MTT-38, pp. 1831-1836, Dec. 1990). In those cases, the spectral gap has been examined in detail. The talk will first review the physics of the spectral-gap behavior in those two cases.

It is not generally known that similar behavior occurs on *periodic* leaky-wave antennas when the radiating beam reaches forward endfire. A periodic leaky-wave structure is more versatile than a uniform one; not only can it radiate in the backward direction also, but more than one radiating beam can be present at the same time. In this paper, we present numerical results showing the endfire behavior for two cases: when only a single radiating beam is present as the beam is scanned to endfire, and when a second radiating beam emerges before the first beam reaches forward endfire. The specific structure for which numerical values will be presented is a grounded dielectric layer periodically loaded by metal strips on its top surface (S. Majumder, D. R. Jackson, A. A. Oliner and M. Guglielmi, IEEE Trans. Microwave Theory Tech., vol. MTT-45, pp. 2296-2307, Dec. 1997). The stress in the talk, however, will be on the general features, showing in what ways the spectral-gap behavior is different in the two cases mentioned above, and how they differ from that occurring in uniform structures.

Fundamental Characteristics of a Printed Antenna On Planar Structures with Periodic Metallic Loading

H. Y. David Yang

M/C 154, Dept. of Electrical Engineering and Computer Science
University of Illinois at Chicago, Chicago, IL 60607

In recent years, there has been significant renew interest in microwave applications of wave band-gap technology, particularly in two or three-dimensional periodic structures. A few years ago, we proposed the use of artificial periodic materials as the integrated-circuit substrates to eliminate surface-waves within the frequency band-gap zone (H.Y.D. Yang, *IEEE Trans. MTT*, vol. 45, 428-435, 1997). It was concluded however that with common material periodic elements, complete surface-wave elimination is not easily feasible. The use of periodic metallic loading, due to large electric-field density and resonances, results in a large variation of phase constant within a short frequency range and surface-wave band-gap in all directions (H.Y.D. Yang, et. al. *IEEE MTT-Symp. Digest*, 2000). However due to large phase constant variation, the bounded modes or complex modes (in the band-gap) may easily turn into leaky-waves that are faster-waves with a small attenuation constant.

This paper presents the fundamental characteristics of a printed antenna on a multi-layer dielectric structure with planar arrays of patches or dipoles. The idea is to design a printed antenna that has high efficiency (without surface-wave) and high-gain (with leak-wave generation) with a thin substrate and small electric spacing between periodic elements. By designing the periodic substrate that supports fast leaky-wave within the surface-wave band-gap, we demonstrate that such a printed antenna is possible. Numerical analysis of the pertinent problem first deals with the same structure but with infinite phased arrays of δ sources (the periods of the sources and periodic patches or dipoles are the same). The field solution of such structures can be found with a standard Floquet mode expansion of the field in conjunction with the moment method. Subsequently, an analytic array-scanning scheme (V. Galindo, *IEEE Trans. AP*, 424-429, July 1968) transforms the fields due to infinite phased arrays to those due to a single δ source while the otherwise periodic structures are unchanged. This procedure is the integration of the phased array solutions over a period of 2π (for a planar array, it is a double integral). The quantities of interest are the far-zone radiated fields (power) and the periodic surface-wave fields (power) extracted from the total fields through asymptotic analyses similar to that for a δ source on a grounded uniform slab.

The effects of the periodic substrate to the antenna directivity, gain, periodic surface-wave directivity and power, and the radiation efficiency (defined according to the power distributions among the radiated waves and surface waves) are highlighted. Antenna gain measurements are performed to support the theory.

RECONFIGURABLE ELECTROMAGNETIC BANDGAP STRUCTURES: MODELING AND EXPERIMENTS

Richard W. Ziolkowski[†], Michael Hill and John Papapolymou

Electromagnetics Laboratory, Department of Electrical and Computer Engineering

The University of Arizona, Tucson, AZ 85721-0104 USA

Tel: (520) 621-6173 Fax: (520) 621-8076

E-mail: ziolkowski@ece.arizona.edu

Nanometer and micron sized optical devices are currently being explored for their applications in a variety of systems associated with communications, data storage, optical computing, etc. It has been demonstrated that photonic bandgap (PBG) structures can be used at these sizes to form extremely narrow bandwidth filters, extremely small laser cavities, and extremely small waveguiding structures by a variety of research groups. The ability of the FDTD approach to model finite-sized PBG structures with the defects required to form these filters and waveguides, and to recover known behaviors has been demonstrated. The FDTD scheme provides a PBG simulation environment that is quite flexible in terms of the allowed variations in the PBG structure and the excitation pulses. There has also been much activity in the microwave area to use the corresponding electromagnetic bandgap (EBG) structures, for examples, as frequency filters, surface wave mitigators, and reflectors.

One EBG structure that has received attention both in the microwave and the optical regimes is the woodpile PBG. We have simulated and built a finite sized log cabin EBG from square metallic rods. A wide bandgap region where little electromagnetic energy is transmitted through the structure has been demonstrated both numerically and experimentally. The structure has also been modeled with a set of passive defects by removing one partial row of rods in the center of the structure. The difference between the structure without and with the defects has been studied numerically. It has been demonstrated that a narrow microwave frequency filter can be achieved with the defective EBG structure. Experiments have confirmed this general behavior.

A reconfigurable frequency filter has been achieved by introducing defects in one row of the woodpile by inserting diodes into a set of rods in that row. The diodes can be switched on or off. When the diodes are on, the rods are completely conducting and the resulting structure looks like the original passband EBG filter. When they are off, gaps in the bars are introduced and the passband appears. Simulations and experiments demonstrating this behavior will be presented.

It has also been shown that the EBG structures can be used successfully for waveguiding environments and that additional defects can be used to actively control the flow of the power in the EBG structures. A millimeter reconfigurable metallo-dielectric waveguide EBG power-divider and switch has been successfully designed numerically. We are currently trying to realize a similar configuration in Duroid at microwave frequencies. The results from all of these simulations and experiments will be reviewed in our presentation.

Integration of Planar Antennas and Defect Resonators in Two-dimensional EBG Substrates

W. J. Chappell*, M. P. Little, J. D. Shumpert, and L. P. B. Katehi
Radiation Laboratory, EECS Department
University of Michigan, Ann Arbor, Michigan, 48109-2122

Two-dimensional electromagnetic band-gap (EBG) structures have yielded a number of applications for improved antenna and circuit applications. In particular, by fabricating a slot antenna over a reflecting back plane and filling the resulting parallel plate waveguide with an appropriately designed two-dimensional EBG substrate, significant enhancements in antenna performance have been achieved (Shumpert, Chappell, and Katehi, *IEEE Trans. Microwave Theory Tech.*, vol. 47, no. 11, pp. 2099-2104). The parasitic parallel plate substrate modes that radiate energy away from the antenna are trapped and the energy is stored within the EBG lattice. Consequently, a planar antenna with virtually no substrate modes is created yielding an estimated efficiency between 85 to 90 percent.

Recent investigations of reduced height defect resonators, created by removing a single element in an EBG lattice, were found to have an unloaded Q of approximately 700 (Chappell, Little, and Katehi, *2000 MTT Symposium*). By integrating a two-dimensional EBG substrate containing a defect resonator with a slot antenna, the antenna can be coupled to another antenna for use in quasi-optical applications or can be coupled through the defect to other planar receiver circuitry. By creating a defect by removing specific elements in the periodic structure surrounding the slot antenna, a high-Q resonance is formed. Since the periodic inclusions in the substrate do not allow energy to propagate through the EBG lattice in specific directions for a range of frequencies, energy radiated into the substrate at a frequency inside this band evanesces into the lattice. By coupling the evanescent fields of the antenna to the defect, an integrated system is created that provides isolation and allows the substrate radiation to be usefully directed. The number of periodic layers and the relative locations of the antenna and the defect in the EBG lattice determine the coupling between the antenna and the resonator. The coupling will be increased if few lattice inclusions separate the antenna and the resonator. Conversely, the coupling will decrease if many lattice inclusions separate them. Additional defects could be implemented to develop specific filtering responses.

Designing appropriate EBG substrates for stronger coupling and utilizing the defect resonator as a feed for the slot antenna are computationally modeled and experimentally verified in the present work. Specifically, the coupling mechanism between the antenna and the defect will be investigated in an attempt to develop useful components for a millimeter wave front-end subsystem.

Surface Wave Mitigation using Photonic Bandgap Structures

P. Keith Kelly, T. Kutrubos, T. Lammers, M. Picket-May
Electrical and Computer Engineering
University of Colorado, Boulder, CO 80309-0425

Simply speaking, photonic bandgap structures are periodic structures in which specific bands of frequencies are not propagated. The filtering capabilities of these structures make them potentially useful in applications that require passive mitigation of surface waves or any type of microwave transmission. In this paper finite-difference time-domain (FDTD) simulations are used to model PBG structures. A variety of photonic band gap structure applications will be discussed to illustrate the simulation capability. These simulations allow us to rapidly determine the frequency and time-domain characteristics of various PBG structures. Measured and simulated PBGs used as novel microstrip filters, with periodic holes drilled in the substrate or ground plane, will be shown. FDTD simulations of PBG surfaces enhancing the directivity of a microstrip patch antenna will be presented. FDTD simulations showing the mitigation of surface waves on cylindrical structures will be shown. Finally, general surface wave mitigation and the use of FDTD-generated band diagrams will be discussed. The importance of the thickness of the PBG material with respect to specific frequency mitigation will be shown.

LGA Rough Surface Scattering

Organizer and Chair: J. West, Oklahoma State University

Page

- | | | | |
|---|------|--|-----|
| 1 | 1:50 | Analytical theory of scattering anomalies for periodic conducting and dielectric surfaces, <i>M. Charnotskii*</i> , NOAA Environmental Technology Laboratory, USA | 292 |
| 2 | 2:10 | An approximation of the NLSSA scattering cross section, <i>S. Broschat*</i> , Washington State University, USA | 293 |
| 3 | 2:30 | Numerical simulation of scattering from an impedance rough surface at low grazing angles, <i>A. Voronovich*</i> , <i>V. Zavorotny</i> , NOAA/Environmental Technology Laboratory, USA | 294 |
| 4 | 2:50 | On the calculation of rough surface cross section under conditions of strong multiple scattering, <i>G. Brown*</i> , Virginia Polytechnic Institute & State University, USA | 295 |
| 5 | 3:10 | Low-grazing angle backscatter from 2D targets on a time-evolving rough sea surface, <i>R. Burkholder*</i> , The Ohio State University, USA, <i>M. Pino</i> , <i>F. Obelleiro</i> , Universidad de Vigo, Spain | 296 |
| | 3:30 | Break | |
| 6 | 3:50 | A multilevel FB/NSA algorithm for the computation of scattering from extremely large-scale rough surfaces, <i>D. Torrungrueng*</i> , <i>J. Johnson</i> , Ohio State University, USA | 297 |
| 7 | 4:10 | Numerical simulations and backscattering enhancement study of electromagnetic waves from one-dimensional random rough surfaces using the FB/NSA method, <i>D. Torrungrueng*</i> , <i>J. Johnson</i> , Ohio State University, USA | 298 |

**ANALYTICAL THEORY OF SCATTERING
ANOMALIES FOR PERIODIC CONDUCTING AND
DIELECTRIC SURFACES.**

M. I. Charnotskii

NOAA Environmental Technology Laboratory/Science and Technology Corp.
325 Broadway, Boulder CO, 80303 USA
E-mail mcharnotskii@etl.noaa.gov

Grazing Perturbation theory was introduced recently for the scattering of vertically polarized waves by a periodic perfectly conducting surface (M. I. Charnotskii, *PIER*, 26, pp. 1-67, 2000). This theory complements the conventional perturbation theory and predicts a nonlinear dependence of the scattering amplitudes on the roughness heights for slightly rough surface in the presence of diffraction orders propagating at low grazing angles. Grazing perturbation theory revealed the existence of the intrinsic surface impedance that strongly affects the scattering when low grazing diffraction order is present. Here we discuss the extension of the grazing perturbation theory to a periodic interface of two media.

We show that conventional perturbation theory fails for vertical polarization for good conductors when surface plasmon is excited, and for good dielectrics in the presence of low grazing modes. Alternative perturbation theory will be presented that complements the conventional perturbation theory, and is accurate in the presence of surface plasmons and/or grazing modes. Similar to Grazing Perturbation theory we show that scattering periodic surface features effective impedance that depends on the geometrical and electrical properties of the surface. Effective Brewster angle associated with this effective impedance serves as a boundary between the validity regions of the conventional and new perturbation results.

Our results indicate that for vertical polarization scattering amplitude of a periodic interface is a non-analytical function of roughness height and incidence angle in the vicinity of scattering anomalies. We found that conventional and new perturbation results can be combined in a relatively simple set of analytical formulas for scattering amplitudes, which compare favorably with direct numerical calculations.

An Approximation of the NLSSA Scattering Cross Section

Shira L. Broschat

School of Electrical Engineering and Computer Science
Washington State University
PO Box 642752
Pullman, WA 99164-2752

Numerical studies have shown that the small slope approximation (SSA) for scattering from rough surfaces gives excellent results over a broad range of scattering angles. However, at large rms slopes and as the correlation length is increased, the SSA becomes less accurate, particularly at low grazing angles. At these angles multiple interactions at distant points on the surface affect the scattering levels. In an effort to explicitly include these multiple, non-local interactions, Voronovich introduced the non-local small slope approximation (NLSSA), a generalization of the SSA. He showed that the lowest-order NLSSA scattering amplitude, or equivalently the T-matrix, reduces to the second-order SSA scattering amplitude under appropriate conditions. It also reduces to the second-order perturbation theory result in the small height limit and to the Kirchhoff approximation result for smooth surfaces and away from low grazing angles. Finally, Voronovich showed that the NLSSA generally accounts for double scattering in the high frequency limit.

Broschat and Thorsos presented numerical results for the lowest-order NLSSA incoherent bistatic scattering cross section for 2-D, perfectly conducting surfaces. These results agreed well with "exact" Monte Carlo integral equation results and, in particular, were more accurate than the higher-order SSA results at low forward grazing angles. However, the computational cost of obtaining these results was prohibitive. In this paper, we discuss an approximation to the NLSSA scattering cross section that reduces the computational complexity of the integration substantially. The original form of the lowest-order NLSSA scattering cross section equation requires evaluation of an extremely challenging multiple integral. The approximation results in a sum of three integrals of successive difficulty; the first integral is actually the lowest-order SSA result. Numerical results for bistatic scattering at low grazing angles are presented for 2-D, perfectly conducting surfaces and TE polarization. These results are compared with results obtained using the SSA and the original NLSSA, and the trade-offs for each of the three methods are discussed.

NUMERICAL SIMULATION OF SCATTERING FROM AN IMPEDANCE ROUGH SURFACE AT LOW GRAZING ANGLES

A. G. Voronovich*

NOAA/Environmental Technology Laboratory, Boulder, CO

V. U. Zavorotny

NOAA/Environmental Technology Laboratory/CIRES, Boulder, CO

Presently there is no a reliable analytical method that can successfully treat the problem of wave scattering from a sea surface at low grazing angles (LGA). For this reason researchers most frequently rely on numerical techniques. The problem of scattering of electromagnetic (EM) waves from a rough dielectric surface can be significantly simplified if considered for a 2-D case. Further simplification is possible if an impedance approximation of the exact boundary condition is involved. When both approximations are used the problem reduces to the solution of a single scalar linear integral equation with respect to a surface field.

There are two issues related to the numerical treatment of this equation. The first issue is a number of unknowns. The size of a radar footprint or the dominant roughness wavelength could reach hundreds of meters. Then, a conventional " $\lambda/10$ " discretization leads to 10^3 unknowns for centimeter EM waves. The linear system of such a dimension cannot be solved by a brute-force approach. The other issue is a calculation of the entries for the interaction matrix that might be very time-consuming. The approaches to the effective solution of this problem suggested recently are based on iterative methods (e.g., D. A. Kapp and G. S. Brown, IEEE Trans. Antennas Propagat., 44, 711-721, 1996; D. Holliday et al., IEEE Trans. Antennas Propagat., 44, 722-729, 1996) that physically correspond to splitting of the total field into forward- and backward-propagating components that are weakly-interacting in the LGA case.

Our approach is based on the same idea. The novel elements are as follows:

- 1) We use smallness of the Rayleigh parameter associated with the small-scale component of sea surface roughness. This allows taking into account the small-scale component of roughness by a perturbative approach. Then, the unperturbed roughness includes only a smooth component. This produces even weaker interaction between forward and backward components of the field.
- 2) The fast-oscillating factor associated with the phase of the incident wave is extracted from the unknown total field at the surface. Then the reduced field becomes a slowly varying function, and the interval of discretization can be made significantly larger.
- 3) The unknown field between discretization points is represented by the second-order polynomial. Hence, an evaluation of the entries of the interaction matrix reduces to a calculation of some "basic" integrals involving products of exponential, power, and Hankel functions. An effective numerical procedure has been developed for the computation of these integrals.

As a result, the numerical solution of the scattering problem for X-band waves and for 100 m of the footprint length is performed on a standard PC for less than ½ hour. The relevance of the results to explanation of the HH/VV polarization-ratio anomaly will be discussed.

On the Calculation of Rough Surface Cross Section Under Conditions of Strong Multiple Scattering

Gary S. Brown
ElectroMagnetic Interactions Laboratory (EMIL)
Bradley Department of Electrical & Computer Engineering
Virginia Polytechnic Institute & State University
Blacksburg, VA 24061-0111

The calculation of rough surface scattering cross section is now being routinely carried out by numerical means both for specific surfaces and also for single realizations from a class of randomly rough surfaces. Generally, such computations are accomplished using either plane wave or beam illumination with the particular type of illumination dictated by the numerical technique used to solve the scattering problem. For example, FDTD methods employ plane waves while moment method approaches employ a simulated beam illumination. For randomly rough surfaces, both approaches generally always assume that the scattering process is statistically homogeneous. In the case of beam illumination this means that moving the center of the beam around on the surface has no effect on any of the moments of the scattering process. It is less easy to define exactly what this means in the case of FDTD calculations because of the unbounded nature of the plane wave illumination. In addition, it is frequently assumed that if the surface is statistically homogeneous, the scattering process will also be statistically homogeneous and one need not be concerned with the exact placement of a beam on the surface. The purpose of this paper is to discuss a situation where this assumption may, in fact, not hold and to consider its implications.

For low grazing scattering from certain classes of rough surfaces, it is very probable that multiple scattering will occur. Under the additional constraint of backscattering, multiple scattering becomes particularly important because it can give rise to scattered energy in a direction that frequently has no other source of energy. For example, in the case of high frequencies and horizontal polarization, the conventional mechanism of Bragg resonance scattering is very weak yet there is frequently a very strong scattered signal. This strongly suggests the mechanisms of wedge diffraction, resonant wave packet diffraction, or incipient wave breaking. While each of these sources of wave scattering acting alone is a source of backscattering, they may also be involved in multiple scattering on the surface. That is, energy forward scatters from one point on the surface to the location of these features and then is scattered a second time into the backscatter direction. If FDTD or moment method techniques are used to calculate scattering from such surfaces, these multiple scatterings will be averaged into the ensemble-averaged $\sigma^o(\theta_i, -\theta_i)$ for the surface. However, if a short pulse radar is used to measure the same quantity, one may well get a different result because the multiple scattered component will appear in a "range bin" that is different from the one it originated in. While averaging may smear this effect out, such is not always the case. This is the problem that this paper will address.

Low-Grazing Angle Backscatter from 2D Targets on a Time-Evolving Rough Sea Surface

Robert J. Burkholder*, M.R. Pino¹, and F. Obelleiro¹

*The Ohio State University Department of Electrical Engineering
ElectroScience Laboratory, 1320 Kinnear Road. Columbus, Ohio 43212
E-mail: burkhold@ee.eng.ohio-state.edu Phone: (614) 292-4597

¹Universidad de Vigo, Dpto. Tecnologías de las Comunicaciones
ETSE Telecomunicacion, Campus Universitario, 36200 Vigo, Spain

The low-grazing angle (LGA) electromagnetic backscatter from a PEC target on a rough sea surface may vary significantly as the surface evolves with time. To study this phenomenon numerically, the generalized forward backward (GFB) method is used to compute the backscatter from a 2D target on a very long rough surface (M.R. Pino, L. Landesa, J.L. Rodriguez, F. Obelleiro, and R.J. Burkholder, *IEEE Trans. Antennas Propag.*, **47**, 961-969, 1999). The surface is randomly generated using the Pierson-Moskowitz ocean wave spectrum for a given wind speed, and evolves with time according to a linear gravity wave dispersion relation. The GFB method computes the plane wave backscatter (2D radar cross section, RCS) from the target at isolated instants in time for a given LGA of incidence. The RCS is then plotted as a function of time.

The LGA case is particularly interesting to study because the incident field that illuminates the target (including the reflection from the sea surface) is nearly coherent, even for relatively high wind speeds. Therefore, the time variation in the RCS of the target must be due to the locally changing sea surface in the vicinity of the target. As the numerical results will show, the primary trend in the RCS vs. time plots is directly related to the height of the target as it moves up and down with the large scale waves, with the minima and maxima corresponding to troughs and swells, respectively. The small scale waves have a less noticeable effect. However, in these results the target is not allowed to roll with the waves. Additional numerical results will show that the variations caused by the rolling of the target are usually more significant than that caused by the time changing sea surface for LGA cases. The RCS vs. roll angle is computed for the target on an infinite flat surface, which is easy to compute using image theory. In reality, since most targets on the sea surface will roll with the waves, the roll angle plot provides a very important tool for predicting the variation of the RCS of a ship on a rough sea surface.

The results of a Monte Carlo study of the RCS as a function of wind speed and elevation angle will also be presented to introduce the LGA region.

A Multilevel FB/NSA Algorithm for the Computation of Scattering from
Extremely Large-Scale Rough Surfaces

D. Torrungrueng* and J. T. Johnson
Ohio State University
Dept. of Electrical Engineering
ElectroScience Lab.
1320 Kinnear Rd.
Columbus OH 43212
Tel: (614)292-7981
Fax: (614)292-7297
dtg@lenz.eng.ohio-state.edu
jtj@silver.eng.ohio-state.edu

The forward-backward method with a novel spectral acceleration algorithm (FB/NSA) has been shown to be a very efficient iterative method of moments for the computation of scattering from both one-dimensional (1-D) and two-dimensional (2-D) rough surfaces. The method creates only one large group of source elements for the weak interaction computations. This source group enlarges as the forward or backward sweep proceeds and recursively builds up the plane wave spectrum associated with the NSA algorithm. Thus, for fixed surface roughness statistics, the operation count and memory storage requirement of the FB/NSA method is $\mathcal{O}(N)$ as the surface size increases.

Preliminary studies based on the physical optics (PO) approximation and the flat surface assumption show that the given 1-D NSA parameters (see H.-T. Chou and J. T. Johnson, *Radio Sci.*, **33**, 1277-1287, 1998) yield inaccurate results for the case of *extremely* large-scale surfaces. Inaccuracy comes from the fact that the 1-D plane wave spectrum of a source group far separated from the receiving element is rapidly decayed along the deformed contour away from the origin in the complex angular domain, which requires higher sampling rates. In this paper, the original FB/NSA method is modified to obtain accurate results for the computation of scattering from *extremely* large-scale rough surfaces. Analytical results based on asymptotic evaluations of the radiation integral associated with the PO and flat surface assumption suggest that the very large weak region associated with *extremely* large-scale surfaces needs to be decomposed into more than one weak region, and appropriate 1-D NSA parameters must be determined for each separate region to gain better accuracy. Comparison of results obtained from the original FB/NSA method and the multilevel FB/NSA algorithm shows that the latter yields more accurate results than the former indeed.

Numerical Simulations and Backscattering Enhancement Study of
Electromagnetic Waves from One-Dimensional Random Rough Surfaces
Using the FB/NSA Method

D. Torrungrueng* and J. T. Johnson
Ohio State University
Dept. of Electrical Engineering
ElectroScience Lab.
1320 Kinnear Rd.
Columbus OH 43212
Tel: (614)292-7981
Fax: (614)292-7297
dtg@lenz.eng.ohio-state.edu
jtj@silver.eng.ohio-state.edu

The forward-backward method with a novel spectral acceleration algorithm (FB/NSA) has been shown to be a very efficient iterative method of moments for the computation of scattering from one-dimensional perfectly conducting and impedance rough surfaces (H.-T. Chou and J. T. Johnson, *Radio Sci.*, **33**, 1277-1287, 1998). Basically, the NSA algorithm is employed to rapidly compute interactions between widely separated points in the conventional FB method, and is based on a spectral domain representation of source currents and the associated Green's function. With the recursive property of the plane wave spectrum associated with the NSA algorithm, it can be shown that, for fixed surface roughness statistics, the computational cost and memory storage of the FB/NSA method is $\mathcal{O}(N)$ as the surface size increases. In addition, The FB/NSA method is still very efficient for moderately-rough large-scale surfaces. This makes studies of backscattering enhancement from large-scale surfaces, as are required in low-grazing-angle (LGA) scattering problems, tractable.

In this paper, variations in the level and angular width of backscattering enhancement with incidence angle, surface material (impedance or perfect electric conductor), polarization, and surface statistics are investigated. Incidence angles ranging from normal incidence (0°) to LGA incidence (85°), and very rough surfaces with a Gaussian spectrum ($\sigma_h \geq 0.5\lambda$ and $\sigma_s \geq 0.5$, where σ_h and σ_s are the rms surface height and the rms surface slope, respectively), are considered in this study. Although the FB/NSA method is a very efficient iterative technique, the numerical problem of interest is still computationally intensive. Parallel computing techniques are incorporated into the 1-D FB/NSA method, primarily to perform the Monte-Carlo simulations in parallel.

Wireless Communications Systems and Applications

Organizer and Chair: Jon Steadman, Tritel Communications

Page

1	8:00	Challenges of the wireless services provider, <i>J. Steadman*</i> , Tritel Communications, Inc., USA	300
2	8:20	Adaptive integrated transceivers for consumer products (Keynote), <i>L. Leyten and G. Dolmans</i> , Philips Research, The Netherlands	301
3	9:00	Nominal radio frequency system design process, <i>M. Murdock</i> , Galaxy Engineering Services, USA	302
4	9:20	Planning commercial broadband fixed wireless networks, <i>P. Cutler</i> , Cisco, USA	303
	9:40	Break	
5	10:00	Dual polarized antenna performance, <i>R. Smith</i> , Allgon Enterprises, Inc. USA	304
6	10:20	Effect of antenna parameters on reuse in broadband wireless access systems, <i>R. Arefi*</i> and <i>K. Etemad</i> , Wireless Facilities, Inc., USA	AP
7	10:40	Antenna technologies for wireless applications, <i>S. C. Olson</i> , Ball Wireless Communications Products, USA	305
8	11:00	Confidence limit testing: the key to efficient CDMA mobile receiver test, <i>K. Thompson, M. Wagner</i> , Agilent Technologies, USA	306
9	11:20	Recent advancements in coaxial cable and connector development, <i>R. Vaccaro</i> , Commscope, Inc., USA	307

Challenges of the Wireless Services Provider

Jon Steadman
Tritel Communications, Inc.

In recent years the wireless communications industry has exploded with activity. With new spectrum opportunities opened up by the Federal Communications Commission (FCC) increased competition for wireless services has become prevalent throughout the United States. Similar growth is experienced throughout much of the world, with rapid expansion throughout many third world countries. With this increased competition, the Wireless Services Provider is challenged with staying on the cutting edge of technology while maintaining operating and capital costs within financially competitive bounds. The FCC mandates coverage objectives, which the Wireless Services Provider must meet. In addition, wireless subscribers demand more and more services, including both voice and data. To meet the requirements of the regulatory bodies and the demands of the competitive marketplace, the Wireless Services Provider must rely on technology advancements in the area of antennas, integrated components, computer aided design tools, and signal processing software. A convergence of technology is underway to bring all communications solutions together in a single package. It is the challenge of the Wireless Service Provider to provide the solutions cost effectively and reliably to an increasingly wireless world.

Adaptive Integrated Transceivers for Consumer Products

L. Leyten and G. Dolmans
Philips Research

Within our department we are doing research on improving the circuits of wireless and cordless products for the consumer market. The constraints for these circuits are mainly low cost, small size and low power. The performance of the individual circuits is only a few dB's from theoretical limits, like thermal noise floor and 100% power added efficiency. We are still improving on the performance and technology of individual circuits, but it becomes more difficult to do this within the constraints given by the consumer market. We identified the inclusion of adaptive algorithms, especially diversity, in the front-end part as one of the possibilities to overcome this problem. Implementation of antenna diversity results in approximately 6 to 9 dB's extra in the link budget at the expenses of more complex circuitry. This amount of improvement is significant with respect to that obtainable in other ways. By compromising between the performance and complexity of an adaptive transceiver we have contributed to a product for the consumer market, the Kala DECT handset of Philips, which has a better performance than previous products.

The implementation of many concepts for adaptive transceivers, like diversity or space-time processing, into consumer products requires specific tools and capabilities. The selection of candidate concepts can be made using stochastic models of the radio channel and the transmitted data. The use of stochastic models becomes less optimal when implementation issues, like resolution, processing-speed and antenna-array size are considered. As a consequence we have developed a deterministic model of the radio channel that enables us to analyze the various implementation issues. With this model we obtain relevant information on, for example, antenna characteristics, the effect of user movement on performance, the speed of adaptation, resolution, etc.

The current status of radio channel modeling is such that not all relevant parameters can be included. Therefore measurements are needed to evaluate the performance of a specific implementation. Several types of measurements can be identified, each measuring different parameters. We have developed a measurement set-up consisting of a computer controlled scanner, personal computer and a network analyzer. This set-up is used to obtain the received voltage as a function of antenna characteristics and location and to obtain the actual performance of the adaptive transceiver in a realistic propagation environment.

When an algorithm can be implemented by adaptive circuitry, then this adds to the overall complexity of the transceiver. Care should be taken not to interfere with the system protocols and to integrate the circuits at a suitable position within the total architecture. Performance loss when combining the adaptive circuitry with other control loops, like an automatic gain control loop or the offset compensation circuitry must be avoided. We have studied some of these issues for the implementation of an equal-gain combiner. Finally, we have also been involved in the development of new technologies that are suitable for the integration of adaptive transceivers.

In the presentation, novel concepts in the challenging area of radio channel modeling and measurement, IC technology, architecture and circuits for cellular and wireless consumer products will be discussed.

Nominal Radio Frequency System Design Process

Monty Murdock
Galaxy Engineering Services

The rapid growth of the wireless industry presents several opportunities and challenges to Electrical Engineers who have found a home in the wireless industry. Engineers are not only faced with the challenges of developing analytical solutions to the growing wireless industries needs, but are also faced with developing practical solutions. The true goal of a wireless design is to take a specific technology platform with inherent characteristics and develop a consumer product that provides quality service. The Nominal Radio Frequency System Design Process must take into account a wide variety of variables in order to achieve this goal.

The Nominal Radio Frequency System Design Process discussed will overview the methodologies developed to incorporate variables such as equipment specifications, market coverage objectives, traffic loading, design tool limitations, land use zoning restrictions, Federal Communications Commission guidelines, Federal Aviation Administration guidelines, and the limited availability of spectrum.

Planning Commercial Broadband Fixed Wireless Networks

Paul Cutler
Cisco

Fixed wireless is becoming more popular as an option for broadband internet access, as well as voice and (in the future) video services. Like today's mobile wireless networks, fixed wireless network technologies and architectures come in a variety of shapes and sizes. This paper will present a brief overview of the fixed wireless market and associated technologies. General fixed network architectures and structures will be discussed and compared to current and future mobile network architectures. Propagation characteristics of OFDM (orthogonal frequency division multiplexing), a popular modulation/multiplexing technique used by some leading hardware vendors will be briefly discussed and compared to traditional TDMA, GSM, and CDMA schemes used in today's mobile networks.

Dual Polarized Antenna Performance

Richard Smith
Allgon Enterprises, Inc.

The dependence of the orthogonality to the cross-polar discrimination level for dual linearly polarized antennas as well as their function in a wireless network is presented. Most of the cross-polarized, dual polarized, antennas being deployed in wireless networks are slant 45 polarized. The multi-path in an antenna range and the phase stability of the range play a large part in accurately determining the orthogonality of the antenna. For linearly polarized antennas, this work will show that the orthogonality or far field coupling of the antenna can be reduced to measuring the cross-polar discrimination angle by angle over the desired field of view. This result will further demonstrate that measuring the radiation properties and the impact on the wireless network for conventional horizontal and vertically polarized antennas is far less demanding from an antenna characterization stand point.

**Antenna Technologies
For
Wireless Applications**

Steven C. Olson
Director of Engineering
Ball Wireless Communications Products
Broomfield, CO
solson@ball.com
(phone) (303) 533-7202
(fax) (303) 533-7112

The most difficult challenge that an antenna designer has in today's commercial wireless market is antennas are becoming a commodity product. Commercial antenna manufacturers are in an extremely competitive market where the selling price continues to fall and yet the expected performance requirements are increasing. Therefore, the technical challenge is to design antennas using technologies that can provide superior performance, are low cost, use minimal components and are simple to manufacture.

Antennas contribute only a small amount to the overall system cost but they play a key role in providing the initial interface between mobile or fixed users and the wireless base station infrastructure. This is true whether an antenna is used in a conventional mobile base station, wireless local loop, or 'smart antenna system' application. Careful selection of antenna technologies is critical in maximizing system performance. These issues become an even bigger concern after the infrastructure is in place and the network capacity continues to increase. In this paper several important antenna characteristics and technologies will be discussed that service providers should be concerned with.

Critical radio frequency (RF) antenna characteristics such as VSWR, gain, beamwidth, pattern shaping and control, and passive intermodulation (PIM) will be addressed. Various design approaches and performance tradeoffs will be presented. To ensure excellent RF performance the RF design must be well thought out with mechanical design integrity and low cost assembly in mind.

Zoning is becoming a greater concern as the number of antenna deployments is increasing. Even though communities want excellent wireless coverage they are demanding that the number of antennas be minimized or concealed. Many of these issues are being addressed by implementing dual slat polarized and/or dual band antenna technologies. Smart antenna technologies are becoming more important as systems are reaching capacity limits. Smart antenna approaches vary from simple switched beam arrays to complex adaptive antenna systems.

CONFIDENCE LIMIT TESTING: THE KEY TO EFFICIENT CDMA MOBILE RECEIVER TEST

Ken Thompson and Marv Wagner
Agilent Technologies

Modern commercial communication systems employ digital modulation and protocol techniques. This allows maximum bandwidth utilization and user security for service providers and consumers. It also creates a challenge for equipment manufacturers & test equipment suppliers. Equipment manufacturers want to minimize test time to reduce the manufacturing cost of their appliances. Test equipment suppliers are then challenged to create solutions that minimize test time without sacrificing thoroughness of testing.

This paper will explore one technique that has been developed to reduce test time without sacrificing test quality, the use of Confidence Limits in error rate testing. Frame Error Rate (FER) testing of CDMA mobile appliances in commercially available test equipment will be used as an example of this technique.

Recent Advancements in Coaxial Cable and Connector Development

Ron Vaccaro
CommScope Inc.

With site build schedules being compressed, installers and system providers are looking for products which allow the job to go in faster and be more reliable in the long run. Recent developments in smooth-walled coaxial cable and advancements in connector designs have addressed these issues. These new products allow for reduced assembly variability associated with connectors and improved environmental and electrical performance of the cable.



Microstrip Element and Array Design

Co-chairs: K. C. Gupta, University of Colorado
R. W. Grow, University of Utah

Page

- | | | | |
|----|-------|---|-----|
| 1 | 8:00 | Planar microstrip Yagi array with notched parasitic elements, <i>R. Lee*</i> , NASA Glenn Research Center, USA | 310 |
| 2 | 8:20 | Using small holes to achieve dual-band reduce-surface-wave antennas, <i>V. Davis, J. Williams*</i> , D. Jackson, S. Long, University of Houston, USA | 311 |
| 3 | 8:40 | Matching antennas over high impedance ground planes, <i>G. Poilasne, E. Yablonovitch</i> , University of California at Los Angeles, USA | 312 |
| 4 | 9:00 | Array performance of a new annular-ring microstrip antenna element, <i>G. Mayhew-Ridgers*</i> , Vodacom (Pty) Ltd, J. Odendaal, J. Joubert, University of Pretoria, South Africa | 313 |
| 5 | 9:20 | A circular polarized dielectric-loaded patch antenna for mobile satellite applications, <i>A. Ittipiboon*</i> , Communications Research Centre, S. Stout, Carleton University, A. Petosa, Communications Research Centre, J. Wight, Carleton University, Canada | 314 |
| | 9:40 | Break | |
| 6 | 10:00 | Modified compact printed disc antennas for HIPERLAN, <i>E. Ibrahim, R. Abd-Alhameed*</i> , N. McEwan, P. Excell, Bradford University, UK | 315 |
| 7 | 10:20 | Electronically tunable rectangular microstrip antennas, <i>L. Basilio, J. Williams*</i> , D. Jackson, S. Long, University of Houston, USA | 316 |
| 8 | 10:40 | Stacked electromagnetically coupled rectangular patch antenna with segmented elements, <i>A. Zaman*</i> , R. Lee, NASA Glenn Research Center, USA | 317 |
| 9 | 11:00 | Antenna patch reduction by inductive and capacitive loading, <i>S. Reed, SEI-IRESTE, France, L. Desclos, NEC USA Inc, USA, C. Terret, Université de Rennes, S. Toutain*</i> , SEI-IRESTE, France | 318 |
| 10 | 11:20 | Resonant modes of a wide class of microstrip patches fabricated on magnetized ferrites with arbitrarily oriented bias magnetic field, <i>R. Boix*</i> , G. León, F. Medina, Facultad de Física, Spain | 319 |

Planar Microstrip Yagi Array with Notched Parasitic Elements

Richard Q. Lee

NASA Glenn Research Center
Cleveland, OH 44135

A planar microstrip Yagi array consisting of a single driven element, a single parasitic reflector element and two parasitic director elements was introduced in 1991 for mobile satellite vehicle application (*IEEE Trans. Antennas & Propagation*, vol. 39, No. 7, 1024-1030, 1991). Unlike the conventional Yagi-Uda array which is used primarily for gain enhancement, this array is designed to produce a directional beam within the angular region between 20° and 60° elevation. The beam is steered away from its broadside direction through mutual coupling of electromagnetic energy from the driven patch to the parasitic patches. In order to produce a beam in a specified direction, proper phase settings of all the parasitic elements, both the reflector and the directors, are required so that radiation from each element are added up coherently. In the case of the Yagi array reported earlier, correct phase delay of each parasitic element was achieved by proper variation of the element size and element spacing. It has been reported that proper phase delay can also be obtained by introducing slots or notches in the antenna element (John L. Kerr, *Antenna Applications Symposium Proceedings*, 1977). A slot cut on a microstrip antenna causes the surface current to flow around the slot resulting in a longer current flow path, a decrease in the resonant frequency, and consequently, a phase delay. In this work, we study, both analytically and experimentally, the scanning capability of a planar microstrip Yagi array using notched parasitic elements as directors and reflector. The microstrip Yagi array of square patches has two directors and one reflector. Preliminary results indicate that a directional beam 45° from its broadside direction can be obtained with notches cut along the radiating and non-radiating edges of the directors and reflector respectively. Based on simulated results, a gain of over 7 dB; was observed at 45° elevation with proper element spacing and slot dimensions. Detailed results will be presented and discussed.

USING SMALL HOLES TO ACHIEVE DUAL-BAND REDUCE-SURFACE-WAVE ANTENNAS

Vickie B. Davis, Jeffery T. Williams, David R. Jackson, and Stuart A. Long

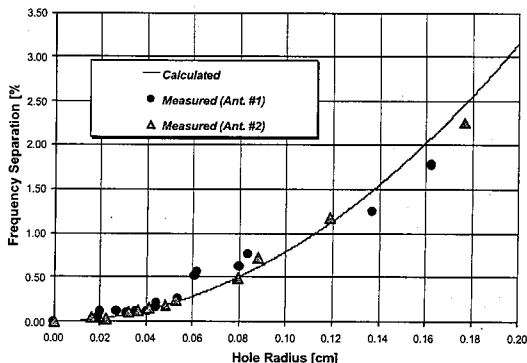
Applied Electromagnetics Laboratory
Department of Electrical and Computer Engineering
University of Houston
Houston, TX 77204-4793, USA

The shorted-annular-ring (SAR) reduced-surface-wave (RSW) microstrip patch antenna was introduced in 1993 [*IEEE Trans. Antennas Propagat.*, vol. AP-41, pp.1026-1037, Aug. 1993]. This antenna consists of an annular ring microstrip patch that is shorted to the ground plane along the circular inner boundary. This design significantly reduces surface- and lateral-wave excitation compared to conventional microstrip patch antennas and, therefore, has a higher radiation efficiency. Later, a modification of this design was made to achieve dual band performance. In this case the circular inner boundary was made elliptical. Results from this study demonstrated the band separation, isolation, and continued RSW characteristics of the dual-band structure [*1996 USNC/URSI Radio Science Meeting Digest, Baltimore, MD, p.150*].

In this presentation, we investigate a different method for achieving dual-band performance. This method entails drilling a small hole in the substrate under the patch, leaving an air-filled void in the patch cavity. The circular hole in the substrate produces two orthogonal modes, with one mode resonant at a frequency higher than the other (unperturbed) mode. This method allows for an accurate prediction of the dual resonant frequencies for very small band separations, such as those necessary for achieving circularly-polarized patch designs. In this case both modes are excited by feeding the antenna along an axis that is at an angle of 45° with respect to the axis on which the hole is placed. The hole radius is then chosen to give the necessary band separation to achieve circular polarization.

One technique that has been used to analyze and design this structure is based on perturbation theory. The agreement between this theory and experiment (two different measurements) is shown in the figure below for a RSW design on a grounded duroid substrate (thickness $h = 0.0635$ cm, permittivity $\epsilon_r = 10.8$).

As with the previous dual-band method, there is little degradation in the RSW performance for the band separations studied. This will be demonstrated by examining the radiation patterns of the RSW antenna on a finite-size ground plane. The RSW antenna patterns show much less back radiation and front-side pattern rippling than do the patterns of a conventional patch, due to less edge diffraction from surface and lateral waves. The present method has the advantage of allowing for easier manufacture, compared to the previous elliptical-boundary method.



MATCHING ANTENNAS OVER HIGH IMPEDANCE GROUND PLANES

G. Poilasne and E. Yablonovitch

Electrical Engineering department, University of California at Los Angeles,
Los Angeles, CA, 90095, USA
Poilasne@ee.ucla.edu

Wireless systems are now widely used in communication. In order to improve their performance and their efficiency, antennas are taking a growing place. Because of their small dimensions, planar antennas are usually used. And to obtain a 3dB improvement of the radiated field, a metallic sheet maybe used as reflector or ground plane. Unfortunately, two important limitations appear when the antenna is placed close to the reflector. Firstly, good performance is obtained only when the distance is a quarter of the wavelength, which does not correspond to a planar antenna anymore. Secondly, surface waves excited by the antenna propagate along the ground plane and are diffracted by the edge. These surface waves create ripples in the radiation pattern and increase the backward radiated field.

These two issues can be solved using a High Impedance Ground Plane. These textured structures -Fig.1- introduced by D. Sievenpiper et al. (IEEE MTT, Vol.47, n.11, Nov. 1999, pp.2059-2074) are based on the behavior of Photonic Band-Gap materials. They allow to reduce drastically surface waves. Moreover, as they behave like a perfect magnetic wall, antennas can be placed right on their top. Therefore, the radiation pattern presents a better front to backward radiated field ratio without any ripples.

While these high impedance ground planes show a lot of promise for all wireless applications, still a lot of issues remain. The antenna matching is one of these. On one hand, at frequencies within the band-gap, the structure is resonating. On the other hand, antennas like dipole or loop resonate as well. When the two elements are placed very near, the action of the ground plane on the antenna changes the radiation characteristics, especially the input impedance. New laws can be determined in order to match antennas on such ground planes. The strong influence of the ground plane on the antenna demonstrated by numerical and experimental results also means that size reduction can be obtained as the resonant frequency of the radiating element can be trapped inside the band-gap. Fig.2 presents the smith chart of a loop antenna over an HIGP. In these case, the loop diameter is $2/3$ of the wavelength.

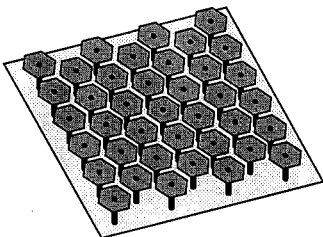


Fig.1: High Impedance Ground Plane

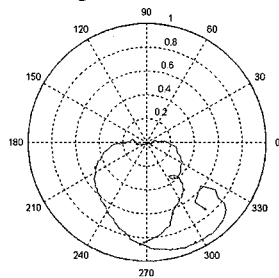


Fig.2: Smith chart of loop antenna input impedance

Array Performance of a New Annular-Ring Microstrip Antenna Element

G. Mayhew-Ridgers[†], J.W. Odendaal[‡] and J. Joubert[‡]

[†] Vodacom (Pty) Ltd, 082 Vodacom Boulevard, Midrand, 1685, South Africa

[‡] Centre for Electromagnetism, Department of Electrical and Electronic Engineering, University of Pretoria, Pretoria, 0002, South Africa

Microstrip patch antennas have found widespread application during the recent past as a result of their many salient features. Of particular interest here is the annular-ring antenna which, when operated in its fundamental TM_{11} mode, is smaller than most of its other counterparts. Unfortunately this mode is associated with a very high and inductive input impedance and is therefore seldom used in antenna applications. The current authors have however recently reported on a new feeding mechanism that overcomes the aforementioned matching problem and also offers enhanced impedance bandwidth performance.

The new feeding mechanism is based upon a rectangular strip that is capacitively coupled to the ring and fed by a probe. This strip is situated on the same layer as the ring and therefore the entire structure can be supported by a single substrate. Matching is accomplished by varying the length of the strip as well as the gap between the strip and the ring. The length of the strip is used to control the input reactance while the gap between the strip and the ring is used to control the input resistance. Tuning of the input impedance is also very easy. It can be accomplished by merely trimming the sides of the rectangular strip.

Numerical modelling have shown that the co-polar radiation patterns of the new structure correspond very well to those of a conventional probe-fed annular-ring antenna, while the cross-polar radiation patterns are only marginally higher. The bandwidth is also somewhat wider than that of the conventional probe-fed annular ring.

As this element is physically smaller than a rectangular or circular patch, it should be well suited for many array applications. Its behaviour and performance in different array configurations will therefore be presented. It is also very easy to construct a dual-polarised array by simply feeding each ring with two rectangular strips, one for each polarisation. The cross-polarisation levels can be reduced by using symmetrical feeds or by appropriate rotation of the individual array elements. A problem that however still needs some attention, is the generation of $\pm 45^\circ$ polarisation together with low cross-polarisation levels by making use of a vertical array. These requirements are often found in the wireless communications environment and is currently the topic of further investigations.

A Circular Polarized Dielectric-Loaded Patch Antenna for Mobile Satellite Applications

A. Ittipiboon*, S. Stout[†], A. Petosa, J.S. Wight[†]

Communications Research Centre, 3701 Carling Avenue, P.O. Box 11490,
Station H, Ottawa, ON, Canada K2H 8S2

[†] Carleton University, 1125 Colonel By Drive, Ottawa, ON, Canada, K1S 5B6

Antennas for L-Band mobile satellite terminals are required to meet challenging design specifications. In order to cover both receive and transmit channels, they must have a fairly broad bandwidth (8 – 10%). Also, antennas must have good coverage at low elevation, since in North America, geo-stationary satellites appear low to the horizon (at about 30° elevation). In order to combat de-polarization effects through the atmosphere, the mobile satellite systems all operate with circular-polarized signals hence circularly-polarized antennas are needed. Since these antennas are intended for a consumer or commercial market, they are also required to have a compact size, and low profile, at a reasonable cost.

Several antennas have been proposed as candidates for mobile satellite communications, such as stacked microstrip patches, short quadrifilar helices, or dielectric resonator antennas. However, a single-layer microstrip patch had not been found suitable, due to its inherently narrow bandwidth performance, and its large size at L-Band.

A new dielectric-loaded microstrip patch antenna was recently introduced to address some of these challenges (Stout et al, USNC/URSI 1999, Orlando, FLA, pp. 322). The structure consisted of a microstrip patch antenna, having a relatively thick air substrate so it could meet the required bandwidth. Instead of a probe feed, a microstrip feed slot aperture was used to excite the patch, in order to reduce unwanted cross-polarization radiation associated with probe feeds. The slot was loaded with a thin layer of high-permittivity dielectric material to achieve strong coupling between the feed and the patch. The sides of the patch were also loaded with high-permittivity dielectric material, to reduce the resonant frequency of the patch and make it more compact. Results of a linearly-polarized prototype antenna were presented, which demonstrated a bandwidth of 8% and a size reduction of 30%.

In this work, this new antenna configuration is successfully extended to produce a circular-polarized antenna, consisting of two dielectric-loaded slot apertures as well as additional dielectric loading to reduce the patch dimensions. Details of the patch configuration and a summary of the radiation performance will be presented at the conference.

MODIFIED COMPACT PRINTED DISC ANTENNAS FOR HIPERLAN

E. M. Ibrahim, R. A. Abd-Alhameed, N. J. McEwan and P. S. Excell
 Electronic and Electrical Eng. Dept., Bradford University, UK

A novel conical beam antenna design was proposed with introduction of a central cylindrical connection to ground (see Fig. 1 and 2). This reintroduces the need for a through - board connection, which is somewhat undesirable in terms of manufacturing costs. However; a fairly inexpensive method may be to metallise or through - plate a hole punched in the substrate. As would be expected, there are significant reductions in bandwidth (see Table 1) and a moderate reduction in radiation efficiency, and these are almost inevitable penalties of miniaturising an antenna that is realised with normal metallic conductors. The major advantage is however a great reduction in antenna size. The reduced size patches show a larger effect of the fringing field effect on the resonant frequency, for the same outer radius. A significant difference between the normal disc and reduced size disc is that the peak radiation of the conical beam (see Fig. 2) occurs at a lower elevation. This might degrade overall performance in cluttered environments where ceiling reflections dominate the coupling, and improve it in more open layouts. The reduced size construction provides a useful degree of freedom in design, since by varying the diameter of the central post, the elevation of peak radiation can be varied continuously to suit the application and the propagation conditions. More propagation data are needed to show what the best values are likely to be in practice. So far the compact disc antenna has only been realised in probe fed form, though a uniplanar form appears feasible.

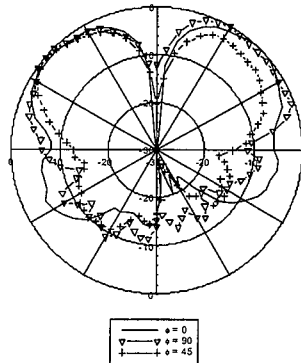
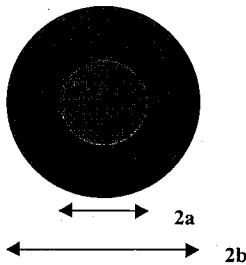


Fig. 1. The modified disc antenna geometry.

Fig. 2. Measured pattern for reduced size patch A

Table 1. The geometry and performance of the prototype disc antennas.

Prototype	a (mm)	b (mm)	Measured frequency (GHz)	Predicted frequency (GHz)	Return loss (dB)	Bandwidth (%) at VSWR ≤ 2
A	7.5	1.9	5.19	5.98	21	1.8
B	18	9	5.095	4.86	44.693	3.61
C	20	4	2.252	2.155	22	1.24
D	19.5	5	1.988	1.903	37.146	0.754
E	20	2	1.565	1.579	17.58	0.479
Normal disc (1)	20	-	5.46	5.2	33	4.029
Normal Disc (2)	58.5	-	2.084	2.0	35.84	1.585

ELECTRONICALLY TUNABLE RECTANGULAR MICROSTRIP ANTENNAS

*Lorena I. Basilio, Jeffery T. Williams, David R. Jackson,
and Stuart A. Long*

Applied Electromagnetics Laboratory
Department of Electrical Engineering
University of Houston
Houston, TX 77204-4793

Although widely used in other areas, microstrip patch antennas are often unable to meet the bandwidth requirements of many modern wireless telecommunication applications. However, electronically tuned microstrip antennas could allow not only for relatively wide-band frequency diversity, which would be ideal for frequency division duplex and frequency hopping schemes, but also for the electronic correction of errors introduced by changes in temperature, environment, and manufacturing imperfections. In some previous studies, tunable patch antenna designs have been realized using ferrite materials, requiring relatively strong biasing magnetic fields that complicate the design. Electronically tunable patches using varactor diodes between the edges of the patch and the ground plane have also been demonstrated. This design, however, is not monolithic, requiring a hole to be drilled into the substrate into which the diode is placed.

In this presentation we will discuss a new rectangular microstrip patch antenna design that contains a slot across the resonant dimension, dividing the patch into two halves. By placing reverse-biased varactor diodes across the slot and changing the bias voltage across the two halves of the patch, the resonant frequency of the patch antenna can be tuned. The slot is placed in the center of the patch in order to maximize the tuning of the dominant mode of the antenna.

We will first present an accurate transmission-line model of the slotted patch that has been recently developed. From this model the tunability and sensitivity of the antenna as a function of dielectric constant, slot size and varactor diode configuration will be examined. Results will then be presented that demonstrate the electrical properties of the slotted patch antenna and the design considerations necessary for fabrication using actual varactor diodes.

Stacked Electromagnetically Coupled Rectangular Patch Antenna with Segmented Elements

Afroz Zaman* and Richard Q. Lee

NASA Glenn Research Center
Cleveland OH 44135

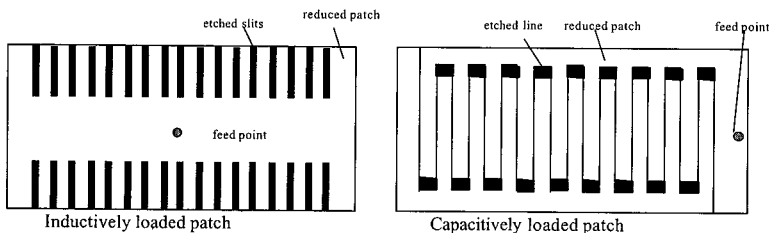
A segmented patch antenna consisting of a driven center element and planar parasitic elements of same resonant length but unequal widths, gap coupled to the non radiating edge of the driven element has been reported previously (*Electron Lett.*, 22, 1064-1065). This antenna showed good impedance matching and radiation characteristics over a wide frequency band. Another approach for bandwidth enhancement using a two-layer, electromagnetically coupled, patch antenna with a gap spacing between the two layers has been reported (*IEEE Trans. Antennas & Propagation*, 38, 8, 1298-1302, 1990). In addition to bandwidth enhancement, the latter technique can significantly improve the gain of the antenna for proper spacing between the layers. The objective of this paper is to investigate the performance characteristics of a stacked antenna configuration with segmented elements. To begin with, a segmented rectangular patch (length=44 mm, width= 58 mm, fabricated on a 10 mil Duroid substrate, $\epsilon_r = 2.22$, at S band) was analyzed. Based on simulated results, an improvement in bandwidth from 0.015 GHz to 0.055 GHz is observed by segmenting the patch into seven unequal sections compared to the solid patch. However, the efficiency of this planar, segmented structure is very poor and shows significant degradation in gain (from 3.9 dB_i for solid patch to -2.9 dB_i for the segmented one). To offset this gain degradation, a stacked configuration made up of similar segmented elements is analyzed. Preliminary results indicate the validity of our approach and will be optimized for obtaining good bandwidth as well as gain performance. Detailed simulated and measurement results of a segmented stacked antenna will be presented and trade off issues will be discussed.

Antenna patch reduction by inductive and capacitive loading

S.Reed (1), L. Desclos(2) , C. Terret(3) and S. Toutain(1)

- (1) SEI-IRESTE, rue Christian PAUC, BP 60601, 44306 Nantes cedex France .
- (2) NEC USA Inc,CCRL, Princeton NJ,USA.
- (3) LAT - Université de Rennes 1 - France.

Since few years, the telecommunication world is evolving toward mobility and multiservices. These leading words have driven the researchers to find solutions to integrate more and more the devices and antennas in small areas. Handy phones and PC cards are the best supporting examples . In this paper, we are concerned with the size reduction of planar patch antenna. This type of antenna present for the mobile communication systems attractive features such as light weight, low production cost and the possibility to be conformed. This size reduction, if effective enough, will then permit a better integration as well as more possibilities to have a space diversity configuration within the same physical embedding communication device. Several reduction techniques have been already proposed such as introducing slots [M. El Yazidi et al. JINA - nov 1994 , pp. 83-86], shorting the electric field at null point [J. George et al. , Electronics Letters, 14th march 1996, vol.32, , PP. 508-509] or even choosing a special patch geometry[A. Gorur et al, IEEE Microwave and Guided Wave Letters, vol8, Aug. 1998 , pp. 278-279]. Our approach is different and is based on the fact that a patch antenna could be seen as two radiating discontinuities which are generally modeled by two virtual slots. As the length of the patch's edge is nearly half wavelength, the slot fields become in phase and the radiation is in its maximum in their median plane. Under these conditions, we can consider the microstrip patch as a phase shifter which has a feeder role for the two virtual slots. Using the line theory, we develop new structures to link these two virtual radiating elements with loaded transmission lines. It is then possible by structuring either the inner part with a capacitive effect as presented in figure 1a or the edges form with inductive effect as presented in figure 1b, to create the desired phase shifting effect. Using these concepts we develop an analytical model, validated also by moment method calculation, enabling to get from 30% to 50% size reduction in comparison to a classical patch, of 35 mm by 70 mm on a 4.4 permittivity substrate, radiating at 470 MHz. The matching and radiation properties are then the same non reduced patch presenting a size of 35 mm by 140 mm. A good agreement between theory and experimental results has been observed. Several examples of calculation and realizations will be presented for different bands, demonstrating the approach.



Resonant modes of a wide class of microstrip patches fabricated on magnetized ferrites with arbitrarily oriented bias magnetic field.

Rafael R. Boix*, Germán León, Francisco Medina

Grupo de Microondas, Departamento de Electrónica y Electromagnetismo.

Facultad de Física, Avda. Reina Mercedes s/n, 41012, Sevilla, Spain.

E-mail: boix@cica.es. Telephone number: 34-954552891. Fax: 34-954239434.

Microstrip patches can be used either as planar resonators for oscillators and filters or as resonant antennas at microwave frequencies. Since the bandwidth of microstrip patch resonators and antennas around their operating resonant frequencies is known to be very narrow [K. A. Michalski, D. Zheng, *IEEE-MTT*, **1**, 112--119, 1992], it is important to develop accurate algorithms for the computation of those resonant frequencies. Microstrip patch resonators fabricated on magnetized ferrites have been found to have an application in the design of tunable filters with band-rejection response [K. Araki, D. I. Kim, Y. Naito, *IEEE-MTT*, **2**, 147-154, 1982] or band-pass response [T. Fukusako, M. Tsutsumi, *IEEE-MTT*, **11**, 2013-2017, 1997]. The use of magnetized ferrites as substrates of microstrip patch antennas is also advantageous because it makes it possible frequency tuning, radar cross section reduction and achievement of circular polarization with one single feed [D. M. Pozar, *IEEE-AP*, **9**, 1084-1092, 1992].

In this work Galerkin's method in the spectral domain [S. Nam, T. Itoh, *JEWA*, **7**, 635-651, 1988] is applied to the determination of the resonant frequencies and quality factors of microstrip patches fabricated on ferrite substrates in the case in which the bias magnetic field of the ferrites is arbitrarily oriented. Rooftop basis functions are used in the approximation of the current density on the patches, which makes it possible to analyze patches with right-angle corners of arbitrary shape. Special asymptotic extraction techniques based on the interpolation of the spectral dyadic Green's function [R. R. Boix, N. G. Alexopoulos, M. Horno, *JEWA*, **8**, 1047-1083, 1996] are applied for making it possible a fast computation of the double infinite integrals arising from the application of Galerkin's method in the spectral domain. In order to check the validity of the algorithm developed, the results obtained in [W. C. Chew, Q. Liu, *IEEE-AP*, **8**, 1045-1056, 1988] for the resonant frequencies and quality factors of rectangular microstrip patches on a dielectric substrate are compared with our numerical results, and good agreement is found. The numerical results obtained for microstrip patches on ferrite substrates show that there are cutoff frequency bands in which resonances are not possible owing to the excitation of magnetostatic wave modes [V. Losada, R. R. Boix, M. Horno, *IEEE-MGWL*, **6**, 226-228, 1998]. Also, the authors have found that the resonant frequencies of microstrip patches on ferrite substrates can be tuned over a wide range by varying the magnitude of the applied bias magnetic field.



Periodic Structures

Co-chairs: W. X. Zhang, Southeast University, Nanjing
P. Besso, CSELT, Italy **Page**

- 1 8:00 Equivalent circuit model of 2D microwave photonic band gap structures, *M. Rahman**, *M. Stuchly*, University of Victoria, Canada 322
- 2 8:20 Design of diachronic filters for deep space antennas, *P. Besso*, CSELT, *M. Bozzi**, University of Pavia, *P. Gianola*, CSELT, Italy, *R. Madde*, European Space Agency, Germany, *L. Perregini*, University of Pavia, *L. Drioli*, University of Florence, Italy 323
- 3 8:40 Frequency selective surfaces and volumes to enhance performance of broadband reconfigurable antennas, *Y. Erdemli**, *K. Sertel*, University of Michigan, *R. Gilbert*, *D. Kopf*, Sanders, A Lockheed Martin Co., *J. Volakis*, University of Michigan, USA 324
- 4 9:00 Design of multi-frequency band photonic band-gap structures, *G. Poilasne**, University of California, Los Angeles, *L. Desclos*, NEC CCRL, USA, *P. Pouliguen*, *C. Terret*, University Rennes 1, France 325
- 5 9:20 Circularly polarized antenna above metallic photonic band-gap materials, *G. Poilasne**, University of California, Los Angeles, *L. Desclos*, NEC, CCRL, USA, *P. Pouliguen*, *C. Terret*, Universite de Rennes 1, France 326
- 6 9:40 Active metallic photonic band-gap structure performs beam diversity, *G. Poilasne**, University of California, Los Angeles, *L. Desclos*, NEC C&C Research Lab, USA 327

Equivalent Circuit model of 2D Microwave Photonic Band Gap Structures

M. Rahman*, and M. A. Stuchly

Department of Electrical and Computer Engineering, University of Victoria,
P.O. Box 3055, Stn. CSC, Victoria, BC, V8W 3P6, Canada

Photonic band gap structures (PBG) are composite periodic structures that exhibit transmission and reflection bands in their frequency response. Recently, a new class of 2D PBG structure has been emerged. These 2D planar (D. Sievenpiper et. al., MTT, 47, 2050-2074, 1999 and R. Coccioli et. al., MTT, 47, 2123-2130, 1999) PBG structures suppress the surface currents and serve as high-impedance electromagnetic surfaces within the stop band. Due to the high impedance property of this type of structures they are used as ground planes for microstrip antennas. Both the structures mentioned above have been analyzed numerically. The first one has also been modeled with lumped L and C parameters that can only predict the first resonant frequency but not the band gaps.

In this paper we explore an analytical model based on the theory of transmission line and periodic circuits for 2D planar microwave PBG structures. The dispersion diagram of the structure is calculated using the proposed method. A finite-difference time domain (FDTD) method is used for numerical calculation of the transmission coefficient of the structure, in order to verify the analytical model.

As one of the examples we analyze a square array of square metal patches connected to the ground plane through thin wires. The shorting pins provide inductive loading while the small gaps between the patches put additional capacitive loading on them. So, the high-impedance surfaces are basically structures periodically loaded with microstrip resonators. The input impedance of each resonator of the periodic circuit is calculated using the transmission line theory. Then the dispersion diagram is calculated using the theory of periodically loaded structures. Fig.1a shows the results, which is compared with transmission coefficient computed with the FDTD method shown in Fig 1b. The shaded area indicates the surface wave stop band for the structure predicted by the proposed model. An excellent agreement is apparent between the proposed model and the numerical computations.

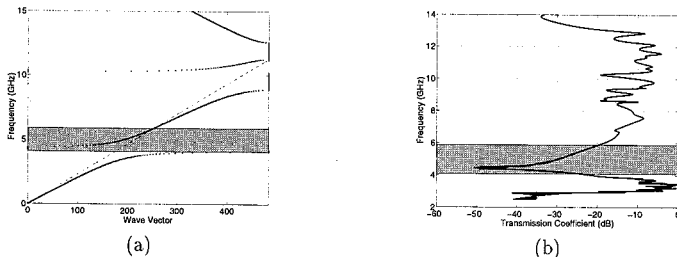


Figure 1: (a) Dispersion diagram, and (b) Transmission coefficient for the analyzed structure.

Design of Dichroic Filters for Deep Space Antennas

Piermario Besso⁽¹⁾, Maurizio Bozzi⁽²⁾, Paolo Gianola⁽¹⁾,
Roberto Maddè⁽³⁾, Luca Perregrini⁽²⁾, and Luca Salghetti Drioli⁽⁴⁾

⁽¹⁾CSELT Centro Studi E Laboratori di Telecomunicazioni
Via Reiss Romoli 274, 10148 Torino (ITALY)

⁽²⁾University of Pavia, Dept. of Electronics
Via Ferrata 1, 27100 Pavia (ITALY)

⁽³⁾European Space Agency, ESOC
Robert Bosch Strasse 5, 64293 Darmstadt (GERMANY)

⁽⁴⁾University of Florence, Dept. of Electronic Engineering
Via S. Marta 3, 50139 Florence (ITALY)

Abstract – This paper presents the preliminary design of a new dichroic plate, transparent for the circular polarization in the Ka-band (31.8–32.3 GHz and 34.2–34.7 GHz) and completely reflecting for the circular polarization in the S- and X-bands.

This dichroic is intended to be used in a Deep Space Antenna (DSA) presently under construction in Australia. The European Space Operations Centre (ESOC) of ESA will use this antenna to support the Rosetta and Mars-Express missions.

The design of this dichroic plate is very critical, due to both electrical and mechanical constraints. With regards to mechanical issues, the plate is huge (3.2 m by 2.25 m, with a perforated area of 2.48 m by 1.75 m) and will be placed at 45° with respect to the horizontal position. With respects to the electrical performance, the antenna cross-polarization level must be lower than -25 dB. This requirement imposes a minimal relative phase shift between TE and TM transmitted fields in the Ka-band and reflected fields in the S- and X-bands, and to control the insertion losses for both the TE and TM fields in the Ka-band.

Three design solutions have been investigated and are presented in this work.

The first solution consists of a metal plate perforated with closely-packed cross-shaped holes. This structure presents a number of degrees of freedom, which allow for a fine-tuning of the electrical performances. Moreover, the crosses can be tightly packed, and this permits to limit the effect of the grating lobes. Nevertheless, some problems arise in the cross-polarization levels in the S- and X-band, due to a not negligible phase shift between the reflected TE and TM modes.

To overcome this drawback, the second design considered rectangular holes, which permit to reduce the cross-polarization effects.

The third design is based on a pair of slots within a periodic cell. This approach permits to separately control the TE and TM modes, thus allowing a better flexibility in the minimization of the cross-polarization level.

The theoretical analysis of these structures, based on the MoM/BI-RME method (M. Bozzi and L. Perregrini, *Electronics Letters*, 35, 1085–1087, 1999), and the automatic optimization routine will be discussed, and the experimental characterization of some prototypes will be presented.

Frequency Selective Surfaces and Volumes to Enhance Performance of Broadband Reconfigurable Antennas

Y. Erdemli*, K. Sertel*, R. Gilbert**, D. Kopf**†, and J. Volakis*

*Radiation Laboratory
Electrical Engineering and
Computer Science Department
University of Michigan
1301 Beal Avenue
Ann Arbor, MI 48109-2122

**†Sanders, A Lockheed Martin Co.
95 Canal Street
P.O. Box 868
Nashua, NH 03060-0868

Conformal antennas are often printed on a planar or curved substrate surface. However, typical substrate configurations are narrowband and thicker substrates result in low efficiencies due to surface wave coupling. Perforated or bandgap substrates have recently been used to increase the efficiency of printed antennas on thicker substrates. However, these approaches are still applicable only to narrowband or multiband antenna structures. When traditional broadband antennas such as log-periodics are printed on substrates, their bandwidth characteristics are altered, and one approach to regain the broadband behavior of the antenna element is to employ frequency dependent substrates or ground planes. This can be achieved by using multiple layers of frequency selective volumes and/or surfaces as part of the substrate in a manner similar to that used for designing broadband microwave filters. Each screen is resonant at a given frequency and is placed a distance $\lambda_r/4$ away from the antenna's surface, where λ_r refers to the wavelength at the screen's resonance frequency.

A multilayer frequency selective surfaces (FSSs) or volumes (FSVs) are needed for optimizing the performance of a broadband antenna. In this paper, we examine various designs of such volumetric periodic surfaces that can be used to enhance the performance of broadband antennas. Of particular concern is the development of frequency selective volumes which reflect with pre-specified phase and amplitude of the reflection coefficient over a broad set of frequencies. Previous emphasis on the design of FSSs has been on the reflectivity performance, whereas in this case, the phase response is of more importance. Modeling of multilayer FSSs and FSVs with different periodicities is another important issue that will be addressed in this presentation.

DESIGN OF MULTI-FREQUENCY BAND PHOTONIC BAND-GAP STRUCTURES

G. Poilasne, L. Desclos[†], P. Pouliguen* and C. Terret*

Electrical Engineering department, UCLA, Los Angeles, CA, 90095, USA

[†]NEC CCRL, Princeton New Jersey, USA, *UPRES-A 6075, Univ. Rennes 1, France

Photonic band-gap materials (PBG) are periodic structures composed of dielectric or metallic material. The different periodicities give them some interesting behaviors similar to electron propagation in semi-conductor materials. They exhibit frequency bands inside which no propagation mode exists. Between these band-gaps are propagation bands with different corresponding modes. These structures are very attractive for antenna applications as they can enhance the gain or shape the radiation pattern. For structure initially composed of dielectric material only, it has been shown that adding metallic wires can enlarge the frequency band-gap. These so called metal-dielectric PBG are a very interesting evolution of PBG since they offer the possibilities to improve the basic behavior of all dielectric PBG. Unfortunately, their design is still hard and yet has to be solved, especially for future multi-mode communications systems applications involving multiple frequency bands. It is then important to clarify the involved mechanisms and give useful tools to design such structures. Therefore, the authors have studied a mixed MPBG - Bragg mirror structure - Fig. 1-, to obtain a wide band-gap, taking into account the effective medium. A realization made out of Pyrex and foam incorporating metallic wires has been characterized. Experiments have shown that the control of propagation bands is not so obvious as propagation peaks still remained. But, the simple behavior of each structure (without taking into account an effective medium) could be sufficient to determine the behavior of the whole structure. Further investigations have been carried out, merging two different PBG. Fig. 2 presents numerical results of a mixed PBG composed of a continuous structure and a discontinuous one. This behavior is compared to the response of the both structures when isolated. It shows that when one structure exhibits a band-gap and the other a propagation band, the mixed structure exhibits a band-gap (left part of figure 2). It also shows that when both MPBG are alone they exhibit a band-gap, however the mixed structure exhibits a propagation band (right part of figure 2).

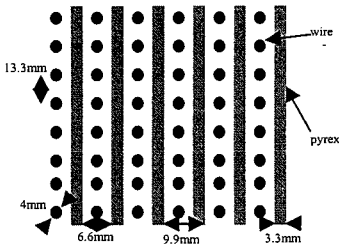


Fig. 1: MPBG and Bragg mirror mixed structure

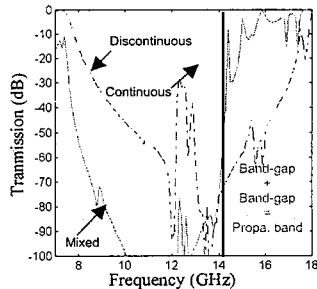


Fig. 2: Transmission coef. of a mixed structure composed of a continuous wire MPBG and a discontinuous wire one.

These results have led to establish laws in order to design complex and multiple frequency structures in a systematic way. For example, to design a double frequency MPBG, two MPBG with the same period can be designed for each frequency band. The mixed structure corresponds to the specifications as long as the targeted band-gaps of isolated MPBG do not overlap undesired gap, otherwise they vanish. More examples will be given in the conferences and the laws will then be drawn.

CIRCULARLY POLARIZED ANTENNA ABOVE METALLIC PHOTONIC BAND-GAP MATERIALS.

G. Poilasne, L. Desclos[†], P. Pouliguen* and C. Terret*
Electrical Engineering department, UCLA, Los Angeles, CA, 90095, USA
[†]NEC, CCRL, Princeton New Jersey, USA
* UPRES-A 6075, Universite de Rennes 1, France

Abstract:

In certain circumstances circularly polarized antennas could be more efficient than simple linear polarized ones, for indoor telecommunications. In fact, it reduces distortions due to reflections on the walls and all other depolarization sources. In order to have a circularly polarized antenna, different possibilities can be considered (Fujimoto and James, artech house 1991). Patch antennas are often used, especially at millimeter wave frequencies. By changing their shapes or introducing a slot on them, they can radiate a circularly polarized field. However, under classical technological assumptions, their working bandwidth remains narrow. Printed spiral antennas can also be used, but they need a reflector, which reduces the working bandwidth. Axial ratio beamwidth can also be a limitation.

In this communication, we propose to use metallic photonic band-gap materials (MPBG) in order to improve axial ratio beamwidth and working bandwidth of circularly polarized antennas. MPBG are periodic structures composed of metallic parts. The reflection characteristics of MPBG depend on frequency, (E. Yablonovitch, Physical Review Letters, Vol.58, n°20, 1987, pp.2059-2062). They exhibit bands in which there is no propagation mode inside the structure. Their behaviors are different when they are excited by two orthogonal polarized waves and the evolution of these behaviors regarded to the frequency and the direction of emission can really be interesting in order to improve antenna characteristics.

Therefore, to design MPBG for circular polarization applications, their reflection and transmission characteristics must be determined for two linear and orthogonal polarizations. For example, in the case of a simple 2D structure composed of metallic wires, when it is excited by a plane wave with the E field parallel to the wire axis, the MPBG exhibits a band-gap starting from 0Hz to a cutoff frequency depending on the physical parameters (period, wire diameter,...). When the E field is orthogonal to the wire axis, frequencies corresponding to the previous band-gap now corresponds to a propagation band. If a circularly polarized antenna is placed above this structure, the MPBG reflects the parallel polarization and transmits the orthogonal one -Fig.1-a)-. This configuration allows improvement of the polarization of the emitting antenna (G. Poilasne et al., Proc. ICEAA, Torino, Italy, September 15-18, 1997). Moreover, the angular characteristics of the reflection coefficient can also improve the axial ratio of the antenna over the whole space.

An improvement of the axial ratio 3 dB aperture has been obtained on more than 80 deg in comparison with a classical 30 deg for the antenna alone. This shows the potential use of MPBG with circularly polarized antennas. Different configurations are now investigated in S and C bands. Numerical and experimental results will be given at the conference

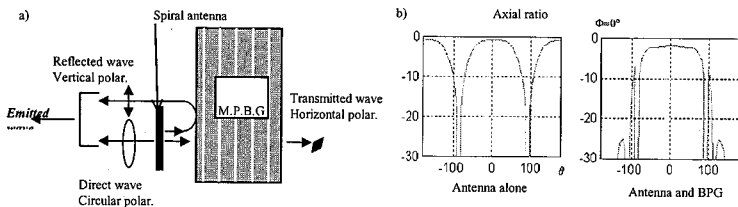


Fig.1: Phenomenon around the antenna and Axial ratio improvement.

ACTIVE METALLIC PHOTONIC BAND-GAP STRUCTURE PERFORMS BEAM DIVERSITY

G. Poilasne and L. Desclos*

Electrical Engineering department, University of California at Los Angeles,
Los Angeles, CA, 90095, USA

*NEC C&C Research Lab., Princeton New Jersey, USA

Abstract: Latest indoor communication systems often need a diversity solution to cope with fading effects. One of these solutions could be the beam diversity switching. It often consists in switching from one antenna to another one or beam forming directly an active array. In this communication we propose another solution which doesn't involve directly the antenna itself but more its surrounding. In order to make an active beam forming we compose actively with the material in which the antenna is embedded. This material is a metallic photonic band-gap material (MPBG). MPBG are periodic structures composed of metallic wires. Their electromagnetic characteristics are frequency dependent. They exhibit bands in which there is or not propagation mode. These characteristics also depend on the direction of propagation (E. Yablonovitch, Physical Review Letters, Vol.58, n°20, 1987, pp.2059-2062).

MPBG composed of continuous wires and MPBG composed of discontinuous wires have opposite responses. Therefore, exploiting these differences can lead to interesting applications if we can switch from one structure to the other (i.e. from continuous to discontinuous wires). In order to obtain this behavior, one solution consists in adding active components on discontinuous wires to connect the different element along their axis. As the active components are used in an ON/OFF state, it can easily be implemented in an electromagnetic simulator based on a moment method to optimize the structure. In our case, field effect transistors have been used as switches. The authors have already demonstrated that, with such a structure, the ON/OFF control and beamwidth control as well, were effective (G. Poilasne et al, IEEE Trans on AP, Jan. 2000). The functionality presented in this communication is more advanced since based on an extended study of propagation modes inside the structure. In fact, it allows to choose between two types of radiation patterns. By adjusting the frequency band-gaps of discontinuous and continuous structures within the same embodiment, it is possible to excite two different modes inside the structure with different directions of propagation at the same frequency, depending of the component states. This basically comes from the fact that, when a dipole is placed inside a continuous MPBG and works at a frequency corresponding to a propagation mode of the structure, a narrow beam is radiated. When the antenna is placed inside a discontinuous wire MPBG and works at a frequency corresponding to the beginning of the band-gap for normal incident plane wave, the field can still propagate in other directions and a dual beam is radiated.

Optimizing the physical dimensions (period, wire diameter, wire length for the discontinuous structure), the desired behaviors can be obtained at the same frequency. The key points of this design will be outlined. Finally as a result we can see in Fig.1 the two different diagrams obtained by introducing a dipole working at 2.4 GHz within an active structure. This shows a state ON for the switch which gives a single beam pattern of 30 deg. at 3dB aperture, as when the switches are commuted it gives two beams at 40 deg from each other, with a 20 deg. aperture. These results encourage the research for an application in base station switching in mobile communication.

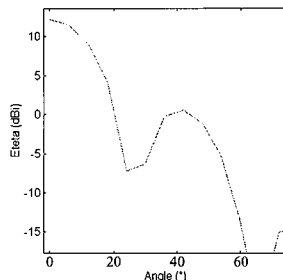


Fig.1 Mono- and dual-beam radiation patterns

Rough Surfaces and Random Media

Co-chairs: L. Carin, Duke University
G. Pan, Arizona State University

Page

1	12:00	Input impedance measurements for half-wave dipole radiating over a rough surface, <i>J. Catton, S-W. Lee, J. Rockway*, Y. Kuga, A. Ishimaru, University of Washington, USA</i>	330
2	12:00	Input impedance of a half-wavelength dipole above a randomly rough surface, <i>T. Chiu*, National Central University, Chung-Li, K. Sarabandi, University of Michigan, USA, E. Li, National Chi-Nan University, Nantou</i>	331
3	12:00	Radar backscatter image comparisons of analytical and numerical models for rough surface scattering, <i>H. Kim*, J. Johnson, The Ohio State University, USA</i>	332
4	12:00	On 3D rough surface scattering using the Coifman wavelets, <i>M. Toupikov, Y. Tretiakov, G. Pan*, Arizona State University, USA</i>	333
5	12:00	Analysis of three dimensional scattering from random rough surfaces with buried penetrable objects for mine detection applications, <i>M. El-Shenawee*, E. Miller, C. Rappaport, Northeastern University, USA</i>	334
6	12:00	Numerical simulations of thermal emission from random dielectric rough surfaces based on physics-based two-grid method, <i>L. Zhou*, L. Tsang, Q. Li, University of Washington, USA, K. Chen, National Central University, Chung-Li, C. Chan, University of Hong Kong, Hong Kong</i>	335
7	12:00	MRTD modeling of wideband scattering from a fractal surface, <i>T. Dogaru, L. Carin*, Duke University, USA</i>	336
8	12:00	Modelling of radiowave scattering from turbulent jet creating of space vehicle in the upper atmosphere, <i>V. Spitsyn*, Tomsk State University, Russia</i>	337
9	12:00	Stochastic model of wave propagation in the jet with inhomogeneous profile of velocity and concentration of turbulences, <i>V. Spitsyn*, L. Kudryashova, Tomsk State University, Russia</i>	338
10	12:00	Computation of light scattered into a detector, <i>E. Marx*, National Institute of Standards and Technology, USA</i>	AP
11	12:00	Moment Method simulations of electromagnetic scattering from conducting random rough surfaces using wavelet basis, <i>M. Xia*, C. Chan, S. Li, City University of Hong Kong, Hong Kong</i>	AP
11	12:00	Multiple Sweep Method of Moments (MSMM) analysis of electromagnetic scattering from targets on ocean-like rough surfaces, <i>D. Colak*, R. Burkholder, E. Newman, The Ohio State University, USA</i>	AP

Input Impedance Measurements for Half-Wave Dipole Radiating over a Rough Surface

J. Catton, S-W Lee, J.D. Rockway*, Y. Kuga and A. Ishimaru

*Department of Electrical Engineering
University of Washington, Box 352500
Seattle, Washington 98195-2500
Email: ishimaru@ee.washington.edu*

In electromagnetics, the Green's function provides the propagation mechanism by which objects interact and scatter. Recently we have investigated several properties of a rough surface Green's function that is applicable to rough surfaces with small rms heights. We now focus on the response of a radiating object within the presence of the rough surface. The description of the scattering process will be provided by the stochastic Green's function. Several approximations are made to develop an electric field integral equation (EFIE) to calculate the coherent and incoherent fields. The stochastic EFIE is solved to determine the mean and incoherent currents for an antenna suspended above the rough surface.

To examine this problem, we calculate the current distributions produced by an excited $\frac{1}{2}$ wave dipole located above a conducting rough surface with small rms heights. The input impedance of the antenna is calculated from recent experimental and numerical simulations. In the experiment, a $\frac{1}{2}$ wave dipole of vertical and horizontal orientations is suspended above a "smooth" rough surface. The input impedance is measured and compared to a flat surface case. These measurements are then compared to the currents produced by the modified EFIE that has been implemented in MININEC. A study of the input impedance versus rms height is studied and analyzed.

Input Impedance of a Half-Wavelength Dipole above a Randomly Rough Surface

Tsenchieh Chiu*

**Department of Electrical Engineering,
National Central University, Chung-Li, 32054, Taiwan**

Kamal Sarabandi,

**Department of Electrical Engineering and Computer Science
University of Michigan, Ann Arbor, MI 48109-2122, USA**

Eric S. Li

**Department of Electrical Engineering,
National Chi-Nan University, Nantou, Taiwan**

The problem of electromagnetic wave propagation, excited by a short dipole, above a dielectric ground plane has been long considered as a research topic of great interest. Recently, this problem has been extended more practically to include dielectric rough surface, since it is considered that the presence of the rough surface could effectively reduce the surface reflectivity. Also the incoherence scattering from the rough surface could play an important role in the short-term fading. To simulate a common ground point-to-point communication, the dipole and the observation point are both close to the ground and are far away to each other. In this case, the incidence angle of the radiated field to the surface is large. However, as predicted by the Rayleigh criterion, the effect of the surface roughness on the radiated field under this situation can almost be ignored.

In this paper, the attention is turned to the effect of the surface roughness on the input impedance of the half-wavelength dipole antenna. When the dipole is close to the dielectric ground surface, the mutual coupling between the antenna and the surface roughness could significantly change the value of the input impedance, which is usually calculated assuming the smooth ground surface. In our study, first, the average scattered field from the rough surface is incorporated into half-space Green's function. Using the method of moment in conjunction with this Green's function, the average input impedance is calculated. Then, the uncertainty of the input impedance caused by the incoherent scattering from the random rough surface is also computed. The description of effect of the different surface roughness and the polarization of the antenna will be given in the presentation.

Radar Backscatter Image Comparisons of Analytical and Numerical Models for Rough Surface Scattering

H. Kim* and J. T. Johnson

ElectroScience Laboratory
The Ohio State University
1320 Kinnear Rd., Columbus, OH 43212
Tel: (614)292-7981, Fax: (614)292-7297
e-mail: hjk@esl.eng.ohio-state.edu

The recent development of efficient analytical and numerical models is allowing new insights into electromagnetic scattering from random rough surfaces. Although analytical models provide physically based prediction of scattering properties for rough surfaces, detailed scattering behaviors, especially at lower grazing angles, have not yet been understood completely. In this paper, we investigate analytical and numerical models for one dimensional rough surface profiles by means of radar imaging based on back-projection tomography using backscattered field calculations. The approximate theories applied include the physical optics (PO) approximation, small perturbation method (SPM), and the small slope approximation (SSA). In particular, we will present initial results for complete 2nd order (3rd order in slope) as well as incomplete 3rd and 4th order SSA in terms of average radar cross sections from given surface statistics.

Radar images are formed through the wide range of frequency- and angular-swept backscatter data with a proper choice of frequency and angular sampling to allow unambiguous down and cross ranges. Due to the memory requirements in 2nd order SSA calculations, the images describing 2nd or higher order SSA will be confined up to moderate incident angles. Images obtained from the analytical methods are compared to numerical results for several surface profiles. The numerical methods involve an iterative method of moments accelerated either with a canonical grid expansion or a spectral acceleration technique. Various scattering features captured from the images will be analyzed to determine the applicability of approximated models. The major and secondary scattering events, angular dependencies and polarization effects observed from the images will also be discussed.

ON 3D ROUGH SURFACE SCATTERING USING THE COIFMAN WAVELETS

M. Toupikov, Y. Tretiakov and *G. Pan

Department of Electrical Engineering, Arizona State University, Tempe, AZ

Rough surface scattering has been studied by analytic techniques, including the Kirchhoff method, small perturbation method, Wiener-Hermite expansion among others. Nonetheless, these methods are limited by parametric constrains, such as a large radius of curvature, small height, non-grazing incident angles. Numerical solutions may overcome these limitations and provide more flexibility. However, due to the extremely large scales and prohibitively high computational costs, most numerical approaches available can only handle 2D Maxwell's equations, i.e., 2D scattering problems.

In this paper, the Coifman wavelets are used as basis and testing functions to solve integral equations via the Galerkin method. Very sparse impedance matrix has been obtained, due to zero moments, multiresolution analysis and localization (strictly in space and approximately in spectrum) property of the Coifman wavelets. Wavelets have already been applied for the scattering problems on rough surfaces by different authors before, where matrix has been filled by using a standard moment method and then sparsified via wavelet transform. This leads to the excessive and unnecessary work of calculating matrix entries of orders $O(N^2)$. In contrast, in this paper authors have utilized the Dirac- δ like property of the Coifman scaling functions. As a result, the majority of entries in the impedance matrix are evaluated by the one-point quadrature, i.e., without using numerical integration such as the Gauss-Legendre quadrature. Zero entries of the impedance matrix are identified a priori without performing numerical integration and subsequent thresholding. The error analysis of the one-point quadrature is also provided.

Numerical results from perfect conducting random 2D surfaces (3D scattering) are compared with analytical solutions and laboratory measurements.

Analysis of Three Dimensional Scattering from Random Rough Surfaces with Buried Penetrable Objects for Mine Detection Applications

M. El-Shenawee, E. Miller and C. Rappaport
Center for Electromagnetics Research
Department of Electrical and Computer Engineering
Northeastern University
360 Huntington Ave., Room 235 Forsyth Bld
Boston, MA 02115
magda@cer.neu.edu

The analysis of scattering and transmission of electromagnetic waves in the presence of a random rough dielectric interface and in the nearfield of the sensing systems is a crucial step for subsurface object detection problems in general and landmine remediation applications in particular. Generally, this fully three dimensional problem must be treated numerically, however the calculation of the required fields using conventional techniques (e.g. moment method, finite elements, or finite differences) is a computationally intensive undertaking especially for large dielectric constants. The complexity of the problem dramatically increases upon inserting objects under the rough interface especially when these objects are penetrable. Therefore a fast and accurate computational technique is needed for such applications.

The integral equation-based Fast Multipole Steepest Descent Method (SDFMM), that was originally developed at the University of Illinois (UIUC), will be modified and expanded here to analyze this intensive scattering problem. The rough surface is assumed a random one characterized with Gaussian statistics for the height with zero mean. A single penetrable object is buried at less than one wavelength beneath the mean plane of the rough interface. The incident wave, which is located above the surface, is assumed to be a Gaussian beam that is carefully tapered to minimize surface edge excitations. The PMCHW (Poggio, Miller, Chang, Harrington, and Wu) integral equations are implemented in this work for three regions; air, soil, and buried object. Upon applying the appropriate boundary conditions of the electric and magnetic fields on the air-soil interface, four integral equations are obtained. Both the rough surface and the buried object are discretized into triangular patches. The moment method surface currents are approximated using the RWG (Rao, Wilton, and Glisson) vector basis functions. The interactions between the rough surface and the buried object are fully taken into account here. Thorough investigation will be conducted to test several approximations to ignore some of these interactions aiming to simplify the involved intensive calculations.

Results for the near field complex vectors will be shown. Monte Carlo simulations will be conducted to obtain the statistics of both scattered and transmitted near fields as functions of receiver position, frequency, and incident angle. This work can be extended to include several buried objects of different dielectric constants and/or perfectly conducting ones. The ultimate objective of this research is to analyze, understand and consequently to be able to differentiate between scattering from buried objects and scattering from rough surfaces, clutter in this case.

Numerical Simulations of Thermal Emission from Random Dielectric Rough Surfaces Based on
Physics-Based Two-Grid Method

Lin ZHOU¹, K. S. CHEN², Leung TSANG¹, Qin LI¹, and C. H. CHAN³
¹Laboratory of Applications and Computations in Electromagnetics and Optics

Department of Electrical Engineering, Box 352500

University of Washington, Seattle, Washington 98195-2500

Fax: (206) 543-3842 Email: tsang@ee.washington.edu

²Center for Space and Remote Sensing Research

National Central University

Chung-Li, Taiwan 32054

³Department of Electrical Engineering, City University of Hong Kong

83 Tat Chee Avenue, Kowloon, Hong Kong

Bistatic scattering and emission of soil surfaces with inhomogeneous soil moisture profiles and ocean surfaces with large permittivities are studied by using numerical simulations. For such cases, the surfaces have to be discretized with a dense grid in order to calculate accurate results for the surface fields because the Green's function of the lower medium and the surface fields have large spatial variation. In addition, the integration for near-field interactions is included in calculations. Accurate bistatic scattering coefficients are particularly important for the calculation of emissivities of rough surface which have to be accurate to within 1% for passive remote sensing applications. Dense grid requires more CPU time and memory. To circumvent the problem, we have developed a physics-based two-grid method (PBTG). This is based on two observations: (1) Green's function of lossy medium is attenuative and (2) the free space Green's function is slowly varying on the dense grid. The first property gives a sparse submatrix for the Green's function of the lossy medium. The second property allows us when using free space Green's function on the dense grid, to first average the values of surface unknowns on the dense grid, and then place them on the coarse grid. After completing multiplication of matrix and vector, the products are placed on the dense grid by interpolation. We use 64 points per square wavelength for the coarse grid and up to 1024 points per square wavelength for the dense grid. A bivariate interpolation is used to transfer values from coarse grid to dense grid. It has been shown that the PBTG can efficiently compute the accurate surface fields on the dense grid in terms of CPU time and memory requirements. The numerical results of emission in terms of physical roughness parameters are illustrated as a function of frequency, soil moisture and ocean wind. Results are compared with those from the second order small perturbation method and from Q and H empirical models. It is found that the empirical parameters Q and H are dependent on soil moistures, frequencies, and observation angles.

MRTD Modeling of Wideband Scattering from a Fractal Surface

Traian Dogaru and Lawrence Carin
Department of Electrical and Computer Engineering
Duke University
Box 90291
Durham, NC 27708-0291

The multiresolution time-domain (MRTD) method was recently introduced in the analysis of various electromagnetic field problems. The MRTD often yields important savings in computational resources, *vis-à-vis* the traditional FDTD, without sacrificing solution accuracy. In the MRTD algorithm, the fields are expanded in a wavelet basis, and Maxwell's curl equations are discretized using a method-of-moments procedure. Higher resolution (in the form of wavelets) is introduced in zones with relatively fast spatial field variation, while keeping a lower-resolution representation (in the form of scaling functions) in the slowly varying regions. This approach can be related to data compression techniques, in which the wavelet basis functions have proven extremely useful for a large number of applications.

The purpose of the paper is to address the advantages of the MRTD algorithm in modeling rough interfaces, as compared with the FDTD scheme. In particular, at the same discretization rate, the MRTD rough-surface model is more accurate than its FDTD staircase counterpart; *i.e.*, relative to the FDTD, MRTD can model scattering from the same rough surface with coarser spatial sampling, without losing accuracy, thereby reducing computer-memory requirements and CPU time. In addition to its advantages concerning the rough surface itself, the MRTD algorithm also only employs a high-resolution spatial grid (in the form of wavelets) in certain regions of the computational domain (as opposed to the classic FDTD scheme which uses a uniform grid everywhere), leading to further savings in computational resources. Short-pulse time-domain scattering is considered from several dielectric fractal surfaces, with MRTD and FDTD results compared.

Modelling of Radiowave Scattering from Turbulent Jet Creating of Space Vehicle in the Upper Atmosphere

Vladimir G. Spitsyn

Tomsk State University, Siberian Physical and Technical Institute,
Revolution square, 1, Tomsk, 634050, Russia,
Tel: 7-3822-412797, Fax: 7-3822-233034,
e-mail: spic@elefot.tsu.ru

In this investigation is suggested the numerical model of scattering radiowave on a turbulent jet creating of space vehicle in a low ionosphere. The surface of conical turbulent jet is supposed to be beams source. The ionosphere out of disturbance domain is supposed to be of spherical layers. In this work there are tabulated the trajectories of radiowaves, refracting in ionosphere. In order to solve this problem is used the method of numerical analysis of electromagnetic wave propagation in the discrete random media (V.G. Spitsyn, IEEE AP-S Intern. Sympos., Atlanta, USA, 1, 112-115, 1998).

We suppose the correspondence of the turbulences to the discrete random scatterers moving down the jet along its surface. These discrete random scatterers have a stochastic component of velocity which distributed by the Gauss law. Here there are investigated the isotropic, Lambert and quasi-mirror types of scatterers indicatrix. Further we turn to the modelling of the radiowave scattering process on the surface of conical turbulent jet created by space vehicle by the method of Monte-Carlo.

The initial parameters of this model are: the co-ordinates of radio transmitter and receiver, the worker frequency of transmitter, the parameters, characterizing ionospheric plasma condition, the co-ordinates of space vehicle and the parameters of conical jet. As a result of work of the model is carried out the graphic construction of lighted domain of the Earth surface. Then we calculate the dependence of Doppler frequency shift, a radar cross section, and zenith and azimuth angles of receiving signal from the time. The comparison of calculating frequency spectrum of scattering signal on the turbulences of space vehicle jet with experimental data demonstrates its satisfactory conformity.

**Stochastic Model of Wave Propagation in the Jet with
Inhomogeneous Profile of Velocity and Concentration of Turbulences**

Vladimir G. Spitsyn, Lubov N. Kudryashova
Tomsk State University, Siberian Physical and Technical Institute,
Revolution square, 1, Tomsk, 634050, Russia,
Tel: 7-3822-412797, Fax: 7-3822-233034,
e-mail: spic@elefot.tsu.ru

In this work there are suggested the stochastic model of electromagnetic and ultrasonic wave propagation in the turbulent jet of weak ionized gas and liquid. Here there are assumed that the wavelength less than the transverse size of jet and the distance between turbulences. We suppose the correspondence of the turbulences to the discrete random scatterers, having the inhomogeneous profile of concentration and velocity. Here there are analysed the turbulent jets with circle, ellipse and rectangular transverse cross-sections.

In order to solve this problem is used the method of numerical analysis of electromagnetic wave propagation and absorption in the turbulent jets (V.G. Spitsyn, IEEE AP-S Intern. Sympos., Orlando, USA, 4, 2532-2535, 1999). Here there are take place the accumulation of Doppler shift of frequency of multiple scattering signal in the process of modelling.

In this investigation are analysed the dependences of angular and frequency spectrums of scattering signal from the optical thickness of turbulent jet, the types of its transverse cross-sections and the parameters, characterizing of inhomogeneous structure of velocity and concentration of scatterers. The comparison of calculating frequency spectrum of scattering ultrasonic signal on the turbulent jet of water with experimental data demonstrates its satisfactory conformity.

Ultra-Wideband Systems and Measurements

Chair: M. Morgan, Naval Postgraduate School

Page

1	12:00	A sampling receiver for subsurface sensor, <i>J-S. Lee*</i> , <i>C. Nguyen</i> , <i>Texas A&M University, USA</i>	340
2	12:00	Ultra-wideband synthetic aperture radar for detection of unexploded ordnance: modeling and measurements, <i>A. Sullivan</i> , <i>R. Damarla</i> , <i>Army Research Laboratory</i> , <i>Y. Dong</i> , <i>L. Carin*</i> , <i>Duke University, USA</i>	341
3	12:00	Impulsive field computation and measurement, <i>M. Morgan*</i> , <i>Naval Postgraduate School, USA</i>	342
4	12:00	Ultra-wide-band synthetic aperture radar imaging through complex media, <i>L. Cai*</i> , <i>E. Walton</i> , <i>The Ohio State University, USA</i>	343
5	12:00	Design and performance of an ultra-wideband random noise foliage penetration radar, <i>J. Henning*</i> , <i>R. Narayanan</i> , <i>X. Xu</i> , <i>University of Nebraska, USA</i>	344
6	12:00	Measurement and modelling of transient TEM horn antennas, <i>I. Morrow*</i> , <i>A. Moumen</i> , <i>P. van Genderen</i> , <i>Delft Technical University, The Netherlands</i>	345
7	12:00	High resolution analysis of antenna measurements using the oversampled Gabor transform, <i>Z. Altman*</i> , <i>B. Fourestié</i> , <i>J. Wiart</i> , <i>France Telecom, France</i>	346
8	12:00	Comparison of time-domain responses of reflector and phased array antennas, <i>D. Leatherwood</i> , <i>L. Corey</i> , <i>R. Cotton*</i> , <i>B. Mitchell</i> , <i>J. Hampton</i> , <i>Georgia Tech Research Institute, USA</i>	AP

A SAMPLING RECEIVER FOR SUBSURFACE SENSOR

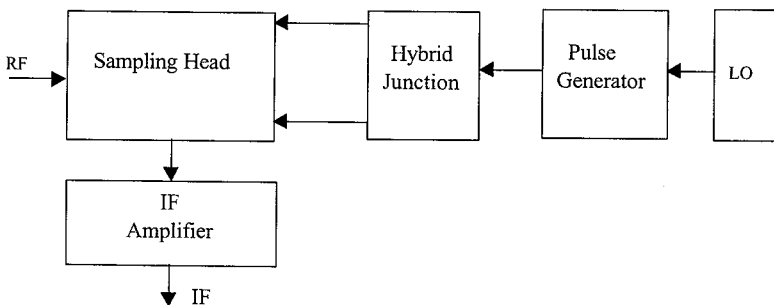
Jeong-Soo Lee* and Cam Nguyen

Department of Electrical Engineering
Texas A&M University
College Station, Texas 77843-3128
E-mail: cam@ee.tamu.edu

ABSTRACT

Sampling receiver is an essential subsystem in pulsed radar. Existing sampling receivers require two-sided circuit processing, resulting in high complexity and fabrication cost.

In this paper, we report the development of a new sampling receiver completely fabricated using coplanar waveguide and slot line. The use of these uniplanar transmission lines allows the entire receiver to be fabricated on only one side of the substrate, which is highly desired for simplicity and low cost. The receiver's block diagram is shown below and consists of LO, pulse generator, hybrid junction, sampling head, and IF amplifier. The pulse generator generates a step function from the LO signal, which is then fed to the hybrid junction to produce two opposite pulses for gating the sampling diodes. The sampling head is used to sample, hold, and convert the RF signal into an IF signal. The receiver exhibits a conversion gain from 12 to 15.5 dB over a RF frequency of 0.01-3 GHz with 10-MHz LO and sampling pulses around 100 ps. It is used in pulsed radar for subsurface sensing applications. Analysis, design, and performance of this receiver will be presented.



Ultra-Wideband Synthetic Aperture Radar for Detection of Unexploded Ordnance: Modeling and Measurements

Anders Sullivan and Raju Damarla
Army Research Laboratory
Microwave and Sensors Branch
Adelphi, Maryland 20783

Yanting Dong and Lawrence Carin
Department of Electrical and Computer Engineering
Duke University
Box 90291
Durham, North Carolina 27708-0291

Although radar-based subsurface sensing is an old technology, until recently there has been very little rigorous modeling done to characterize the target response as a function of frequency, polarization, incidence angle, target geometry and soil type. In previous work, we initially restricted ourselves to those targets that had body-of-revolution (BoR) symmetry, thereby significantly reducing the computational complexity of the problem. For unexploded ordnance (UXO) targets, whose shape and orientation in the soil may be completely arbitrary, the BoR analysis is inappropriate. In the work presented here, we therefore consider a MoM analysis for arbitrary perfectly conducting targets in a layered medium, with the lossy, dispersive layers representing the typical layered character of many soils. In addition to the aforementioned MoM model, we have developed fast multipole method (FMM) and multi-level fast multipole algorithm (MLFMA) models for electrically large conducting targets above or embedded within a lossy half space. The FMM and MLFMA schemes are particularly important at higher frequencies, for which the MoM is computationally less efficient.

Synthetic aperture radar images from actual UXO are presented for data collected with the US Army Research Laboratory BoomSAR, it a fully polarimetric experimental radar system, characterized by four TEM antennas placed atop a 40 m boom lift. The measurements have been performed in Yuma, AZ and at Eglin Air Force Base in northern Florida (both in the United States). The BoomSAR operates directly in the time domain, covering an instantaneous bandwidth of 50-1200 MHz. Several comparisons are made between measured and computed SAR images, the latter simulated via the MoM forward solver.

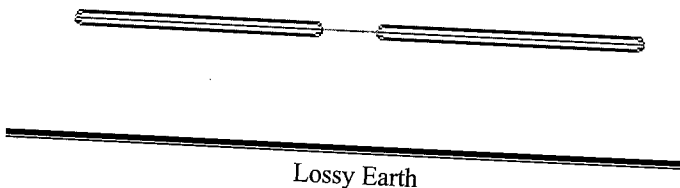
IMPULSIVE FIELD COMPUTATION AND MEASUREMENT

Michael A. Morgan
ECE Department, Naval Postgraduate School
833 Dyer Road, Monterey, CA 93943-5121

Near-fields of UWB impulse-driven antennas located over ground are computed and compared to experiments. Time-domain fields are calculated by first employing stepped-frequency NEC-4 calculations using wire-grid modeling of the antennas over the earth as depicted in the figure below.

Near-field frequency-domain data is extracted from the NEC output file and post-processed using inverse FFT based algorithms programmed in MatLab. Specific impulsive excitation is introduced in post-processing by either circuit modeling of the impulse generator or by way of measured terminal voltages or currents. The procedure employed includes the frequency-dependent effects of impedance mismatch, lossy earth and penetration of impulsive fields into structures.

Comparisons of computations and experimental data will be shown for measurements of near-fields produced by impulsively driven asymmetric horizontal dipoles over ground. Animations of computed fields in the region near to the dipoles will be displayed and discussed.



Ultra-Wide-Band Synthetic Aperture Radar Imaging through Complex Media

Lixin Cai and Eric K. Walton

The Ohio State Univ., Dept. of Electrical Eng., ElectroScience Lab.
1320 Kinnear Rd., Columbus, OH, 43212-1191, U.S.A.

Classical Ultra-Wide-Band (UWB) Synthetic Aperture Radar (SAR) imaging techniques based on free space propagation and tomographic back-projection may suffer significant distortion when a target of interest is located in a complex environment such as behind a building wall, underground or embedded in foliage.

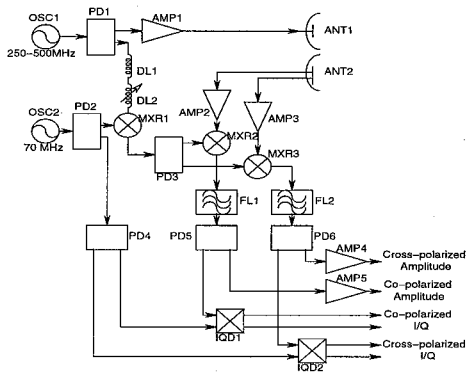
An independently derived analytical solution for radar signal propagation (and back-projection) through a uniform dielectric wall or a uniform dielectric half-space is obtained by the authors. A new and computationally efficient model-based iterative SAR image refocusing algorithm based on the above first-order solution is developed. The algorithm permits non-uniform spatial sampling of imaging data, and cases where a radar unit may be in the radiating near-field of a target. This technique requires knowledge of a specific medium (or media) involved. Parameters such as average wall, ground or foliage dielectric constant and wall physical (or electrical) thickness may be estimated directly from imaging data or separately from other probing techniques. A priori knowledge of medium parameters (from experience) is normally a useful starting point.

This algorithm is applied to both simulated and measured data. Resulting SAR images are shown to be significant improvement over those generated by classical free-space tomographic back-projection techniques.

Design and Performance of An Ultra-Wideband Random Noise Foliage Penetration Radar

Joseph A. Henning*, Ram M. Narayanan, and Xiaojian Xu
Department of Electrical Engineering and Center for Electro-Optics
University of Nebraska, Lincoln, NE 68588-0511
Tel: 402-472-5141, Fax: 402-472-4732, Email: rnarayanan@unl.edu

The University of Nebraska-Lincoln has developed and field tested a coherent ultra-wideband polarimetric random noise radar system which shows great promise in its ability to covertly image targets and terrain obscured by foliage. The block diagram of the radar system is shown in the following figure.



The system operates over the 250-500 MHz frequency band with a transmit power of 1 W and uses broadband dual-polarized log-periodic antennas with a gain of 7.5 dB. The noise figure of the front-end receiver is 3 dB. The system uses the technique of heterodyne correlation at an intermediate frequency of 70 MHz to preserve phase coherence and allow polarimetric imaging. Range scanning is performed using a 7-bit coaxial cable delay lines that can be stepped from 0-127 nsec in steps of 1 nsec. The range resolution of the system is 60 cm in air.

Detection and localization of targets hidden by foliage is accomplished by correlating the reflected waveform with a time-delayed replica of the transmitted waveform. The ultra-wide bandwidth of the transmitted signal provides fine range resolution. Since the receiver utilizes heterodyne cross-correlation, coherent processing algorithms can be used to enhance the detection of targets, reduce clutter effects, and sharpen azimuth resolution. A modified apodization-filtering technique has been implemented for reducing range sidelobes and thereby enhancing the image. Simulation studies, theoretical analyses, and experimental measurements show that the system is capable of imaging obscured objects with high resolution, and that its performance is comparable to coherent stepped frequency systems operating over the same frequency band. The principal advantages of the random noise radar include its ability for covertness and simplified signal processing.

Measurement and Modelling of Transient TEM Horn Antennas

I. L. Morrow, A. Moumen and P. van Genderen
Delft Technical University
ITS-IRCTR, Mekelweg 4, P.O. Box 5031
2600 GA Delft, The Netherlands
Email: I.Morrow@its.tudelft.nl

Ultra-wide-band transient antennas are increasingly finding applications as high-fidelity sensors with many potential applications in telecommunications and direction finding but herein with particular reference to ground penetrating radar. The problem of determining transient radiation from a three-dimensional geometrical structure is accomplished via two independent treatments. Numerical computation using the Finite-difference Time-domain (FDTD) technique to predict time- and frequency-domain responses are presented to show that careful shaping of antenna metallization can be used to design TEM horns with a prescribed impulsive electromagnetic field. The role of time-domain diffraction from the edges of the aperture in shaping the pulse and the nature and extent of the near-field, radiating near-field and far-field are discussed. The effect on bandwidth, radiation resistance and impulsive radiated waveform is considered and the ringing action of the antenna recognised as the crucial parameter constraining the usefulness of the design.

Experimentally the radiated far-field from the transient antennas is verified using a time domain planar near-field measurement technique. The approach utilised time domain formulas derived from the inverse Fourier transforms of the corresponding frequency domain formulas. Sampled time domain data may contain systematic or random error sources and to minimise these we outline the likely pitfalls and necessary remedies. An additional complication is that the receiving probe antenna must be compensated for its frequency response. Which once known can then be deconvolved from the measured data. Examples demonstrating these issues are provided during the course of the presentation.

High Resolution Analysis of Antenna Measurements Using the Oversampled Gabor Transform

Zwi Altman, Benoît Fourestié and Joe Wiart
CNET-DMR/IIM, France Telecom, 38-40 rue du General Leclerc,
92794 Issy les Moulineaux, France

The Oversampled Gabor Transform (OGT) is proposed as a powerful tool for analyzing antenna measurements in amplitude and phase. This technique allows one to perform a high resolution analysis of a measured signal leading to the identification and separation of its propagating wave constituents.

The proposed technique has been compared to a short time Fourier analysis, namely, the Windowed Short Time Fourier Transform (WSTFT), and to a super resolution technique, the Matrix Pencil (MP) method. The comparison has been carried out for two canonical signals, i.e., sinusoids with frequencies very close to each other, and contiguous chirp signals. It is shown that the OGT can provide a better resolution than the WSTFT, and that the problem of mathematical artifacts which may appear in the MP method is avoided.

The OGT has been applied to measurements performed in a semi-anechoic chamber using log-periodic antennas in the frequency range of 100-1,000 MHz. It is shown that the component reflected on the ground can be systematically identified and removed to retrieve the measurements performed in a fully anechoic chamber in the frequency range of 350-1,000 MHz. The identification procedure of the wave components and the signal reconstruction by removing of its reflection contributions is carried out using an automatic procedure. The reconstructed signal and the signal measured in a fully anechoic chamber agree to less than 1.3 dB with an average of 0.44 dB, and a standard deviation of 0.33 dB. The proposed method can be used to correlate measurements in different test sites.

Integral Equation MethodsCo-chairs: D. Wilton, University of Houston
R. Miller, Lockheed Martin**Page**

- | | | | |
|----|-------|---|-----|
| 1 | 12:00 | Using half plane currents as basis functions in Moment Method solutions of two-dimensional strips, <i>J. Natzke*</i> , <i>George Fox University, USA</i> | 348 |
| 2 | 12:00 | Integral equation solutions for diffraction problems involving semi-infinite structures, <i>S. Maci*</i> , <i>University of Siena, Italy</i> | 349 |
| 3 | 12:00 | An integral equation method for electromagnetic scattering from a trough in a ground plane, <i>A. Wood</i> , <i>Air Force Institute of Technology, W. Wood, Jr. *</i> , <i>Air Force Research Laboratory, USA</i> | 350 |
| 4 | 12:00 | A pedestrian introduction to the accuracy and convergence of integral equation methods, <i>K. Warnick*</i> , <i>W. Chew</i> , <i>University of Illinois at Urbana-Champaign, USA</i> | 351 |
| 5 | 12:00 | Comparison of load models for a thin-wire antenna, <i>F. Pisano III*</i> , <i>C. Butler</i> , <i>Clemson University, USA</i> | 352 |
| 6 | 12:00 | Computer simulation of 2D-SNOM using metal-coated dielectric-probe with aperture, <i>M. Tanaka*</i> , <i>K. Tanaka</i> , <i>Gifu University, Japan</i> | 353 |
| 7 | 12:00 | Generation of adaptive basis functions to create a sparse impedance matrix using Method of Moments, <i>S. Rao*</i> , <i>M. Waller</i> , <i>Auburn University, USA</i> | 354 |
| 8 | 12:00 | Application of local trigonometric bases to EM scattering on electrically large bodies, <i>Y. Tretiakov</i> , <i>M. Toupikov</i> , <i>G. Pan*</i> , <i>Arizona State University, USA</i> | 355 |
| 9 | 12:00 | Wavelet packets used in the solution of integral equations, <i>R. Miller*</i> , <i>Lockheed Martin, USA</i> | 356 |
| 10 | 12:00 | Numerical properties of new combined source & field equations, <i>F. Canning*</i> , <i>HyperSparse Tech.</i> , <i>T. Bazoe</i> , <i>Metron Inc.</i> , <i>L. Couchman</i> , <i>Naval Research Lab., USA</i> | 357 |
| 11 | 12:00 | Analysis of finite linearly tapered slot antenna (LTSA) arrays using finite element methods in conjunction with fast integral techniques, <i>E. Topsakal*</i> , <i>sJ. Volakis</i> , <i>The University of Michigan, USA</i> | 358 |

Using Half Plane Currents as Basis Functions in Moment Method Solutions of Two-Dimensional Strips

John R. Natzke, George Fox University, Newberg, OR 97132

The current induced on a wide, perfect electrically conducting strip can be accurately expressed as an infinite series of half plane currents given the appropriate edge reflection coefficients for the higher order terms. The series is a geometric one after the second order and can then be expressed in closed form. The resulting expression consists of six diffracted current terms plus the physical optics current. The accuracy of the high frequency model suggests that a moment method solution of a wide strip could be completed with a minimum of terms given the appropriate basis functions. Thus in this paper, the half plane currents are used as entire domain basis functions in the moment method solution of wide strips. Although the number of necessary expansion terms is minimized, the computation time of each in forming the impedance matrix is increased with the need for a numerical integration of the electrical field integral equation. These trade-offs are presented and discussed.

The technique is first validated for the perfect electrically conducting strip under plane wave illumination at oblique incidences. It is then applied to other two-dimensional, electrically large geometries that may not lend themselves well to high frequency solutions or that require large impedance matrices. Of particular interest are multiple strips and strips made of resistive materials. The technique is tested for its accuracy in predicting the far field of these geometries by comparing to pulse basis, point matching moment method solutions.

INTEGRAL EQUATION SOLUTIONS FOR DIFFRACTION PROBLEMS INVOLVING SEMI-INFINITE STRUCTURES

Stefano Maci

Dept. of Information Engineering, Univ. of Siena, Via Roma 56, 53100, Siena, Italy
macis@ing.unisi.it

The solutions of semi-infinite problems which exhibit a uniform geometry along the axis parallel to the truncation is often used in high-frequency diffraction theories. From these solutions diffraction coefficients can be derived and applied in the framework of the Geometrical Theory of Diffraction (GTD). This presupposes the knowledge of suitable analytical form for applying asymptotic evaluations. When the analytical form is not available, one can perform *a priori* high-frequency approximations on the solution in order to manage analytical quantities. In this case it is necessary to test these approximate solutions in order to determine their range of validity. Typically, this validation is carried out by the solution of an integral equation (IE) via the Method of Moments (MoM) of a finite, but large structure, sometimes encountering unavoidable problems of interaction mechanisms with other truncations. Applying an ordinary sub-domain meshing formulation to the original semi-infinite structure, leads to impairments essentially due to the infinite extension of the spatial integration domain. In this paper we suggest a quite general procedure to overcome these impairments. This procedure benefits from the physical information contained in 1) the exact solution of an infinite problem which constitutes the infinite continuation of the truncated one, and 2) the high-frequency solution of the same problem, but treated under a "windowing" approximation, which consists on a semi-infinite truncation of the integration domain applied to the current of the infinite structure.

The procedure is based on the MoM solution of two uncoupled IEs. The first one is that obtained by imposing the boundary conditions on the infinite structure; its solution can be given in analytical form or, in case of periodicity, by a very efficient MoM solution. The second "fringe" integral equation (FIE) is the difference between the previous IE and the IE pertinent to the semi-infinite structure. This allows one to isolate an unknown function which is the difference between the solution of the semi-infinite structure and that of the associated infinite structure. This unknown has a diffractive nature and a quite localized behavior, being physically associated to the truncation. Furthermore, the forcing term of the FIE is the field radiated by the complementary portion of the truncated structure with currents equal to those of the infinite structure. This realizes a "windowing" approximation of the semi-infinite structure solution, which can be calculated by asymptotic closed-form approximations or by convenient numerical integrations on steepest descent paths. The asymptotic form also suggests the definition of semi-infinite domain basis functions for an efficient expansion of the FIE unknown.

Several examples will be shown to support the effectiveness of the method, which include line sources placed on truncated grounded dielectric slab, semi-infinite arrays of open-ended waveguides on an infinite ground plane, semi-infinite metallic circular cylinders.

An Integral Equation Method for Electromagnetic Scattering from a Trough in a Ground Plane

Aihua W. Wood

Air Force Institute of Technology
2950 P Street, Building 640
Wright-Patterson AFB OH 45433-7765

William D. Wood, Jr.

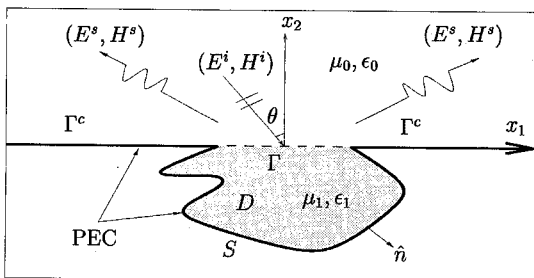
Air Force Research Laboratory
2591 K Street, Building 254
Wright-Patterson AFB OH 45433-7602

Prediction of the radar cross section of aircraft is limited in accuracy by the fidelity in predicting the scattering from cracks and gaps in the aircraft skin. Such cracks and gaps are often filled with penetrable materials to improve the aerodynamic properties of the aircraft. Modeling each individual crack and gap is computationally intractable, especially at high (e.g., X-band) frequencies. However, valuable insight can be gained by examining the two-dimensional analogue of a trough in an infinite ground plane.

We present a set of scalar integral equations governing the electromagnetic scattering from a two-dimensional trough in an infinite conducting screen. The trough region may be filled with an arbitrary homogeneous material and be of arbitrary cross section shape. The boundary between the material filling and the medium above the trough aperture must coincide with the plane of the screen. The geometry is shown in Figure .

We recently presented these integral equations for the transverse magnetic polarization (W.D. Wood, Jr., and A.W. Wood, "Development and Numerical Solution of Integral Equations for Electromagnetic Scattering from a Trough in a Ground Plane," *IEEE Trans. Antennas Propagat.*, vol. 47, pp. 1318-1322, Aug. 1999). The set of three coupled integral equations degenerate to a single integral equation when the material filling is absent (J.S. Asvestas and R.E. Kleinman "Electromagnetic Scattering by Indented Screens," *IEEE Trans. Antennas Propagat.*, vol. 42, pp. 22-30, Jan. 1994). We present numerical results that show the well-posedness of the integral equations at all frequencies, including those corresponding to the eigenmodes of the interior trough region.

We compare the numerical results from these integral equations to those from other methods, including the generalized network formulation, finite-domain integral equations (using a finite ground plane and vector background subtraction), and the hybrid finite element/boundary integral (FE/BI) method.



A Pedestrian Introduction to the Accuracy and Convergence of Integral Equation Methods

Karl F. Warnick* and Weng Cho Chew
Center for Computational Electromagnetics
University of Illinois, 1406 West Green St., Urbana, IL 61801-2991

Error estimation for integral equation-based numerical methods has been a concern in computational electromagnetics for many years. Despite common misconceptions that this problem is theoretically intractable, and that only benchmarking and test cases are available to assess accuracy, both classical and recent results provide rigorous proofs of convergence, deep insights into numerical behavior, and even quantitative error estimates.

Over the last several decades, the mathematics community has studied the fundamental question of numerical analysis for these methods: *Does the solution error decay as the mesh is refined, and if so, at what asymptotic rate?* The rigorous answer to the first part of the question—with only a few qualifications—is yes. Thus far, this remarkable achievement has had little impact in CEM. One obstacle is that this work is founded on some of the previous century's deepest results in analysis and operator theory. Surprisingly, the key theorem (quasioptimality) could not be more intuitive: the numerical solution is close to the projection of the exact solution into the trial space used to discretize the integral equation. This simple principle leads immediately to predictions of the solution convergence rate.

With these result in place, we can turn to harder questions: *When does quasioptimality break down? What is the absolute magnitude of the error for a given mesh? How do geometry and electrical size affect the error? Scattering resonances? The choice of basis functions, including higher order bases? Approximate integration of matrix elements?* By making use of basic methods in EM analysis such as high frequency asymptotic approximation, one can go beyond the classical convergence theory to answer these and other questions as well. The true solution error consists not only of the approximation error implied by quasioptimality, but also another contribution due to sampling of the singularity of the kernel of the integral equation. These depend differently on parameters such as mesh length and incidence angle. On smooth regions of a scatterer, the approximation error for low order bases is second order in the mesh length, and the sampling error is higher order. With approximate numerical integration of moment matrix elements, however, the sampling error becomes first order and can be dominant. In addition, the approximation error cancels for specular scattering cross sections (if the scattered field is discretized using the same expansion functions as the current), so that the RCS is only affected by the sampling error. These effects make empirical convergence observations difficult to interpret, but once understood, solution error can be predicted quantitatively—allowing CEM to move beyond the venerable rule-of-thumb of “10 points per wavelength.”

Comparison of Load Models for a Thin-Wire Antenna

Frank A. Pisano III* and Chalmers M. Butler
Department of Electrical and Computer Engineering
Clemson University
Clemson, SC 29634-0915

Loads in thin-wire antennas can serve many purposes. From shifting a resonance to acting as a choke, loads are versatile design devices. In many cases, circuit models can replace these loads in numerical solutions that predict antenna characteristics. Representation of features by circuit models where feasible in an analysis offers computational efficiency over a complete electromagnetic field characterization of a loaded antenna. Often, however, one arrives at the value of a load impedance needed in an application before consideration is given to the structure of candidate circuit elements of the load only to encounter difficulties in attempts to physically realize a load which exhibits these desired characteristics. A robust load implementation whose impedance can be varied with only minor modification of the antenna structure is desirable. To this end, the authors have devised simple load structures and computationally efficient load models for use in integral equation analyses of loaded wire antennas.

The aforementioned loaded antenna is constructed by creating a gap in a cylindrical tube. The tube serves as the antenna proper, and the gap is the manifestation point of the load. The load itself is created inside the antenna, i.e., inside the tube, by insertion into the tube of another cylinder, coaxial with the cylindrical tube. The inserted cylinder and tube form an interior coaxial guide of finite length. A signal can enter at the gap and excite the coaxial guide at a predetermined location along its length. The load impedance seen at the gap can be controlled by adjustment of the parameters of the coax and by adjustment of the terminations at the ends of the coax remote from the gap. Loading of the coax itself offers even more freedom to one who wishes to arrive at a desired impedance.

Several models useful in analysis of this loaded antenna are considered. Two rely entirely upon full characterization by Maxwell's equations and lead to solutions which can be used to assess the accuracy of those models which do incorporate circuit approximations to simplify the analysis. The first of the two "field" methods is a rigorous mixed potential integral equation analysis of the total structure in which it is treated as coaxial cylinders. The second field method is a complete aperture solution in which the gap electric field and cylinder current are unknowns to be determined from solutions of coupled integral equations. In this method, the field in the interior of the coax is represented in the usual way in terms of eigenfunction expansions. These two solution methods provide the basis for comparison for the efficient load models devised.

To characterize this structure efficiently, the gap in the outer tube is viewed as an input port to the coaxial interior and the effects of this interior are represented as a circuit which manifests itself to the exterior at the gap. The impedance of this circuit is used as a lumped load in the wire antenna which is analyzed by integral equation methods. Four load models have been devised, and all are variations on the conventional lumped load model: the lumped load located at the center of the tube gap, two lumped loads separated by the width of the gap in the cylindrical tube, two lumped loads at the ends of a section of wire whose radius is that of the inner cylinder's, and a distribution of lumped loads along the span of the gap. Each of the four models incorporating circuit loads offers increased computational efficiency over the corresponding complete electromagnetic field models in exchange for a varying amounts of reduced accuracy.

Computer Simulation of 2D-SNOM Using Metal-Coated Dielectric-Probe with Aperture

Masahiro Tanaka and Kazuo Tanaka

Department of Information Science, Gifu University
1-1 Yanagido, Gifu-shi, Gifu 501-1193, Japan

Near-Field Optics (NFO) such as a Scanning Near-field Optical Microscope (SNOM) and an optical manipulator is a technology in which many researchers are interested recently. SNOM can make images with the subwavelength resolution, and the optical manipulator can control a position of a tiny particle by electromagnetic force. In order to understand the basic characteristics of NFO circuits, it is very important subject to develop the accurate simulator and their basic theory.

It is considered that NFO circuits are composed of the observed or controlled particles, and semi-infinite probe that is made from fiber in the case of 3-dimensional structure or waveguide slab in the case of 2-dimensional structure. Many papers concerning the analysis of NFO circuits have been published so far. However, to our knowledge, there are only small number of papers which treat the energy of the guided-wave as the output image.

We have proposed new integral equations called Guided-Mode Extracted Integral Equations (GMEIEs) for the analysis of 2-dimensional SNOM (2D-SNOM) and optical manipulator using the uncoated dielectric-probe, and have reported results of the computer simulation. In this paper, GMEIEs are extended to the case of 2D-SNOM using the metal-coated dielectric-probe with aperture, and the computer simulation is performed by the boundary element method (moment method). The metal is treated as the perfect electric conductor in this paper.

Results of computer simulation show that it is possible to detect the position of two particles separated by 0.16λ , when the each object size which is square is given by $0.16\lambda \times 0.16\lambda$, where λ represents the wavelength of incident field. One-dimensional (1-D) scanning images that are obtained by scanning the metal-coated dielectric-probe with aperture are compared with those that are obtained by scanning the uncoated dielectric-probe. It is found that 1-D scanning images obtained by 2D-SNOM using the metal-coated dielectric-probe with the aperture are higher resolution than those obtained by 2D-SNOM using the uncoated dielectric-probe.

When the aperture size of the coated dielectric-probe becomes small, the contrast quality becomes worse. However, the detected positions of two particles obtained by 2D-SNOM using the metal-coated dielectric-probe with the smaller aperture, is better agreement with the true positions of two objects.

Generation of Adaptive Basis Functions to Create a Sparse Impedance Matrix Using Method of Moments

S. M. Rao* and M. L. Waller, Department of E & CE, Auburn University, Auburn, AL 36849.

The most popular method to solve electromagnetic field problems via integral equation solution approach is the method of moments (MoM). One major problem with MoM is the generation of a dense matrix and for complex problems, the dimension of this matrix can be prohibitively large. Usually, for electromagnetic scattering problems, it is necessary to divide the solution region into small enough subdomains in order to obtain accurate results. By *small enough*, we mean about 200-300 subdomains per square wavelength. In usual practice, we may typically solve for several thousand unknowns for large, complex problems. Quickly, this requirement becomes expensive in terms of computational resources and may even become impossible to handle. Hence, we look for alternate schemes to reduce the computational resources by generating a sparse matrix instead of a full matrix.

The generation of a sparse matrix in the method of moment solution procedure may be achieved in two ways *viz.* a) by defining a special set of basis functions to represent the unknown quantity or b) by handling the influence of the kernel function in a novel way. The usage of wavelet-type basis functions which provide some sparsity belong to the former category and the application of fast multipole method (FMM) belongs to the later category.

In this work, we develop a set of adaptive basis functions which, when used in the regular moment method solution, automatically generates a sparse moment matrix. The central idea in this scheme is to group a number of subdomain basis functions into one cluster. Then, we attach appropriate complex weights to these individual basis functions in the cluster so that the integrated field value (*i.e.* the basis function multiplied by the kernel function and integrated over the basis function domain) produces a null outside the cluster. This null translates to zero elements in the moment matrix thus enabling us to generate a sparse system of equations. We note here that the sparsity of the moment matrix depends upon the number of basis functions used to form the cluster. It is fairly simple to achieve over 95% sparsity in the impedance matrix using this procedure. Obviously, the evaluation of the appropriate weights is essential to the crucial step in this method and we discuss a simple procedure to calculate these weights. One major advantage this new method is we only need to generate the non-zero elements in the moment matrix which reduces the computer storage requirements substantially. This is in contrast to other similar methods, such as using wavelet transforms, wherein one usually generates the full matrix and applies threshold to obtain the sparsity. We demonstrate the efficiency and advantages of this new procedure using several numerical examples.

APPLICATION OF LOCAL TRIGONOMETRIC BASES TO EM SCATTERING ON ELECTRICALLY LARGE BODIES

Youri Tretiakov, Mikhail Toupikov and *George Pan
Department of Electrical Engineering, Arizona State University, Tempe AZ

The Electromagnetic field scattering by arbitrarily shaped conductors is usually obtained by solving an integral equation with respect to the unknown induced current distribution. The solution is performed by discretizing the integral equation into a matrix form by the method of moments. The choice of basis functions is very important. The well-known approach of using pulse and δ -functions as basis and testing functions leads us to a dense system matrix. For electrically large problems this approach results in a prohibitively excessive usage of computer resources (memory and computational time).

Application of classical wavelets as basis and testing functions gives us very good results for the case of low frequency scattering and antenna problems. Wavelet application leads to very sparse system matrices, which can be efficiently solved by sparse solvers. However the sparsity of the system matrix for wavelet bases is decreased as we go to higher frequencies. This is due to the fact that high frequency oscillatory integral kernels require high level of wavelets for a good approximation.

In this work authors have applied smooth local cosine bases of Coifman and Meyer (Remarques sur l'analyse de Fourier à fenêtre, série I, *C.R. Acad. Sci. Paris* **312** (1991), 259-261)) to solve electromagnetic scattering problems from two-dimensional arbitrary shaped electrically large conducting bodies. Smooth local cosine bases have such advantages as frequency localization, orthogonality and the availability of fast numerical algorithms. Numerical scattering results for several 2D cross sections are given. Authors also performed comparison of effectiveness of the smooth local cosine and wavelet approaches.

Wavelet Packets Used in the Solution of Integral Equations

Richard E. Miller
Lockheed Martin Government Electronic Systems
199 Borton Landing Road
P.O. Box 1027
Moorestown, NJ 08057-0927

Wavelet basis functions have successfully been used to reduce the size of moment method impedance matrices through direct expansion of the integral equation and the discrete wavelet transform (DWT). The extension from wavelets to wave packets has begun to demonstrate the potential for higher reductions in the size of moment method impedance matrices. This paper compares the matrices generated by the discrete wavelet packet transform (DWPT). Orthogonal and semi-orthogonal wavelet packets are used to generate the transformed impedance matrices.

A wavelet basis is composed of entire domain and sub domain basis functions. The larger scale or lower frequency functions are generated by decomposing the previous higher level basis into smooth (low frequency) and detail (high frequency) functions. The decomposition path proceeds through the smooth functions only. A wavelet packet basis is a more general form of the wavelet basis in that the decomposition can proceed through both the smooth and detail functions.

The wavelet packet impedance matrices generated by orthogonal and semi-orthogonal DWPTs will be compared. The following metrics are used in comparing the matrices: matrix condition number, sparsity, and solution error. The impedance matrix for this study will be constructed for a two-dimensional finite-width flat plate scatterer with plane wave excitation.

Numerical Properties of New Combined Source & Field Equations

Francis X. Canning*
HyperSparse Tech.
Newbury Park
CA 91320
fxc@ieee.org

Terry Bazow
Metron Inc.
Reston
VA 22090
bazow@metsci.com

Luise Couchman
Naval Research Lab.
Washington, DC
couchman@
ccf.nrl.navy.mil

A new combined field integral equation is examined for its numerical properties. For scattering from a closed conducting body, it is known that a combined field integral equation has a better condition number than either the electric field integral equation or the magnetic field integral equation alone. This is understood by proofs involving energy inequalities. The standard combined field integral equation receives somewhat more strongly from the exterior of that closed body than from its interior. The use of the Impedance Matrix Localization (IML) along with a diagonal matrix as a combination coefficient allows a new combined field integral equation which receives very significantly more strongly from the exterior than from the interior. We present the condition numbers for all these equations and show that the new combined equation has a very significantly improved condition number than all other approaches, including the standard combined field integral equation.

In the past, combined source integral equations always were for an electric field. That is, the standard electric field integral equation, which has an electric current as a source, was combined with a different electric field integral equation, one which has a magnetic current as a source. The very method of derivation for these combined equations required that they both be for the same field quantity. However, we show that there is another possibility. The Impedance Matrix Localization Method (IML) shows how to transform a far field scattered electric field into a magnetic field. More importantly, in the IML formulation, this transformation becomes a diagonal matrix. Using this fact, we show how to derive other combined equations. For example, it is even possible to combine an electric field integral equation for an electric current source with a magnetic field integral equation with a magnetic source. More to our purposes, we show a novel combination of three integral equations. This combination is designed to achieve both testing functions which preferentially receive from the exterior and sources which preferentially transmit to the exterior. Numerical results show that this combination has an even better condition number than any others seen before.

ANALYSIS OF FINITE LINEARLY TAPERED SLOT ANTENNA (LTSA) ARRAYS USING FINITE ELEMENT METHODS IN CONJUNCTION WITH FAST INTEGRAL TECHNIQUES

Erdem Topsakal* and John L. Volakis

(topsakal@umich.edu, volakis@umich.edu)

Radiation Laboratory

Department of Electrical Engineering and Computer Science

The University of Michigan, Ann Arbor, MI 48109-2122

In this paper we present a finite-element boundary integral (FE-BI) formulation for the analysis of finite linearly tapered slot antenna (LTSA) arrays. TSAs are widely used in many applications because of their ultra-wide bandwidth and high power handling capabilities. They are also used as feeds to reflector antennas due to their narrow beamwidths. Previous analysis of these TSA arrays has been carried out using moment method techniques in conjunction with Floquet's theorem. To allow the capability of modeling material and treatments between the array elements, in this paper we consider the finite element method modeling of the LTSA along with periodic boundary conditions for handling the periodic boundaries. Also, a new fast spectral domain method [Eibert and Volakis, 1998] with $O(N \log N)$ CPU requirements is employed for truncating the aperture mesh.

Of particular importance in this study is the use of higher order/multi-resolution elements [Andersen and Volakis, 1999] for accurate feed modeling and for efficient modeling of thin dielectric layers. Automatic adaptivity will be employed to control the accuracy of the solution by modifying only a few elements of the solution volume and results will be shown on the efficiency of this approach. Also, materials modeling will be considered to decrease coupling effects and scan performance. The computational aspects of the method in dealing with such broadband elements with fine detail will be addressed as well.

L. Andersen and J. L. Volakis, "Development and Application of a Novel Class of Hierarchical Tangential Vector Finite Elements for Electromagnetics" *IEEE Trans. Antennas and Propagat.*, v 47, n 1, pp 104-108, Jan 1999

T. Eibert and J. L. Volakis, "A Fast Spectral Domain Algorithm for Rapid Solution of Integral Equations," *IEE Electronics Letters*, v 34, n 13, pp 1297-1299, 25 Jun 1998.

Conformal Arrays and Elements

Chair: S. Sanzgiri, Boeing Defense and Space Group

Page

- | | | | |
|---|------|--|-----|
| 1 | 1:50 | Mutual coupling between antennas on an elliptic cylinder, <i>C-W. Wu*</i> , <i>L. Kempel</i> , <i>E. Rothwell</i> , <i>Michigan State University, USA</i> | 360 |
| 2 | 2:10 | Conformal wide bandwidth antennas on circular cylinders, <i>C. Macon*</i> , <i>L. Kempel</i> , <i>Michigan State University</i> , <i>K. Trott</i> , <i>Mission Research Corp.</i> , <i>S. Schneider</i> , <i>Air Force Research, USA</i> | 361 |
| 3 | 2:30 | Radiation characteristics of field radiated from and received by resistively loaded thin half-wave coplanar orthogonal dipoles excited by ultra wide band signals, <i>A. Choudhury*</i> , <i>Howard University, USA</i> | 362 |
| 4 | 2:50 | Optimization of the radius of a circular array, <i>R. Vescovo*</i> , <i>Universita di Trieste, Italy</i> | 363 |
| 5 | 3:10 | Mutual admittance between two concentric annular slots, <i>S. Zeilinger*</i> , <i>Visteon Automotive Systems</i> , <i>D. Sengupta</i> , <i>University of Detroit Mercy, USA</i> | 364 |
| 6 | 3:30 | Computational models for practical antenna loads, <i>S. Rogers*</i> , <i>J. Young</i> , <i>C. Butler</i> , <i>Clemson University, USA</i> | 365 |

Mutual Coupling Between Antennas on an Elliptic Cylinder

Chi-Wei Wu*, Leo C. Kempel, Edward J. Rothwell
Electromagnetics Laboratory
Michigan State University
East Lansing, MI

An approximate asymptotic solution based on the geometrical theory of diffraction (GTD) for surface fields due to a source on a smooth perfectly conducting surface with arbitrary curvature has been developed by Pathak and Wang (*IEEE Trans. Antenna Propag.*, 29(6), pp. 911-922, Nov. 1981). Based on this development, we find an approximate asymptotic solution for the electromagnetic fields that are induced on the surface of an electrically large perfectly conducting elliptic cylinder by an infinitesimal magnetic current moment on the same surface. The superposition of such current elements represents the surface current in the aperture of a conformal antenna. This solution can be employed to calculate mutual coupling between two or more antenna elements. Such information is essential for designing conformal antenna arrays and for studying the electromagnetic compatibility (EMC) of multiple conformal antennas. In this solution, the surface fields propagate along each ray's geodesic path, and their description remains uniformly valid within the shadow boundary transition region including the immediate vicinity of the source. The surface field due to a magnetic current element is expressed in terms of Fock functions in the form of a rapidly convergent creeping wave series.

This solution is used to form the dyadic Green's function for the elliptic cylinder. The Green's function is then used in a hybrid finite element-boundary integral formulation. In this, the fields within the cavity are expanded in terms of finite element basis functions while the boundary integral is used to close the aperture mesh and provide the necessary radiation conditions. This formulation is analogous to the one developed for conformal antennas mounted on circular cylinders by Kempel, Volakis, and Sliva (*IEE Proc.-Microw. Antennas Propag.*, 142(3), pp. 233-239, June 1995).

Conformal Wide Bandwidth Antennas on Circular Cylinders

Charles Macon*, Leo Kempel
Michigan State University

Keith Trott
Mission Research Corp.

Stephen Schneider
Air Force Research Laboratory

In this paper, the effect of curvature on the behavior of broadband antennas will be investigated. A broadband antenna exhibits a performance, as defined by the radiation pattern and input impedance, that is practically independent of frequency over a large bandwidth. The motivation for this study lies in the fact that designers may sometimes find it necessary to place conformal antennas on curved surfaces. The effect of curvature on the input impedance of such antennas is needed in order to ensure a proper match with the antenna feed network. The finite-element boundary integral (FE-BI) method will be utilized to model the behavior of the antennas with respect to variations in curvature. This method is versatile in that it permits the specification of anisotropic materials within the computational domain and is capable of modeling composite metallic and dielectric structures.

The affect of curvature on broadband antenna performance will be quantified through an analysis of the dependence, as a function of rotational state, of key performance parameters (e.g. input impedance, gain, phase linearity, etc.). In particular, a log-periodic antenna (LPA) will be analyzed. The LPA was chosen as a good candidate for investigation among various types of broadband antennas due to its rotational asymmetry. A rotational state may be considered as aligned with the points on a compass. In this investigation, there will be three rotational states for a four arm self-complementary LPA, namely 0, 22.5, and 45 degrees. These are illustrated in Figure 1.

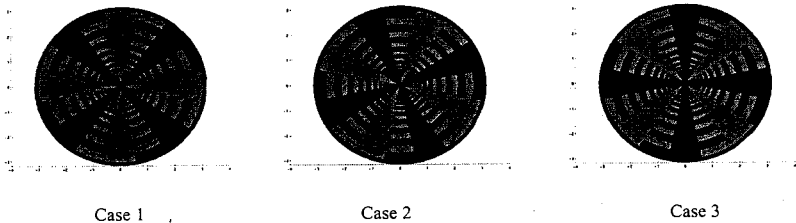


Figure 1. Three orientations of the LPA on a cylinder: 0, 22.5, and 45 degrees.

The input resistance is a parameter that characterizes the performance of broadband antennas. The variation in input resistance over the frequency range 6-20 GHz for each rotational state was presented recently (Macon, et al, "Curvature Effects on a Conformal Log-Periodic Antenna, ACES Conference, Monterey, CA, March 2000). Further results, illustrating the effect of curvature on the radiation pattern and far-zone phase behavior, will be presented at this meeting.

From this investigation, we hope to better understand the effect of curvature on broadband antennas. This knowledge would have many practical applications, such as more efficiently aligning conformal antennas on supporting structures to maximize performance.

RADIATION CHARACTERISTICS OF FIELD RADIATED FROM AND RECEIVED
BY RESISTIVELY LOADED THIN HALF-WAVE COPLANAR ORTHOGONAL
DIPOLES EXCITED BY ULTRA WIDE BAND SIGNALS

Ajit K. Choudhury
Department of Electrical Engineering
College of Engineering, Architecture and Computer Sciences
Howard University, Washington, D.C. 20059

ABSTRACT

Characteristics of the radiated electric field in free space at far distances from resistively loaded thin half-wave coplanar orthogonal dipoles excited by pulses are investigated. The receiving antenna consists of a thin half wave resistively loaded coplanar orthogonal dipoles situated at a far distant point, not necessarily in the same plane of the transmitting coplanar orthogonal dipoles. It is shown that the radiated field can become circularly polarized in the broadside direction ($\theta = \phi = 90^\circ$) when the exciting input voltage is sinusoidal, and the input to the x-axis dipole is the same as the input to the z-axis dipole but delayed by a quarter cycle.

The Wu-King [2] loading profile is considered here. The far field of the loaded orthogonal dipoles excited by a finite cycle-sine input (N cycles) to each dipole is derived. When the input is fed directly into the dipoles and the observed direction is broadside, the time-domain field is extended in time to $(N+0.5)/f_0$ with respect to the duration of the source N/f_0 and circular polarization occurs only for $(N+0.5)/f_0$. For the UWB case ($N=1$), the radiated field's duration is 1.5 times the duration of the source, and circular polarization occurs only for two-quarter of the period of the source i.e., two-quarter of a cycle. This is different from that of the unloaded orthogonal dipoles case [1]. In the case of unloaded orthogonal dipoles when the dipoles and the feed network are perfectly matched and the observation direction is broadside, the time-domain field is extended to $(N+0.75)/f_0$ with respect to the duration of the source N/f_0 and circular polarization occurs for $(N+0.75)/f_0$. For the UWB case ($N=1$), the radiated field's duration is 1.75 times the duration of the source, and circular polarization occurs only for one-quarter of the period of the source. Similar results are derived for the voltages out of the receiving antenna and compared with the corresponding results of the unloaded case.

1. E.L. Mokole, A.K. Choudhury and S.N. Samaddar, "Transient radiation from thin, half-wave, orthogonal dipoles," *Radio Science*, Volume 33, Number 2, pp. 219-229, March-April 1998.

2. T.T. Wu and R.W.P. King, "The cylindrical antenna with non-reflecting resistive loading," *IEEE Trans. Antennas and Propagat.*, Volume 13, pp. 369-373, (1965)

OPTIMIZATION OF THE RADIUS OF A CIRCULAR ARRAY

Roberto Vescovo
 Dipartimento di Elettrotecnica Elettronica ed Informatica
 Università di Trieste
 Via A. Valerio, 10 - 34127 Trieste - Italy

In a process of pattern synthesis for circular arrays, the array radius plays an important role in determining the quality of the synthesized pattern. We here examine the problem of optimizing this radius. Let us consider a circular array of N equispaced elements placed on a circular ring of radius R , lying in the x - y plane of a Cartesian system $O(x, y, z)$ and having the center coincident with the origin O . The far-field pattern of the array in the x - y plane is given by

$$P(a)(\phi) = \sum_{n=1}^N a_n p(\phi - \phi_n) \exp(j\beta R \cos(\phi - \phi_n)) \quad (1)$$

where $a = [a_1, \dots, a_N]^T$ is the complex excitation vector, ϕ is the azimuth angle, ϕ_n ($= 2\pi N^{-1}n$) and $p(\phi - \phi_n)$ are the angular position and the far-field pattern, respectively, of element n ($n = 1, \dots, N$), and $\beta = 2\pi\lambda^{-1}$ with λ the wavelength.

Given a desired radiation pattern $F_0(\phi)$, the array pattern $P(a_0)(\phi)$ minimizing the mean-square distance $\|P(a) - F_0\|$ can be determined in closed form by a DFT (discrete Fourier transform) approach described in (R. Vescovo, *Int. Journal of Infrared and Millimeter Waves*, **20**, 1957-1976, 1999). By following this approach it can be shown that the squared distance between the optimal array pattern $P(a_0)$ and F_0 is given by

$$\rho^2(a_0) = \|P(a_0) - F_0\|^2 = \|F_0\|^2 - \sum_{k=1}^N |a_0^{(k)}|^2 \|g_k\|^2 \quad (2)$$

where the coefficients $a_0^{(k)}$ and $\|g_k\|$ can be calculated by formulas involving the DFT (see reference above) which therefore are suitable for implementing FFT (fast Fourier transform) algorithms.

Note that the quantity βR in (1) affects the optimal excitation vector a_0 , which therefore is indicated by $a_0(\beta R)$. Accordingly, the distance in (2) is indicated by $\eta(\beta R) = \rho(a_0(\beta R))$. The relation (2) allows a fast computation of the distance $\eta(\beta R)$ for different values of βR , thus providing a diagram of $\eta(\beta R)$. This allows to easily determine an approximation of the value $(\beta R)_0$ minimizing $\eta(\beta R)$. The value $(\beta R)_0$ yields the best synthesized pattern, and therefore it can be considered as the optimal value of βR .

Numerical results were obtained, which validate the above method.

Mutual Admittance Between Two Concentric Annular Slots

Steve Zeilinger*
Visteon Automotive Systems
Dearborn, Michigan 48126
USA

Dipak L. Sengupta
Department of Electrical and Computer Engineering
University of Detroit Mercy
Detroit, Michigan 48219-0900
USA

Abstract

This paper presents results obtained from the induced emf solution for the mutual admittance between two concentric annular slots on an infinite ground plane. The inner (smaller) slot is delta gap driven while the outer (larger) slot is arbitrarily loaded at its terminals.

The mutual admittance Y_{21} is obtained from the following expression:

$$Y_{21} = \frac{1}{I_1 I_2} \int_{-\pi}^{\pi} I_2(\phi) H_2(\phi) c d\phi$$

where;

I_1 and I_2 are the magnetic currents (at $\phi = 0$) on the inner (slot 1) and outer (slot 2) slot terminals respectively,

$I_2(\phi)$ and $H_2(\phi)$ are the magnetic current and field distributions on slot 2,

c is the mean radius of the outer (parasitic) slot.

The required field and magnetic current distributions are determined by using the appropriate MFIE's and boundary conditions. Magnetic currents and magnetic fields are expanded via Fourier series and the Fourier coefficients determined by use of the orthogonality principle.

The mutual admittance has been calculated by using standard numerical techniques for annular slots of variable size. A variety of numerical results will be presented.

COMPUTATIONAL MODELS FOR PRACTICAL ANTENNA LOADS

Shawn D. Rogers*, John C. Young, and Chalmers M. Butler
Department of Electrical and Computer Engineering
Clemson University, Clemson, SC 29634-0915

It is well known that loading an antenna with tuned circuits has many useful applications, e.g., increasing bandwidth, altering resonant frequency, etc. Such tuning is particularly effective for monopole and dipole antennas, which are typically narrow-band devices but which are often the structures of choice when the application requires a vertically polarized, omnidirectional (in azimuth), low-profile antenna. There has been much attention in the literature in recent years devoted to the application of genetic algorithms for determining the optimum placement on the antenna and component values of these circuits. However, there is little information available pertaining to the design and construction of practical antenna loads. Also, data are not available for the experimental validation of computational models of loaded antennas.

The purposes of this study are to verify computational models of loaded antennas with measured results and to present example designs for practical antenna loads. One practical load of interest is the simple helical coil. Results are presented for monopoles loaded with a helical coil treated as a single inductor in the load model. Another model of the helical coil incorporating the interwinding capacitance between the turns of the coil is assessed. In order to provide parallel capacitance for a tuning circuit, a shield is placed over the helical coil. In both cases the inductance of the coil and the inductance and capacitance of the shielded coil are predicted by computational methods. Data determined from integral equation solutions of loaded antennas are compared with data obtained from measurements on laboratory models.

Numerical results reported in the literature suggest that load circuits containing resistors are more effective for achieving broadband operation of an antenna than non-resistive loads. Measured and computed results for antennas containing these types of loads are presented.



Specialized Antennas

Chair: A. Djordjevic, University of Belgrade, Yugoslavia

Page

- | | | | |
|---|------|--|-----|
| 1 | 1:50 | Dual-band glass-mounted car antenna for mobile phone, <i>L. Niccolai, Alfa Accessori, Italy, A. Djordjevic, B. Kolundzija*, University of Belgrade, Yugoslavia, T. Sarkar, Syracuse University, USA</i> | 368 |
| 2 | 2:10 | Double slot antenna integration on thick film substrate LTCC at 60 GHz, <i>L. Desclos*, NEC USA Inc., USA, K. Maruhashi, M. Ito, K. Ikuina, N. Senba, N. Takahashi, K. Ohata, M. Madhian, NEC Corporation, Japan</i> | 369 |
| 3 | 2:30 | Artificial dielectrics for graded index lens design, <i>T. Ozdemir*, K. Sabet, P. Frantzis, EMAG Technologies, K. Sarabandi, L. Katehi, The University of Michigan, J. Harvey The Army Research Office, USA</i> | 370 |
| 4 | 2:50 | Folded conical helix antenna, <i>J. Dobbins*, R. Rogers, The University of Texas at Austin, USA</i> | 371 |
| 5 | 3:10 | Telemetry & command antenna for a micro satellite at the VHF/UHF frequencies (design & manufacturing), <i>A. Aminaie*, M. Solaimani, Advanced Electronic Research Center, Iran</i> | 372 |
| 6 | 3:30 | Multifeed unit for wideangle SAT-TV antenna, <i>S. Guerouni*, Radiophysics Measurement Institute, Armenia</i> | 373 |

DUAL-BAND GLASS-MOUNTED CAR ANTENNA FOR MOBILE PHONE

Luca Niccolai
Alfa Accessori, S.R.L., Via Parini 1/5, 60027 Osimo, Italia

Antonije Djordjevic
Branko Kolundzija*
School of Electrical Engineering, University of Belgrade
P.O. Box 35-54, 11120 Belgrade, Yugoslavia

Tapan Sarkar
Department of Electrical Engineering and Computer Science
Syracuse University, Syracuse, New York 13244-1240, USA

To avoid drilling holes in the metallic body of a car, antennas can be mounted at the top part of the windshield or another glass surface. For mobile-phone applications, the antenna is usually at the outside of the car. It is coupled to the feeding cable located inside the car using a through-the-glass capacitor. Such a design is common for the 900 MHz band, where the radiating element is an external monopole (whip). The design is complicated when the antenna should operate at both the 900 MHz and 1800 MHz bands.

The whip should resonate at two frequencies, which are approximately in the ratio 2:1. This is achieved by interrupting the monopole by a tank circuit, resonant at 1800 MHz. This circuit is made in the form of a simple coil, which has an antiresonance at 1800 MHz. At the base of the whip, there is a metallized surface touching the windshield glass. This surface plays the role of one electrode of the capacitor. The other electrode of the capacitor is a metallized flat surface at the glass interior. This electrode is placed on the top of a box-like structure. This structure is used for the mechanical connection of the feeding coaxial line, but it also plays the role of the antenna counter-balance and a choke that prevents signal leakage along the feeder. The box walls and floor are metallic, and the feeder connection is at the box floor.

The most critical part of the antenna design is the connection between the electrode and the feeder. The main problem is to force the major radiation to come from the external whip, and not from the box interior. This is required to control the radiation pattern of the antenna. The radiating segment should be positioned as high as possible, to minimize shadowing by the car body. This connection is made in the form of a conical metallic surface, with the apex at the feeder.

The design was carried out theoretically, using program WIPL (B.M. Kolundzija, J.S. Ognjanovic, T.K. Sarkar, and R.F. Harrington, Boston: Artech House, 1995), by carefully modeling all metallic and dielectric parts of the antenna and the windshield. Theoretical results were then verified experimentally. A very good agreement was obtained between the theoretical and experimental data.

Double slot antenna integration on thick film substrate LTCC at 60 GHz

L. Desclos, K. Maruhashi*, M. Ito*, K. Ikuina+, N. Senba+,
N. Takahashi+, K. Ohata*, M. Madihian
NEC USA Inc., CCRL, Princeton, * Kansai elec. Labs, + Fundamental research lab,
NEC Corporation Japan

Summary: Development of short range communication systems requires to investigate technological issue to reduce the overall cost of the proposed module. These modules should include the active part as well as the antenna. Several solutions have been proposed based on a total GaAs solution specially for millimeter wave range, (C. Peixeiro, et al, 26th EuMC, Prague, 9-12 Sept. 1996). However it appears that a full GaAs solution creates several blocking points. First of all the reliability as if one of the used component is with defect all the chain is affected, and the second point is the cost. Then several investigations have been carried out on different low cost modules or materials, and one of the candidates is LTCC substrate. This one is issued from the low frequency range as it is used with a thick film printed technique. By adapting this low frequency technique toward the high frequency we can keep the cost as interesting as possible. The antenna can then be printed on the module itself and the MMIC will be mounted with a flip-chip technique - Fig. 1-. One of the difficulties encountered in designing the antenna is then how to respect the printing tolerances (related to low frequency) to have the best performances reliability. All this considering that it has to be on a single plane and in a finite size. The proposed V band antenna has to stand within 3.5x5 mm, on a 320 μm thickness substrate of 7.1 permittivity. To keep the cost as low as possible, the minimum separation or printing was over 90 μm . This means that we could use the same thick film line as in the low frequency. The antenna chosen was a double slot and a the first investigation showed that keeping the design rules was not permitting to get any good results. We then used techniques to shift the characteristics. Several proposals are made and demonstrated by experimental realizations. Using the possibility of including short points around each slot permits to have a shift in the frequency of resonance as it adds a degree of freedom in the control of coupling. Another technique used has been the ridged slot antenna, by introducing several orthogonal slots loaded in the slot it is possible to smooth more the overall results. Finally, the evaluation as been made using an on probe time domain technique (L. Desclos et al., Microwaves and RF Feb. 1999) and results show at 60 GHz a gain of 4 dB for the gain and 15 dB for the matching -Fig. 2-.

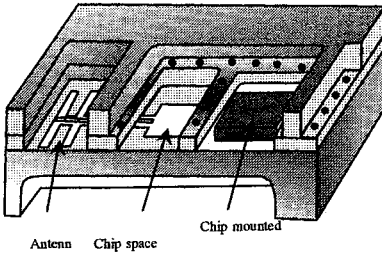


Fig. 1

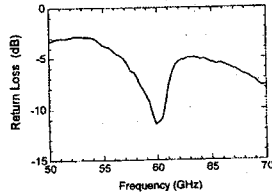


Fig. 2

ARTIFICIAL DIELECTRICS FOR GRADED INDEX LENS DESIGN

T. Ozdemir^{*§}, K.F. Sabet[§], P. Frantzis[§], K. Sarabandi^{§§}, L.P.B. Katehi^{§§}, J.F. Harvey^{§§§}

[§]EMAG Technologies Inc, 3055 Plymouth Rd., Ste. 205, Ann Arbor, MI 48105

^{§§} Dept. of EECS, The University of Michigan, Ann Arbor, MI 48109-2122

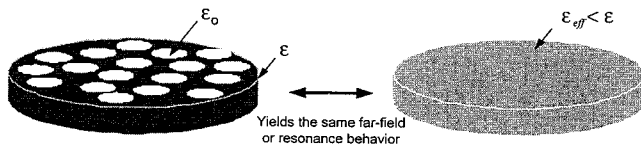
^{§§§} The Army Research Office, P.O. Box 12211, Research Triangle Park, NC 27709-2211

tayfun@emagtechnologies.com, ksabet@emagtechnologies.com

Today's communication systems call for multifunction, low profile antennas, where reduction of size and cross talk are major design concerns. A typical system may involve a multitude of printed radiators that have to be packaged and operate in close proximity. In a parallel paper [T. Ozdemir, *et al.* "Compact wireless antennas using a superstrate dielectric lens", submitted to 2000 APS Symp.], it has been proposed to use a graded index planar dielectric lens to achieve both size reduction and isolation of adjacent radiators. A high permittivity superstrate lens provides miniaturization of individual radiators. On the other hand, a properly designed varying index profile prevents propagation of surface waves and hence minimizes the cross talk.

Controlling the dielectric constant of a material is a challenging task. Depending on the index profile, the process may be very expensive and difficult from a manufacturing point of view. In this paper, we propose a cost-effective way of controlling and realizing index profiles. The approach involves introducing air voids inside a uniform host dielectric, the shape, size and density of which are optimized to achieve the given profile (K.F. Sabet, K. Sarabandi, L.P.B. Katehi, "A planar antenna including a superstrate lens having an effective dielectric constant", *U.S. Patent Pending, 1998*). Using artificial dielectrics of this kind makes it possible to achieve any particular index profile. As opposed to the "material injection" or "molding" techniques, this approach promises to be cost-effective and manufacturing-friendly.

This paper presents a simulation-based approach to the synthesis of an artificial dielectric lens with a uniform or graded index profile. The underlying premise is to establish the equivalence between an artificial dielectric lens and a uniform lens made of a solid material with an effective dielectric constant such that both yield similar resonance and radiation characteristics (see the figure below). To prove the concept of controlling the dielectric constant, we designed different sets of numerical experiments on a dielectric disc overlaid on and excited by a slot ring antenna. The structure was analyzed rigorously via a full-wave technique based on the finite element method (FEM). In one set of experiments, first the permittivity of the uniform disc was varied and the front-to-back ratio (FBR) of the combined antenna was recorded. Then, air voids of varying density were introduced inside the disc of the same size but of a uniform permittivity and again FBR has been recorded. Finally, a data-driven model was constructed by relating the effective dielectric constant to the volume fraction based on identical front-to-back ratio. Indeed a computation performed on two lenses, deemed equivalent by the model, showed that the radiation patterns differed by a maximum of 0.1dB. Similar experiments were carried out where equivalent models were constructed based on other characteristics such as the resonant frequency of the combined lens antenna. Extensive numerical and experimental data will be presented at the symposium.



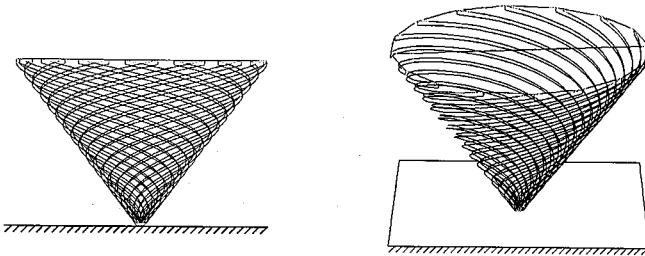
Folded Conical Helix Antenna

Justin A. Dobbins *, Robert L. Rogers
Applied Research Laboratories
The University of Texas at Austin
PO Box 8029
Austin, TX 78713-8029

Much of the recent work in the field of small antennas has been based upon the top-loaded, folded monopole design. Both broad-banding and miniaturization techniques have been developed and applied to these antennas. Our work is focused on the development of a novel wire antenna, specifically, a folded conical helix (see figure below) optimized for HF to VHF with some of the same broad-banding and miniaturization techniques. This antenna has an electrical bounding sphere radius (kr) of 0.71 radians, and it exhibits a half-power bandwidth of 58% of the $2/Q$ value, where Q is the ratio of near-field stored energy to radiated energy per cycle for this size of antenna. The antenna is matched to 50 ohms.

The folded conical helix antenna is made of multiple spiral-wound wires that are fashioned in the shape of a cone. The wires are fed from a single point at the apex of the cone. At the top of the cone each wire is folded back down in parallel with itself and connected to the ground plane. In addition to the well-known impedance transformation effect, this type of folding also creates shorted two-wire transmission lines connected in parallel with the cone. The length of the spiral wires is chosen so that the transmission line segments help to cancel the susceptance curve at the first antenna resonance as shown in (H. D. Foltz, J. S. McLean, and G. Crook, IEEE Trans. AP, vol. 46, No. 12, pp. 1894-1896, December 1998).

Folding techniques used to optimize a folded conical helix antenna will be presented. Simulated and measured results of input impedance, bandwidth, efficiency, and beam pattern data for this antenna will also be presented.



Telemetry & Command Antenna for a Micro Satellite at the VHF / UHF Frequencies
(Design & Manufacturing)

Amin Aminaie* , Mohammad Solaimani
Advanced Electronic Research Center

Turnstile Antenna is one of the most common antennas for creating circular polarization. it consists of two crossed dipoles that is fed by 90° phase difference or four monopoles that is fed by 0° , 90° , 180° & 270° phase difference respectively. Turnstile Antenna is simple reliable and has a good size comparing with the micro satellite.

The designed antenna consists of four slant monopoles. The length & configuration of the monopoles are optimized with respects to the parameters of the antenna at transmitting & receiving by NEC-WIN software. (Fig.1 & 2)

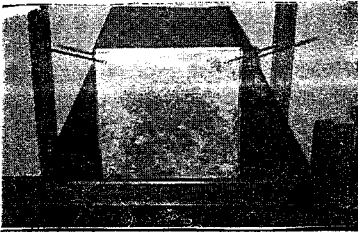


Fig. 1 Constructed Model

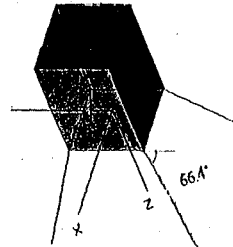


Fig.2 Configuration of the monopoles

At the frequencies of transmitting & receiving (435 ,145 MHz respectively) , many satellite antennas especially UOSAT antenna are considered. For transmitting , the power gain of the designed antenna is more uniform than UOSAT's. (Fig.3 & Fig.4)

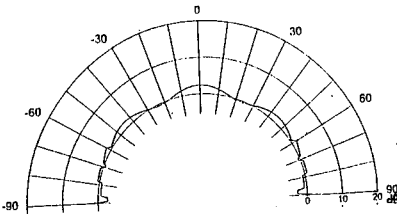


Fig. 3 Power gain for transmitting

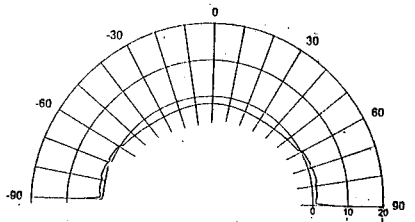


Fig.4 Power Gain for Receiving

Other parameters :

- VSWR for transmitting & receiving : 1.53 & 2.99 without using matching element (30 pf capacitance in seri with each monopole will reduce VSWR to 1.34 & 1.85)

- Axial ratio for transmitting & receiving : is cosinoidal for both frequencies.

for transmitting between -30 & 30 degree so that at 0 degree (Z axis) polarization is circular. for receiving , between -50 & 50 degree so that at 0 degree polarization is circular.

- Antenna is tested for pattern & VSWR . Results verify theoretical datas.

MULTIFEED UNIT FOR WIDEANGLE SAT-TV ANTENNA

Souren P. GUEROUNI. Head of Dept. of Radiophysics
Measurement Institute. Yerevan. Armenia

Microwave unit, including 16 feeds, one collector and one LNC, was elaborated and tested for the joint operation with a wideangle spherical reflector for SAT-TV signals reception in Ku-Band.

Spherical mirror in its immovable state allows to carry out the turn of the pattern without of reducing the Gain-factor in wideangle sector of as minimum as 120° . In such a sector of synchronous orbit might be located nearly 40 geostationary satellites (GSS). In this project it was set the problem of creating multifeed unit for simultaneous positioning onto 16 GSS, using only one LNC.

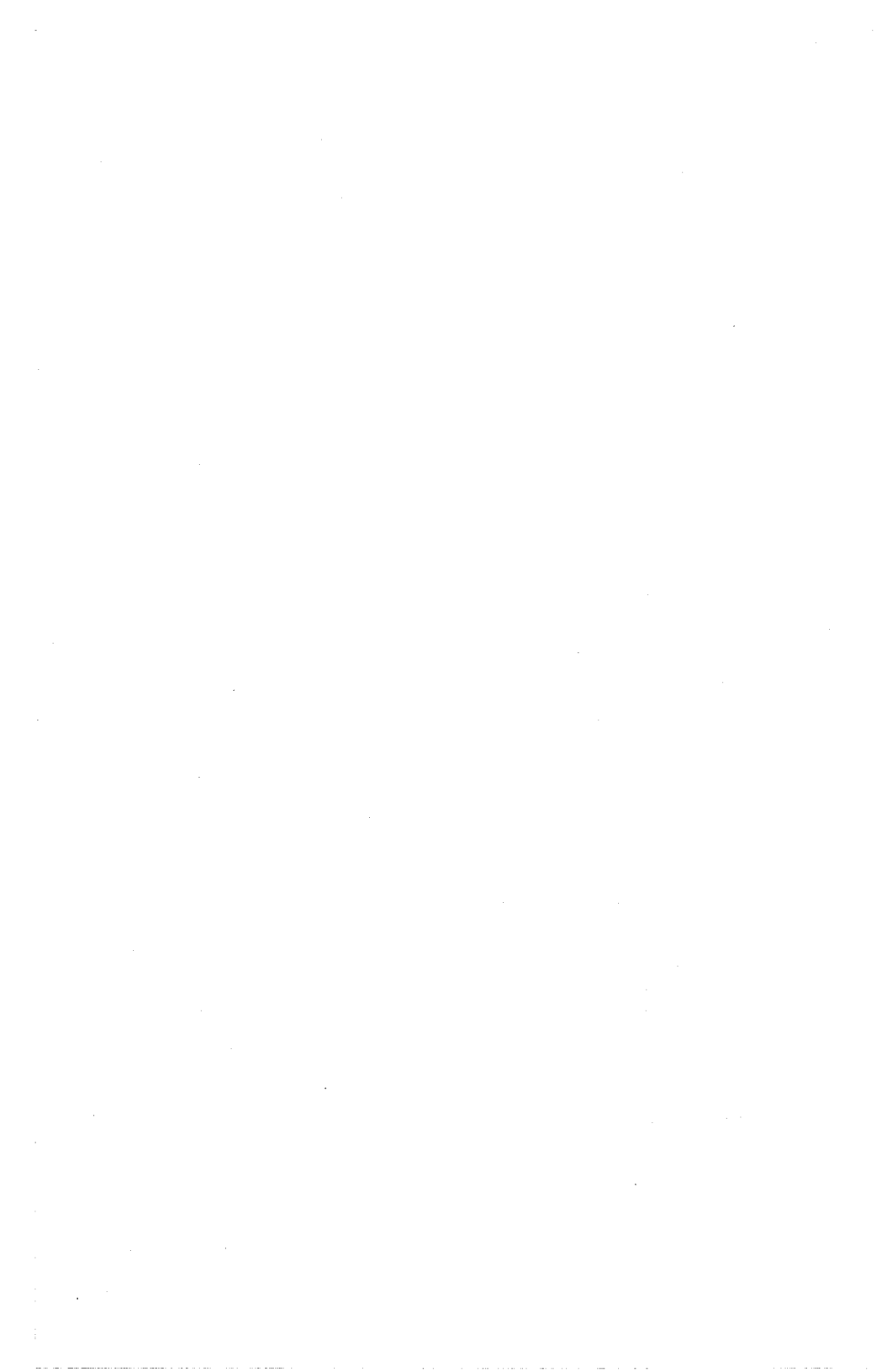
On the basis of rectangular waveguide of 19×9.5 mm was manufactured the signals collector, including 16 electromagnetic valves in the wide wall of waveguide. Over the valves were mounted 16 sections of flexible corrugated waveguide to which there were connected 16 feeds in the shape of circular open-ended waveguides. The implementation of flexible feeder allows to orientate feeds axes to the position of selected GSS. The given 16 feeds can control the angular orbit sector of GSS of nearly 60° .

The positions of feeds are fixed on a concentric guide both in azimuth and in elevation in the small angle sector in case of necessity.

In the operating state of the antenna the microwave feeders of all feeds, except one, are locked by electromagnetic valves. The signal from opened feed is transmitted to the collector and further to LNC, joined to the collector output. The collector channel length makes up nearly 300 mm. As shown by the measurements of the signal attenuation, the losses on the way from the farthest switch to LNC made 1.5 dB. With this in view the solution on setting the second LNC was accepted, that allowed to reduce the losses up to 0.5 dB at the farthest valve (No.8). So each of LNC serves 8 positions with a quite satisfactory quality.

Reflector is the cutting out of the spherical surface with the aperture size of 1500×2300 mm.

This antenna with multifeed unit may be used for creation of wireless communication net.



Guiding Structures and Circuits

Chair: R. Nevels, Texas A&M University

Page

- | | | | |
|----|------|--|-----|
| 1 | 1:50 | A novel equation for non-uniform lossless transmission line analysis, <i>J. Miller*</i> , <i>R. Nevels, Texas A&M University, USA</i> | 376 |
| 2 | 2:10 | Generalized telegrapher equations suitable for non-reciprocal ferrite loaded transmission lines, <i>R. Marqués*</i> , <i>F. Mesa, F. Medina, Facultad de Física, Spain</i> | 377 |
| 3 | 2:30 | Propagation parameters of microstrip transmission lines fabricated on magnetized ferrites with arbitrarily oriented bias magnetic field, <i>R. Boix*</i> , <i>G. León, F. Medina, Facultad de Física, Spain</i> | 378 |
| 4 | 2:50 | Efficient spectral domain analysis of strip-guided magnetostatic surface waves on a grounded multilayer ferrite loaded substrate/superstrate structure, <i>R. El Idrissi, R. Marqués*</i> , <i>Facultad de Física, Spain</i> | 379 |
| 5 | 3:10 | Full-wave analysis of microstrip lines and coplanar waveguides with arbitrarily shaped metallizations, <i>A. Dreher*</i> , <i>A. Ioffe, German Aerospace Center, Germany</i> | 380 |
| | 3:30 | Break | |
| 6 | 3:50 | Mutual coupling between open-ended coaxial and circular waveguides terminated in a layered medium, <i>Z. Shen*</i> , <i>P. Luo, C. Law, Nanyang Technological University, Singapore</i> | 381 |
| 7 | 4:10 | Electromagnetic modal analysis of a circular-rectangular waveguide T-junction using the finite plane wave expansion technique, <i>K-L. Wu*</i> , <i>The Chinese University of Hong Kong, Hong Kong</i> | 382 |
| 8 | 4:30 | Millimeter-wave response of the dielectric resonator in the slot line, <i>Y. Horii*</i> , <i>Kansai University, Japan</i> , <i>M. Tsutsumi, Kyoto Institute of Technology, Japan</i> | 383 |
| 9 | 4:50 | Finite-element analysis on a three-phase underground pipe-type cable for the computation of its zero-sequence impedance, <i>X-B. Xu*</i> , <i>G. Liu, Clemson University, USA</i> | 384 |
| 10 | 5:10 | Phase constant equalization of three coupled microstrip lines, <i>I. Barseem*</i> , <i>Electronics Research Institute, Egypt</i> | 385 |

A Novel Equation for Non-Uniform Lossless Transmission Line Analysis

J. A. Miller* and R. D. Nevels
 Department of Electrical Engineering
 Texas A&M University
 College Station, Texas 77843-3128

Transmission line analysis is traditionally performed using the pair of wave equations

$$V(z, t) = V^+ \left(t - \frac{z}{v} \right) + V^- \left(t + \frac{z}{v} \right) \quad (1)$$

$$I(z, t) = I^+ \left(t - \frac{z}{v} \right) + I^- \left(t + \frac{z}{v} \right)$$

derived from the telegrapher's equations. Each of these wave equations yield general solutions of positive (superscript plus) and negative traveling (superscript minus) voltages or currents where v is the velocity of either the voltage or current waves. Equations (1) are interpreted as follows: the voltage at a certain time (t) and position (z) is the sum of the positive traveling and negative traveling waves that existed at time $t - (z/v)$ and at positions $z \pm vt$. Implicit in (1) is that the transmission line is uniform and the wave functions for the positive and negative traveling voltages and currents are known. Another solution to the telegrapher's equations will be illustrated here.

Assuming a lossless transmission line, the transmission line equations can be combined into a single vector equation. A propagator can then be found which takes any given initial voltage and current distribution and generates a new set of distributions that are the voltage and current after one time step. This process can be repeated indefinitely, thereby producing the entire time history of the initial voltage-current distribution. The explicit pair of equations is as follows:

$$\begin{aligned} V(z, t) &= \frac{1}{2} [V_0(z+vt) + V_0(z-vt) + Z_0(I_0(z+vt) - I_0(z-vt))] \\ I(z, t) &= \frac{1}{2} [(V_0(z+vt) - V_0(z-vt))/Z_0 + I_0(z+vt) + I_0(z-vt)] \end{aligned} \quad (2)$$

where Z_0 is the characteristic impedance of the line. This solution is also valid for a non-uniform transmission line. In practice this would mean that Z_0 is a function of position z on the transmission line, but (2) are also valid when the permeability or permittivity is z dependent, as is realized through the velocity v . It is especially interesting that on a homogeneous line the positive and negative traveling waves are automatically distinguished and propagated without error in their respective directions given only the total initial voltage and current distributions.

In this presentation, a method for deriving (2) and a simple numerical evaluation technique will be outlined. Examples will include numerical simulation of a square pulse on a transmission line with two sections, and the response of a filter and a transmission line with a non-uniform section to a Gaussian pulse excitation. The results will be compared with those obtained using the commercial Libra[®] software package.

Generalized telegrapher equations suitable for non-reciprocal ferrite loaded transmission lines.

Ricardo Marqués, Francisco Mesa and Francisco Medina
Grupo de Microondas, Departamento de Electrónica y Electromagnetismo.
Facultad de Física, Avda. Reina Mercedes s/n, 41012, Sevilla, Spain.
Telephone number: 34-954552891. Fax: 34-954239434.
E-mail: marques@cica.es

The well-known telegrapher equations are widely used in the analysis of reciprocal transmission lines in the low frequency range. After the appropriate approximations of Maxwell equations, the line parameters (i.e., the shunt capacitance and conductance and the series inductance and resistance) may be calculated in a high variety of lines, such as microstrip and CPW on anisotropic and lossy substrates, including ferrite layers magnetized along the line axis, [T.Kitazawa, *IEEE-MTT*, **37**, 1749-1754, 1989], [M.Horno, et al., *IEEE-MTT*, **38**, 1059-1068, 1990], [J.Aguilera, et al., *IEEE-MGWL*, **9**, 57-59, 1999]. Nevertheless, the telegrapher equations in their standard form are not applicable to the analysis of non-reciprocal ferrite loaded transmission lines, since these equations are essentially reciprocal in nature.

In this work, the authors develop a modified telegrapher equations suitable for the analysis of non-reciprocal lines. The key of the proposed modification is the introduction of a new circuit concept, named the "characteristic memductance" of the line, which relates the per unit length (p.u.l.) flux density with the p.u.l. charge density along the line. Since the electric charge is a scalar magnitude and the magnetic flux a pseudo-scalar one, the characteristic memductance shows an essential non-reciprocal behavior, that can account for the non-reciprocity of the line. The characteristic memductance is so named after the earlier work of L.O.Chua "Memristor - the missing circuit element" [L.O.Chua, *IEEE-CT*, **18**, 507-519, 1971].

Numerical results will be presented for both the "characteristic memductance" and the rest of the line parameters, for some non-reciprocal structures. A comparison with the full wave analysis results will be also included.

Propagation parameters of microstrip transmission lines fabricated on magnetized ferrites with arbitrarily oriented bias magnetic field.

Rafael R. Boix*, Germán León, Francisco Medina

Grupo de Microondas, Departamento de Electrónica y Electromagnetismo.

Facultad de Física, Avda. Reina Mercedes s/n, 41012, Sevilla, Spain.

E-mail: boix@cica.es. Telephone number: 34-954552891. Fax: 34-954239434.

Microstrip lines fabricated on magnetized ferrite substrates have proved to have a wide variety of applications such as the design of magnetostatic wave transducers based on the excitation of magnetostatic waves [E. B. El-Sharawy, R. W. Jackson, *IEEE-MTT*, **6**, 730-737, 1990], tunable non-reciprocal phase shifters [I. Y. Hsia, H. Y. Yang, N. G. Alexopoulos, *JEWA*, **4/5**, 465-475, 1991], edge-guided mode isolators [T. M. Elshafey, J. T. Aberle, E. B. El-Sharawy, *IEEE-MTT*, **12**, 2661-2668, 1996], tunable band-pass filters [T. Fukusako, M. Tsutsumi, *IEEE-MTT*, **11**, 2013-2017, 1997], etc.

In this work the authors apply the spectral domain approach (SDA) to the full-wave numerical computation of the propagation constant and characteristic impedance of microstrip lines fabricated on ferrite substrates in the case in which the bias magnetic field of the ferrites is arbitrarily oriented. The current-power definition is used in the determination of the characteristic impedance since this definition seems to be more suitable than the voltage-current definition [I. Y. Hsia, H. Y. Yang, N. G. Alexopoulos, *JEWA*, **4/5**, 465-475, 1991] for microstrip lines [L. Zhu, K. Wu, *IEEE-MGWL*, **2**, 87-89, 1998]. The numerical overflow problems arising from the computation of the spectral domain electromagnetic fields inside the ferrite layers for large values of the spectral variables [H. Y. D. Yang, *IEEE-AP*, **8**, 520-526, 1997] are solved by invoking the physical concept of asymptotically equivalent guiding structures [R. R. Boix, N. G. Alexopoulos, M. Horno, *JEWA*, **8**, 1047-1083, 1996]. The numerical results obtained for the propagation constant of microstrip lines on double-layered dielectric-ferrite substrates have been compared with those obtained in [I. Y. Hsia, H. Y. Yang, N. G. Alexopoulos, *JEWA*, **4/5**, 465-475, 1991], and good agreement has been found between the two sets of results. The authors have observed that for every microstrip line fabricated on a substrate containing a ferrite layer, there is a frequency interval in which propagation is not possible, the limits of this frequency interval being strongly dependent on both the orientation and the magnitude of the bias magnetic field. The existence of this cutoff frequency interval is mainly attributed to the excitation of surface and volume magnetostatic wave modes along the substrates containing the ferrite layers. Also, the numerical results obtained have shown that for every frequency, both the propagation constant and the impedance can be varied over a wide range by changing the bias magnetic field magnitude.

Efficient spectral domain analysis of strip-guided magnetostatic surface waves on a grounded multilayer ferrite loaded substrate/superstrate structure

Rachid Rafii El Idrissi and Ricardo Marqués

Grupo de Microondas, Departamento de Electrónica y Electromagnetismo.

Facultad de Física, Avda. Reina Mercedes s/n, 41012, Sevilla, Spain.

Telephone number: 34-954552891. Fax: 34-954239434.

E-mail: marques@cica.es

Magnetostatic surface waves (MSSW) are useful in the design of delay lines, filters, resonators and other circuit devices at microwave frequencies. Strip-guided MSSW may provide a higher field confinement than conventional slab-guided MSSW and were first proposed and analyzed in [M.Uehara, K.Yashiro and S.Ohkawa, *J. Appl. Phys.*, **54** (5), 2582-2587, 1983], after an approximate magnetostatic analysis. They were also reported in [F.Mesa, R.Marqués and M.Horno, *IEEE-MTT*, **40**, 1630-1641, 1992] after a full wave analysis.

In this work the authors apply an efficient spectral domain analysis (SDA) to the analysis of strip guided MSSW propagating in multilayer structures, including slabs with arbitrary magnetization. For this analysis an "intensity function" is defined on the strip. This function gives the per unit length flux of charge between an arbitrary point on the strip and one of its edges. Since the divergence of the magnetostatic surface current density must vanish, the "intensity function" on a point on the remaining strip edge must vanish: i.e., the total intensity on the strip is null. This "intensity function" is then related to the magnetic flux density in the normal direction by means of a Green's function, which is obtained in the spectral domain. Since this component of the magnetic flux density must vanish on both, the strip and the ground plane, it results in an implicit integral equation for the wave phase constant, which is solved in the spectral domain by using the well known Galerkin method.

Numerical results include the validation of the proposed magnetostatic analysis by a full wave analysis, as well as the computation the of strip-guided MSSW characteristics on a high variety of multilayer non-reciprocal substrates with arbitrary magnetization. The range of frequencies and magnetization orientations for the excitation of non-radiating strip-guided MSSW is established, and the main characteristic of the analyzed strip-guided MSSW are discussed.

Full-Wave Analysis of Microstrip Lines and Coplanar Waveguides with Arbitrarily Shaped Metallizations

A. Dreher*, A. Ioffe

German Aerospace Center (DLR), Institute of Communications and Navigation,
Oberpfaffenhofen, D-82234 Wessling, Germany

Transmission lines with non-planar metallizations are of increasing interest in multilayer MMIC or HTS applications. A microstrip line designed with a V-shape strip conductor or ground plane shows lower edge-current densities and thus reduced losses. The shape of the back conductor can be formed to a complete shield to obtain several types of microshield lines. This reduces the coupling of adjacent lines and gives better dispersion characteristics with enhanced bandwidth. In conductor backed coplanar waveguides (CBCPW), the shielding provides proper grounding without via-holes and eliminates the radiation losses caused by parallel plate modes.

The analysis of these structures is often done by a quasi-TEM approach using conformal mapping techniques, since full-wave analysis methods like finite elements or method of moments are time-consuming. The shapes of lines and groundplanes are therefore restricted to simple geometries. In this paper, the discrete mode matching method (DMM) is used for the analysis. DMM is an efficient full-wave analysis method and has successfully been applied to planar multilayer and multiconductor waveguide structures (A. Dreher, *IEEE MTT-S Digest*, 193-196, 1996) as well as to structures with non-planar stratified dielectric layers (A. Dreher and A. Ioffe, *IEEE AP-S Digest* 1840-1843, 1999). Its principle is based on solving Helmholtz' wave equation separately in each layer of the structure and matching the tangential field components at the interfaces. The fields are represented by finite series of eigensolutions of the wave equation with suitable lateral boundary conditions. For the matching at the interfaces the fields are discretized by sampling. In contrast to finite difference procedures, the differential operators are not approximated by finite differences. The resulting system equation involves a small matrix containing either the tangential electric field components in the slots or the current components on the lines similar to moment-method solutions. Because of its flexibility the DMM can also be used to optimize the shape of the metallizations.

Microstrips and coplanar waveguides with non-planar metallizations are analyzed using the discrete mode matching method. The influence of different shapes on the effective permittivity and the current distribution will be discussed.

Mutual Coupling between Open-Ended Coaxial and Circular Waveguides Terminated in a Layered Medium

Zhongxiang Shen, Ping Luo, and Choi Look Law
School of Electrical and Electronic Engineering
Nanyang Technological University
Nanyang Avenue, Singapore 639798

Evaluation of the mutual coupling between open-ended coaxial and circular waveguides is important for the design of waveguide horn antenna arrays and is also useful for the measurement of dielectric material's complex permittivity. T. S. Bird has carried out an extensive study of the coupling between open-ended rectangular, coaxial, and circular waveguides based on a complicated integral formulation (T. S. Bird, *IEEE Trans. Antennas and Propagat.*, vol.42, no. 7, pp.1000-1006, 1994; *IEE Proc. Microwave, Antennas and Propagat.*, vol.143, pp. 265-271 and pp.457-464, 1996). Furthermore, most of the cases he considered are limited to the situation that homogeneous half space was assumed.

This paper describes a modal-expansion method for evaluating the cross-coupling between open-ended coaxial and circular waveguides terminated in a layered medium. The method begins with the introduction of a large circular waveguide to approximate the layered half-space. With the introduced large waveguide, the problem considered reduces to a bifurcated waveguide junction that can be solved by the formally exact modal-expansion method. The E-Field mode-matching matrices for the off-centered coaxial/circular-to-circular waveguide junction are derived analytically with the aid of Graf's addition theorem for Bessel functions. The complexification and extrapolation technique (Z. Shen and R. H. MacPhie, *IEEE Trans. Microwave Theory and Tech.*, vol.45, no.4, pp.546-548, 1997) is then employed to avoid the slow convergence problem and to improve the accuracy of this method. Numerical results for three coupling structures (two open-ended coaxial waveguides, two open-ended circular waveguides, one coaxial line and one circular waveguide) are presented and discussed.

Electromagnetic Modal Analysis of A Circular-Rectangular Waveguide T-Junction Using the Finite Plane Wave Expansion Technique

Ke-Li Wu

Dept. of Electronic Engineering, The Chinese University of Hong Kong, Shatin, Hong Kong, PRC

Abstract

An effective electromagnetic model of a circular-rectangular waveguide T-junction is a key module in many practical problems, such as a waveguide orthomode transducer in an antenna feed network and some high performance waveguide multiplexer network employing circular waveguide dual mode filters. In this paper, we provide a new modal analysis called extended boundary condition modal analysis (EBMA) for the T-junction. The analysis employs the finite plane wave expansion technique and matches the boundary conditions on the extended virtual boundary. Therefore, there is no numerical integration required. Since it is virtually an analytic solution, it can be used for a wide rectangular opening on the side-wall of a circular waveguide.

It should be noted that there are two boundary surfaces between rectangular waveguide WG2 and the circular waveguide: S2 and S2', as shown in Fig.1. In another word, there is a overlap region. It is postulated, in the analysis, that if fields in the two regions match on one surface, they must match on the other one. Therefore, instead of matching the field on S2, the new modal analysis matches the fields on S2' whenever needed. To match the fields on S2', the solutions for the three types of field solution are expressed in two different forms: one is in cylindrical coordinates that is used to match the fields on S1 and S3; the other is in rectangular coordinates that will facilitate the matching of the cavity fields to that of rectangular waveguide. For example, the TE mode electric field mode function in circular waveguide can be expressed, in cylindrical coordinate, as

$$\bar{\Phi}_{q_s}^{1h} = N_{nm}^{1h} \left[\hat{r} \frac{n}{r} J_n(k_{nm}^h r) \begin{pmatrix} \sin(n\phi) \\ -\cos(n\phi) \end{pmatrix} + \hat{\phi} k_{nm}^h J_n'(k_{nm}^h r) \begin{pmatrix} \cos(n\phi) \\ \sin(n\phi) \end{pmatrix} \right] sh[\gamma(z-L)]$$

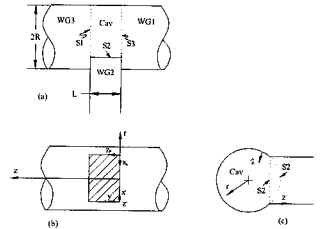
Its tangential component on the boundary S2 can be expressed in local rectangular coordinate as

$$\Phi_{q_s}^{1h} = N_{nm}^{1h} A_{mn} \sum_{l=0}^{N-1} S_{ls} \begin{pmatrix} C_{ln} \\ S_{ln} \end{pmatrix} E_{mjs} e^{-jk_{nm}^h C_{ls} x_s} sh[\gamma(z-L)]$$

so that the field matching can be undertaken analytically.

To verify the proposed modal analysis, a large number of configurations are investigated using the proposed analysis and commercial FEM software. Excellent agreement has been obtained.

Figure 1 Perspective views of the circular to rectangular T-junction.



Millimeter-wave Response of the Dielectric Resonator in the Slot Line

Yasushi Horii
Kansai University

Ryozenji-cho, Takatsuki, Osaka 569-1095 Japan
Tel & Fax: +81-726-90-2476
E-mail: horii@res.kutc.kansai-u.ac.jp

Makoto Tsutsumi
Kyoto Institute of Technology

Matsugasaki, Sakyo-ku, Kyoto, 606-8585 Japan
Tel : +81-75-724-7451 Fax : +81-75-724-7400
E-mail: tutumi@dj.kit.ac.jp

Introduction

For an optical control of electromagnetic (EM) waves, the slot line with semiconductor substrate is very sensitive to the laser illumination in millimeter wave band[1]. Using this slot line, this paper proposes a novel band stop filter based on the dielectric resonator (DR). As the EM-field is concentrated around the slot, the propagation mode strongly couples with the DR, and the band stop characteristic can be easily obtained. We have demonstrated this filter both theoretically and experimentally using the small DR chip and the silicon wafer for the semiconductor substrate.

Model

The slot line with the width of 1.0mm is fabricated on the silicon substrate (0.6mm thickness, $\epsilon_r = 11.8$), and the rectangular DR (1.0mm \times 1.0mm \times 2.0mm, $\epsilon_{DR} = 40$) is placed on the slot line as shown in Fig.1. For the FDTD analysis, this filter is modeled on the Yee's mesh constructed by 70 \times 90 \times 200 cells (0.1mm cubic cell). Experiment was also carried out using the same model.

Results

Fig.2 shows the frequency characteristic of the transmission parameter S_{21} of this filter. From the experimental result (rigid line), the resonance could be observed around 36GHz, 42GHz, and 48GHz, and the notch responses around 42GHz and 49GHz were more than -20dB. This frequency characteristic agrees with the theoretical prediction (dotted line).

Conclusion

Though the theoretical and experimental results in Fig.2 are not optimized, the resonant frequency and the notch characteristic will be designed by tuning dimensions of the DR and its dielectric constant ϵ_{DR} . Proposed slot line filter having the simple structure and small in size is useful for millimeter wave signal processing including optical control of millimeter waves.

Reference

[1] M.Tsutsumi, *et. al.*, *APMC 1999*, pp.327-330, Singapore.

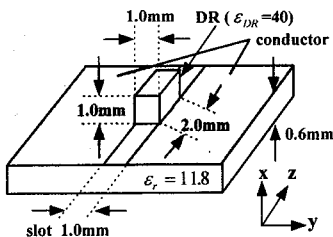


Fig.1 Theoretical model

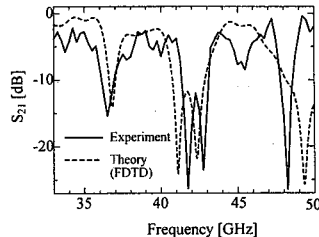


Fig.2 Frequency characteristic of S_{21}

Finite-Element Analysis on A Three-Phase Underground Pipe-Type Cable
For The Computation of Its Zero-Sequence Impedance

Xiao-Bang Xu* and Guanghao Liu
Holcombe Department of Electrical and Computer Engineering
Clemson University
Clemson, SC 29634-0915

Three-phase underground pipe-type cables are widely used in power transmission systems in urban areas. To protect such systems, utilities engineers need to properly size circuit breakers based on knowledge of fault currents. For an accurate calculation of the fault currents, it is necessary to know the zero-sequence impedance of the underground pipe-type cable. The method currently most widely used in industry for calculating the zero-sequence impedance is based on a paper by J.H. Neher published in 1964 (J.H. Neher, "The phase sequence impedance of pipe-type cables," IEEE Transactions on Power Apparatus and Systems, Vol. PAS-83, pp. 795-804, August 1964). Neher indicates that in the usual case where the pipe is made of steel, the zero-sequence impedance depends upon the permeability of the steel. It is well known that the permeability of steel changes with the magnetic field intensity. Since the magnetic field intensity varies in the steel pipe, the permeability should be different from point to point in the pipe. But, unfortunately, in Neher's computational model, a *constant* "effective permeability" is used for the *whole* steel pipe and the magnetic field intensity used for calculating the "effective permeability" is obtained from an empirical formula. As a result, such calculated zero-sequence impedance has a considerable difference compared with measurement data.

In this paper, we present an improved method for computing the zero-sequence impedance of a three-phase underground pipe-type cable, based on finite-element analysis and iterative solution procedure. The zero-sequence impedance can be computed from knowledge of the source current densities in the conducting regions within the pipe-type cable. To determine the source current densities, integro-differential equations are formulated. They are solved numerically by employing finite-element method, subject to appropriate boundary conditions. In the numerical solution, special attention is paid to the nonlinear B-H characteristic of the steel pipe. An iterative solution procedure is developed for determining the relative permeability in each element of the pipe. Computational results of the zero-sequence impedance at different current levels are presented and analyzed. Also, they are validated by being compared with measurement data.

Phase Constant Equalization of Three Coupled Microstrip Lines

I.M. Barseem
Electronics Research Institute
El-Tahrir street, Dokki, Cairo, Egypt
Tel: 202-3310506, Fax: 202-3351631, e-mail: bibrahim@eri.sci.eg

Abstract:

Three coupled microstrip lines can be used as a six-port reflectometer. It is an alternative tool of the network analyzer to measure the amplitude and phase of the unknown complex impedance only by using the reading of power meters and a simple calibration procedure. The design of microstrip six-port reflectometer requires good isolation between certain ports. Because of the difference in the phase constant of the three propagating modes exist in the three coupled microstrip lines, the required degree of isolation can not be achieved. Also the coupling length which specify the center frequency of the reflectometer is calculated by an approximated method (the average of the three phase constants) which will cause a shift in the center frequency. A three coupled microstrip lines with equal mode phase constant is introduced in (I Barseem, ANTEM98, pp. 173-176, Ottawa, August 1998) by adjusting an air gap between the dielectric substrate and the ground plane. Although this method give accurate results, there is some difficulty on calibrating the air gap length specially if a teflon dielectric substrate is used . Also it has some restrictions when integration with another microstrip circuits is required. An alternative method for phase equalization is the use of dielectric overlay. A two coupled microstrip lines with equal phase constant using dielectric overlay is implemented experimentally in (J.L. Klein, K. Chang Elec. Lett, Vol. 26, PP. 274-276, March, 1990)

In this paper we annalize the three coupled microstrip lines with dielectric overlay structure to obtain equal phase constant of the three propagating modes. The method of lines is used in our analysis to obtain the propagation phase constant and the characteristic impedance.



Radar Cross Section

Chair: N. Uzunoglu, National Technical University of Athens, Greece

Page

- | | | | |
|---|------|---|-----|
| 1 | 1:50 | Application of the PO to the computation of the monostatic RCS of arbitrary bodies modeled by plane facets of dielectric and magnetic materials, <i>F. Saez de Adana*</i> , <i>P. Lozano</i> , <i>F. Gisbert</i> , <i>I. Sudupe</i> , <i>J. Perez</i> , <i>M. Catedra</i> , <i>Universidad de Alcala, Spain</i> | 388 |
| 2 | 2:10 | Method based on physical optics to calculate the monostatic RCS of arbitrary targets bodies modeled by NURBS surfaces of dielectric and magnetics materials, <i>F. Saez de Adana*</i> , <i>J. Perez</i> , <i>M. Catedra</i> , <i>Universidad de Alcala, Spain</i> | 389 |
| 3 | 2:30 | Electromagnetic scattering from large targets with low cross section: a geometrical case study, <i>W. Wood Jr.*</i> , <i>K. Hill</i> , <i>Air Force Research Laboratory, USA</i> | 390 |
| 4 | 2:50 | The Method of Auxiliary Sources (MAS) applied to radar cross-section (RCS) evaluation of jet engine inlets, <i>H. Anastassi*</i> , <i>D. Kaklamani</i> , <i>N. Uzunoglu</i> , <i>National Technical University of Athens, Greece</i> | 391 |
| 5 | 3:10 | Calculation and analysis of second order diffractions and reflections on radar cross-section, <i>P. Pouliguen*</i> , <i>P. Jaffrezou</i> , <i>Centre d'Electronique de l'Armement, France</i> | 392 |
| 6 | 3:30 | Model of radiowave scattering from ionospheric plasma disturbance creating of space vehicle exhaust plume, <i>V. Spitsyn*</i> , <i>Tomsk State University, Russia</i> | AP |

**APPLICATION OF THE PO TO THE COMPUTATION OF THE
MONOSTATIC RCS OF ARBITRARY BODIES MODELED BY
PLANE FACETS OF DIELECTRIC AND MAGNETIC MATERIALS.**

F. Saez de Adana , P. Lozano, F. Gisbert, I. Sudupe, J. Pérez, M.F. Cátedra

*Dept. Teoría de la Señal y Comunicaciones
Escuela Politécnica, Universidad de Alcalá
28806 Alcalá de Henares. Madrid. Spain
Fax: +34 91 885 6699. E-mail: felipe.catedra@uah.es*

A Physical Optics (PO) approach for the computation of the monostatic Radar Cross Section (RCS) is presented. This method is applied to three-dimensional structures modeled by plane facets of dielectric and magnetic materials including losses.

The RCS of a target plays a predominant role in its detection by radar. A method based on the PO is developed to solve the problem. To represent the body a model of plane facets is used. The validity of this geometrical model has been proved previously for perfectly conductive facets. In this work the effect of having facets composed by any dielectric and magnetic material (including losses) is considered in the description of the model.

The main mechanism that contributes to RCS is the reflection in facets. In this approach, this contribution is computed using the PO expressions, but including the Fresnel coefficients in order to consider the influence of the material. However, the analysis will be erroneous if the model edges are not considered. The computation of diffraction produced by edges is carried out with a heuristic formulation. This formulation introduces the influence of the reflection coefficients of the facets that form the edge in the Equivalent Currents Method (ECM). These facets can be composed by different materials.

The scattering mechanisms of higher order like double reflections or double interaction between facets and edges are not less important because at fixed angular margins can represent a substantial change in the RCS of the body. These effects are introduced combining the Geometrical Optics (GO) with the PO and the ECM employing the Image Theory. This theory has also been modified to include the Fresnel coefficients in it.

**METHOD BASED ON PHYSICAL OPTICS TO CALCULATE THE
MONOSTATIC RCS OF ARBITRARY TARGETS BODIES MODELED
BY NURBS SURFACES OF DIELECTRIC AND MAGNETICS
MATERIALS.**

F. Saez de Adana, J. Pérez, M.F. Cátedra

*Dept. Teoría de la Señal y Comunicaciones
Escuela Politécnica, Universidad de Alcalá
28806 Alcalá de Henares. Madrid. Spain
Fax: +34 91 885 6699. E-mail: felipe.catedra@uah.es*

This communication presents a method for the analysis and prediction of monostatic Radar Cross Section (RCS) of targets of complex geometry. These targets can be formed by multilayer structures of dielectric and magnetic materials. Nowadays one technique used to reduce the RCS of a body is cover it with a dielectric material which mitigates the reflection of the incident wave on the body, reducing in this way the RCS value. Therefore, it is very important to have a tool to predict the electromagnetic behavior of a body covered by dielectric material to control the increase or reduction of its RCS. In the past this problem has been treated for perfectly conductive bodies.

The geometry representation of the targets is given as a collection of NURBS (Non Uniform Rational B-Spline) surfaces. These are parametric surfaces of arbitrary degree widely used in the world of the Computer Aided Geometric Design (CAGD). With this kind of surfaces complex targets can be modeled with a very low amount of surfaces and very high accuracy. Another advantage of this representation is that not artificial edges are introduced.

The scattering electric field can be obtained integrating the currents in the body induced by an incident plane wave. The PO assumes simple expressions to calculate the induced currents as functions of the incident fields, taking into account that the surface is not perfectly conductive introducing in the PO equations the Fresnel reflection coefficients of the material. The integral to obtain the scattered field is expressed as a function of the parametric coordinates of the surface and is solved using the Stationary Phase method, which is an asymptotic method that provides excellent results in the high frequency range where the PO is valid.

To determine the reflection coefficients, a general situation is considered. The material, which forms the layers, can have dielectric and magnetic losses. The computation of the reflection coefficients of the multilayer structure is done using an analogy with transmission lines. Each layer is like a stretch of line with a length equal to the thickness of the layer.

The method has been validated with different complex structures comparing the PO results with those obtained with the Conjugate Gradient with the Fast Fourier Transform (CG-FFT) method.

Electromagnetic Scattering from Large Targets with Low Cross Section: A Geometrical Case Study

William D. Wood, Jr. and Kueichien C. Hill
Air Force Research Laboratory
2591 K Street, Building 254
Wright-Patterson AFB OH 45433-7602

Recent advances in computational electromagnetics (CEM) have lead to dramatic increases in the ability to predict, with arbitrary accuracy, the scattering characteristics of electrically large targets. For example, the fast multipole method, especially in its multiple level form, has greatly improved the problem sizes that can be treated on current workstations and parallel supercomputers. Even the most advanced CEM algorithms, however, are put to the test when applied to electrically large targets having low radar cross section (RCS). This is due to the extreme sensitivity of RCS to errors in surface current density for such targets, exacerbated by the more uniform contribution from the entire surface compared to the more discrete, scattering-center property of conventional targets. The result has been an increased awareness of the importance of accurate geometrical modeling of large, low-RCS targets.

We present results from a study involving the Denmark Dart, an approximately four foot long object sharply pointed at one end and bluntly rounded at the other end. The monostatic RCS of a physical model of the Dart has been measured at the AFRL Advanced Compact Range at Wright-Patterson AFB, Ohio, providing reference data to which computed data can be compared. The shape of the physical model has been sampled using three separate techniques, resulting in three slightly different computer models of the Dart. Surface grids were generated from each computer model, suitable for input to several advanced moment-method computer codes. Convergence and accuracy assessments are based on code-to-code and code-to-measurement comparisons. The results show that the RCS predictions are sensitive to the fidelity of the computer model, and that this sensitivity is especially strong when the RCS is low and the frequency is high.

The Method of Auxiliary Sources (MAS) Applied to Radar Cross Section (RCS) Evaluation of Jet Engine Inlets

Hristos T. Anastassiou*, Dimitra I. Kaklamani and Nikolaos K. Uzunoglu

Institute of Communication and Computer Systems,
National Technical University of Athens,
Iroon Polytechniou 9, GR-15780 Zografou, Athens, Greece
hristosa@esd.ece.ntua.gr

Accurate Radar Cross Section (RCS) computations of aircraft structures is an issue of great importance in both civilian and military applications. Recent investigations have demonstrated that a very significant contribution to the overall aircraft RCS is due to the engine inlets. Since the inlet is not amenable to high frequency solutions, because of its electrically small geometrical details, various numerical techniques, such as the Finite Element Method (FEM), the Moment Method (MoM) and the Adaptive Integral Method (AIM) have been recently invoked in the analysis of simplified cavity models. Nevertheless, the extremely large size of a realistic inlet renders all standard numerical solutions impractical, unless drastic reduction of the computational cost is achieved.

The Method of Auxiliary Sources (MAS) is a numerical technique with attractive properties, well-suited to the particular difficulties of the inlet geometry. While its accuracy is comparable to MoM, MAS computational demands are much lower than MoM's for a wide range of applications. The fundamental concept of the method is the expression of the scattered field as a superposition of elementary contributions from fictitious sources, located inside the scattering surface boundary. The unknown source weights are determined through the solution of a linear system, constructed on the basis of all pertinent boundary conditions satisfaction. The low computational complexity of the technique is due to the extremely fast calculation of the relevant matrix elements.

In this paper, MAS is applied to the jet engine inlet analysis, in conjunction with modal field representation, and exploitation of the inlet cylindrical periodicity. The inlet aperture is illuminated by a plane wave exciting waveguide modes, which propagate towards the inlet opposite end. These incoming modes constitute the incident field in the MAS-modeled scattering procedure from the hub/blade termination, which gives rise to scattered outgoing modes. It can be shown that only one period ("slice") of the termination is necessary in the calculation, resulting in further reduction of the computational requirements. The global scattered field is the sum of all outgoing modal contributions, radiated from the aperture into free space.

The low CPU time requirements of MAS, combined with the significant reduction of the structure effective size due to the "slicing" scheme, yields a powerful computational tool, capable of characterizing very large engine inlets. Numerical results and comparisons with reference data will be presented at the conference.

CALCULATION AND ANALYSIS OF SECOND ORDER DIFFRACTIONS AND REFLECTIONS ON RADAR CROSS SECTION

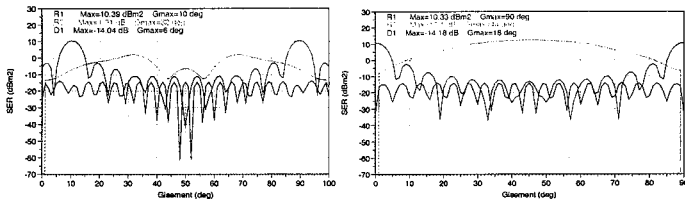
P. POULIGUEN, P. JAFFREZOU

Centre d'Electronique de l'Armement (CELAR), Division GEOS,
35170 Bruz, FRANCE

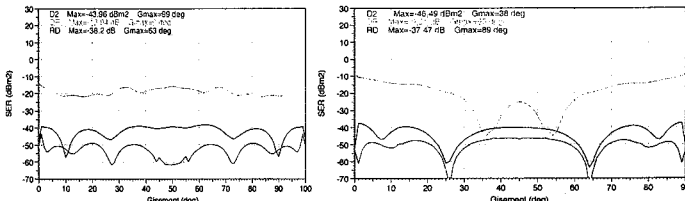
ABSTRACT

A high frequency model, using Physical Optics (P.O.) and the Method of Equivalent Currents (M.E.C.), is proposed to calculate Radar Cross Section (R.C.S.) of targets, including single and double diffractions, single and double reflections and "diffractions - reflections". This model furnishes monostatic or bistatic scattered electromagnetic fields of the target under test. The calculation can be accomplished versus the range between the Radar and the target centre of symmetry ; giving the possibility of a near field simulation.

Targets studied in this paper have been selected for their ability to produce second order interactions. These targets are two conducting dihedrals of 20 cm in side, the first with an internal angle of 90° in order to maximise the double reflections, the second with an internal angle of 100° to reduce the double reflections amplitude. Figures 1 and 2 compare the different E.M. interactions for the two dihedrals, at 7 GHz in VV polarization. Figure 1 superimposes the single reflections "R1", the double reflections "R2" and the single diffractions "D1" contributions to R.C.S. Figure 2 superimposes the double diffractions "D2", the "reflections - diffractions" "RD" and the "diffractions - reflections" "DR" contributions to R.C.S.



- Figure 1 : R.C.S. of dihedral 100° (left) and 90° (right) : R1, R2, D1 -



- Figure 2 : R.C.S. of dihedral 100° (left) and 90° (right) : D2, RD, DR -

Inverse Scattering

Chair: A. Ishimaru, University of Washington

Page

- | | | | |
|---|------|---|-----|
| 1 | 1:50 | Inverse scattering of dielectric targets embedded in a multi-layered medium,
<i>T. Yu, L. Carin*, Duke University, USA</i> | 394 |
| 2 | 2:10 | Nonlinear inversion of borehole induction measurements using a new fast
forward algorithm, <i>Z. Zhang*, Q. Liu, Duke University, USA</i> | 395 |
| 3 | 2:30 | Inverse scattering by total variation-based conjugate gradient algorithm on
parallel systems, <i>J-H. Lin*, C. Tsai, National Taiwan Ocean University,
Keelung</i> | 396 |
| 4 | 2:50 | Reflection from PMLs in lossy media, <i>J.-P. Berenger*, Centre d'Analyse de
Défense, B. Martinat, A. Reineix, IRCOM, France</i> | 397 |

Inverse Scattering of Dielectric Targets Embedded in a Multi-Layered Medium

Tiejun Yu and Lawrence Carin
Department of Electrical and Computer Engineering
Duke University
Box 90291
Durham, NC 27708-0291

There are many applications for which one may be interested in sensing a low-loss dielectric target embedded in a lossy host medium. For example, buried plastic land mines, plastic pipes and underground tunnels generally constitute conducting voids in the presence of a lossy soil background. While such targets can in principle be detected by a radar sensor, radar suffers well-known difficulties due to soil-induced attenuation. An electromagnetic-induction (EMI) sensor, on the other hand, affords the potential for significant soil penetration. Such sensors are typically used as metal detectors, with example applications including detection of buried *conducting* land mines and unexploded ordnance. As elucidated here, such sensors can also be used to detect the *absence* of conductivity (a conducting void) in the presence of a conducting host medium. Our focus here is on generally small, shallow targets (e.g. plastic mines), although the computer model is quite general.

We have developed three forward models used in the inversion of such targets. Two of the models are based on the method of moments (MoM). In particular, we have developed a volumetric electric-field integral equation (EFIE), as well as a surface combined-field integral equation (CFIE). While a MoM analysis is accurate, it generally requires the inversion of a large matrix. This task is circumvented by employing the extended-Born method, this an approximate method that only requires inversion of simple 3x3 matrices. The attendant speed enhancement accrued by extended-Born, *vis-a-vis* the MoM, is critical if the model is to be utilized in the context of signal processing and/or inverse scattering.

The forward models are employed in iterative Born and distorted Born inversion of general dielectric targets embedded in an arbitrary layered medium. The basic forward and inverse framework will be discussed in detail, and results will be presented for several subsurface targets of interest.

Nonlinear Inversion of Borehole Induction Measurements Using a New Fast Forward Algorithm

Zhong Qing Zhang* and Qing Huo Liu
Department of Electrical and Computer Engineering
Duke University
Durham, NC 27708-0291

Tel:(919) 660-5440; Fax:(919) 660-5293; Email:qhliu@ee.duke.edu

In this work we investigate the inverse problem of borehole induction measurements. Previously, several methods have been developed to invert for the formation conductivity distribution using inversion methods. These include the linear inversion with the Born approximation or simple geometrical factor theory, and nonlinear inversion using the Born iterative method (BIM), distorted Born iterative method (DBIM) (Chew and Liu, *IEEE, GE*, **32**, 878-884, 1994), and modified gradient method (van den Berg et al, *Radio Sci.*, **30**, 1355-1369, 1995). The forward solutions have been obtained by the numerical mode-matching method and conjugate-gradient fast Fourier Hankel transform (CG-FFHT) method.

The main contribution of this work is to combine the extended Born approximation (EBA) (Habashy et al, *J. Geoph. Res., Solid Earth*, **98**, 1759-1775, 1993) and the CG-FFHT method (Liu and Chew, *Radio Sci.*, **29**, 1009-1022, 1994) in both the forward and inverse solutions. In the forward solution, the fast Fourier/Hankel transform algorithm is first used to speed up the EBA. This reduces the computational complexity of the EBA from $O(N^2)$ to $O(N \log_2 N)$, where N is the number of unknowns. Then, this improved EBA is used as a partial preconditioner for the CG-FFHT method to reduce the number of CG iterations. The hybrid EBA-CGFFHT method is thus more accurate and efficient than the EBA or CG-FFHT alone. Since the initial solution is given by the FFHT enhanced EBA, it automatically stops the CG iteration if the EBA solution is accurate; otherwise the CG iterations proceed until the solution converges.

In the inversion, the initial solution is obtained by a two-step linear inversion involving the FFHT enhanced EBA. For many moderate contrasts, this solution suffices. For other high contrasts, an iterative nonlinear inversion procedure is then invoked with the EBA-CGFFHT as the forward solver. Hence, the combination of the EBA and CG-FFHT reduces the forward computation to a complexity of $O(N \log_2 N)$. Additional constraints (nonnegative conductivity and permittivity) must be taken into consideration in practical inversion. Numerical results will be shown to demonstrate the advantages of this novel nonlinear inversion scheme.

This work was supported by U.S. EPA through a PECASE grant CR-825-225-010, and by the NSF through a CAREER grant ECS-9702195.

Inverse Scattering by Total Variation-Based Conjugate Gradient Algorithm on Parallel Systems

JIUN-HWA LIN* AND CHIH YUNG TSAI
DEPARTMENT OF ELECTRICAL ENGINEERING
NATIONAL TAIWAN OCEAN UNIVERSITY
KEELUNG 202, TAIWAN, REPUBLIC OF CHINA

In recent years, the total variation method applied in inverse scattering [P.M. van den Berg and R.E. Kleinman, *Inverse Problems*, vol. 11, 5-10, 1995] or data de-blurring gains much attention in that it is capable of reconstructing piecewise constant profile objects. This method leads to images of better resolution and clearly exhibits the object sharp boundary, for which previous works utilizing the Tikhonov regularization fail to reconstruct satisfactorily and always give rise to oscillating structures.

In this work, we apply the total variation method in a two-dimensional TM electromagnetic problem in microwave regime. A cost function is defined as the difference between the measured data and the simulated one under current ϵ profile. A total variation penalty term is included to emphasize the piecewise-constant profile characteristics. The cost function is minimized to a specified tolerance by iteratively updating ϵ . Each iteration calculates the gradient to find the conjugate direction, and the step size along the direction via the Hessian of the cost function. The most computationally intensive part for the iterative algorithm lies in calculating the gradient and Hessian, which involves forward scattering problems for all transmitters and receivers. The forward solver such as CG-FFT once invoked requires $O(N_i N \log N)$ operations, where N_i inner iterations and N unknowns are assumed. Hence, N_T transmitters and N_R receivers would incur $O((N_T + N_R)N_i N \log N)$ operations for each outer iteration.

In view of transmitters and receivers acting independently in linear media, parallel processing scheme is employed to reduce the wall-clock time in profile reconstruction by seminating $N_T + N_R$ forward problems among all available processors and simultaneously solving the assigned forward problems. In addition, N_i can be kept fixed by retaining previous solutions as initial guesses for next outer iteration. Therefore, as the problem size grows and processors increase proportionately, the time in obtaining the reconstructed profile scales as $O(N \log N)$.

We shall investigate several aspects of this algorithm including: the image quality versus choices of weighting factors; reconstructions from real measurement data; parallel efficiency analysis; frequency hopping scheme in the larger object reconstruction.

REFLECTION FROM PMLs IN LOSSY MEDIA

J.-P. BERENGER*, B. MARTINAT**, A. REINEIX**

* Centre d'Analyse de Défense
16 bis, Avenue Prieur de la Côte d'Or 94114 Arcueil, France

** IRCOM
123, Avenue Albert Thomas 87060 Limoges, France

The extension of the PML concept to lossy media was derived by Fang and Wu (*IEEE Trans. MTT* 12-1, 1996). In such media the PML equations in frequency domain can be found as in a vacuum by stretching the coordinates. From this, the time domain equations and then the FDTD equations can be derived. In this paper, both the theoretical reflection and the actual FDTD reflection from such "lossy PMLs" will be studied and discussed, and the application to a problem of probing the Mars underground will be shown.

On the contrary to PMLs in a vacuum, in lossy PMLs the absorption depends on frequency, i.e. the theoretical reflection coefficient $R(\theta)$ becomes $R(\theta, \omega)$. As a result, choosing the parameters of the PML is more complicated than in a vacuum. Ideally, the absorption must be sufficient at all the frequencies of interest, while not needlessly strong at some frequencies, not to produce an important amount of numerical reflection. In the paper, the evolution of reflection $R(\theta, \omega)$ in function of the parameters of the problem will be discussed, with an emphasize on some special cases (reflection reduced to that of a PML in a vacuum, or to that of the lossy medium).

The second part of the paper will be devoted to the numerical reflection, i.e. the actual reflection in the FDTD discretized medium. The theoretical formulae giving this reflection have been derived and validated by FDTD tests. Comparisons of theoretical reflection (i.e. in ideal continuous media) with FDTD reflection, will be provided. The actual possibilities of "lossy PMLs" will be discussed in function of such parameters as the conductivity of the lossy medium, the PML conductivity, or the PML thickness.

The last part of the paper will present an application to the design of a device meant for probing the underground of the Mars planet. A transmitter above the ground radiates a wave that is reflected from the different layers, up to several kilometers in depth. This problem has been solved by applying the FDTD method within a computational domain reduced to a narrow well surrounded by a "lossy PML".



Author Index

Abd-Alhameed, R.	315	Brickerd, D. D.	188
Abdulla, M.	12	Broschat, S.	293
Adams, R.	162	Brown, G.	295
Adler, E. D.	188	Buber, T.	8
Afonin, D.	55, 277	Bunting, C.	128
Aksun, M.	41	Burke, M.	7
Al-Ansari, K.	121	Burkholder, R.	168, 296
Alonso, B.	222	Butler, C.	352, 365
Altintas, A.	41	Buxton, C.	10
Altman, Z.	151, 346	Cable, V.	88
Altshuler, E.	226	Cai, L.	343
Aminae, A.	372	Caliskan, F.	125
Anastassiou, H.	391	Cangellaris, A.	126
Anderson, A.	112	Canning, F.	357
Arnold, D.	114, 115, 116, 117, 118, 269	Cao, Q.	93
Arnold, J.	144	Capolino, F.	232
Arvas, E.	8, 235	Caputa, K.	89, 156, 213
Arvas, S.	8	Carin, L.	92, 162, 164, 165, 167, 336, 341, 394
Ashcraft, I.	113	Casciato, M.	244
Aydin, E.	238	Caswell, E.	227
Aygin, K.	176	Catedra, M.	222, 388, 389
Bae, D.	31	Catton, J.	330
Baertlein, B.	153	Cetiner, B.	87
Balakrishnan, N.	29, 91	Chae, H.	263
Barbosa, A.	65	Chair, R.	81
Bardati, F.	72	Chakravarty, S.	238
Barka, A.	265	Chan, C.	202, 335
Barnett, T.	210	Chan, K.	202
Barseem, I.	385	Chang, C.	158
Basilio, L.	316	Chang, W.	192
Bassey, C.	213	Chappell, W.	288
Bazin, V.	265	Charnotskii, M.	292
Bazow, T.	357	Chatterjee, D.	50
Beck, F.	215, 258	Chavannes, N.	86
Benarroch, A.	121	Chen, G.	158
Berenger, J-P.	397	Chen, Y.	93
Bernhard, J.	99	Chen, N-W.	99
Besso, P.	323	Chen, L-Y.	104
Bindiganavale, S.	124	Chen, L.	136, 186
Blaunstein, N.	246	Chen, H-H.	273
Boag, A.	53, 54	Chen, K.	158, 209, 335
Bobillot, G.	265	Cheng, J.	98
Boix, R.	319, 378	Chew, W.	163, 252, 257, 351
Bozzi, M.	323	Chiao, J-C.	104, 136
Branch, E.	259	Chio, I-M.	104
Brehonnet, A.	150	Chiu, T.	331

Chiu, T-C.....	48	Dou, W.....	70
Cho, W-S.....	217	Dreher, A.....	380
Choi, J.....	135	Drioli, L.....	323
Choi, S.....	135	Drossos, A.....	150
Choo, H.....	78	Eibert, T.....	40
Choo, E.....	43	El Idrissi, R.....	379
Chou, H-T.....	18, 133, 134	El-Shenawee, M.....	334
Choudhury, A.....	362	Elamaran, B.....	104
Chrisey, D.....	192	Elkins, J.....	210
Christ, A.....	25	Engheta, N.....	147
Chung, S-J.....	273	Erdemli, Y.....	324
Cicchetti, R.....	61	Ergin, A.....	166, 177, 178
Ciccotosto, M.....	239	Erker, E.....	193
Clark, R.....	99	Erricolo, D.....	5, 51, 141
Coccioli, R.....	87	Erturk, V.....	80
Cockreel, C.....	258	Evans, N.....	74
Cockrell, C.....	215	Excell, P.....	315
Coetzee, J.....	103	Ezzedine, T.....	260
Colak, D.....	168	Fan, G-X.....	169, 182
Cole, M.....	110, 196	Farane, A.....	61
Coleman, C.....	13, 17	Farhat, N.....	160
Colton, J.....	274	Fazarinc, Z.....	4
Corona, P.....	236	Feng, M.....	99
Couchman, L.....	357	Ferrara, G.....	236
Creech, G.....	98	Fink, P.....	256
Cummings, N.....	77, 229	Fiumara, V.....	145
Curry, M.....	239	Fourestié, B.....	346
Cutler, P.....	303	Franchi, P.....	108
Cwik, T.....	200	Frandsen, P.....	198
D'Agostino, F.....	233	Frantzis, P.....	370
da Silva, H.....	102	Frasch, L.....	209
da Silveira, M.....	137	Freni, A.....	106
Damarla, R.....	341	Furse, C.....	84
Daming, L.....	253	Galdi, V.....	145
Dana, R.....	67	Garcia, P.....	121
Datta, S.....	7	Garg, V.....	51
Davis, V.....	311	Gennarelli, C.....	233
Davis, W.....	77, 227	Gersten, B.....	190
Dawson, T.....	156	Geyer, R.....	191
Desclos, L.....	105, 318, 325, 326, 327, 369	Gheorma, I.....	276
Deshpande, M.....	215	Ghione, G.....	276
Detweiler, P.....	225	Gianola, P.....	323
Dick, A.....	37	Gilbert, R.....	97, 324
Ding, Z.....	36	Gingrich, M.....	281
Djordjevic, A.....	368	Gisbert, F.....	388
Djukic, S.....	15	Gisin, F.....	214
Dobbins, J.....	371	Gonzalez, I.....	222
Dogaru, T.....	92, 336	Graglia, R.....	276
Dolmans, G.....	301	Gres, N.....	176
Dong, Y.....	341	Guerouni, S.....	373
		Guo, Y.....	81

Gupta, K.	205
Hagness, S.	154, 270
Hanazawa, M.	216
Hankui, E.	105
Harada, T.	105
Hart, A.	107
Harvey, J.	370
Hashimoto, O.	71, 216
Havrilla, M.	68
Hawkins, J.	81
He, J.	164, 165
Henning, J.	344
Heyman, E.	34
Hilgner, M.	22
Hill, M.	287
Hill, K.	124, 390
Hirata, A.	152, 155
Horii, Y.	152, 383
Horwitz, J.	192, 195
Hosaka, S.	157
Housmand, B.	87
Hubbard, C.	110, 196
Hudson, H.	129
Hurst, M.	170
Hurt, G.	245
Hussey, T.	37
Huynh, M.	223
Hwang, N-L.	251
Ibrahim, E.	315
Ibrahim, T.	153
Ikuina, K.	369
Infante, D.	66
Ioan, D.	271
Ioffe, A.	380
Ishihara, T.	52
Ishimaru, A.	330
Iskander, M.	3, 190
Issaev, Y.	277
Ito, K.	157
Ito, M.	369
Itoh, T.	87
Ittipiboon, A.	314
Jackson, D.	285, 311, 316
Jaffrezou, P.	392
Janaswamy, R.	60
Janev, L.	11
Jang, S.	82
Janpugdee, P.	133
Jensen, M.	114, 122, 249
Jin, J.	257
Jin, J-M.	259

Johnson, W.	129
Johnson, J.	168, 297, 298, 332
Johnston, R.	228
Jorgenson, R.	129
Joshi, P.	110, 196
Joubert, J.	137, 313
Ju, S.	31
Judah, S.	90
Kadambi, G.	221, 224
Kaklamani, D.	391
Kanda, M.	89, 217
Kanellopoulos, J.	120
Karwowski, A.	151
Katehi, L.	98, 272, 288, 370
Katz, D.	246
Kavet, R.	156
Kelley, D.	85
Kelly, P.	289
Kempel, L.	360, 361
Kesler, M.	274
Khebir, A.	260
Kim, W.	192, 195
Kim, S.	211
Kim, H.	31, 332
Kim, K.	171
Kirchoefer, S.	192, 195
Klepal, M.	248
Koala, B.	239
Koh, J.	132
Kolundzija, B.	368
Kopf, D.	97, 324
Korea, S.	263
Kotulski, J.	129, 261
Kouki, A.	260
Koymen, H.	41
Kravchenko, V.	19, 55
Kritikos, T.	120
KruhlaK, R.	23
Kudryashova, L.	338
Kuga, Y.	63, 239, 275, 330
Kunhardt, E.	37
Kuroda, R.	203
Kuster, N.	25, 86
Kutumbos, T.	289
Lam, K.	202
Lammers, T.	289
Langlet, S.	265
Law, C.	381
Lee, A.	188
Lee, C.	250
Lee, H.	250

Lee, J-S.	268, 340
Lee, K.	81
Lee, R.	153, 310, 317
Lee, S.	63, 275
Lee, S-W.	330
Lee, T.	270
Lee, W.	179
Legault, S.	140
Leininger, K.	154
León, G.	319, 378
Letrou, C.	53
Leviaton, Y.	266
Leyten, L.	301
Li, H.	250
Li, L.	167
Li, Q.	335
Li, X.	154
Li, E.	48, 331
Lin, J-H.	396
Lin, Y-Y.	134
Lindell, I.	58, 142
Lindmark, B.	79
Ling, H.	78
Little, M.	288
Liu, C.	99
Liu, G.	384
Liu, Q.	169, 182, 183, 395
Liu, T.	250
Liu, Y.	193
Long, D.	112, 113, 116
Long, S.	311, 316
Long, Y.	14
Lovestead, R.	16
Lowe, L.	210
Lozano, P.	388
Lu, M.	166
Luebbers, R.	85
Lugara, D.	53
Luk, K.	81
Lundgreen, R.	116
Luo, P.	381
Macelloni, G.	119
MacGregor, S.	37
Maci, S.	106, 349
Macon, C.	361
Madde, R.	323
Madhian, M.	105, 369
Mailloux, R.	108
Maloney, J.	274
Malyshkin, A.	277
Marhefka, R.	49
Marliani, F.	119
Marqués, R.	377, 379
Martín, A.	241
Martinat, B.	397
Martinaud, J-P.	199
Martínez-Búrdalo, M.	241
Maruhashi, K.	369
Masek, T.	221
Mason, C.	28
Matsuyama, S.	155
Matthes, R.	5
Mautz, J.	235
Mayes, P.	99
Mayhew-Ridgers, G.	313
Mazanek, M.	248
Mazotta, J.	136
McEwan, N.	315
McKinzie, W.	191
Medina, F.	319, 377, 378
Meese, J.	209
Merrill, W.	42
Mesa, F.	377
Michielssen, E.	99, 166, 176, 177, 178
Miller, R.	356
Miller, E.	334
Miller, J.	180, 181, 376
Millet, F.	115
Miner, G.	118
Mioc, F.	46, 141
Miranda, F.	194
Mittra, R.	59, 204, 238
Moini, R.	67
Mondal, J.	99
Montoya, T.	30, 230
Mooney, J.	36, 210
Morgan, M.	62, 342
Mori, S.	152
Morrow, I.	345
Moumen, A.	345
Mullen, R.	275
Munteanu, I.	271
Murdock, M.	302
Nagra, A.	193
Nagy, L.	17
Nam, S.	263
Narayanan, R.	344
Natzke, J.	348
Naylor, D.	6
Naylor, S.	5
Nehrbass, J.	27

Nelson, S.	208	Periaswamy, P.	193
Nepa, P.	133	Perreggrini, L.	323
Nestico, D.	88	Peterson, A.	125
Nevels, R.	180, 181, 376	Petosa, A.	314
Newman, E.	127, 168	Pierro, V.	145
Newman, H.	195	Piket-May, M.	289
Ngo, E.	110, 196	Pino, M.	296
Nguyen, C.	211, 212, 268, 340	Pinto, I.	145
Niccolai, L.	368	Pisano III, F.	352
Nishizawa, S.	71	Poilasne, G.	312, 325, 326, 327
Nonidez, L.	241	Polat, B.	47
Notaros, B.	15, 234	Poljak, D.	159
Nyquist, D.	66, 68, 209	Pond, J.	192, 195
Oakley II, B.	2	Pontoppidan, K.	198
Obelleiro, F.	264, 296	Potrepka, D. M.	188
Odendaal, J.	137, 313	Potter, M.	24
Ohata, K.	369	Pouliguen, P.	325, 326, 392
Okhmatovsky, V.	126	Puska, L.	142
Okoniewski, M.	24, 28, 228	Qadri, S.	192
Olakangil, J.	84	Rafi, G.	67
Oliner, A.	284, 285	Rahman, M.	322
Ololoska, L.	11	Rahmat-Samii, Y.	201
Olson, S.	305	Ramahi, O.	208
Olyslager, F.	142	Rao, J.	189
Ong, J.	43	Rao, S.	29, 91, 354
Oughstun, K.	146	Rappaport, C.	334
Ow, S.	90	Recchioni, M.	237
Ozdemir, K.	8	Reddy, C.	258
Ozdemir, T.	98, 370	Reed, S.	318
Pack, J.	122	Reinecke, D.	26
Paiva, C.	65	Reineix, A.	397
Paloscia, S.	119	Rembold, B.	14
Pampaloni, P.	119	Riccio, G.	233
Pan, G.	333, 355	Riemann, A.	74
Panagopoulos, A.	120	Riera, J.	121
Pantic-Tanner, Z.	214	Riggs, L.	36, 210
Papapolymerou, J.	287	Riley, D.	37, 261
Park, J.	212, 263	Robitailec, P.	153
Partal, H.	235	Rockway, J.	330
Pate, R.	37	Rod, B.	188
Patel, D.	189	Rodriguez, J.	264
Pathak, P.	49, 133	Rogers, R.	371
Patterson, M. S.	188	Rogers, S.	365
Patterson, P.	37	Rohde, M.	221, 224
Paul, A.	245	Rojas, R.	80
Pearson, L.	47, 107	Roje, V.	159
Pechac, P.	248	Romanofsky, R.	194
Peixeiro, C.	102	Rosario, M.	102
Pelosi, G.	233	Ross, J.	17
Penno, R.	225	Rothwell, E.	17, 158, 209, 360
Perez, J.	222, 388, 389	Sabet, K.	98, 370

Sachdeva, S.	29	Stuchly, M.	89, 156, 322
Sachdeva, N.	91	Stupfel, B.	262
Sacz de Adana, F.	388, 389	Stutzman, W.	10, 77, 223, 227, 229
Safaai-Jazi, A.	16	Su, T.	78
Saito, K.	157	Sudupe, I.	388
Salghetti, L.	106	Suk, J.	158
Sarabandi, K.	48, 98, 244, 331, 370	Sullivan, J.	221, 224
Sarkar, T.	82, 132, 171, 179, 368	Sullivan, A.	341
Sarolic, A.	159	Sultan, M.	76
Sastre, A.	156	Sun, W.	158
Savi, P.	276	Sun, S-W.	134
Savrun, E.	63	Swenson, C.	84
Schindler, J.	108	Swiatkowski, M.	230
Schneider, S.	361	Syed, H.	247
Schneider, J.	23	Symons, W.	240
Schuhmann, R.	22	Synowczynski, J.	188, 190
Schultz, J.	274	Taboada, J.	264
Schuster, C.	25	Takahashi, N.	369
Scott, W.	30	Takamizawa, K.	77, 227
Scullion, T.	212	Talor, T.	193
Senba, N.	369	Tanaka, K.	353
Sengupta, D.	364	Tanaka, M.	353
Senior, T.	140	Tanigughi, T.	157
Sertel, K.	324	Tauber, A.	188
Shanker, B.	176, 177, 178	Terret, C.	318, 325, 326
Shen, Z.	381	Tham, C.	159
Shepard, R.	156	Thiele, G.	225
Shifman, Y.	266	Thoma, P.	26
Shiozawa, T.	152, 155	Thompson, D.	116, 117
Shlivinski, A.	34	Thompson, K.	306
Shumpert, J.	288	Tian, B.	183
Simmons, K.	221, 224	Tiberio, R.	46, 232
Slattman, P.	79	Tidrow, S. C.	188
Smith, R.	269	Timothy, K.	43
Smith, R.I.	304	Tirkas, P.	203
Smith, P.	146	Toccafondi, A.	46
Smith, J-K.	96	Tognolatti, P.	72
Solaimani, M.	372	Tokgoz, C.	49
Song, J.	163, 252, 257	Topa, A.	65
Soudais, P.	265	Topcu, S.	41
Speck, J.	193	Topsakal, E.	358
Spitsyn, V.	73, 337, 338	Toroshchin, P.	19
Spitsyna, N.	73	Torungrueng, D.	297, 298
Steadman, J.	300	Toso, G.	233, 236
Steenman, D.	62	Toupikov, M.	333, 355
Steyskal, H.	108	Toutain, S.	318
Stout, S.	314	Trabelsi, S.	208
Stronach, S.	129	Tretiakov, Y.	333, 355
Stuchly, S.	213	Trintinalia, L.	78
		Trosko, J.	158

Trott, K.....	361	Worasawate, D.....	8
Tsai, C.....	396	Wu, I.....	71
Tsang, L.....	239, 335	Wu, K-L.....	382
Tsutsumi, M.....	383	Wu, H.....	192
Turhan-Sayan, G.....	38	Wu, F.....	64
Turner, C.....	261	Wu, C-W.....	360
Tyo, J.....	143	Wu, T.....	35
Ugur, A.....	8	Xie, T.....	162
Upham, B.....	158	Xu, H.....	103
Uslenghi, P.....	5, 51, 141	Xu, X.....	169, 344
Uzunoglu, N.....	391	Xu, X-B.....	384
Vaccaro, R.....	307	Yablonovitch, E.....	312
Vagnoni, A.....	72	Yan, M.....	186
Van, T.....	175	Yang, Y.....	59
van Genderen, P.....	345	Yang, H.....	286
Van Keuls, F.....	194	Yang, M.....	93
Velamparambil, S.....	163	Yang, S.....	35
Vescovo, R.....	363	Yasan, E.....	272
Villar, R.....	241	Yetginer, E.....	41
Volakis, J.....	97, 247, 324, 358	Yin, X.....	257
Voronovich, A.....	294	Yoho, P.....	112
Wada, K.....	216	York, R.....	193
Wagner, M.....	306	Yoshimura, H.....	157
Wahid, P.....	7	Yoshioka, R.....	52
Walkenhorst, B.....	118	Young, J.....	365
Wallace, J.....	122, 249	Yu, T.....	394
Waller, M.....	354	Yu, W.....	204
Walton, E.....	343	Yun, Z.....	190
Wang, C-C.....	251	Yurchenko, V.....	41
Warne, L.....	129	Yylmaz, O.....	41
Warnick, K.....	351	Zaman, A.....	317
Watson, P.....	98	Zaugg, D.....	114
Weiland, T.....	22, 26, 271	Zavorotny, V.....	294
Weile, D.....	177	Zeilinger, S.....	364
Weng, C-L.....	273	Zelkin, E.....	19
Werges, S.....	6	Zhang, Q.....	205
Werner, D.....	59, 281	Zhang, Y.....	252
Werner, P.....	281	Zhang, Z.....	190, 395
Whalen, S.....	15	Zhou, L.....	335
Whites, K.....	64, 240	Zhu, X.....	165
Wiat, J.....	151, 346	Ziolkowski, R.....	287
Wight, J.....	314	Zirilli, F.....	237
Williams, J.....	311, 316		
Williams, C.....	5		
Wilton, D.....	256		
Wittig, T.....	271		
Wong, M.....	151		
Wong, T.....	186		
Wood, A.....	175, 350		
Wood, W.....	350		
Wood Jr., W.....	390		



